

AD-A055 523

ARMY ENGINEER WATERWAYS EXPERIMENT STATION VICKSBURG MISS F/G 8/3
PHYSICAL MODEL SIMULATION OF THE HYDRAULICS OF MASONBORO INLET,--ETC(U)
NOV 77 R A SAGER, W C SEABERGH

UNCLASSIFIED

WES-GITI-15

NL

1 OF 5
AD
A055523





FOR FURTHER TRAN

12

B.S.

AD A 055523

PHYSICAL MODEL SIMULATION OF THE HYDRAULICS OF MASONBORO INLET, NORTH CAROLINA

by

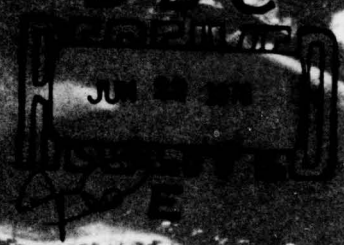
Richard A. Sager, William C. Seabergh

AD No. _____
DDC FILE COPY

GIT REPORT 15



November 1977



GENERAL INVESTIGATION OF TIDAL INLETS

A Program of Research Conducted Jointly by

U. S. Army Coastal Engineering Research Center, Fort Belvoir, Virginia

U. S. Army Engineer Waterways Experiment Station, Vicksburg, Mississippi

Department of the Army
Corps of Engineers

78 06 19 140

APPROVED FOR PUBLIC RELEASE

Reprint or republication of any of this material shall give appropriate credit to the U.S. Army Coastal Engineering Research Center.

Limited free distribution within the United States of single copies of this publication has been made by this Center. Additional copies are available from:

*National Technical Information Service
ATTN: Operations Division
5285 Port Royal Road
Springfield, Virginia 22151*

Contents of this report are not to be used for advertising, publication, or promotional purposes. Citation of trade names does not constitute an official endorsement or approval of the use of such commercial products.

The findings in this report are not to be construed as an official Department of the Army position unless so designated by other authorized documents.

• Cover Photo: Masonboro Inlet, North Carolina, July 1974

Unclassified

SECURITY CLASSIFICATION OF THIS PAGE (When Data Entered)

REPORT DOCUMENTATION PAGE		READ INSTRUCTIONS BEFORE COMPLETING FORM
1. REPORT NUMBER GITI Report 15 ✓	2. GOVT ACCESSION NO.	3. RECIPIENT'S CATALOG NUMBER
4. TITLE (and Subtitle) 6 PHYSICAL MODEL SIMULATION OF THE HYDRAULICS OF MASONBORO INLET, NORTH CAROLINA.	5. TYPE OF REPORT & PERIOD COVERED 7 Final report	
7. AUTHOR(s) 10 Richard A. Sager William C. Seabergh	8. CONTRACT OR GRANT NUMBER(s)	
9. PERFORMING ORGANIZATION NAME AND ADDRESS U. S. Army Engineer Waterways Experiment Station Hydraulics Laboratory P. O. Box 631, Vicksburg, Mississippi 39180	10. PROGRAM ELEMENT, PROJECT, TASK AREA & WORK UNIT NUMBERS	
11. CONTROLLING OFFICE NAME AND ADDRESS U. S. Coastal Engineering Research Center Kingman Building Fort Belvoir, Virginia 22060	12. REPORT DATE 11 November 1977	
14. MONITORING AGENCY NAME & ADDRESS (if different from Controlling Office) 14 WES-GITI-25	13. NUMBER OF PAGES 552	
15. SECURITY CLASS. (of this report) Unclassified		15a. DECLASSIFICATION/DOWNGRADING SCHEDULE
16. DISTRIBUTION STATEMENT (of this Report) Approved for public release; distribution unlimited. 12 258 P.		
17. DISTRIBUTION STATEMENT (of the abstract entered in Block 20, if different from Report) DDC RECEIVED JUN 22 1978 E		
18. SUPPLEMENTARY NOTES		
19. KEY WORDS (Continue on reverse side if necessary and identify by block number) Fixed-bed models Hydraulic models Hydraulic similitude Masonboro Inlet, N. C.		
20. ABSTRACT (Continue on reverse side if necessary and identify by block number) This report is part of the General Investigation of Tidal Inlets "Inlet Hydraulics Study." The study involves the investigation of the tide- and wave-generated flow regime and water-level fluctuations in the vicinity of coastal inlets. Masonboro Inlet was selected as an inlet to be used in determining the usefulness and reliability of physical and mathematical models in predicting hydraulic characteristics of inlet/bay systems. This report presents results obtained from the physical model study. 138 200 (Continued)		

DD FORM 1 JAN 73 1473 EDITION OF 1 NOV 65 IS OBSOLETE

Unclassified

SECURITY CLASSIFICATION OF THIS PAGE (When Data Entered)

78 06 19 140

Abstract

CINT

Unclassified

SECURITY CLASSIFICATION OF THIS PAGE(When Data Entered)

20. ABSTRACT (Continued).

cont

→ The Masonboro Inlet fixed-bed model, constructed to scales of 1:300 horizontally and 1:60 vertically, reproduced an area extending to the -45 ft contour in the Atlantic Ocean and to the nodal points in each interior channel. The wetlands were accurately reproduced near the inlet; but those areas farther bayward, being relatively flat, were reproduced schematically and artificially bent into the research flume to provide storage for the tidal prism. The model was equipped with appurtenances necessary for accurate reproduction and measurement of tides, tidal currents, waves, and other significant prototype phenomena. Model verification tests assured that the model hydraulic regimen was in satisfactory agreement with that of the prototype. Five velocity ranges with three stations at each range were verified in the model (readings were taken at three depths at each station); and seven tidal elevation gages in the ocean and bay were also verified. ←

A detailed examination of the effects of waves on model current and tidal height data was then made. A circulation pattern was set up in the lee of the single jetty which ebbed out along the edge of the jetty, then returned along the outer portion of the ocean bar back toward shore and the inlet. This occurred for a variety of wave directions. Waves approaching from a S16°E direction, directly into the ebb current, produced the greatest effect on tidal heights in the bay, causing a superelevation of the heights when compared with data taken without waves.

After testing the 1969 condition, the model was remolded to the November 1964 condition, which represents a time preceding the construction of improvements--a north jetty, a deposition basin, and a dredged channel. Base data were collected, then the improvements were installed upon this condition and tests were run to predict the effect of the improvements on the tidal elevations, tidal currents, and wave-induced currents. The model was then remolded to the July 1966 postconstruction condition and tests were conducted to gather data to compare with the predicted data since no immediate prototype postconstruction hydraulic data were available.

The fixed-bed model predictions of a filling of the dredged navigation channel, filling of the deposition basin, and a tendency for the navigation channel to shift toward the north jetty were substantiated by comparison with the 1966 model results and with prototype data.

ACCESSION for	
NTIS	White Section <input checked="" type="checkbox"/>
DDC	Buff Section <input type="checkbox"/>
UNANNOUNCED	<input type="checkbox"/>
JUSTIFICATION	
BY	
DISTRIBUTION/AVAILABILITY CODES	
Dist.	AVAIL. and/or SPECIAL
A	

Unclassified

SECURITY CLASSIFICATION OF THIS PAGE(When Data Entered)

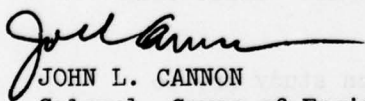
FOREWORD

This report was prepared by the Estuaries and Wave Dynamics Divisions of the Hydraulics Laboratory at the U. S. Army Engineer Waterways Experiment Station (WES) as one in a series of reports on the General Investigation of Tidal Inlets (GITI). The GITI research program is under the technical surveillance of the U. S. Army Coastal Engineering Research Center (CERC), and is conducted by CERC, WES, and other Government and private organizations.

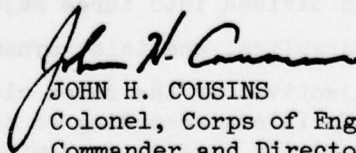
The Masonboro Inlet fixed-bed model tests were conducted by Messrs. W. C. Seabergh, Project Engineer, E. F. Lane, and L. M. Neal. The report was prepared by Messrs. Seabergh and R. A. Sager (WES), with extensive revisions and editing by M. L. Giles (CERC). The study and report preparation were supervised by E. C. McNair and MAJ F. C. Perry (former WES GITI Program Managers), C. L. Vincent (present WES GITI Program Manager), R. A. Sager, Chief of the Estuaries Division, R. W. Whalin, Chief of the Wave Dynamics Division, and H. B. Simmons, Chief of the Hydraulics Laboratory. CERC technical surveillance was conducted by Messrs. C. Mason and R. M. Sorensen. Civilian members of the Coastal Engineering Research Board, Dean Morrough P. O'Brien, Professor Robert G. Dean, and Professor Arthur T. Ippen (former member, deceased), were intimately involved in both the planning and review of this report, and Professor Robert L. Wiegel contributed extensive review comments. Technical Directors of CERC and WES were Messrs. T. Saville, Jr., and F. R. Brown, respectively.

Comments on this publication are invited.

Approved for publication in accordance with Public Law 166, 79th Congress, approved 31 July 1945, as supplemented by Public Law 172, 88th Congress, approved 7 November 1963:



JOHN L. CANNON
Colonel, Corps of Engineers
Commander and Director
Waterways Experiment Station



JOHN H. COUSINS
Colonel, Corps of Engineers
Commander and Director
Coastal Engineering Research Center

PREFACE

1. The Corps of Engineers, through its Civil Works program, has sponsored, over the past twenty-three years, research into the behavior and characteristics of tidal inlets. The Corps' interest in tidal inlet research stems from its responsibilities for navigation, beach erosion prevention and control, and flood control. Tasked with the creation and maintenance of navigable U. S. waterways, the Corps dredges millions of cubic yards of material each year from tidal inlets that connect the ocean with bays, estuaries, and lagoons. Design and construction of navigation improvements to existing tidal inlets are an important part of the work of many Corps offices. In some cases, design and construction of new inlets are required. Development of information concerning the hydraulic characteristics of inlets is important not only for navigation and inlet stability but also because inlets control the daily exchange of water between bay and ocean. Accurate predictions of the effects of storm surges and runoff also require an understanding of inlet hydraulics during extreme conditions.

2. A research program, the General Investigation of Tidal Inlets program, was developed to provide quantitative data for use in design of inlets and inlet improvements. It is designed to meet the following objectives:

To determine the effects of wave action, tidal flow, and related phenomena on inlet stability and on the hydraulic, geometric, and sedimentary characteristics of tidal inlets; to develop the knowledge necessary to design effective navigation improvements, new inlets, and sand transfer systems at existing tidal inlets; to evaluate the water transfer and flushing capability of tidal inlets; and to define the processes controlling inlet stability.

3. The GITI is divided into three major study areas: inlet classification, inlet hydraulics, and inlet dynamics.

- a. The objectives of the inlet classification study are to classify inlets according to their geometry, hydraulics, and stability, and to determine the relationships that exist among the geometric and dynamic characteristics and

the environmental factors that control these characteristics. The classification study keeps the general investigation closely related to real inlets and produces an important inlet data base useful in documenting the characteristics of inlets.

- b. The objectives of the inlet hydraulics study are to define the tide-generated flow regime and water-level fluctuations in the vicinity of coastal inlets and to develop techniques for predicting these phenomena. The inlet hydraulics study is divided into three areas: idealized inlet model study, evaluation of state-of-the-art physical and numerical models, and prototype inlet hydraulics.

- (1) The idealized inlet model. The objectives of this model study are to determine the effect of inlet configurations and structures on discharge, head loss, and velocity distribution for a number of realistic inlet shapes and tide conditions. An initial set of tests in a trapezoidal inlet was conducted between 1967 and 1970. However, in order that subsequent inlet models are more representative of real inlets, a number of "idealized" models representing various inlet morphological classes are being developed and tested. The effects of jetties and wave action on the hydraulics are included in the study.
- (2) Evaluation of state-of-the-art modeling techniques. The objectives of this portion of the inlet hydraulics study are to determine the usefulness and reliability of existing physical and numerical modeling techniques in predicting the hydraulic characteristics of inlet/bay systems, and to determine whether simple tests, performed rapidly and economically, are useful in the evaluation of proposed inlet improvements. Masonboro Inlet, N. C., was selected as the prototype inlet which would be used along with hydraulic and numerical models in the evaluation of existing techniques. In September 1969 a complete set of hydraulic and bathymetric data was collected at Masonboro Inlet. Construction of the fixed-bed physical model was initiated in 1969, and extensive tests have been performed since then. In addition, three existing numerical models were applied to predict the inlet's hydraulics. Extensive field data were collected at Masonboro Inlet in August 1974 for use in evaluating the capabilities of the physical and numerical models.
- (3) Prototype inlet hydraulics. Field studies at a number of inlets are providing information on prototype inlet/bay tidal hydraulic relationships and the effects of friction, waves, tides, and inlet morphology on these relationships.

c. The basic objective of the inlet dynamics study is to investigate the interactions of tidal flow, inlet configuration, and wave action at tidal inlets as a guide to improvement of inlet channels and nearby shore protection works. The study is subdivided into four specific areas: model materials evaluation, movable-bed modeling evaluation, reanalysis of a previous inlet model study, and prototype inlet studies.

- (1) Model materials evaluation. This evaluation was initiated in 1969 to provide data on the response of movable-bed model materials to waves and flow to allow selection of the optimum bed materials for inlet models.
- (2) Movable-bed model evaluation. The objective of this study is to evaluate the state-of-the-art of modeling techniques, in this case movable-bed inlet modeling. Since, in many cases, movable-bed modeling is the only tool available for predicting the response of an inlet to improvements, the capabilities and limitations of these models must be established.
- (3) Reanalysis of an earlier inlet model study. In 1957, a report entitled "Preliminary Report: Laboratory Study of the Effect of an Uncontrolled Inlet on the Adjacent Beaches" was published by the Beach Erosion Board (now CERC). A reanalysis of the original data is being performed to aid in planning of additional GITI efforts.
- (4) Prototype dynamics. Field and office studies of a number of inlets are providing information on the effects of physical forces and artificial improvements on inlet morphology. Of particular importance are studies to define the mechanisms of natural sand bypassing at inlets, the response of inlet navigation channels to dredging and natural forces, and the effects of inlets on adjacent beaches.

4. As a part of the inlet hydraulics portion of the GITI, the primary goal of the model study was an investigation of the predictive capabilities of physical models of inlets and the modeling techniques necessary to accomplish this. This report is the first of two reports presenting detailed results and covers model verification and 1964 and 1966 conditions. A second report will discuss the model verification (model predictions versus prototype data) based on 1974 conditions.

CONTENTS

	<u>Page</u>
FOREWORD	1
PREFACE	2
CONVERSION FACTORS, U. S. CUSTOMARY TO METRIC (SI) UNITS OF MEASUREMENT	7
PART I: INTRODUCTION	8
Purpose and Scope of Study	8
Approach	8
PART II: THE PROTOTYPE	11
PART III: THE MODEL	19
Design of Model	19
Model Construction	19
Appurtenances	22
Limitations of the Accuracy of Model Measurements	26
PART IV: HYDRAULIC VERIFICATION	28
Prototype Data	28
Procedure	30
PART V: ADDITIONAL 1969 TESTS	41
Tides and Currents	41
Influence of Waves	41
Waves with No Tide	45
Waves with Tide	45
Supplemental Information	48
Summary	49
PART VI: BASE TESTS OF 1964 HYDROGRAPHY	51
Model Modification	51
Hydraulic Tests	51
Wave Tests	53
Summary	62
PART VII: PLAN TESTS OF 1964 HYDROGRAPHY	64
Model Modification	64
Hydraulic Tests	64
Wave Tests	68
Predictions	76
Summary	77
PART VIII: TESTS OF 1966 HYDROGRAPHY	78
Hydraulic Tests	81
Wave Tests	85
Summary	87

CONTENTS

	<u>Page</u>
PART IX: CONCLUSIONS AND RECOMMENDATIONS	89
Model Predictions	89
Prototype Data Collection	89
Model Procedures	90
Effects of Waves on Inlets	92
Basic Research Needs	92
REFERENCES	95
TABLES 1-5	
PHOTOS 1-105	
PLATES 1-349	

CONVERSION FACTORS, U. S. CUSTOMARY TO METRIC (SI)
UNITS OF MEASUREMENT

U. S. customary units of measurement used in this report can be converted to metric (SI) units as follows:

<u>Multiply</u>	<u>By</u>	<u>To Obtain</u>
inches	25.4	millimetres
feet	0.3048	metres
miles (U. S. statute)	1.609344	kilometres
square feet	0.09290304	square metres
square miles (U. S. statute)	2.589988	square kilometres
cubic feet	0.02831685	cubic metres
feet per second	0.3048	metres per second
cubic feet per second	0.02831685	cubic metres per second
degrees (angle)	0.01745329	radians

PHYSICAL MODEL SIMULATION OF THE HYDRAULICS OF
MASONBORO INLET, NORTH CAROLINA
Hydraulic Model Investigation

PART I: INTRODUCTION

Purpose and Scope of Study

1. The purpose of the Masonboro Inlet fixed-bed model study was to determine the ability of existing physical modeling techniques to predict the hydraulic characteristics of an inlet/bay system, and to determine whether simple tests, performed rapidly and economically, could be useful in predicting the effects of proposed inlet improvements. This report presents model verification and prediction data as well as analyses concerning a comparison of model results and effects of waves on model hydraulics. Some of the data were used by Harris¹ to assess the relative accuracy of physical and numerical model verifications. Results of a number of supplementary tests conducted in the physical model are discussed by Seabergh in Reference 2.

Approach

2. The normal sequence of events in a physical fixed-bed model study conducted for the purpose of developing a plan of improvement for a tidal inlet is to:

- a. Obtain the necessary prototype data required to verify the model (include bathymetries, tidal velocities, wave characteristics, and tidal heights).
- b. Construct the model to the bathymetric condition that existed when all prototype data were obtained for the pre-improvement inlet conditions.
- c. Verify (adjust) the model to obtain agreement between model and prototype data, which ensures that the physical parameters of the inlet are properly reproduced in the model.

- d. Obtain a complete set of base data consisting of all conditions of interest in the model.
- e. Install a plan of improvement, obtain a set of data similar to the base data, and predict the effects of the plan on the important physical parameters, i.e., tidal velocities and tidal elevations, waves, etc.

Since this study was an evaluation of physical model capabilities, a seventh step would normally be required:

- f. Obtain prototype hydraulic and bathymetric data for post-improvement conditions and compare this with the model predictions.

3. In this study, a significant change in the order of events given above was necessary, resulting in a model evaluation that was less than ideal. The sequence of events followed in this study is compared with those above in order to provide the reader with an understanding of the problems and limitations of the study.

- a. (Steps 2a, 2b, and 2c: Obtain prototype data for pre-improvement conditions; construct and verify model). The improvements at Masonboro Inlet were constructed between 1965 and 1966 and although satisfactory preimprovement bathymetries of the inlet were available, no comprehensive tide and current data had ever been collected. Therefore, the model could not be verified in September 1969 to pre-improvement conditions. Instead, a complete set of tide and current data was collected just after this study began (1969), and the model was built and verified to these conditions. Then, a detailed preimprovement bathymetry was selected (1964) and the area immediately adjacent to the inlet throat and ebb and flood tidal deltas was remodeled to this condition. The modeled bay area remained the same since there was very little change in the bay during the 1964-1969 period. Although no hydraulic data were available to verify this preimprovement condition, the area that was changed from the 1969 to the 1964 condition was small relative to the entire model. Also, the 1969 verification provided considerable experience in the adjustment of model roughness. Therefore, the 1964 model hydraulic conditions were assumed to be close to those of the prototype.
- b. (Steps 2d to 2f: Obtain complete model data for base conditions, then for base condition with improvements; evaluate model predictions using postimprovement prototype data). Model data were collected from the 1964 condition to

provide a basis for comparison of additional data collected with the improvement plan installed in the 1964 model. However, for an accurate evaluation of the model's predictive capability, prototype data obtained immediately after the actual improvements were made should be available. Since no data were available, the model was remolded to the bathymetry in existence just after the improvements were completed in 1966, and model data were collected which are assumed to represent postimprovement prototype tides and currents. These data are compared with the improved 1964 condition data to evaluate the model's effectiveness. Thus, a complex series of actions have been necessary which make a direct evaluation of the model capabilities difficult; however, many useful and interesting results have been obtained that merit publication.

4. As indicated above, Step 2f is not included in this report. However, in view of the limitations cited above, prototype data were later obtained for hydrographic conditions significantly different from that of model verification, allowing a direct comparison of predicted and prototype data. Results of this comparison were published by Seabergh and Mason,³ and a more detailed analysis, including numerical model results, will be published in a forthcoming GITI report.

PART II: THE PROTOTYPE

5. Masonboro Inlet, a natural inlet through the coastal barrier beach of North Carolina, is located in the southern portion of the state, 8 miles* northeast of Wilmington, North Carolina (Figure 1). The inlet

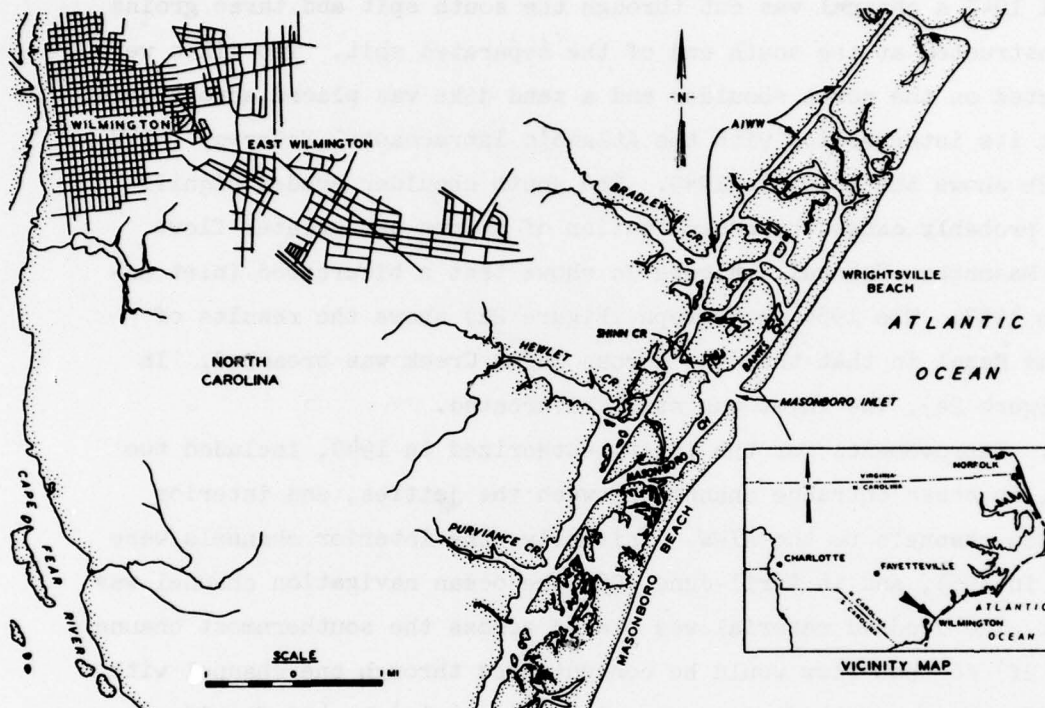


Figure 1. Location map

is at the southern end of Wrightsville Beach, an important resort beach located in New Hanover County.

6. A short history of Masonboro Inlet and its local environment derived from reports of the Wilmington District^{4,5} and other publications^{6,7} follows. It appears that the inlet has been open continuously since 1733, although it has migrated extensively. In 1909 it was 4000 ft.

* A table of factors for converting U. S. customary units of measurement to metric (SI) units is presented on page 7.

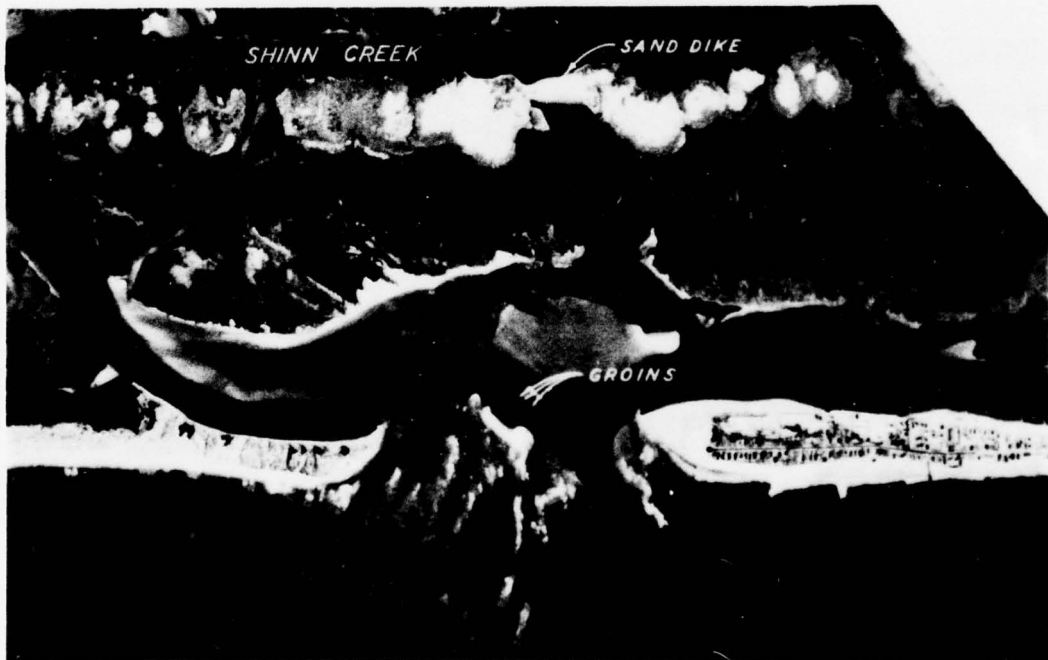
south of its present location. Since 1928 the north shoulder of the inlet (Wrightsville Beach tip) has been relatively stable. The history of the south shoulder indicates that its position has been much more erratic, due both to man and nature. Figure 2a shows the protrusion of the south shoulder into the inlet in 1945 which subsequently caused erosion of the north shoulder of the inlet. In order to abate this problem, in April 1947 a channel was cut through the south spit and three groins were constructed at the south end of the separated spit. Two dikes were constructed on the north shoulder and a sand dike was placed across Shinn Creek at its intersection with the Atlantic Intracoastal Waterway (AIWW). Figure 2b shows the inlet in 1949. The south shoulder eroded significantly, probably caused by a combination of storms and greater flows through Masonboro Channel. Figure 2c shows that a bifurcated inlet existed in 1953. The 1954 photograph (Figure 2d) shows the results of Hurricane Hazel in that the dike across Shinn Creek was breached. In 1956 (Figure 2e), the inlet was still bifurcated.

7. Improvements for the inlet, authorized in 1949, included two jetties, an ocean entrance channel between the jetties, and interior navigation channels to the AIWW. Initially, the interior channels were dredged in 1957, and in April-June 1959 the ocean navigation channel was dredged. The dredged material was placed across the southernmost channel (Figure 2f) so that flow would be concentrated through one channel with design dimensions of 14 ft deep mean low water (mlw) by 400 ft wide at the bottom. This channel shoaled quickly and the channel was reestablished in 1959. Again, heavy shoaling of the entrance occurred so that construction of the two authorized jetties was recommended by the U. S. Army Engineer District, Wilmington. Due to funding limitations, it was proposed to construct the north jetty initially since it was on the updrift side of the inlet.

8. The plan of improvement extracted from the Wilmington District General Design Memorandum is shown in Figure 3. The improvement plan consisted of a north jetty with a low interior weir, a deposition basin adjacent to the north jetty, and reestablishment of the navigation channel. The jetty was constructed using concrete sheet piles for the

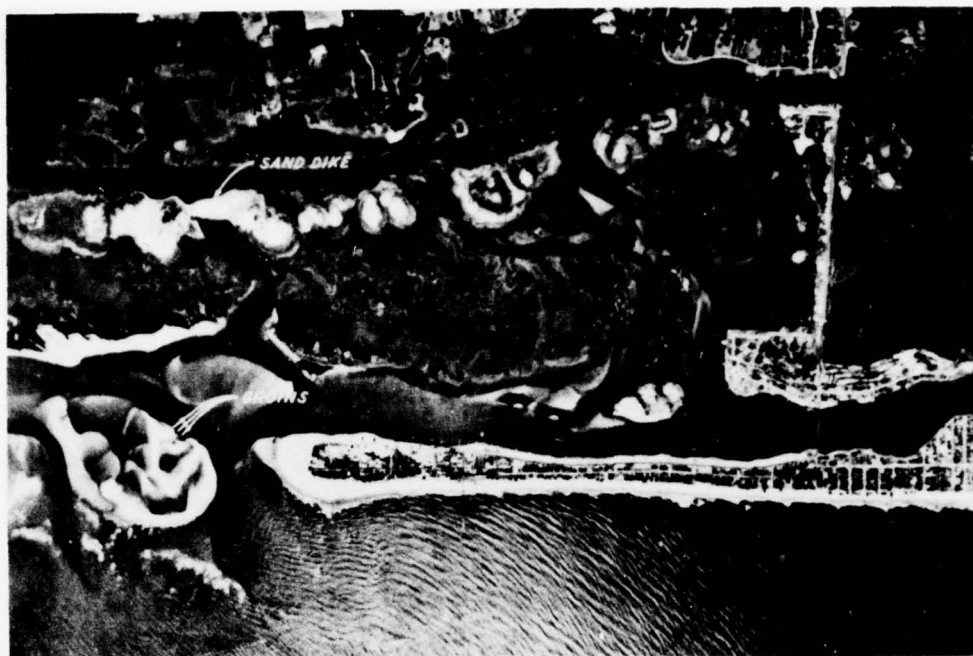


a. 23 Jan 1945

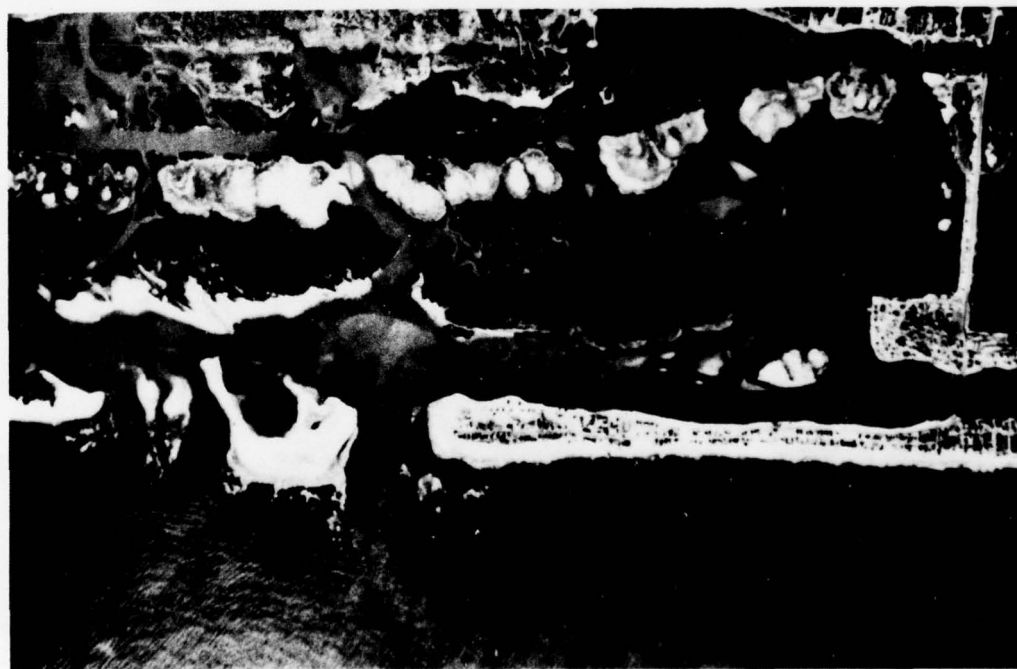


b. 15 Nov 1949

Figure 2. Masonboro Inlet, 1945-1959 (sheet 1 of 3)



c. 31 May 1953



d. 30 Nov 1954

Figure 2 (sheet 2 of 3)



e. 25 Mar 1956



f. 16 Aug 1959

Figure 2 (sheet 3 of 3)

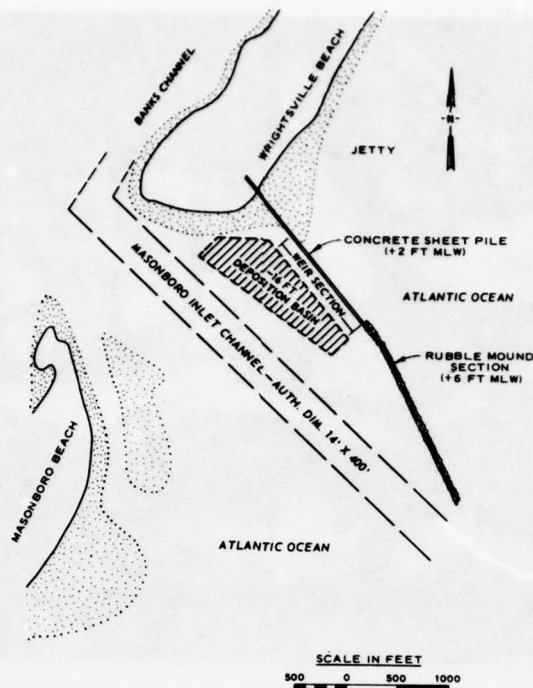
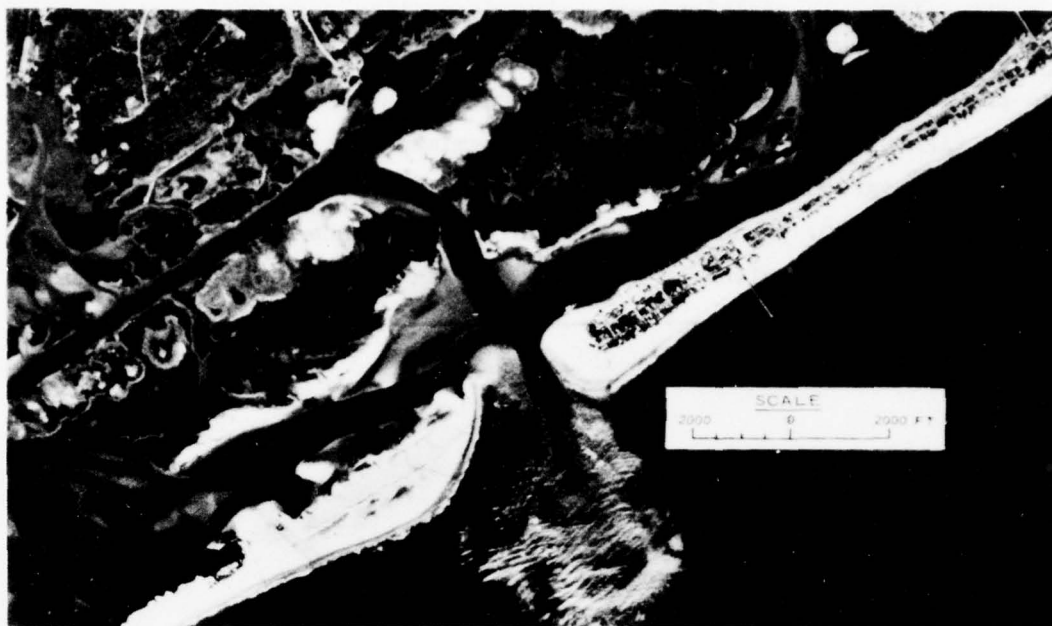


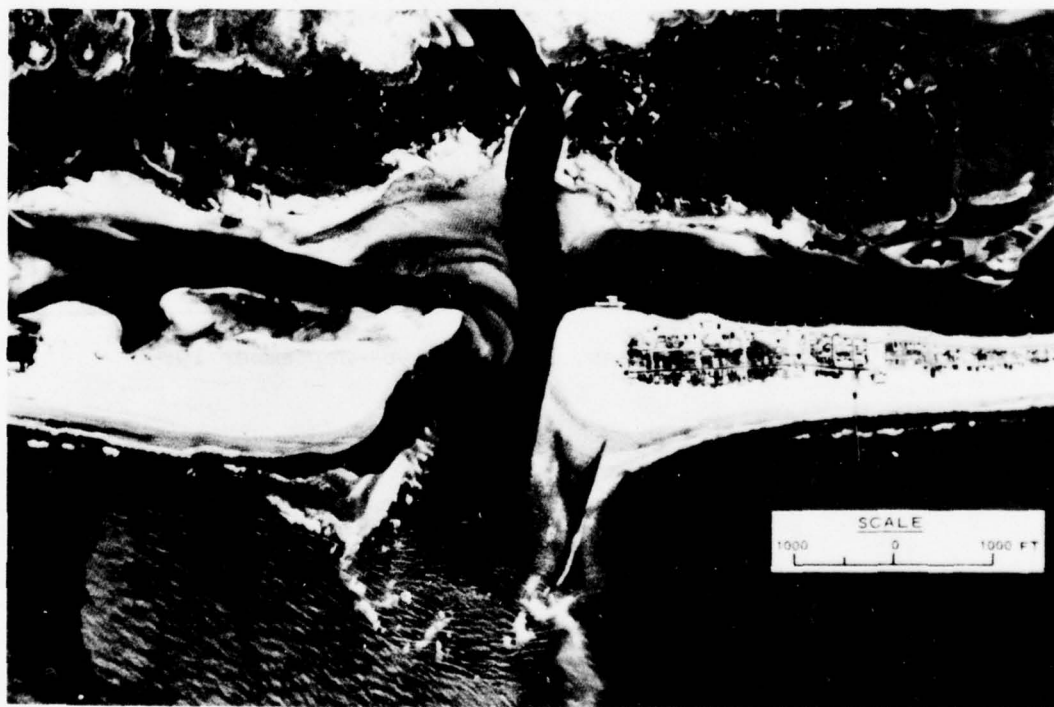
Figure 3. 1965-1966 plan of improvement

shoreward portion from +12 ft beach elevation to the existing -5 ft mlw, a distance of about 1700 ft, and quarrystone from -5 ft mlw to -12 ft mlw, a distance of 1700 ft. The top of the sheet pile for the shoreward 600 ft varied from +12 ft to +2 ft mlw and then remained at +2.0 ft mlw to the -5 ft mlw depth. From the -5 ft mlw contour to the -12 ft mlw contour, the jetty was constructed to an elevation of +6 ft mlw. The concrete sheet pile portion of the jetty, graded at +2.0 ft mlw, was designed to act as a weir and would allow the passage of littoral drift within the zone from the beach to the -5 ft contour. Sand moving southward along the beach and over the weir would be trapped in the deposition basin dredged between the jetty and the northern limit of the inlet channel. Figures 4a and 4b show the inlet during construction from August 1965 to June 1966.

9. A year and a half after construction of the jetty the existing channel had migrated northward through the deposition basin and against



a. Weir portion of jetty under construction 26 Oct 1965



b. Rubble-mound portion of jetty under construction 20 Mar 1966

Figure 4. Construction phase

the north jetty. In addition, extensive deposition occurred on the large shoal on the south side of the inlet. By 1969 the inlet channel was in close proximity to over half the jetty length, as shown by the channel thalwegs (lines connecting points of the maximum depth) in Figure 5. Prototype hydrographic surveys from November 1964 to September 1969 are shown in Plates 1-8. A detailed discussion of the channel response to jetty construction is given by Kieslich and Mason.⁸

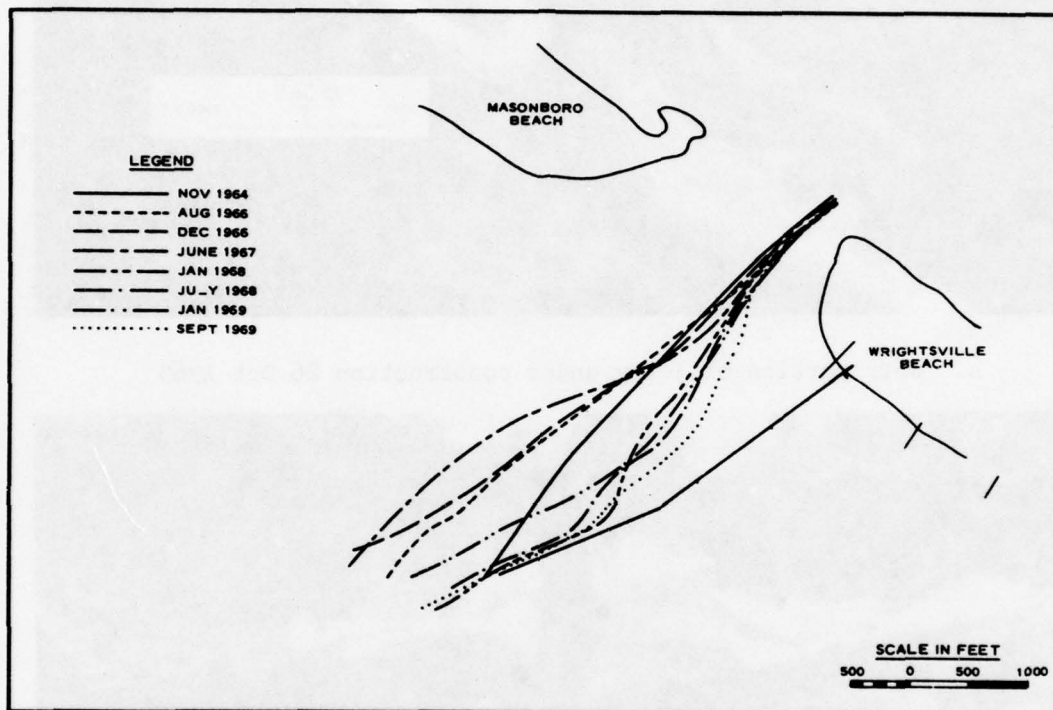


Figure 5. Channel thalwegs, December 1964-September 1969

PART III: THE MODEL

Design of Model

10. Linear scale ratios, model to prototype, of 1:300 horizontal and 1:60 vertically were selected for the Masonboro Inlet model. Scale selections were based on:

- a. Size of model facility available,
- b. Cost of model construction,
- c. Ocean and bay areas to be reproduced to ensure accuracy of model results,
- d. Depths in channel and bay areas, and
- e. Convenience of model operation.

Following selection of the linear scales, the model was designed and operated in accordance with Froude's model law. The scale relations used for design and operation of the model were as follows:

<u>Characteristic</u>	<u>Scale Relations</u>
Horizontal	$L_H = 1:300$
Vertical	$L_V = 1:60$
Volume	$L_H L_H L_V = 1:5,400,000$
Velocity	$L_V^{1/2} = 1:7.746$
Discharge	$L_V^{3/2} L_H = 1:139,427$
Time--tides	$L_H / L_V^{1/2} = 1:38.73$
Slope	$L_V / L_H = 5:1$
Time--wind wave (modeling refraction, see paragraphs 42 and 43)	$L_V / L_V^{1/2} = 1:7.746$

Model Construction

11. The model, constructed in a 50-ft-wide by 150-ft-long enclosed facility, was molded in cement mortar to metal templates forming

a fixed-bed model. The model represented the September 1969 hydrographic survey (Plate 8) and approximately 14.5 square miles of the prototype including the bay area to the limits of the inlets' influence and offshore to the -45 ft mlw contour. North Carolina grid coordinates were used for horizontal control and the mlw Beaufort datum was used for vertical control during model construction. After construction, the control was converted to mean sea level (msl) by subtracting the difference between the datum planes of 1.88 ft.

12. Determining the limit of influence, or nodal points, of Masonboro Inlet is difficult due to the lack of tidal data in the AIWW and other connecting inlets. However, estimates of the nodal points were made using the discharge measurements. In addition, maps were examined for locations of frequent dredging or other low-velocity indicators to help locate the bay boundaries. Due to the limitation of the lateral extension of the facility, artificial bending of the bay areas north and south of the inlet was necessary. Since the principal area of interest was the immediate vicinity of the inlet, this primarily schematic reproduction of the bay allowed significant savings to be achieved in model construction. In the prototype, the bay extended north and south from the inlet entrance parallel to the coast (Figure 6). In the model, the northern and southern extremities of the bay were reproduced in the rear of the model facility (Figure 7) rather than on the sides, due to space limitations. The wetland areas of the bay were thus maintained in the correct model-to-prototype proportion and provided the proper tidal prism storage area. A general view of the model is shown in Figure 8.

13. Since the model was of distorted scales, it was necessary to add three types of artificial roughness to obtain a greater energy loss due to friction than could be achieved from the relatively smooth concrete model bed. While the molded concrete was still soft, 1/2-in.-wide flat metal roughness strips were inserted in the main flow channel regions perpendicular to the expected flow directions. The strips extended from the bottom of the channel to just below the mlw level. Spacing of the strips was governed by previous experience with roughness adjustment;

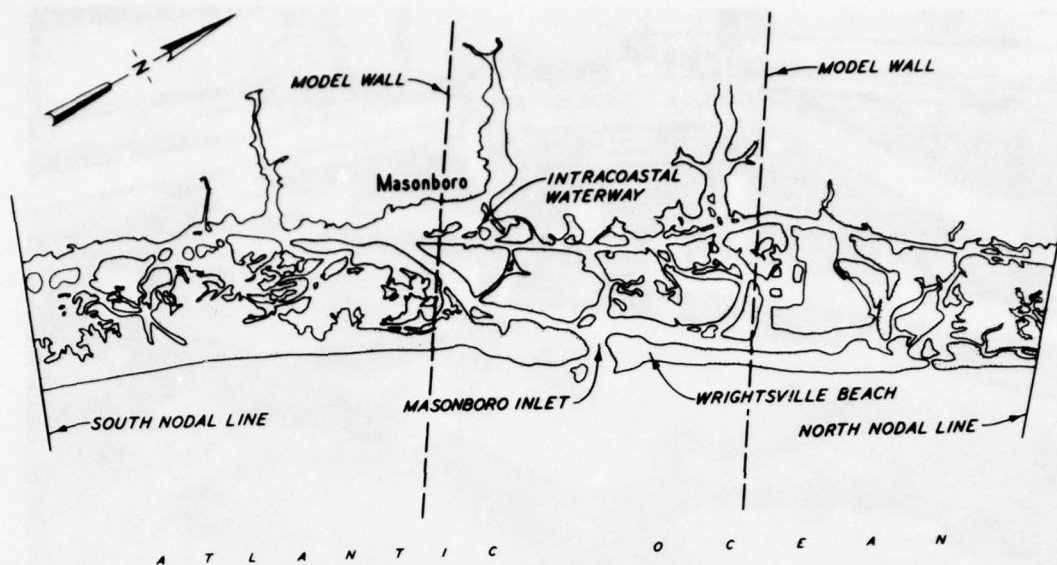


Figure 6. Model wall locations

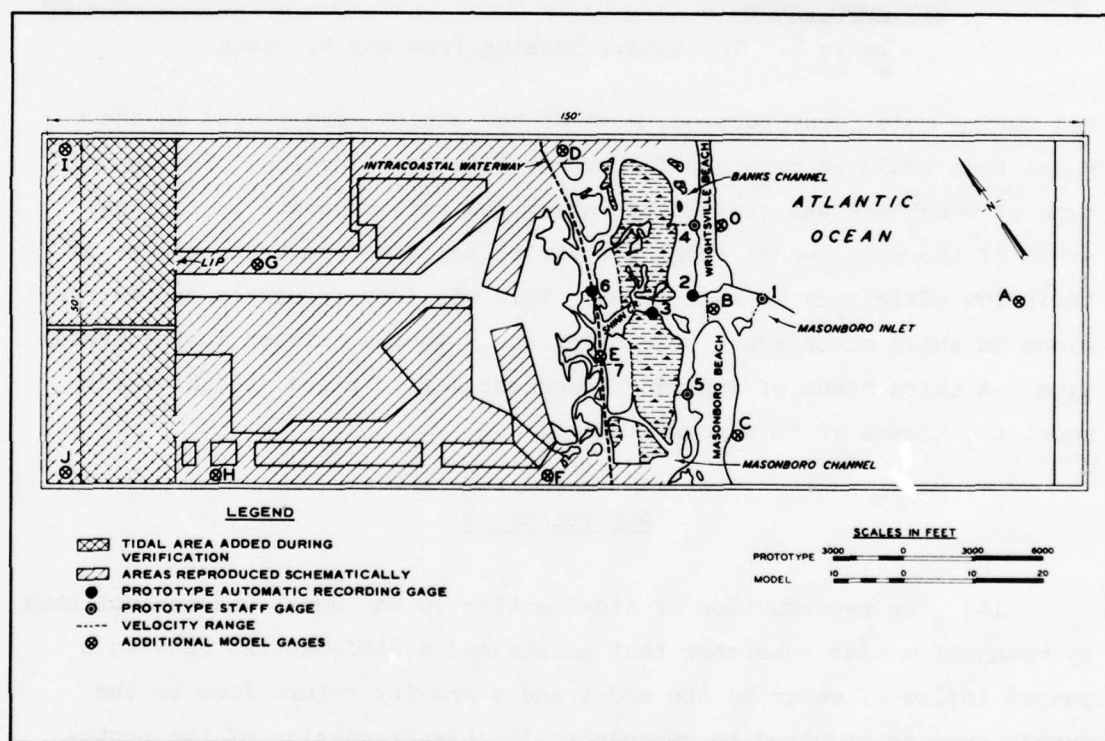


Figure 7. General model layout

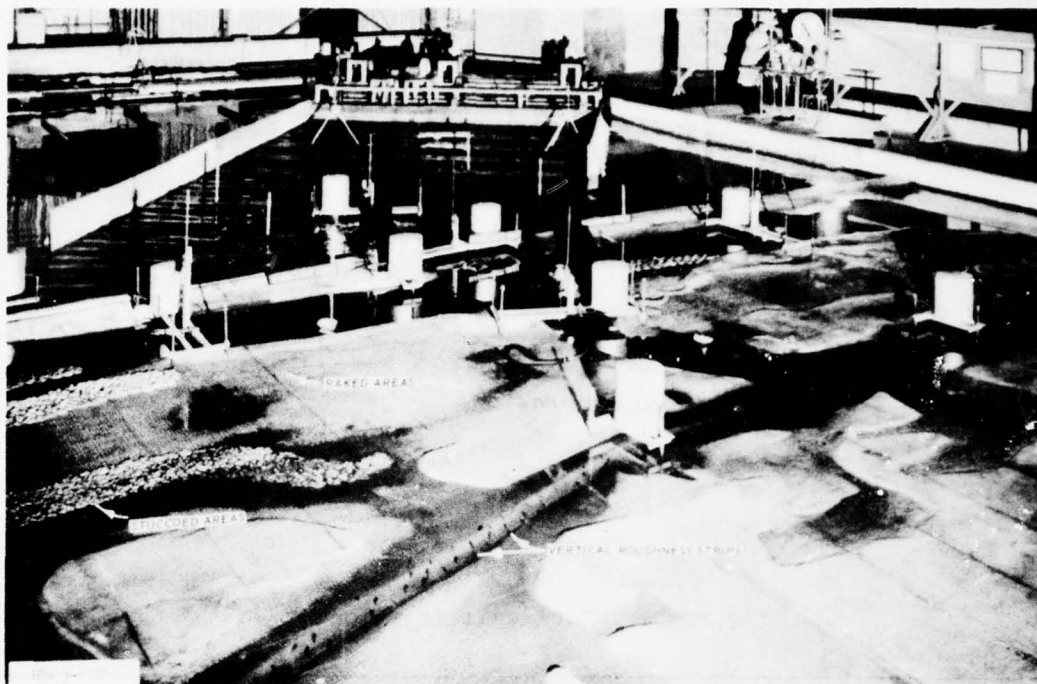


Figure 8. The model, looking from bay to ocean

and during model construction, more of the strips were placed in the model than would be required for proper flow reproduction. The second type of roughness was created by raking the soft concrete in shallow areas of the model where roughness strips could not be used because of their low efficiency in such areas. This was done primarily on the regions in which marsh grass or shallow sandy shoals existed in the prototype. A third means of applying roughness was to place stucco on the model and trowel it to a rough finish.

Appurtenances

14. The reproduction of tidal action in the model was accomplished by means of a tide generator that maintained a differential between a pumped inflow of water to the model and a gravity return flow to the supply sump as required to reproduce all characteristics of the prototype tides at the ocean control tide gage. A schematic drawing of this

system and description of the operation of the tide generator are shown in Figure 9.

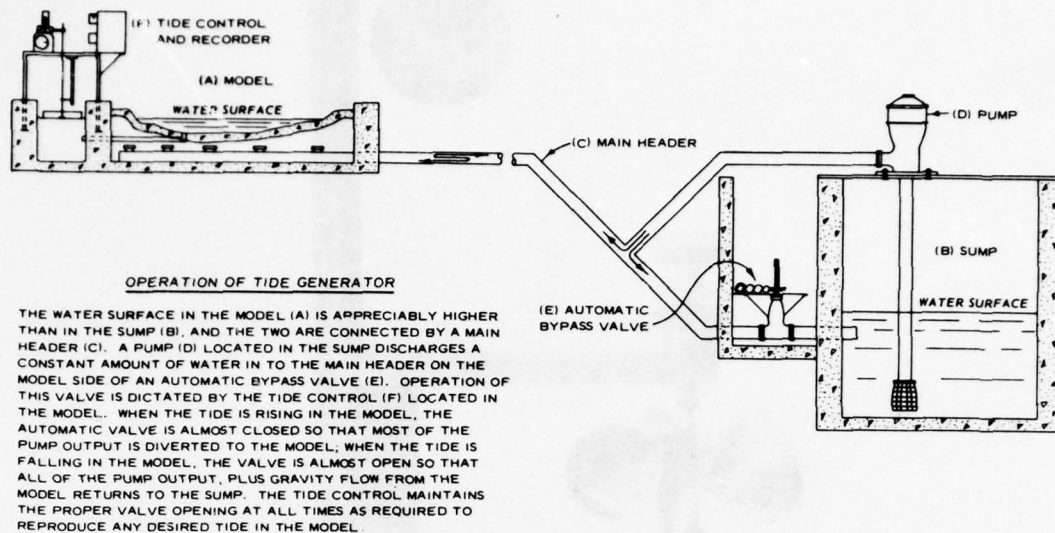
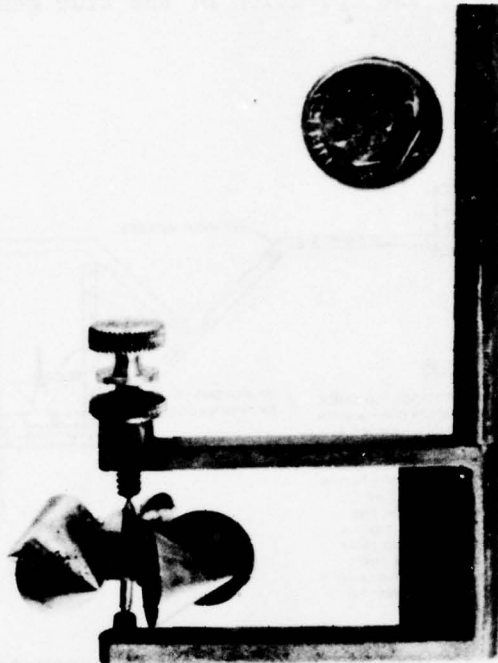


Figure 9. Operation of the tide generator

15. Current measurements were made in the model with miniature Price-type current meters (Figure 10). The meter cups were about 0.04 ft in diameter (2.4 ft prototype). The center of the cups was about 0.045 ft from the bottom of the frame, or 2.7 ft prototype. The meters were calibrated frequently to ± 0.01 fps to ensure their accuracy and were capable of measuring speeds as low as about 0.05 fps (0.4 fps prototype).

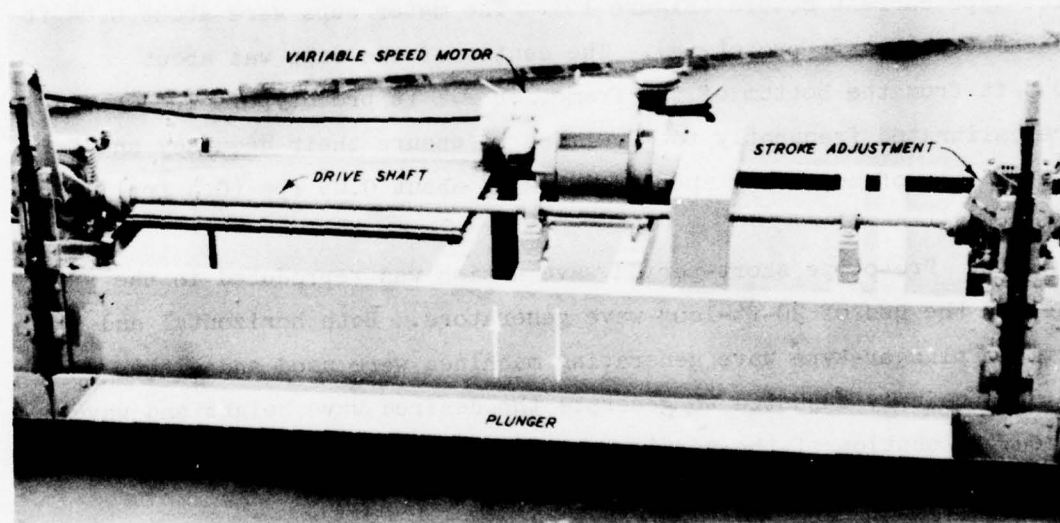
16. Prototype short-period wave action was reproduced in the model by the use of 20-ft-long wave generators. Both horizontal and vertical plunger-type wave generating machines were used and either could be quickly adjusted to generate the desired wave height and wave period. A section of the vertical plunger wave machine is shown in Figure 11.

17. The tidal stage time-history was measured by the use of an electronic system consisting of a transmitter (Figure 12) and a recorder (Figure 13) with a telemetering circuit consisting of two selsyn motors, one in the transmitter and the other in the recorder, connected by an



2461-124A

Figure 10. Miniature Price-type current meter



2461-130

Figure 11. Wave generator

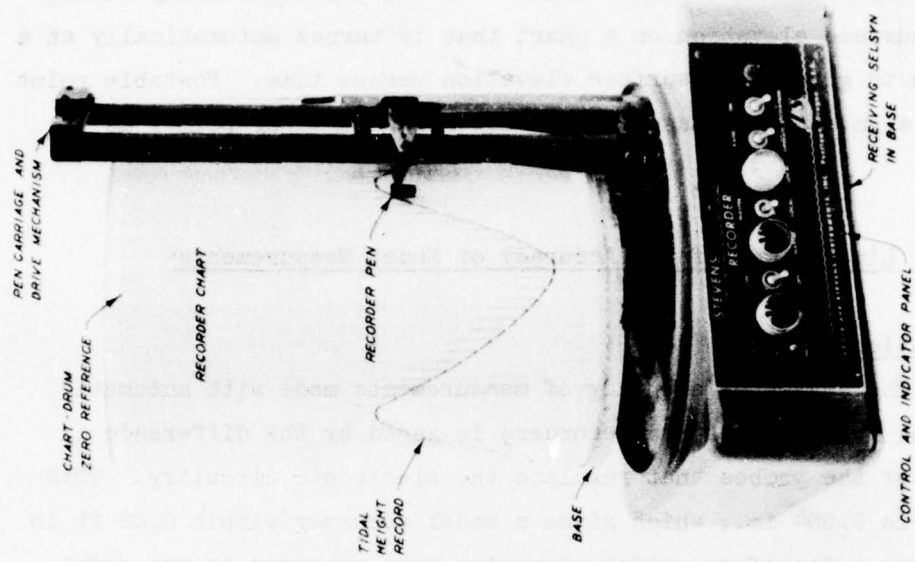


Figure 13. Water-height recorder

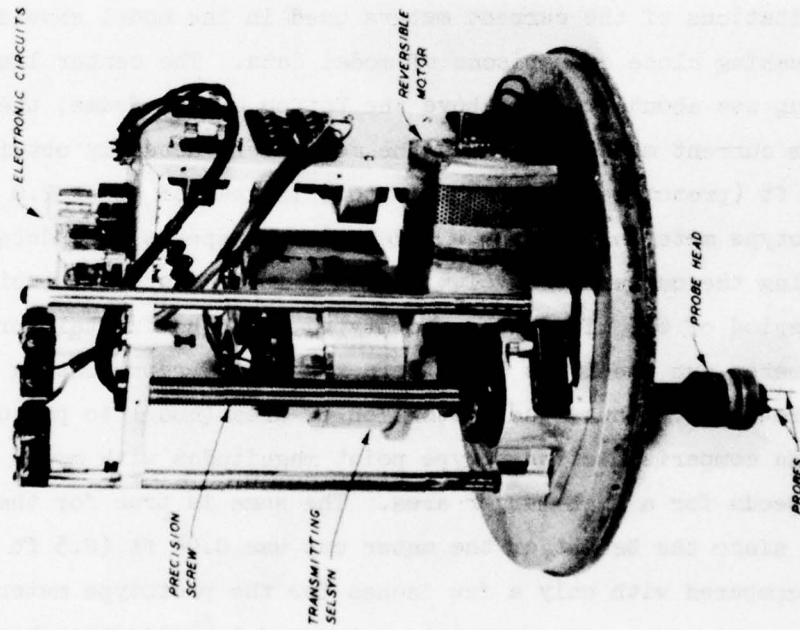


Figure 12. Water-height transmitter
with cover removed

electrical cable. The tidal stage transmitter, located over the desired data gathering point, measures the water-surface elevation by means of an electronic sensing probe and transmits this elevation to a recorder located in a control or instrument house. An ink pen continually records the water-surface elevation on a chart that is turned automatically at a preset rate to give water-surface elevation versus time. Portable point gages were also used to measure tidal elevation at other points as required.

Limitations of the Accuracy of Model Measurements

Tidal elevations

18. The degree of accuracy of measurements made with automatic telemetering transmitters and recorders is gaged by the difference in the length of the probes that regulate the electronic circuitry. This difference is 0.004 in., which gives a model accuracy within 0.02 ft in the prototype. Therefore, tidal elevation data gathered on the model are well within the degree of accuracy of the prototype data of 0.1 ft.

Current magnitudes

19. Limitations of the current meters used in the model should be considered in making close comparisons of model data. The center line of the meter cup was about 0.05 ft above the bottom of the frame; therefore the bottom current measurements in the model were actually obtained at a point 3.0 ft (prototype) above the bottom, instead of about 2.0 ft as in the prototype metering program. Model current speeds were determined by counting the number of revolutions in a 10-sec interval (which represents a period of 6.5 min in the prototype). The horizontal spread of the entire meter cup wheel was 0.11 ft in the model, representing 33 ft in the prototype. Thus, the distortion of area (model to prototype) results in comparison of prototype point magnitudes with model mean current speeds for a much larger area. The same is true for the vertical area, since the height of the meter cup was 0.04 ft (2.5 ft prototype) as compared with only a few inches for the prototype meter. Possible measurement error may enter into current data collection because

of the chance of error during observation of the meter while revolutions are counted. If the revolutions are counted to $\pm 1/4$ revolution during a 10-sec measurement period, this converts to ± 0.02 fps or ± 0.15 fps prototype.

Discharges and flow volumes

20. The variance in current measurement causes a variance in subsequent discharge and flow volume calculations. For example, for a cross-sectional area of 8,000 sq ft and current speed of 3.00 ± 0.15 fps, the discharge would be some value between 22,800 cfs and 25,200 cfs, any error in cross-sectional area notwithstanding. For flow volumes, consider an average ebb current of 1.50 ± 0.15 fps over a duration of 22,500 sec prototype (1/2 tidal cycle) and a cross-sectional area of 8,000 sq ft, the flow volume would be some value between 243 and 297 million cu ft (mcf) ($270 \pm 10\%$).

Surface tension

21. Water-surface films, from dust and oils, can cause severe surface tension effects that distort model measurements. However, frequent draining and washing of the model can remove the surface film.

PART IV: HYDRAULIC VERIFICATION

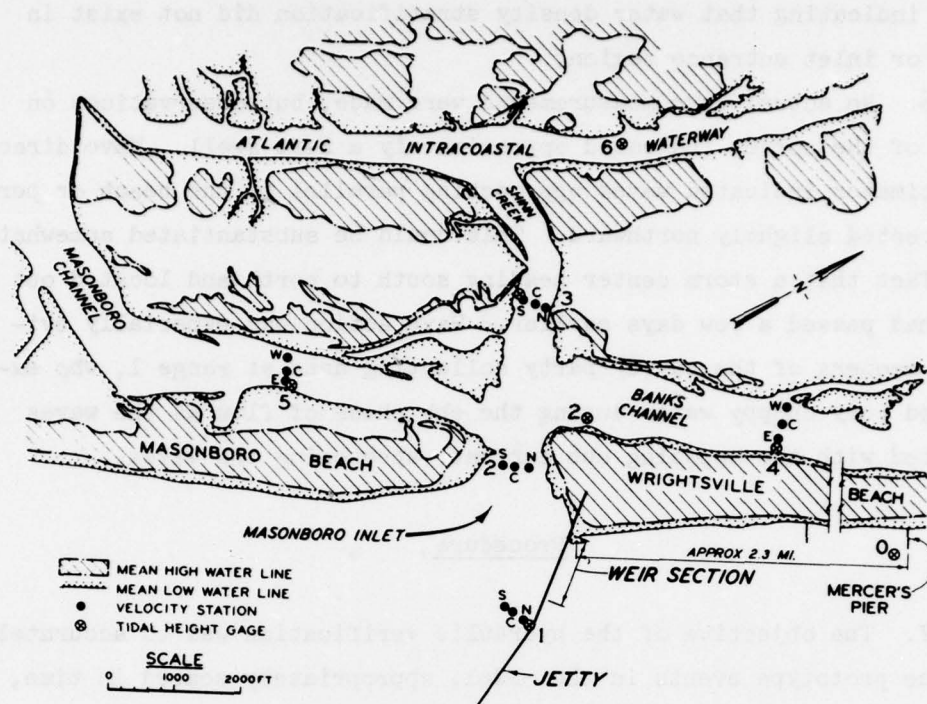
Prototype Data

22. In order to adjust the model, a set of prototype data was collected. A prototype survey was conducted jointly by personnel of the Wilmington District and the U. S. Army Engineer Waterways Experiment Station on 12 September 1969. This date was selected to take advantage of the symmetry of ocean tides. The two successive high-water levels, predicted to be within 0.1 ft of each other, facilitated model adjustment, since the same tide is repeated continually during model operation. Also, the tidal range (4.15 ft) was close to the mean range (3.8 ft) for the region. The seasonal aspect of data collection did not enter into this survey, since there is little freshwater flow into the inlet system.

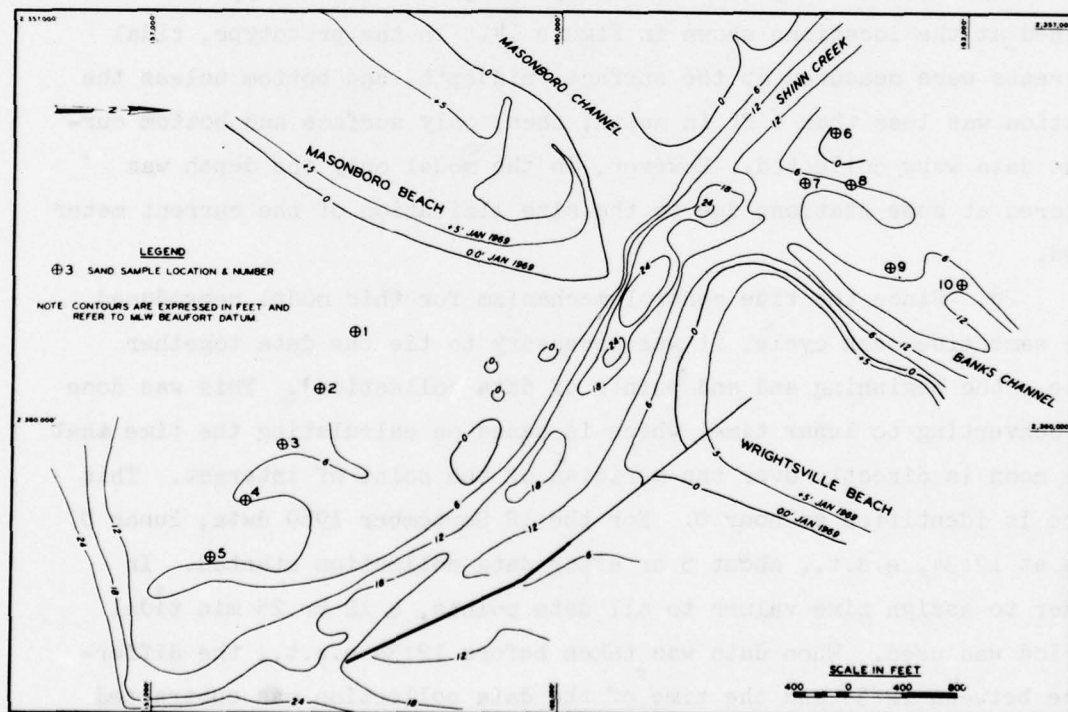
23. Sufficient personnel were available to permit simultaneous observations of tidal currents and elevations at the locations shown in Figure 14a. Plots of prototype data appear in Plates 9-33. "Range" is indicative of a line of current measuring stations across a channel, perpendicular to the flow. Range 1 was in a channel whose sides are formed by the jetty on the north side and a shoal on the south side whose elevation was slightly above mean low water.

24. Other data collected as a part of the prototype survey included wind data, surficial sand samples, salinity and temperature measurements, limited estimates of wave activity, and a complete bathymetric survey. Wind data, shown in Table 1, indicate that winds were generally from the north and at times were gusty. The winds did not appear to have any significant effects on survey results, especially since the bay is channelized and does not offer a broad surface for the wind stresses to produce a setup. Surficial sand samples were collected on the ocean bar and bay channels at the points shown in Figure 14b. A gradation curve for each sample is shown in Plates 34-43; generally, the median diameter ranges from 0.20 to 0.25 mm for the samples.

25. Salinity and temperature data are shown in Table 2. Both salinity and temperature measurements showed little change during the



a. Range and gage locations



b. Locations of sand sampling sites

Figure 14. Prototype survey of 12 September 1969

survey, indicating that water density stratification did not exist in the bay or inlet entrance region.

26. No actual wave measurements were made, but observations on the day of the survey indicated approximately a 2-ft swell. Wave direction estimates indicated waves approaching parallel to the beach or perhaps directed slightly northward. This could be substantiated somewhat by the fact that a storm center heading south to north and located out to sea had passed a few days earlier. Wave action was especially evident to members of the survey party collecting data at range 1, who experienced very choppy water during the ebb phase of flow as the waves interacted with the opposing ebb current, steepening the waves.

Procedure

27. The objective of the hydraulic verification was to accurately reproduce prototype events in the model, appropriately scaled in time, magnitude, and direction. To verify the model, tidal elevations and tidal currents were reproduced corresponding to the prototype data obtained at the locations shown in Figure 14. In the prototype, tidal currents were measured at the surface, middepth, and bottom unless the station was less than 6 ft in depth; then, only surface and bottom current data were collected. However, in the model only one depth was metered at some stations due to the size limitation of the current meter used.

28. Since the tide control mechanism for this model reproduced the same tide each cycle, it was necessary to tie the data together (i.e., the beginning and end points of data collection). This was done by converting to lunar time, which is based on calculating the time that the moon is directly over the meridian of the point of interest. This time is identified as hour 0. For the 12 September 1969 data, lunar 0 was at 12:34, e.s.t., about 5 hr after data collection started. In order to assign time values to all data points, a 12 hr 25 min tidal period was used. When data was taken before 12:34 e.s.t., the difference between 12:34 and the time of the data collection was subtracted

from 12 hr 25 min. For example, data collected at 11:30 a.m., e.s.t., would be 12 hr 25 min - 1 hr 4 min = 11 hr 21 min lunar time. Prototype velocity data taken before 12:34 are indicated by the symbol "O" in Plates 46-60, while data taken later are indicated by a "Δ."

29. The initial step following model construction was the reproduction of the ocean tide at gage 0, located on Mercer's Pier, 2.3 miles north of the inlet. This gage was the control gage and all other model results were dependent on proper adjustment of the tide at this location. Plots of the verification tide at gage 0 are shown in Plates 9 and 44.

30. Two primary controls may be used to verify a fixed-bed model. The first control is adjustment of the boundary roughness of the flow channels. This is accomplished by bending the 1/2-in. strips placed in the model during construction. The frictional effect of the strips is necessary to compensate for scale effects and aids in obtaining the proper flow distribution and magnitude, and tidal elevations and phases in the model.

31. The second control is that of variation of the tidal prism or volume of water flowing through the inlet. Tidal prism adjustments are usually necessary to compensate for the lack of data in the far reaches of extensive bays such as those at Masonboro Inlet. Adjustment is achieved either mechanically or by change of physical geometry (i.e., either by extending or reducing the limits of the model bay). Mechanical adjustments are made using an auxiliary pump which (in the case of increasing the tidal prism) pumps water from the bay during flood flow, then into the bay during ebb flow. Since the use of an auxiliary pump to adjust the tidal prism is a complicated procedure, a trial-and-error adjustment to the model bay area was employed to adjust the tidal prism of Masonboro Inlet.

32. Adjustments to both the boundary roughness and the tidal prism were incorporated to verify the model. The roughness strips were extremely helpful in achieving local current magnitude corrections and proper flow distributions. One case in point occurred at sta N of range 2, which is located in the gorge of the inlet. This location, designated problem area 1, and other problem areas to be discussed are

shown in Figure 15. Flow through this station was much too fast during the ebb phase. In reality, the area along the north side of the inlet should have been an eddy region; after insertion of additional roughness, the proper velocities were obtained and the desired eddy developed on

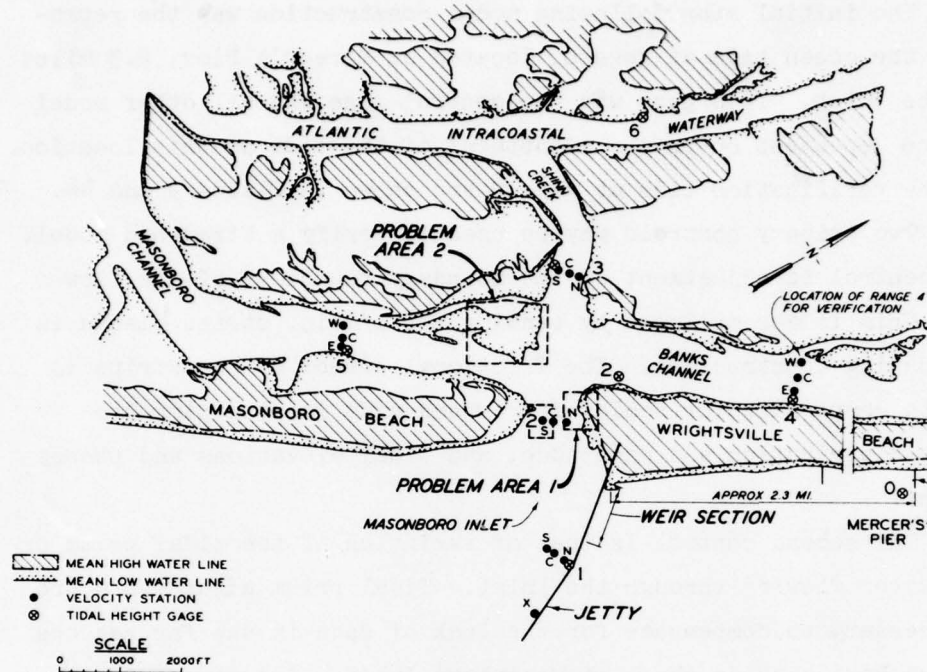


Figure 15. Verification problem areas

the north bank of the inlet during ebb flow. A comparison of before and after data is shown in Figures 16a and 16b, respectively. The decrease in ebb current speeds should be noted. The increase in flood current speeds (as much as 1.5 fps greater) although appearing paradoxical is actually also a result of this roughness. Referencing Figure 15, most of the roughness added was placed to the Wrightsville Beach side of sta 2N. The placement was such that ebb flow was sufficiently impeded at sta 2N but a portion of flood flow which came into the inlet between sta 2N and Wrightsville Beach was shifted by the roughness effect so that flood velocities increased at sta 2N.

33. Tidal inlet models have many areas that are very shallow and pose modeling problems due to difficulty in achieving the proper

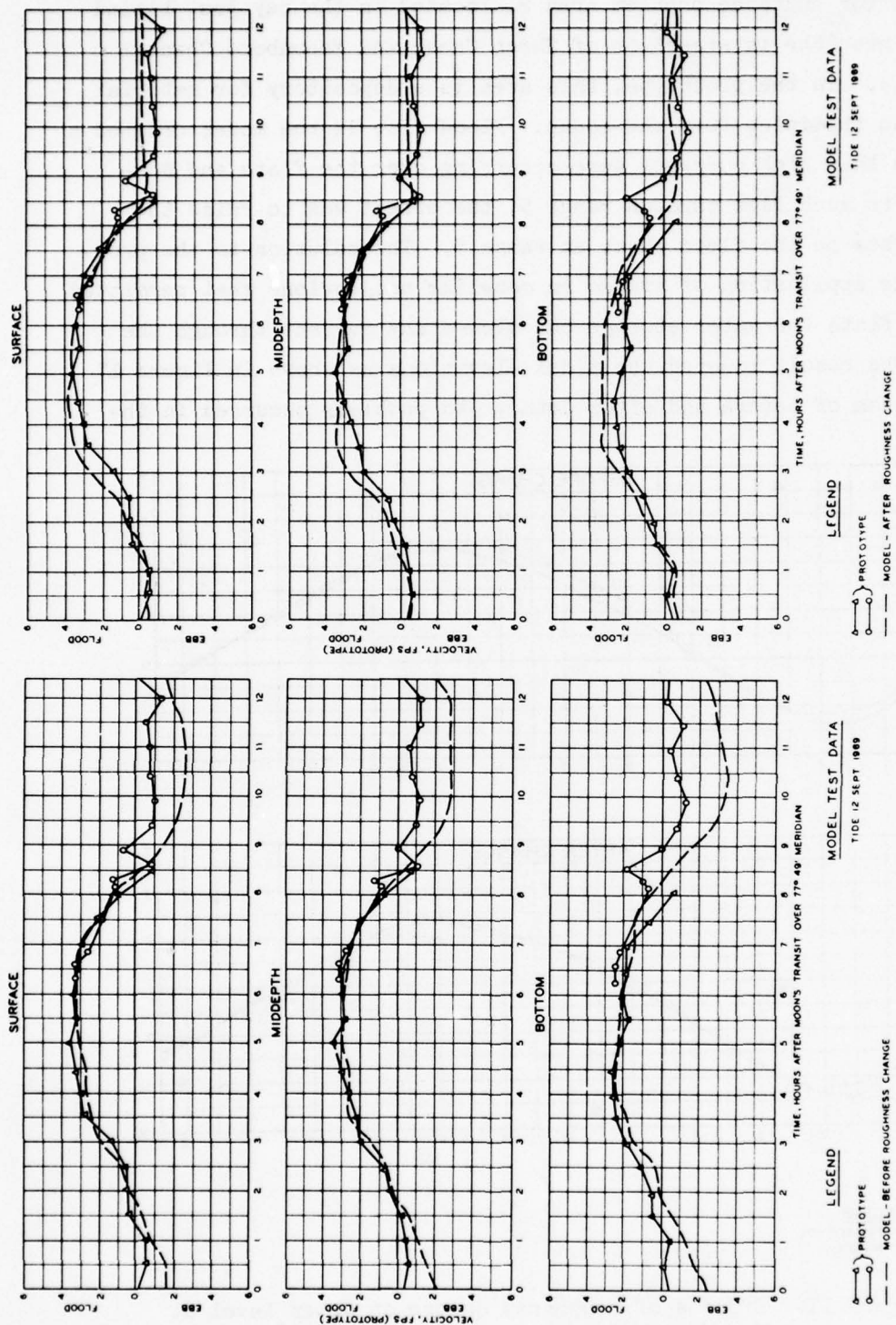


Figure 16. Verification of tidal currents, problem area 1, sta N, range 2

roughness, for instance problem area 2, located in the bay just behind the inlet near the intersection of Shinn Creek and Masonboro Channel (Figure 15). In the prototype, this area is a depository for material coming into the inlet from the south. Flood flow in the model created a problem in that high currents were occurring over the flats and contributing to much flow through range 5; the effect was to raise the tidal heights on the flood phase at range 5. The solution to the problem was the application of stucco in conelike projections that permitted using the flats for water storage but slowed any current through the region. The result lowered the tidal elevations as shown in Figure 17 (a comparison of before and after data). No problems occurred in the

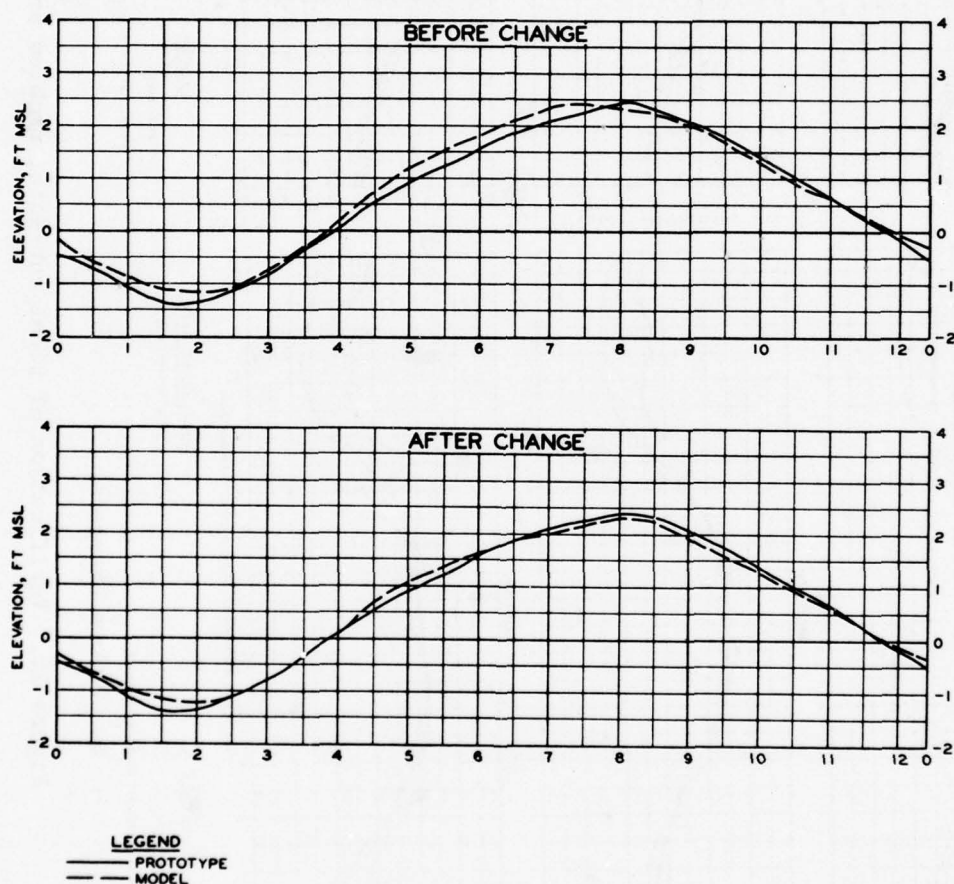


Figure 17. Effects of roughness change on water level at problem area 2, gage 5

bay tidal flats off to the side of the channels as lateral flood currents into these areas were very slow.

34. Early in the adjustment period, it was noted that current speeds at range 2 were too low. No matter how much roughness was removed, by bending the roughness strips flat against the model bed, the currents did not increase enough to agree with the prototype. To increase these currents required an increase in the tidal prism, and rather than using auxiliary pumping to achieve this, an increase in the bay area was used. The exact amount of bay area was difficult to determine because of the influence of the AIWW and insufficient prototype tide and current data in the bay. However, as a first attempt the rear model wall was removed, resulting in the expanded area shown in Figure 7. It should be noted that the bay enlargement was only a trial and if the resulting currents were too high or low, then additional area would have been subtracted or added accordingly. Currents at range 2, sta S, are shown before and after bay enlargement in Figure 18.

35. Even after bay enlargement, maximum current speeds were lower than prototype currents, especially at the middepth locations of range 2, center and south stations. At both stations the model velocity during flood flow remained constant at 2 fps for hours 4-7 (Plates 50 and 51) while the prototype velocity was higher. The reason for this discrepancy was the development of an eddy at this model location due to the turbulent interaction of flow coming over the south shoal and flow through the channel. As the flow from the shoal approached the range at the inlet gorge, there was an abrupt change to a greater depth, which produced this turbulent flow. The cup meter used in the model was large enough to be affected by the turbulence and a somewhat erratic spin could be observed as forces fluctuated. Most likely, the true flow through this station was higher than that indicated by the meter.

36. With the larger bay area, flows were increased, but difficulty in obtaining high-water elevations in the north portion of the bay arose. Therefore, a lip was installed in the model (Figure 7) to control the flow of water into this area. Addition of the lip had the same effect as adding friction to the back bay portion of the model during peak tide

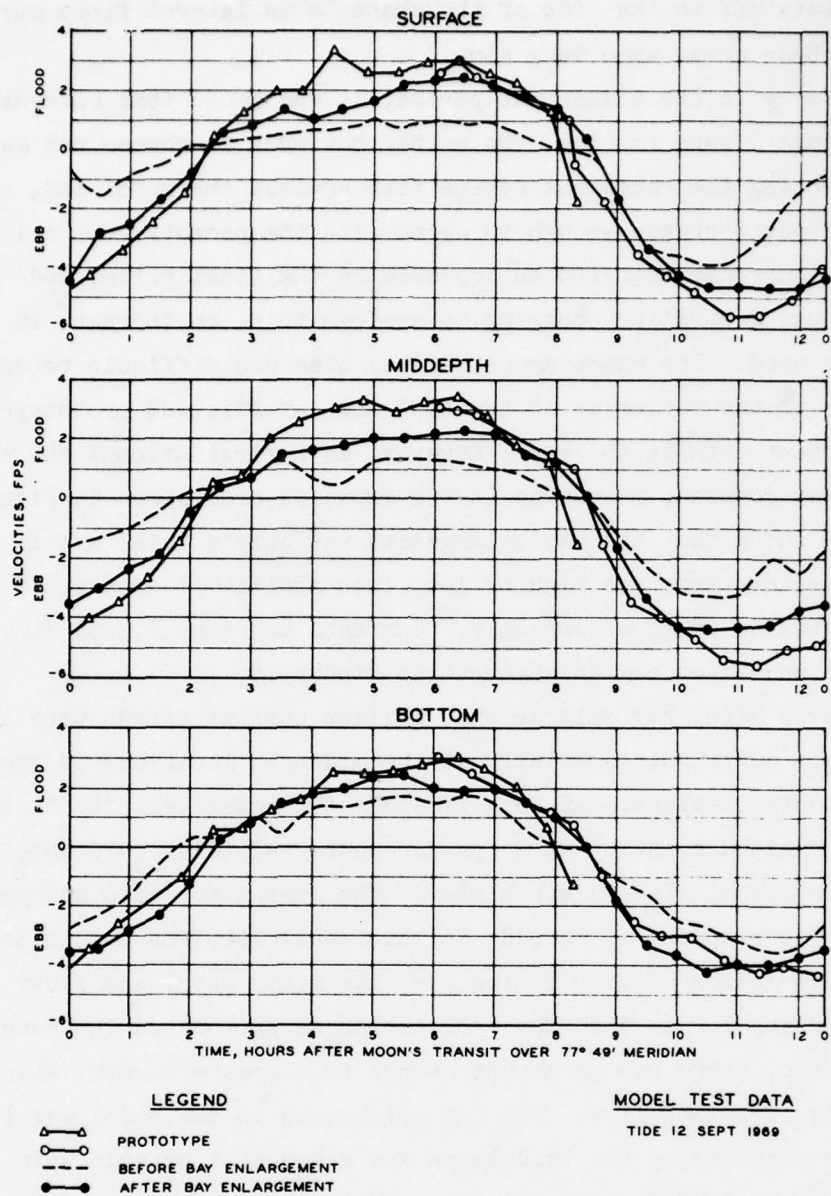


Figure 18. Verification of tidal currents, sta S, range 2

flow. The correct elevation of the lip was determined by trial-and-error procedures, since the elevation of the lip determined the high-water elevation. Figure 19 shows the tidal current and tidal elevation at range 4 with the lip at -3.9 ft msl, while Figure 20 shows the results with the lip at its final verified elevation of +0.1 ft msl. Due to a slight reduction in the tidal prism as the lip height was increased, the tidal currents at range 4 were slightly less than those taken with the lip at the lower elevation. In addition, the tidal elevation at range 4 still did not quite achieve the high-water level of that of the prototype.

37. This inability to reproduce bay high-water elevations was resolved by arbitrarily increasing the high-water elevation at tidal

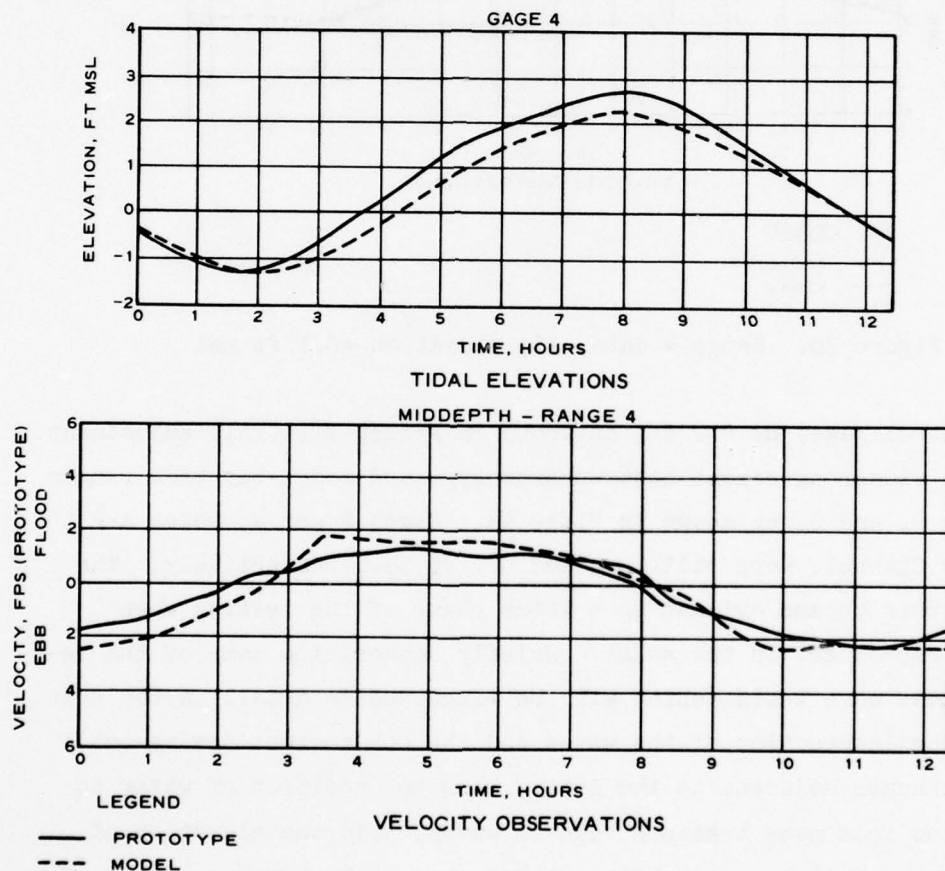


Figure 19. Range 4 data, lip elevation -3.9 ft msl

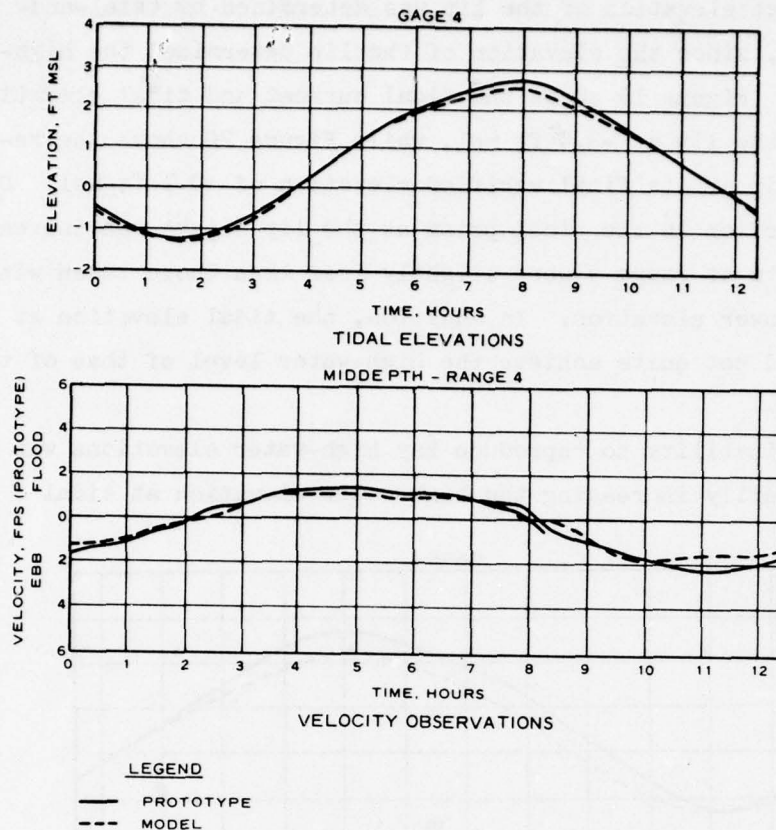


Figure 20. Range 4 data, lip elevation +0.1 ft msl

gage 0 (control gage) by 0.2 ft, as shown in Figure 21. This adjustment resulted in closer agreement between prototype and model bay tide ranges at gages 3, 4, and 5, as shown in Plate 44. Gages 2 and 4, which are along Banks Channel, were still 0.1 and 0.2 ft low, respectively. The reason for this became evident in a later phase of the testing when waves were reproduced in the model. Briefly summarizing some of the results of these wave tests (which will be discussed in detail in the next section), the interaction of the waves and the ebb current coming out along the channel adjacent to the jetty, plus the addition of water to this ebb flow from mass transport due to waves, held the elevation of the Banks Channel system at a higher level than without waves. Most of the water flowing from Banks Channel exits through the north side of the

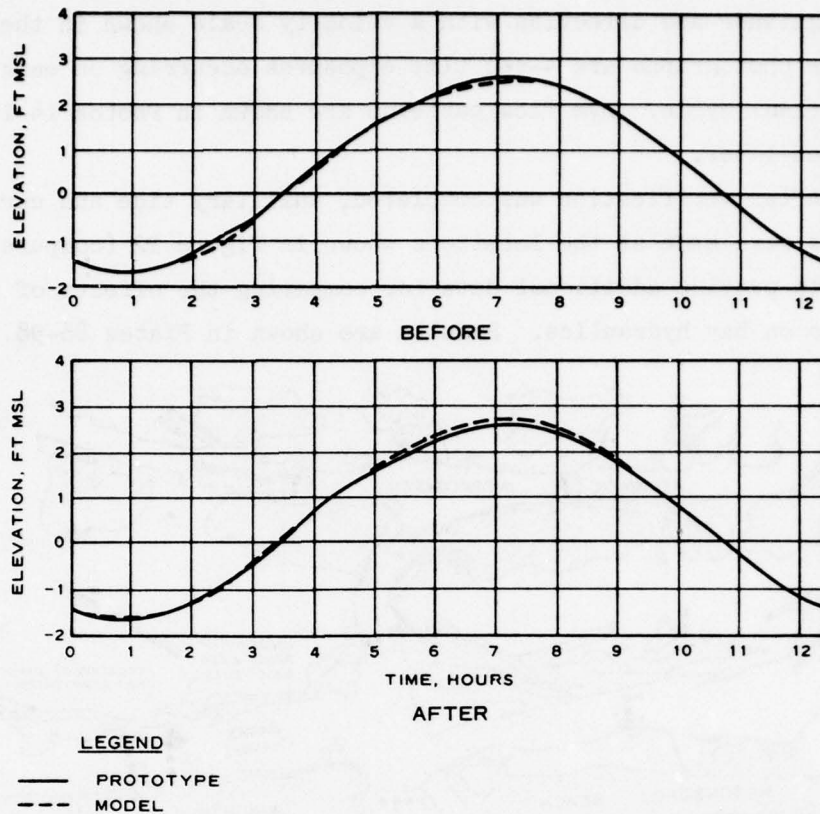


Figure 21. Tidal elevations, adjustment of control gage 0

inlet and along the jetty, so that any interaction with this flow also affects the flow in Banks Channel. The capacity of the channel along the jetty is partially taken up by water brought toward the channel by mass transport of the waves. As mentioned earlier, evidence of wave activity on the day of prototype data collection was observed during the ebb phase of flow at range 1. The final results of the verification of tidal heights, discharges, and tidal currents are presented in Plates 44-65.

38. Surface current patterns were taken at hourly intervals (Photos 1-13). These photographs were made prior to the insertion of stucco between Shinn Creek and Masonboro Channel, but the only change this would bring would be the eradication of any significant velocity streaks over this area. The white velocity tracks are indicative of the

velocity magnitude and direction with a velocity scale shown in the legend. The photographs are 4-sec time exposures occurring on each hour during the tidal cycle. Dye flow patterns are shown in Photos 14-17 and are discussed later.

39. After verification was completed, auxiliary tide and current measurements were made at the locations shown in Figure 22 (compare with Figure 14) to provide additional data for comparing the effects of inlet improvements on bay hydraulics. Results are shown in Plates 86-98.

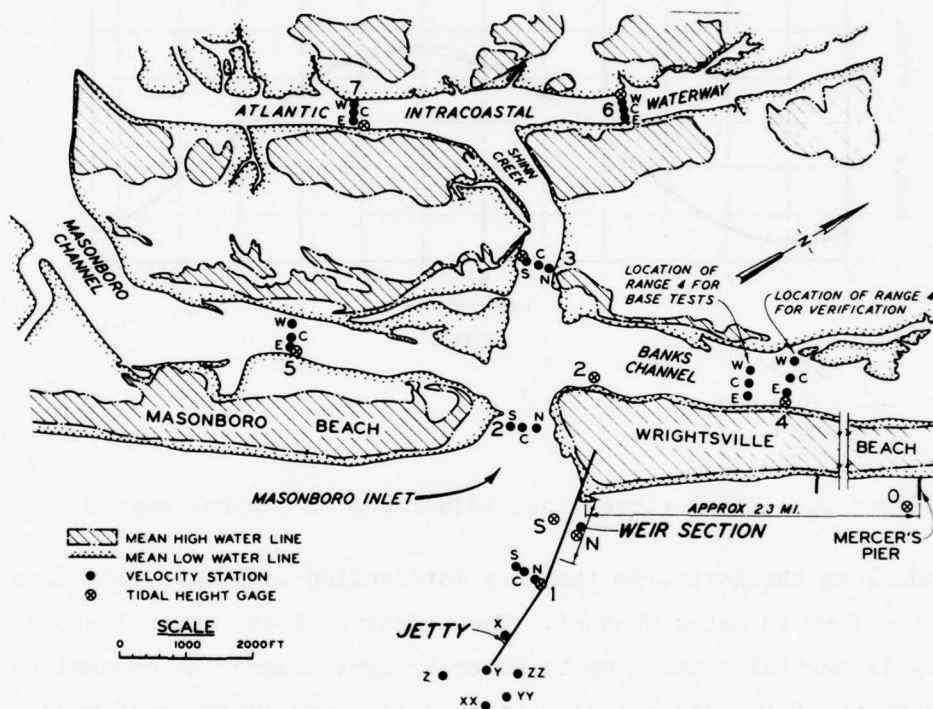


Figure 22. Model range and gage locations

PART V: ADDITIONAL 1969 TESTS

Tides and Currents

40. After completion of the hydraulic verification, the tide control was adjusted to reproduce the average spring ocean tide (4.5-ft range) and then the mean ocean tide (3.8-ft range), both tides centered about mean sea level. These tides were operated to facilitate comparisons between various model configurations for tides which represented the average and maximum conditions. The tidal heights and current measurements for these two conditions are shown in Plates 66-98 and discharge comparisons for ranges 1-7 are shown in Plates 99-105. The change in the mean tidal plane (from +0.4 ft msl for verification to msl for mean and spring conditions) caused some minor effects in flows over the ocean shoals (Photos 18-43). It did not appear that lowering the mean plane drastically changed the effect of the roughness which had been adjusted for the higher mean level. However, as shown in Plate 100 the spring tide (4.5-ft range) tidal prism was smaller than the verification prism (4.15-ft range) because: (a) since the mean sea of the entrance of range 2 was smaller, less flow was able to pass through the throat; and (b) the lower mean level resulted in less storage area in some of the tidal flat regions.

Influence of Waves

41. After completion of model verification, a decision was made to assess the importance of waves on model hydraulics. Because the model was not originally designed for wave tests, the lengths of shoreline on either side of the inlet were insufficient to adequately reproduce wave refraction patterns and longshore currents along the beaches. However, throughout the region of major wave/current interactions the important wave processes were reproduced.

42. In order to scale waves, it must be determined whether refraction or diffraction is to be reproduced, since both cannot be modeled

simultaneously in a distorted-scale model. For refraction, wavelength is scaled from the vertical scale. The refractive effects were considered most important for the Masonboro Inlet model and this is substantiated by work of others in field studies of tidal inlets, particularly work by Hayes,⁹ which illustrates how important refractive effects are in relation to material movement at inlets. Also, the refraction of waves by the presence of tidal currents is very important, since currents up to 5 fps normally exist in the inlet entrance region. Further, when refraction is modeled diffraction effects are conservatively simulated and diffractive wave energy is greater by a factor of the square root of the distortion of the model than if diffraction scaling were used.

43. Harris¹ has shown that when modeling refraction in distorted-scale models, wave rays (orthogonals) are similar in model and prototype but kinematic similarity is sacrificed. This means that distances traveled by wave crests are not the same in model and prototype for corresponding times. The fact that refraction of wave rays is similar in model and prototype when scaling waves by the vertical dimension is illustrated by examining the ratio of wave celerity at two similar depths for model and prototype (Table 3). The ratio of celerities at depths of 20 and 10 ft for both the prototype wave and the model wave scaled by the vertical is 1.35. This similarity of ratios is indicative of the similarity of refractive patterns, since the amount of refraction is governed by the change of wave celerity with depth. Therefore, when scaling for refraction in a distorted-scale model, the height and wavelength are scaled the same as the vertical geometric scale (1:60) and the period scale is

$$T_r = L_v/L_v^{1/2}, \quad T_r = 1:7.74$$

where

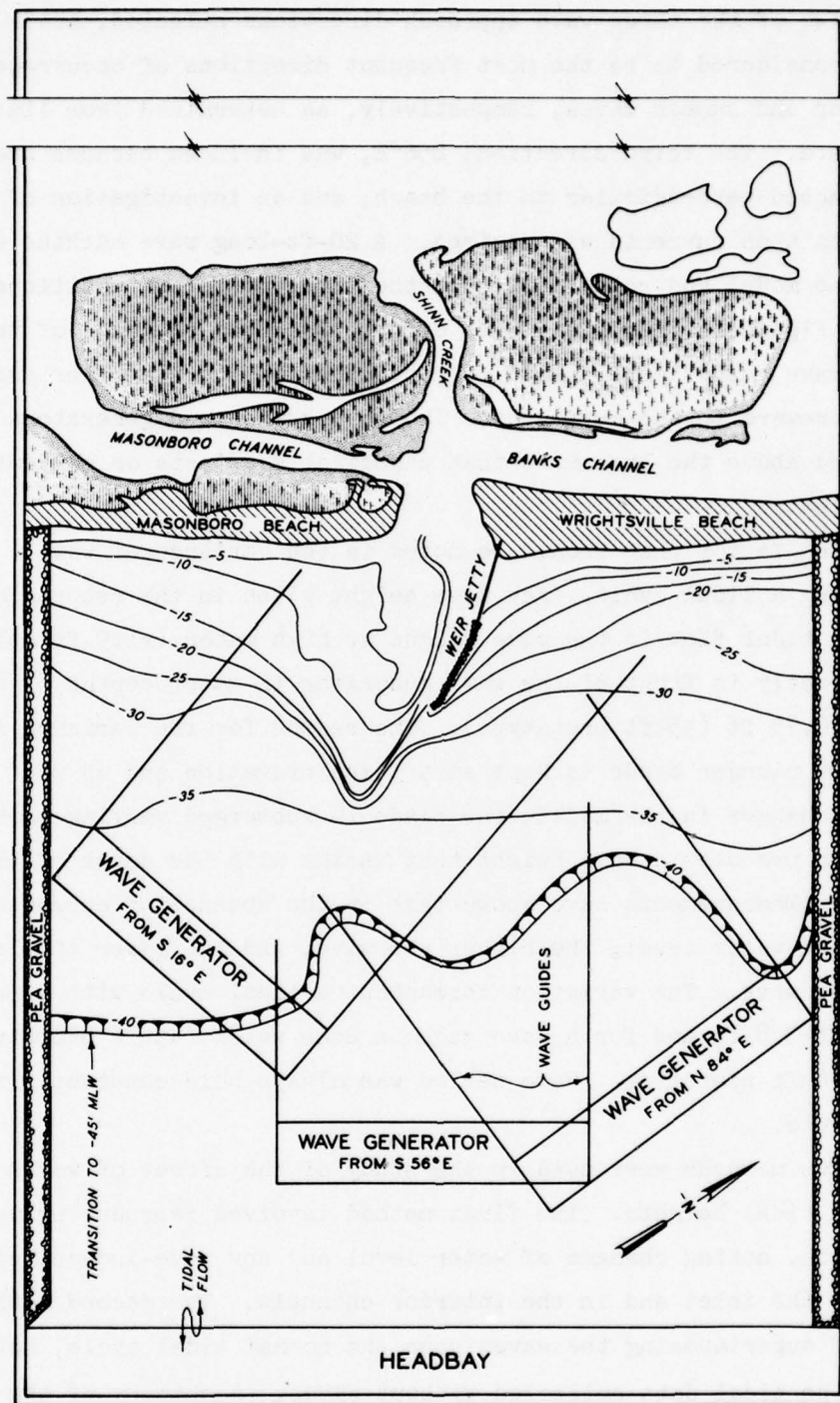
T_r = time ratio, model to prototype

L_v = vertical distance ratio, model to prototype

44. Two of the three wave approach directions selected, N84°E and S16°E were considered to be the most frequent directions of occurrence of the winter and summer waves, respectively, as determined from limited available data. The third direction, S56°E, was included because such waves approached perpendicular to the beach, and an investigation of their effects upon currents was desired. A 20-ft-long wave machine was placed in the model and rotated through the three different positions, as shown in Figure 23. To avoid wave diffraction from the ends of the generator, wave guides were placed perpendicular to the generator and extended shoreward to the surf zone. The wave guides and generators were elevated above the bottom so that undesirable effects on currents were minimized.

45. One factor that should be noted is the variance of wave heights during a tidal cycle. Any wave height given in the report for tests having tidal flow is the wave height at high water (+1.9 ft msl) measured directly in front of the wave generator in water depths of approximately 0.75 ft (45 ft prototype). The reason for the variance is that the wave plunger blade is kept at a fixed elevation and as the water level changes in the model, the blade is submerged varying amounts, which in turn produces a wave height that varies with the depth of blade submergence. Measurements have shown that in the absence of currents, the higher the water level, the higher the wave; and the lower the level, the lower the wave. The variation throughout a tidal cycle with a mean tide range of 3.8 ft and for a wave gage in deep water (45 ft prototype) is about ± 0.6 ft prototype. Wave period was always held constant during the tidal cycle.

46. Two methods were used in the study of the effect of waves on currents and tidal heights. The first method involved reproducing waves without a tide, noting changes of water level and any wave-induced circulations in the inlet and in the interior channels. The second method consisted of superimposing the waves upon the normal tidal cycle, noting changes to the tidal data collected without waves. A summary of the model observations follows.



NOTE: CONTOURS AND ELEVATIONS ARE IN FEET REFERRED TO MLW
 VERTICAL SCALE OF MODEL 1:60
 HORIZONTAL SCALE OF MODEL 1:300
 THERE IS ADEQUATE CLEARANCE BETWEEN WAVE GENERATOR
 AND MODEL FLOOR TO PERMIT TIDAL FLOW

SCALES IN FEET
 PROTOTYPE 0 1000 2000 3000
 MODEL 0 5 10

Figure 23. Wave generator locations

Waves with No Tide

Wave direction S56°E
(perpendicular to the beach)

47. With waves from this direction and no tide, a complex circulation pattern was generated in the model, probably because of the combined effects of refraction and diffraction. An ebb flow was created along the interior of the north jetty. At the tip of the jetty, the current turned south and returned bayward offshore from the bar. At the gorge of the inlet, a bayward current at the surface and an oceanward current at the lower depths were generated, with the total flows balanced. No setup in the bay due to waves was observed during the test.

Wave direction S16°E

48. With the wave approaching from the south, a wave nearly perpendicular to the outer trunk of the jetty, current patterns were similar to those described above for the S56°E direction. Observations of setup indicated a very slight increase in bay setup.

Wave direction N84°E

49. The circulation pattern formed by the waves was similar to the two previous tests. This pattern is shown in Figure 24. As the waves were approaching from the north, there was a slight increase in wave overtopping of the weir section which generated a current toward the gorge; but this current was turned back by the ebbing flow on the north side of the inlet. There was no measurable water-level setup in the bay.

50. The above circulation observations were made by injecting dye into the model and observing its movement. Water-level elevations were checked in the bay at sta 2, 3, 4, 5, and 6.

Waves with Tide

51. After this somewhat qualitative analysis of the wave effects on the inlet, a more detailed effort was made to obtain quantitative results. For these tests, the waves from the three above-mentioned

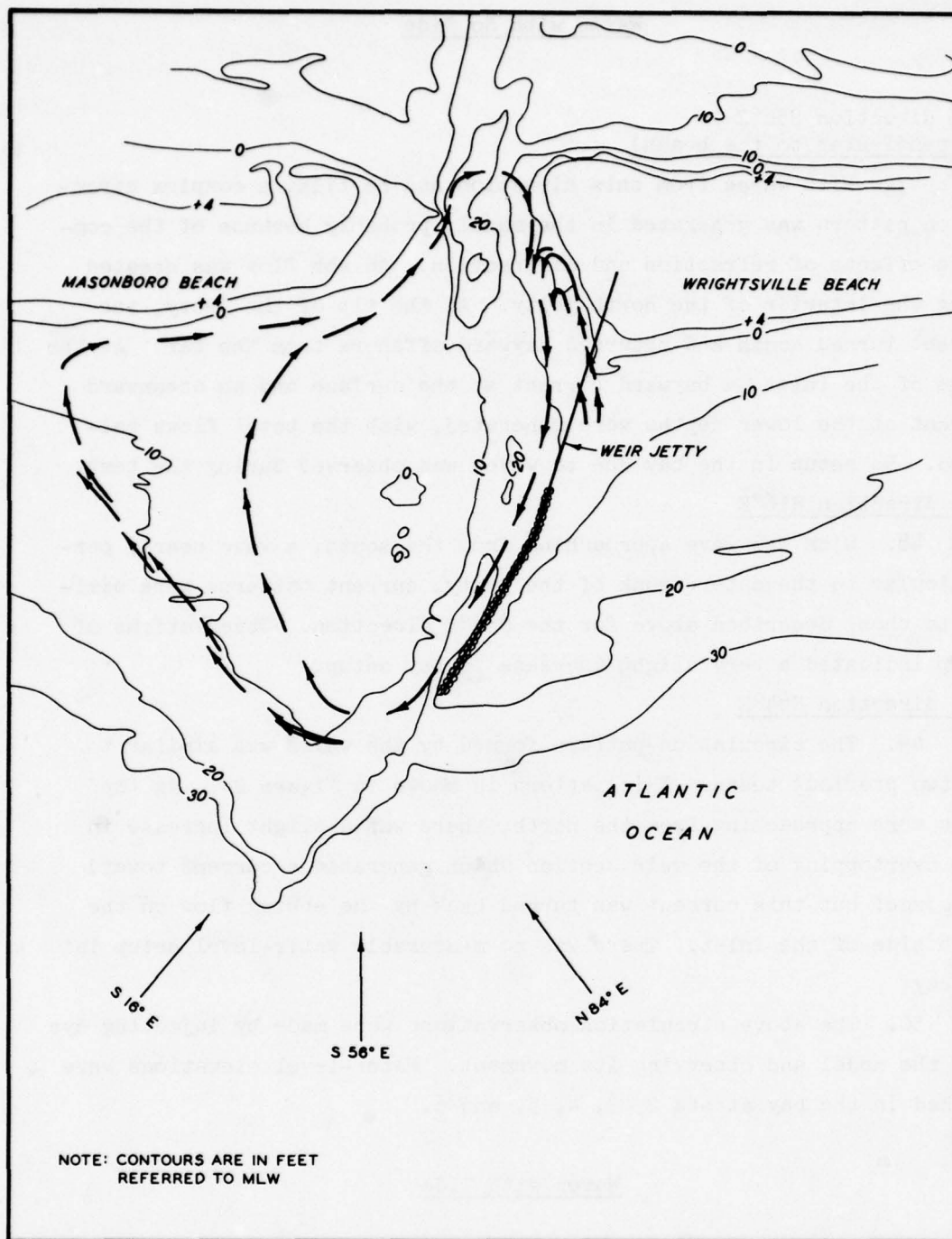


Figure 24. Current pattern caused by waves, without tide; typical of waves from all directions

directions together with a mean tide (3.8-ft range) were reproduced in the model. These tests showed that the circulation patterns observed with the nontidal wave tests were still in evidence. Ebb currents at range 1 were increased for each wave direction. There were slight changes in current speeds at range 2 in the inlet gorge. With respect to tidal heights, waves from the N84°E and S56°E directions caused little change to bay elevations. However, the S16°E wave caused a noticeable change in bay tidal elevations, raising some elevations by as much as 0.4 ft (prototype) during a part of the tidal cycle. This superelevation of tidal heights had its greatest increase in the interim between high water and low water, indicating that the direct interaction of the ebbing currents and the opposing S16°E wave field were responsible for this buildup.

52. There are also some relevant changes in current speeds when waves are introduced. Model data taken with the more northerly waves show a greater tendency for current values at ranges 1 and 2 to be in better agreement with the prototype data than does the verification test without waves. The more northerly waves do not improve the model tidal heights as the southerly waves do. However, since the wave field in the prototype is complex and the model wave is monochromatic, it seems improbable that one model wave condition could alter every tidal current and tidal height in the same manner as the prototype was altered by a spectrum of waves.

53. The above discussion suggests that since waves affect tidal heights and currents in the prototype, their absence from the model for a particular prototype survey may cause some discrepancies in prototype model agreement. It is not indicated, however, that model data taken without waves reproduced should be considered inconclusive, though the use of waves in a tidal model does show up certain problem areas which may not be seen in testing without waves.

54. Tidal height and current data taken with waves are shown in Plates 106-136. The data are compared with the mean tide data taken without waves. With respect to wave direction, the data appear in the following order: 3-ft, 7-sec, S16°E waves tidal elevation data

(Plates 106-108), current data (Plates 109-122); 3-ft, 7-sec S56°E waves tidal elevation data (Plates 123 and 124), current data (Plates 125-127); and 3-ft, 7-sec N84°E waves tidal elevation data (Plates 128-130), current data (Plates 131-136).

Supplemental Information

55. Although the hydraulic characteristics of Masonboro Inlet were complex, many details were exceptionally well reproduced in the model. Some of these facets will be detailed in this section, both for the information they give on inlet behavior and as an illustration of what a hydraulic model can show. This information, related to the dynamics of the inlet, includes such topics as bay circulation, isovels, and flow patterns.

Bay circulation

56. The bay of Masonboro Inlet is heavily channelized compared with some inlets that flow into an expanse of open water. As shown in Plate 31, the prototype discharges through ranges 3 and 4 do not balance on ebb and flood flow. Range 3 has a net flood discharge of 50 mcf, while range 4 shows a net ebb discharge of 50 mcf. This indicates a net clockwise circulation through range 3, the AIWW, then back through Banks Channel. Model discharge observations made at range 6 (Plate 104) showed a net flood of 57 mcf (136 mcf flood, 79 mcf ebb). The entrance of Shinn Creek into the AIWW appears to contribute to the circulation. The hook to the south permits the flow ebbing from the south through range 7 (Plate 105) to predominate over the flow from the north and actually prevents flow from range 6 to return via the flood route through Shinn Creek and range 3. The model reproduced this circulation effect very well.

Flow distribution through the inlet

57. An examination of the flow through the model in the absence of waves was made using dye. Photos 14-17 show how the flow was distributed. Dye was injected at times of high current speeds at the locations shown, then allowed to disperse. Photo 14 shows that flow approaching from south of the inlet flows into Masonboro Channel and Shinn

Creek; flow coming over the weir is relegated to entering Banks Channel. Thus, most suspended sediment coming over the weir eventually reaches Banks Channel and is deposited there as current speeds decrease. This is supported by prototype dredging records. Photo 15 shows that flood flow along the jetty disperses through all three interior channels. The ebb flow emitting from each interior channel is shown in Photos 16 and 17. The flow from each channel is relegated to its own section of the inlet as it flows oceanward. This same pattern on the ebb was noted on aerial photographs of the inlet illustrating good model-prototype agreement.

Isovels

58. Isovels comparing the model and prototype current distributions are shown in Plates 137-161. They show good agreement on the ebb but do not agree as well on the flood phase due to the vertical eddies experienced in the region of sta 2C, middepth.

Summary

59. The following observations are made based on the results of tests conducted with the 1969 hydrograph conditions installed.

- a. Reproduction of the velocities at the throat of the inlet was not achieved fully. Apparently because of the scale distortion of the model, the flows at middepth were adversely affected by surrounding model hydrography. Also, the relatively large size of model velocity meters restricts the ability to measure velocities in turbulent areas.
- b. The simulation of waves in the model improved the agreement between model and prototype results.
- c. Because of the distortion of the model scales, refraction, diffraction, and reflection cannot be reproduced simultaneously. The waves investigated in the study are based on the best possible reproduction of refraction.
- d. The ocean area of the model was not sufficient to allow optimum reproduction of waves for model tests. The investigation of wave effects was not included in the original planning for the model study. The S16°E waves are more effective in producing accurate results than the N84°E waves.

- e. A net clockwise circulation over the ebb tidal delta results solely from tidal effects, toward the entrance channel due primarily to the greater flux of water across the shoal during flood than during ebb (due to greater water depths), and in part to the separation of the jet during ebb flow.
- f. Addition of waves produced a noticeable setup in the bay, especially during ebb flow and for waves approaching from a $S16^{\circ}E$ direction, or perpendicular to the outer portion of the jetty and channel.
- g. Ebb currents through range 1, which was located in the ocean channel along the jetty, showed significant increases when waves were added.
- h. A wave-generated current whose circulation is generally toward the inlet over the shoals and along the jetty, as shown in Figure 19, may tend to help direct the ebb current toward the jetty. This probably occurs most significantly during the first few hours of ebb flow, when the wave-induced mass transport over the ebb tidal delta and along Masonboro Beach prevents currents from ebbing in a fanlike pattern and which may also contribute to the ebb flows in the main channel.

PART VI: BASE TESTS OF 1964 HYDROGRAPHY

Model Modification

60. After the model was verified for the 1969 hydrographic conditions, it was converted to the 1964 hydrographic conditions by removing approximately 400 sq ft of concrete and remolding the inlet region to the extent covered by the 1964 survey map (Figure 25). Roughness in the interior of the model remained the same, and roughness was added to the newly molded region in the same general locations and quantities as had been required for the verification conditions.

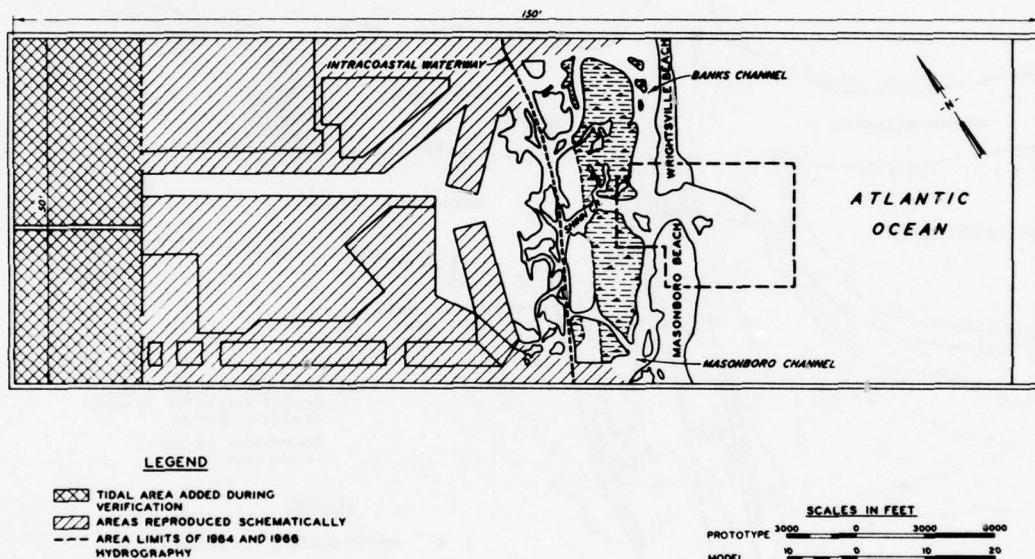


Figure 25. Model areas reproduced to 1964 and 1966 hydrography

Hydraulic Tests

61. Once the model was prepared, base tests were conducted with the mean tide (3.8-ft range) and the mean tide level of 0 ft msl at gage 0. The same tidal elevation gage locations as had been monitored for the 1969 condition were monitored for this test and are shown in Figures 7 and 26. The same current range and station locations were also monitored, as well as additional current sta 2SS and 8-21 (Figure 26).

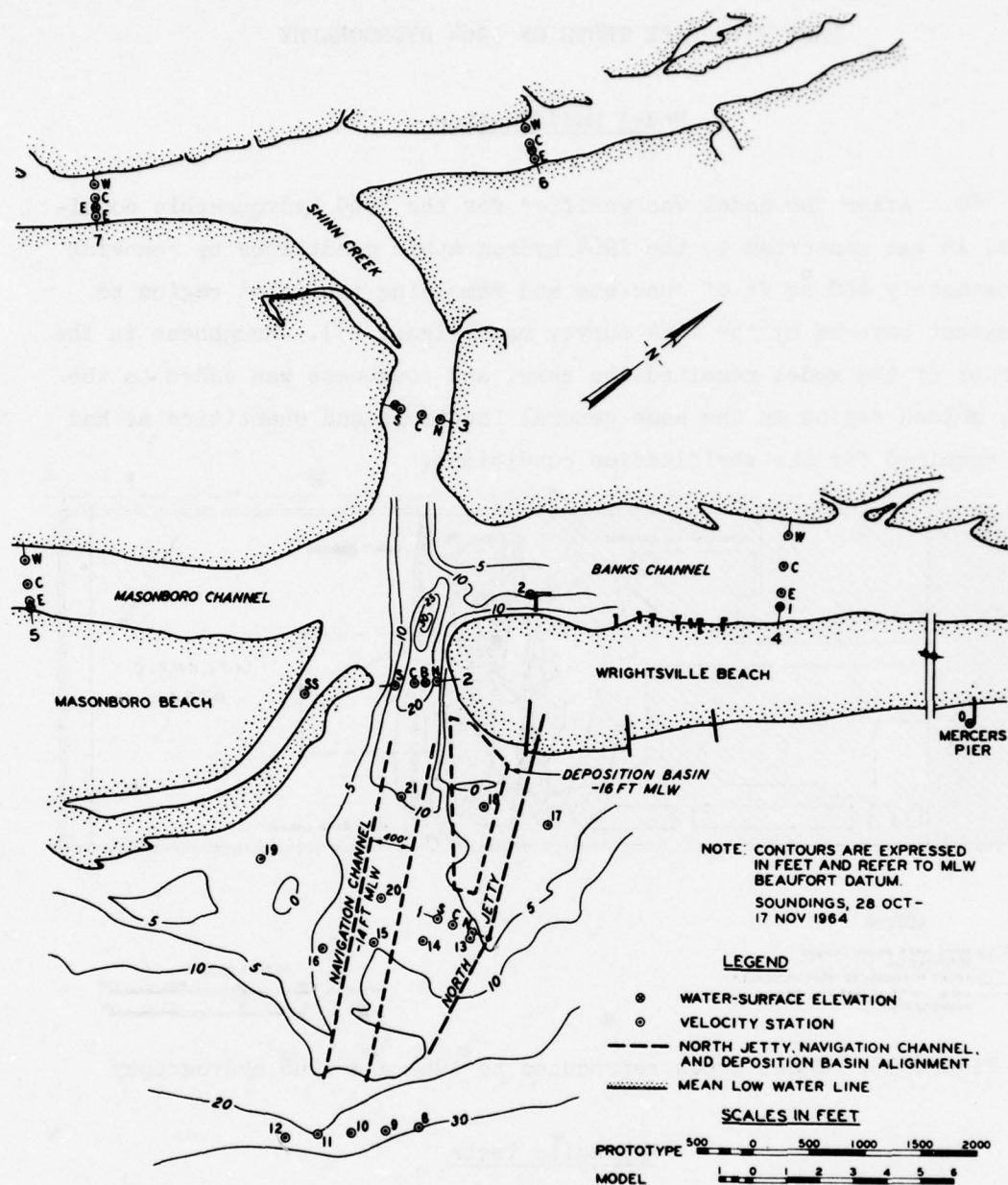


Figure 26. Tidal current and tide station location, 1964 hydrography

The new current sta 2SS was located in the southerly portion of a bifurcation in the entrance channel that did not exist for the 1969 conditions. Tidal data are shown in Plates 162-167; current data, in Plates 168-198; discharge data, in Plates 199-204; surface current patterns, in Photos 44-56; and dye movement patterns, in Photos 57-64.

Wave Tests

62. The influence of two waves, i.e. S16°E, 7.4 sec, 3 ft high, and N84°E, 7.4 sec, 3 ft high, on the base test data was investigated in detail. Limited information was obtained for N84°E, 7.4-sec, 5-ft-high waves. Results of the tests for tidal heights are shown in Plates 205-209; for currents, in Plates 210-215; and for the discharge at range 2, in Plate 216. Model current patterns are shown in Plates 217-219 without tides and in Plates 220-245 at hourly intervals throughout a tidal cycle; dye movement patterns are presented in Photos 57-64.

Tidal heights

63. Although tide sta C and O (Plate 205) were intended to be model control stations, small differences were observed when waves were reproduced. About the greatest change noted was that the elevation of high water at gage O was increased by approximately 0.2 ft by S16°E waves. The differences observed are not considered to be significant in the overall results.

64. Inspection of the data at tide sta B (Plate 205) located at the throat of the inlet shows that both waves resulted in increases in water-surface elevations throughout the tidal cycle. The waves from S16°E resulted in a considerably more pronounced setup, especially around low water (about 0.4 ft). The waves from N84°E resulted in the lesser water-level setup, generally less than 0.2 ft, with a higher setup occurring at high water than at low water.

65. The tide stations located just bayward from the throat, i.e., sta 2 in Banks Channel, and sta 3, 4, and 5, located in Shinn Creek, Banks Channel, and Masonboro Channel, respectively, were all influenced by the waves (Plates 206 and 207). The waves from S16°E caused a setup

throughout the tidal cycle at each of these stations, except at high water at sta 3. The largest setup occurred at low water (about 0.4 ft). The waves from N84°E caused less setup. A setup of less than 0.2 ft was observed in Masonboro Channel (sta 5) with a slightly smaller setup measured immediately behind the throat (sta 2). Records from both Banks Channel and Shinn Creek (sta 3 and 4) show slight setdown in the water-surface elevations.

66. At sta 6 and E in the AIWW behind the inlet, both records (Plate 207) show that the S16°E waves resulted in an average setup of more than 0.2 ft (about 0.4 ft at low water). The N84°E waves resulted in an average water-level setup of approximately 0.1 ft at both stations, with sta E results showing a slightly larger setup.

67. Records for tide stations in the bay northward from the inlet (sta D, G, and I in Plates 208 and 209) show both waves resulted in a setup of the water level at the junction of Banks Channel and the AIWW (sta D), but only the S16°E wave resulted in a setup for the remainder of the bay (sta G and I). The S16°E wave also caused a setup of the water level in the bay south of the inlet (sta F, H, and J in Plates 208 and 209, with only minor influence of the N84°E wave measured.

68. In general, the S16°E wave resulted in a more significant setup of the water-surface levels in the inlet and bay. In addition, the setup at low water was generally considerably greater than that at high water, after the ebb flow when the greatest wave-current interaction took place.

Current patterns without tide

69. Three wave tests (Plates 217-219) conducted without tidal currents were included to investigate the effects of wave direction and height on general current patterns. Results of the S16°E wave (Plate 217) show a pattern of currents generally perpendicular to the contour lines over both shoal areas. Flow is toward the inlet over the shoal north of the channel. The N84°E, 3-ft wave (Plate 218) resulted in flow toward the inlet over both shoals with flow toward the ocean between the two shoals. Two areas of no flow (or eddy) existed approximately 300 ft apart in the secondary channel near Masonboro Beach. When

the amplitude of the north wave was increased from 3 to 5 ft (Plate 219), a distinct large eddy developed immediately south of the throat of the inlet and a distinct splitting of the flow of the channel along Masonboro Beach was observed.

Currents during flood flow

70. The tide-generated surface current patterns at strength of flood (Photo 50) show a generally uniform flow pattern approaching the inlet. The waves from N84°E (Plate 226) influenced the current pattern only immediately adjacent to Masonboro Beach where a reversal of current direction occurred. When waves from S16°E were simulated, a similar effect occurred immediately offshore from Wrightsville Beach--currents were in a direction away from the inlet (Plate 239). Early in the flood phase of the tide cycle (Photo 47 and Plate 236), the influence of the south wave on the currents was most evident; but approaching the strength of flood (Photos 47-50 and Plates 237-239), the influence of south waves on the current direction decreased and tidal currents dominated. The reversal of flow direction at the appropriate beach for each wave direction was evident during this period. Immediately after strength of flood (Photo 51 and Plates 227 and 240), the reversal of flow progressed down the beach away from the inlet. Near the end of the flood phase of the tidal cycle (Photo 52 and Plates 228 and 241), an eddy developed near Masonboro Beach for waves from N84°E and in an extensive area oceanward from Wrightsville Beach for waves from S16°E.

71. Dye placed immediately oceanward from Masonboro Beach during the early portion of strength of flood (Photo 59) showed a similar movement with and without waves. Dye was injected into the model at hour 4.5, and photographed 1.0 hr (prototype) later. The tests were not conducted such that intensity of dye at selected locations could be determined. Similar tests with dye placed off Wrightsville Beach were conducted (Photo 61). In this case, dye was injected into the model just before strength of flood (hour 3.5), and photographs were taken 1.0 hr later. The test with no waves simulated resulted in the dye moving along Wrightsville Beach toward the inlet, and essentially all dye that passed through the throat of the inlet moved into Banks Channel.

When N84°E waves were simulated, the dye was much more extensively dispersed through the throat of the inlet and a significant portion of the dye moved into Shinn Creek in addition to Banks Channel. When waves from S16°E were simulated, all of the dye moved away from the inlet north along Wrightsville Beach. Tests with dye placed directly oceanward from the throat of the inlet were conducted also (Photo 64). The dye was injected during strength of flood (hour 5.0) and photographed 1.5 hr later. Without waves simulated, the dye moved directly through the throat of the inlet; and essentially all of the dye moved into Shinn Creek. The waves from N84°E caused the dye to shift distinctly toward Masonboro Beach and to favor Masonboro Beach as it passed through the throat of the inlet. The dye was then dispersed into each of the three internal channels, i.e. Banks Channel, Shinn Creek, and Masonboro Channel. When waves from S16°E were simulated, the dye oceanward from the throat shifted toward Wrightsville Beach. Once the dye passed through the throat of the inlet, it moved into Banks Channel and Shinn Creek. No dye was observed to move into Masonboro Channel.

72. Detailed current measurements were made at ranges 1 and 2. An increase in maximum flood speeds at each of the range 1 current stations (Plates 210-212) was observed for both wave directions. The increase in the maximum current (about 1.5 fps) was higher at each station with the S16°E wave simulated. Significant reductions occurred in the duration of the flood phase from approximately 6.5 hr without waves to approximately 5 hr with the S16°E wave simulated. It should be noted that limited area is covered by the three current stations (Figure 26).

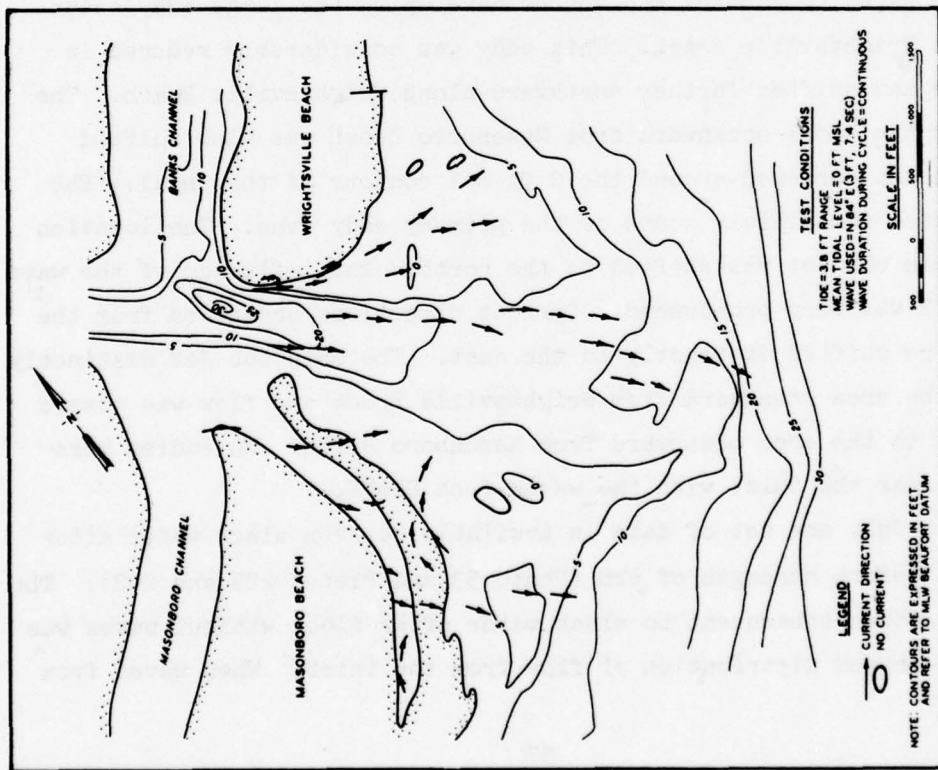
73. Current data for stations at the throat of the inlet (range 2) are shown in Plates 212-215. Waves from N84°E had essentially no effect on sta 2C and 2S. Current speeds at the surface at sta 2N were reduced in magnitude (about 0.5 fps at strength of flood); middepth flood magnitudes were essentially unchanged; and the maximum bottom flood current speed was increased by about 1.0 fps. The duration of flood flow was essentially unchanged at these three stations; however, at sta 2SS it was increased from approximately 6.5 hr to about 9 hr. The peak current magnitude at sta 2SS was unchanged.

74. The effect of the S16°E wave was a net increase to the overall flood currents at sta 2N (increased maximum surface current by about 0.6 fps) and a decrease at sta 2C and 2S. Although the maximum flood current speeds at sta 2C and 2S were not significantly changed, the duration of the maximum currents was significantly reduced. The peak magnitude of the current at sta 2SS was increased from approximately 2.5 to 3.6 fps by the S16°E wave, and the duration of flood flow was increased from approximately 6.5 to 9 hr. The total flood discharge at range 2 (Plate 216) was essentially the same for the no-wave condition (620 mcf) and with waves from N84°E (619 mcf), whereas the S16°E wave resulted in about a 4 percent decrease (593 mcf). This apparent reduction in discharge is within the limits of accuracy of the current measurements.

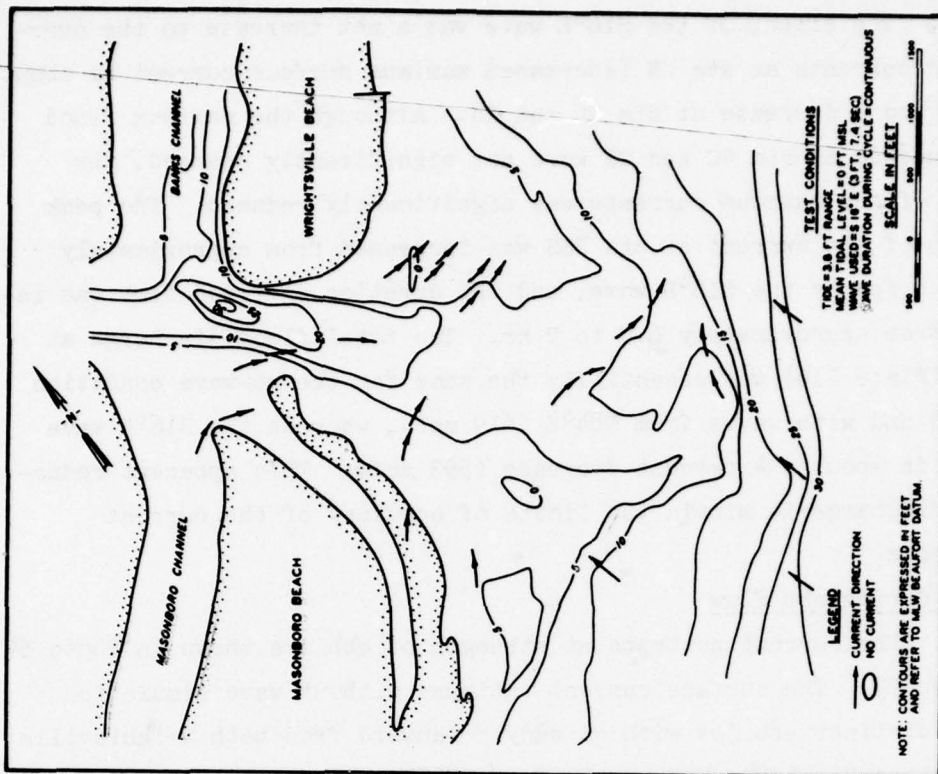
Currents during ebb flow

75. The current patterns at strength of ebb are shown in Photo 54 and Figure 27. The surface current patterns without wave simulation show the distinct ebb jet with an eddy oceanward from both Wrightsville and Masonboro Beaches. When waves from N84°E were simulated, the wave action appeared to counter the forces developing the large eddy oceanward from Wrightsville Beach. This eddy was considerably reduced in magnitude and shifted farther northward along Wrightsville Beach. The eddy over the shoal oceanward from Masonboro Beach was also shifted northward and centered around the 0 ft msl contour of the shoal. Ebb flow existed immediately south of the primary eddy zone. The location of the main ebb jet was shifted to the north. The influence of the wave from S16°E was very pronounced. Current directions oceanward from the throat were shifted distinctly to the east. The main ebb jet distinctly favored the area oceanward from Wrightsville Beach and flow was toward the inlet in the area oceanward from Masonboro Beach. No eddies were observed near the inlet with the waves from S16°E.

76. Only one set of data is available between slack water after flood and before strength of ebb (Photo 53 and Plates 229 and 242). The general pattern subsequent to slack water after flood without waves was for a fan-shaped distribution of flow from the inlet. When waves from



a. North wave



b. South wave

Figure 27. Model current patterns, 1964 hydrography, hour 10

N84°E were simulated, a distinct flow separation zone developed immediately oceanward from Masonboro Beach with a splitting of the flow near the beach. Flow was toward the inlet along the minor channel near Masonboro Beach with flow in the flood direction until the main ebb flow through Masonboro Channel was encountered. The general trend for waves from S16°E was also observed early in the ebb phase. The area oceanward from Masonboro Beach has a large area of no current located just oceanward from the shoal. This area was conducive to the deposition of sediment. Flow was observed to be northward along Wrightsville Beach north of the inlet.

77. After strength of ebb (hours 11-1), the data without wave effects (Photos 55-56 and 44-45) show a general progressive abatement of the magnitude of the ebb currents and relatively small, rather weak eddies on either side of the ebb jet. The data with wave effect (Plates 220, 221, 231, 234, 244, and 245) show important effects of the waves. With waves from N84°E, the effects of wave refraction over the shoal oceanward from Masonboro Beach were more pronounced than at strength of ebb. A distinct circular flow pattern developed around the shallowest portion of the shoal which was particularly conducive to trapping and deposition of sediment on the shoal. Flow in the secondary channel next to Masonboro Beach was subjected to minimal or no flow at hours 12 and 0, and reversed to flood flow at hour 1 (2 hr before reversal in the throat). The area oceanward from Wrightsville Beach showed a progressive shift of flow to the north with an area of generally no flow at the shoreline near the northward toe of the shoal off Wrightsville Beach. Although the flow patterns were not conducive to a general deposition on the shoal area, the deposition of sediment at the toe of the shoal would be reinforced by the current patterns. Immediately after strength of ebb, the S16°E waves caused currents to continue over the north shoal and swing parallel to Wrightsville Beach (see Plates 243 and 244). The effects of the waves over the south shoal were less pronounced as ebb flow existed along the north side of the shoal. South of the shoal, flow continued toward the inlet. As ebb flow continued to abate, the depth of water decreased with an associated

decrease of the influence of the waves on the flow. The major effect of the waves on the currents was essentially confined to the ocean side of the south shoal.

78. Current magnitude data are limited to observations (Plates 210-215) obtained at current ranges 1 and 2 (Figure 26). During ebb flow at range 1, the current data for waves from N84°E showed slight increases of the maximum ebb current magnitudes. The current speeds for the S16°E wave showed marked increases at all stations (up to 3.6 fps increase in maximum ebb currents). The general current patterns discussed in paragraph 86 indicate that the ebb flow was shifted to the area of range 1. These data substantiate the current patterns.

79. The current data obtained at range 2 in the throat of the inlet (Plates 213-215) showed minimal changes when either wave direction was simulated in the model. The data obtained at sta 2SS in the small channel along Masonboro Beach (Plate 212) during ebb flow show the previously discussed (paragraphs 72-74) shift of the dominant flow from ebb to flood. The magnitude and duration of ebb flow were reduced by the waves from both directions.

80. The dye movement photographs further confirm the general ebb pattern defined by the current pattern photographs. In the first of these tests, dye was injected into Banks Channel just after the beginning of ebb flow (hour 9) and was photographed 1 hr later (Photo 57). Without waves, dye passed through the northern half of the gorge, moved oceanward in the natural channel, and expanded until it covered a width about equal to the width of the gorge near the ocean end of the shoal. Very limited evidence of flow moving northward across the shallow area oceanward from Wrightsville Beach was observed. N84°E waves affected the pattern in two minor areas. The width of the throat covered was slightly increased and the ocean end of the plume was more confined. The S16°E wave influenced the flow pattern of the dye more significantly. The dye was deflected around Wrightsville Beach and split into two plumes when depths of 10-15 ft were reached; one plume remained adjacent and parallel to Wrightsville Beach and the second plume moved oceanward. A second dye test was conducted with dye placed in Banks Channel

(Photo 48). In this test, the dye was introduced at about the strength of ebb (hour 11.5) and was photographed 0.5 hr later. The dye pattern for the test without waves was similar to that in the test before strength of ebb, with the exception that some dye moved onto the shoal oceanward from Wrightsville Beach and the dye extended farther into the ocean (because of the greater current magnitudes). The N84°E wave caused a widening of the dye at the throat of the inlet, a significant confining of both the dye moving directly oceanward and along Wrightsville Beach, and lesser movement offshore in the main channel. The S16°E wave resulted in a dye width in the throat intermediate between those for the no-wave and north-wave conditions. Like the test before the strength of ebb, the south waves forced the dye to move over the shoal oceanward from Wrightsville Beach. The dye did not extend as far into the ocean nor as close to Wrightsville Beach as in the prestrength-of-ebb test. A test was conducted in which dye was placed in Shinn Creek just before strength of ebb (hour 9.75) and was photographed 0.75 hr later. Photo 60 shows that, for the test without waves, dye spread across almost the entire portion of the throat which was submerged at the time, was distributed fairly uniformly in the main channel offshore from the throat, and occupied both Masonboro Channel and the secondary channel offshore from Masonboro Beach. The N84°E wave deflected the dye away from Masonboro Channel and the secondary channel at Masonboro Beach and moved some of the dye onto the shoal oceanward from Wrightsville Beach. The S16°E wave diverted the dye over the shoal oceanward from Wrightsville Beach where it split with one leg directed oceanward and the second leg located approximately 2000 ft offshore and parallel to the beach. Dye was placed in Masonboro Channel just prior to strength of ebb (hour 9.5) and was photographed 0.75 hr later (Photo 62). When waves were not simulated in the model, the dye was confined to the inner half of the shoal oceanward from Masonboro Beach and the southern portion of the natural channel from the throat to the ocean. The N84°E wave caused the dye to be shifted from the shoal area northward into the natural offshore channel. The S16°E wave forced the dye northward to the base of the shoal located oceanward from Wrightsville Beach. A second dye injection was made in

Masonboro Channel, this one at about the conclusion of strength of ebb (hour 11.5). The dye pattern was photographed 0.5 hr later (Photo 63). Because water levels at this phase of tide were lower than during the time of the previous ebb release in Masonboro Channel (Photo 62), the dye for the test without wave action was more confined to areas of deeper water. The dye was in evidence in the small channel along Masonboro Beach and in the natural channel extending from the throat to the ocean. The N84°E wave had minimal influence on the dye pattern with the effects essentially confined to a small shifting of the plume in the main channel to the north. The S16°E wave had more of an influence. The movement of dye out of the small channel along Masonboro Beach was retarded, and the main plume was deflected northward to the base of the shoal oceanward from Wrightsville Beach.

Summary

81. The following observations are made, based on the results of the 1964 base tests:

- a. The limitations placed on the ability to simulate the N84°E wave must be considered in all results involving waves from N84°E.
- b. Both the N84°E and S16°E waves resulted in a setup of the mean tide levels in the bay. The S16°E waves resulted in the higher setups of the mean tide levels.
- c. Both the N84°E and S16°E waves caused the flow through the small channel along Masonboro Beach to become strongly flood-dominated.
- d. Waves tested from either direction generated shoreward currents over both offshore shoals during at least part of the tidal cycle when tidal currents without waves were in the ebb direction.
- e. Results of the hydraulic tests with only tide reproduction indicate that particularly during ebb flow, the shoals oceanward from Wrightsville and Masonboro Beaches were areas of relatively low current speeds; therefore, material can be expected to be deposited and remain on the shoals.
- f. Results of the tests to determine the influence of waves on current patterns show a distinct increase in the extent

and duration that low flows and eddies developed over the shoals oceanward from both Wrightsville and Masonboro Beaches.

- g. The $S16^{\circ}E$ wave appeared to influence all model results more than the $N84^{\circ}E$ wave. However, the limitations on the ability to simulate the $N84^{\circ}E$ wave must temper this observation. It does appear, however, that results from tests with the $N84^{\circ}E$ wave more effectively simulated would still show the $S16^{\circ}E$ to be more significant.

PART VII: PLAN TESTS OF 1964 HYDROGRAPHY

Model Modification

82. After data for the 1964 natural condition were collected, a 14-ft-deep by 400-ft-wide navigation channel, a 16-ft-deep deposition basin, and a 3400-ft-long weir jetty (Figure 3) were installed in the model. These are the improvements that would have been tested prior to their construction in 1965, had a verified model been available in 1964. Thus, model data for both the natural and improved 1964 conditions will be compared to assess the influence of the improvements on the hydraulic and wave characteristics.

Hydraulic Tests

83. Tidal data for the base and plan conditions are shown in Plates 162-167. Limited tidal changes occurred when the plan was installed.

84. Current data obtained at sta 8-12 (Plates 188-192) located oceanward from the jetty (Figure 26) show that the plan shifted both flood and ebb flow in a southerly direction (toward sta 12). During flood flow, all of these stations exhibited an increase in maximum current speed of less than 0.5 fps. Surface current patterns for the flood phase of the tidal cycle (Photos 47-52 for the base test and Photos 68-73 for the plan test) show that current directions in this vicinity shifted approximately 90 degrees in the area throughout essentially all of the flood phase. Crosscurrents can be expected to occur in the outer end of the navigation channel throughout essentially the complete flood phase of the tidal cycle. Prior to installation of the plan, flow was directed toward the throat of the inlet. With the plan installed, current directions were directed toward Masonboro Beach for some distance before swinging around the end of the jetty toward the inlet. Ebb current data for the northern three stations (8-10) show marked maximum current magnitude decreases with the plan in place (0.5 to 2.5 fps),

whereas significant increases in maximum ebb flow were observed for the two south stations, 11 and 12 (1.9 fps at the surface of sta 12). Surface current patterns for ebb flow (Photos 44-46 and 53-56 for the base test and 65-67 and 74-77 for the plan test) confirm the shift in ebb flow to the south with the plan in place. Minor changes in the direction of the ebb flow with the plan in place were observed; and strong ebb currents impinged on the outer end of the jetty.

85. Current data obtained near the bend in the jetty show the continuing trend for flow to be shifted in a southerly direction away from the jetty. Current measuring stations in this area are sta 13 and 14 (Plate 193), sta 15 (Plate 194), sta 16 (Plate 195), sta 1N and 1C (Plate 168), sta 1S (Plate 169), sta 20 (Plate 197), and sta 19 (Plate 196). During flood flow, reduced current magnitudes were observed away from the jetty (sta 14, 15, 20, 16, and 19) with the plan installed in the model. The most significant change in this area occurred at sta 16 where the plan increased the maximum flood current magnitude from approximately 0.8 to 1.6 fps. Surface current data for the flood phase of the tidal cycle (Photos 68-73) show that, early in the flood phase, flow was relatively uniform through the area; however, as strength of flood was attained, a low-magnitude eddy developed between the channel and the jetty. The size of the eddy was progressively larger throughout the flood phase. Maximum ebb currents near the jetty (sta 13, 14, 1S, 1C, and 1N) were reduced by less than 0.8 fps by the plan. The two current stations in the navigation channel (sta 15 and 20) showed a slight increase in maximum ebb magnitudes near the surface and a slight decrease near the bottom with the plan in place. Sta 16, located south of the navigation channel, and sta 19, located near Masonboro Beach, showed only minor current changes with the plan installed in the model. Comparison of Photos 51 and 72 and Photos 54 and 75 illustrates the effectiveness of the jetty in blocking flow at sta 17 and 18 during flood and ebb, respectively.

86. Current data in the navigation channel approaching the throat of the inlet (sta 21, Plate 198), in the area of the weir (sta 17, Plate 195), and in the deposition basin (sta 18, Plate 196) show the

significant decrease in flood (1.0 fps) and ebb (0.5 fps) magnitudes away from the navigation channel with the plan installed and the trend for slightly reduced currents in the navigation channel. Current data for sta 17 located oceanward from the weir show the significant decrease in current speeds with the plan installed. This was caused by the weir and jetty blocking essentially all tidal flow to and from the inlet in the area of sta 17; only minor tidal flow over the weir occurred. Because the deposition basin is located in the angle between the jetty and the tip of Wrightsville Beach, sta 18 is also cut off from strong ebb and flood flows with the plan installed. Current data in the navigation channel adjacent to the deposition basin show that the plan caused small decreases in current magnitude during flood, but a small decrease at the bottom and small increases at the surface for ebb flow. Surface current patterns for flood (Photos 47-52 for the base test and Photos 68-73 for the plan test) and ebb (Photos 44-46 and 53-56 for the base test and 65-67 and 74-77 for the plan test) confirm the surface current data.

87. The minimum cross-sectional area for the inlet is located at range 2, just oceanward from the gorge of the inlet (Figure 26). The maximum current magnitudes in the model were observed at range 2, although current speeds at range 3 (Figure 26) located in Shinn Creek were of nearly the same magnitude. Current data for sta 2C (Plate 171) show essentially no change in magnitude for the center of the channel when the plan was installed. Current data for sta 2N (Plate 170) show that ebb current speeds at all depths were essentially unchanged with the plan installed; however, maximum flood currents were reduced by about 1.0 fps at the middepth and surface and were increased by about 1.5 fps near the bottom. These differences are probably a result of the source of flow to this area. At middepth and surface in the base test, flood flow came from the shallow area oceanward from range 2 and along Wrightsville Beach. When the plan was installed, this source of flow was greatly reduced which caused a reduction of flood current magnitude at the middepth and surface. For the base condition, the source of flow to the bottom depth at sta 2N was probably from the same general area, possibly with some increased contribution from the area directly oceanward

from the station. When the plan was installed (Figure 26), the alignment of the navigation channel focused bottom flood flow toward sta 2N as shown by the contours (Figure 26). Because the surface width was much greater than the bottom width, the navigation channel did not exert a great influence on surface currents. Current data for sta 2S (Plate 172) show reductions of maximum magnitudes for both flood and ebb of 0.2 to 0.6 fps with the plan installed. The maximum ebb magnitude at sta 2SS (Plate 173) was reduced by about 1.0 fps with the plan installed in the model, whereas the maximum flood magnitude was essentially unchanged. Surface current patterns shown in Photos 44-46, 53-56, and 74-77 do not yield any additional information about flow in the throat. Discharge data for range 2, presented in Plate 199 and Table 4, show a small reduction (about 8 to 9 percent) in the tidal prism with the plan installed.

88. Current magnitude data at range 3 (Figure 26) located in Shinn Creek are shown in Plates 174-176. With the plan installed, minor changes are observed for ebb flow. The magnitude of flood flow shows a general trend to distribute flow more evenly across the range with the plan installed. Maximum flood currents at sta 3C (Plate 175) were generally reduced and those at the outer sta 3N and 3S (Plates 174 and 176) were increased to approximately 2.0 to 2.5 fps. The total flood discharge past range 3 (Plate 200 and Table 4) was increased by about 9 percent; but the total ebb discharge was essentially unchanged. No additional information could be obtained from the surface current patterns shown in Photos 44-56 and 65-77.

89. Currents in the remaining interior channels, i.e., ranges 4, 5, 6, and 7 (Plates 177-187), showed slight local changes, but on the whole there was minimal variation from the base data to the plan data. There was some indication that the flow past range 4 was shifted slightly toward the east side of the channel by the plan (Plates 177-179). This would logically follow from the altered direction of the entrance and exit flows just seaward of range 2. Comparison of discharges for each of the ranges (4, 5, 6, and 7, Plates 201-204, respectively) and Table 4 generally shows little change in discharges through these ranges when considering about a ± 10 percent possible model measurement error for

discharges in these relatively low-velocity regions. The ebb and flood discharges at range 6 were reduced by 19 and 14 percent, respectively; but these changes are actually insignificant because the total discharges were quite small. Total flood discharge at range 7 was increased by 19 percent. The absolute magnitude of this increase (32 mcf) is almost equal to the increase at range 3 (23 mcf) plus the reduction of discharge at range 6 (12 mcf). This is remarkable agreement considering the possible error in these data. The degree of possible experimental error is shown by comparison of the discharge data for range 2 (Plate 199) at the throat of the inlet and discharge data for the three interior channels bayward from the throat, i.e. ranges 3, 4, and 5 (Plates 200-202). The total flood flow through the throat is decreased by about 9 percent with the plan in place and each of the three bayward channels shows an increase in flood flow of about 6 to 9 percent. This discrepancy results from experimental error in measuring current magnitudes, which is ± 10 percent when Price-type cup meters are read visually.

Wave Tests

90. Data with waves obtained for the base condition were also obtained with the plan installed in the model, with the exception that only the S16°E, 7.4-sec, 3-ft waves and N84°E, 7.4-sec, 3-ft waves were investigated. The effects of these waves on tidal heights are presented in Plates 246-250. Current magnitudes measured at ranges 1 and 2 are shown in Plates 251-256. The discharges at range 2 are shown in Plate 257. Wave-induced current patterns without tidal currents are shown in Plates 258 and 259. Tide and wave-induced current patterns for each hour of the tidal cycle are shown in Plates 260-272 for the N84°E, 7.4-sec, 3-ft waves, and Plates 273-285 for the S16°E, 7.4-sec, 3-ft waves.

Effects on tidal heights

91. Modification of the two ocean tide height records measured near Wrightsville Beach (sta O) and Masonboro Beach (sta C) is shown in Plate 246. Both the N84°E and S16°E waves caused an average of

approximately 0.1-ft setup of the Wrightsville Beach water heights. The S16°E wave caused a very small setdown of the water level at the Masonboro Beach gage, while the N84°E wave resulted in a small setup at high water and a small setdown at low water. The water level at the gorge of the inlet (sta B) was unaffected by waves from N84°E for water levels below 0 ft msl; for most of the tidal cycle above 0 ft msl, a small setup was observed. Since the weir was set with a top elevation of 0 ft msl, transmission of water over the weir by the N84°E wave was a probable major influence on this setup. The wave from S16°E resulted in a maximum setup at the inlet of approximately 0.4 ft at low water. Within 2 hr after low water, setup had decreased to 0.2 ft until essentially strength of flood. From strength of flood to beginning of ebb flow the setup was minimal. The setup increased as the ebb tide progressed, reaching a maximum setup of 0.4 ft at low water.

92. The setup at sta 2, located a short distance down Banks Channel from the throat of the inlet, was more pronounced than that at the throat. There is no apparent explanation for this occurrence. Near strength of ebb, both waves caused a definite setup of the water surface. At low water, the S16°E waves caused a setup of 0.5 ft, and the N84°E waves resulting in a slight setdown of the water surface around high water. The same general pattern exists for the records obtained in each of the three interior channels (sta 3, 4, and 5) for the S16°E wave. For the N84°E wave, only the setup pattern for Shinn Creek (sta 3) was similar to that for sta 2. Both Banks Channel (sta 4) and Masonboro Channel (sta 5) experienced only minor setup for the N84°E wave.

93. In the AIWW, both locations monitored (sta 6 and E) resulted in setup of the water surface similar to that of sta 2. The magnitudes throughout the tidal cycle were essentially the same as those observed at sta 2. The N84°E waves resulted in about a 0.2-ft setup of the water levels north of the intersection of the AIWW and Shinn Creek (sta 6), with the exception of about 2 hr around high water. South of the intersection (sta E), essentially no setup was measured.

94. The S16°E wave resulted in the same general water-level patterns at five of the six interior bay gage locations (sta D, F, G, H,

and J) as those at sta 2. Sta I, located in the extreme inland end of the bay north of the inlet, experienced both setdown and setup during the course of the tidal cycle. The largest setup at these stations for the N84°E wave occurred at sta D (0.2 ft). Sta G, H, and J experienced small setups of the water surface; sta F did not show any appreciable change; and sta I showed about a 0.2-ft setdown.

95. In summary, the S16°E wave resulted in a general setup throughout the bay with an average setup throughout the tidal cycle of 0.34 ft near the throat to 0.4 ft in the extreme of the south bay. Similar data for the N84°E waves were an average setup throughout the tidal cycle near the throat of 0.05 ft and in the far south bay of 0.05 ft.

Current patterns without tide

96. Two tests were conducted without tidal effects--one with the N84°E waves and the other with the S16°E waves. Results of the S16°E wave (Plate 258) showed a well-developed, large eddy over the shoal south of the inlet. Fairly strong currents existed in the secondary channel along Masonboro Beach. A definite flow existed over the interior end of the weir with minimum flow over the outer end of the weir. Flow exiting oceanward along the channel side of the north jetty was also noted. The N84°E waves (Plate 259) resulted in an eddy located between the south shoal and the throat of the inlet. A second small eddy existed between the outer end of the deposition basin and the navigation channel. Areas of no flow included the interior end of the deposition basin, along the inside of the raised portion of the jetty, in the outer end of the navigation channel, and in deeper water off the end of the navigation channel. These patterns are similar to those taken under the same test conditions with the 1969 bathymetry with the exception that the eddy for the N84°E wave was shifted more southwesterly for the 1964 bathymetry than for the 1969 bathymetry.

Currents during flood flow

97. Comparison of results for strength of flood without waves (Photo 71) with results of tests with N84°E waves (Plate 266) shows, generally, that the flow directions were unchanged over the south shoal for either condition. Both the N84°E and the S16°E wave improved the

flow alignment along the navigation channel, with the S16°E wave providing more of an improvement. A flow separation occurred at the end of the jetty with the N84°E wave, with a highly confined eddy existing at the end of the jetty. Low-magnitude currents existed along the jetty and through the deposition basin. Flow existed over the weir section, as well as away from the weir north along Wrightsville Beach. Flow oceanward from Wrightsville Beach was toward the beach with a well-defined area of no flow existing to the east near the end of the jetty. Flow patterns in the entrance area south of the jetty and over the weir were very similar with the north waves and without waves. The S16°E wave resulted in a more dormant area along the jetty. Very low flow existed along the jetty, with no flow in the deposition basin. A well-defined landward flow existed east of the north jetty, and flow away from the inlet occurred along Wrightsville Beach. During the period from low-water slack to strength of flood, the N84°E waves (Plates 263-265) developed the same patterns that occurred at strength of flood, except that the flow separation and eddy at the end of the jetty did not develop until strength of flood. During this same period, the results of waves from S16°E (Plates 276-278) show a current parallel to the beachline across the south shoal toward the navigation channel. Currents between the navigation channel and the jetty were late in reversing from ebb to flood. After strength of flood, the data for the N84°E wave (Plates 267 and 268) follow the same general pattern that developed at strength of flood. When the S16°E waves were simulated in the model, the results after strength of flood (Plates 280 and 281) showed a continuation of the pattern existing at strength of flood. However, near slack water (hour 8), ebb flow on both sides of the outer end of the jetty developed while flood flow existed throughout most of the remainder of the inlet area.

98. Dye was placed near Masonboro Beach (Photo 79) at hour 4.5 (during the early portion of the strength of flood) and was photographed 1.0 hr later. Results show similar patterns with and without waves. The dye was confined to the immediate area of Masonboro Beach, particularly in the small channel along Masonboro Beach. After moving through

the throat of the inlet, all of the dye was confined to Masonboro Channel. The resulting dye movement pattern was quite similar to that which occurred for prejetty conditions (Photo 59), except that the dye did not move quite so far into Masonboro Channel for the plan test. Dye was placed near Wrightsville Beach (Photo 81) at hour 3.5 (just before strength of flood) and photographed 1.0 hr later. Results without waves show limited movement offshore, with the majority of the dye moving across the low weir and in Banks Channel exclusively. When N84°E waves were simulated in the model, the same general pattern was observed, with the exception that somewhat more movement northward along Wrightsville Beach was observed. When S16°E waves were introduced, the dye all moved northward along Wrightsville Beach, with no dye moving into the inlet. Compared with dye movement for prejetty conditions (Photo 61), the jetty caused no change in movement from the south waves, slightly more offshore movement with no waves, and eliminated movement into Shinn Creek with the north waves. During the strength of flood (hour 5.0), dye was placed in the navigation channel southeast of the outer end of the jetty and photographed 1.5 hr later. Results show that the dye movement was essentially confined to the area between the south shoal and the jetty for the test without waves (Photo 84). After moving through the throat, the dye dispersed into Shinn Creek and Banks Channel. When waves from N84°E were introduced, a similar pattern resulted. The S16°E waves caused modification of the patterns. Dye moved around the end of the jetty toward the north to a limited extent and was transported over the weir and down Wrightsville Beach. Much less dye penetrated Shinn Creek and more entered Banks Channel. Compared with prejetty conditions, dye in the offshore channel was shifted significantly toward the jetty with and without waves; dye movement from the south waves into Shinn Creek was eliminated; and dye was moved without waves into Banks Channel.

99. The waves from N84°E resulted in small increases in maximum flood currents at each station and depth on range 1 (Plates 251-253). The S16°E wave had a progressively increasing influence on the currents at the stations, moving from the south to the north station. Maximum flood currents at sta 1S were increased by 1.2 to 1.5 fps; those at

sta 1C were increased by 1.3 to 2.0 fps; and those at sta 1N were increased by 2.6 fps. The S16°E waves also decreased the duration of flood flow 2.5, 2.0, and 1.5 hr for sta 1S, 1C, and 1N, respectively. Range 1 stations cover a very limited portion of the inlet entrance. The major change at the throat of the inlet (range 2) was at sta 2SS (Plate 253). The effect of both waves was to shift the flow from an essentially balanced flow to a strongly flood-dominated condition. The N84°E waves increased the maximum flood velocity by 0.6 fps, and the S16°E waves increased it by 0.9 fps. The duration of flood was increased by 1.5 hr for the S16°E waves and by approximately 2.0 hr for the N84°E waves. The influence of the N84°E waves at the three stations in the throat of the inlet (Plates 254-256) was relatively small. At sta 2N, increases of roughly 0.5 fps in maximum flood velocity were observed at the surface and middepth measuring points; elsewhere, the effects of the N84°E waves were minimal. The influence of the S16°E waves was more pronounced. Increases of maximum flood magnitude of about 0.5 to 0.9 fps were observed at sta 2S. After the initial 1.5 to 2.0 hr of the flood phase, reductions varying from approximately 1.0 fps at the surface to approximately 0.5 fps at the bottom were measured for sta 2C. Maximum flood current magnitudes, however, were only reduced by about 0.2 fps. At sta 2N, the trend was to increase the current magnitudes early in the flood phase and reduce the speeds later in the flood phase. Maximum magnitudes were increased by about 0.5 fps at the surface and middepth and reduced by the same amount at the bottom. The duration of the flood phase was decreased by approximately 0.75 to 1.0 hr at sta 2N, 2C, and 2S.

Currents during ebb flow

100. The surface current patterns for the inlet during ebb flow without waves are shown in Photos 65-67 and 74-77. The current patterns with north waves are shown in Plates 260-262 and 269-272, and those with south waves are shown in Plates 273-275 and 282-285. At strength of ebb (hour 11), the N84°E wave resulted in minimal changes to the flow patterns without waves, with a somewhat more defined eddy developing over the shallow portion of the shoal. Currents in the small channel along

Masonboro Beach were in the flood direction, as were currents north of the north jetty. The small channel along Masonboro Beach had ebb flow, as it did without waves. Currents in the deposition basin were essentially eliminated. Both wave directions generated flow from the south shoal into the navigation channel. As without waves, ebb flow directed offshore was rapidly established immediately following the slack flood (hour 9) with the north wave. More current was observed in the deposition basin early in the ebb phase than occurred at strength of ebb. Immediately following high-water slack at the inlet throat (hour 9) with the S16°E wave, flood flow continued to occur over the shoal along Masonboro Beach (Plate 282), while ebb flow existed over the remainder of the inlet. As strength of ebb was reached, ebb flow existed in the portion of the south shoal near the inlet. After strength of ebb (hours 12, 0, 1, and 2), the influence of the N84°E wave was more effective in recessing the ebb flow over the south shoal. As the ebb flow abated, the extent of the ebb jet became more confined to the navigation channel. Immediately after strength of ebb (hour 12), the S16°E wave caused currents toward the inlet to develop immediately oceanward of the south shoal. This flow persisted and expanded throughout the remainder of the ebb phase of tide. Near the end of ebb (hour 2), flow existed across the entire south shoal toward the inlet and navigation channel. In general, the flow conditions during ebb over the south shoal were not particularly conducive to removal of material from the shoal and were such that material could be transported to the shoal from offshore.

101. Dye placed in Banks Channel just before strength of ebb (hour 9) without waves (Photo 78) and photographed 1.0 hr later was confined to the northern half of the throat of the inlet and dispersed somewhat over the south shoal by the time it reached the end of the jetty. None of the dye passed over the weir, and very little moved adjacent to the jetty. Both wave directions had a confining effect on the dye near the outer end of the jetty. The N84°E wave confined the dye to the navigation channel and the jetty. The S16°E wave forced the dye out of the navigation channel near the end of the jetty and confined the dye to the area between the navigation channel and the jetty. The S16°E wave also

forced dye over the weir section to a limited extent along Wrightsville Beach. Dye placed in Shinn Creek just before the strength of ebb (hour 9.75) and photographed 0.75 hr later (Photo 80) generally was confined to the central portion of the inlet area. The effects of both waves were similar to the effects on dye placed in Banks Channel, except that the pattern was displaced to the southwest. The S16°E wave displaced the dye more toward the jetty than the N84°E wave. None of the dye for any test reached the jetty or passed over the weir. Dye placed in Masonboro Channel prior to strength of ebb (hour 9.5) and photographed 0.75 hr later (Photo 82) without waves was essentially confined to the south shoal. Very little of the dye moved as far north as the navigation channel. The major change resulting from the N84°E waves was to restrict the movement of the dye over the south shoal. Considerably more dye moved into the navigation channel. The length of dye movement was essentially the same for the N84°E wave test and the test without waves. The S16°E wave displaced the dye toward the navigation channel, but displacement was less than that caused by the north wave. Limited dye was observed in the navigation channel for any of the tests. Results of dye placed in Masonboro Channel at the end of strength of ebb (hour 11.5) and photographed 0.5 hr later (Photo 83) were significantly different. Without waves, dye covered all but the shallowest portions of the south shoal and extended over the shoal into the ocean. In addition, dye moved a considerable distance along Masonboro Beach from the inlet; little dye moved into the navigation channel. The N84°E wave caused the dye to split into two well-defined bands around the shallowest portion of the shoal; no dye reached the navigation channel. The S16°E wave essentially eliminated any dye over the south shoal. The dye was confined to a limited distance down the small channel along Masonboro Beach and a short band of dye reaching the navigation channel did not extend much beyond the outer end of the deposition basin.

102. All detailed current measurements obtained at range 1 (Plates 251-253) showed drastic increases in maximum ebb magnitudes of 1.4 to 3.0 fps for tests with the south wave and 0.9 to 1.5 fps with the north wave. The decrease in flood duration, with an associated increase

in ebb duration, was discussed in paragraph 99. The influence of the waves at range 2 at the throat of the inlet (Plates 253-256) was relatively minor at the gorge, except that the south wave increased the maximum bottom current speeds at sta 2C and 2S by about 1.2 fps and the north wave increased the maximum bottom currents at sta 2C by 0.8 fps. The duration of ebb flow was increased by 0.75 to 1.0 hr at sta 2N, 2C, and 2S. Significant changes, however, occurred in the small channel along Masonboro Beach (sta 2SS). The waves from N84°E had a significant retarding effect on the ebb flow, and the maximum ebb magnitude was reduced by 1.0 fps. The S16°E wave reduced currents during the early phase of the ebb flow but increased the maximum ebb current by 1.5 fps. The duration of ebb was reduced by 2 hr by the north waves and by 1.5 hr by the south waves.

Discharge data

103. Based on the current magnitudes obtained at range 2, the discharge past the throat of the inlet was determined as shown in Plate 257. The data show that approximately a 10 percent imbalance between the ebb and flood flows without waves occurred. A similar imbalance resulted for the data with waves from N84°E. In both cases, the ebb discharge was greater than the flood discharge. When the S16°E wave data were calculated, significant differences between total ebb and flood flow resulted (almost 37 percent). This imbalance of flow volumes was due to the circulation at the entrance. Wave activity forced the mass transport of water into the south portion of the entrance, and this mass of water was recirculated through the more northern stations of range 2. Also, waves breaking southwest of sta 2SS recirculated water as ebb flow through sta 2SS, increasing its ebb current.

Predictions

Hydraulic tests

104. Based on analysis of data from the hydraulic tests without waves, predictions for the improvement of the natural 1964 conditions at Masonboro Inlet are:

- a. Tidal heights would be unchanged throughout the area.
- b. Both ebb and flood flows seaward of the throat would be shifted from the southeast toward the south.
- c. Crosscurrents in the navigation channel would exist at the outer end of the jetty during flood flow.
- d. High current speeds (3.0 to 4.0 fps) would exist during ebb at the outer end of the jetty.
- e. Low current speeds (less than 1.0 fps) would exist in the deposition basin.

Wave tests

105. Based on analysis of data for the hydraulic tests with waves, predictions for the improvement of the inlet are:

- a. The S16°E waves result in a setup of the water level in the bay of 0.4 ft compared with the nonwave condition.
- b. The S16°E waves modify the current patterns over the south shoal so that shoaling can be expected.
- c. The N84°E waves modify the current patterns over the south shoal so that shoaling can be expected; however, the influence is less than that for the S16°E waves.
- d. The S16°E waves and the N84°E waves cause a shift of the current toward the jetty from the throat of the inlet to the ocean end of the jetty for both ebb and flood.

Summary

106. The more significant predictions are:

- a. The navigation channel can be expected to shift toward the jetty, as noted by increased velocities at sta 1N, 1C, and 1S (Plates 251-253) when waves are present.
- b. The shoal located oceanward from Masonboro Beach can be expected to elongate due to the gyre-type currents existing on the bar noted in Plates 258-285 which would tend to aid in material accumulation.
- c. High currents can be expected along the outer end of the jetty during ebb flow based on the same reasoning as item a.
- d. The deposition basin can be expected to fill since tidal currents were low in the vicinity of the basin and material coming over the weir could thus settle in the dredged basin.

PART VIII: TESTS OF 1966 HYDROGRAPHY

107. If ideal verification of the 1964 model predictions were possible, the 1964 plan data would be compared with prototype data collected in 1966, just after all improvements had been made. However, since this study was not initiated until 1969, the only data available from 1966 are shown in the postimprovement bathymetry (Figure 28). Therefore, it must be assumed that model data for the 1966 condition accurately represent the 1966 prototype data, and these model data are compared with the 1964 plan results in the following paragraphs.

108. Differences between the 1964 plan and 1966 hydrography are shown in Figures 29a and 29b which are comparisons of cross-section templates used to mold the model; Figure 30 shows the location of the templates. The comparison shows that depths were generally shallower for the 1966 condition, and that at cross-section C, which is the current range 2 location, there was a significant shift in the channel to the north (about 150 ft). The difference in the planned channel and basin cross sections and the actual cross sections is also shown. The actual channel was not as wide as the plan, probably due to the natural sloping of sand under wave and tidal current action subsequent to completion of dredging. In the model the basin was distinctly separated from the channel while in the prototype this was not possible, since it was necessary to dredge a path for access to the basin area from the channel in order to perform the necessary dredging. In addition, natural erosion of the shallow depths between the deposition basin and the navigation channel occurred prior to the survey. The 1966 data show that a channel was developing through the seaward end of the deposition basin and along the jetty, as seen at cross-section 7YA (Figure 29a). Model data obtained during tests conducted with this modified inlet geometry were compared directly with the data collected with the plan installed in the model with the 1964 geometry.

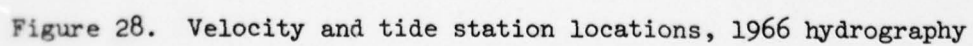
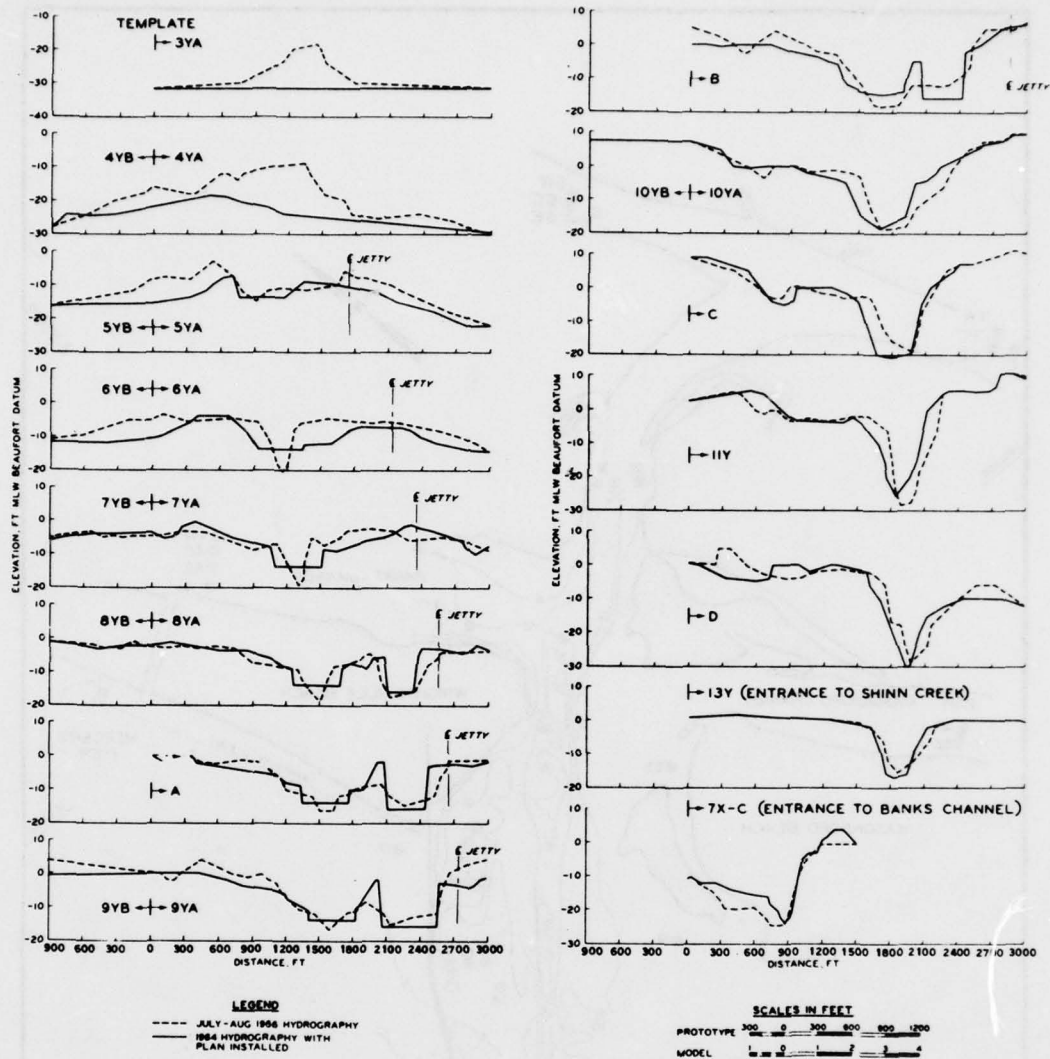


Figure 28. Velocity and tide station locations, 1966 hydrography

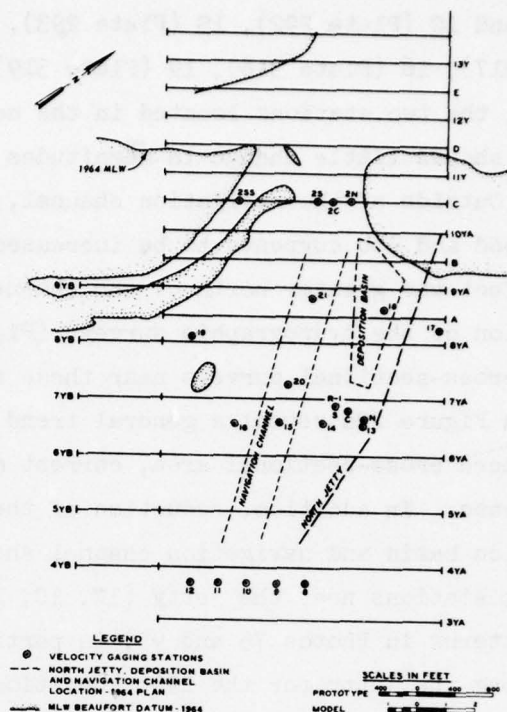


a. Templates 3YA-9YA, 4YB-9YB,
and A

b. Templates B, C, D, 10YA, 10YB,
11Y, 13Y, and 7X-C

Figure 29. Cross-section comparisons

Figure 30. Model template locations for 1964 and 1966 hydrography



Hydraulic Tests

Tidal heights

109. Results of the 1966 tidal data compared with the 1964 condition with the plan (Plates 286-291) were essentially unchanged.

Tidal currents

110. Current magnitude data at sta 8-12 located oceanward of the jetty (Plates 311-315) show essentially no change between the 1964 condition with the plan and the 1966 condition. The current patterns at strength of ebb (Photos 76 and 96) show that the ebb jet seaward of the jetty was more nearly aligned with the outer leg of the jetty than with the navigation channel, as it was for the 1964 plan condition. The crosscurrent at the outer end of the navigation channel which was observed during the flood phase for the 1964 plan conditions (Photos 69-73) was also evident for 1966 conditions (Photos 89-94).

111. Current data near the bend in the jetty were obtained at

sta 1N and 1C (Plate 292), 1S (Plate 293), 13 and 14 (Plate 316), 15 (Plate 317), 16 (Plate 318), 19 (Plate 319), and 20 (Plate 320). In general, the two stations located in the navigation channel (sta 15 and 20) showed little change in magnitudes compared with 1964 plan results. Outside of the navigation channel, a general trend existed for both flood and ebb currents to be increased by about 0.5 to 1.0 fps. This effect was greater north of the channel than south of the channel. Inspection of the hydrographic surveys (Figures 26 and 28) and comparison of cross-sectional surveys near these stations (ranges 7YA-7YB) shown in Figure 29a reveal a general trend for shallower depths. With the reduced cross-sectional area, current magnitudes would be expected to increase. In addition, reduction of the shallow barrier between the deposition basin and navigation channel should further increase ebb currents at stations near the jetty (1N, 1C, 1S, 13, and 14). Surface current patterns in Photos 75 and 95, in particular, show the increased ebb flow along the jetty for the 1966 conditions and the general trend for increased magnitudes for both flood and ebb outside the navigation channel.

112. Current data for sta 17 (Plate 318) located just north of the jetty near the shore showed essentially no change. The current data for sta 18 (Plate 319) located in the deposition basin showed that maximum flood magnitudes were increased by about 0.5 fps. Magnitudes in the basin, however, were still quite low. The reduction in height of the ridge between the deposition basin and the navigation channel undoubtedly contributed to this increase. Data from the navigation channel opposite the deposition basin at sta 21 (Plate 321) showed essentially no change in either ebb or flood currents. Surface current pattern photographs (hours 11 to 1) showed a slightly expanded area of circular flow in the deposition basin for the 1966 conditions.

113. The cross-sectional profiles near the gorge shown in Figure 29b (range C) showed the shift of the gorge 150 ft to the north and a considerably smaller cross section for the 1966 conditions. Current data for range 2 (Plates 293-296) showed the resulting trend for more uniform magnitudes through the inlet for the 1966 condition. The

maximum magnitudes at the center station (Plate 295) were only slightly increased while those at the two adjoining stations, sta 2N and 2S (Plates 294 and 296), were increased by 0.5 to 1.5 fps in both flood and ebb directions to more closely approximate those of the center station. The increased current magnitudes were expected because of the reduced cross section. Surface current patterns shown in Photos 65-77 and 85-97 do not indicate any additional information.

114. Current data for ranges 3-7 (Plates 297-310), in which the cross-sectional areas were the same for both the 1964 and 1966 conditions, were essentially unchanged.

115. Discharge data for ranges 2-7 (Plates 322-327) and Table 5 indicated changes that were generally less than 10 percent, and thus were less than the limits of accuracy for the measurement of model discharges. At range 6, flood and ebb discharges increased 20 and 23 percent, respectively, but the absolute magnitude of the increased discharge was too small to be significant.

116. Dye movement tests for 1966 conditions were made with tide only, i.e., no wave tests were conducted. In the interest of saving time, these dye tests were conducted quite close together. As a result, considerable residual dye from previous tests is apparent in each of these photographs. It was thus necessary to outline the dye limits on each photograph based on close inspection of the full-scale photographs and visual observations during the tests. Dye was placed in Banks Channel prior to strength of ebb (hour 9.0) and photographed 1.0 hr later. Similar results were obtained for the 1964 plan test (Photo 78) and the 1966 test (Photo 98), except that in the 1966 test dye moved into essentially all of the area between the channel and jetty seaward of the deposition basin and the southern edge of the dye was closer to the channel. A second dye release in Banks Channel conducted for the 1966 condition (Photo 99) immediately after strength of ebb (hour 11.5) resulted in patterns similar to the data obtained prior to strength of ebb, except that the dye did not move very far out of the channel toward the jetty. The results are not directly comparable since the photograph for the test after strength of ebb was taken 0.5 hr after placement of the dye

while the photograph for the test prior to strength of ebb was taken 1.0 hr after placement of the dye. Dye patterns after strength of ebb were not obtained for the 1964 condition. Dye was placed in Shinn Creek just before strength of ebb (hour 9.75) and was photographed 0.75 hr later. The results (Photo 101) showed that dye was dispersed somewhat more adjacent to the outer leg of the jetty during the 1966 tests than during the 1964 plan test (Photo 80). This resulted from elimination of the abnormal ridge between the deposition basin and the navigation channel as well as a general restructuring of the entrance area hydrography by current and wave action. When dye was placed in Masonboro Channel prior to strength of ebb (hour 9.5) and photographed 0.75 hr later (Photos 82 and 103), resulting data show the effect of the shallower depths that existed near the inner end of the spit north of the secondary channel at Masonboro Beach for the 1966 hydrographic condition (see cross section B in Figure 29b and cross sections 9YA-9YB and A in Figure 29a). As the dye progressed oceanward, a wider pattern was observed due to the deeper depths in the outer portion of the south shoal (see cross sections 7YA-7YB shown in Figure 29a). Dye placed in Masonboro Channel at the end of strength of ebb (hour 11.5) and photographed 0.5 hr later (Photos 83 and 104) shows somewhat less effect resulting from the depth differences because of the decreased water-surface elevations at this time.

117. Results of dye placed near Masonboro Beach during the early portion of the strength of flood (hour 4.5) and photographed 1.0 hr later (Photos 79 and 100) are not exactly comparable, since the location of the placement was different for the two tests. Dye was placed approximately 300 ft farther offshore and 600 ft closer to the inlet for the 1966 test with the result that dye was somewhat more dispersed for this test. In addition, cross-sectional data for the inner end of the south shoal (section B shown in Figure 29b and sections 9YA-9YB shown in Figure 29a) show the more predominant secondary channel and ridge located nearer to the navigation channel for the 1966 condition. This feature resulted in a more dispersed flow for the 1966 test. The data obtained for the dye placed along Wrightsville Beach just before

strength of flood (hour 3.5) (Photos 81 and 102) were very similar. The dye moved through the northern half of the inlet and into Banks Channel only for both tests. Results of dye placed at the end of the jetty in the navigation channel during the strength of flood (hour 5.0) and photographed 1.5 hr later are shown in Photos 84 and 105. The patterns are similar except that, in the area near the point of placement, dye moved slightly more onto the outer tip of the south shoal for the 1966 condition. The cross section in the immediate area (sections 5YA-5YB shown in Figure 29a) shows that although shallower depths exist for the 1966 hydrography, the minimum depth is located approximately 200 ft farther to the southwest. In addition, the slope from the deepest point of the navigation channel to the minimum depth is appreciably flatter for the 1966 condition. Both conditions contribute to the broader expanse of dye for the 1966 condition.

Wave Tests

118. Data obtained for the 1966 hydrographic condition consisted of defining the effect of the N84°E, 7.4-sec, 3-ft waves and the S16°E, 7.4-sec, 3-ft waves on each tide station shown in Figure 7 and on current magnitudes at ranges 1 and 2. The tide and current data obtained in these tests are compared with the data from similar tests with waves for the 1964 plan condition. Results of the tidal data for the S16°E waves are shown in Plates 328-332, current velocity data for the S16°E waves in Plates 333-337, and discharges at range 2 in Plate 338. For the N84°E waves tidal data are shown in Plates 339-343, current velocity data in Plates 344-348 and discharges in range 2 in Plate 349. During the course of the test program the decision was made to eliminate the tests to determine the effects of waves on both dye movement patterns and current patterns throughout the tidal cycle; therefore, data similar to that obtained for the 1964 condition were not obtained for the 1966 condition.

Tidal heights

119. Tidal data for both the S16°E and N84°E waves (Plates 328-332

and 339-343, respectively) reveal minimal differences between tests with the 1964 hydrography with the plan installed and the 1966 hydrography. No particular trends of differences could be discerned for either wave direction. Tidal differences resulting from the two hydrographies were apparently random and were generally on the order of 0.1 to 0.2 ft or less.

Tidal currents

120. Measurement of currents at range 1 with S16°E waves simulated in the model for 1966 conditions resulted in some difficulties. At and near low water (hours 1, 2, and 3), the water level was actually below the cups of the current meter used to measure the current. As a result, it was not possible to measure current magnitudes during this time period; thus, no data are shown in Plates 333 and 334. For the 1966 conditions, there was a slight shift of ebb flow to the north and a slight shift of flood flow to the south. Maximum ebb magnitudes at sta 1N were increased by about 0.5 fps but were reduced by about 0.7 fps at sta 1C and 1S. Conversely, maximum flood magnitudes were increased by about 0.5 fps at sta 1S but were reduced by about 1.0 fps at sta 1N. For the N84°E wave (Plates 344 and 345), flood currents were essentially unchanged, maximum ebb current magnitudes at sta 1N and 1C were increased by about 1.0 fps, and ebb currents at sta 1S were unchanged. These results are considerably different from the changes between 1964 plan and 1966 conditions without waves (Plates 292 and 293). These latter tests show consistently increased magnitudes for 1966 conditions. Based on the elimination of the ridge between the deposition basin and the navigation channel for 1966 conditions, increased current magnitudes at range 1 should be expected. The hydrographic differences that exist between the 1964 and 1966 model conditions on the south shoal and immediately seaward of the range 1 stations are probably a more important factor with wave conditions. The cross-sectional data, particularly ranges 4YA-4YB, 5YA-5YB, and 6YA-6YB (Figure 29a), show the changes. These differences will cause significant effects on wave refraction, which in turn will cause changes in current directions and magnitudes.

121. The influence of the changed hydrography on the currents

with waves at range 2 closely agreed with the effects on currents without waves. Comparisons of the data at each station of range 2 for the N84°E waves (Plates 345-348) with the data without waves (Plates 293-296) show that the changes were similar; therefore, the altered bed configuration influenced tidal currents but did not significantly affect the influence of north waves on currents at range 2. The same general trend was true for the S16°E waves (Plates 334-337 and 293-296), but in this case the consistency of the changes with and without waves was not quite as good as with the north waves. The differences in hydrography for the two surveys between the throat (range 2) and the ocean would result in greater modification to the refraction of south waves and north waves with resulting changes to the interaction of the waves and tidal currents.

Summary

122. Predictions based on the results of the tests with the 1964 bathymetry with and without the plan installed were presented in paragraphs 104-106. In general, the results of the tests with the 1966 bathymetry confirm these predictions and indicate a greater likelihood of their occurrence. Data from the hydraulic tests without waves show:

- a. Tidal heights for the 1964 plan and 1966 tests are essentially unchanged for any condition.
- b. Concentration of both the ebb and flood flow seaward of the throat are shifted from the southeast toward the south for both the 1964 plan and 1966 tests.
- c. Crosscurrents in the navigation channel at the outer end of the jetty are essentially the same for the 1964 plan and 1966 tests.
- d. Both the 1964 plan and the 1966 tests indicate that high velocities exist during ebb at the outer end of the jetty; however, the 1966 data show the velocities to be higher than the 1964 plan data.
- e. The 1966 data show slightly higher velocities in the deposition basin than the low velocities that occurred during the 1964 plan tests.

123. Data obtained with waves indicate the 1964 predictions to be valid; that is, the $S16^{\circ}E$ waves were the most significant and caused a setup of the water level in the bay and modification of the current patterns over the south shoal. In addition, waves from both the $S16^{\circ}E$ and $N84^{\circ}E$ test directions caused a shift of the current toward the jetty from the throat of the inlet to the ocean end of the jetty for both ebb and flood.

PART IX: CONCLUSIONS AND RECOMMENDATIONS

Model Predictions

124. One of the purposes of this study was to define the effectiveness of present distorted-scale fixed-bed model procedures in predicting hydraulic characteristics of inlets when significant modifications are made to the inlet. This purpose was not fully achieved since the necessary prototype data to compare model predictions with measured prototype results did not exist; however, the model tests discussed in this report indicate:

- a. Predictions of hydraulic changes from tests with and without waves obtained from the model with a deposition basin, low weir jetty, and navigation channel incorporated into the model compared favorably with data obtained from the model after the effects of the improvement plan on hydrography in the prototype were measured and reproduced in the model. Details of the differences observed are discussed in paragraphs 109-121.
- b. When significant natural changes occur in the hydrography, a corresponding change in the hydraulics of the inlet should be expected. A fixed-bed model thus cannot be used to make precise long-range predictions of hydraulic conditions when it is anticipated that major changes to the bed configuration might occur subsequent to construction of the proposed improvement plan.

Prototype Data Collection

125. Verification of the model has revealed several shortcomings of the prototype data collection procedure. If the following information is incorporated into future prototype data collection efforts, verification and possibly model construction should be simpler and easier.

126. Organized wave observations should be obtained concurrent with tide and current data collection. The region near an inlet entrance has highly irregular bathymetry, so observations must be taken with care. One observation at a given location might not give any

indication of the original wave direction due to refraction. Ideally, aerial photographs throughout the data collection period covering the entire area and use of proper techniques to show the wave field and its direction would be necessary. More than likely, observers on the beach would provide sufficient worthwhile information, and possibly some wave gages in deeper water would be useful in determining wave heights so that the wave generators in the model could be set appropriately.

127. Tidal current ranges should be located away from any areas that may have eddies. As an example, range 3 was located just below a constriction in Shinn Creek. On ebb flow, there was an expansion of flow below the neck in the channel and an eddy region developed near the south station of range 3. This type of flow is reproducible but it does cause some difficulties, e.g. accurately calculating discharges through the range. Also, ranges should be located away from regions that have lateral inflow, e.g. small drainage streams entering the main channel. Such was the case at range 4W.

128. Benchmark errors can cause difficulties in data interpretation and in some cases are discovered during the model verification through observation of model behavior. In any case, benchmark elevations should be double-checked to prevent error.

129. Knowledge of the flow distribution through the two branches of the AIWW north and south of its intersection with Shinn Creek would have been useful in adjusting the tidal prism. Thus, ideally it would be desirable to know the distribution of flows through all interior channels of channelized bay systems.

130. Knowledge of the extent of influence of a tidal inlet when there is a series of inlets behind a coastal barrier would aid in locating the inlet nodal lines. This could be done by a boat checking for low current magnitude zones in the far reaches of the bay. However, it should be noted that the locations of current nodal lines can be greatly affected by even mild winds at the time observations are taken.

Model Procedures

131. During the course of the study, certain aspects of modeling

tidal inlets have been observed. These aspects, model design, measurements and observations, and model tests using waves, are discussed below.

132. Comments concerning model design are:

- a. The method of addition of area to the bay of the model (Figure 7) did not appear to influence the results of data near the inlet; however, some local effects in the immediate area of the bay addition appear to have occurred. Since this study was not concerned with detailed changes that occurred in the extremes of the bay, the local effects were not important for this study. If a future study is to include detailed investigation in the bay, care must be taken to assure that the reproduction of prototype conditions throughout the bay is achieved.
- b. Artificial bends introduced in the bays north and south of the model (see paragraph 12) did not appear to influence the results discussed in this report. Since only a general interest in the bay existed during the course of this study, artificial change in detailed bay current patterns was not of concern; however, if details of current patterns are of interest, artificial bends must be avoided. If the primary interest during an inlet model study is confined to the area of the inlet with only general interest in the tidal prism, artificial bending of the bay portions of the model appears to be an acceptable procedure.
- c. Design of the ocean portion of the model must include a sufficient area to allow for adequate wave reproduction to extend both directions from the inlet. Although the variability of the wave characteristics in the ocean was not investigated in this study, as test procedures are refined, the characteristics of the waves in the ocean can be expected to become much more important.

133. Comments concerning measurements and observations are:

- a. Prior to establishing the model tide and particularly current stations to be monitored, in-depth studies of possible plans of improvement need to be considered to assure adequate coverage of all areas prior to conducting the base tests.
- b. The capability to obtain more accurate measurement of current magnitudes in the presence of waves and at locations of high turbulence should be investigated.
- c. Detailed current patterns with waves throughout the tidal cycle with the use of dye were of significant value. Better methods are needed to obtain more comprehensive data.

134. Comments concerning wave tests are:

- a. Wave directions and characteristics expected for an inlet are necessary to allow evaluation of the effects of the waves on hydraulic conditions. However, it was not possible to define the effects of waves on the inlet in more detail because of the lack of reliable field information on the wave conditions that could be expected for Masonboro Inlet.
- b. The model test results showed the importance of including waves in the test program. When the primary area of interest in the inlet is focused from the throat oceanward, the test program should concentrate on tests with waves.
- c. Since the scales of the model are distorted, refraction, diffraction, and reflections could not be scaled simultaneously. Therefore, wave tests were conducted to achieve the best reproduction of refractive effects. Detailed studies of tidal inlets must include more in-depth investigations of the effects of model distortion on wave effects.

Effects of Waves on Inlets

135. Based on the 1964 model tests, several general comments can be made concerning the influence of waves on models of natural inlets. However, care must be used in applying these conclusions to prototype cases. Waves have a significant influence on conditions that exist oceanward of the inlet throat. Waves may result in a setup of the bay water level. Waves cause the flow in areas along both approach beaches through the sides of the throat to be strongly flood-dominated. The angle of wave approach to the inlet appears to be of relatively minor importance to flow direction in a well-developed secondary channel. Waves from essentially all directions cause flow patterns over the ocean shoals near the inlet that are conducive to inflow and deposition of sand on the shoals.

Basic Research Needs

136. Based on the results of this study, recommendations for basic research studies on the characteristics and behavior of inlets are:

AD-A055 523

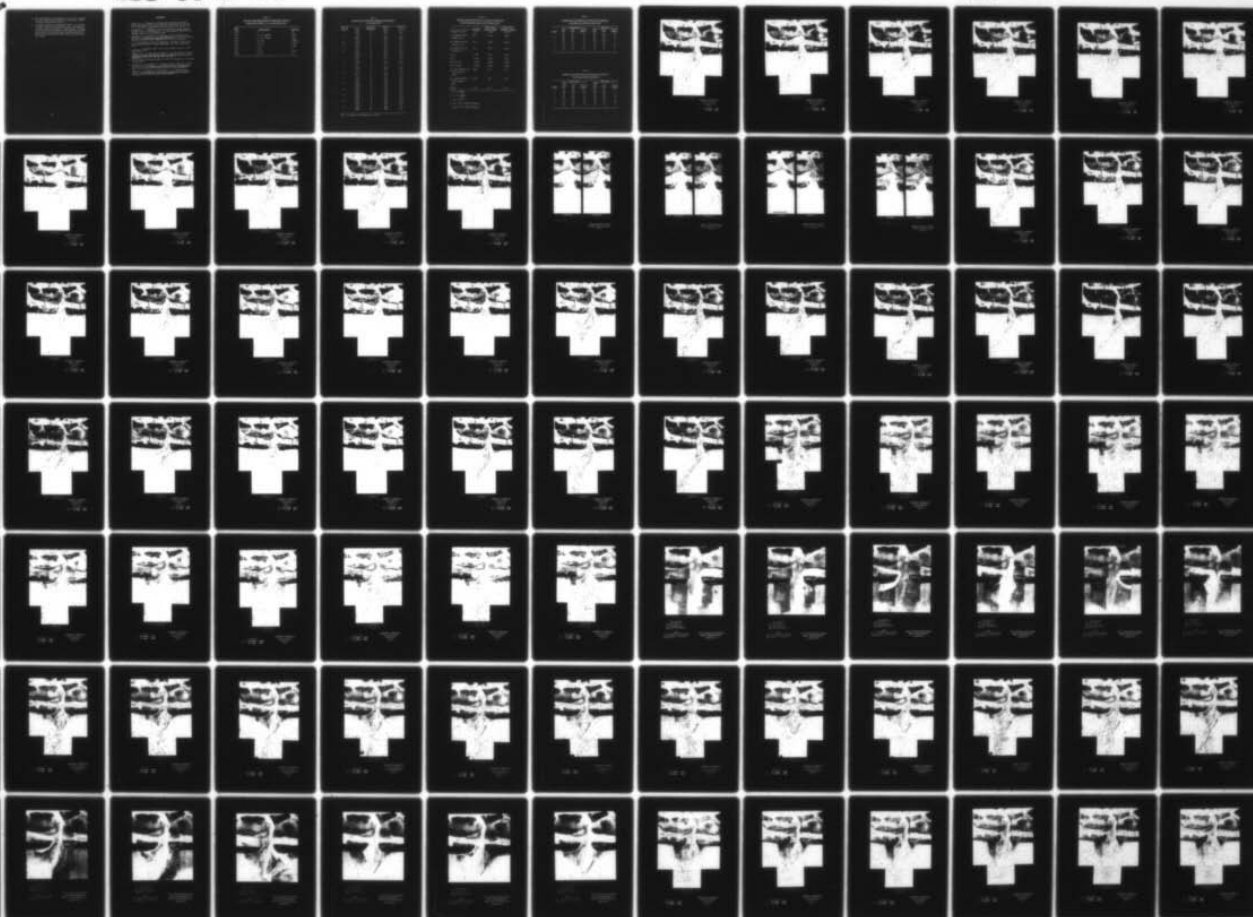
ARMY ENGINEER WATERWAYS EXPERIMENT STATION VICKSBURG MISS F/G 8/3
PHYSICAL MODEL SIMULATION OF THE HYDRAULICS OF MASONBORO INLET,--ETC(U)
NOV 77 R A SAGER, W C SEABERGH

UNCLASSIFIED

WES-GITI-15

NL

2 OF 5
AD
A055523





- a. Any investigation of the portions of the inlet oceanward from the throat should include the simulation of waves to achieve satisfactory results.
- b. A research program to investigate further the influence of waves on the current patterns at the ocean approach to inlets should be conducted. Specifically, the study should include the influence of wave direction, period, and height for both normal tidal conditions and water-surface time histories associated with storm and hurricane surges.

REFERENCES

1. Harris, D. L., "Comparison of Numerical and Physical Hydraulic Models--Masonboro Inlet, North Carolina" GITI Report 6, Jun 1977, U. S. Army Coastal Engineering Research Center, Fort Belvoir, Va.
2. Seabergh, W. C., "Masonboro Inlet Fixed-Bed Model Study; Supplementary Tests" (in preparation), U. S. Army Engineer Waterways Experiment Station, CE, Vicksburg, Miss.
3. Seabergh, W. C. and Mason, C., "Masonboro Inlet Fixed Bed Model Evaluation," Symposium on Modeling Techniques, San Francisco, Calif., American Society of Civil Engineers, Vol I, 1975, pp 294-314.
4. U. S. Army Engineer District, Wilmington, "Masonboro Inlet, North Carolina--North Jetty," Design Memorandum, Jan 1965, Wilmington, N. C.
5. _____, "Masonboro Inlet, South Jetty--Restudy Report," 1970, Wilmington, N. C.
6. Magnuson, N. C., "Planning and Design of a Low Weir Section Jetty," Journal, Waterways and Harbors Division, American Society of Civil Engineers, Vol 93, No. WW2, May 1967, pp 27-40.
7. Project Document--House Document No. 341, 81st Congress, 1st Session, 20 Sep 1949.
8. Kieslich, J. M. and Mason, C., "Channel Entrance Response to Jetty Construction," Proceedings, Civil Engineering in the Oceans/III, American Society of Civil Engineers, Vol I, 1975, pp 689-705.
9. Hayes, M. O., Goldsmith, V., and Hobbs, C. H., "Offset Coastal Inlets," Proceedings, 12th ASCE Coastal Engineering Conference, Washington, D. C., Vol II, 1970, pp 1187-1200.

Table 1
Wind Data from Gage Located on South Water Tower at
Wrightsville Beach, N. C., 12 September 1969

<u>Time</u> <u>EDST</u>	<u>Speed (mph)</u>	<u>Direction</u>
0748	4	NE
0825	4 to 11 (gusty)	N-NE
1010	4 to 12 (gusty)	N-NE
1214	6 to 12	N-NE-N
1347	8 to 15 ⁴	N-NE-N
1527	4 to 5	N-NW
1738	3 to 7	N
1855	3 to 5	N-NW
2045	1 to 6	N

Table 2
Prototype Data, Salinity and Temperature Measurements
12 September 1969

<u>Range and Station</u>	<u>Time</u>	<u>Location of Measurement</u>	<u>Salinity ppt</u>	<u>Temperature °C</u>
5C	10:01	S	36.8	25.7
	10:00	M	36.9	25.6
	9:59	B	36.9	25.4
3C	10:51	S	36.9	25.8
	10:50	M	36.8	25.8
	10:49	B	36.9	25.8
2S	10:59	S	36.8	25.8
	10:58	M	36.9	25.6
1C	11:11	S	36.8	25.4
	11:10	M	36.9	25.4
4C	11:24	S	36.6	25.2
	11:23	M	36.7	25.2
	11:22	B	36.7	25.2
	15:20	S	36.4	24.8
	15:19	M	36.5	24.9
	15:18	B	36.4	24.8
3C	15:29	S	36.4	24.8
	15:28	M	36.5	24.8
	15:27	B	36.5	24.8
5C	15:37	S	36.6	24.6
	15:36	M	36.8	24.6
	15:35	B	36.8	24.5
2C	15:44	S	36.6	24.9
	15:43	M	36.7	24.9
	15:42	B	36.8	24.8
1C	15:41	S	36.5	24.9
	15:40	M	36.6	24.9
	15:39	B	36.6	24.9
4C	18:09	S	36.8	25.4
	18:09	M	36.9	25.4
	18:08	B	36.9	25.5
3C	18:18	S	36.9	25.7
	18:17	M	36.9	25.7
	18:16	B	36.9	25.5
5C	18:29	S	36.8	25.5
	18:28	M	36.9	25.6
	18:26	B	37.0	25.5
2C	18:37	S	36.8	25.6
	18:36	M	36.8	25.7
	18:35	B	36.8	25.7
1C	18:44	S	36.9	25.6
	18:43	M	36.8	25.7
	18:41	B	36.9	25.5

Note: S = surface; M = middepth; and B = bottom.

Table 3
Modeling Wave Refraction in a Distorted Scale Model
1:300 Horizontal Scale, 1:60 Vertical Scale

	Prototype	Model Using Vertical Scale	Model Using Horizontal Scale
T (period in sec)	7.40	0.956*	0.427**
L_o (deepwater wave length, ft)†	280.4	4.679	0.934
d_{20} (depth at 20-ft contour, ft)	20.0	0.333	0.333
d_{10} (depth at 10-ft contour, ft)	10.0	0.167	0.167
d_{20}/L_o	0.071	0.071	0.357
d_{10}/L_o	0.036	0.036	0.179
$\tanh 2\pi d_{20}/L$	0.6181	0.6181	0.9797
$\tanh 2\pi d_{10}/L$	0.4577	0.4577	0.8627
C_{20} (wave celerity at 20-ft contour, fps)††	23.42	3.03	2.14
C_{10} (wave celerity at 10-ft contour, fps)‡	17.34	2.24	1.89
C_{20}/C_{10}	1.35	1.35	1.13

* $T = 7.4/\sqrt{60}$.

** $T = 7.4/\sqrt{300}$.

† $L_o = 5.12 T^2$.

†† $C_{20} = 5.12 T \tanh (2\pi d_{20}/L)$.

‡ $C_{10} = 5.12 T \tanh (2\pi d_{10}/L)$.

Table 4

Comparison of Distribution of Total Flow Volume for
1964 Base and 1964 Plan Conditions

<u>Range</u>	<u>Flood Flow</u>			<u>Ebb Flow</u>		
	<u>Base mcf</u>	<u>Plan mcf</u>	<u>Percent Change</u>	<u>Base mcf</u>	<u>Plan mcf</u>	<u>Percent Change</u>
2	620	563	-9	683	629	-8
3	270	293	+9	241	235	-2
4	227	241	+6	265	266	0
5	136	147	+8	164	159	-3
6	88	76	-14	54	44	-19
7	169	201	+19	178	177	-1

Table 5

Comparison of Distribution of Total Flow Volume for
1964 Plan and 1966 Conditions

<u>Range</u>	<u>Flood Flow</u>			<u>Ebb Flow</u>		
	<u>1964 Plan mcf</u>	<u>1966 mcf</u>	<u>Percent Change</u>	<u>1964 Plan mcf</u>	<u>1966 mcf</u>	<u>Percent Change</u>
2	563	626	+11	629	654	+4
3	293	258	-12	235	236	0
4	241	220	-9	266	243	-9
5	147	138	-6	159	156	-2
6	76	91	+20	44	54	+23
7	201	186	-7	177	177	0



VELOCITY SCALE
0 4 8 12 FTS

SURFACE CURRENTS
VERIFICATION TEST
TIDE: 12 SEPT 69
HOUR 0

SCALES IN FEET

PROTOTYPE	600	0	600	1200	1800
MODEL	1	0	2	4	6

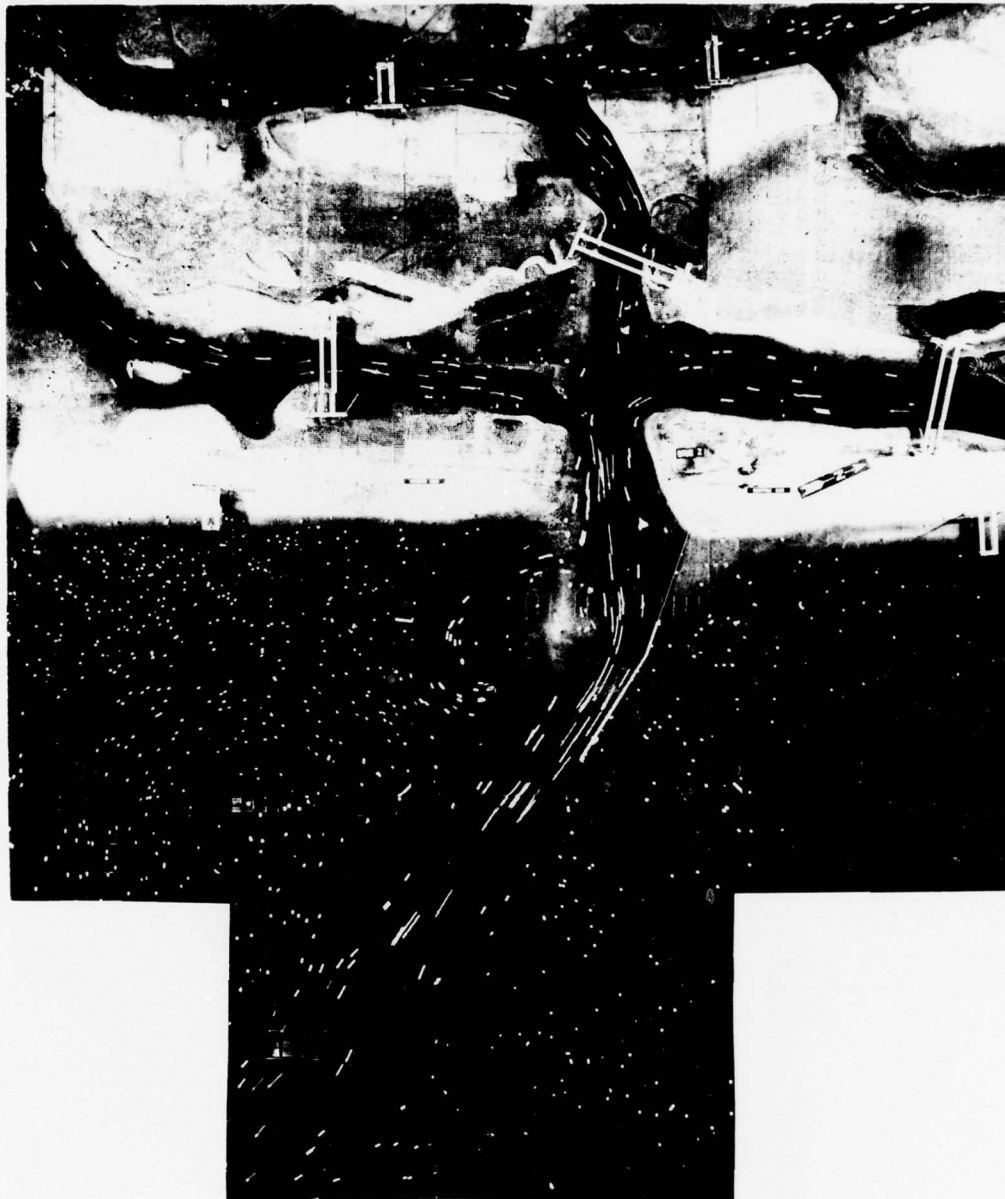


VELOCITY SCALE
0 4 8 12 FPS

SURFACE CURRENTS
VERIFICATION TEST
TIDE: 12 SEPT 69
HOUR 1

SCALES IN FEET

PROTOTYPE	0	200	400	600
MODEL	0	2	4	6



VELOCITY SCALE
0 4 8 12 FPS

SURFACE CURRENTS
VERIFICATION TEST
TIDE: 12 SEPT 69
HOUR 2

SCALES IN FEET

PROTOTYPE	600	0	600	1200	1800
MODEL	4	0	4	8	12



VELOCITY SCALE
0 4 8 12 FPS

SURFACE CURRENTS
VERIFICATION TEST
TIDE: 12 SEPT 69
HOUR 3

SCALES IN FEET
PROTOTYPE 0 500 1000 1500
MODEL 0 2 4 6



VELOCITY SCALE
0 4 8 12 FPS

SURFACE CURRENTS
VERIFICATION TEST
TIDE: 12 SEPT 69
HOUR 4

SCALES IN FEET

PROTOTYPE	0 500 1000 2000 3000
MODEL	0 2 4 6



VELOCITY SCALE
0 4 8 12 FPS

SURFACE CURRENTS
VERIFICATION TEST
TIDE: 12 SEPT 69
HOUR 5

SCALES IN FEET
PROTOTYPE 0 500 1000 1500 2000
MODEL 0 2 4 6



VELOCITY SCALE
0 4 8 12 FPS

SURFACE CURRENTS
VERIFICATION TEST
TIDE: 12 SEPT 69
HOUR 6

SCALES IN FEET
PROTOTYPE 600 0 600 1200 1800
MODEL 2 0 2 4 6



VELOCITY SCALE
0 4 8 12 FPS

SURFACE CURRENTS
VERIFICATION TEST
TIDE: 12 SEPT 69
HOUR 7

SCALES IN FEET
PROTOTYPE 0 600 1200 1800
MODEL 0 2 4 6



VELOCITY SCALE
0 4 8 12 FPS

SURFACE CURRENTS
VERIFICATION TEST
TIDE: 12 SEPT 69
HOUR 8

SCALES IN FEET
PROTOTYPE 0 600 1200 1800
MODEL 0 2 4 6



VELOCITY SCALE
0 4 8 12 FPS

SURFACE CURRENTS
VERIFICATION TEST
TIDE: 12 SEPT 69
HOUR 9

SCALES IN FEET
PROTOTYPE 0 500 1000 1250 1500
MODEL 0 2 4 6



VELOCITY SCALE
0 4 8 12 FPS

SURFACE CURRENTS
VERIFICATION TEST
TIDE: 12 SEPT 69
HOUR 10

SCALES IN FEET

PROTOTYPE 600 0 600 1200 1800
MODEL 2 0 2 4 6



VELOCITY SCALE
0 4 8 2 FPS

SURFACE CURRENTS
VERIFICATION TEST
TIDE: 12 SEPT 69
HOUR 11

SCALES IN FEET

	0	600	1200	1800
PROTOTYPE	0	600	1200	1800
MODEL	0	6	12	18



VELOCITY SCALE
0 4 8 2 FPS

SURFACE CURRENTS
VERIFICATION TEST
TIDE: 12 SEPT 69
HOUR 12

SCALES IN FEET
PROTOTYPE 0 500 1000 2000 3000
MODEL 0 2 4 6



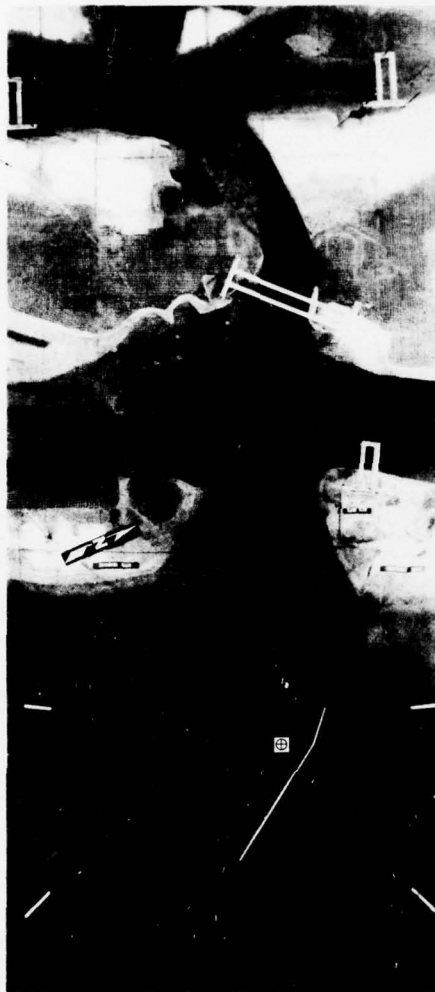
FLOOD FLOW



FLOOD FLOW

⊕ DYE INJECTION STATION

VERIFICATION TESTS
12 SEPT 1969 CONDITIONS
GROUP I



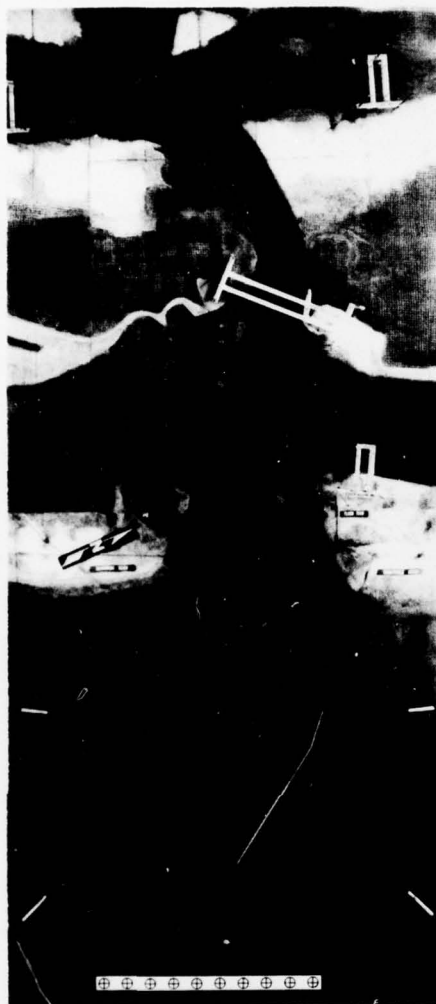
FLOOD FLOW



FLOOD FLOW

⊕ DYE INJECTION STATION

VERIFICATION TESTS
12 SEPT 1969 CONDITIONS
GROUP 2



FLOOD FLOW



EBB FLOW

⊕ DYE INJECTION STATION

VERIFICATION TESTS
12 SEPT 1969 CONDITIONS
GROUP 3



EBB FLOW



EBB FLOW

⊕ DYE INJECTION STATION

VERIFICATION TESTS
12 SEPT 1969 CONDITIONS
GROUP 4



VELOCITY SCALE
0 4 8 12 FPS

SURFACE CURRENTS
1969 CONDITIONS
MEAN TIDE
HOUR 0

SCALES IN FEET

PROTOTYPE	0	600	1200	1800
MODEL	0	2	4	6



VELOCITY SCALE
0 4 8 12 FPS

SURFACE CURRENTS
1969 CONDITIONS
MEAN TIDE
HOUR 1

SCALES IN FEET

PROTOTYPE	0	600	1200	1800
MODEL	0	2	4	6



VELOCITY SCALE
0 4 8 12 FPS

SURFACE CURRENTS
1969 CONDITIONS
MEAN TIDE
HOUR 2
SCALES IN FEET

PROTOTYPE 0 600 1200 1800
MODEL 2 0 2 4 6



VELOCITY SCALE
0 4 8 12 FPS

SURFACE CURRENTS
1969 CONDITIONS
MEAN TIDE
HOUR 3

SCALES IN FEET

PROTOTYPE	600	0	600	1200	1800
MODEL	2	0	2	4	6



VELOCITY SCALE
0 4 8 12 FPS

SURFACE CURRENTS
1969 CONDITIONS
MEAN TIDE
HOUR 4

SCALES IN FEET
PROTOTYPE 0 500 1000 1500
MODEL 0 2 4 6



VELOCITY SCALE
0 4 8 12 FPS

SURFACE CURRENTS
1969 CONDITIONS
MEAN TIDE
HOUR 5
SCALES IN FEET

PROTOTYPE	500	0	500	200	1000
MODEL	2	0	2	1	4



VELOCITY SCALE
0 4 8 12 FPS

SURFACE CURRENTS
1969 CONDITIONS
MEAN TIDE
HOUR 6

SCALES IN FEET

PROTOTYPE	600	0	600	1200	600
MODEL	2	0	2	4	2



VELOCITY SCALE
0 4 8 12 FPS

SURFACE CURRENTS
1969 CONDITIONS
MEAN TIDE
HOUR 7

SCALES IN FEET

PROTOTYPE	0	500	1000	1500
MODEL	0	2	4	6



VELOCITY SCALE
0 4 8 12 FPS

SURFACE CURRENTS
1969 CONDITIONS
MEAN TIDE
HOUR 8

SCALES IN FEET

PROTOTYPE	0	600	1200	1800
MODEL	2	2	4	6



VELOCITY SCALE
0 4 8 12 FPS

SURFACE CURRENTS
1969 CONDITIONS
MEAN TIDE
HOUR 9

SCALES IN FEET

PROTOTYPE	0	600	1200	1800
MODEL	0	2	4	6



VELOCITY SCALE
0 4 8 12 FPS

SURFACE CURRENTS
1969 CONDITIONS
MEAN TIDE
HOUR 10

SCALES IN FEET

PROTOTYPE	0	500	1000	1500
MODEL	0	2	4	6



VELOCITY SCALE
0 4 8 12 FPS

SURFACE CURRENTS
1969 CONDITIONS
MEAN TIDE
HOUR 11

SCALES IN FEET
PROTOTYPE 0 600 1200 1800
MODEL 0 2 4 6



VELOCITY SCALE
0 4 8 12 FPS

SURFACE CURRENTS

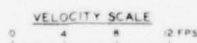
1969 CONDITIONS

MEAN TIDE

HOURL 12

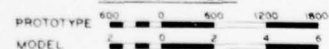
SCALES IN FEET

PROTOTYPE	0	500	1000	1500
MODEL	0	2	4	6



SURFACE CURRENTS
1969 CONDITIONS
SPRING TIDE
HOUR 0

SCALES IN FEET



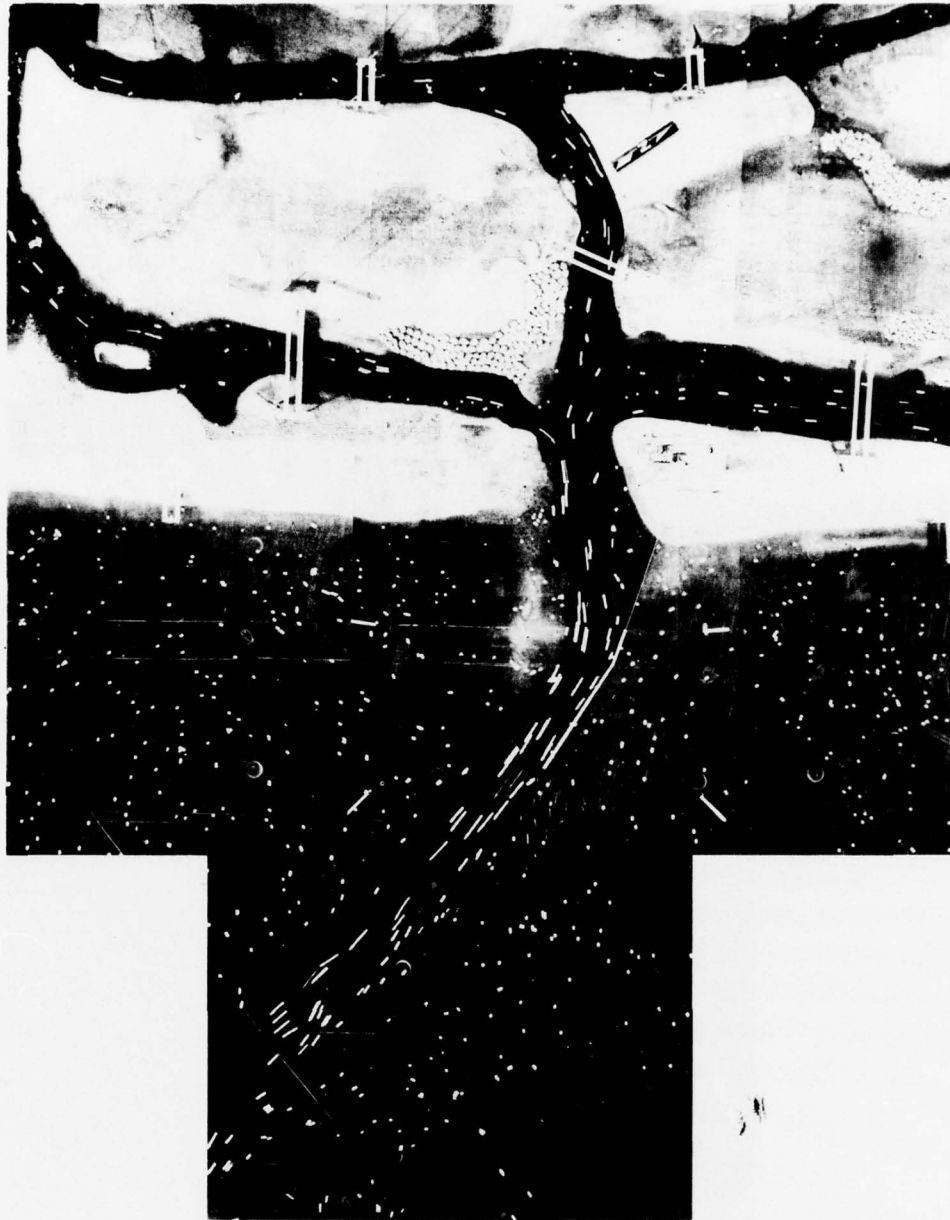


VELOCITY SCALE
0 4 8 12 FPS

SURFACE CURRENTS
1969 CONDITIONS
SPRING TIDE
HOUR 1

SCALES IN FEET

PROTOTYPE 0 600 1200 1800
MODEL 0 2 4 6



VELOCITY SCALE
0 4 8 12 FPS

SURFACE CURRENTS
1969 CONDITIONS
SPRING TIDE
HOUR 2

SCALES IN FEET

PROTOTYPE	0	500	1000	1500
MODEL	0	2	4	6



VELOCITY SCALE
0 4 8 12 FPS

SURFACE CURRENTS

1969 CONDITIONS

SPRING TIDE

HOOR 3

SCALES IN FEET

PROTOTYPE	0	500	1000	1500	2000
MODEL	0	2	4	6	8



VELOCITY SCALE
0 4 8 12 FPS

SURFACE CURRENTS
1969 CONDITIONS
SPRING TIDE
HOUR 4

SCALES IN FEET

PROTOTYPE 0 600 1200 1800
MODEL 0 2 4 6



VELOCITY SCALE
0 4 8 12 FPS

SURFACE CURRENTS
1969 CONDITIONS
SPRING TIDE
HOUR 5

SCALES IN FEET

PROTOTYPE	0	400	800	1200	1600
MODEL	0	2	4	6	



VELOCITY SCALE
0 4 8 12 FPS

SURFACE CURRENTS
1969 CONDITIONS
SPRING TIDE
HOUR 6

SCALES IN FEET

PROTOTYPE	600	5	600	1200	1800
MODEL	2	0	2	4	6



VELOCITY SCALE
0 4 8 12 FPS

SURFACE CURRENTS
1969 CONDITIONS
SPRING TIDE
HOUR 7

SCALES IN FEET
PROTOTYPE 0 600 1200 1800
MODEL 0 2 4 6



VELOCITY SCALE
0 4 8 12 FPS

SURFACE CURRENTS
1969 CONDITIONS
SPRING TIDE
HOUR 8

SCALES IN FEET

PROTOTYPE 0 600 1200 1800
MODEL 0 2 4 6



VELOCITY SCALE
0 4 8 12 FPS

SURFACE CURRENTS
1969 CONDITIONS
SPRING TIDE
HOUR 9

SCALES IN FEET
PROTOTYPE 600 0 600 1200 1800
MODEL 2 0 2 4 6



VELOCITY SCALE
0 4 8 12 FPS

SURFACE CURRENTS
1969 CONDITIONS
SPRING TIDE
HOUR 10

SCALES IN FEET

PROTOTYPE 0 500 1000 1500
MODEL 0 2 4 6



VELOCITY SCALE
0 4 8 12 FPS

SURFACE CURRENTS
1969 CONDITIONS
SPRING TIDE
HOUR 11

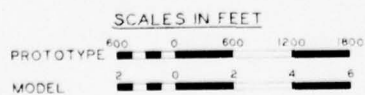
SCALES IN FEET
PROTOTYPE 0 500 1000 1500
MODEL 0 2 4 6



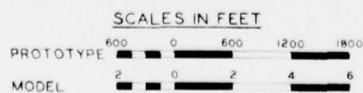
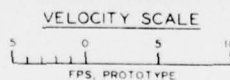
VELOCITY SCALE
0 4 8 12 FPS

SURFACE CURRENTS
1969 CONDITIONS
SPRING TIDE
HOUR 12

SCALES IN FEET
PROTOTYPE 0 600 1200 1800
MODEL 0 2 4 6



SURFACE CURRENTS
1964 CONDITIONS
MEAN TIDE
HOUR 0



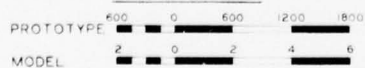
SURFACE CURRENTS
1964 CONDITIONS
MEAN TIDE
HOUR 1



VELOCITY SCALE



SCALES IN FEET



SURFACE CURRENTS

1964 CONDITIONS

MEAN TIDE

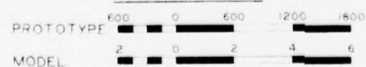
HOOR 2



VELOCITY SCALE



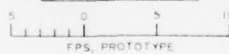
SCALES IN FEET



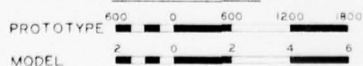
SURFACE CURRENTS
1964 CONDITIONS
MEAN TIDE
HOUR 3



VELOCITY SCALE



SCALES IN FEET



SURFACE CURRENTS

1964 CONDITIONS

MEAN TIDE

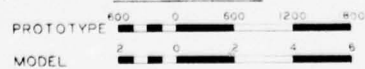
HOUR 4



VELOCITY SCALE



SCALES IN FEET



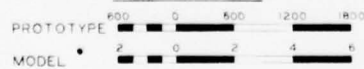
SURFACE CURRENTS
1964 CONDITIONS
MEAN TIDE
HOUR 5



VELOCITY SCALE



SCALES IN FEET



SURFACE CURRENTS

1964 CONDITIONS

MEAN TIDE

HOOR 6



VELOCITY SCALE
 5 0 5 10
 FPS, PROTOTYPE

SCALES IN FEET
 PROTOTYPE 0 500 1000
 MODEL 0 2 4 6

SURFACE CURRENTS
 1964 CONDITIONS
 MEAN TIDE
 HOUR 7



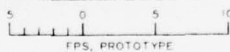
VELOCITY SCALE
 5 0 5 10
 FPS, PROTOTYPE

SCALES IN FEET
 PROTOTYPE 0 500 1000 1500
 MODEL 2 0 2 4 6

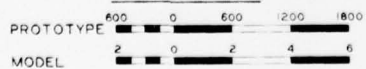
SURFACE CURRENTS
 1964 CONDITIONS
 MEAN TIDE
 HOUR 8



VELOCITY SCALE



SCALES IN FEET



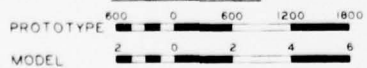
SURFACE CURRENTS
1964 CONDITIONS
MEAN TIDE
HOUR 9



VELOCITY SCALE



SCALES IN FEET



SURFACE CURRENTS
1964 CONDITIONS
MEAN TIDE
HOUR 10



VELOCITY SCALE
 5 0 5 10
 FPS, PROTOTYPE

SCALES IN FEET
 PROTOTYPE 600 0 600 1200 1800
 MODEL 2 0 2 4 6

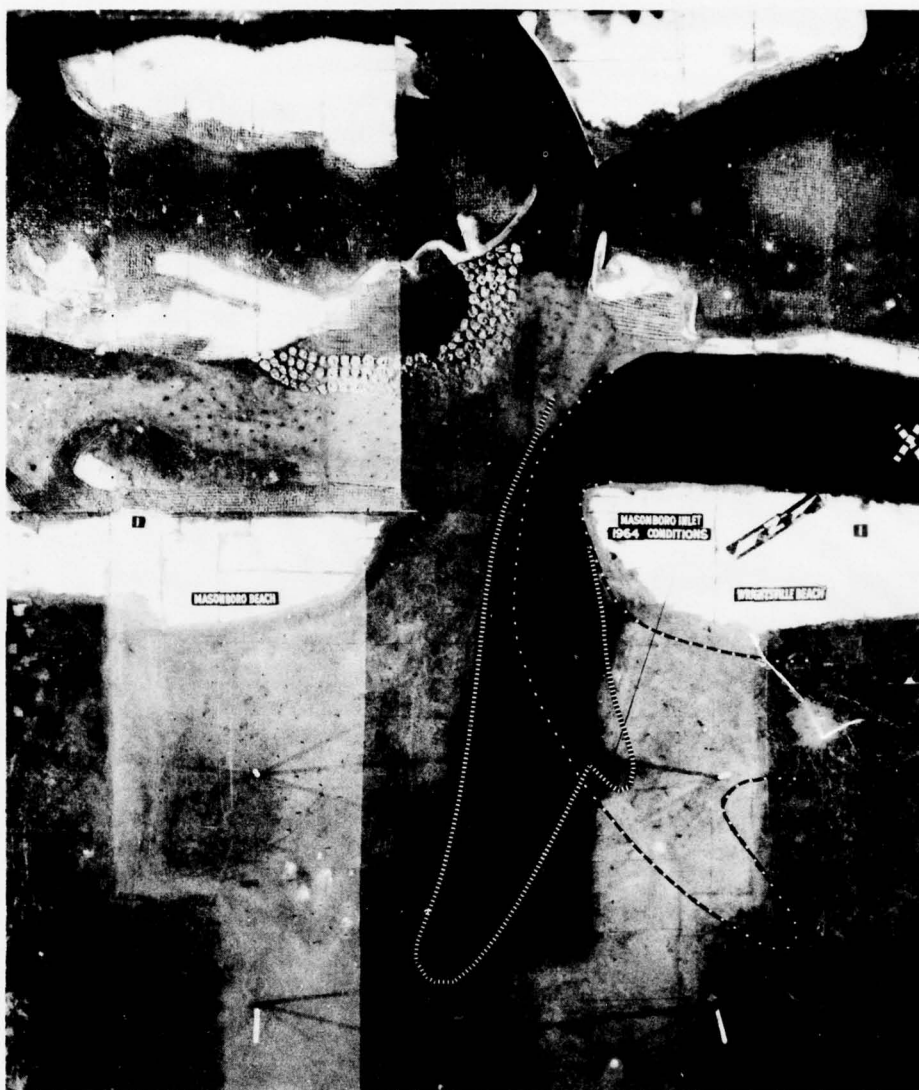
SURFACE CURRENTS
 1964 CONDITIONS
 MEAN TIDE
 HOUR 11



VELOCITY SCALE
5 0 5 10
FPS, PROTOTYPE

SCALES IN FEET
600 0 600 1200 1800
PROTOTYPE
2 0 2 4 6
MODEL

SURFACE CURRENTS
1964 CONDITIONS
MEAN TIDE
HOUR 12



TEST CONDITIONS

TIDE - 3.8-FT RANGE
 MEAN TIDAL LEVEL - 0-FT MSL
 X - SITE OF DYE INSERTION
 9:00 - TIME OF DYE INSERTION
 10:00 - TIME OF STREAK OBSERVATION
 EBB FLOW

LEGEND

..... TEST WITH 3-FT, 7.4-SEC, N84°E WAVE
 ----- TEST WITH 3-FT, 7.4-SEC, S16°E WAVE
 TEST WITHOUT WAVES - DYE PATTERN AS
 SHOWN IN PHOTO

DYE STREAK PATTERNS
 1964 HYDROGRAPHY
 CONDITION 1



TEST CONDITIONS

TIDE - 3.8-FT RANGE
 MEAN TIDAL LEVEL - 0-FT MSL
 X - SITE OF DYE INSERTION
 11:30 - TIME OF DYE INSERTION
 12:00 - TIME OF STREAK OBSERVATION
 EBB FLOW

LEGEND

..... TEST WITH 3-FT, 7.4-SEC, N84°E WAVE
 ---- TEST WITH 3-FT, 7.4-SEC, S16°E WAVE
 TEST WITHOUT WAVES - DYE PATTERN AS
 SHOWN IN PHOTO

DYE STREAK PATTERNS
 1964 HYDROGRAPHY
 CONDITION 2



TEST CONDITIONS

TIDE - 3.8-FT RANGE
 MEAN TIDAL LEVEL - 0-FT MSL
 X - SITE OF DYE INSERTION
 4:30 - TIME OF DYE INSERTION
 5:30 - TIME OF STREAK OBSERVATION
 FLOOD FLOW

LEGEND

..... TEST WITH 3-FT, 7.4-SEC, N84°E WAVE
 ---- TEST WITH 3-FT, 7.4-SEC, S16°E WAVE
 TEST WITHOUT WAVES - DYE PATTERN AS
 SHOWN IN PHOTO

DYE STREAK PATTERNS
 1964 HYDROGRAPHY
 CONDITION 3



TEST CONDITIONS

TIDE - 3.8-FT RANGE
 MEAN TIDAL LEVEL - 0-FT MSL
 X - SITE OF DYE INSERTION
 9:45 - TIME OF DYE INSERTION
 10:30 - TIME OF STREAK OBSERVATION
 EBB FLOW

LEGEND

..... TEST WITH 3-FT, 7.4-SEC, N84°E WAVE
 ---- TEST WITH 3-FT, 7.4-SEC, S16°E WAVE
 TEST WITHOUT WAVES - DYE PATTERN AS
 SHOWN IN PHOTO

DYE STREAK PATTERNS
 1964 HYDROGRAPHY
 CONDITION 4



TEST CONDITIONS

TIDE - 3.8-FT RANGE
 MEAN TIDAL LEVEL - 0-FT MSL
 X - SITE OF DYE INSERTION
 3:30 - TIME OF DYE INSERTION
 4:30 - TIME OF STREAK OBSERVATION
 FLOOD FLOW

LEGEND

———— TEST WITH 3-FT, 7.4-SEC, N84°E WAVE
 - - - - - TEST WITH 3-FT, 7.4-SEC, S16°E WAVE
 TEST WITHOUT WAVES - DYE PATTERN AS
 SHOWN IN PHOTO

DYE STREAK PATTERNS
 1964 HYDROGRAPHY
 CONDITION 5



TEST CONDITIONS

TIDE - 3.8-FT RANGE
 MEAN TIDAL LEVEL - 0-FT MSL
 X - SITE OF DYE INSERTION
 9:30 - TIME OF DYE INSERTION
 10:15 - TIME OF STREAK OBSERVATION
 EBB FLOW

LEGEND

..... TEST WITH 3-FT, 7.4-SEC, N84°E WAVE
 ---- TEST WITH 3-FT, 7.4-SEC, S16°E WAVE
 TEST WITHOUT WAVES - DYE PATTERN AS
 SHOWN IN PHOTO

DYE STREAK PATTERNS
 1964 HYDROGRAPHY
 CONDITION 6



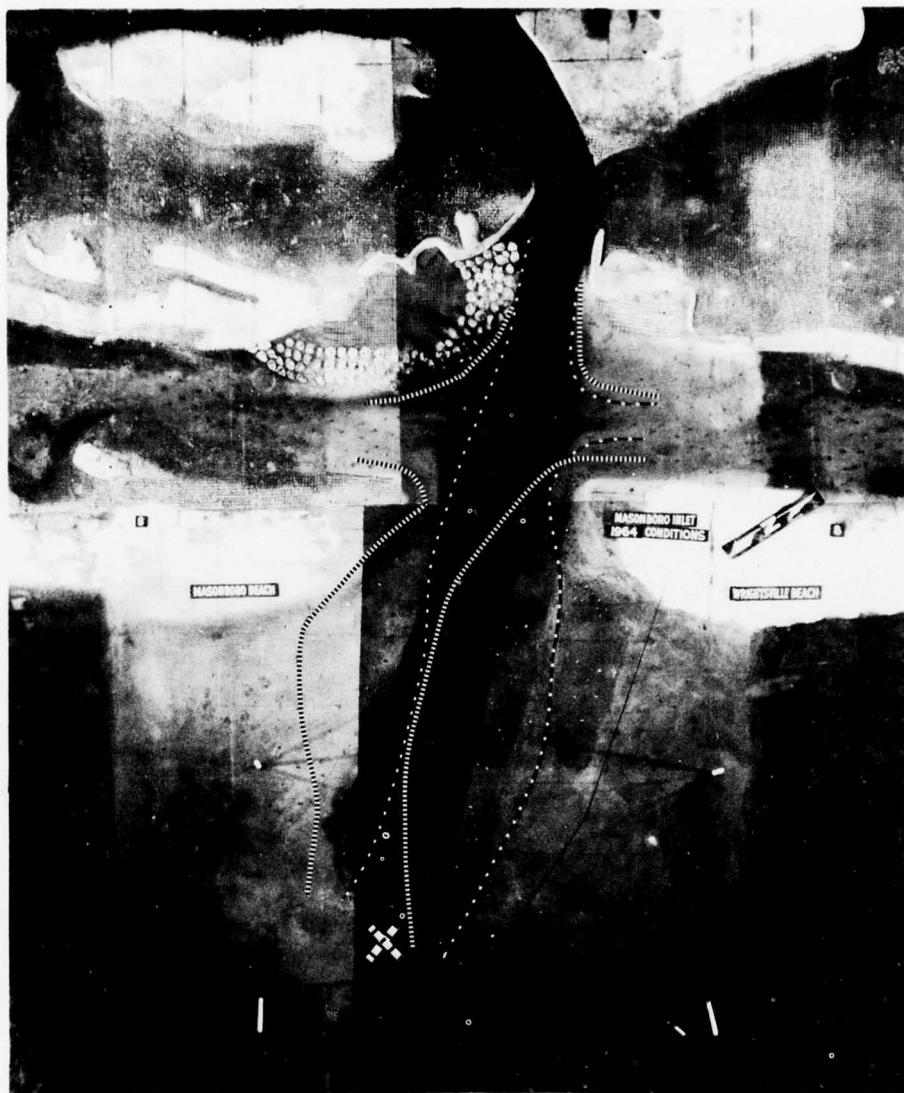
TEST CONDITIONS

TIDE - 3.8-FT RANGE
 MEAN TIDAL LEVEL - 0-FT MSL
 X - SITE OF DYE INSERTION
 11:30 - TIME OF DYE INSERTION
 12:00 - TIME OF STREAK OBSERVATION
 EBB FLOW

LEGEND

..... TEST WITH 3-FT, 7.4-SEC, N84°E WAVE
 ---- TEST WITH 3-FT, 7.4-SEC, S16°E WAVE
 TEST WITHOUT WAVES - DYE PATTERN AS
 SHOWN IN PHOTO

DYE STREAK PATTERNS
 1964 HYDROGRAPHY
 CONDITION 7



TEST CONDITIONS

TIDE - 3.8-FT RANGE
 MEAN TIDAL LEVEL - 0-FT MSL
 X - SITE OF DYE INSERTION
 5:00 - TIME OF DYE INSERTION
 6:30 - TIME OF STREAK OBSERVATION
 FLOOD FLOW

LEGEND

..... TEST WITH 3-FT, 7.4-SEC, N84°E WAVE
 ---- TEST WITH 3-FT, 7.4-SEC, S16°E WAVE
 TEST WITHOUT WAVES - DYE PATTERN AS
 SHOWN IN PHOTO

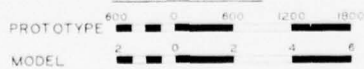
DYE STREAK PATTERNS
 1964 HYDROGRAPHY
 CONDITION 8



VELOCITY SCALE



SCALES IN FEET



SURFACE CURRENTS

1964 CONDITIONS
WITH PLAN INSTALLED
MEAN TIDE

HOOR 0



VELOCITY SCALE
 5 0 5 10
 FPS, PROTOTYPE

SCALES IN FEET
 600 0 600 1200 1800
 PROTOTYPE
 2 0 2 4 6
 MODEL

SURFACE CURRENTS
 1964 CONDITIONS
 WITH PLAN INSTALLED
 MEAN TIDE
 HOUR 1



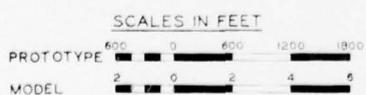
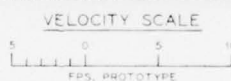
VELOCITY SCALE



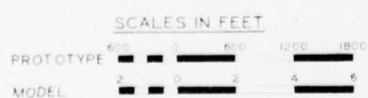
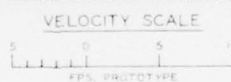
SCALES IN FEET

PROTOTYPE	0	5	10	15	20
MODEL	0	1	2	3	4

SURFACE CURRENTS
1964 CONDITIONS
WITH PLAN INSTALLED
MEAN TIDE
HOUR 2



SURFACE CURRENTS
 1964 CONDITIONS
 WITH PLAN INSTALLED
 MEAN TIDE
 HOUR 3



SURFACE CURRENTS
 1964 CONDITIONS
 WITH PLAN INSTALLED
 MEAN TIDE
 HOUR 4



VELOCITY SCALE



SCALES IN FEET

PROTOTYPE	0	5	10	15	20
MODEL	2	10	20	40	60

SURFACE CURRENTS
1964 CONDITIONS
WITH PLAN INSTALLED
MEAN TIDE
HOUR 5



VELOCITY SCALE
 0 1 2 3 4 5 6 7 8 9 10
 FTS. PROTOTYPE

SCALES IN FEET
 PROTOTYPE 0 600 1200 1800
 MODEL 2 0 2 4 6

SURFACE CURRENTS
 1964 CONDITIONS
 WITH PLAN INSTALLED
 MEAN TIDE
 HOUR 6



VELOCITY SCALE
 5 0 5 10
 FPS, PROTOTYPE

SCALES IN FEET
 PROTOTYPE 600 0 600 1200 1800
 MODEL 2 0 2 4 6

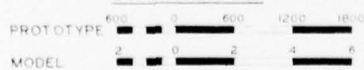
SURFACE CURRENTS
 1964 CONDITIONS
 WITH PLAN INSTALLED
 MEAN TIDE
 HOUR 7



VELOCITY SCALE



SCALES IN FEET



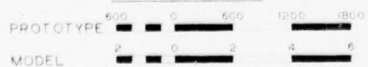
SURFACE CURRENTS
1964 CONDITIONS
WITH PLAN INSTALLED
MEAN TIDE
HOUR 8



VELOCITY SCALE



SCALES IN FEET



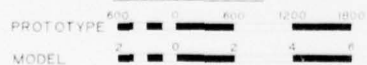
SURFACE CURRENTS
1964 CONDITIONS
WITH PLAN INSTALLED
MEAN TIDE
HOUR 9



VELOCITY SCALE



SCALES IN FEET



SURFACE CURRENTS
1964 CONDITIONS
WITH PLAN INSTALLED
MEAN TIDE
HOUR 10



VELOCITY SCALE
 5 0 5 10
 FPS, PROTOTYPE

SCALES IN FEET
 600 0 600 1200 1800
 PROTOTYPE
 2 0 2 4 6
 MODEL

SURFACE CURRENTS
 1964 CONDITIONS
 WITH PLAN INSTALLED
 MEAN TIDE
 HOUR 11



VELOCITY SCALE
 5 0 5 10
 FPS, PROTOTYPE

SCALES IN FEET
 PROTOTYPE 0 100 200 300 400
 MODEL 0 1 2 3 4

SURFACE CURRENTS
 1964 CONDITIONS
 WITH PLAN INSTALLED
 MEAN TIDE
 HOUR 12



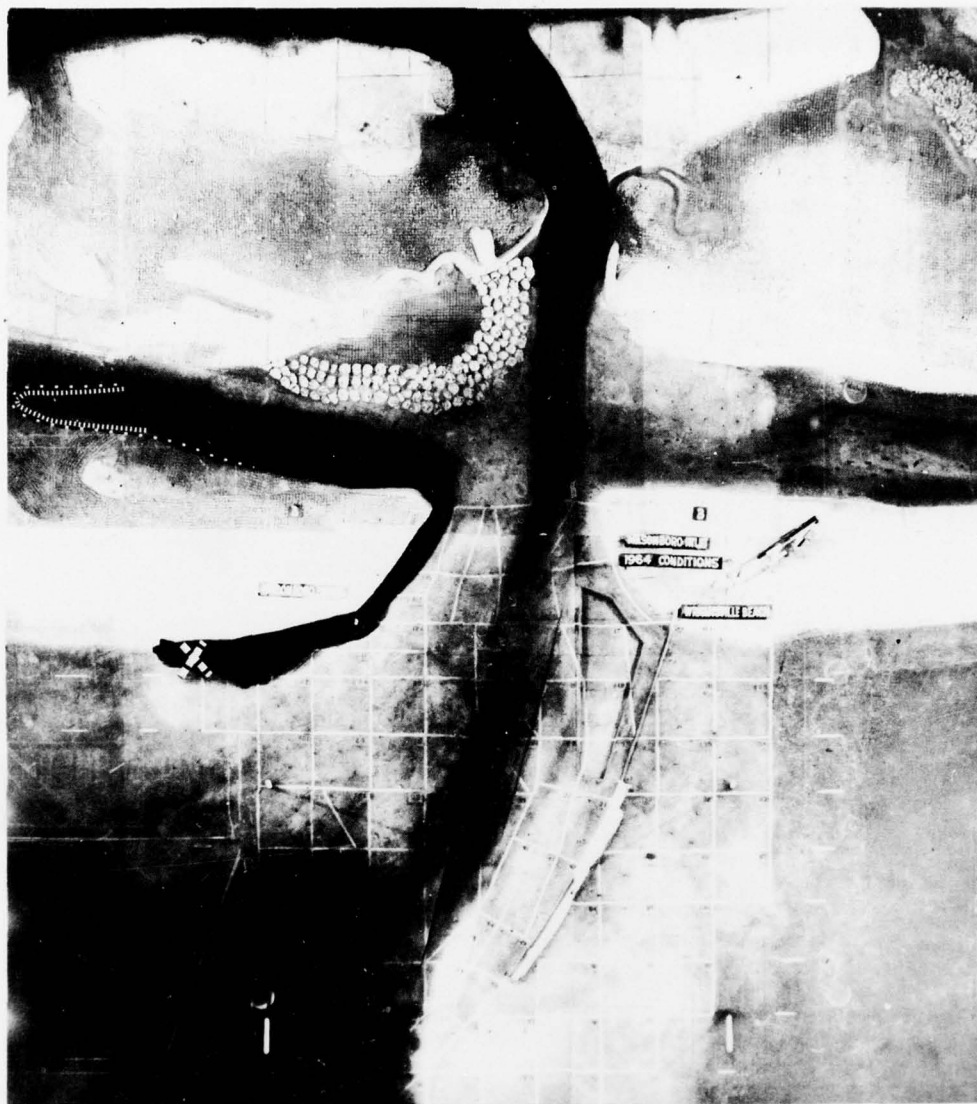
TEST CONDITIONS

TIDE - 3.8-FT RANGE
 MEAN TIDAL LEVEL - 0-FT MSL
 X - SITE OF DYE INSERTION
 9:00 - TIME OF DYE INSERTION
 10:00 - TIME OF STREAK OBSERVATION
 EBB FLOW

LEGEND

..... TEST WITH 3-FT, 7.4-SEC, N84°E WAVE
 ---- TEST WITH 3-FT, 7.4-SEC, S16°E WAVE
 TEST WITHOUT WAVES - DYE PATTERN AS
 SHOWN IN PHOTO

DYE STREAK PATTERNS
 1964 HYDROGRAPHY
 WITH PLAN INSTALLED
 CONDITION I



TEST CONDITIONS

TIDE - 3.8-FT RANGE
 MEAN TIDAL LEVEL - 0-FT MSL
 X - SITE OF DYE INSERTION
 4:30 - TIME OF DYE INSERTION
 5:30 - TIME OF STREAK OBSERVATION
 FLOOD FLOW

LEGEND

||||| TEST WITH 3-FT, 7.4-SEC, N84°E WAVE
 ---- TEST WITH 3-FT, 7.4-SEC, S16°E WAVE
 TEST WITHOUT WAVES - DYE PATTERN AS
 SHOWN IN PHOTO

DYE STREAK PATTERNS
 1964 HYDROGRAPHY
 WITH PLAN INSTALLED
 CONDITION 3



TEST CONDITIONS

TIDE - 3.8-FT RANGE
 MEAN TIDAL LEVEL - 0-FT MSL
 X - SITE OF DYE INSERTION
 9:45 - TIME OF DYE INSERTION
 10:30 - TIME OF STREAK OBSERVATION
 EBB FLOW

LEGEND

———— TEST WITH 3-FT, 7.4-SEC, N84°E WAVE
 - - - - - TEST WITH 3-FT, 7.4-SEC, S16°E WAVE
 TEST WITHOUT WAVES - DYE PATTERN AS
 SHOWN IN PHOTO

DYE STREAK PATTERNS
 1964 HYDROGRAPHY
 WITH PLAN INSTALLED
 CONDITION 4



TEST CONDITIONS

TIDE - 3.8-FT RANGE
 MEAN TIDAL LEVEL - 0-FT. MSL
 X - SITE OF DYE INSERTION
 3:30 - TIME OF DYE INSERTION
 4:30 - TIME OF STREAK OBSERVATION
 FLOOD FLOW

LEGEND

———— TEST WITH 3-FT, 7.4-SEC, NB4°E WAVE
 - - - - TEST WITH 3-FT, 7.4-SEC, S16°E WAVE
 TEST WITHOUT WAVES - DYE PATTERN AS
 SHOWN IN PHOTO

DYE STREAK PATTERNS
 1964 HYDROGRAPHY
 WITH PLAN INSTALLED
 CONDITION 5



TEST CONDITIONS

TIDE - 3.8-FT RANGE
 MEAN TIDAL LEVEL - 0-FT MSL
 X - SITE OF DYE INSERTION
 9:30 - TIME OF DYE INSERTION
 10:15 - TIME OF STREAK OBSERVATION
 EBB FLOW

LEGEND

||||| TEST WITH 3-FT, 7.4-SEC, N84°E WAVE
 ---- TEST WITH 3-FT, 7.4-SEC, S16°E WAVE
 TEST WITHOUT WAVES - DYE PATTERN AS
 SHOWN IN PHOTO

DYE STREAK PATTERNS
 1964 HYDROGRAPHY
 WITH PLAN INSTALLED
 CONDITION 6



TEST CONDITIONS

TIDE - 3.8-FT RANGE
 MEAN TIDAL LEVEL - 0-FT MSL
 X - SITE OF DYE INSERTION
 11:30 - TIME OF DYE INSERTION
 12:00 - TIME OF STREAK OBSERVATION
 EBB FLOW

LEGEND

===== TEST WITH 3-FT, 7.4-SEC, N84°E WAVE
 ----- TEST WITH 3-FT, 7.4-SEC, S16°E WAVE
 TEST WITHOUT WAVES - DYE PATTERN AS
 SHOWN IN PHOTO

DYE STREAK PATTERNS
 1964 HYDROGRAPHY
 WITH PLAN INSTALLED
 CONDITION 7



TEST CONDITIONS

TIDE - 3.5-FT RANGE
 MEAN TIDAL LEVEL - 0-FT MSL
 X - SITE OF DYE INSERTION
 5:00 - TIME OF DYE INSERTION
 6:30 - TIME OF STREAK OBSERVATION
 FLOOD FLOW

LEGEND

||||||| TEST WITH 3-FT, 7.4-SEC, N84°E WAVE
 ----- TEST WITH 3-FT, 7.4-SEC, S16°E WAVE
 TEST WITHOUT WAVES - DYE PATTERN AS
 SHOWN IN PHOTO

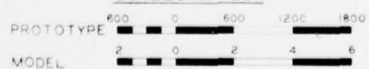
DYE STREAK PATTERNS
 1964 HYDROGRAPHY
 WITH PLAN INSTALLED
 CONDITION 8



VELOCITY SCALE



SCALES IN FEET



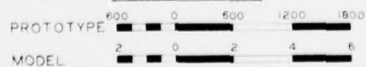
SURFACE CURRENTS
1966 CONDITIONS
MEAN TIDE
HOUR 0



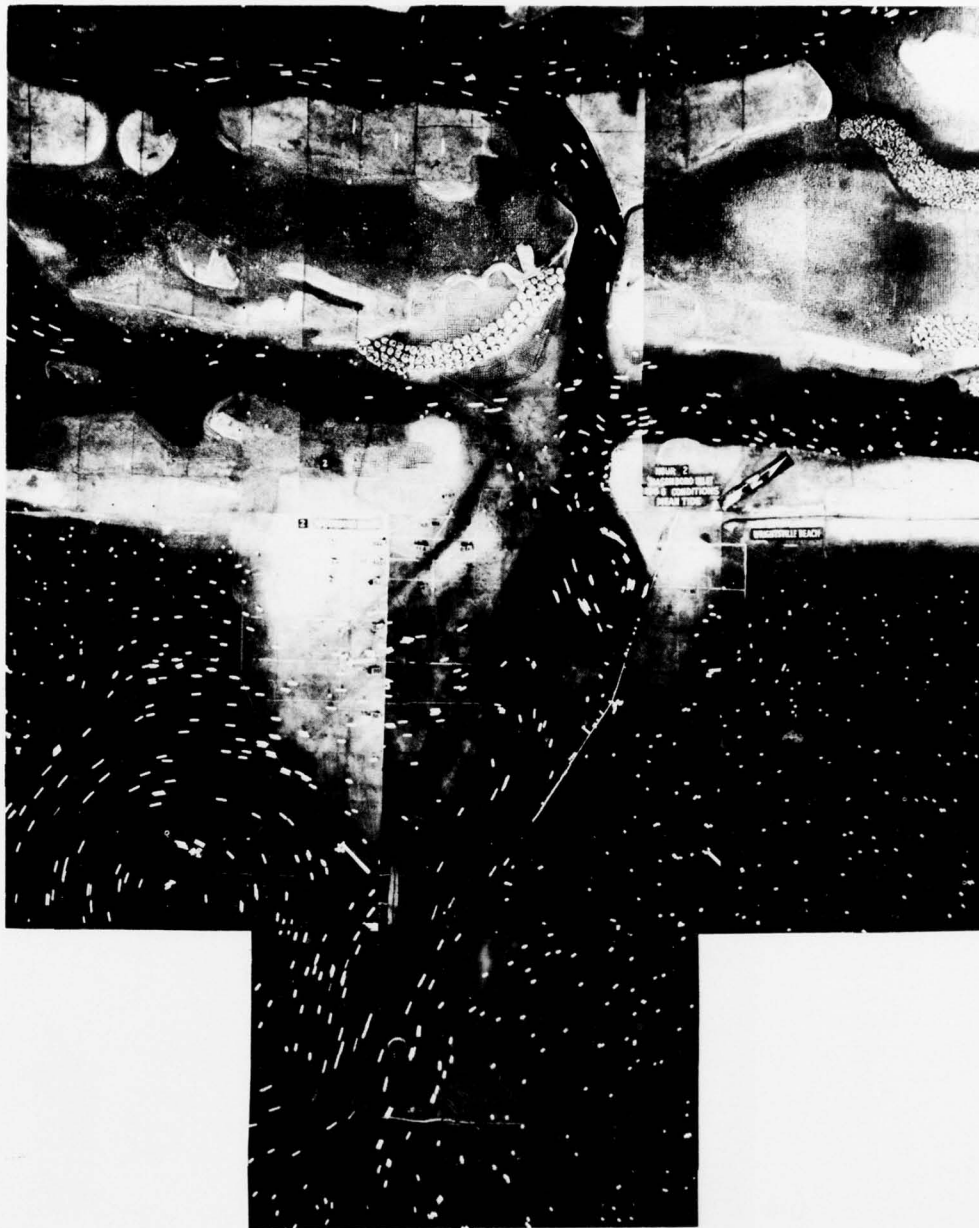
VELOCITY SCALE



SCALES IN FEET



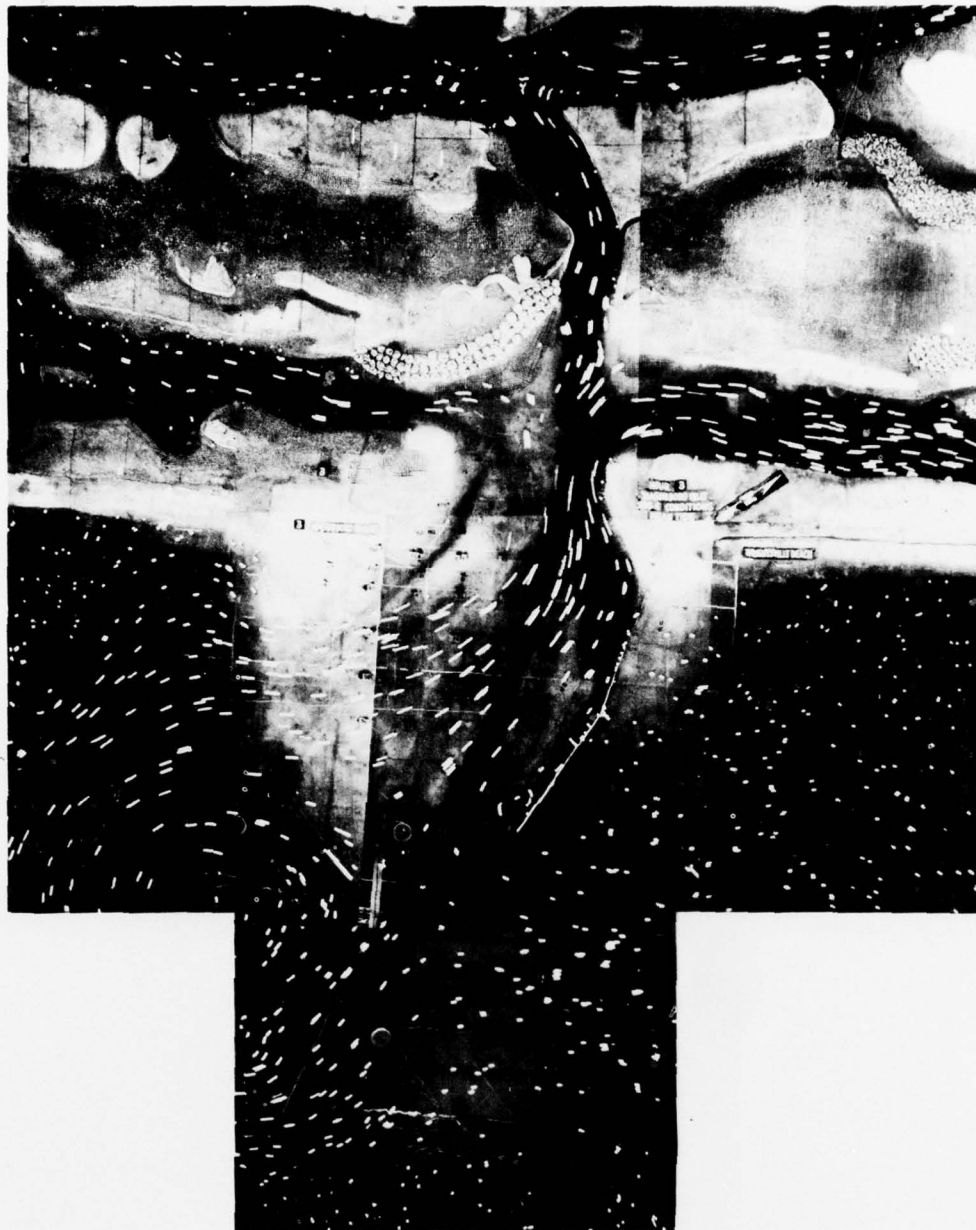
SURFACE CURRENTS
1966 CONDITIONS
MEAN TIDE
HOUR 1



VELOCITY SCALE
 5 0 5 10
 FPS, PROTOTYPE

SCALES IN FEET
 PROTOTYPE 0 600 1200 1800
 MODEL 2 0 2 4 6

SURFACE CURRENTS
 1966 CONDITIONS
 MEAN TIDE
 HOUR 2



VELOCITY SCALE
 5 0 5 10
 FPS, PROTOTYPE

SCALES IN FEET
 PROTOTYPE 0 600 1200 1800
 MODEL 2 0 2 4 6

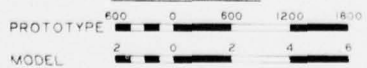
SURFACE CURRENTS
 1966 CONDITIONS
 MEAN TIDE
 HOUR 3



VELOCITY SCALE



SCALES IN FEET



SURFACE CURRENTS
1966 CONDITIONS
MEAN TIDE
HOUR 4



VELOCITY SCALE
 5 0 5 10
 FPS, PROTOTYPE

SCALES IN FEET
 PROTOTYPE 600 0 600 1200 1800
 MODEL 2 0 2 4 6

SURFACE CURRENTS
 1966 CONDITIONS
 MEAN TIDE
 HOUR 5

AD-A055 523

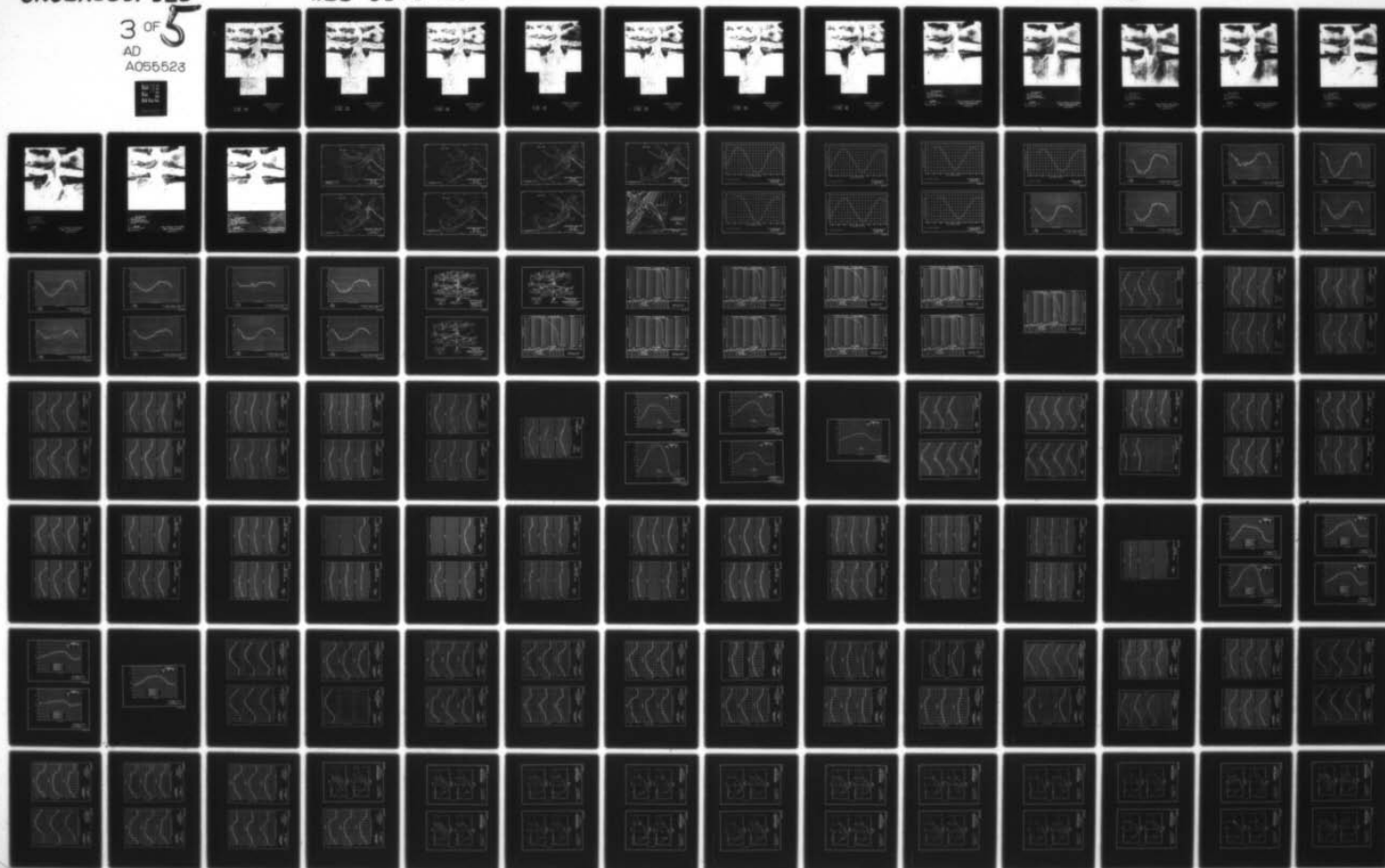
ARMY ENGINEER WATERWAYS EXPERIMENT STATION VICKSBURG MISS F/G 8/3
PHYSICAL MODEL SIMULATION OF THE HYDRAULICS OF MASONBORO INLET,--ETC(U)
NOV 77 R A SAGER, W C SEABERGH

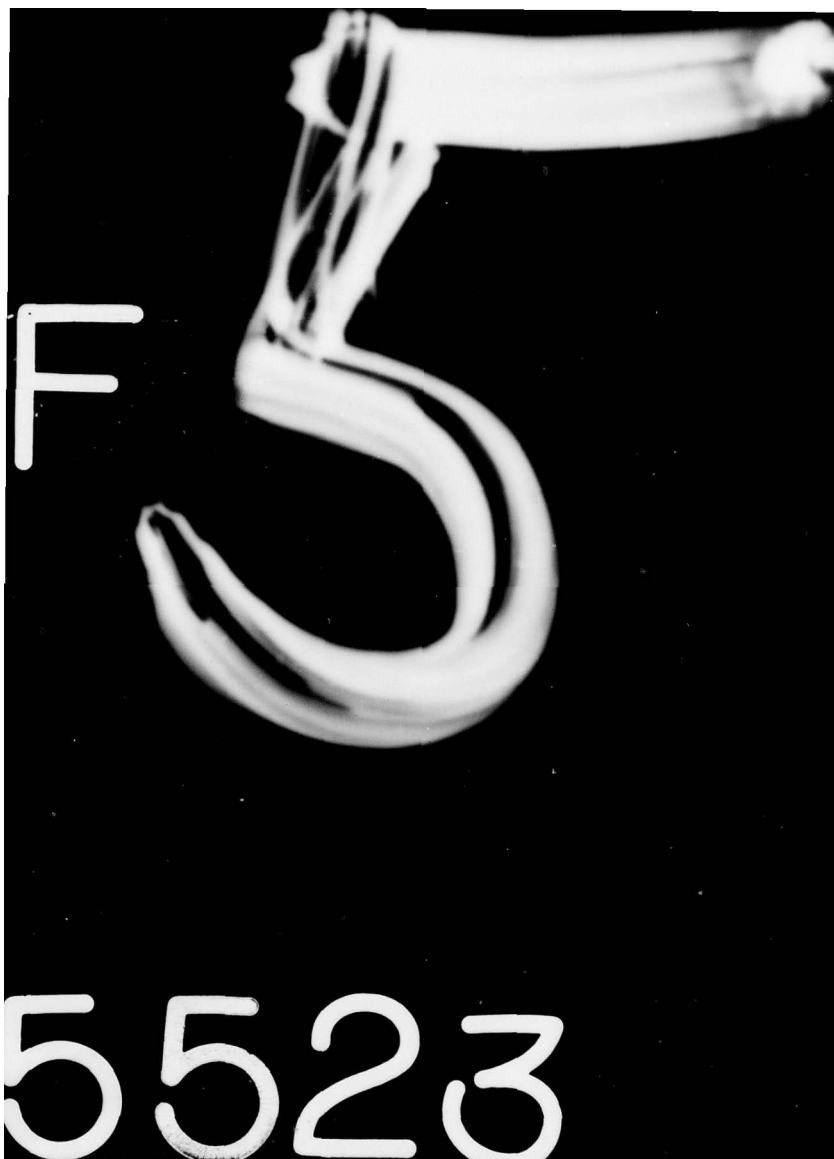
UNCLASSIFIED

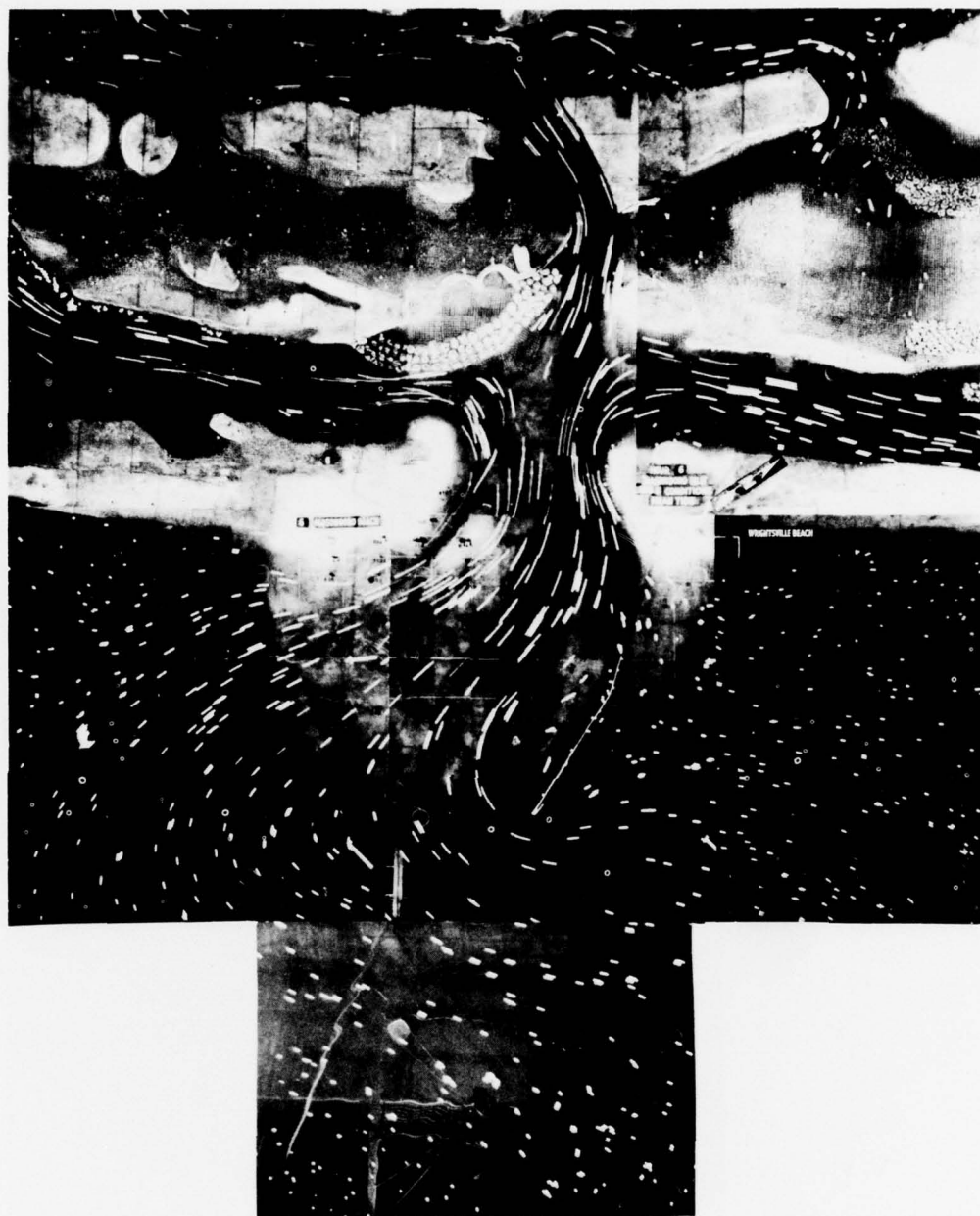
WES-GITI-15

NL

3 of 5
AD
A055523



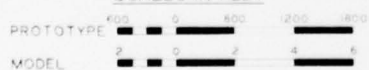




VELOCITY SCALE



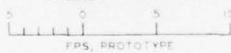
SCALES IN FEET



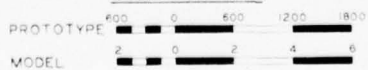
SURFACE CURRENTS
1966 CONDITIONS
MEAN TIDE
HOUR 6



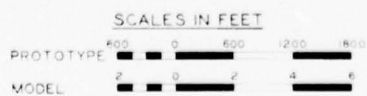
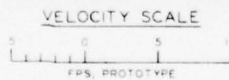
VELOCITY SCALE



SCALES IN FEET



SURFACE CURRENTS
1966 CONDITIONS
MEAN TIDE
HOUR 7



SURFACE CURRENTS
1966 CONDITIONS
MEAN TIDE
HOUR 8



VELOCITY SCALE
 5 0 5 10
 FPS, PROTOTYPE

SCALES IN FEET
 PROTOTYPE 0 500 1000 1500
 MODEL 2 5 10 15

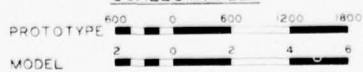
SURFACE CURRENTS
 1966 CONDITIONS
 MEAN TIDE
 HOUR 9



VELOCITY SCALE



SCALES IN FEET



SURFACE CURRENTS
1966 CONDITIONS
MEAN TIDE
HOUR 10



VELOCITY SCALE
 5 0 5 10
 FPS, PROTOTYPE

SCALES IN FEET
 PROTOTYPE 0 500 1000 1500
 MODEL 2 0 2 4 6

SURFACE CURRENTS
 1966 CONDITIONS
 MEAN TIDE
 HOUR 11



VELOCITY SCALE
 5 0 5 10
 FPS, PROTOTYPE

SCALES IN FEET
 PROTOTYPE 0 500 1000 1500
 MODEL 2 0 2 4 6

SURFACE CURRENTS
 1966 CONDITIONS
 MEAN TIDE
 HOUR 12



TEST CONDITIONS

TIDE - 3.6-FT RANGE
 MEAN TIDAL LEVEL - 0-FT MSL
 X - SITE OF DYE INSERTION
 9:00 - TIME OF DYE INSERTION
 10:00 - TIME OF STREAK OBSERVATION
 EBB FLOW

LEGEND

--- OBSERVED DYE STREAK
 TEST WITHOUT WAVES

DYE STREAK PATTERNS
 1966 HYDROGRAPHY
 CONDITION I



TEST CONDITIONS

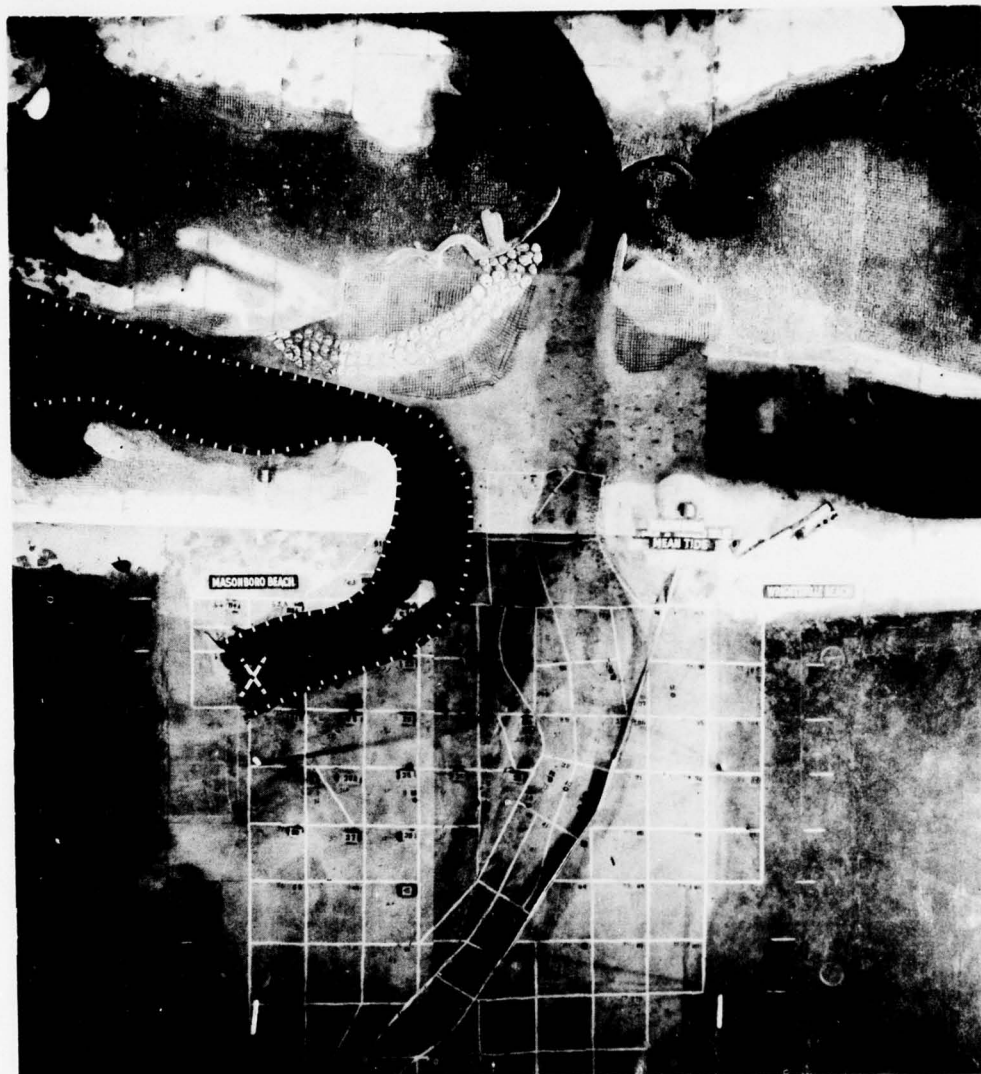
TIDE - 3.6-FT RANGE
 MEAN TIDAL LEVEL - 0-FT MSL
 X - SITE OF DYE INSERTION
 11:30 - TIME OF DYE INSERTION
 12:00 - TIME OF STREAK OBSERVATION
 EBB FLOW

LEGEND

--- OBSERVED DYE STREAK

TEST WITHOUT WAVES

DYE STREAK PATTERNS
 1966 HYDROGRAPHY
 CONDITION 2



TEST CONDITIONS

TIDE - 3.8-FT RANGE
 MEAN TIDAL LEVEL - 0-FT MSL
 X - SITE OF DYE INSERTION
 4:30 - TIME OF DYE INSERTION
 5:30 - TIME OF STREAK OBSERVATION
 FLOOD FLOW

LEGEND

--- OBSERVED DYE STREAK
 --- TEST WITHOUT WAVES

DYE STREAK PATTERNS
 1966 HYDROGRAPHY
 CONDITION 3



TEST CONDITIONS

TIDE - 3.8-FT RANGE
 MEAN TIDAL LEVEL - 0-FT MSL
 X - SITE OF DYE INSERTION
 9.45 - TIME OF DYE INSERTION
 10.30 - TIME OF STREAK OBSERVATION
 EBB FLOW

LEGEND

--- OBSERVED DYE STREAK
 --- TEST WITHOUT WAVES

DYE STREAK PATTERNS
 1966 HYDROGRAPHY
 CONDITION 4



TEST CONDITIONS

TIDE - 3.8-FT RANGE
 MEAN TIDAL LEVEL - 0-FT MSL
 X - SITE OF DYE INSERTION
 3:30 - TIME OF DYE INSERTION
 5:30 - TIME OF STREAK OBSERVATION
 FLOOD FLOW

LEGEND

--- OBSERVED DYE STREAK
 TEST WITHOUT WAVES

DYE STREAK PATTERNS
 1966 HYDROGRAPHY
 CONDITION 5



TEST CONDITIONS

TIDE - 3.8-FT RANGE
 MEAN TIDAL LEVEL - 0-FT MSL
 X - SITE OF DYE INSERTION
 9:30 - TIME OF DYE INSERTION
 10:15 - TIME OF STREAK OBSERVATION
 EBB FLOW

LEGEND

--- OBSERVED DYE STREAK
 TEST WITHOUT WAVES

DYE STREAK PATTERNS
 1966 HYDROGRAPHY
 CONDITION 6



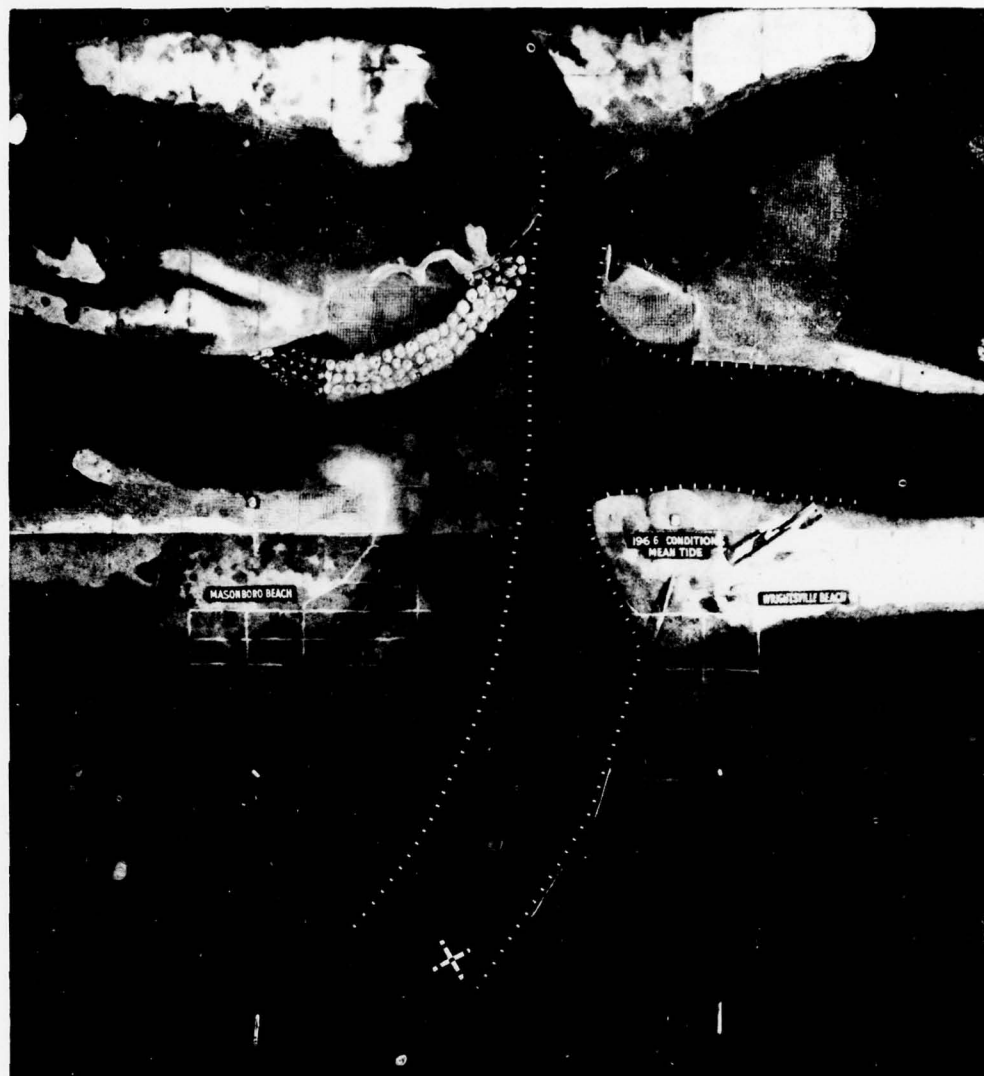
TEST CONDITIONS

TIDE - 3.8-FT RANGE
 MEAN TIDAL LEVEL - 0-FT MSL
 X - SITE OF DYE INSERTION
 11:30 - TIME OF DYE INSERTION
 12:00 - TIME OF STREAK OBSERVATION
 EBB FLOW

LEGEND

--- OBSERVED DYE STREAK
 TEST WITHOUT WAVES

DYE STREAK PATTERNS
 1966 HYDROGRAPHY
 CONDITION 7



TEST CONDITIONS

TIDE - 3.8-FT RANGE
 MEAN TIDAL LEVEL - 0-FT MSL
 X - SITE OF DYE INSERTION
 5:00 - TIME OF DYE INSERTION
 6:30 - TIME OF STREAK OBSERVATION
 FLOOD FLOW

LEGEND

--- OBSERVED DYE STREAK

— TEST WITHOUT WAVES

DYE STREAK PATTERNS
 1966 HYDROGRAPHY
 CONDITION 8

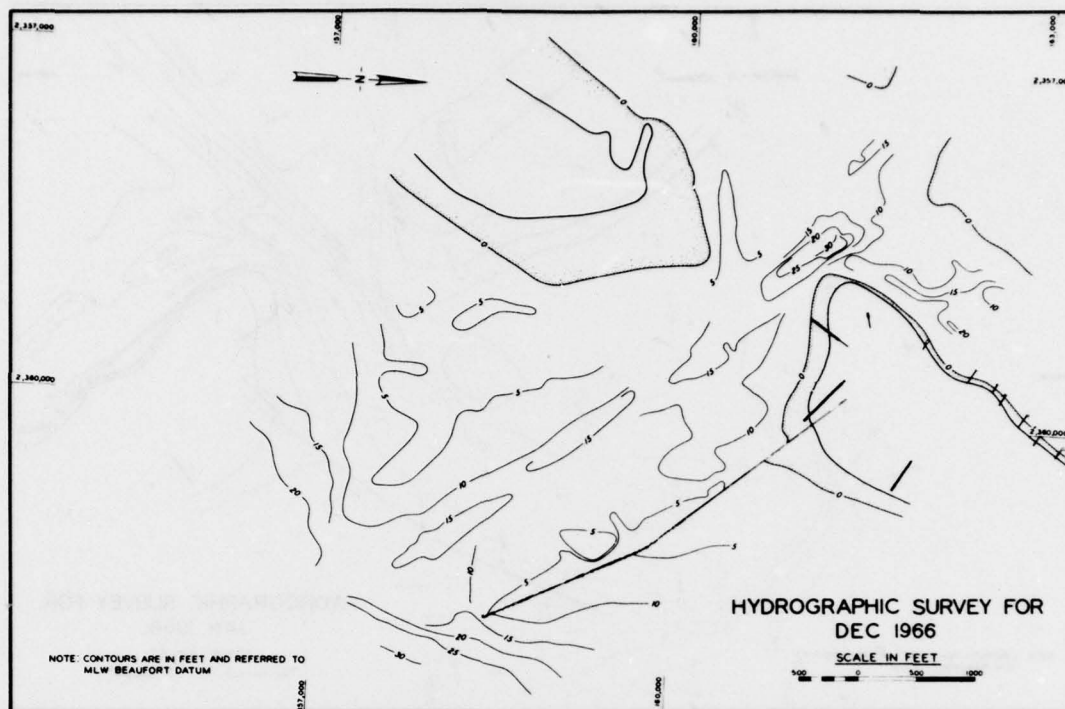


PLATE 3

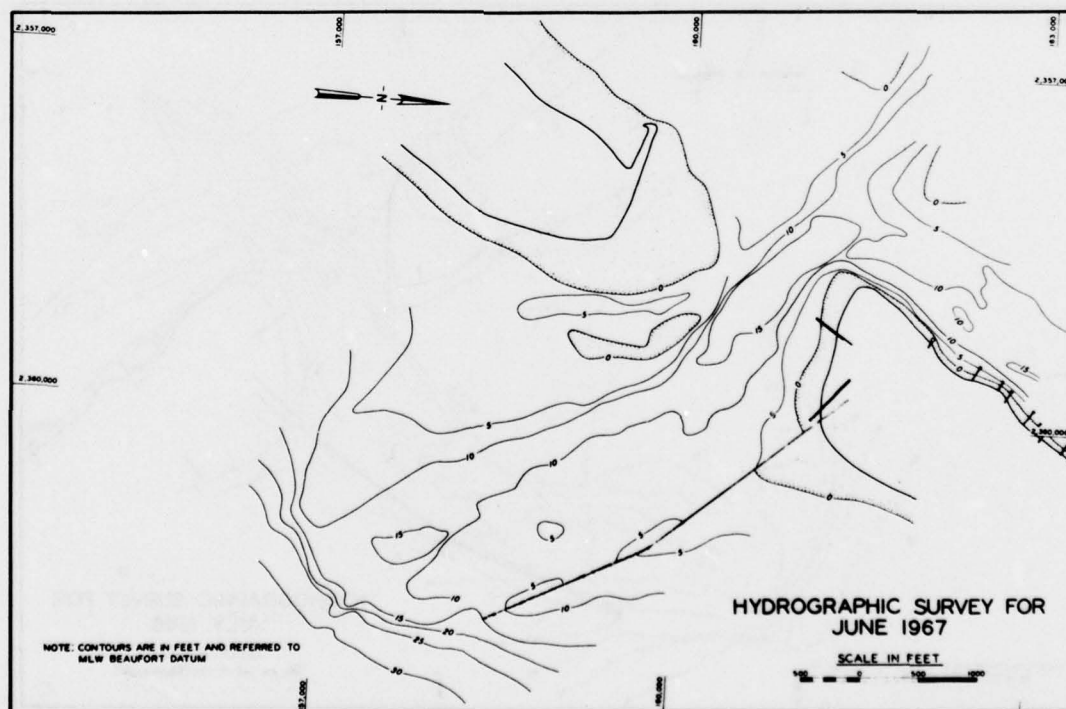


PLATE 4

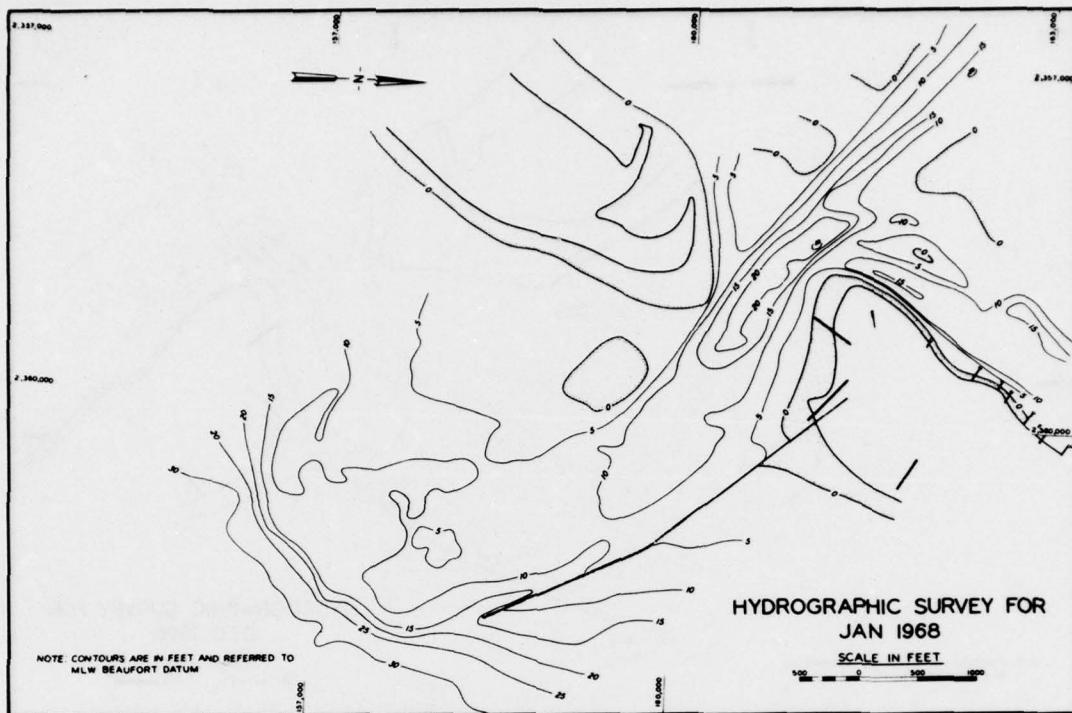


PLATE 5

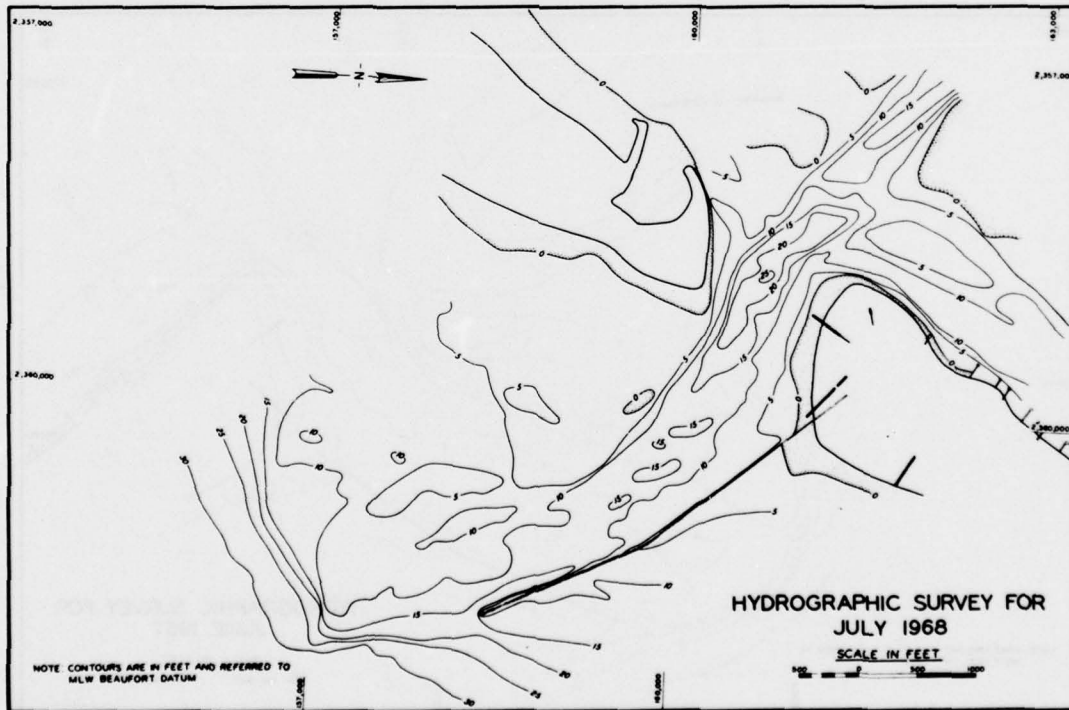
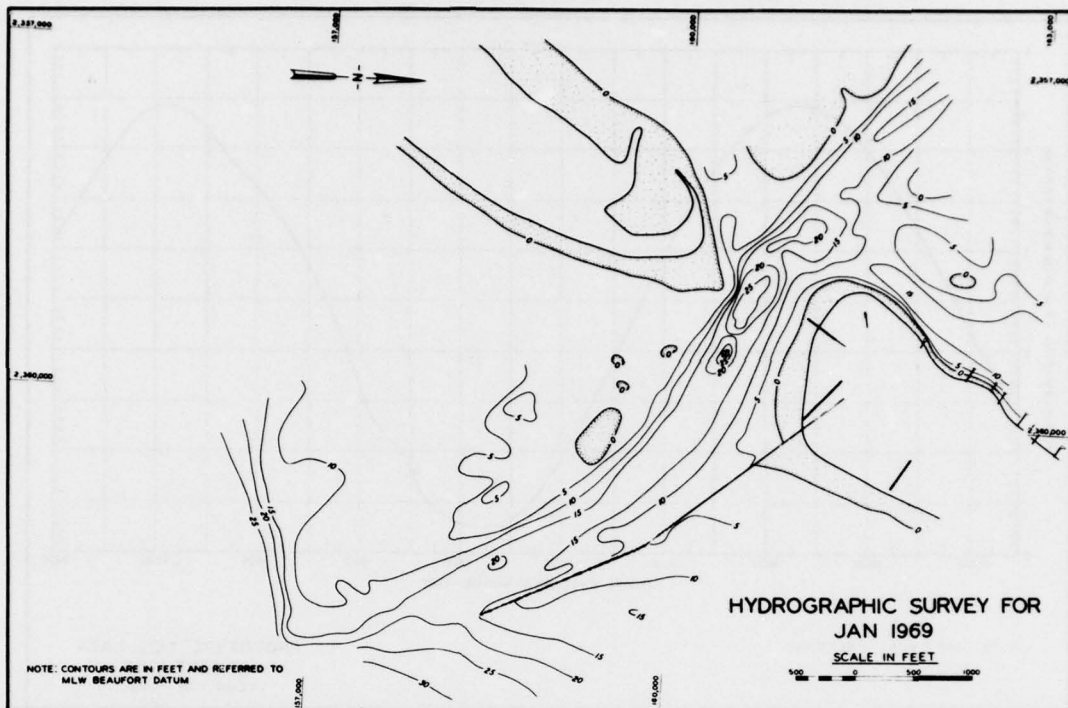


PLATE 6



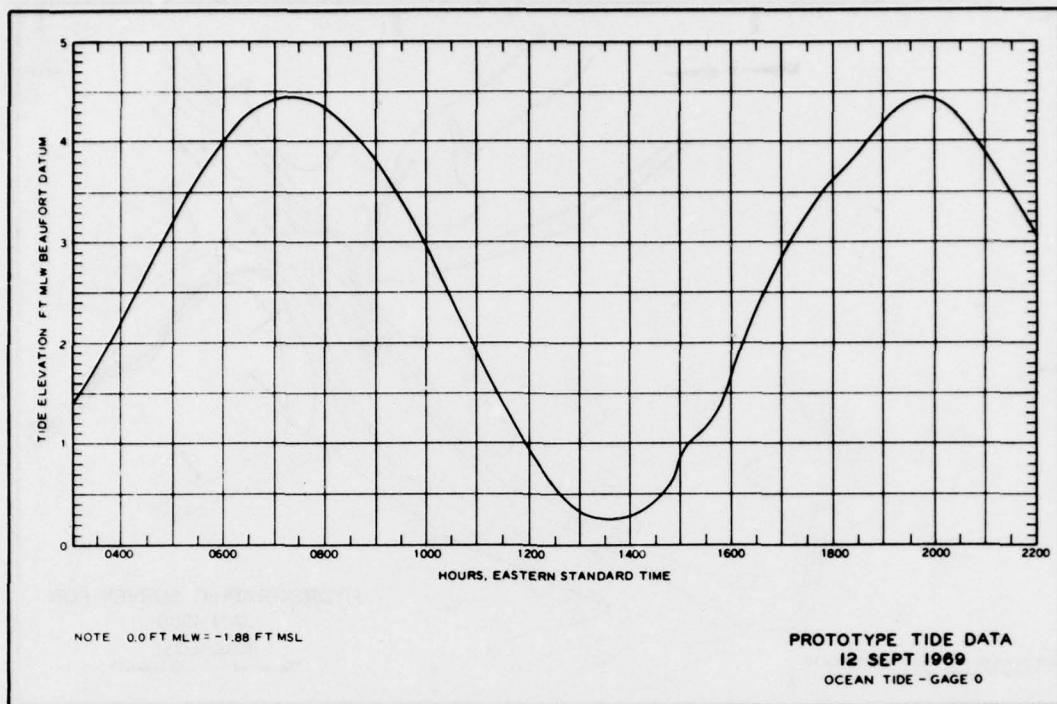


PLATE 9

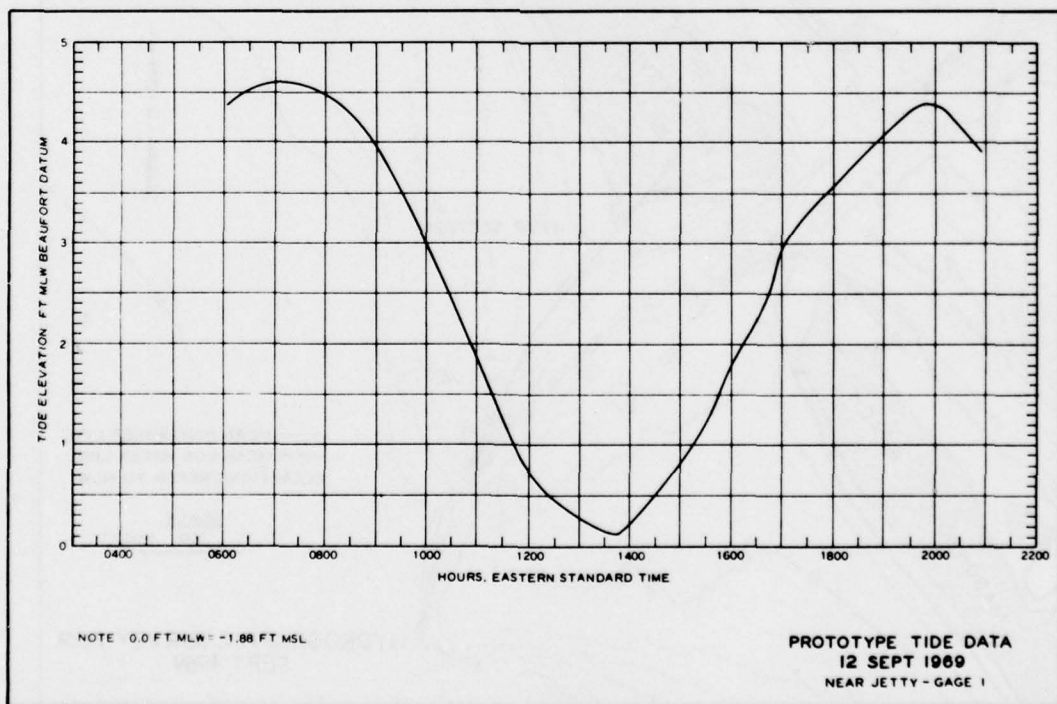


PLATE 10

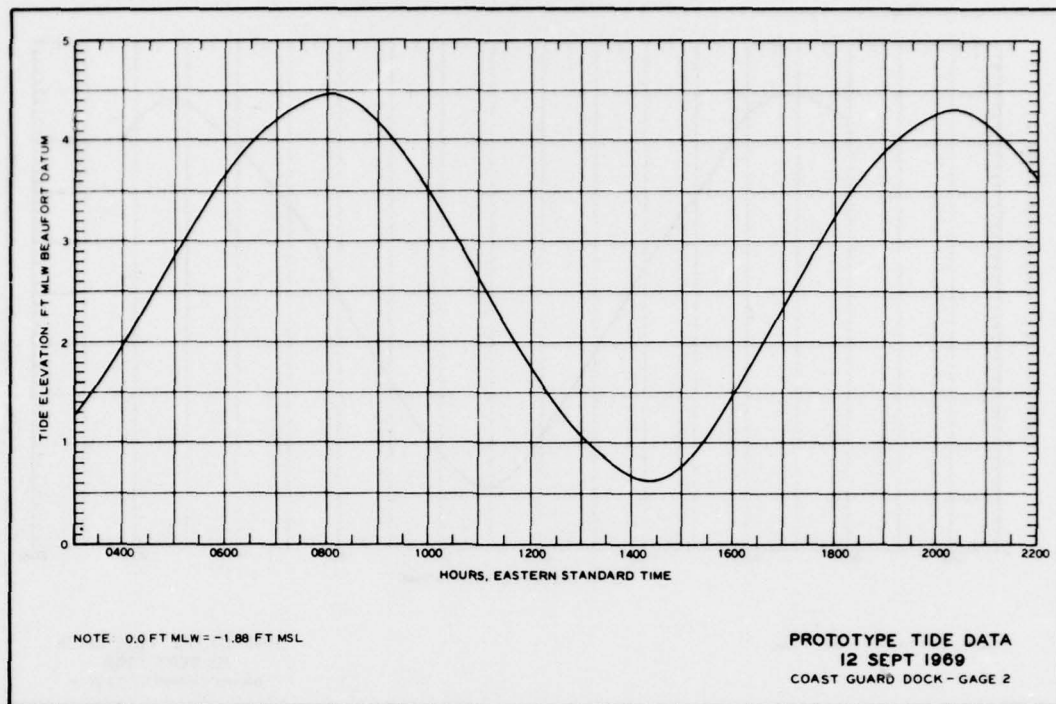


PLATE 11

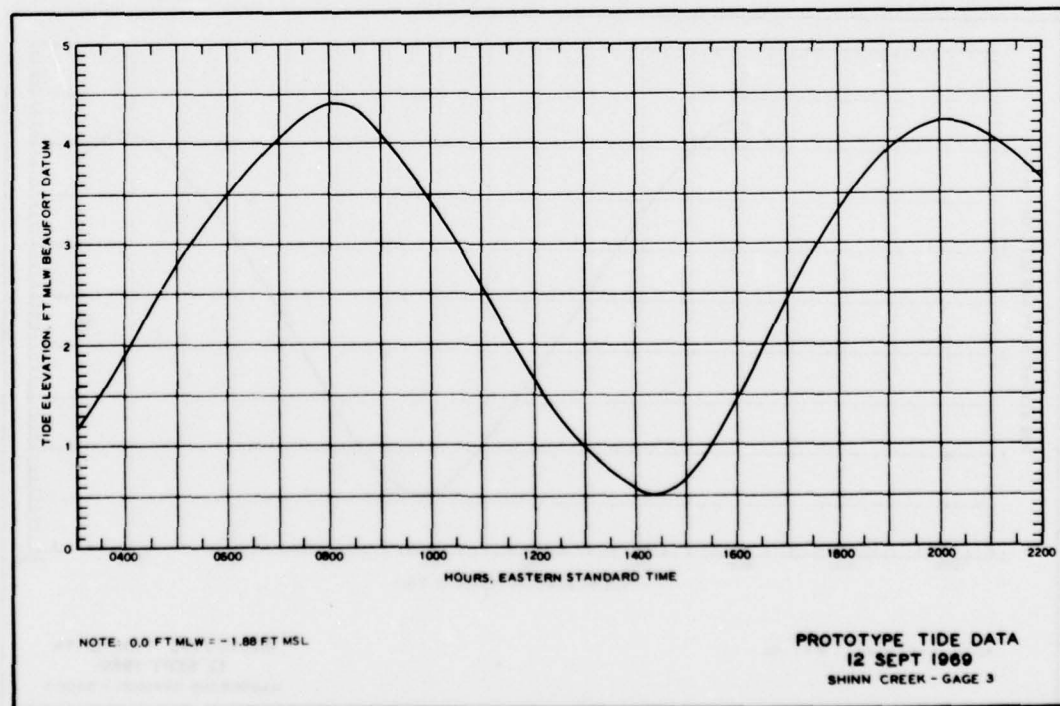


PLATE 12

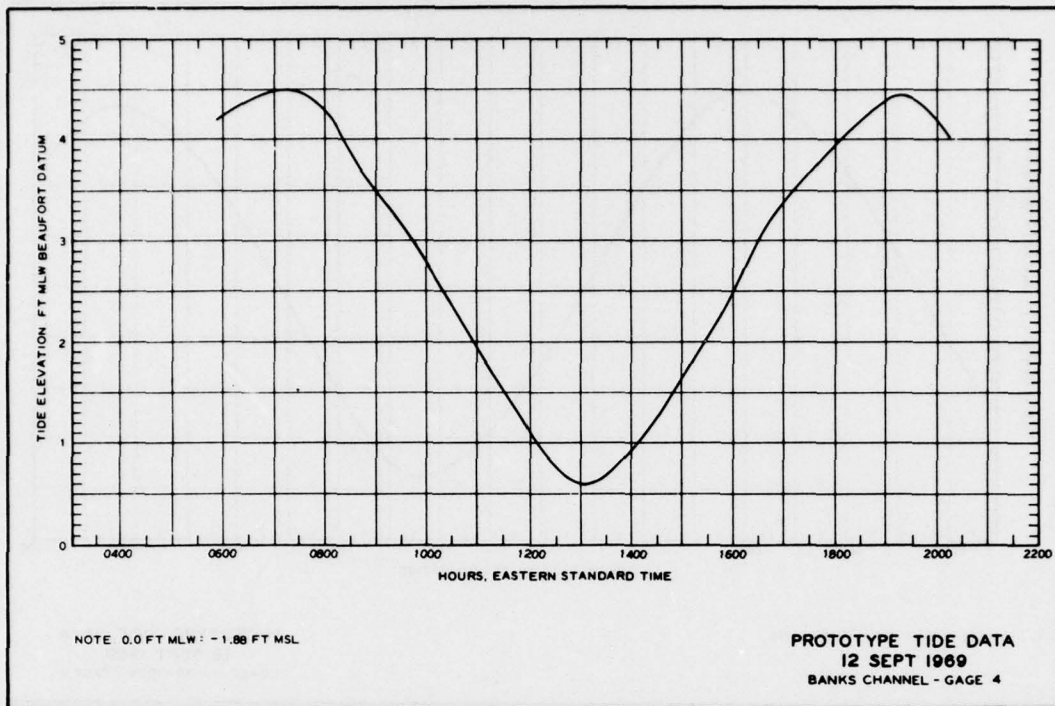


PLATE 13

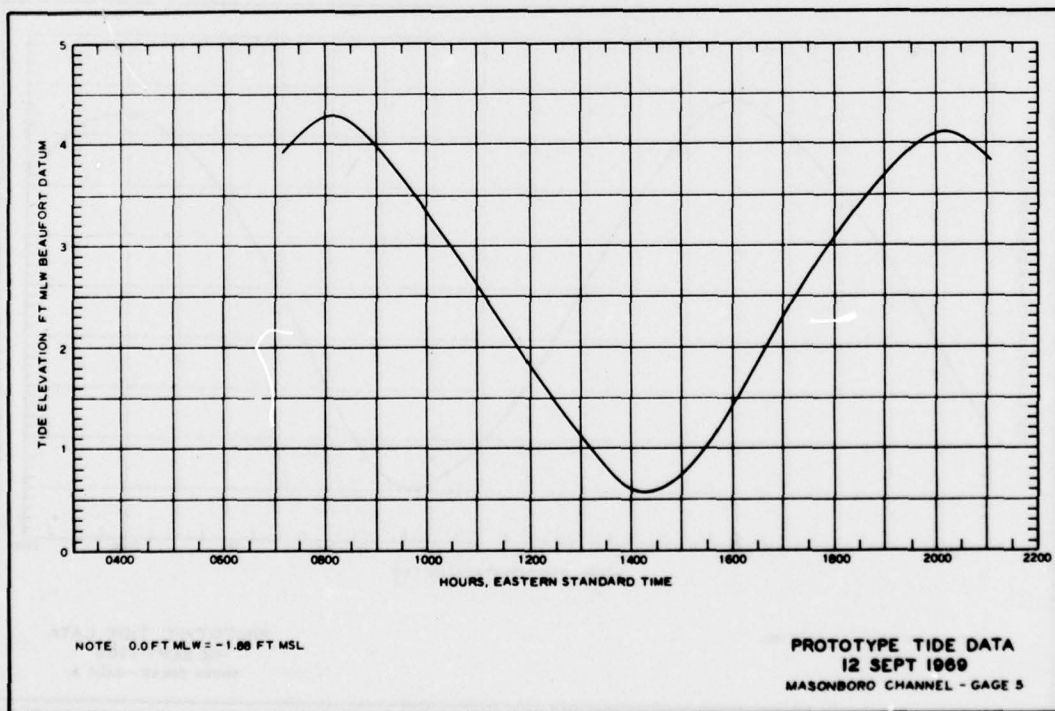


PLATE 14

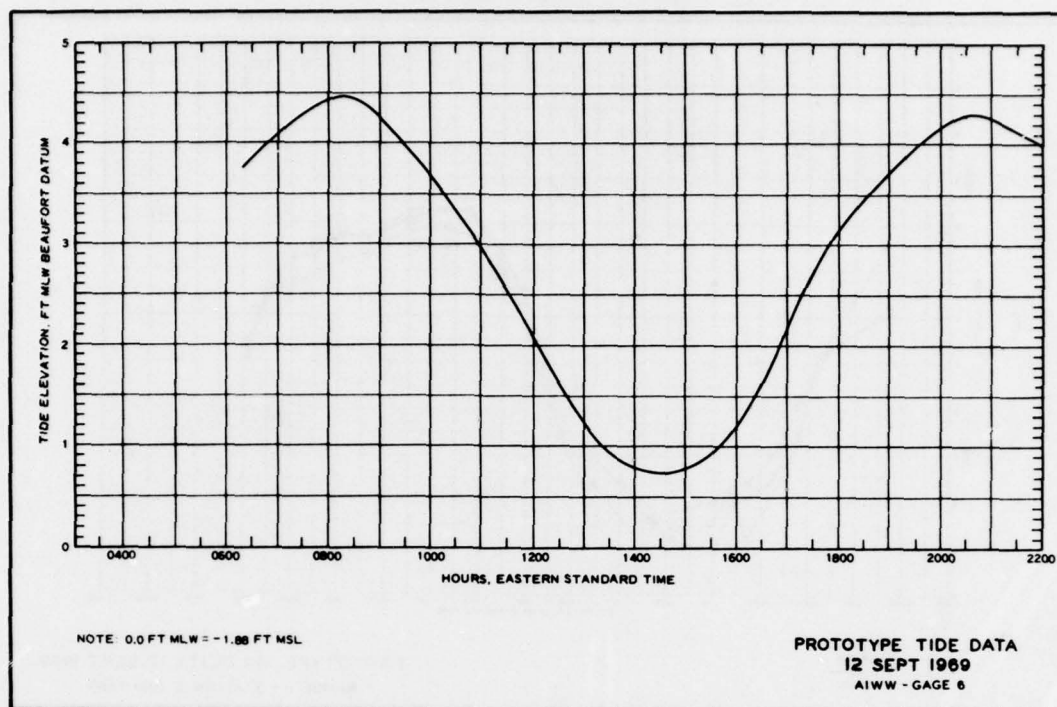


PLATE 15

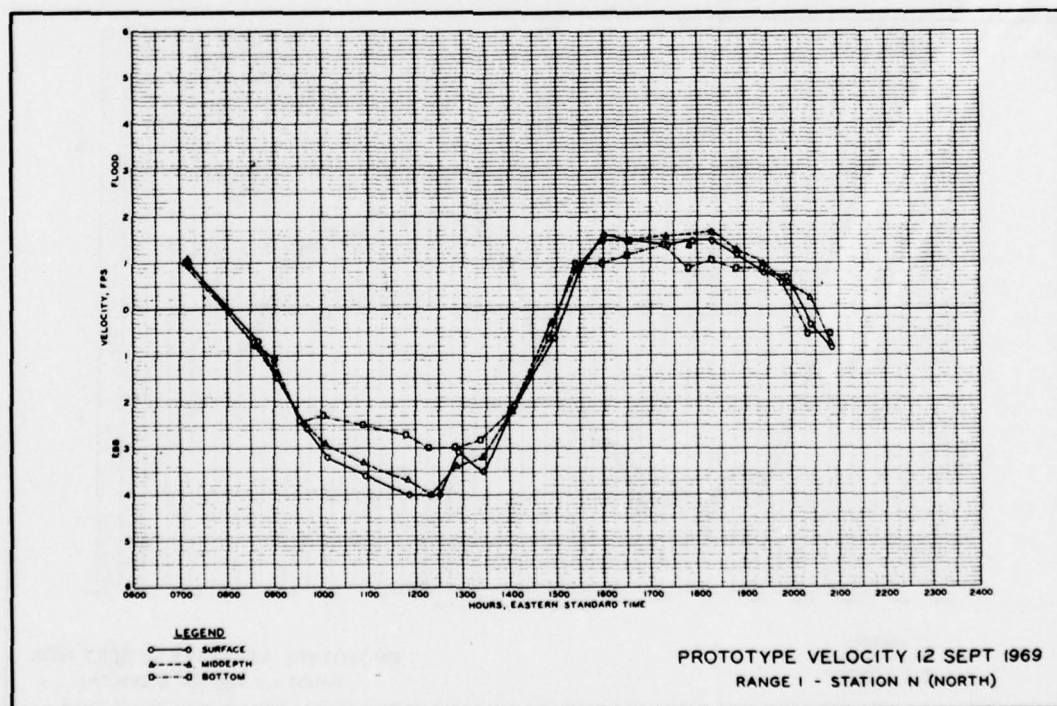


PLATE 16

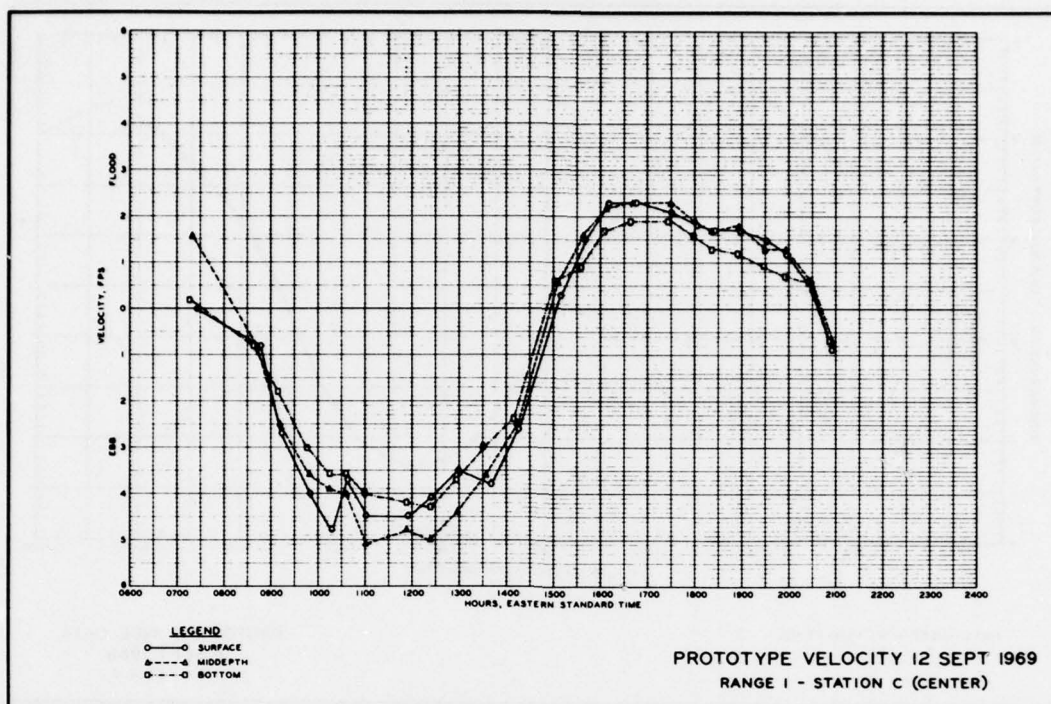


PLATE 17

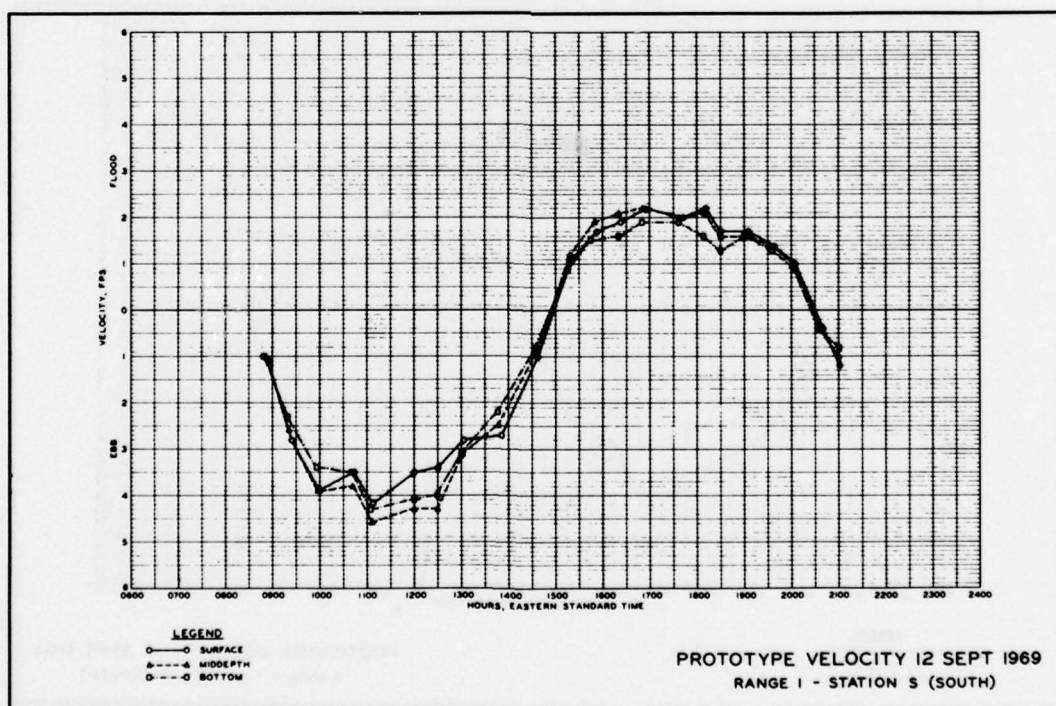


PLATE 18

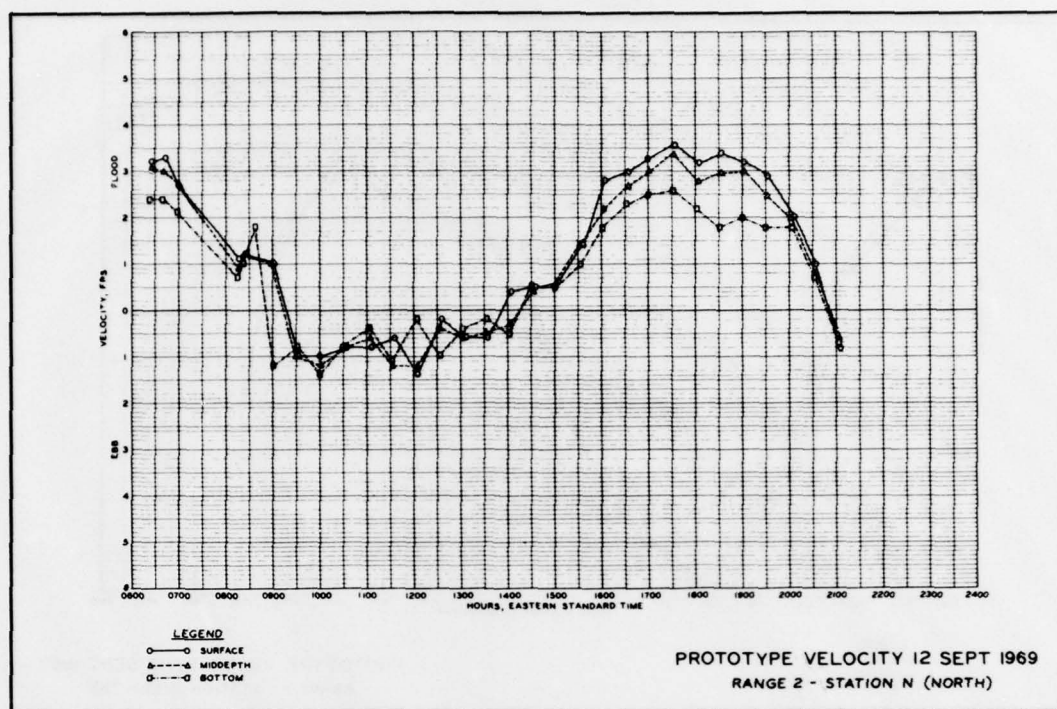


PLATE 19

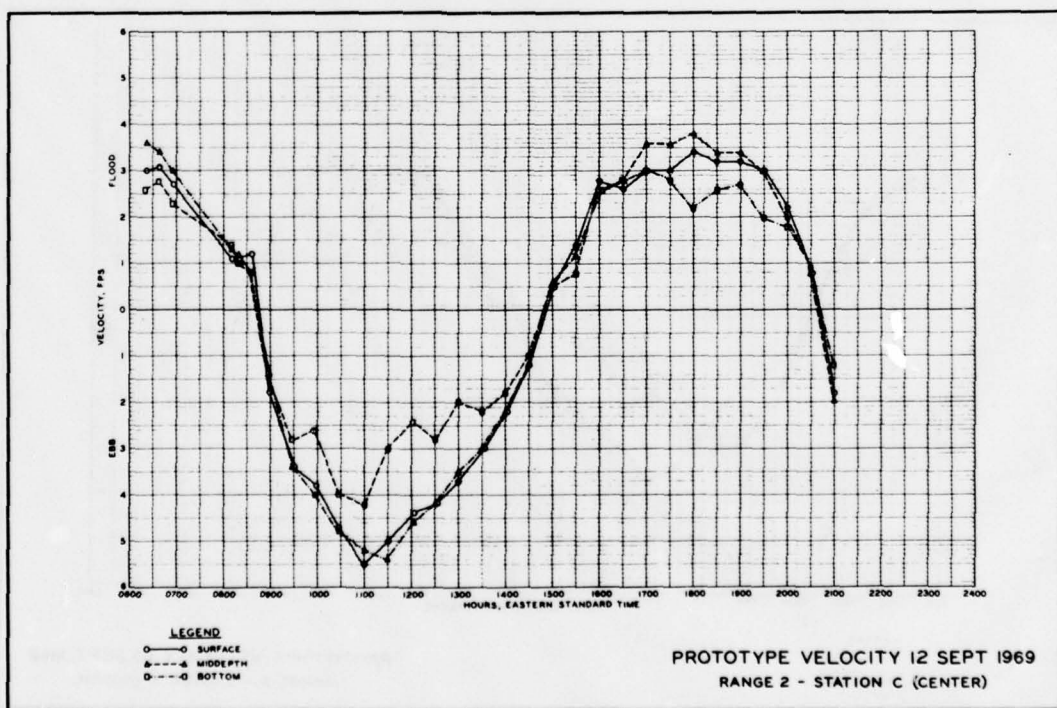


PLATE 20

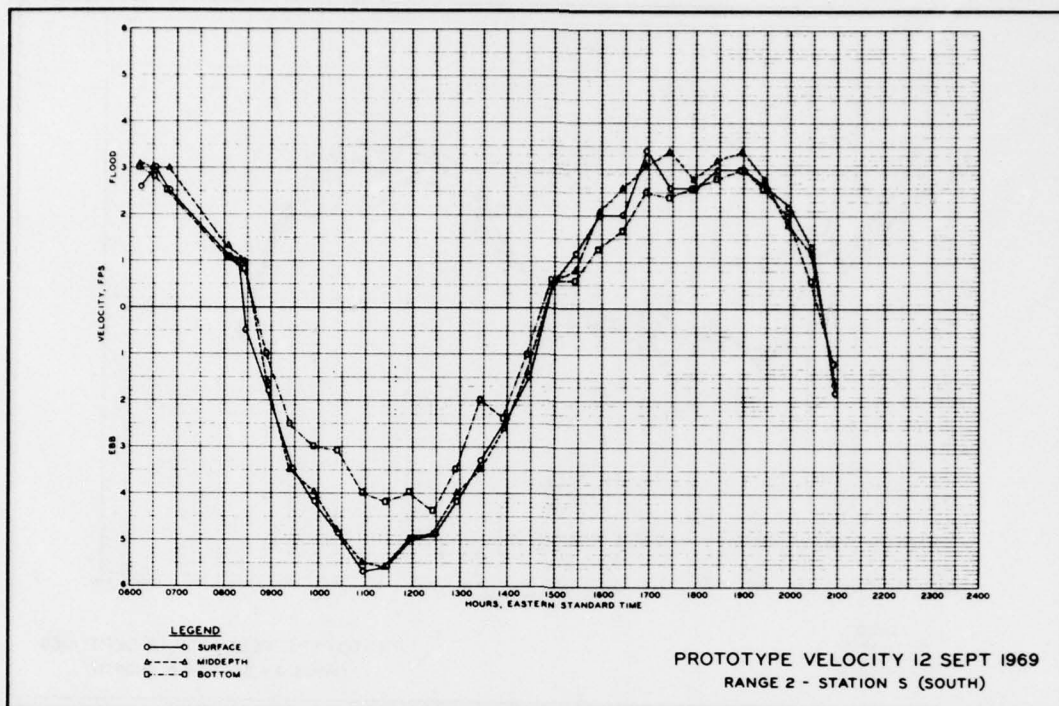


PLATE 21

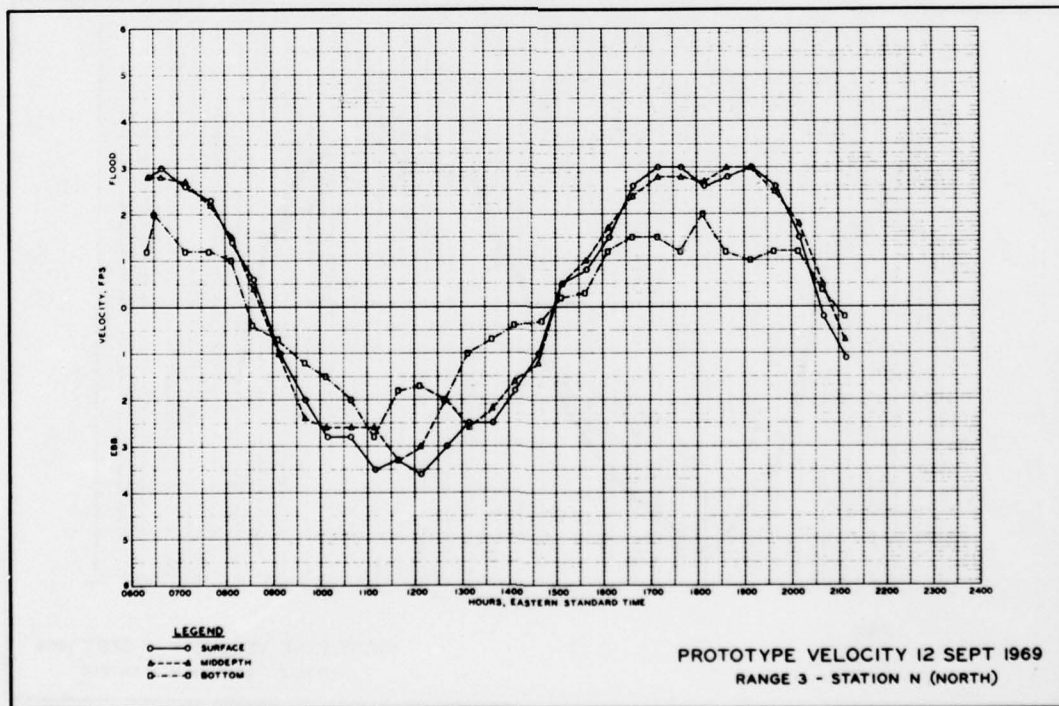


PLATE 22

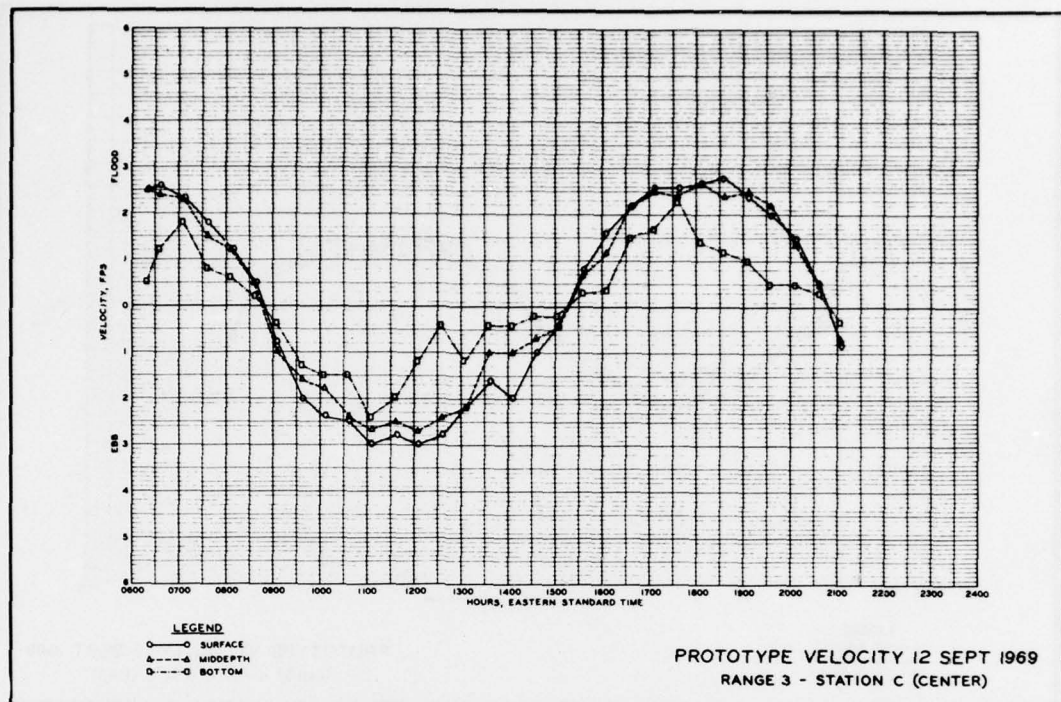


PLATE 23

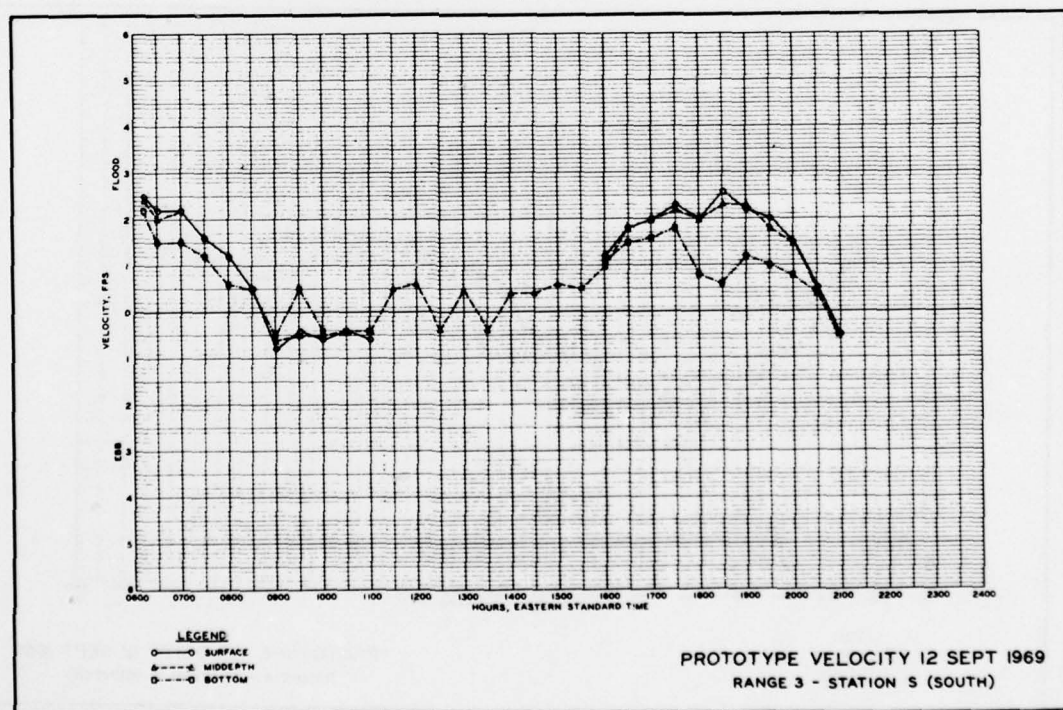


PLATE 24

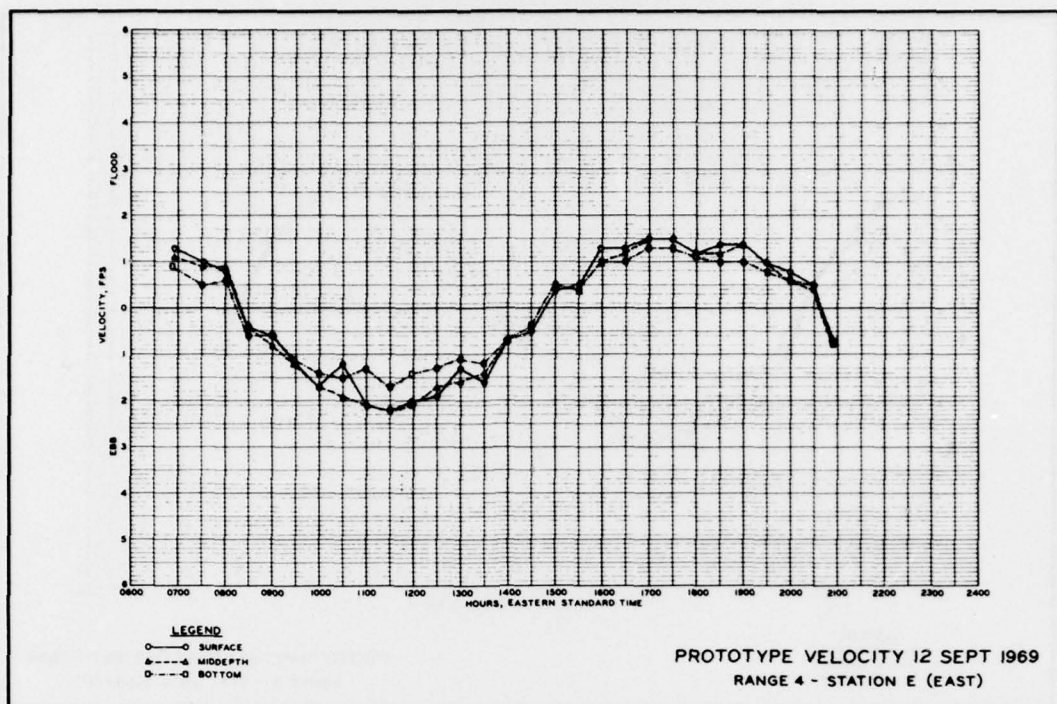


PLATE 25

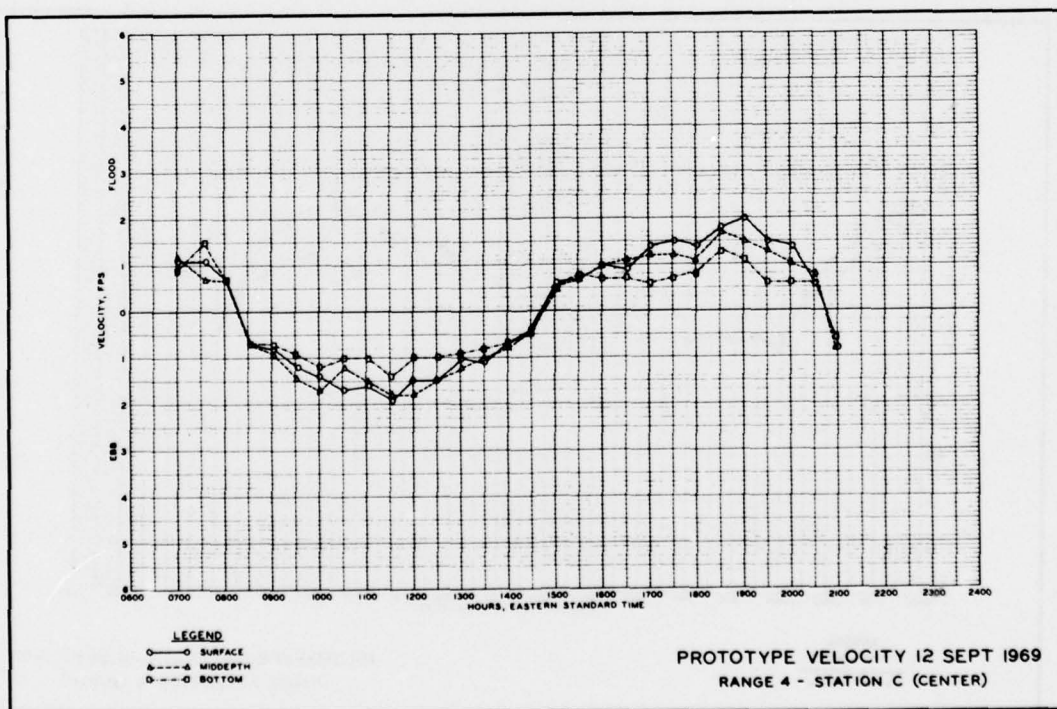


PLATE 26

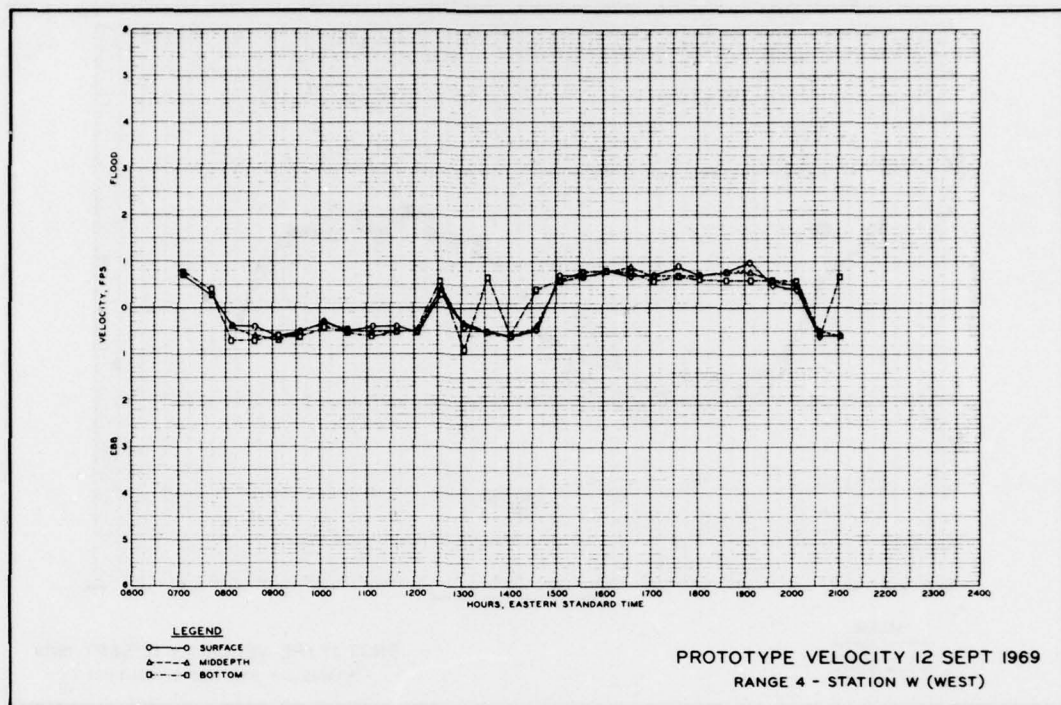


PLATE 27

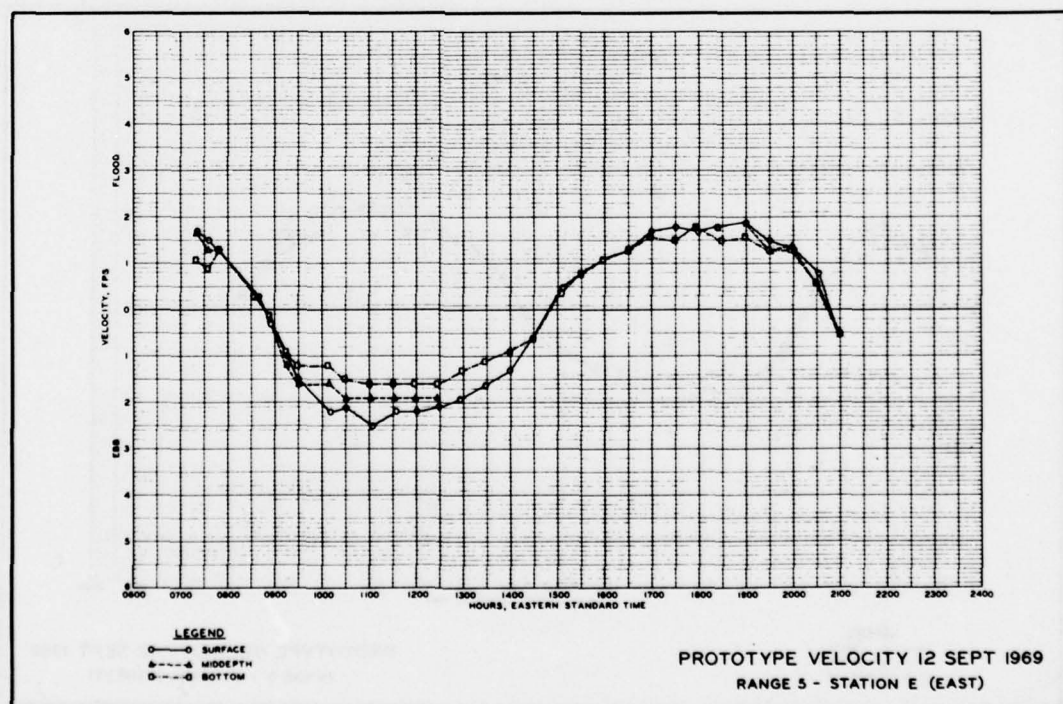


PLATE 28

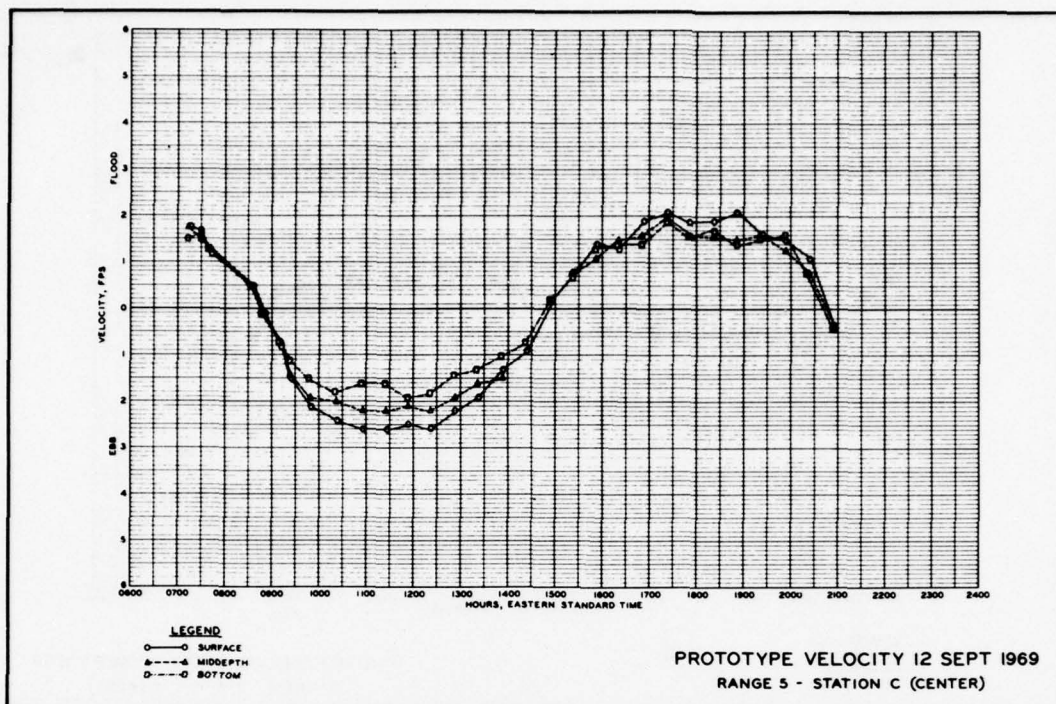


PLATE 29

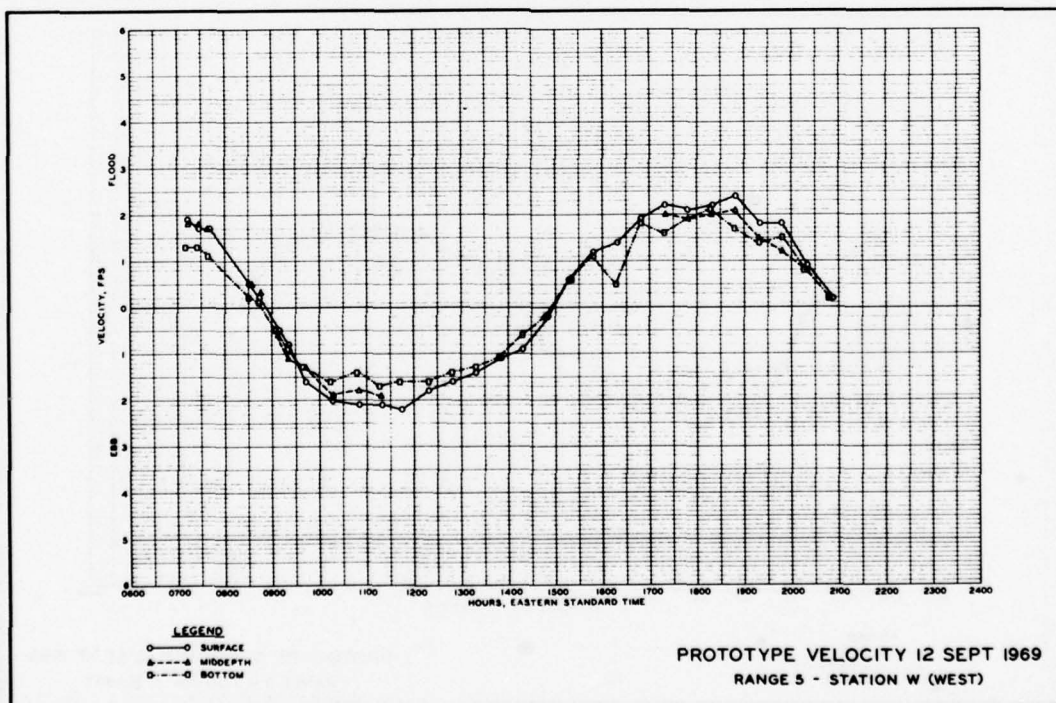


PLATE 30

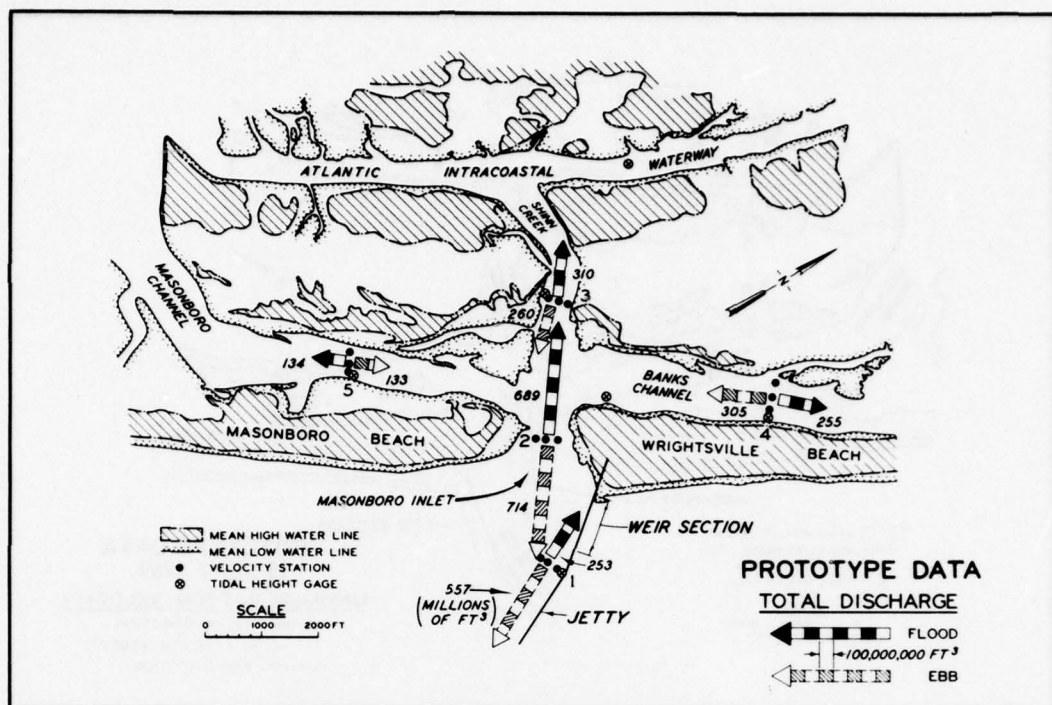


PLATE 31

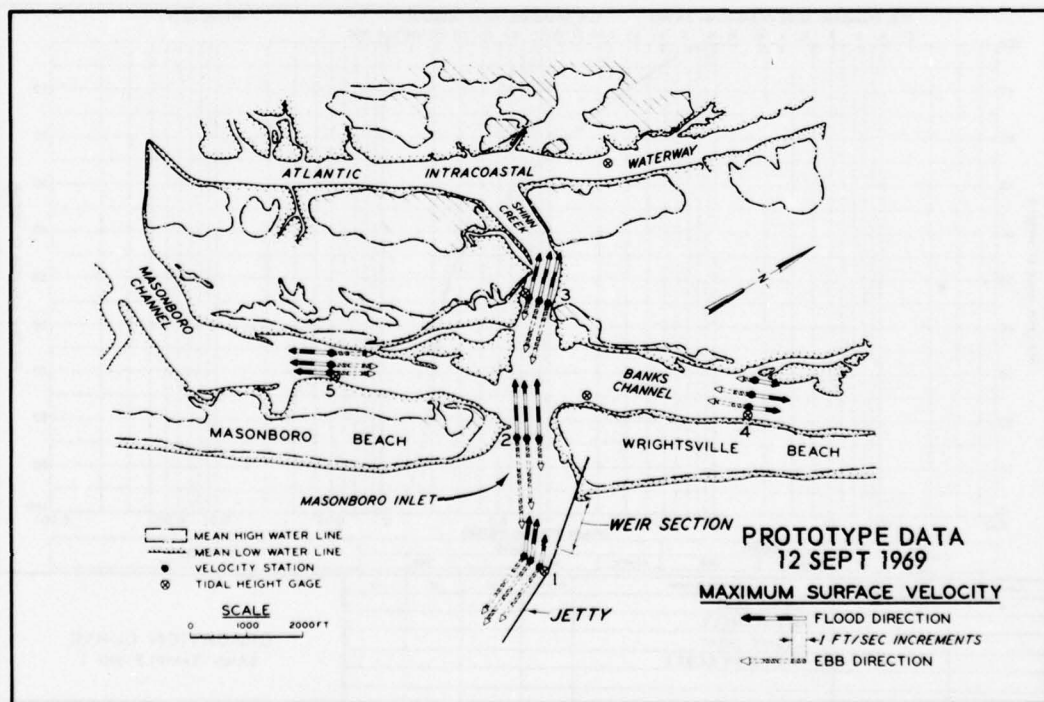


PLATE 32

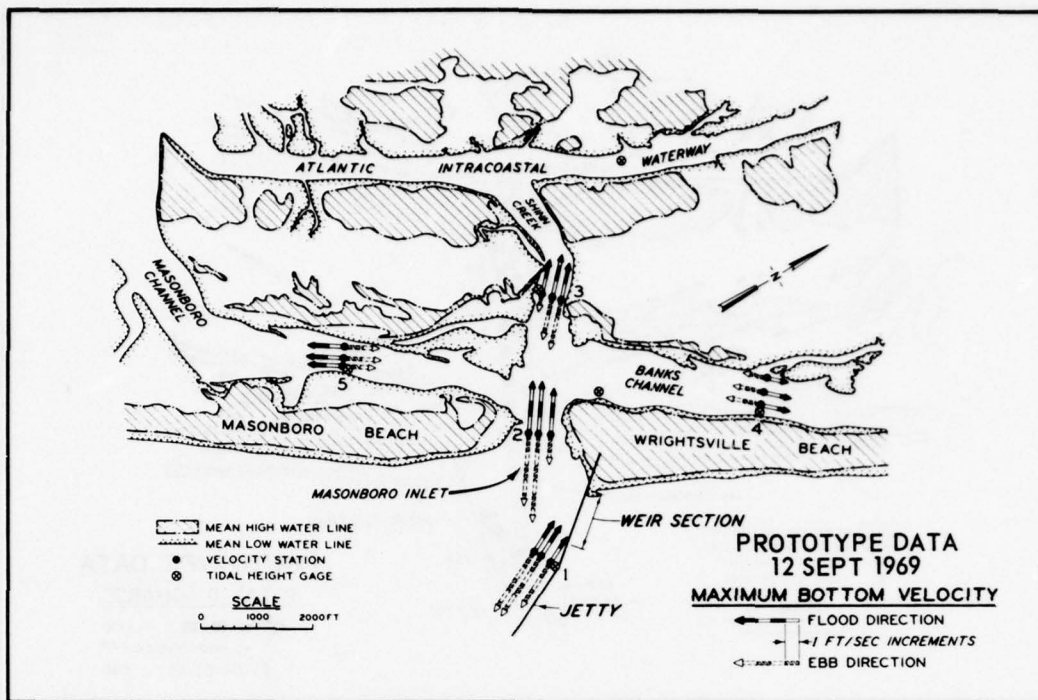


PLATE 33

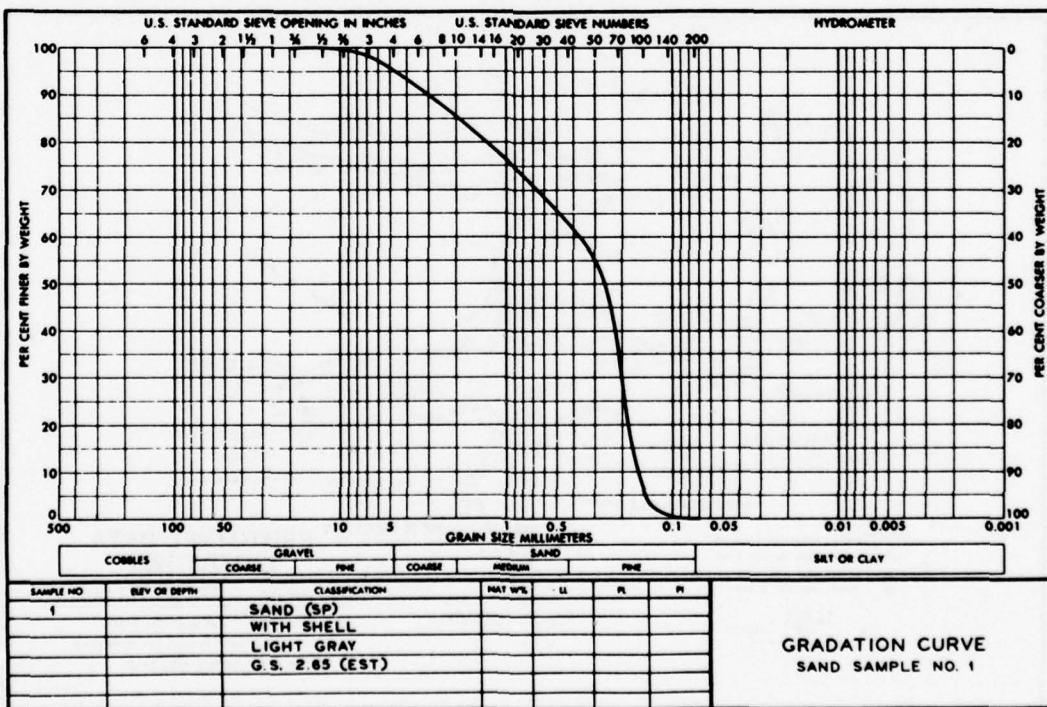
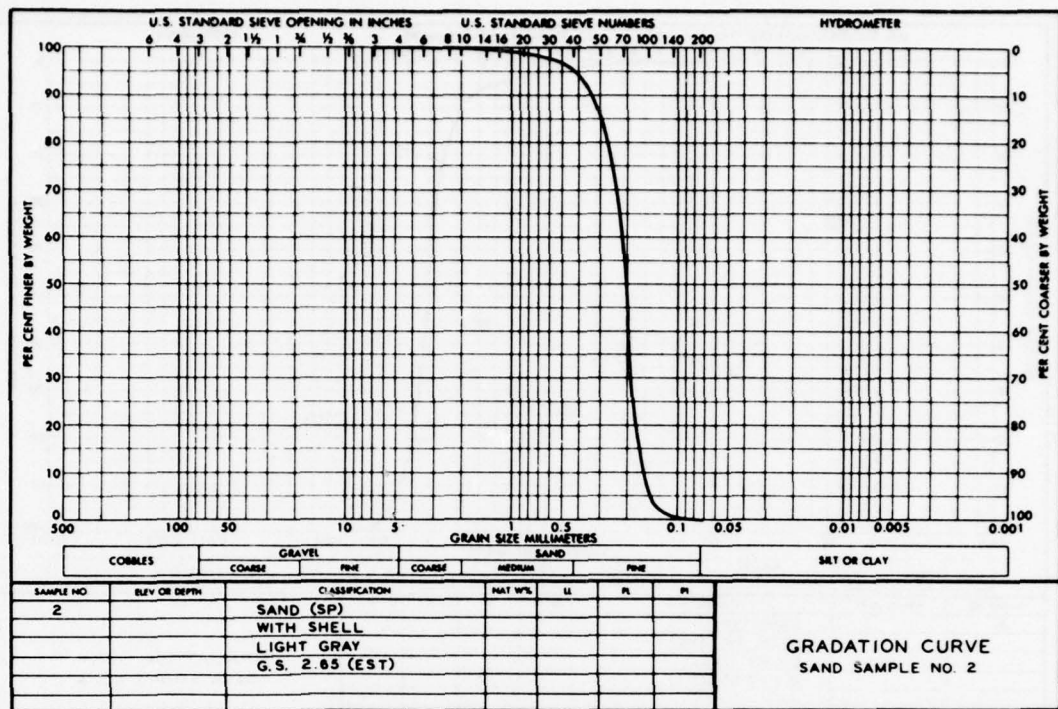


PLATE 34



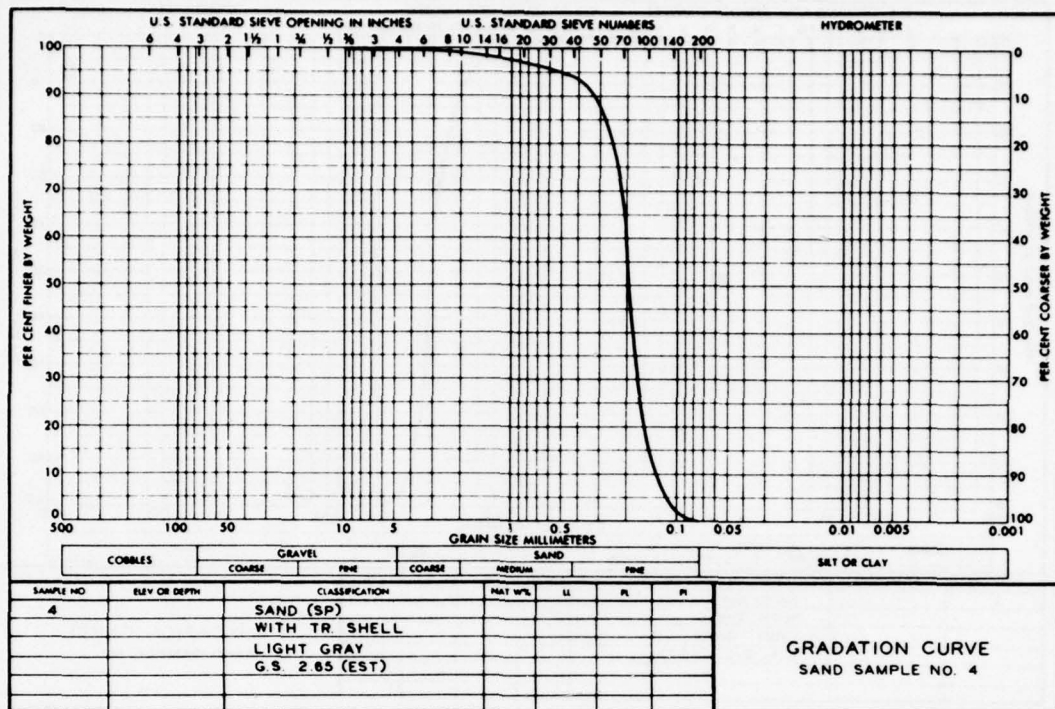


PLATE 37

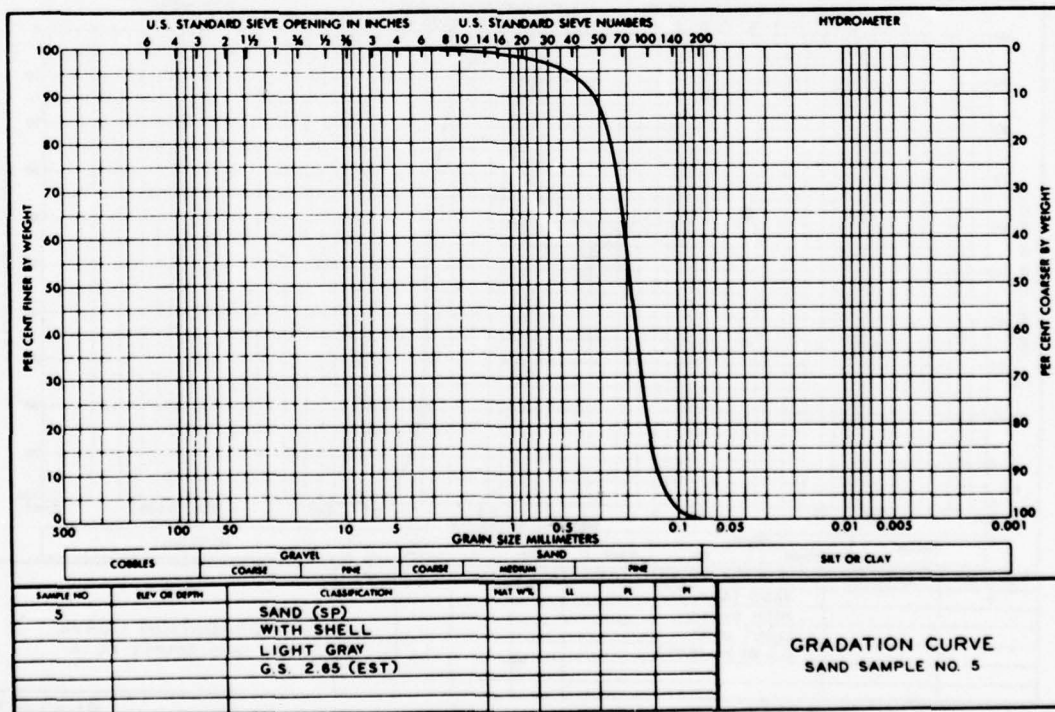


PLATE 38

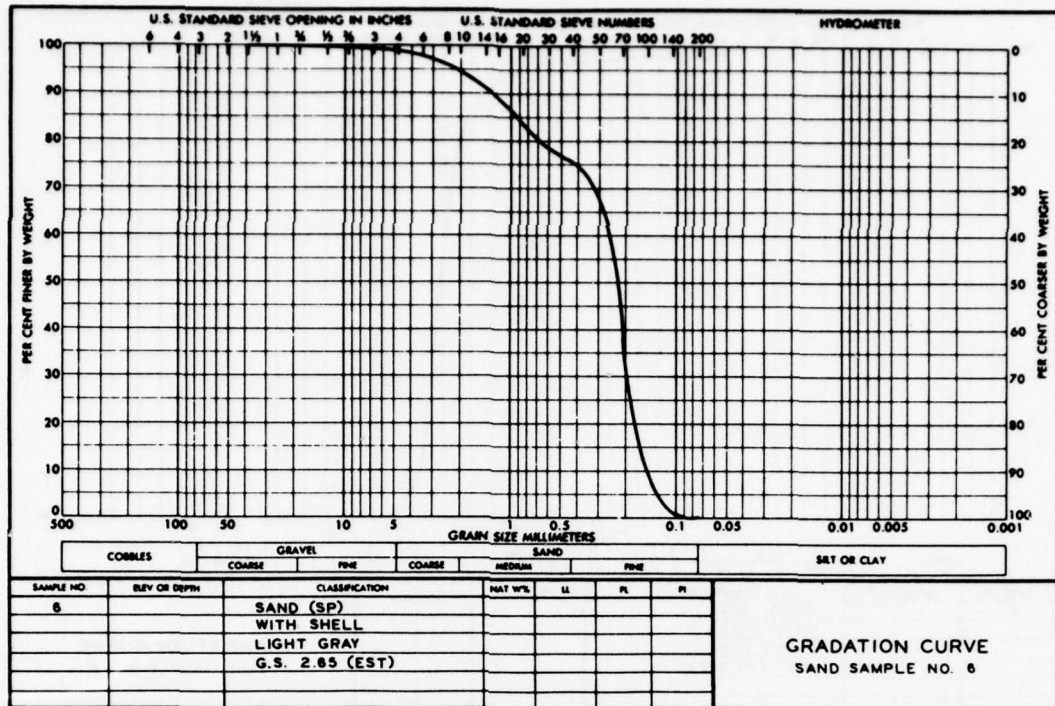


PLATE 39

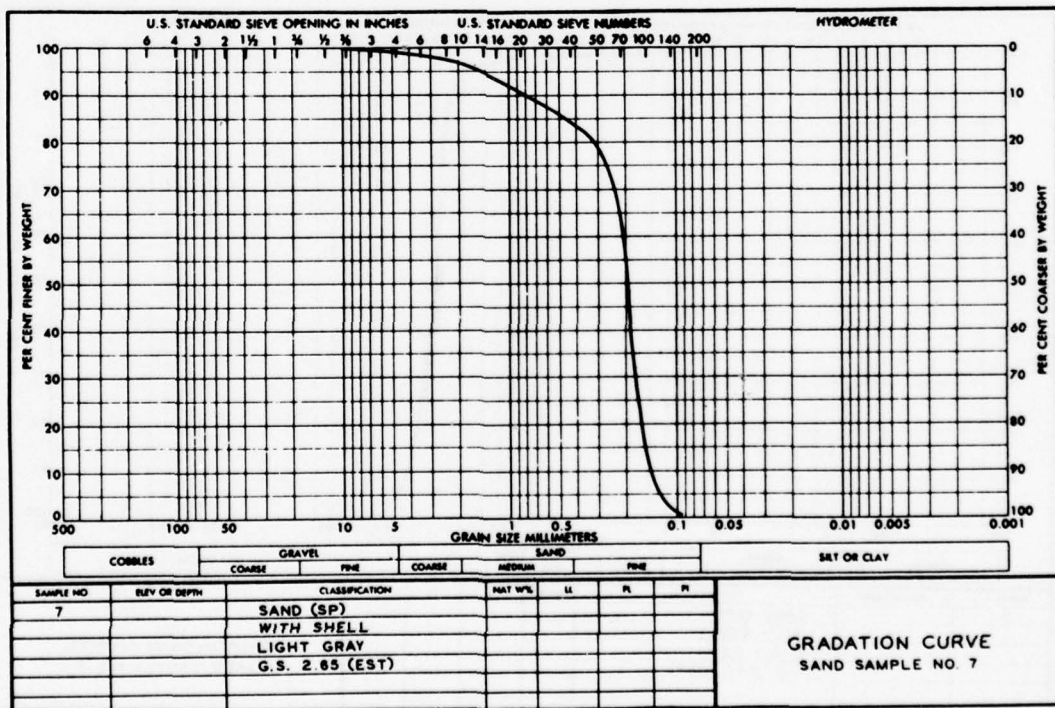


PLATE 40

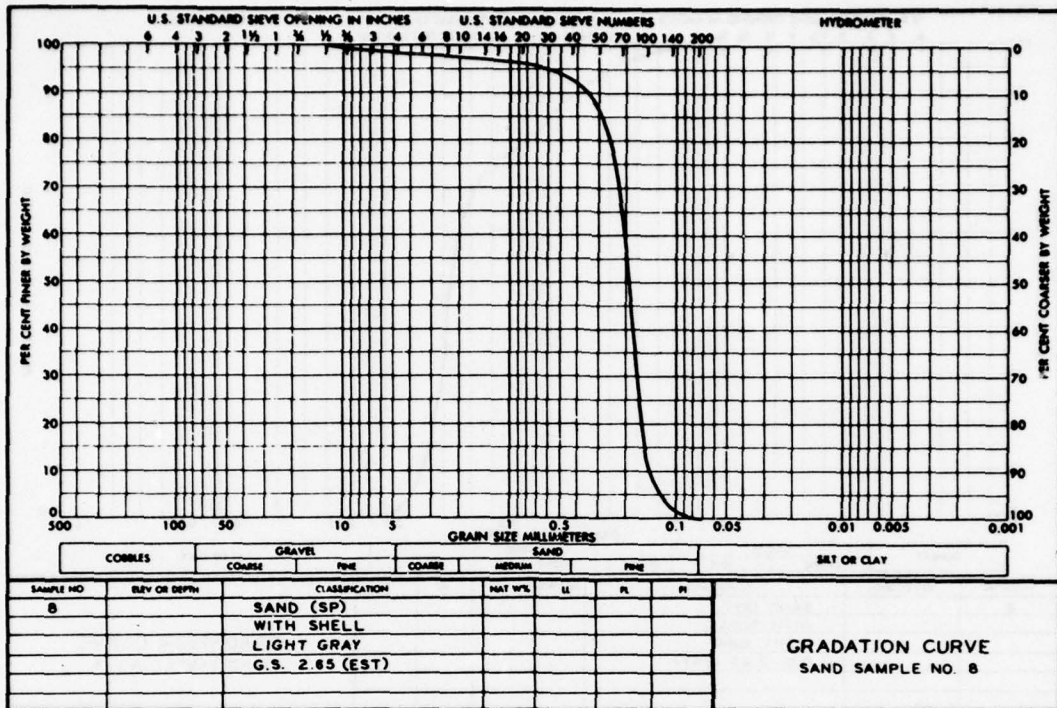


PLATE 41

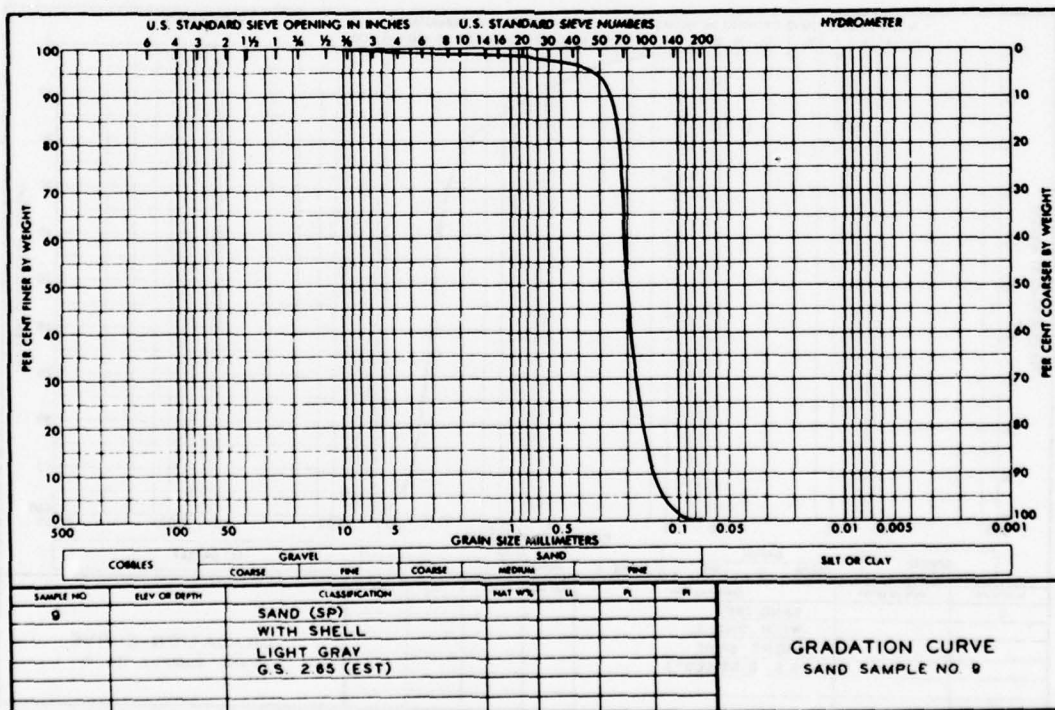


PLATE 42

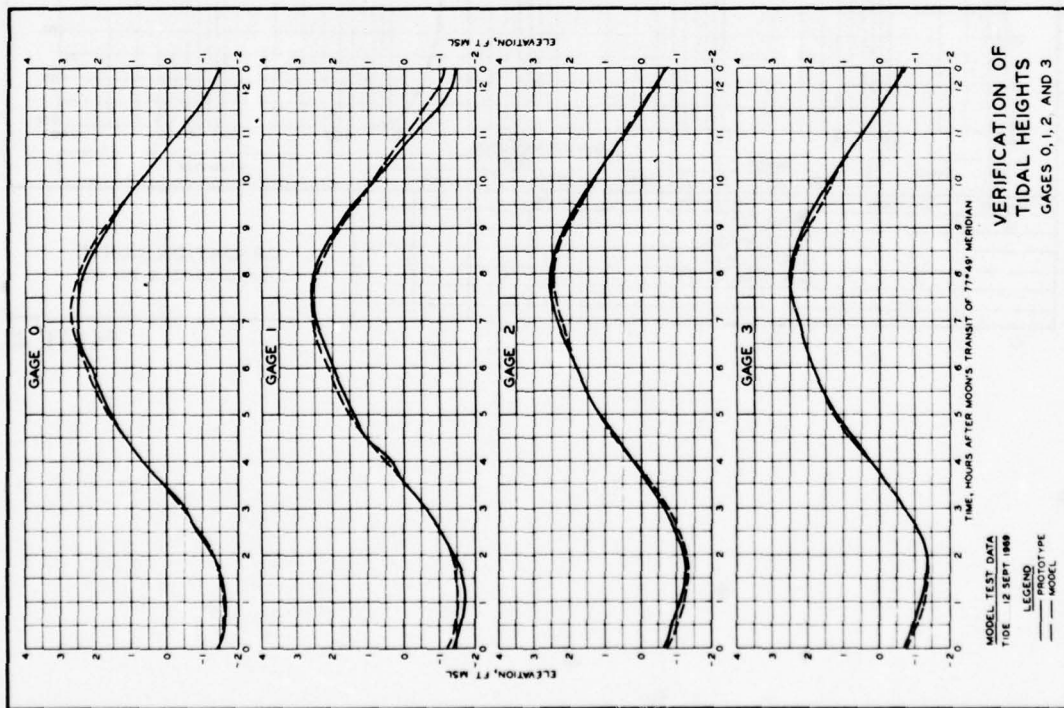


PLATE 44

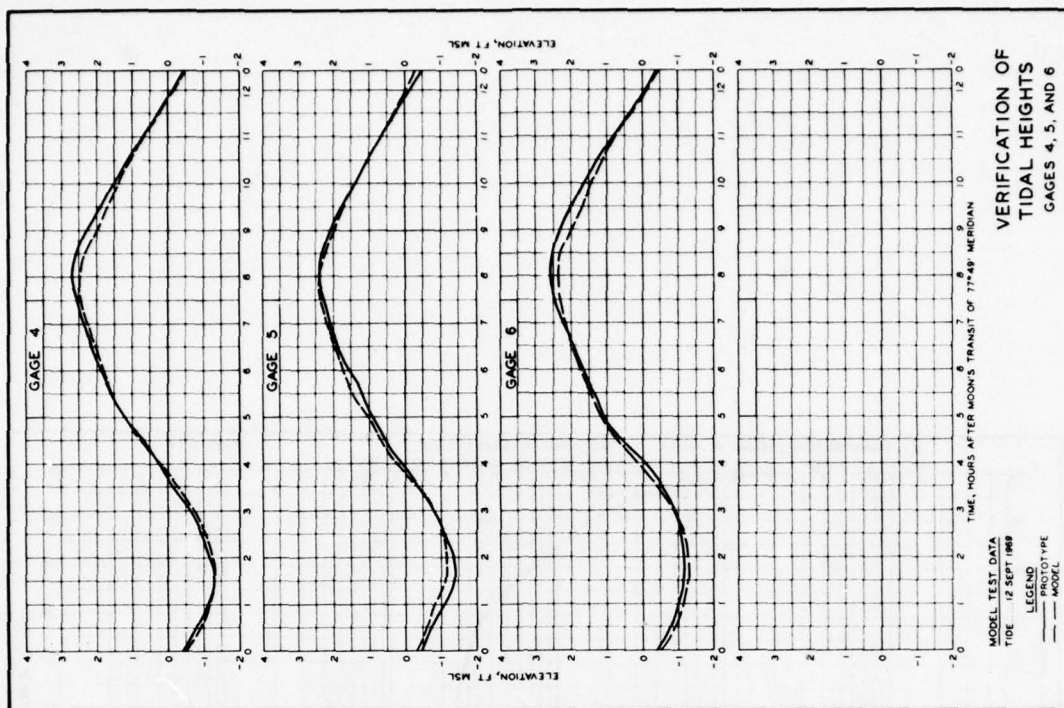


PLATE 45

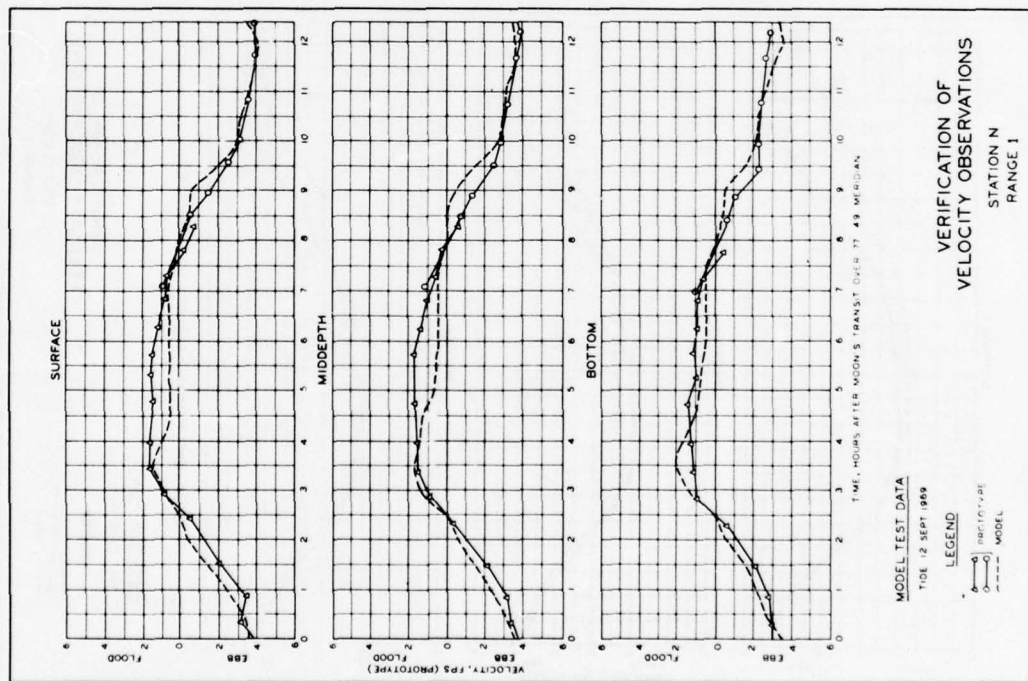


PLATE 46

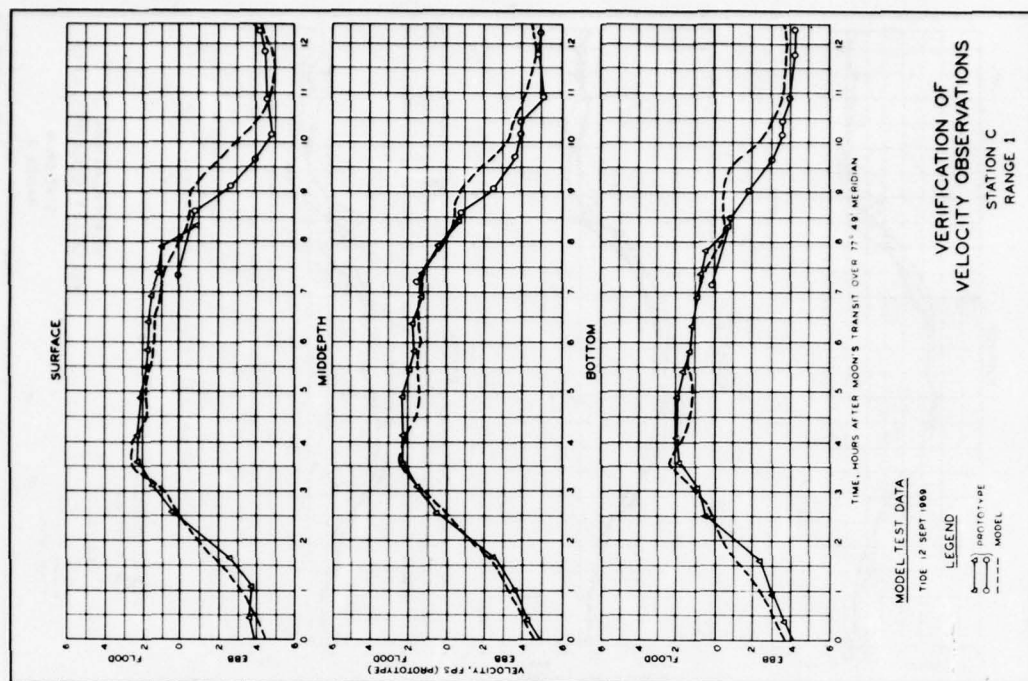


PLATE 47

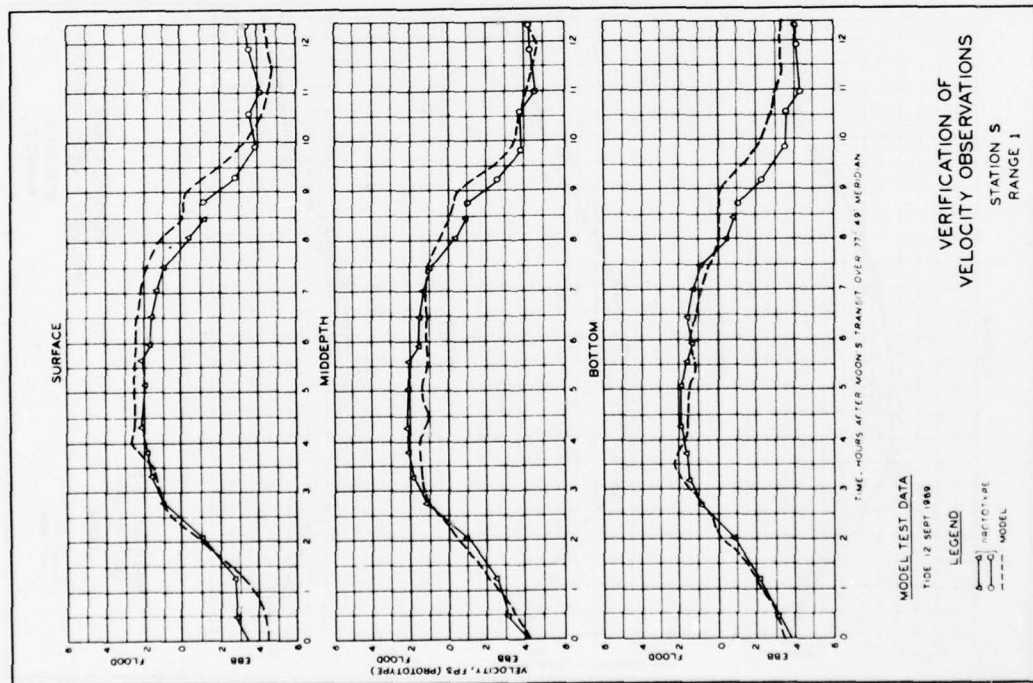


PLATE 48

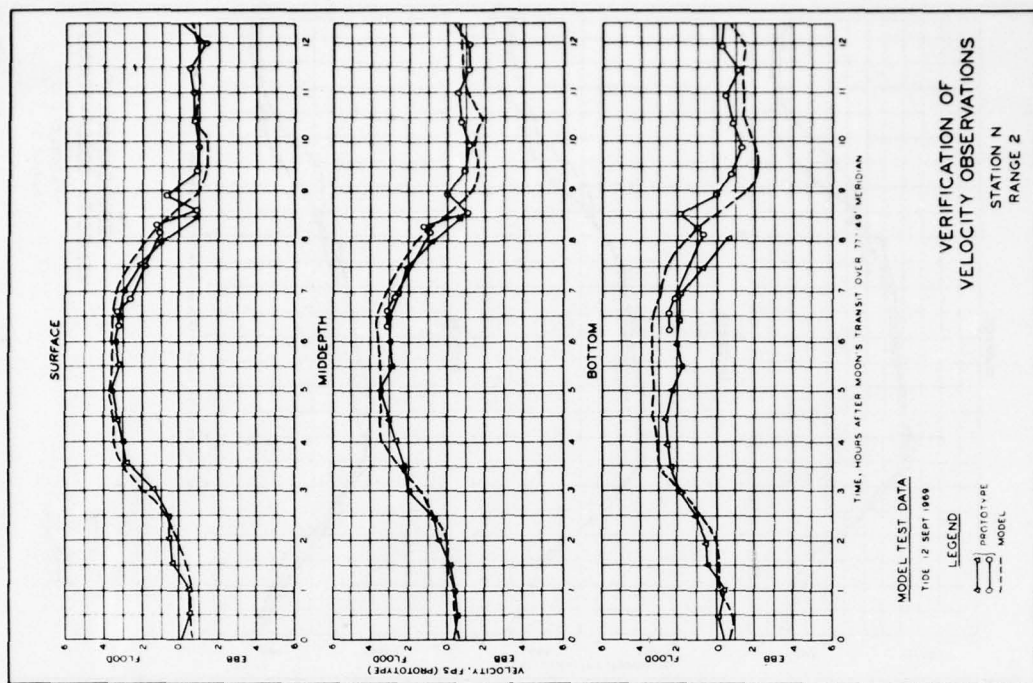


PLATE 49

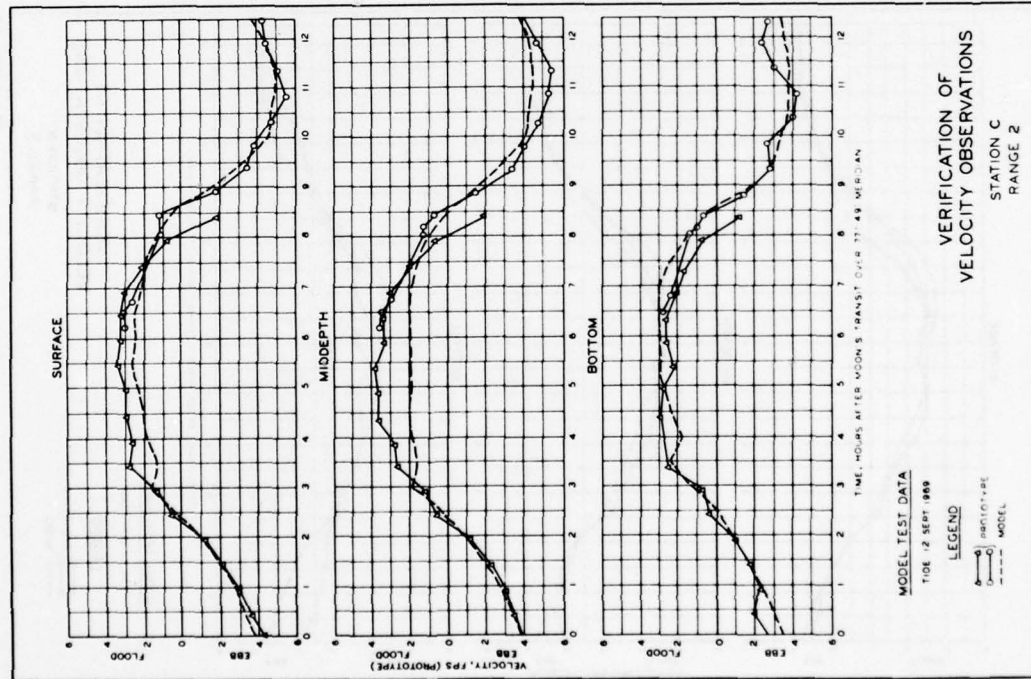


PLATE 50

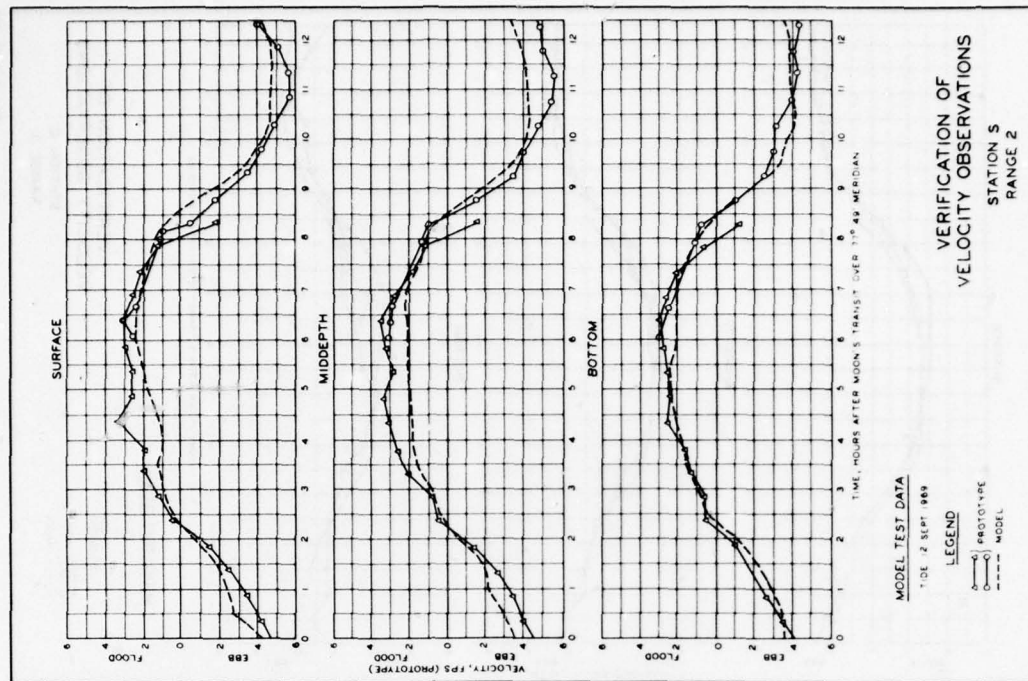


PLATE 51

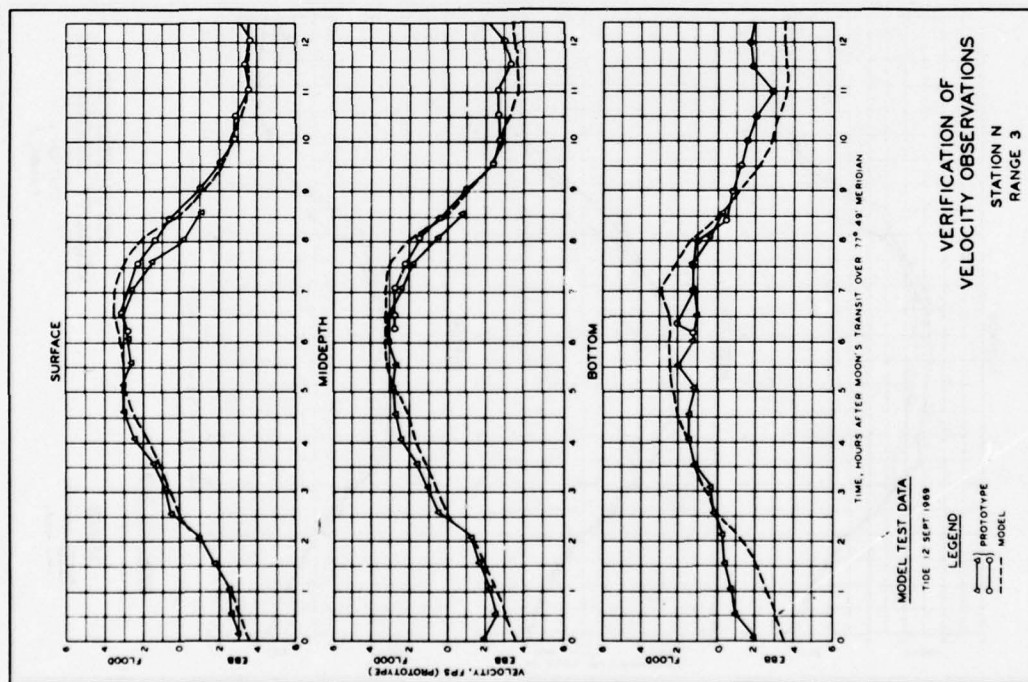


PLATE 52

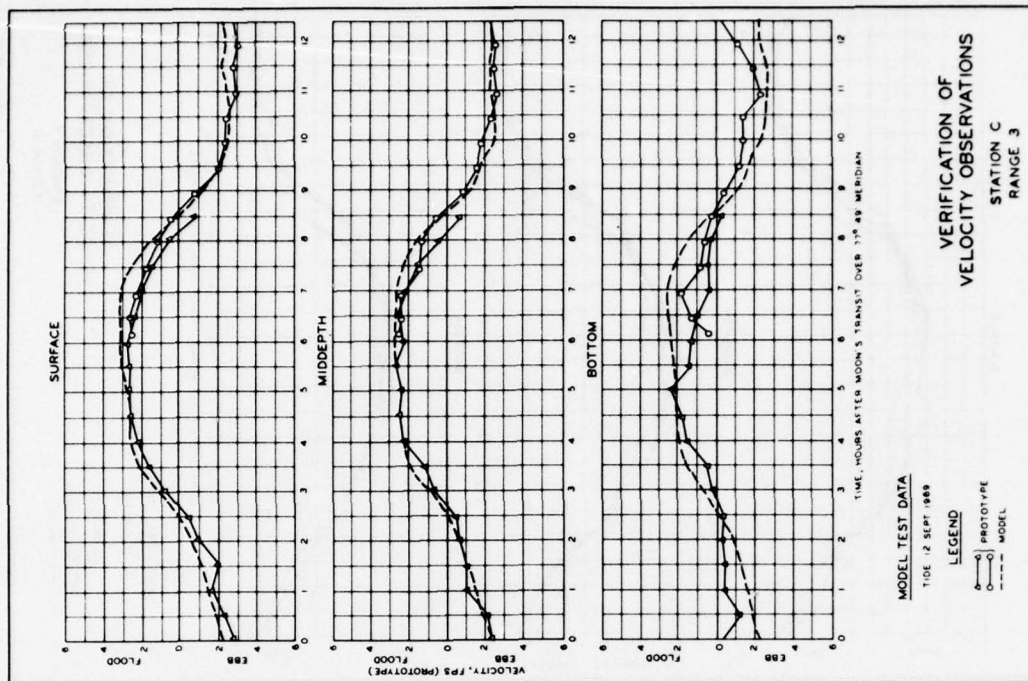


PLATE 53

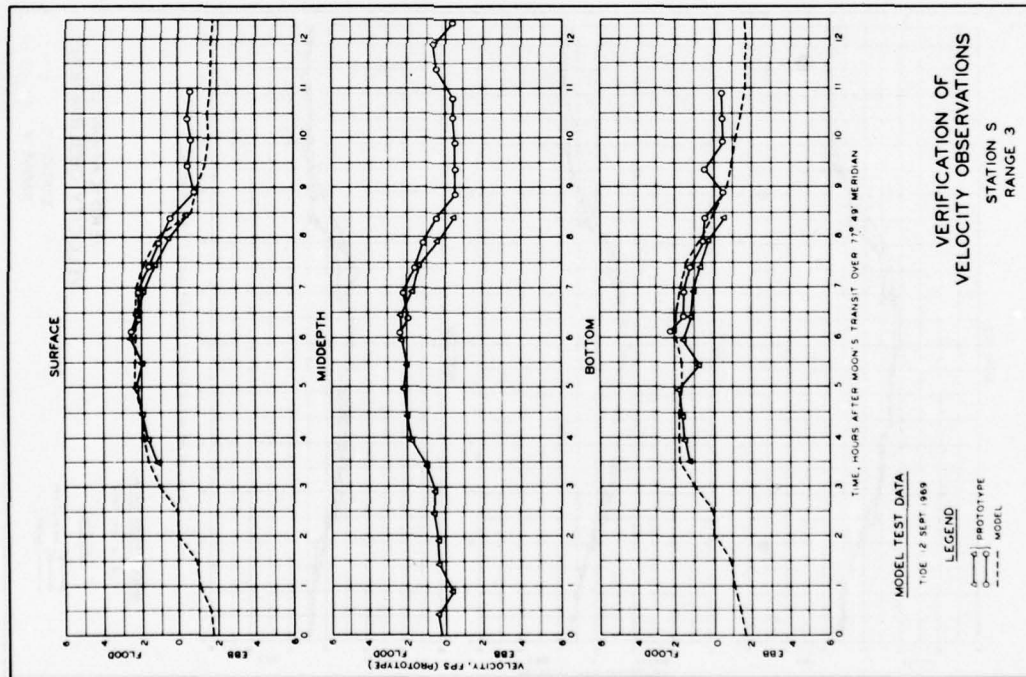


PLATE 54

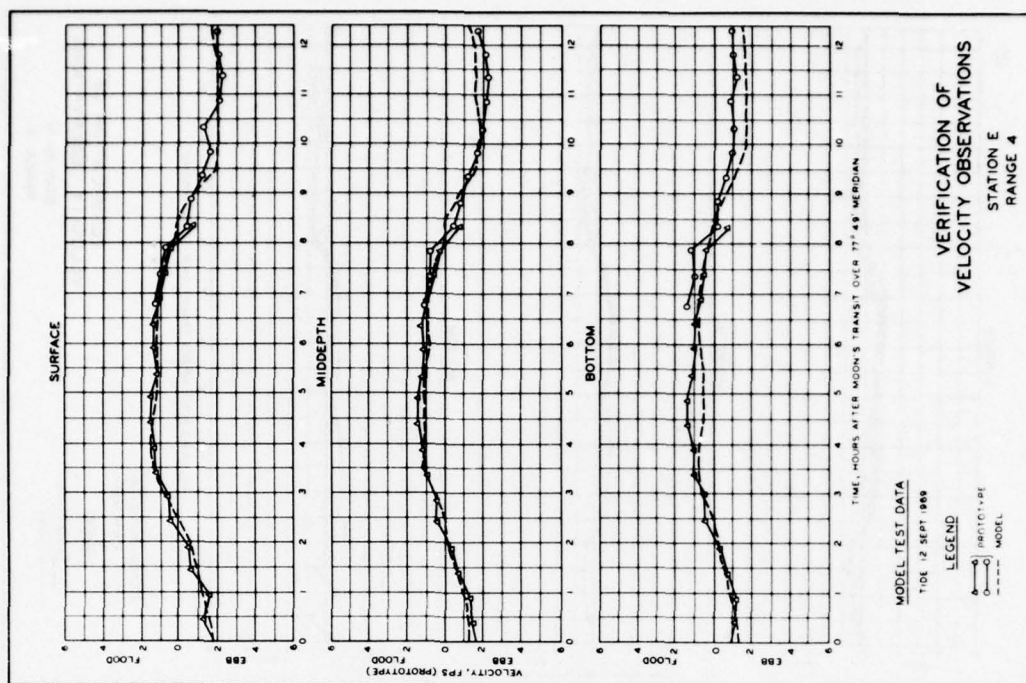


PLATE 55

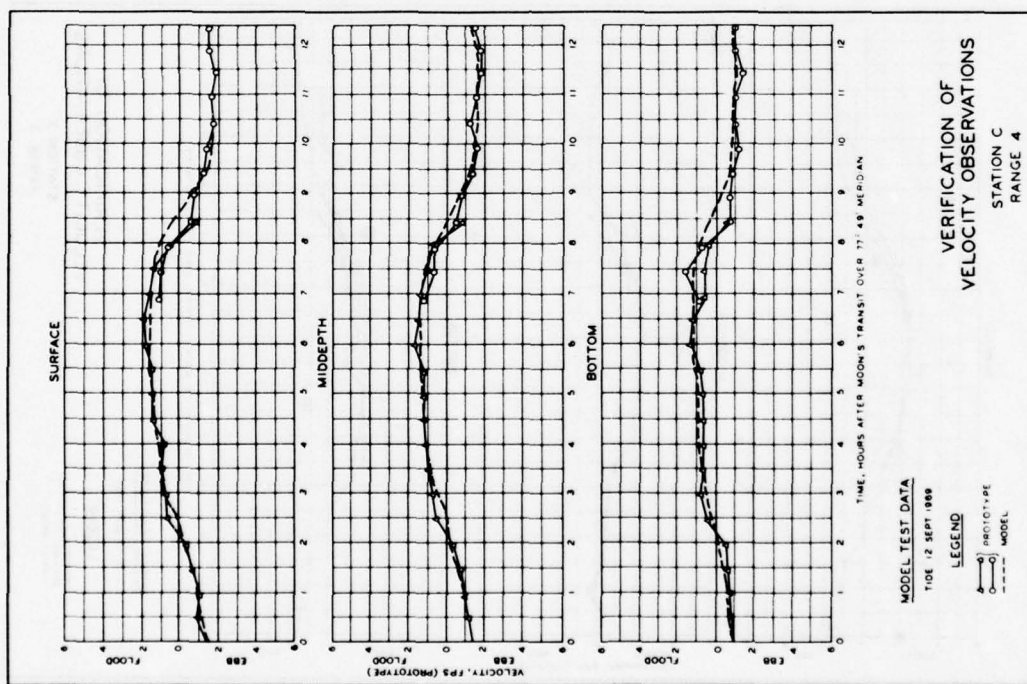


PLATE 56

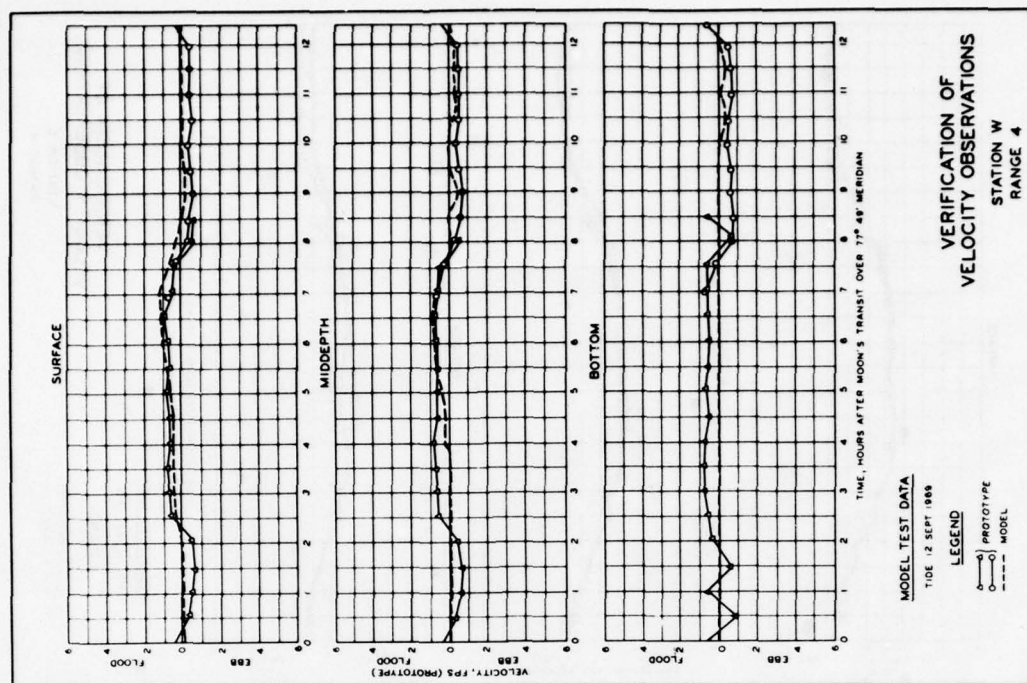


PLATE 57

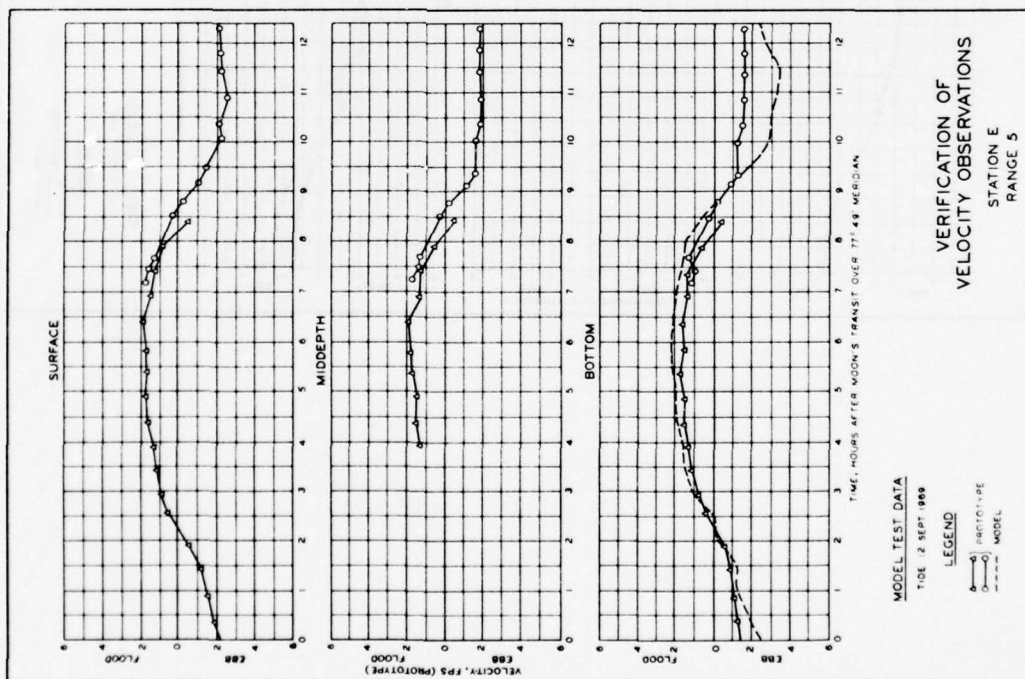


PLATE 58

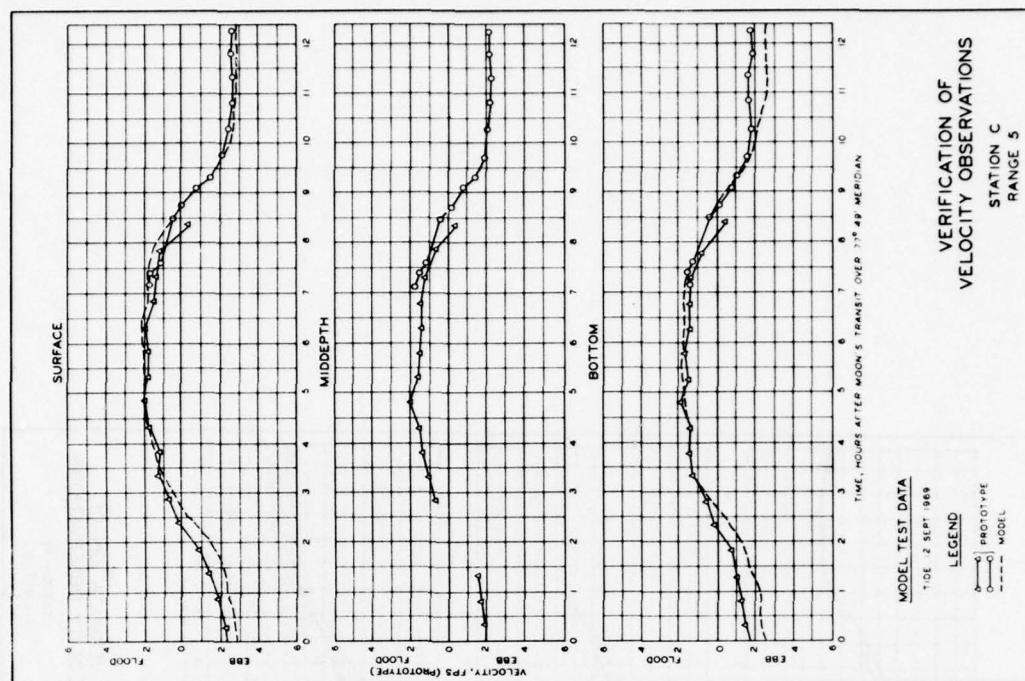
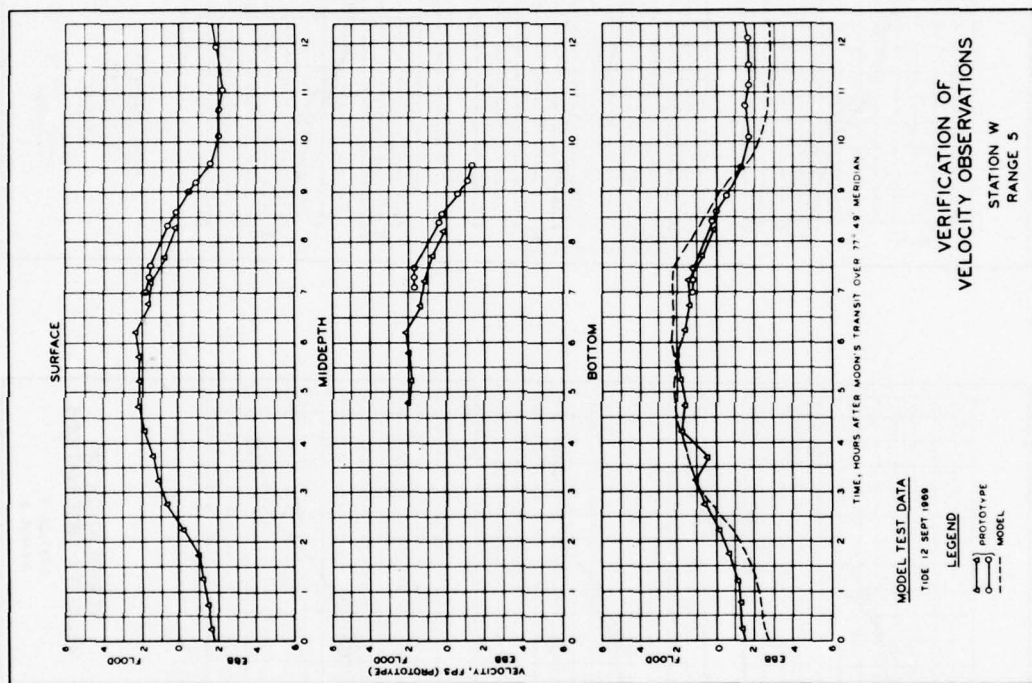


PLATE 59



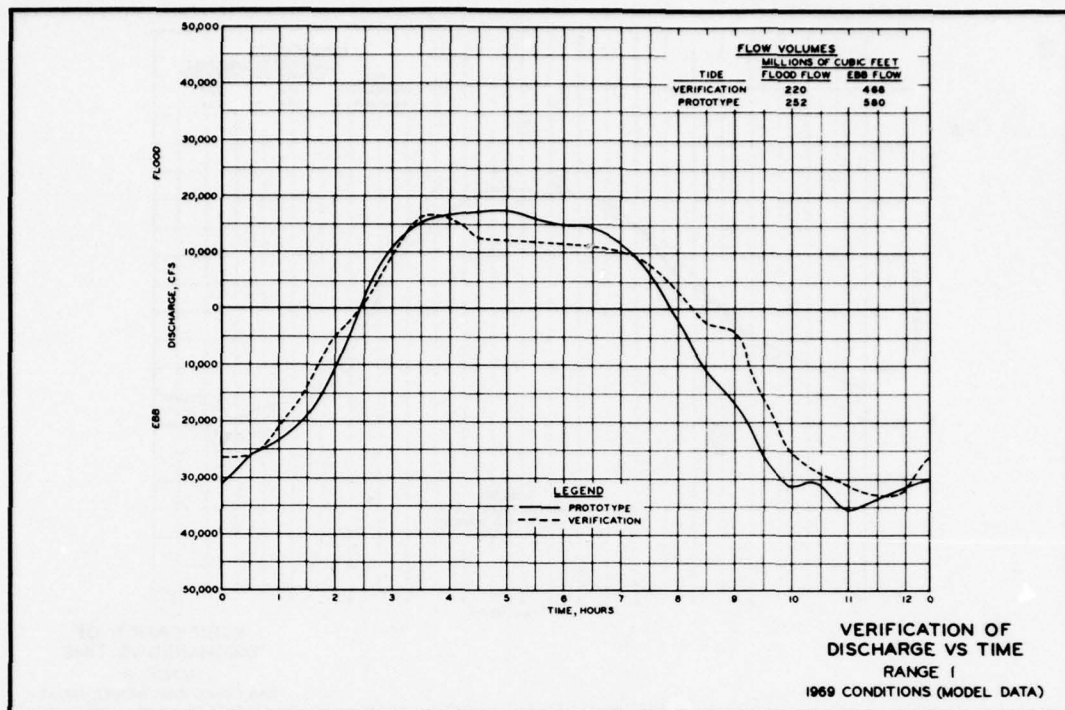


PLATE 61

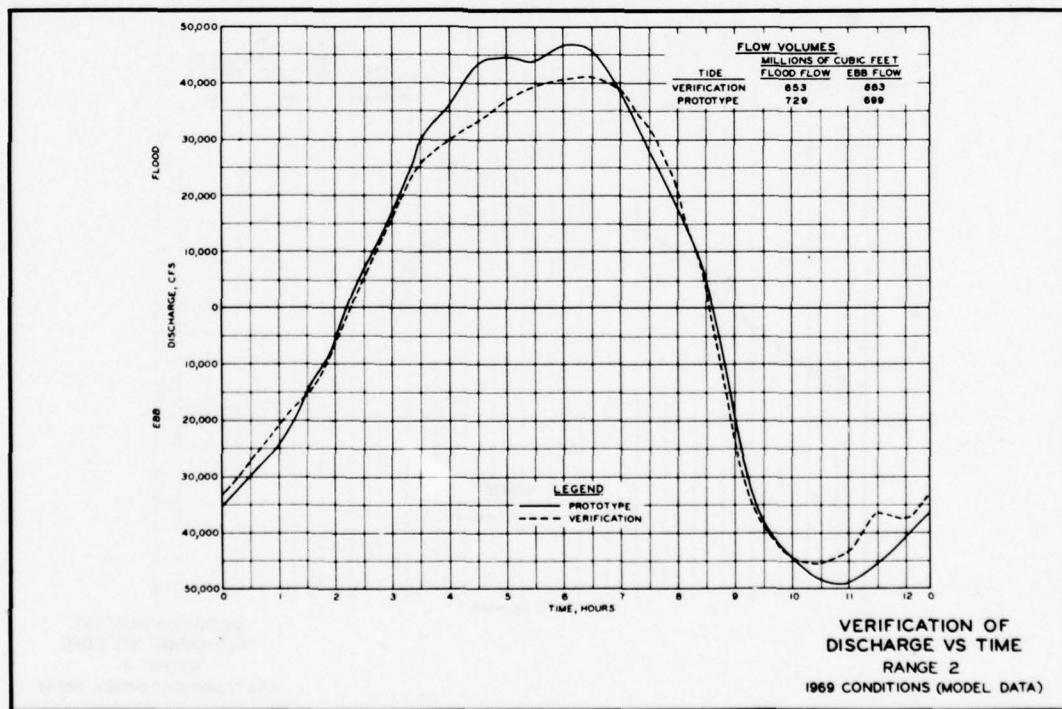


PLATE 62

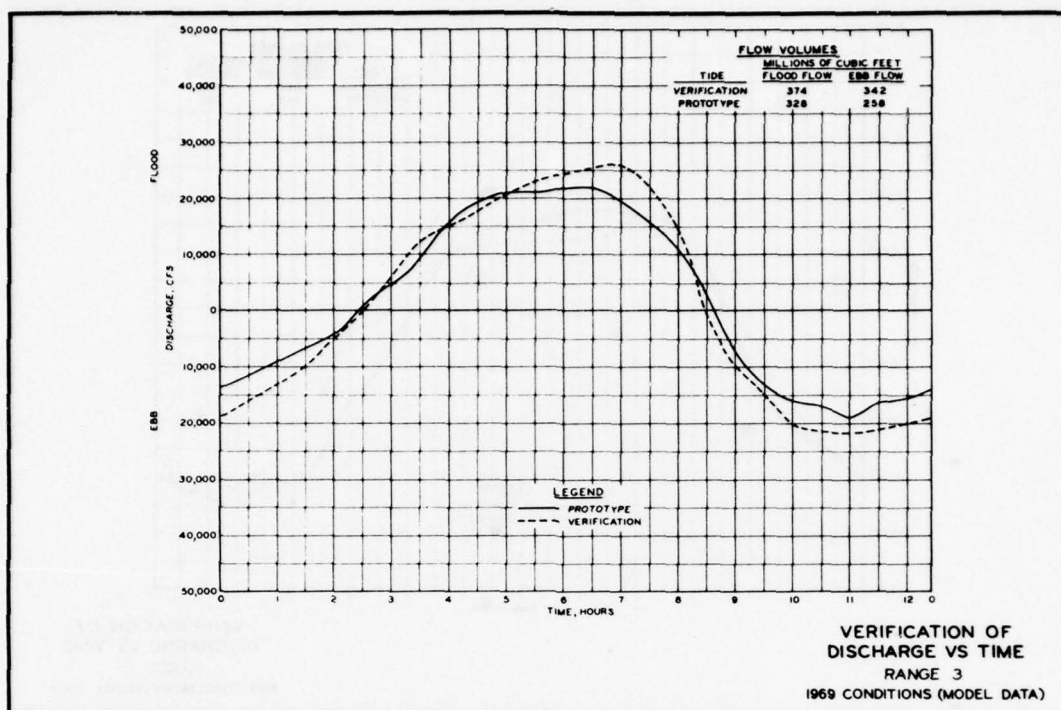


PLATE 63

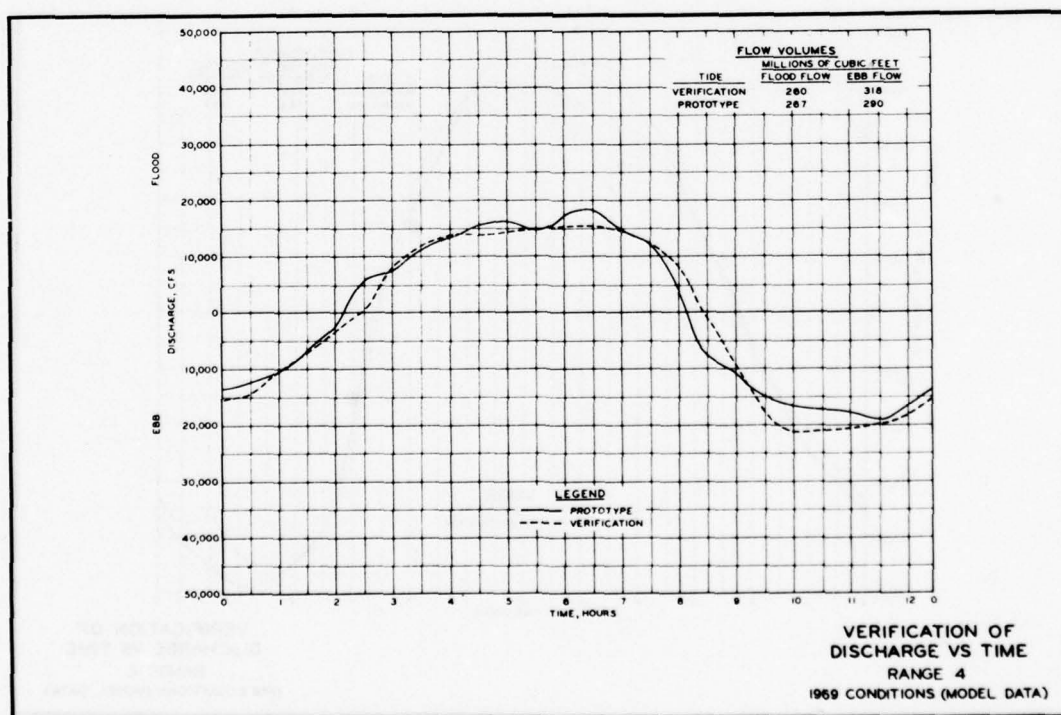
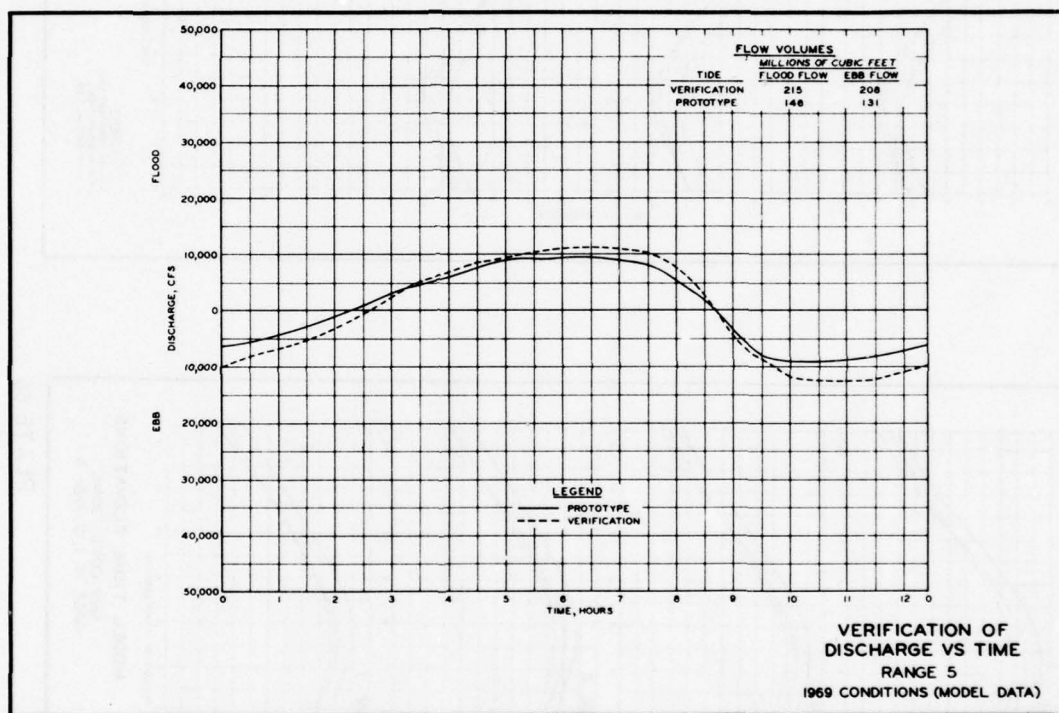


PLATE 64



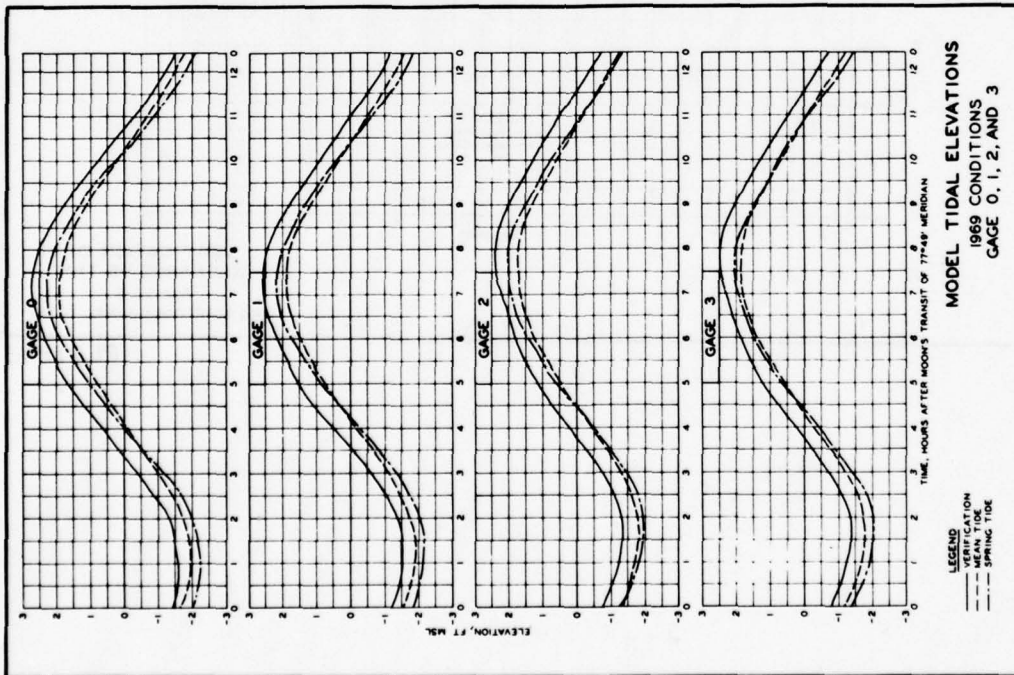


PLATE 66

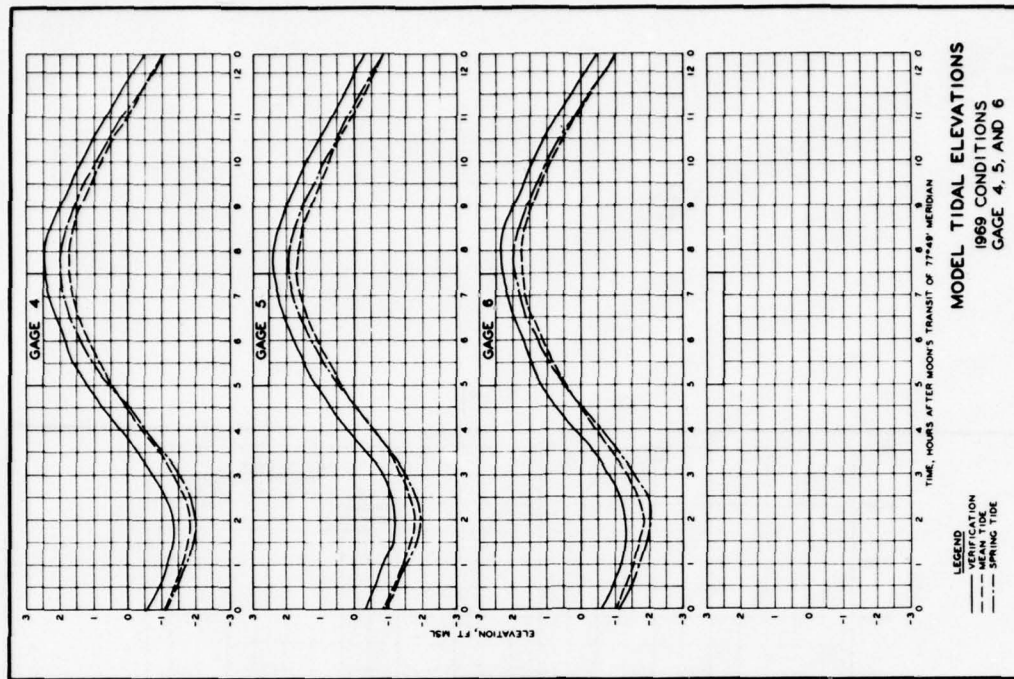


PLATE 67

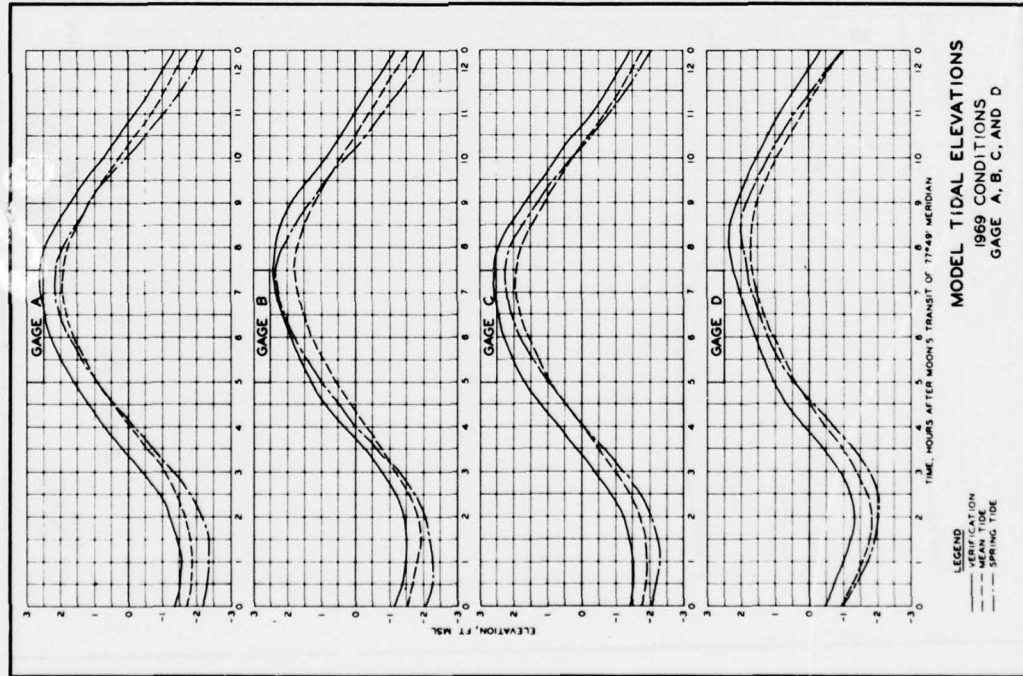


PLATE 68

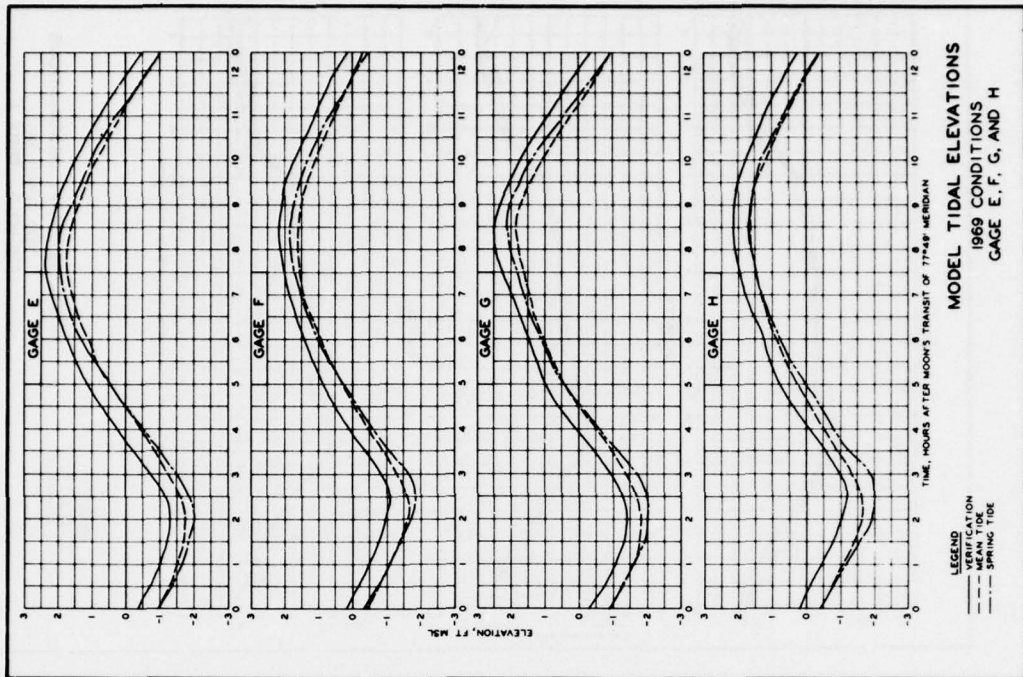


PLATE 69

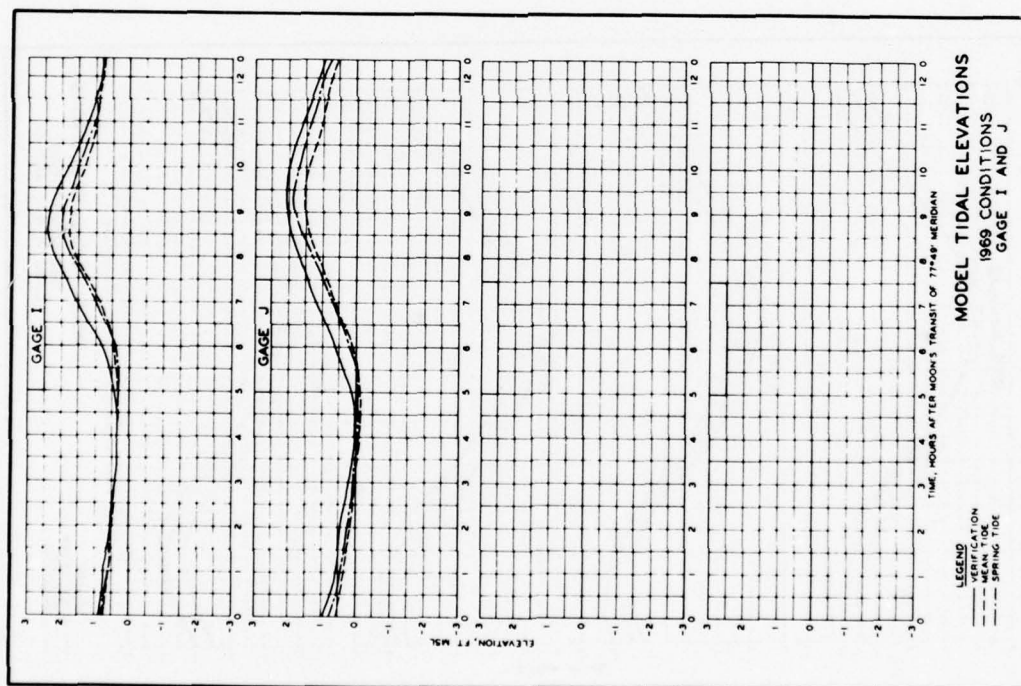


PLATE 70

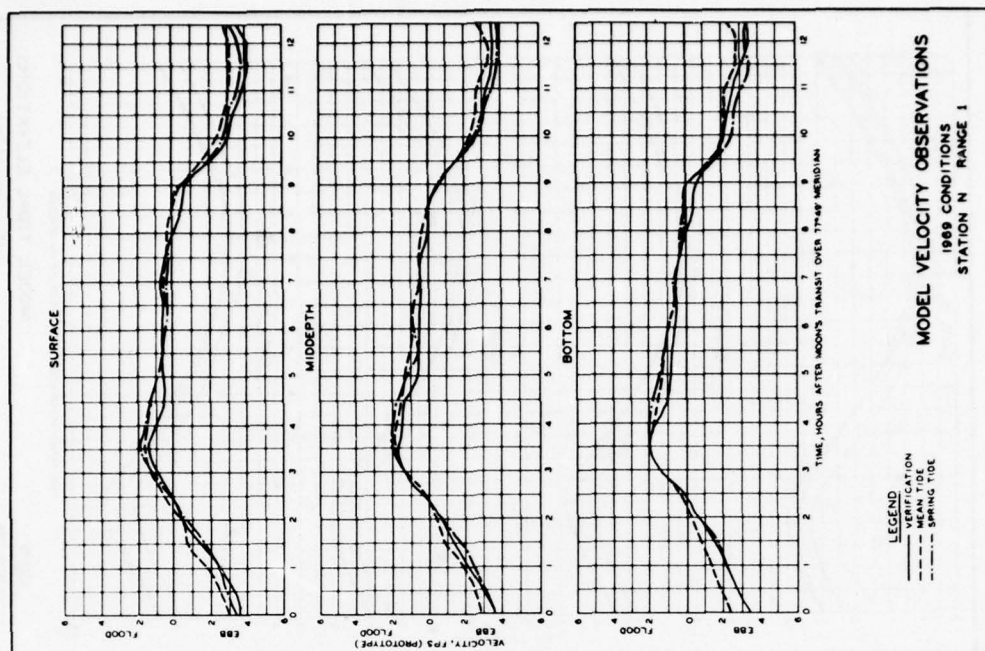


PLATE 71

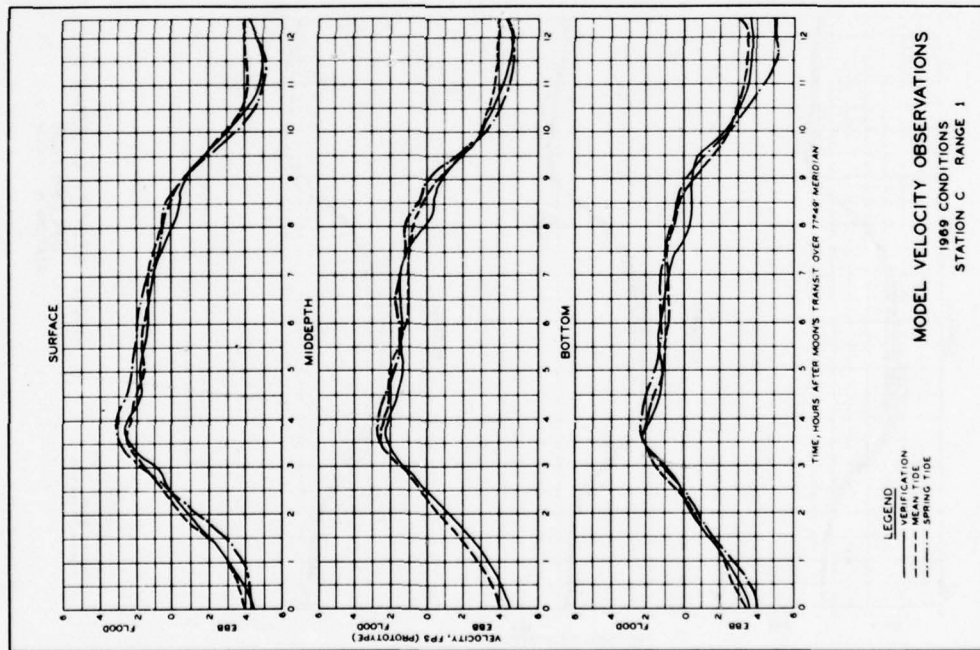


PLATE 72

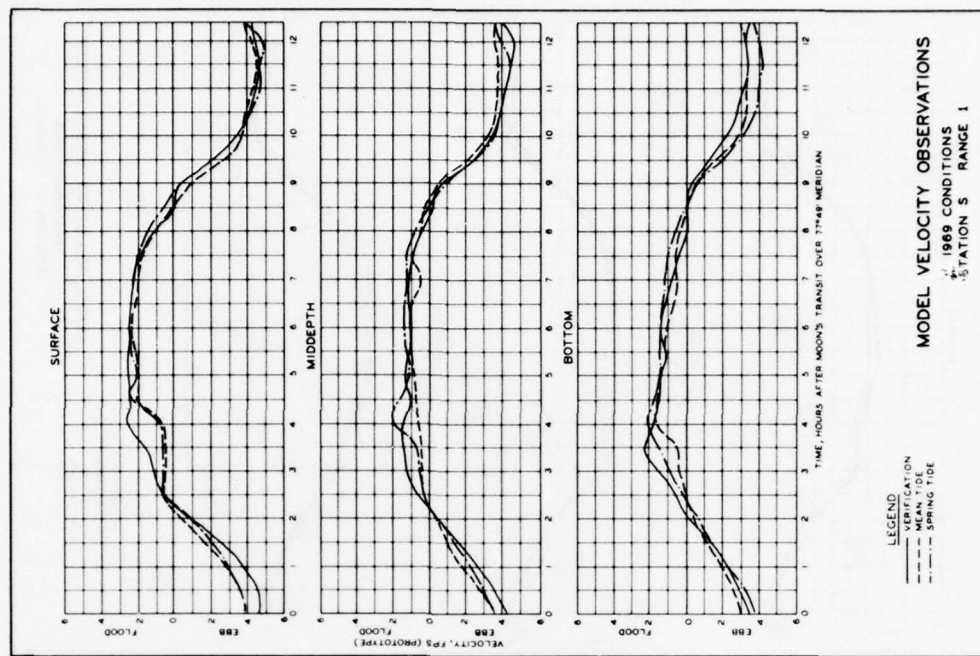


PLATE 73

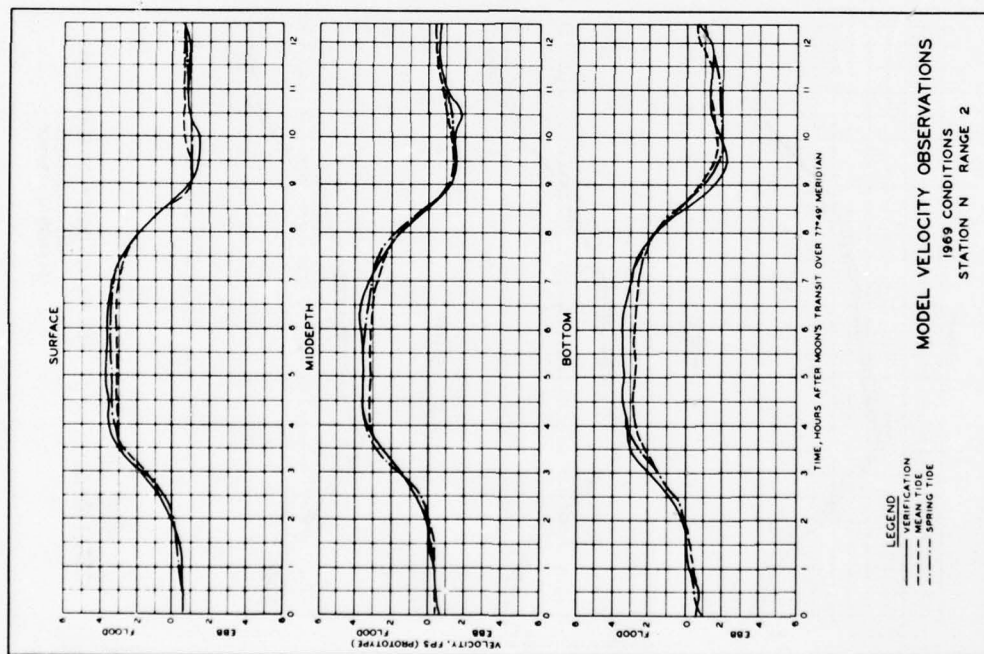


PLATE 74

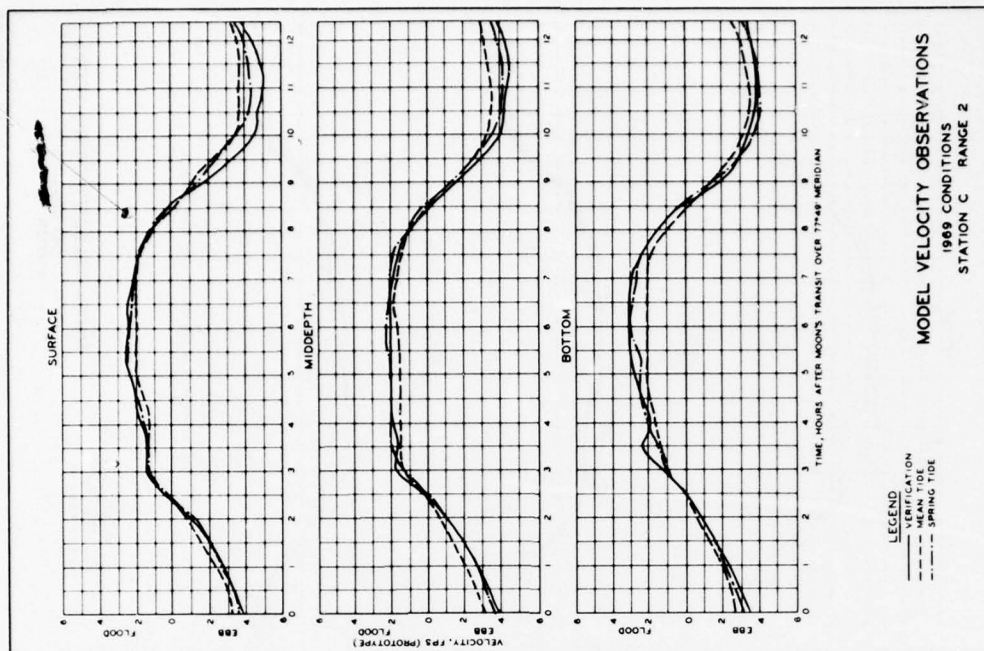


PLATE 75

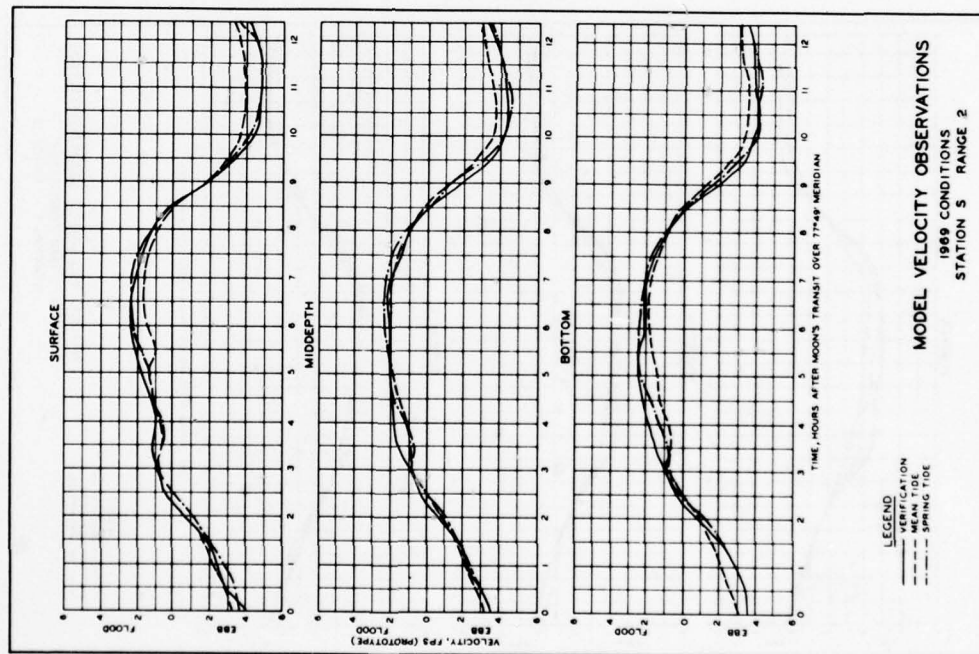


PLATE 76

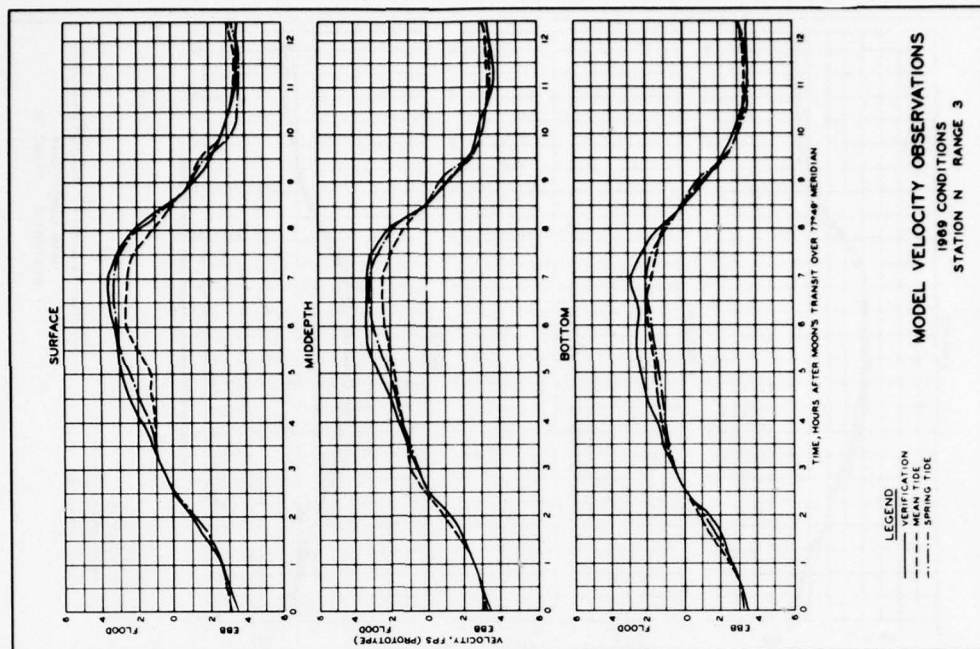


PLATE 77

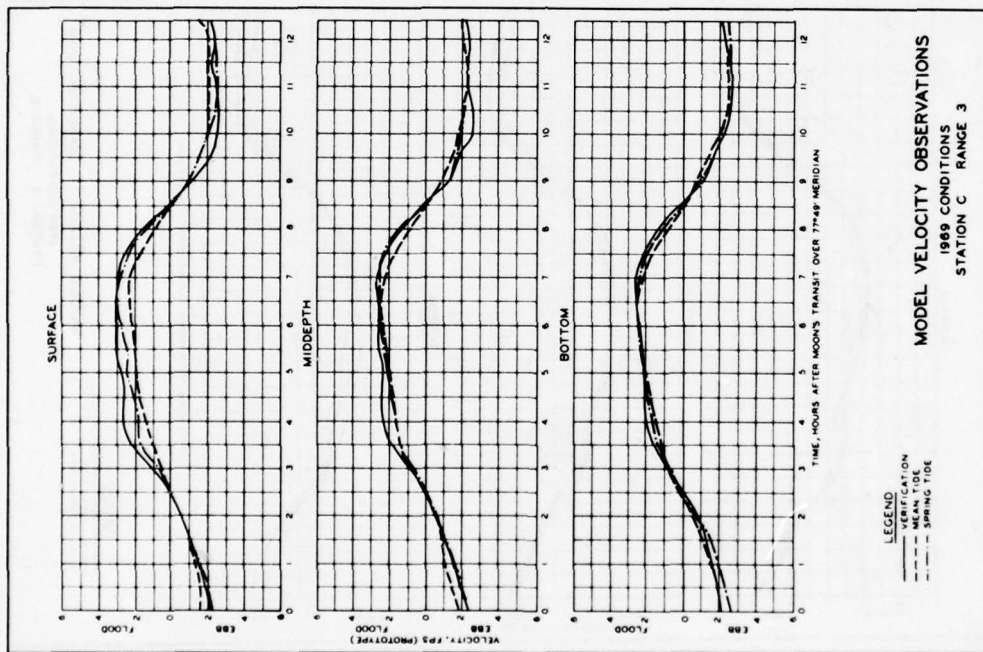


PLATE 78

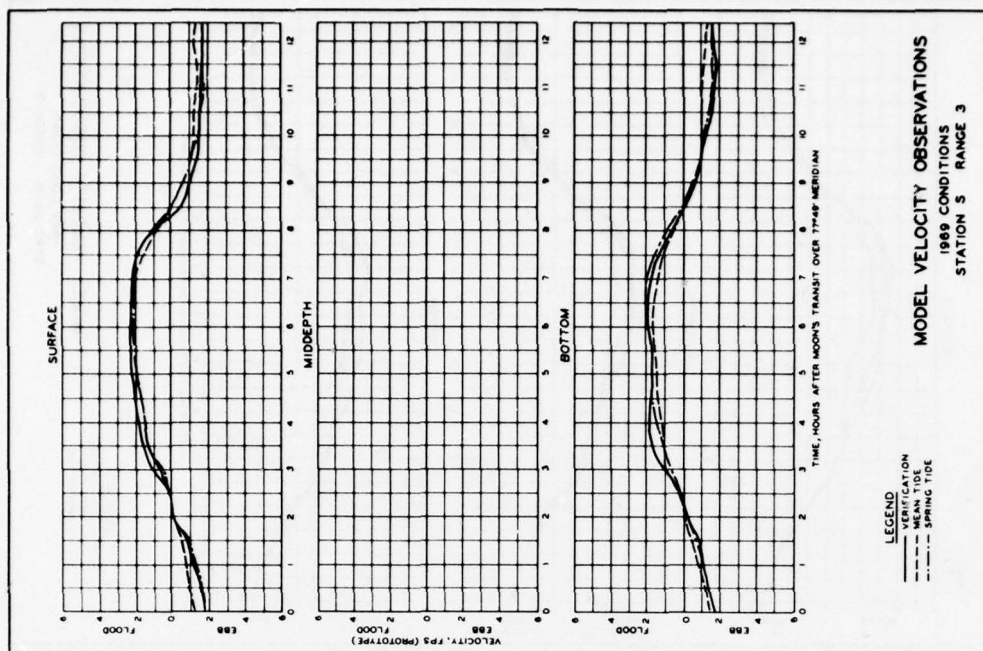


PLATE 79

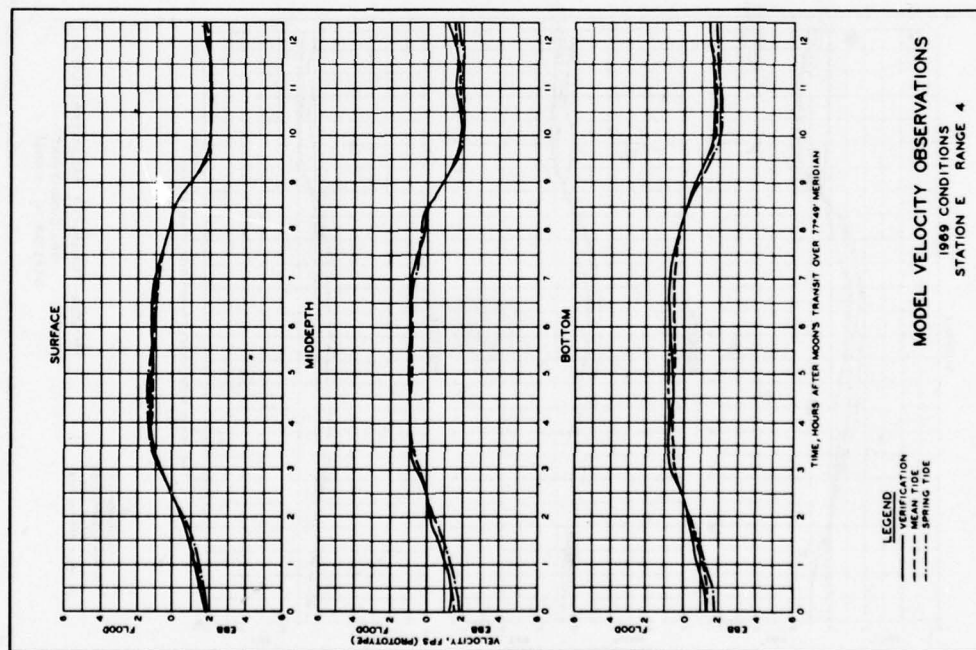


PLATE 80

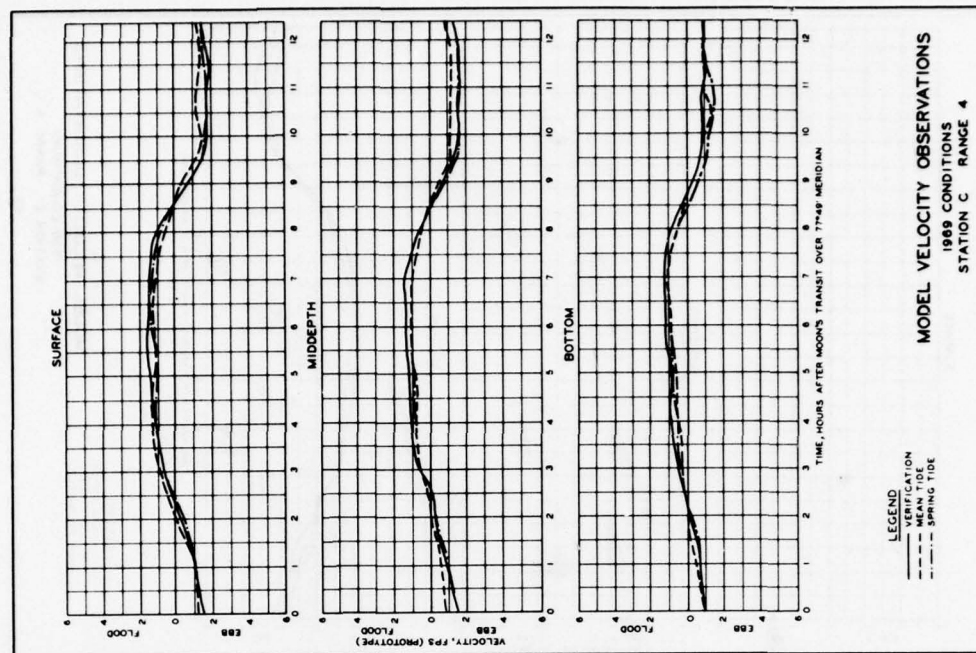


PLATE 81

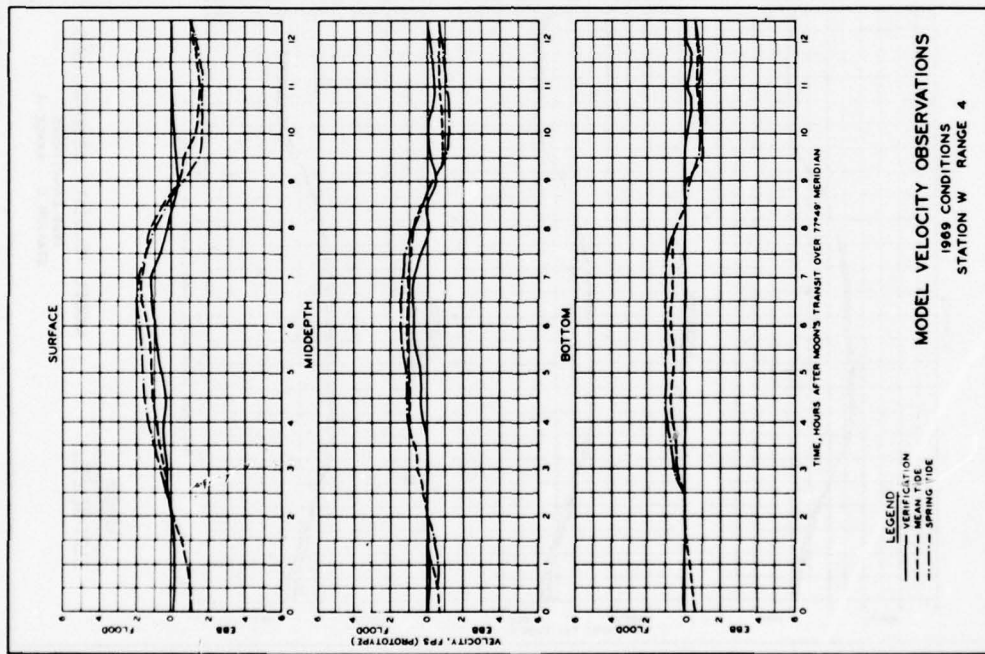


PLATE 82

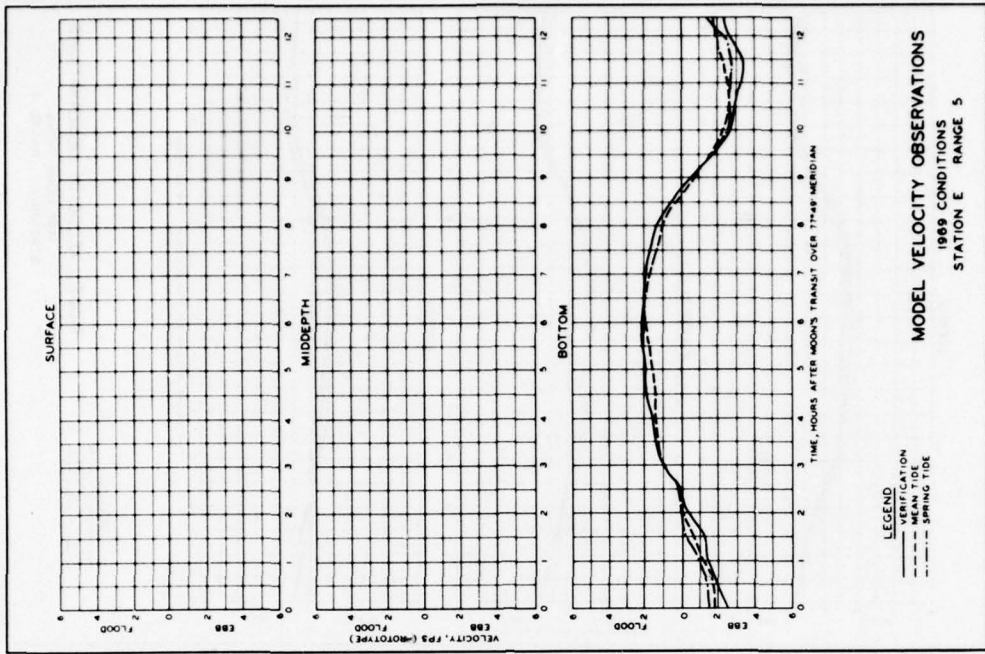


PLATE 83

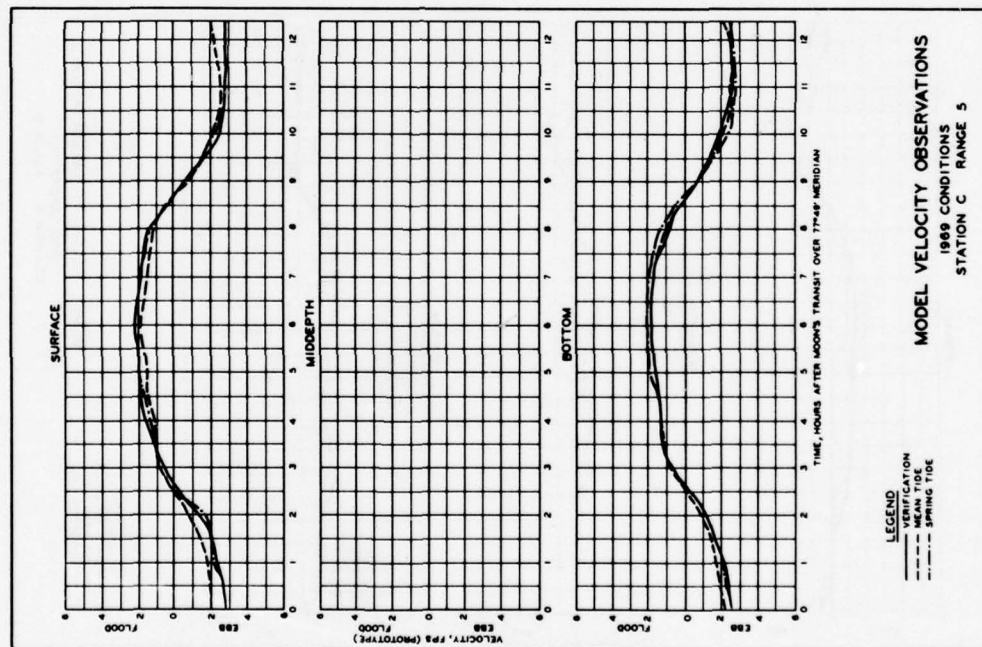


PLATE 84

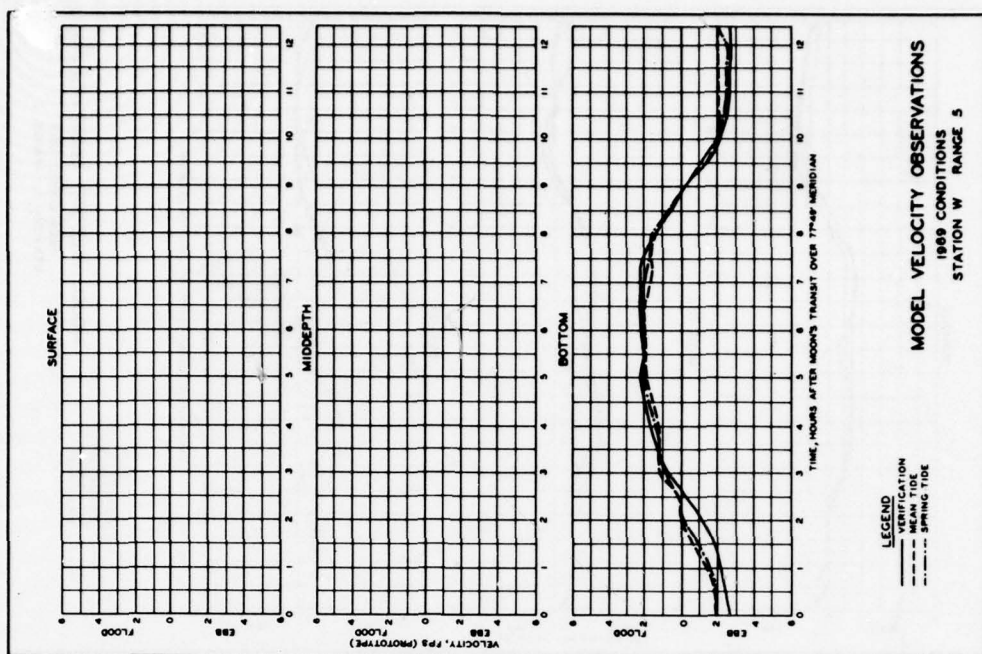


PLATE 85

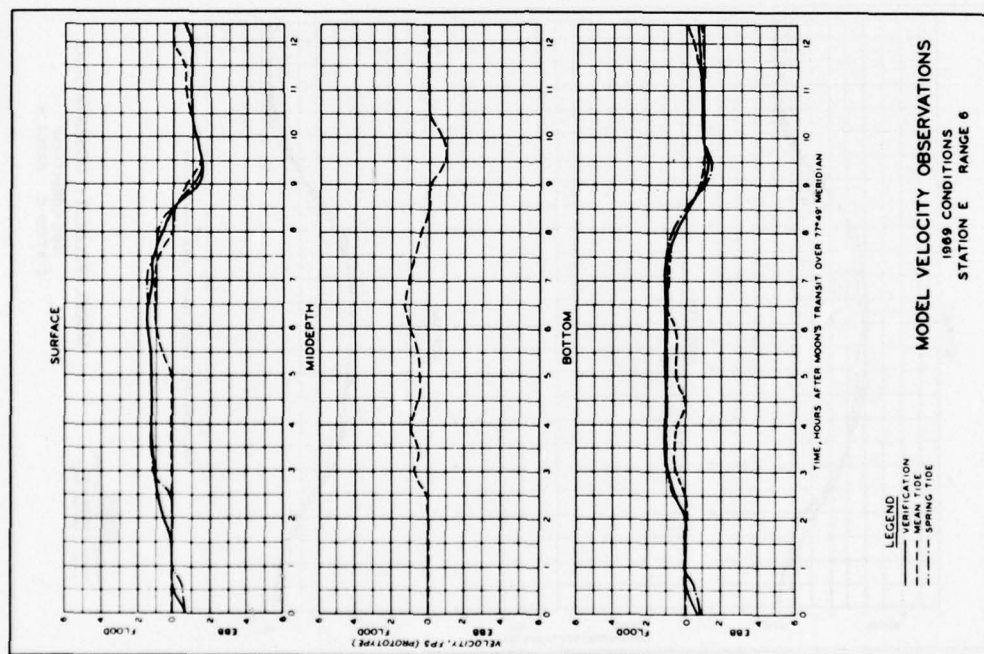


PLATE 86

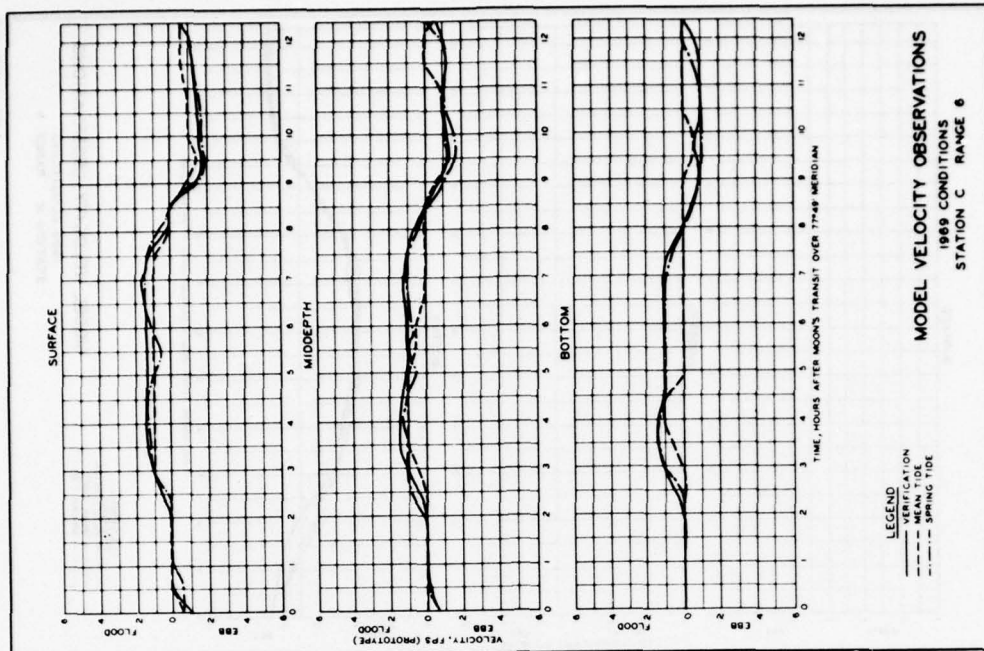


PLATE 87

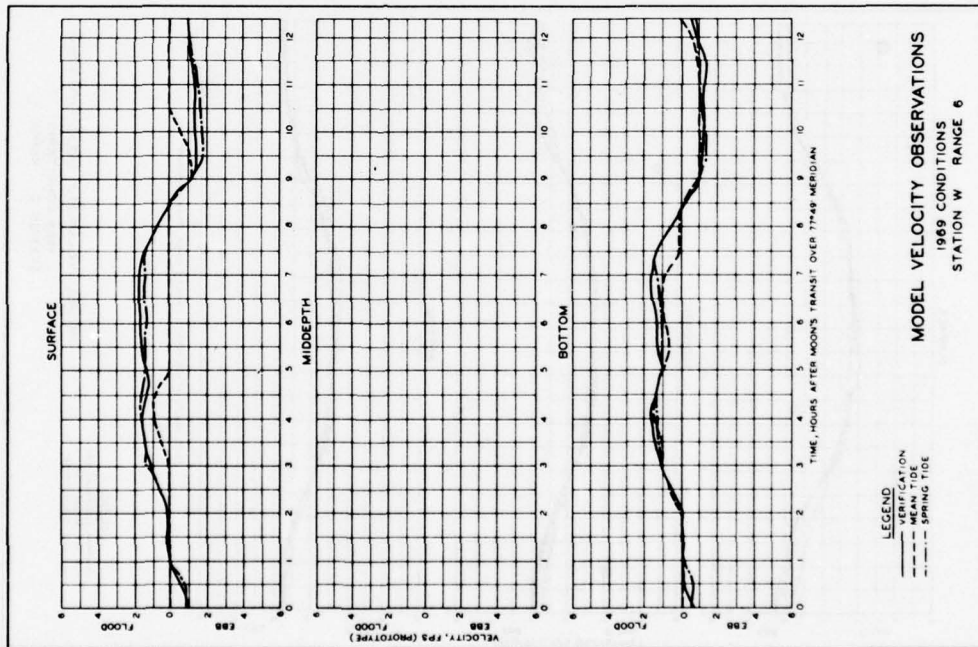


PLATE 88

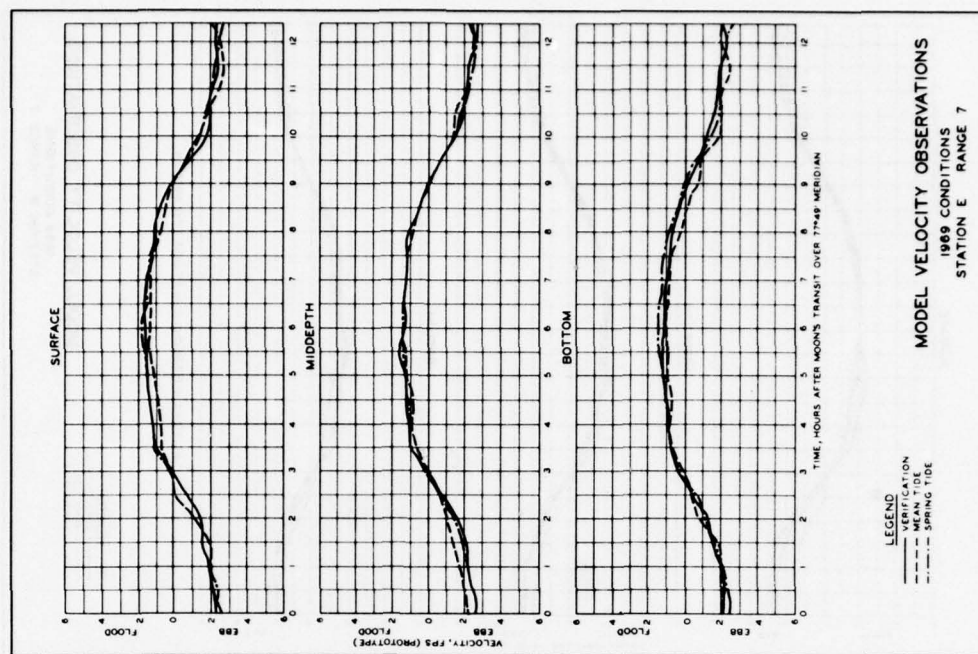


PLATE 89

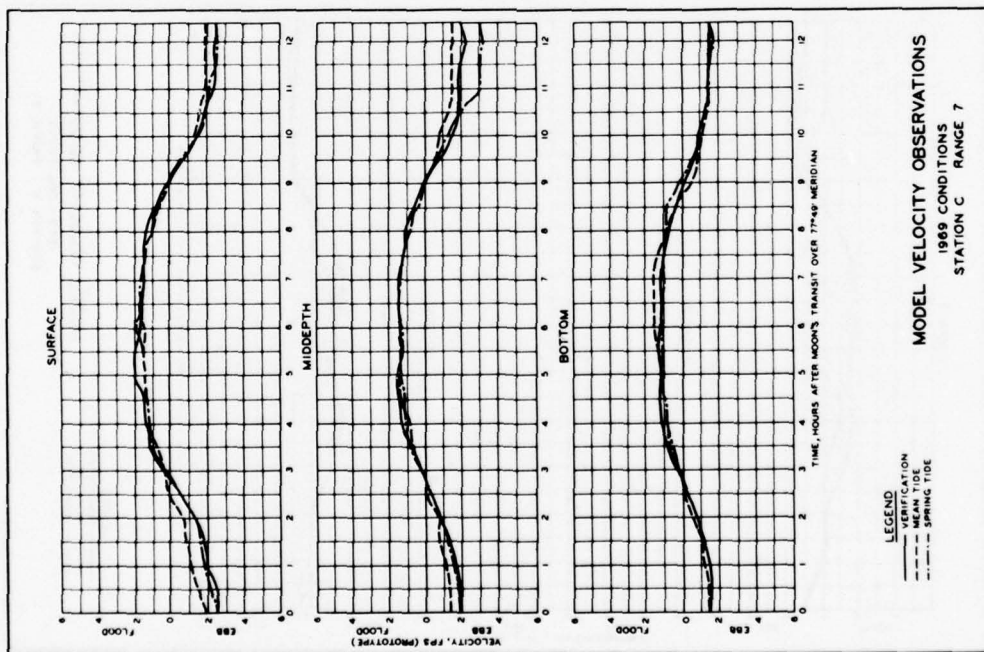


PLATE 90

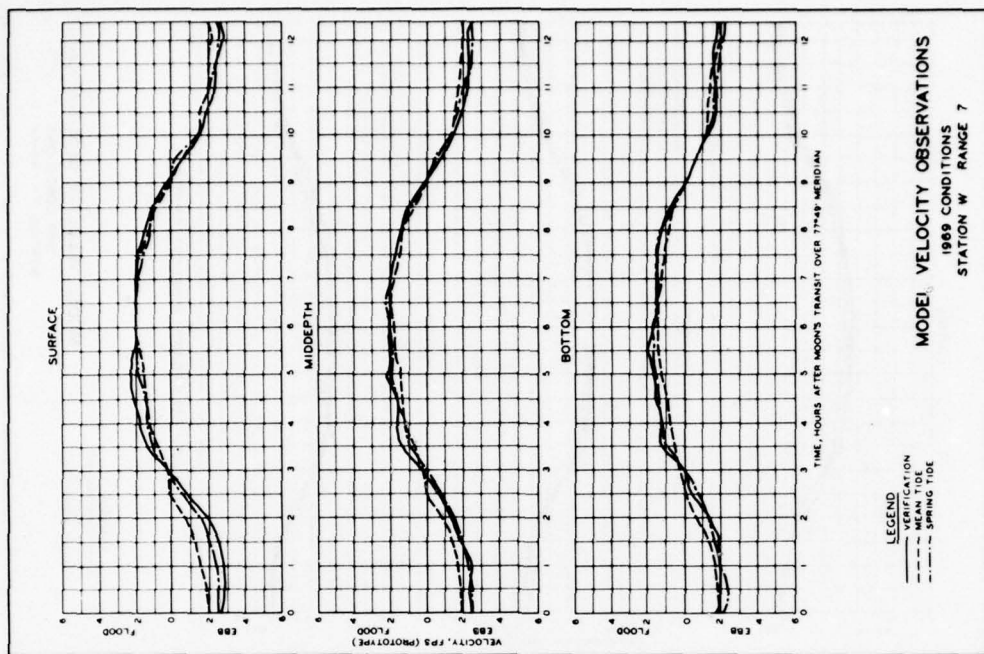


PLATE 91

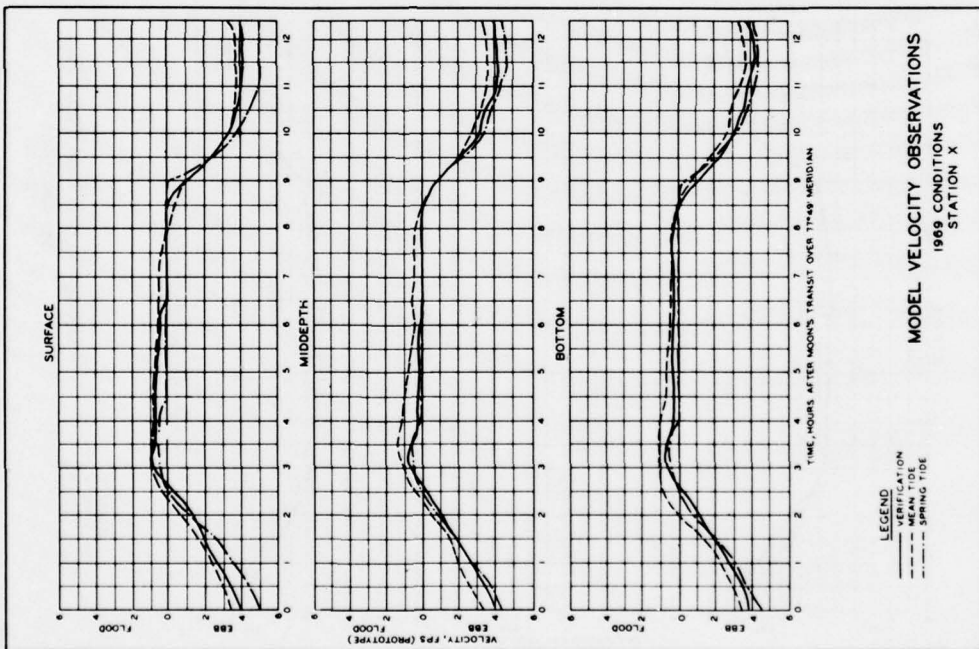


PLATE 92

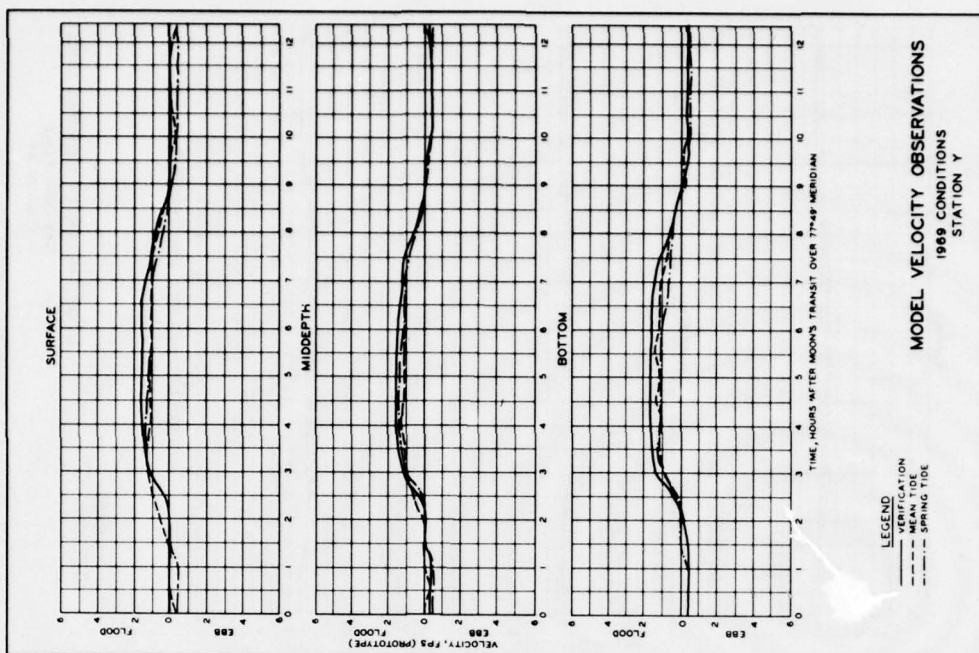
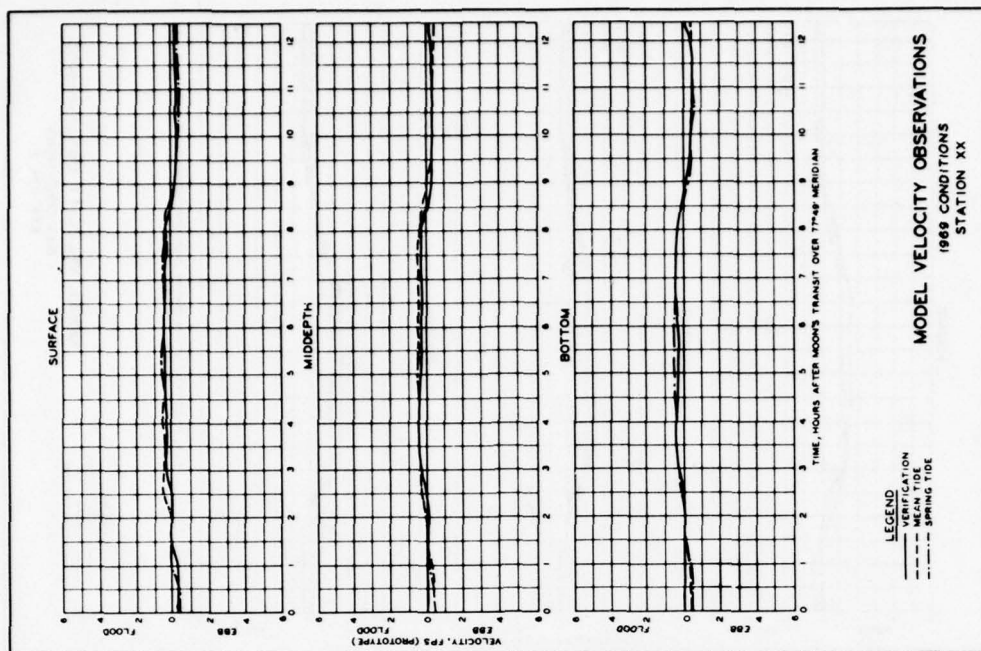
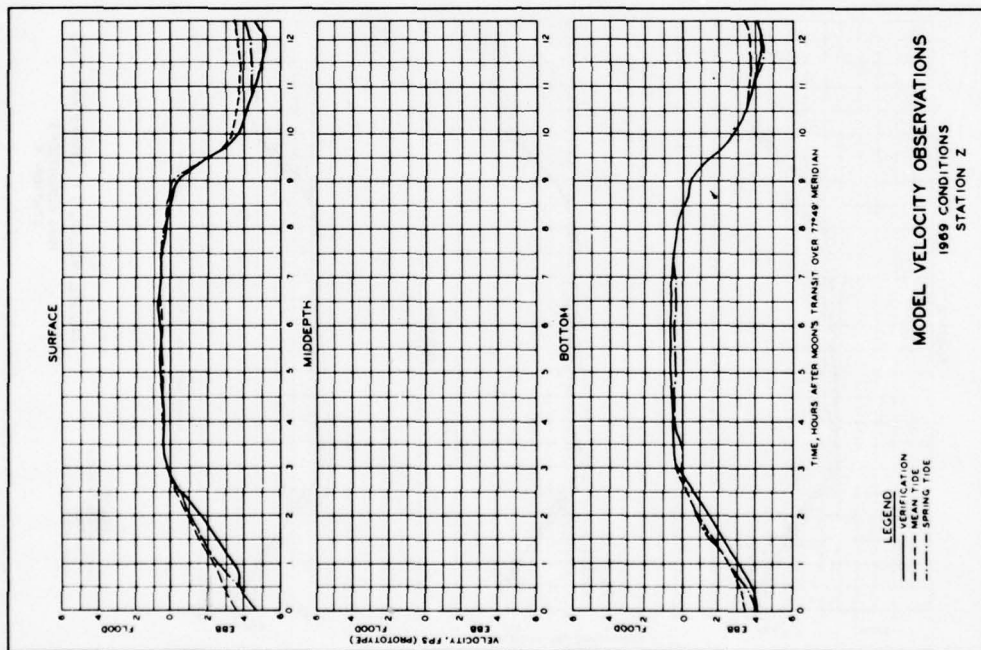


PLATE 93



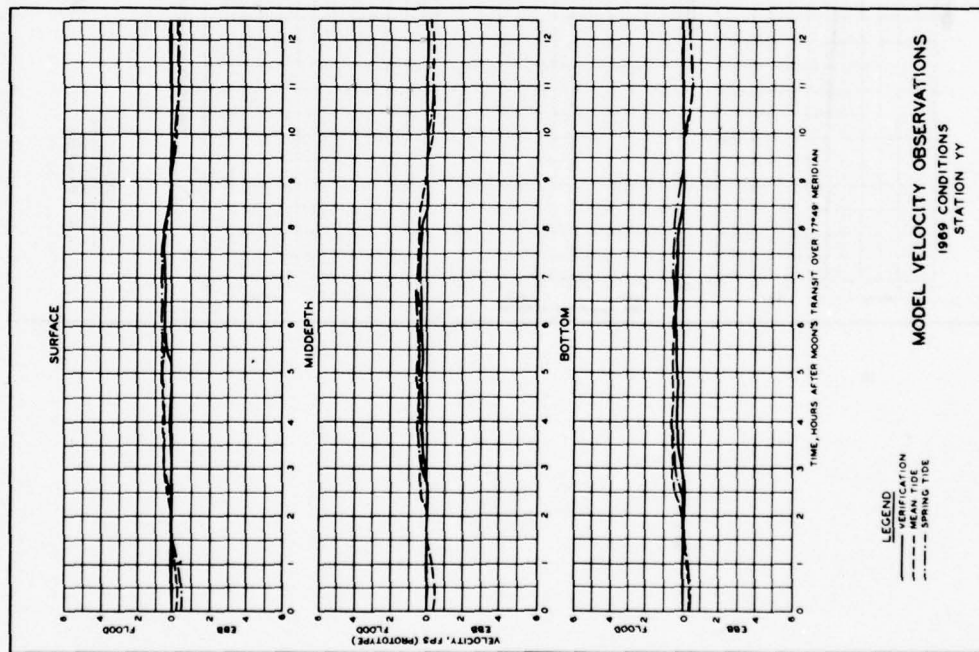


PLATE 96

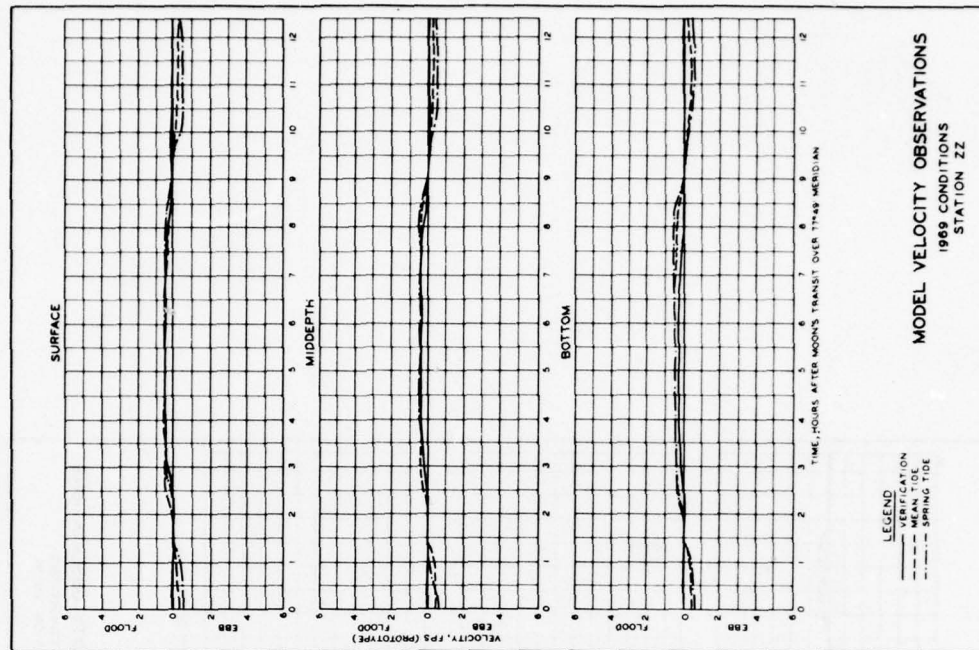
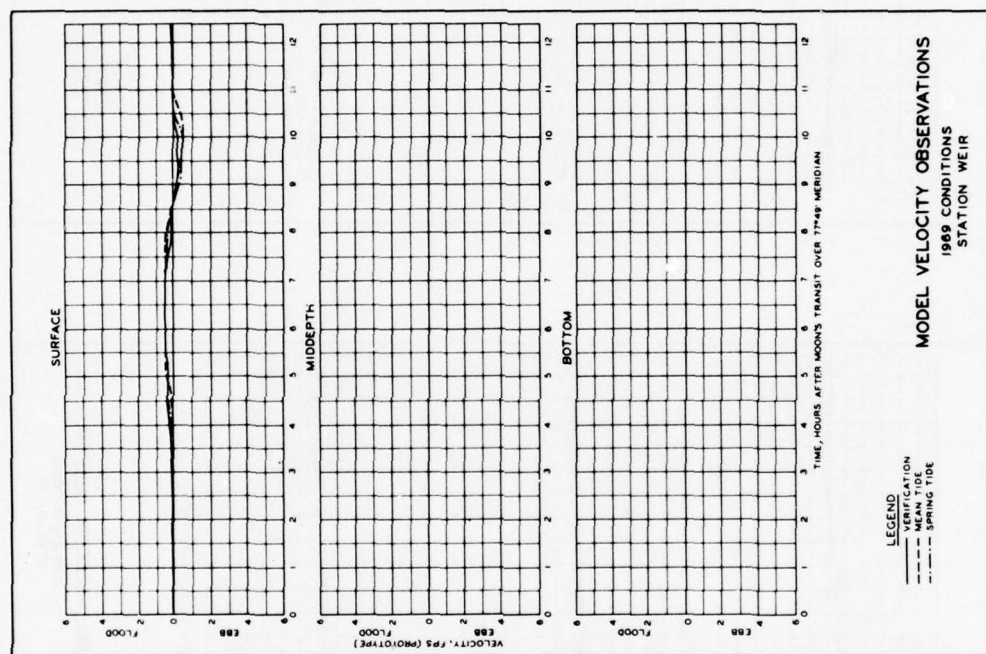


PLATE 97



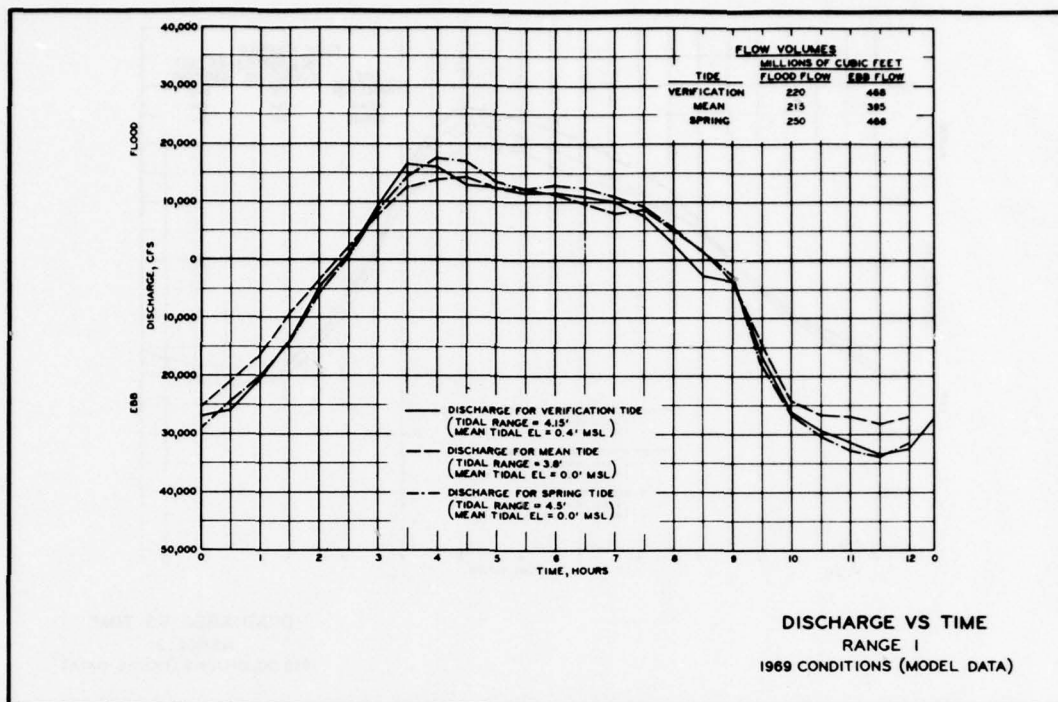


PLATE 99

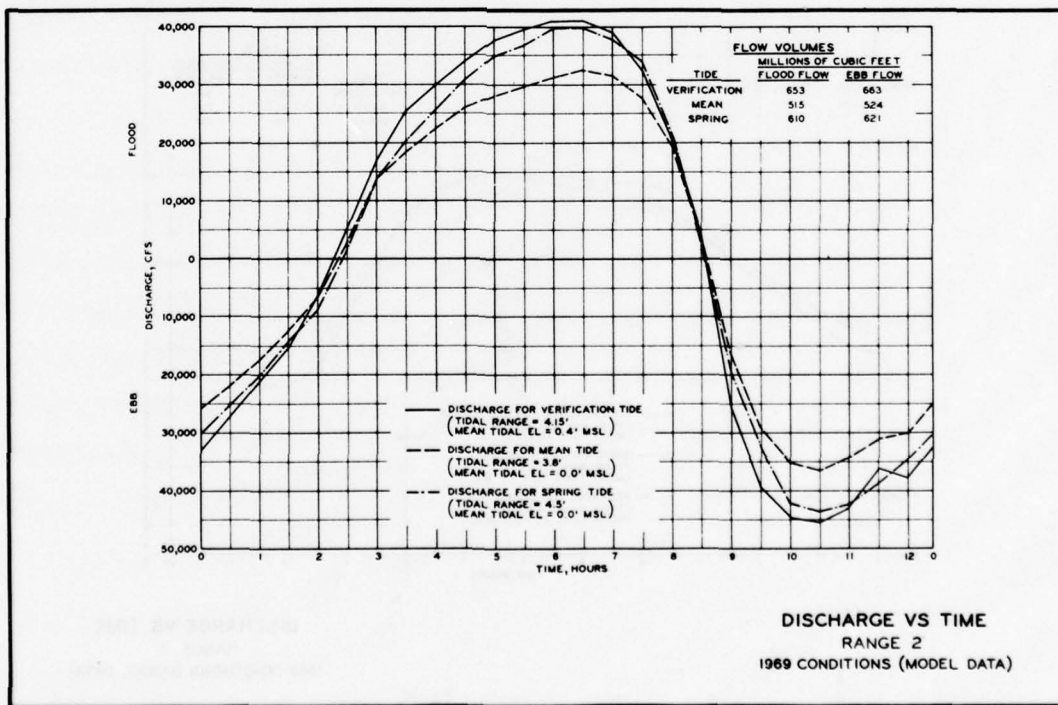


PLATE 100

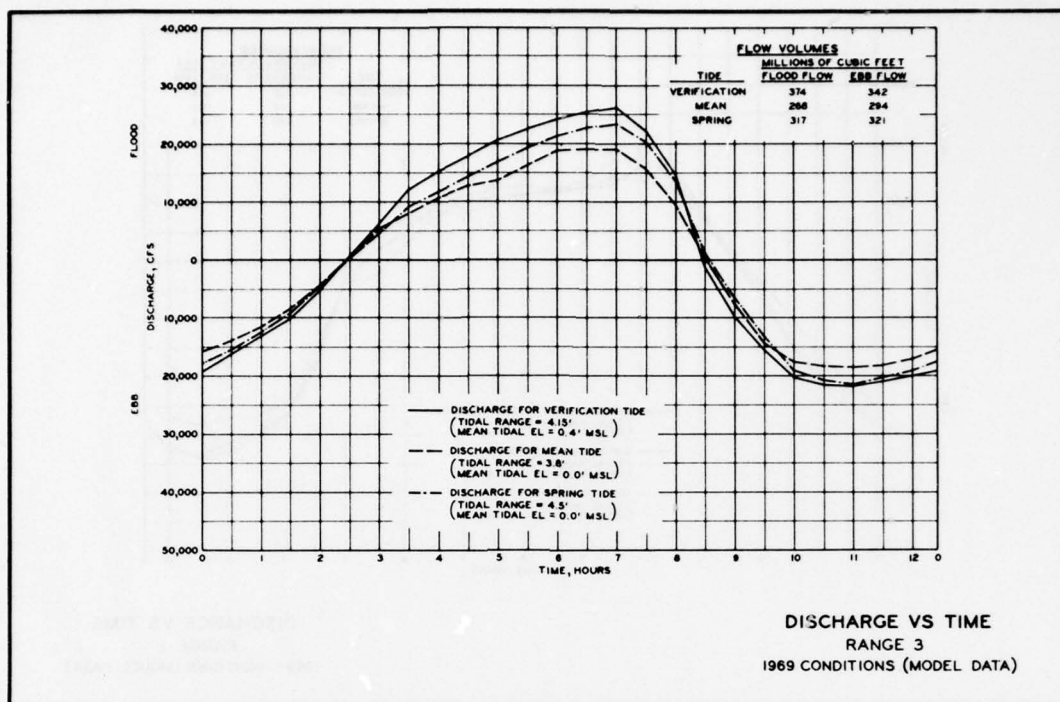


PLATE 101

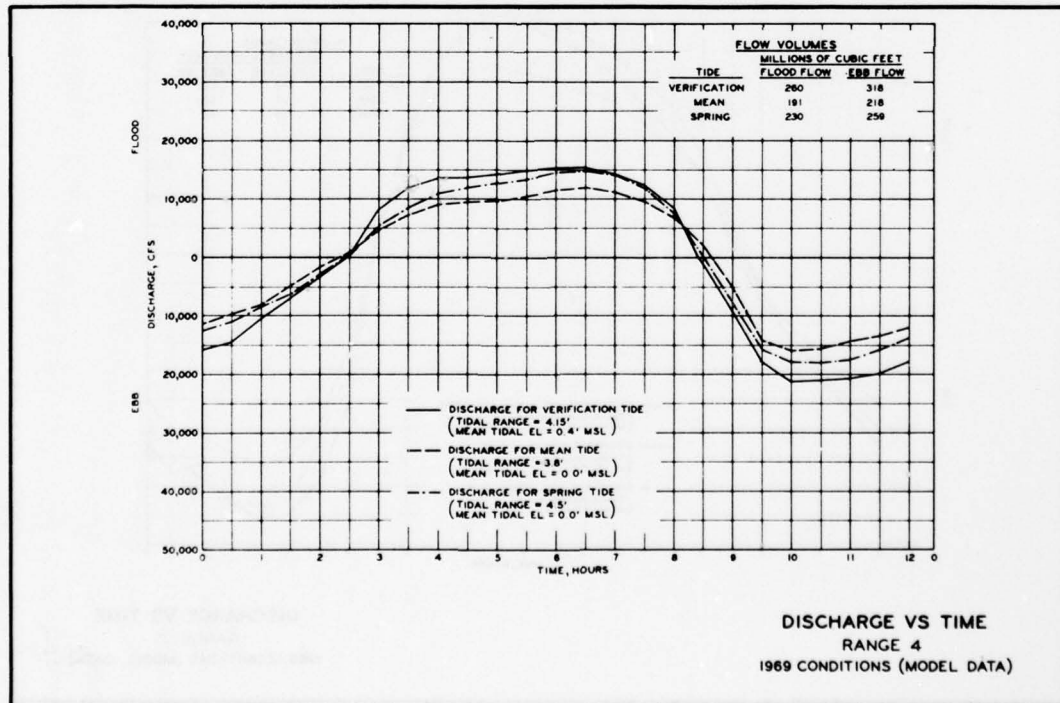


PLATE 102

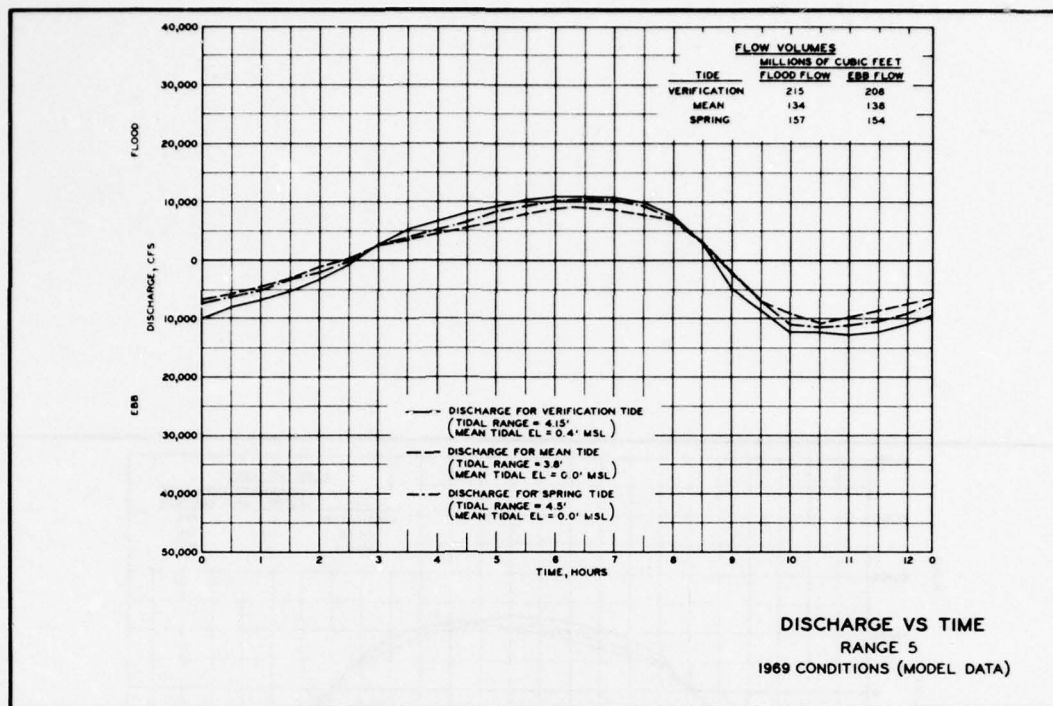


PLATE 103

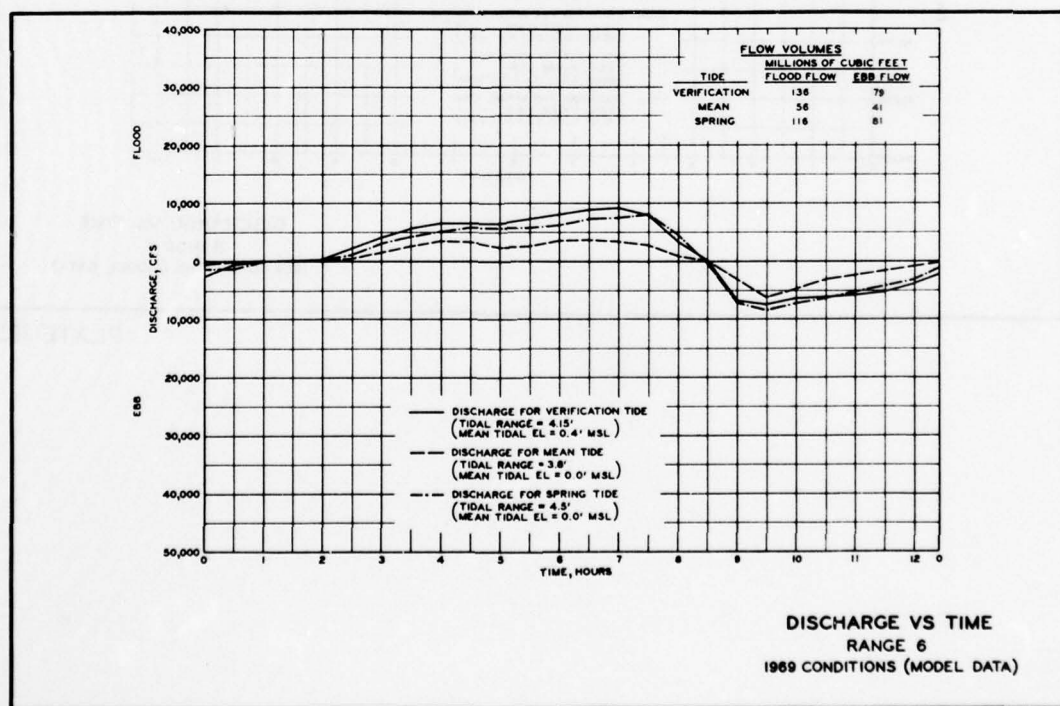
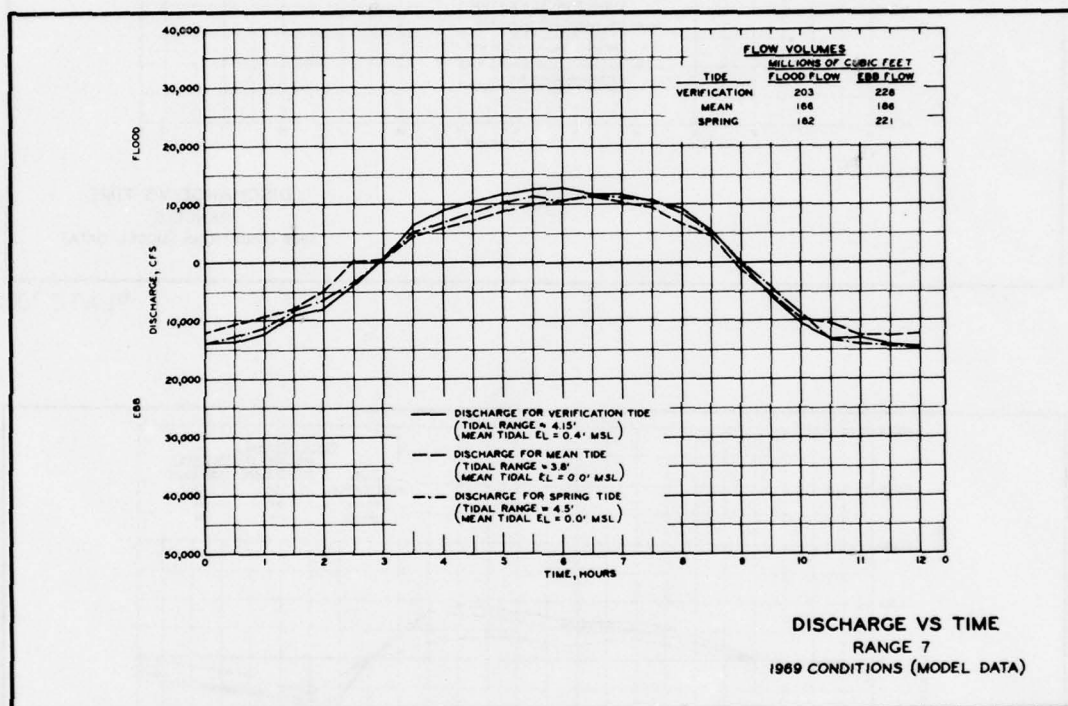


PLATE 104



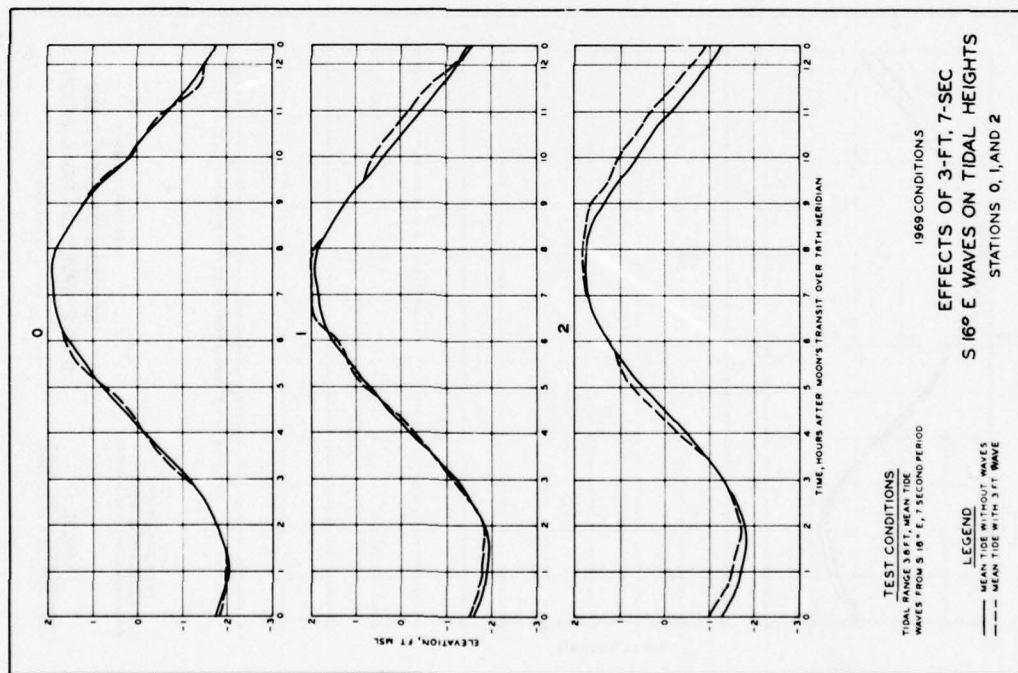


PLATE 106

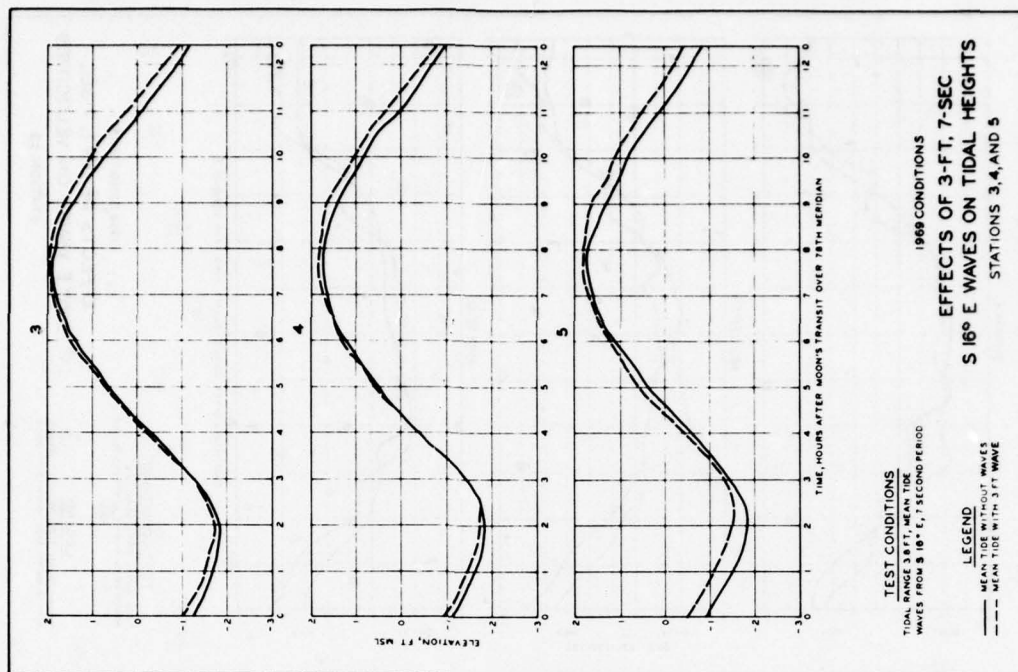


PLATE 107

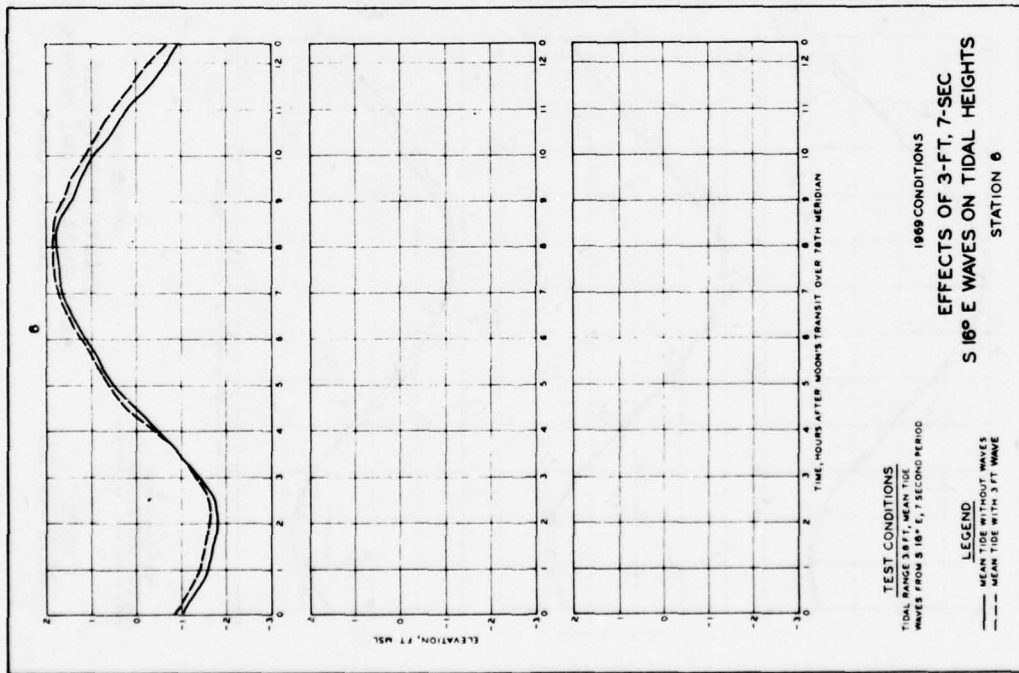


PLATE 108

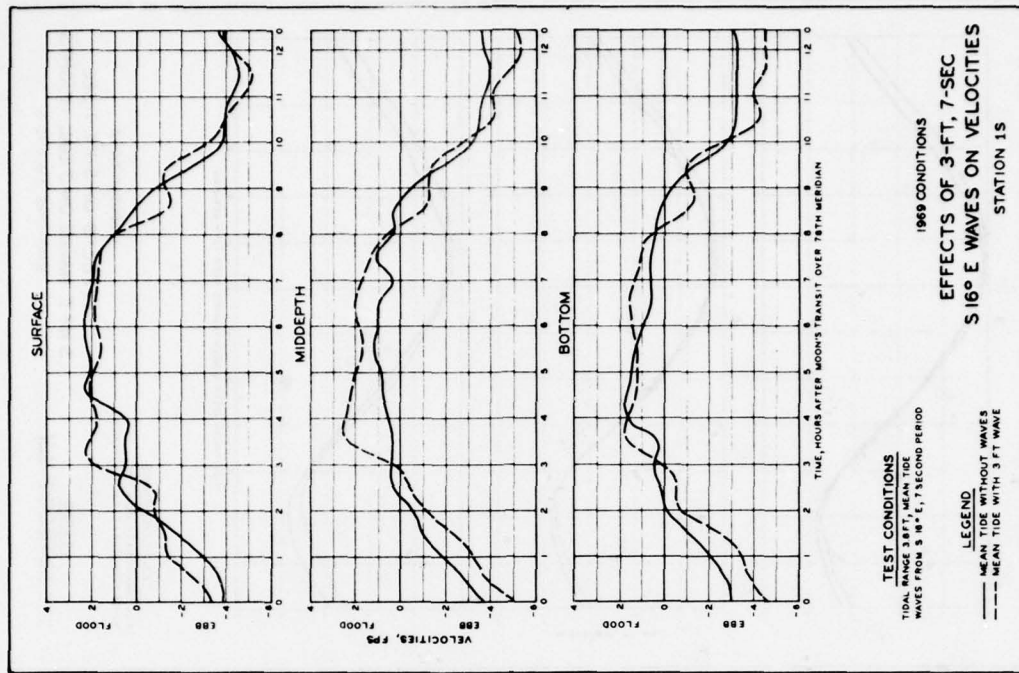


PLATE 109

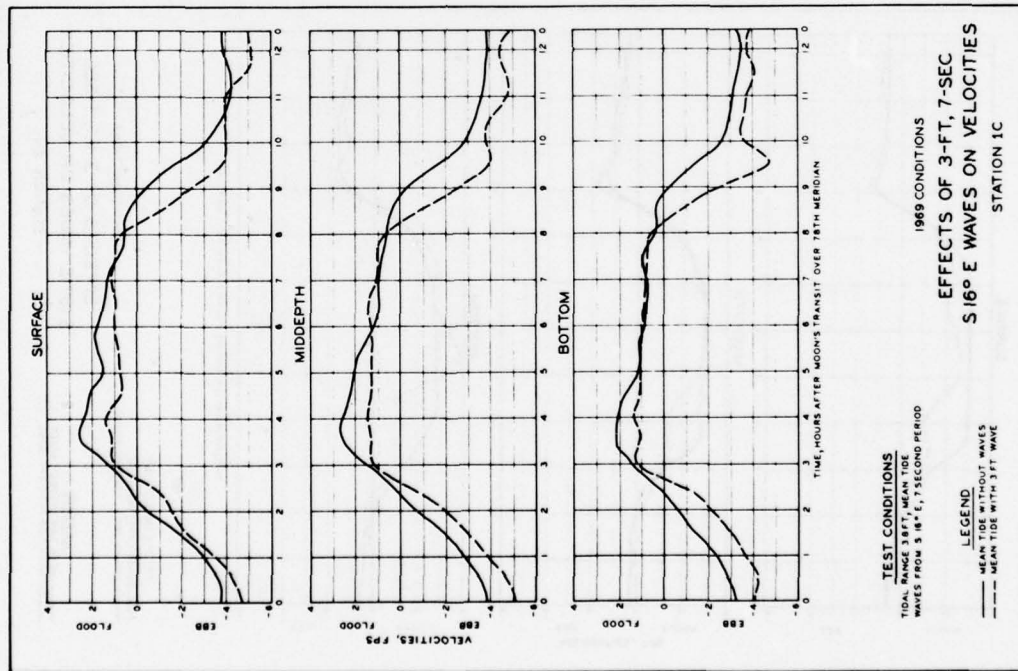


PLATE 110

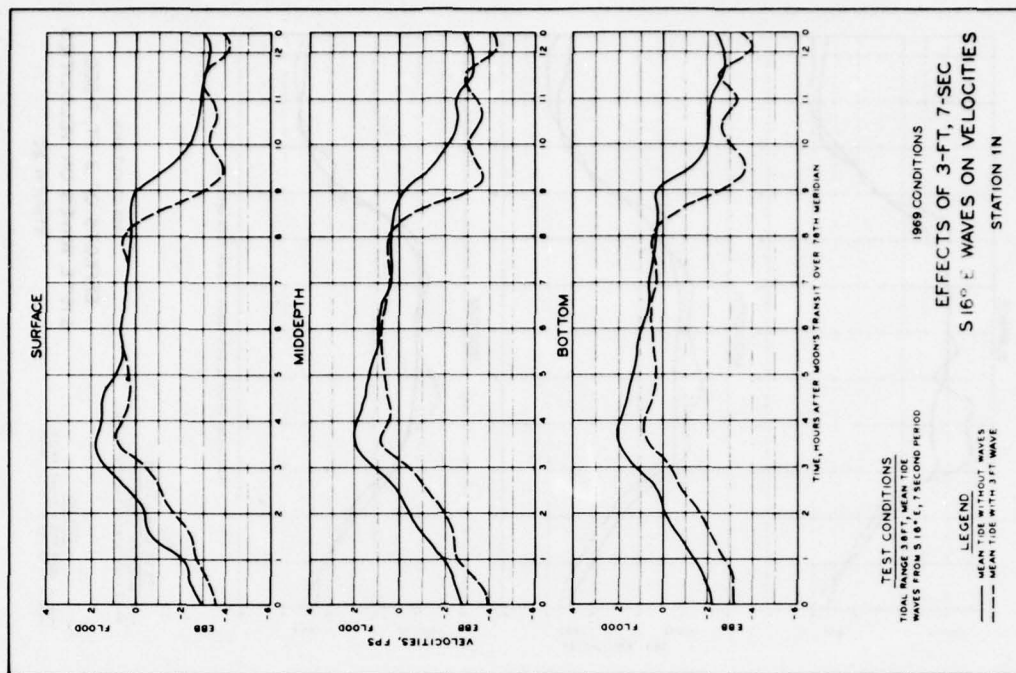


PLATE 111

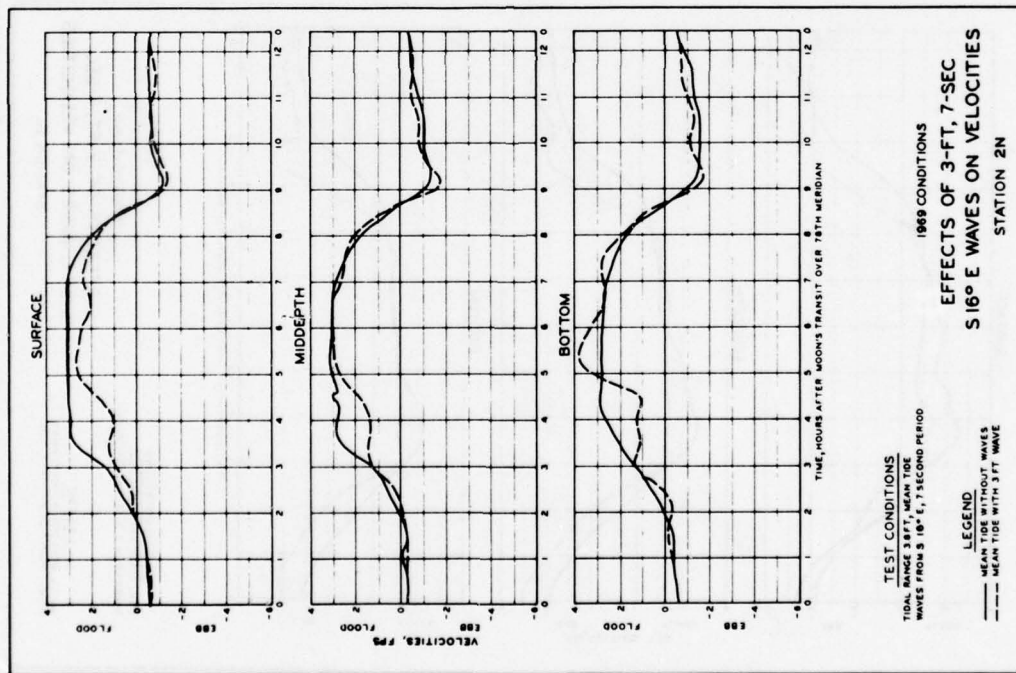


PLATE 112

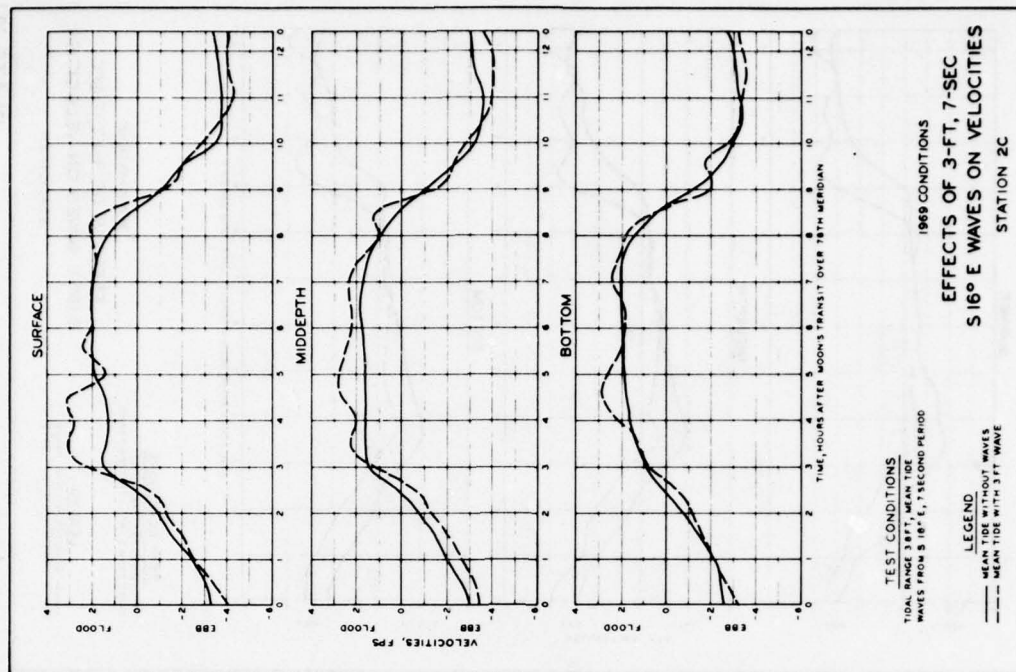


PLATE 113

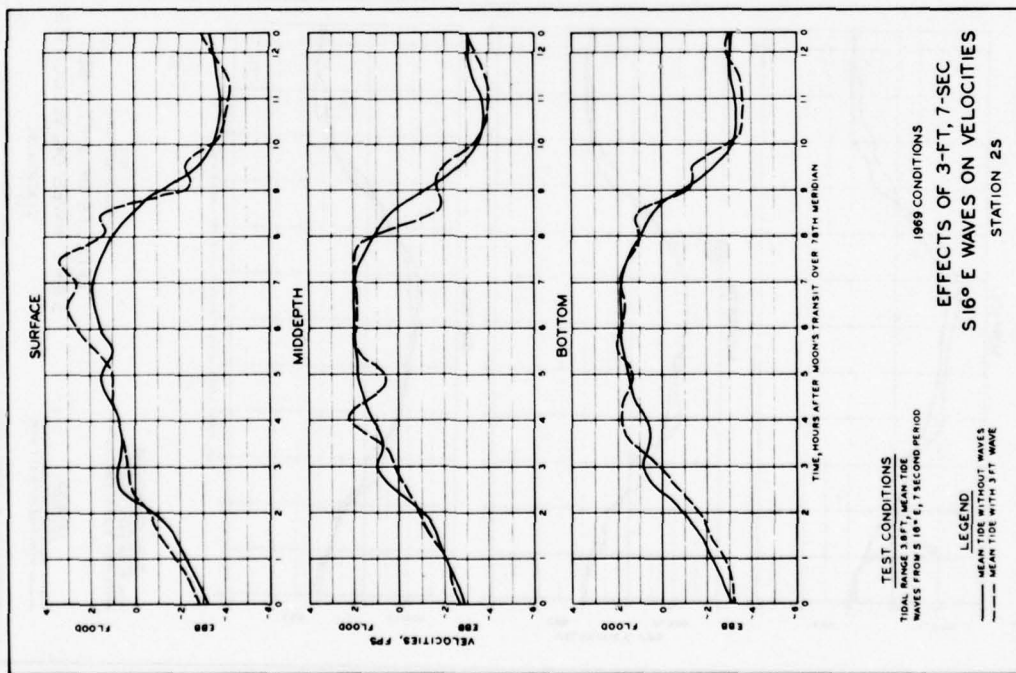


PLATE 114

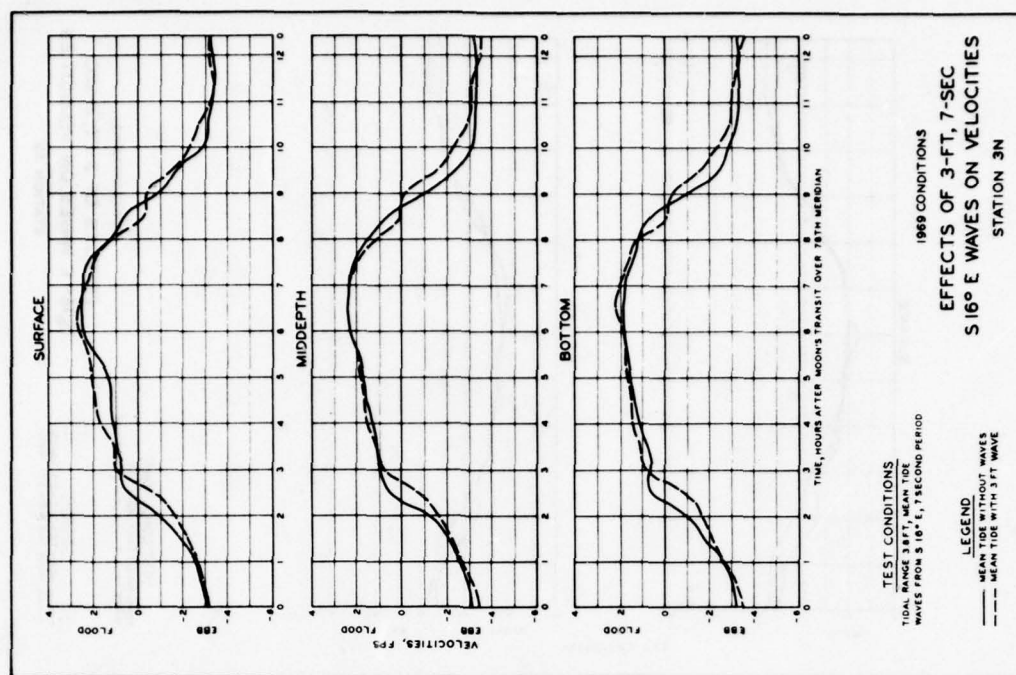


PLATE 115

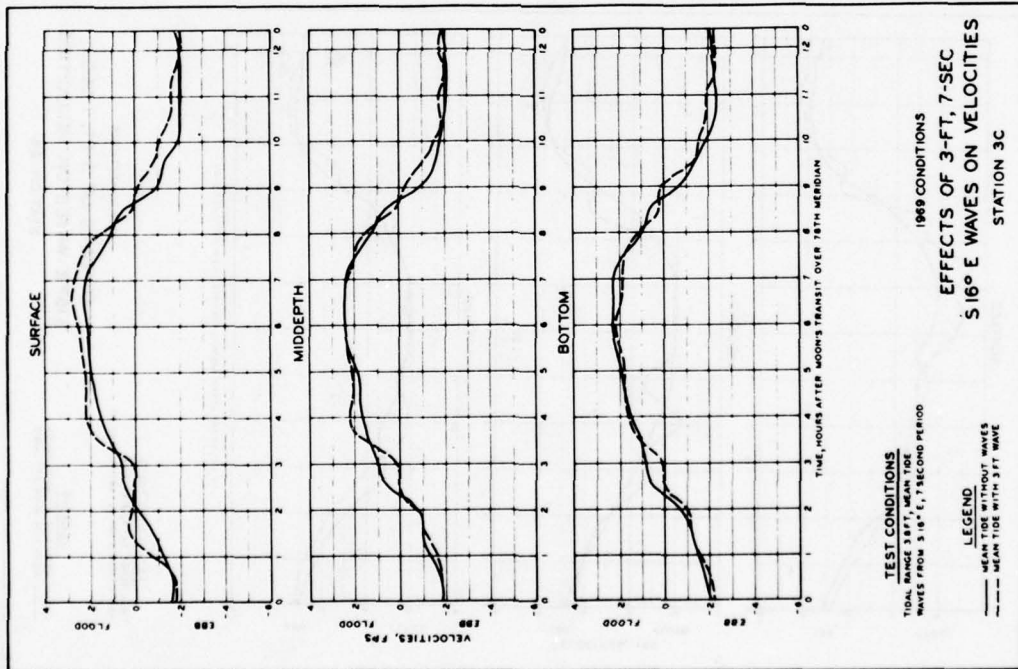


PLATE 116

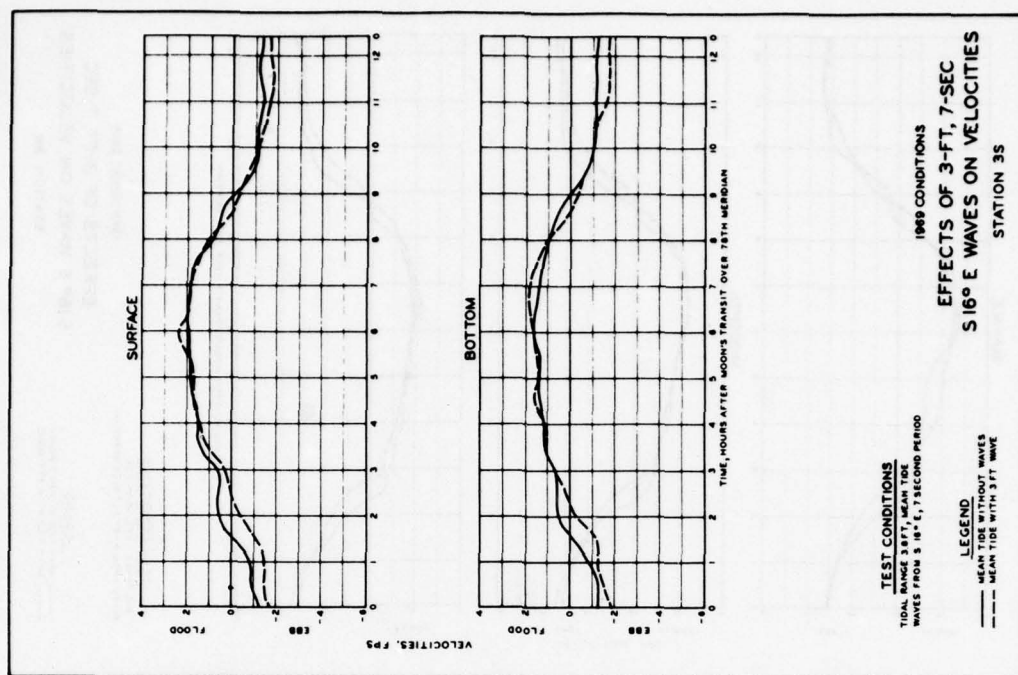


PLATE 117

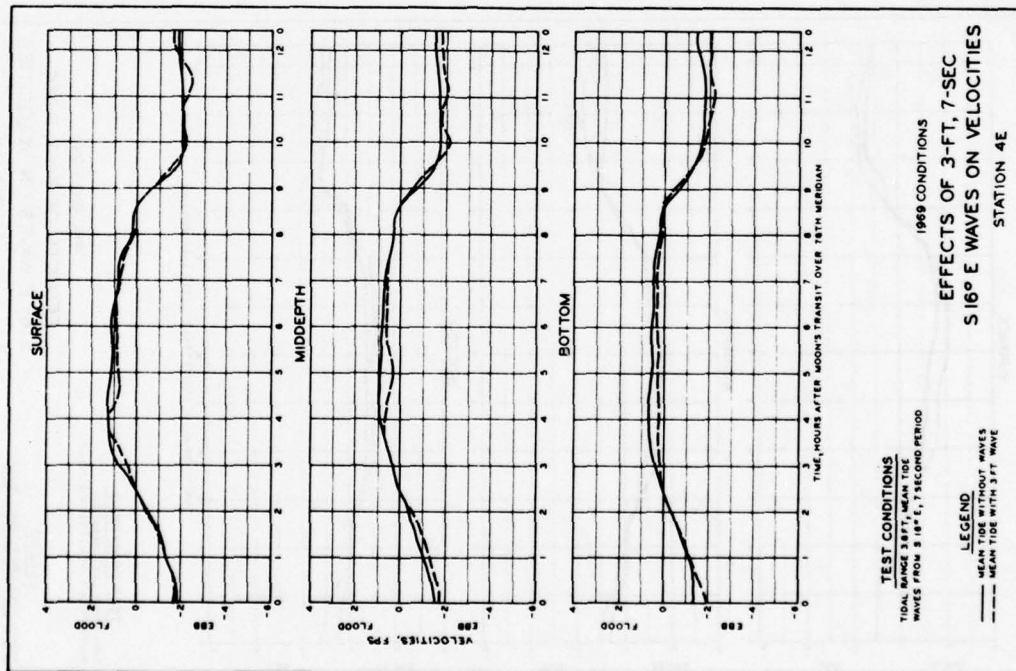


PLATE 118

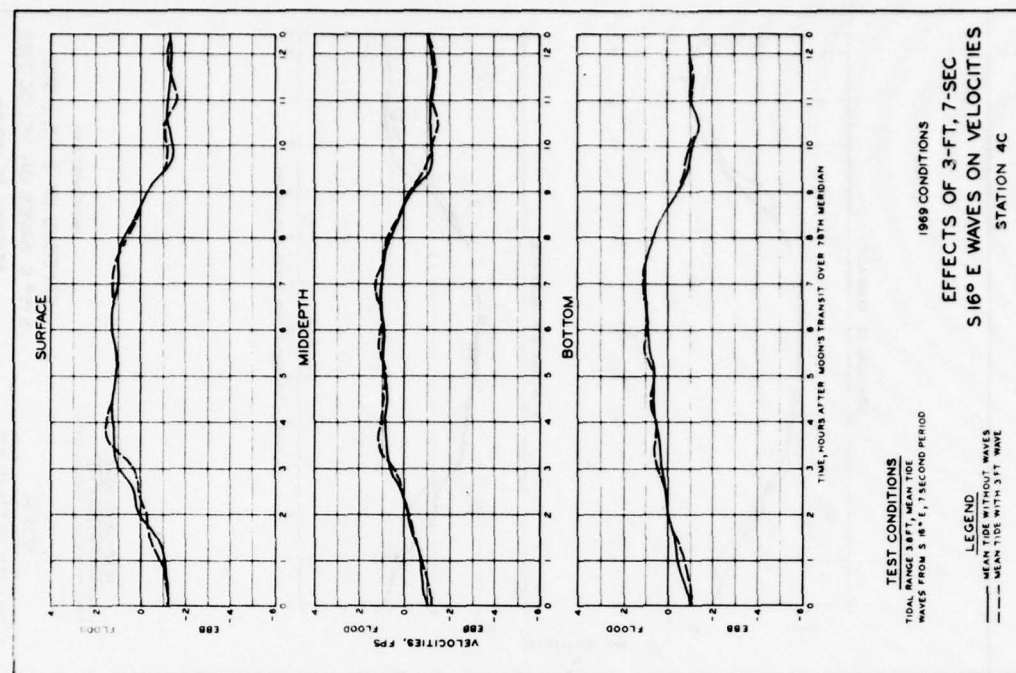


PLATE 119

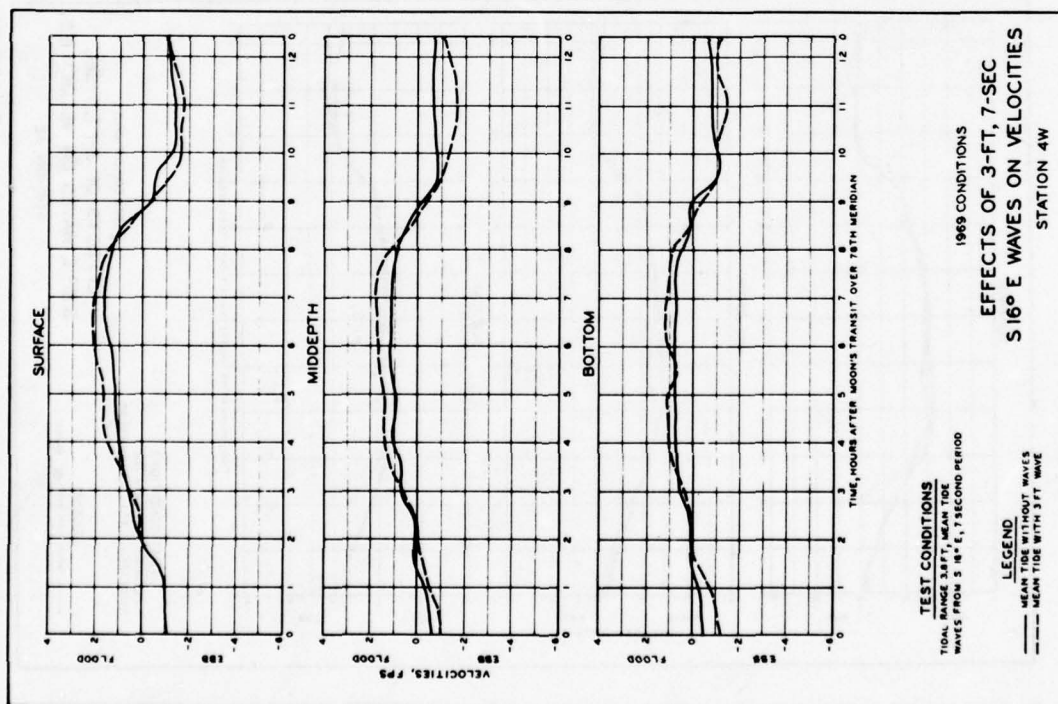


PLATE 120

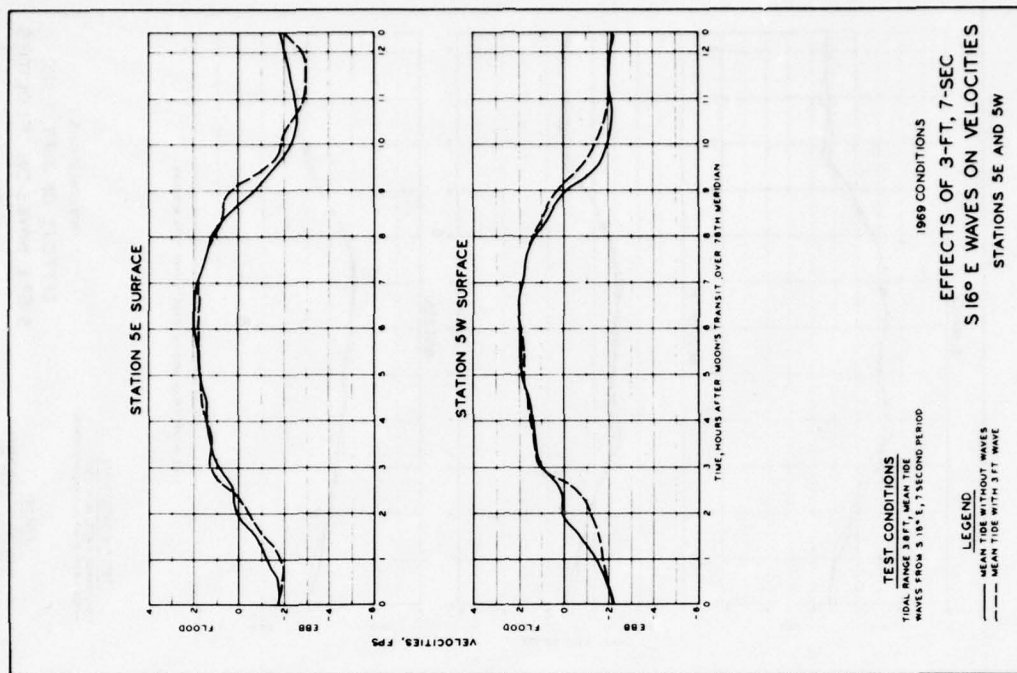


PLATE 121

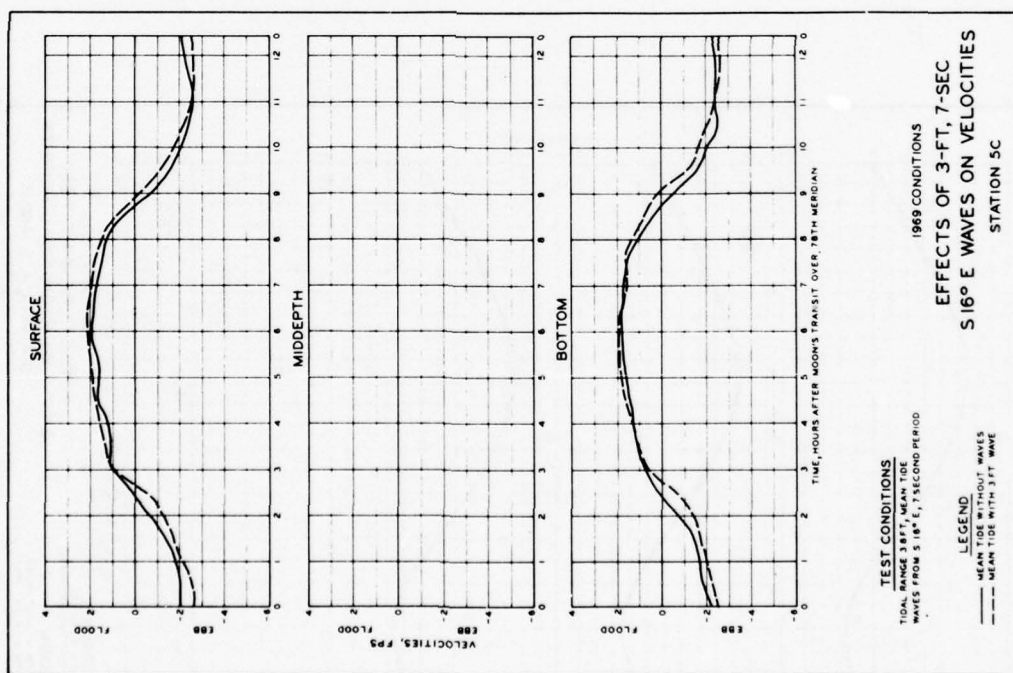


PLATE 122

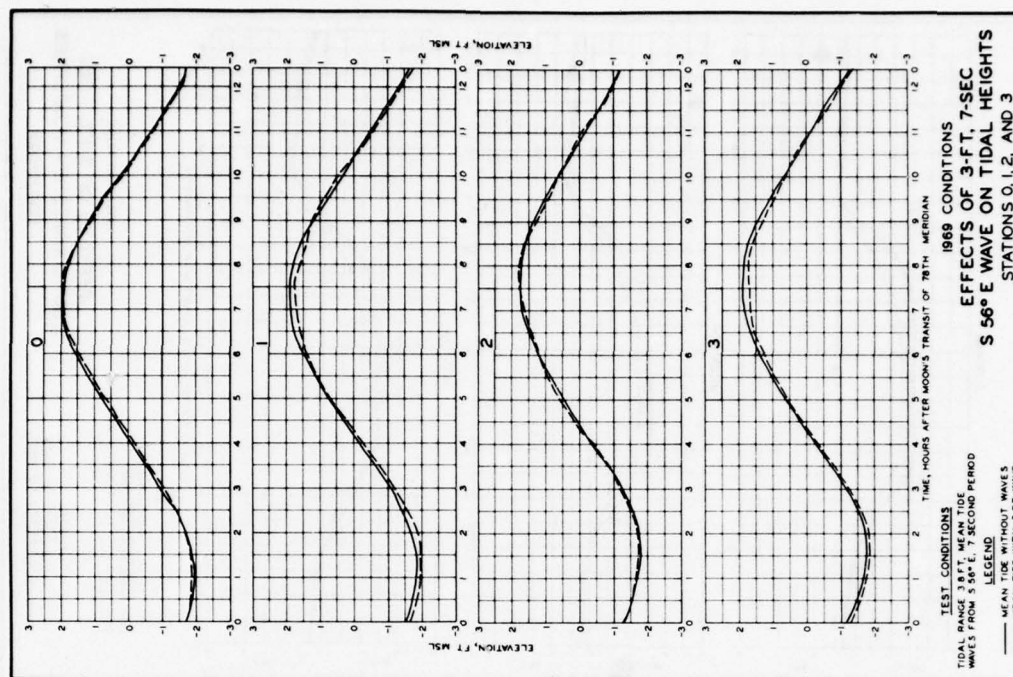


PLATE 123

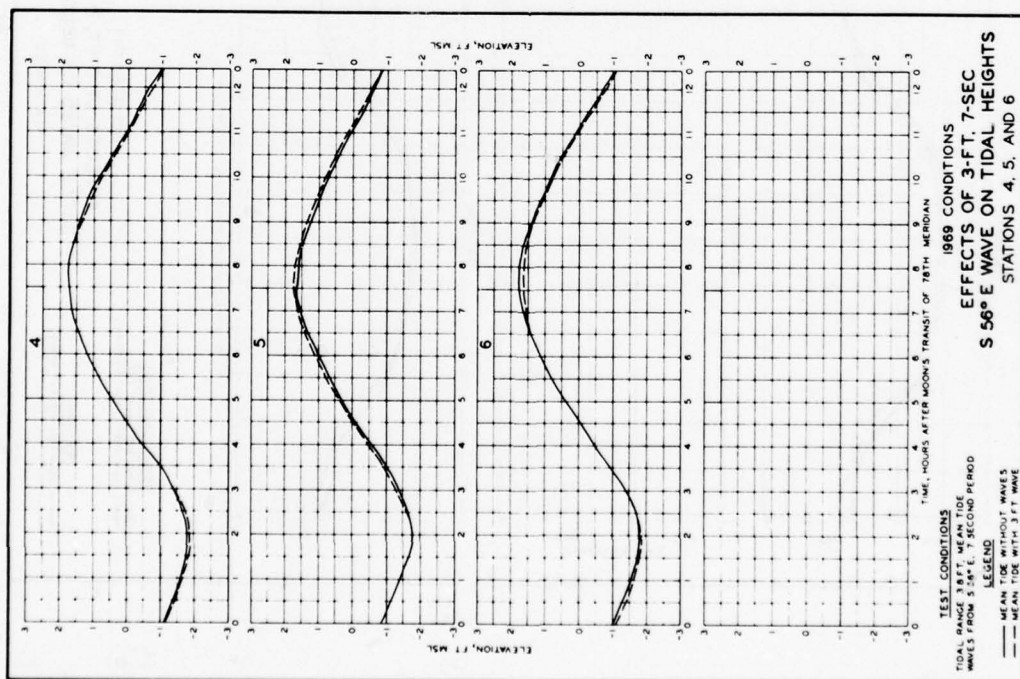


PLATE 124

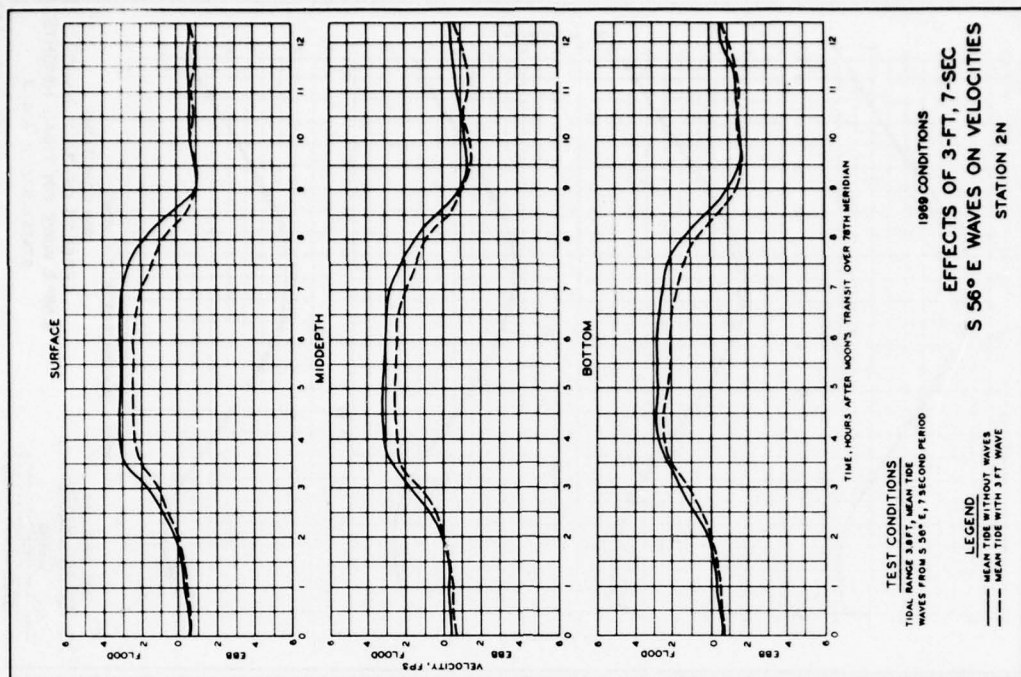


PLATE 125

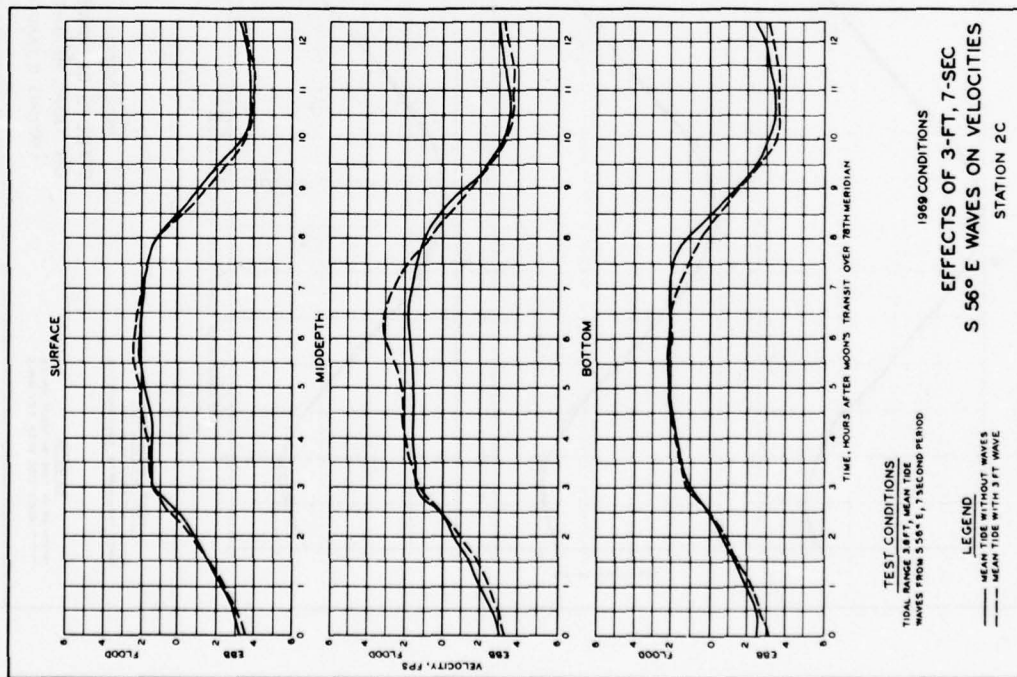


PLATE 126

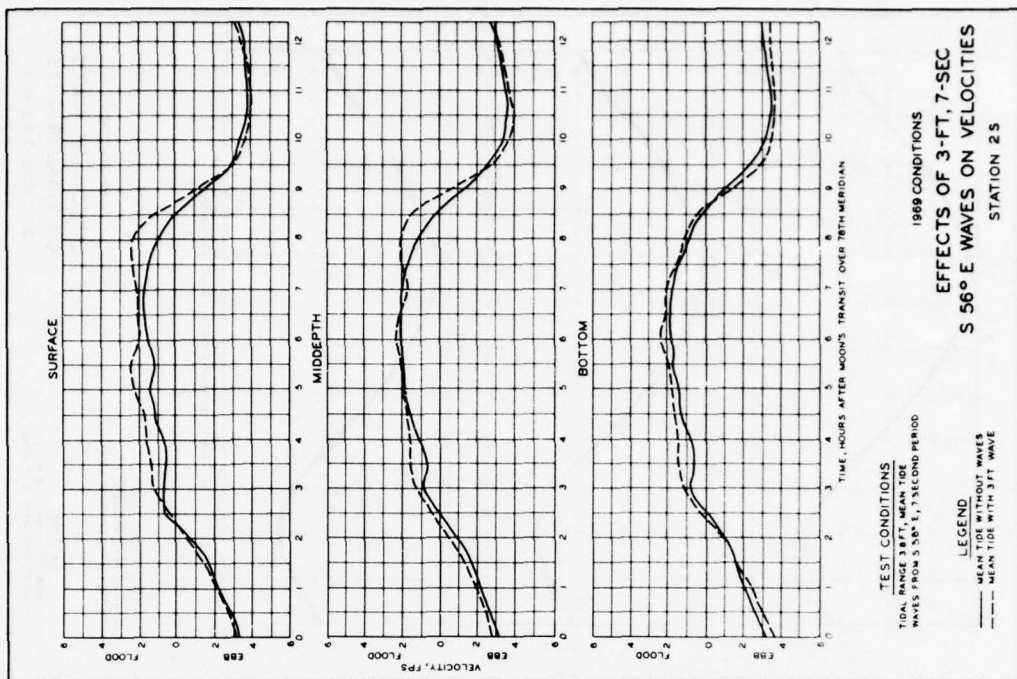


PLATE 127

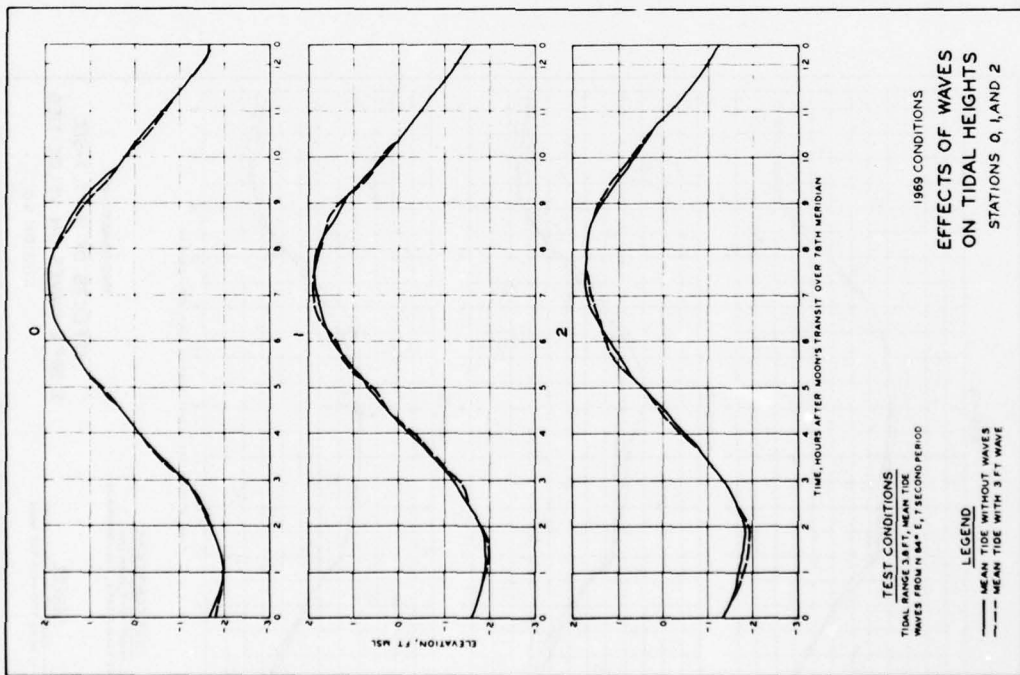


PLATE 128

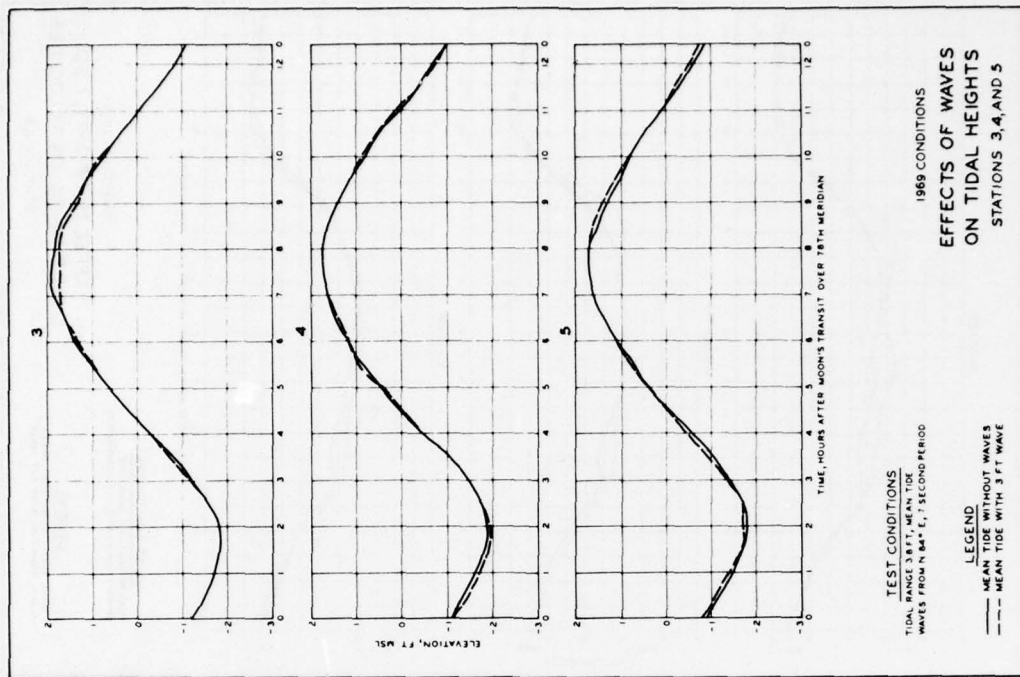


PLATE 129

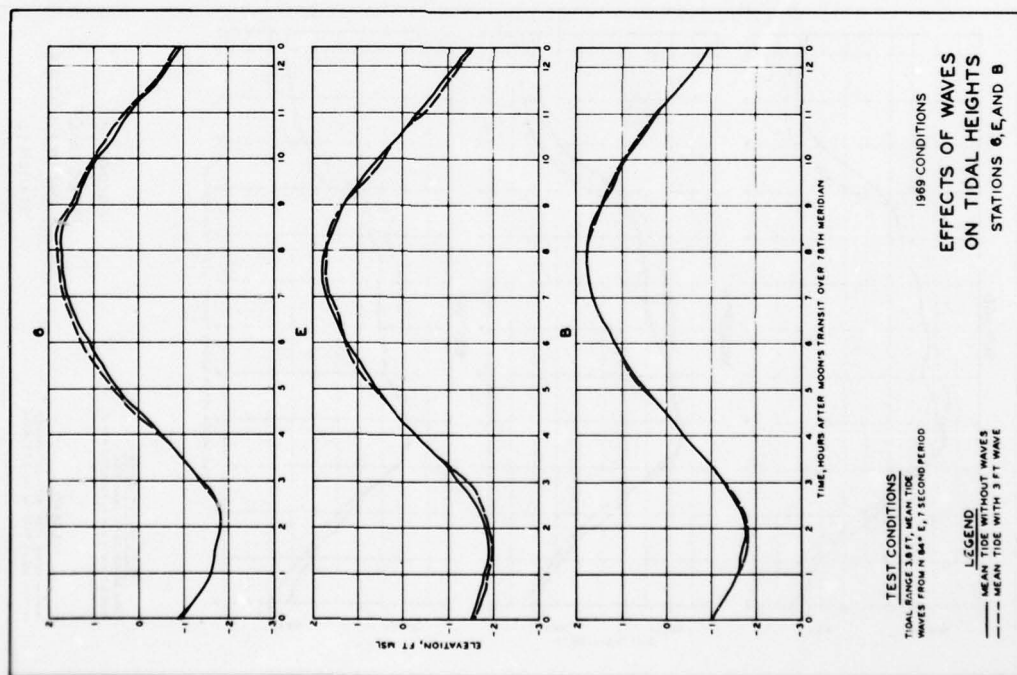


PLATE 130

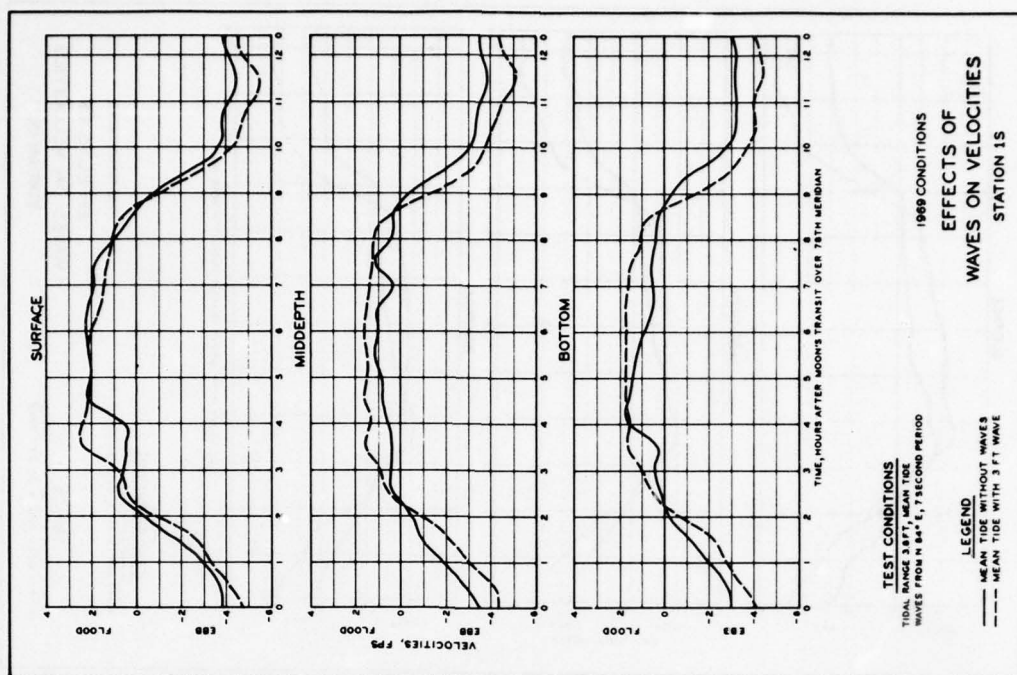


PLATE 131

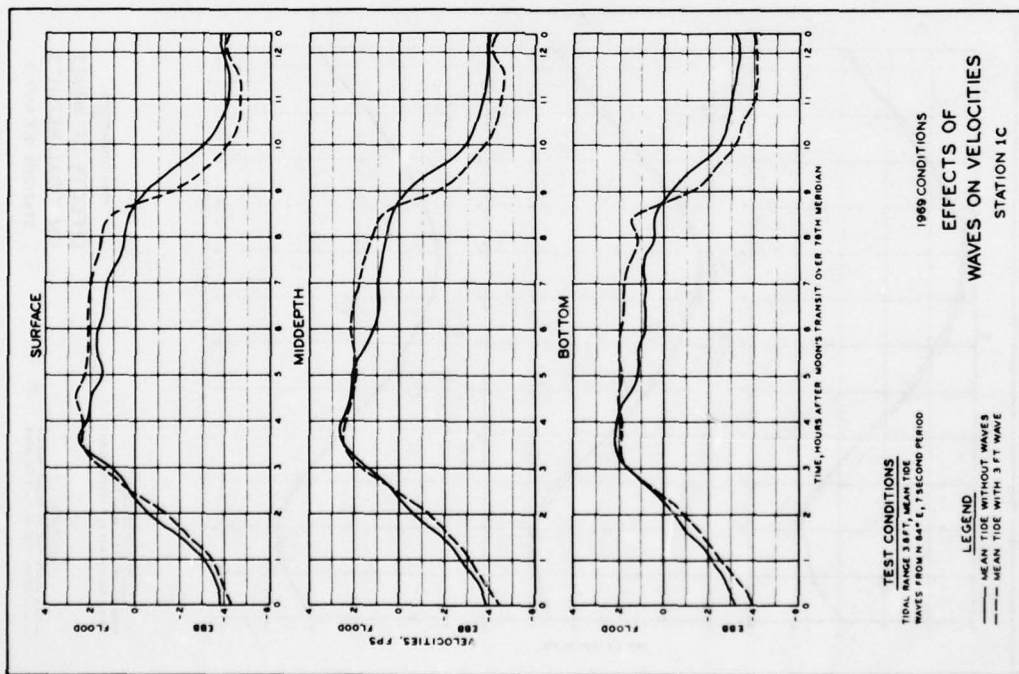


PLATE 132

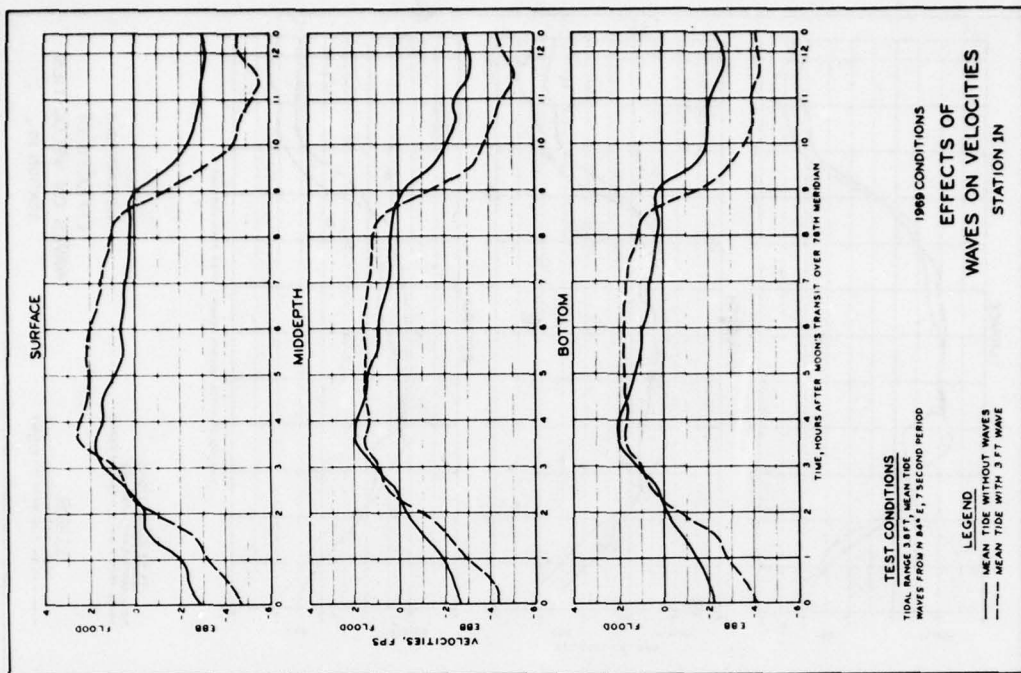


PLATE 133

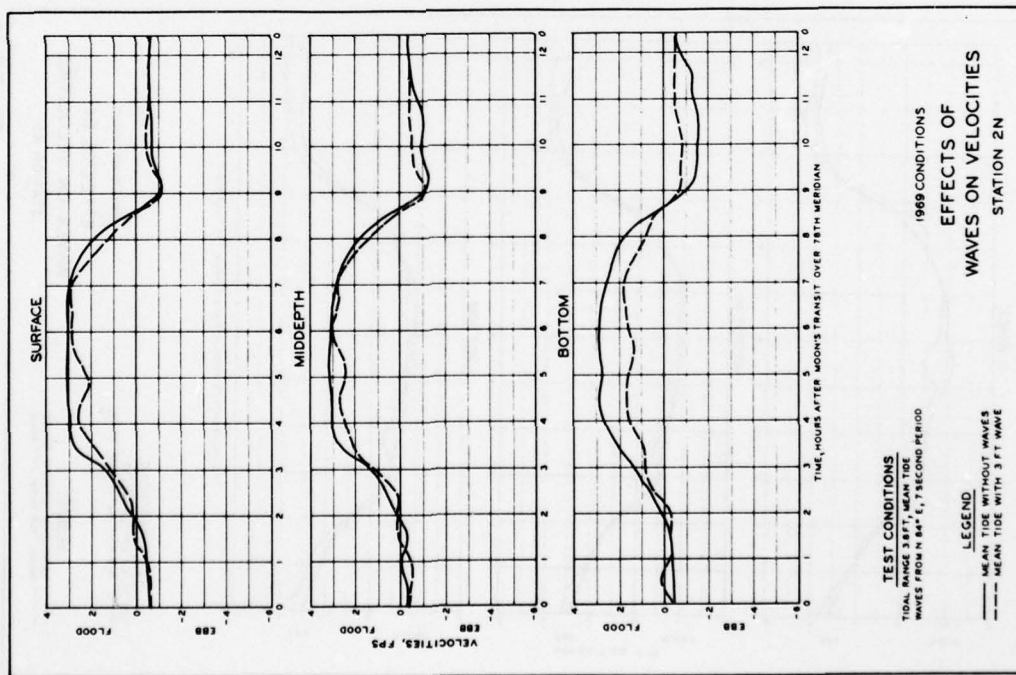


PLATE 134

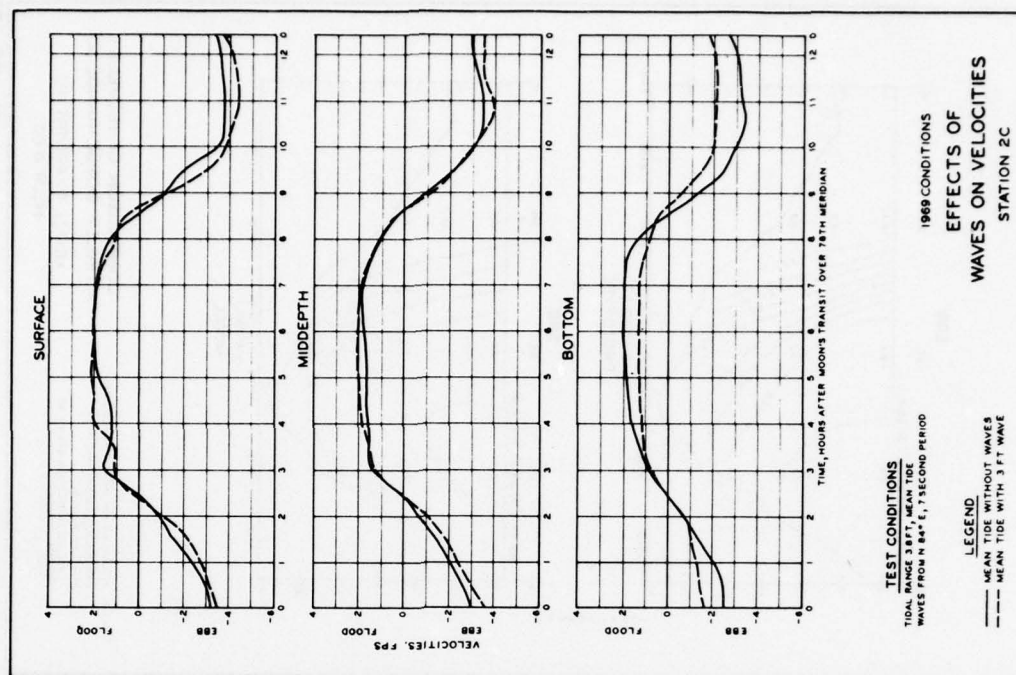


PLATE 135

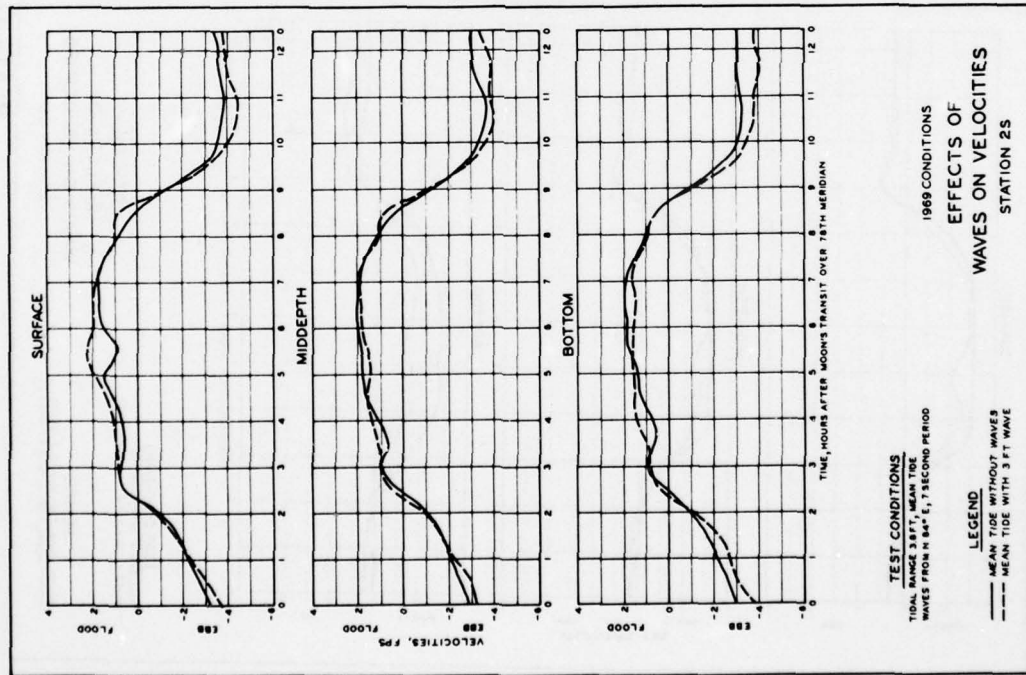


PLATE 136

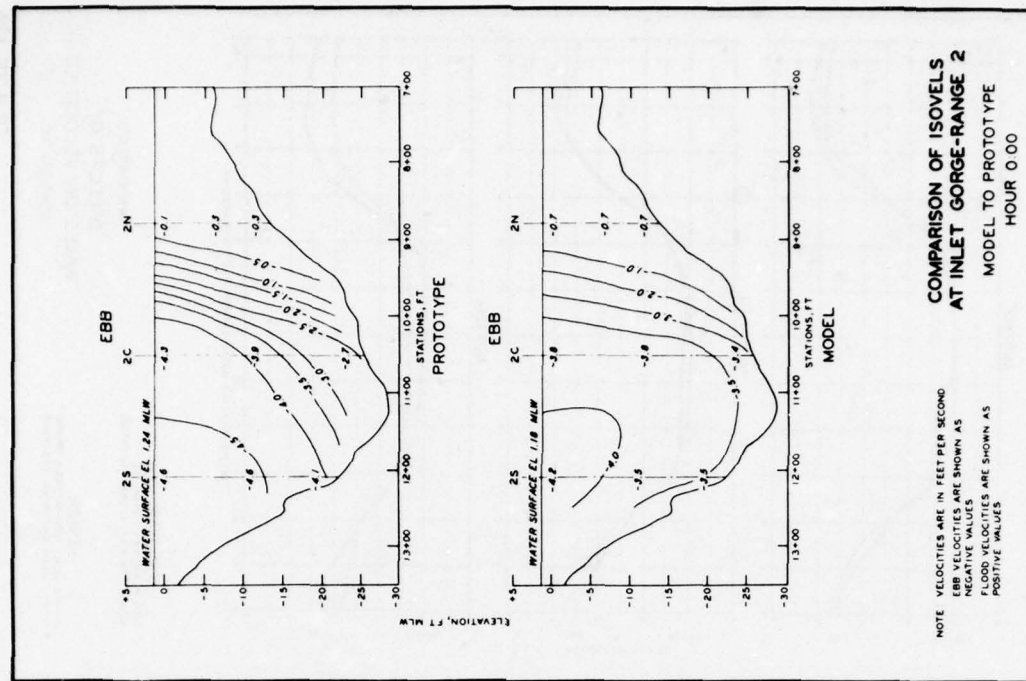


PLATE 137

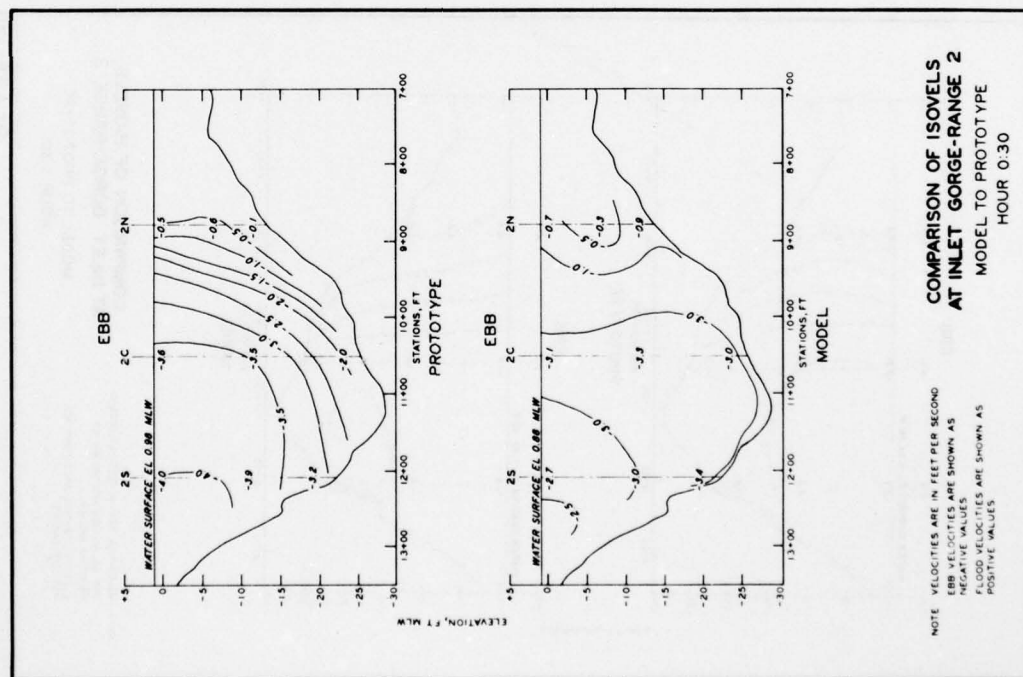


PLATE 138

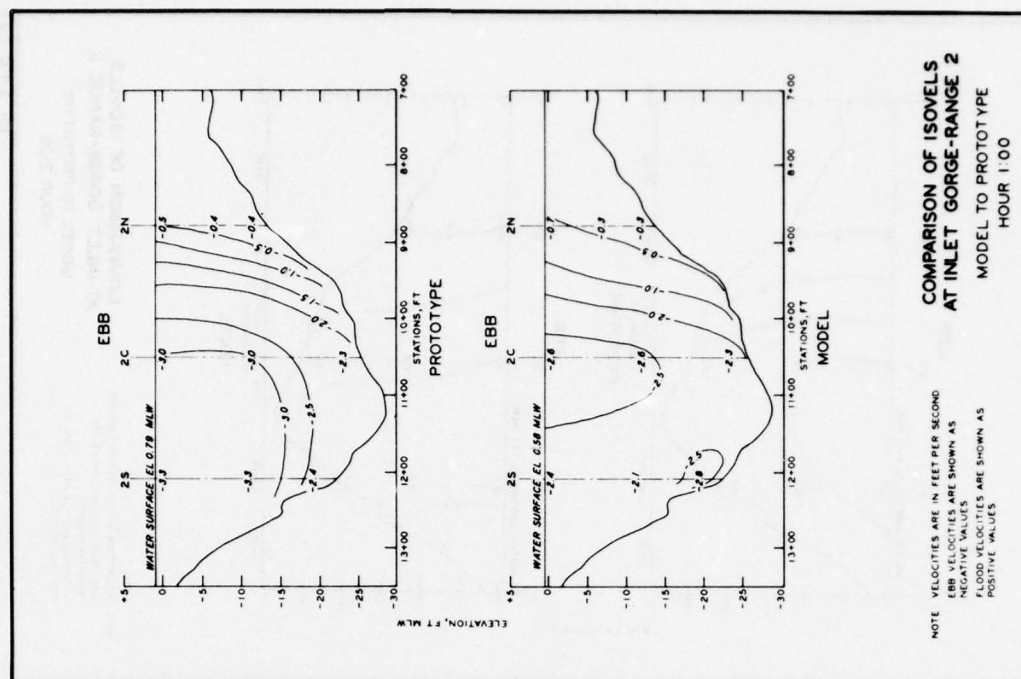
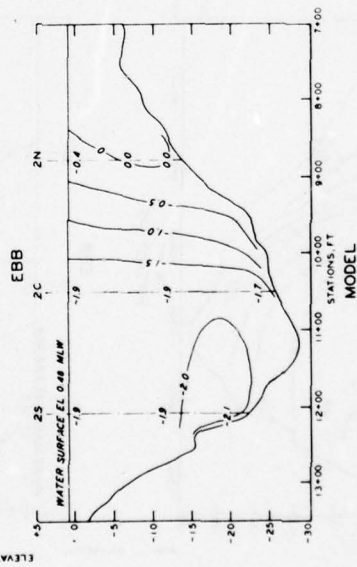
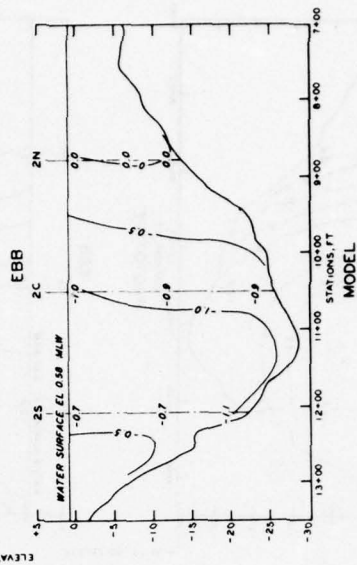


PLATE 139



NOTE: VELOCITIES ARE IN FEET PER SECOND

PLATE 140



NOTE: VELOCITIES ARE IN FEET PER SECOND
EBB VELOCITIES ARE SHOWN AS
NEGATIVE VALUES
FLOOD VELOCITIES ARE SHOWN AS
POSITIVE VALUES

PLATE 141

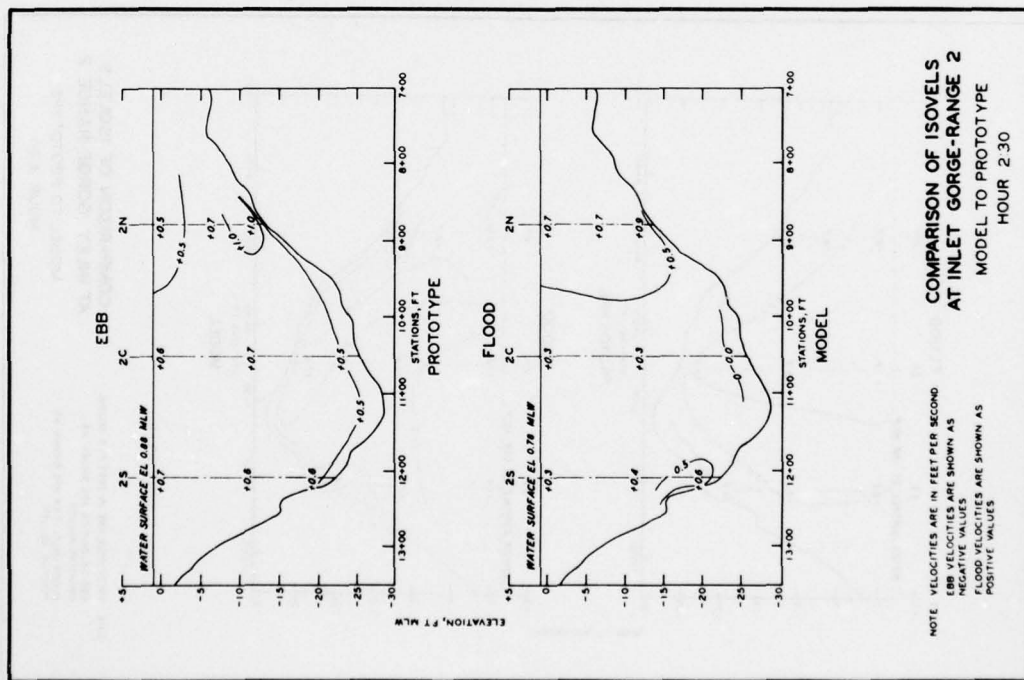


PLATE 142

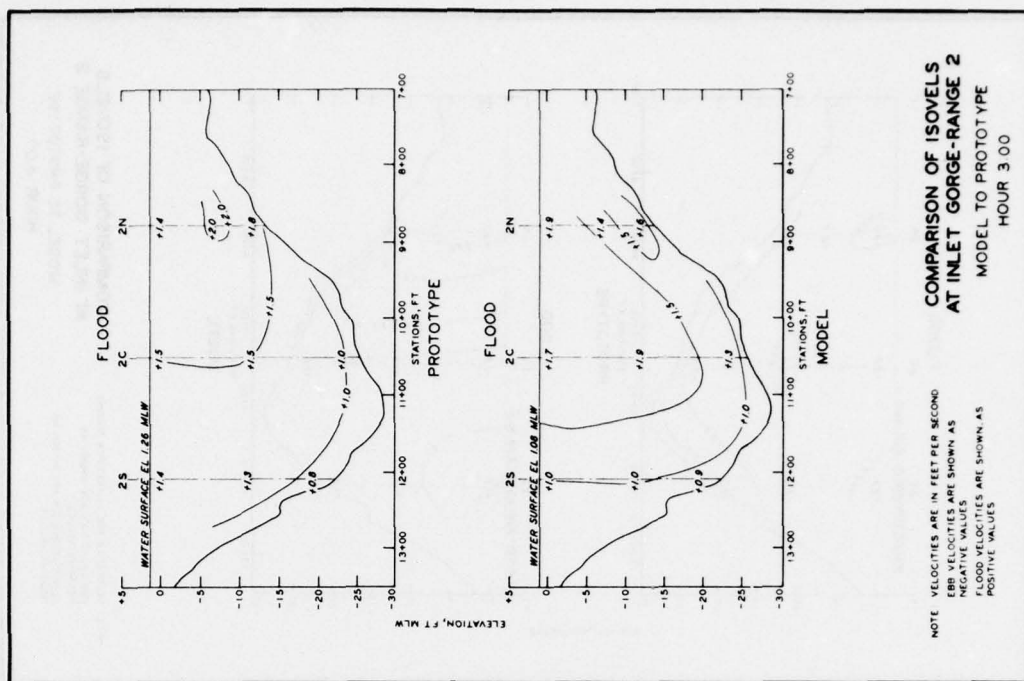


PLATE 143

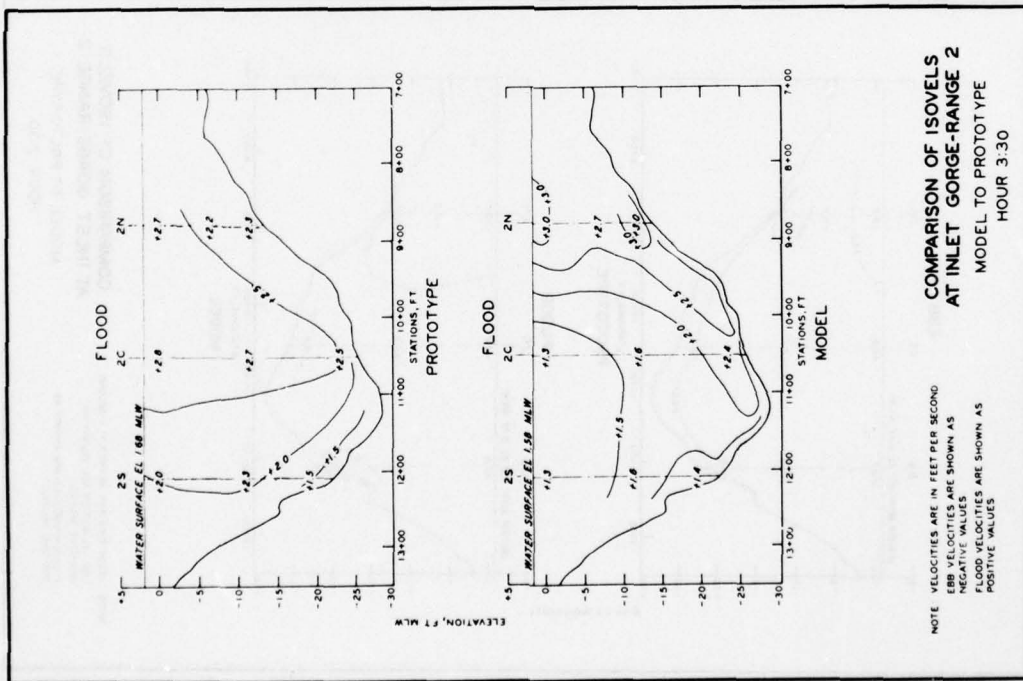


PLATE 144

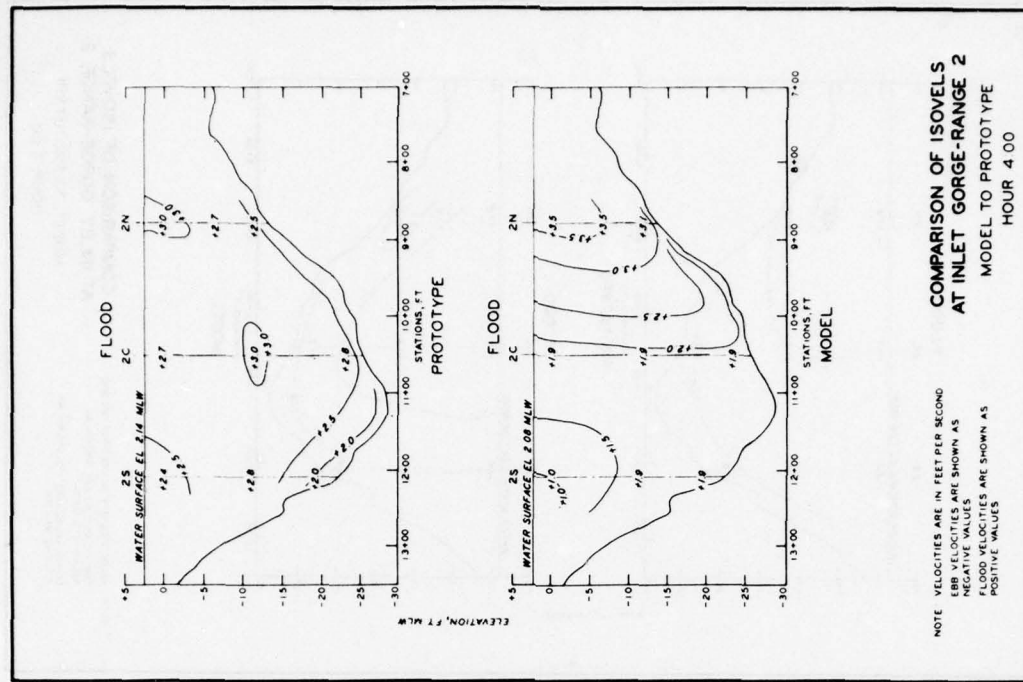


PLATE 145

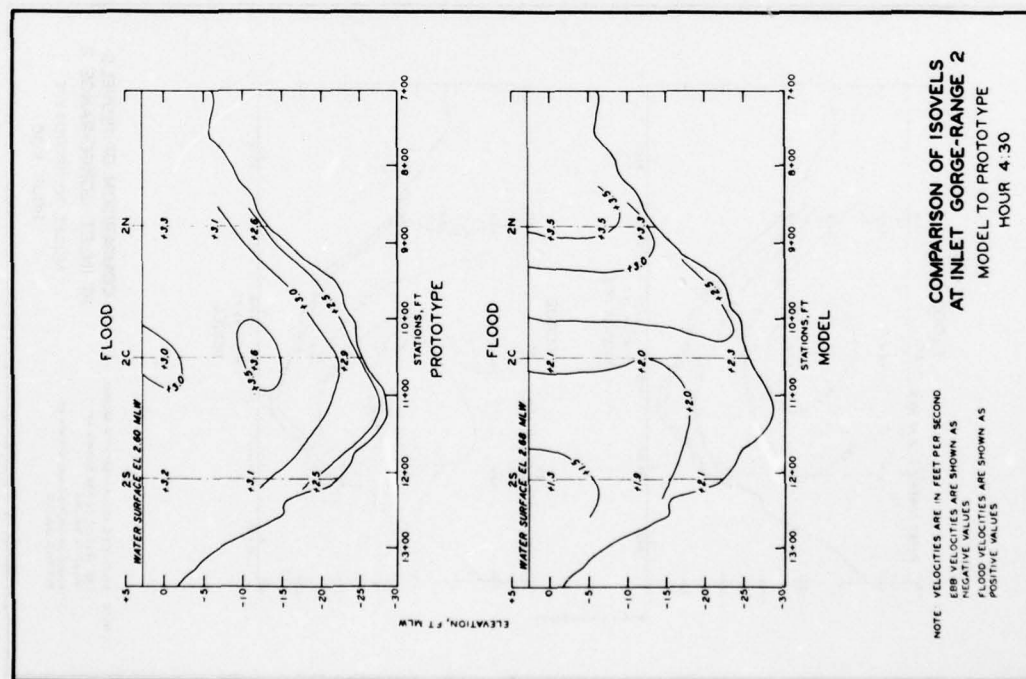


PLATE 146

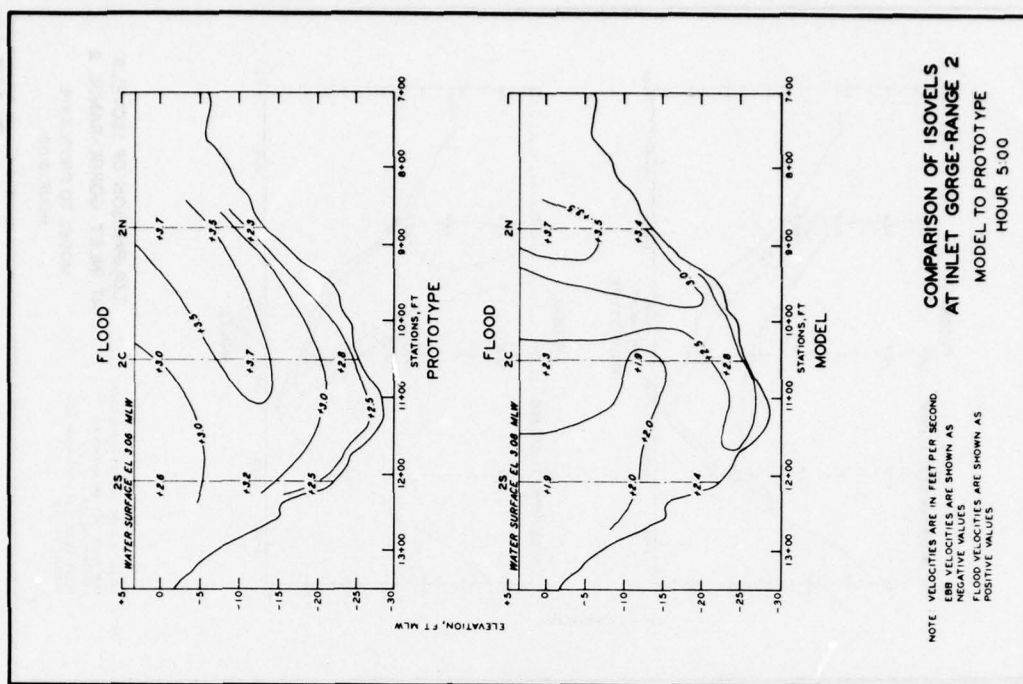


PLATE 147

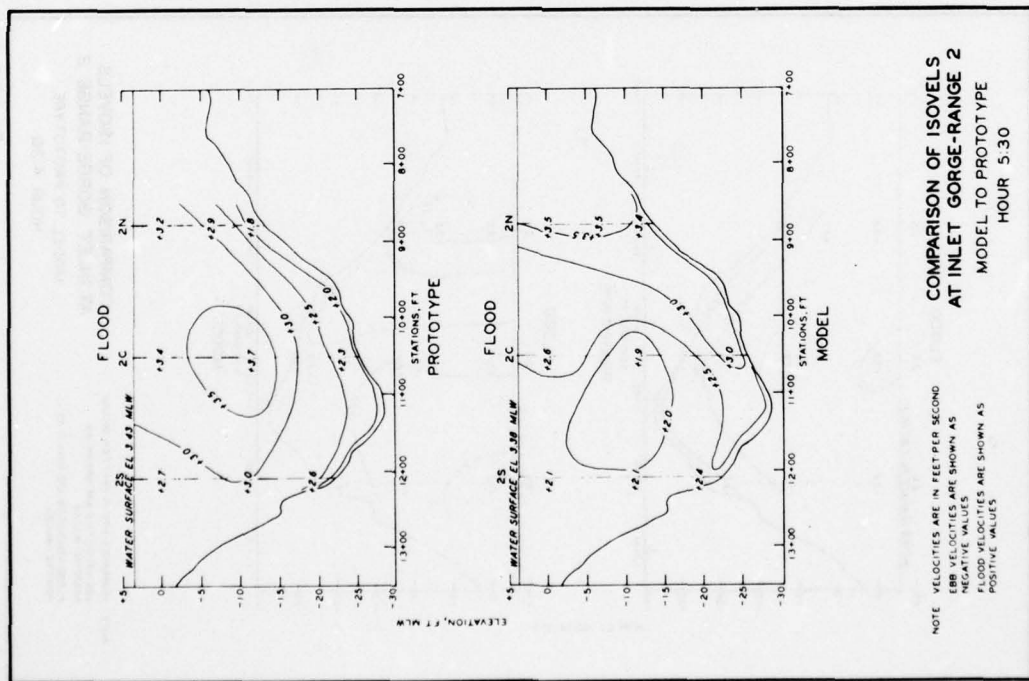


PLATE 148

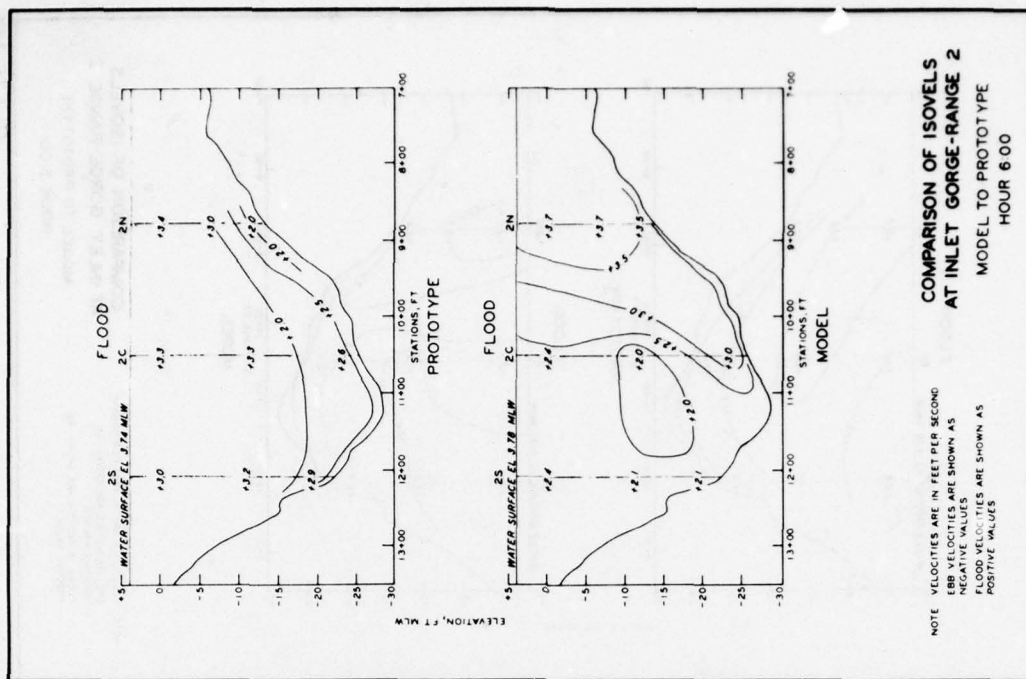


PLATE 149

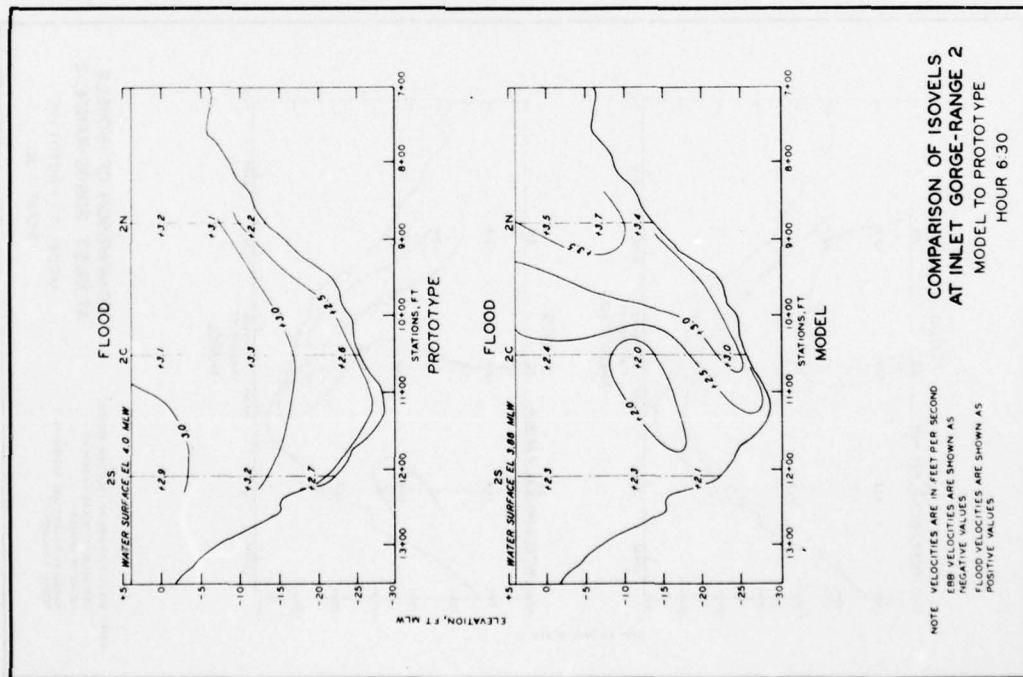


PLATE 150

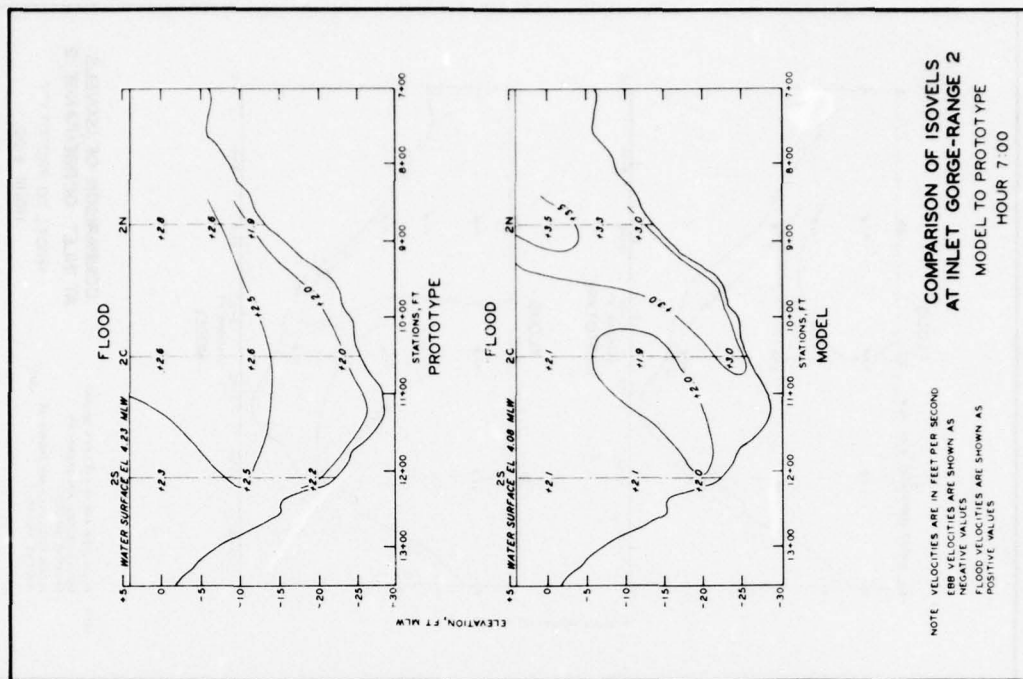


PLATE 151

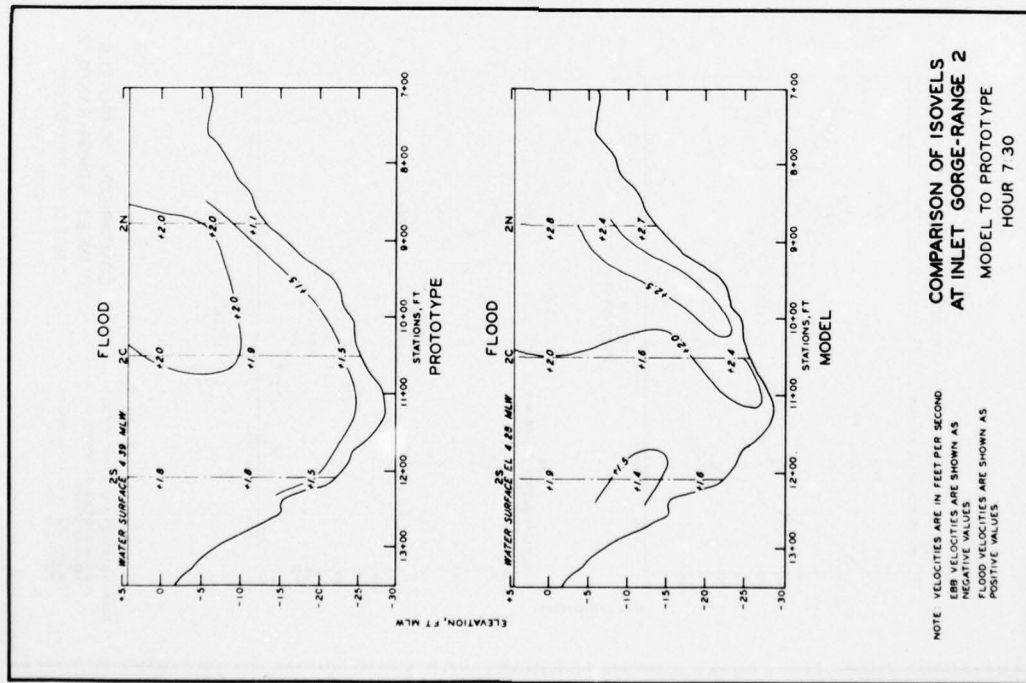


PLATE 152

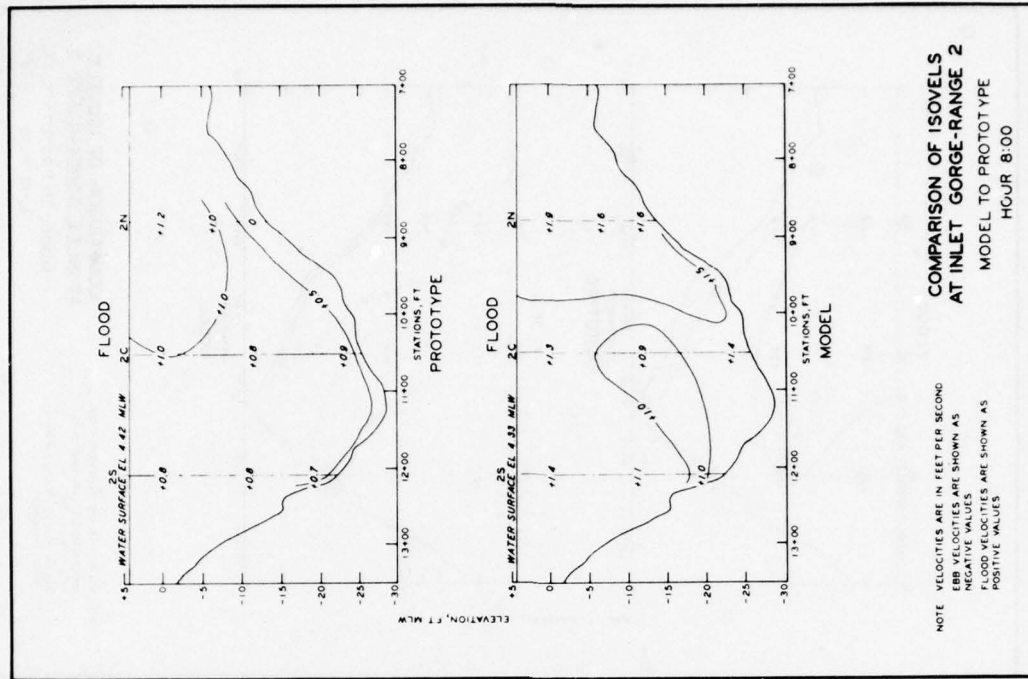


PLATE 153

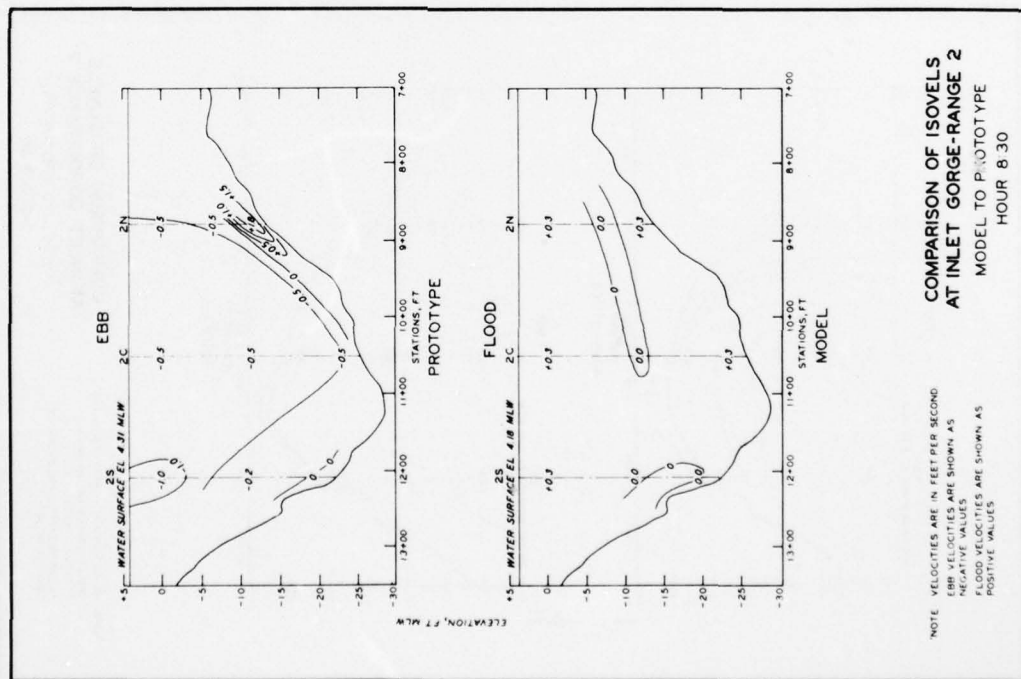


PLATE 154

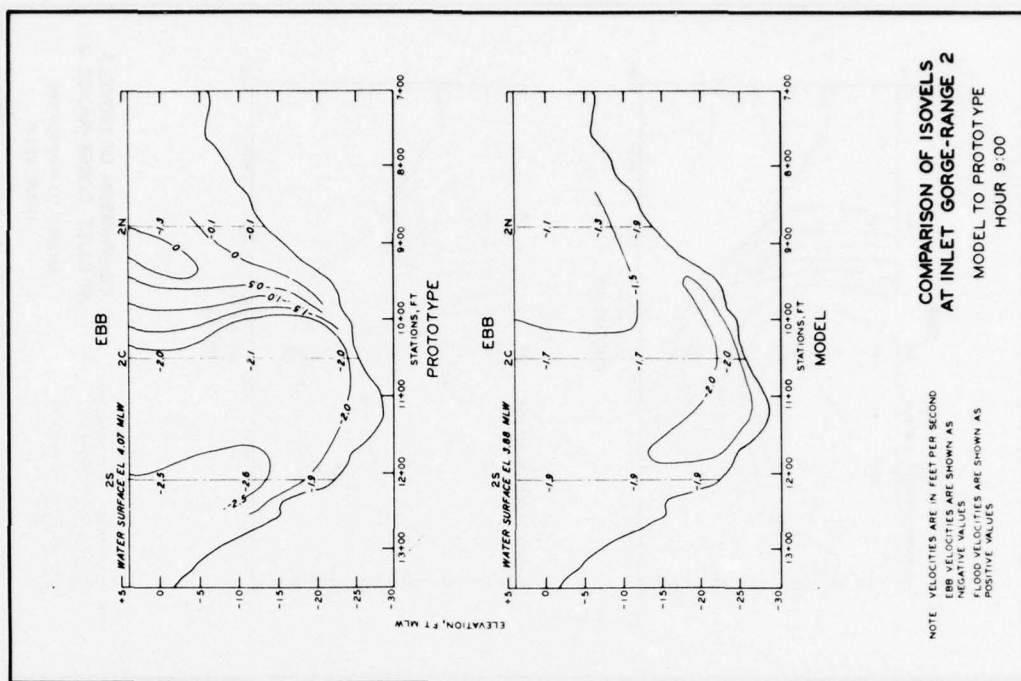


PLATE 155

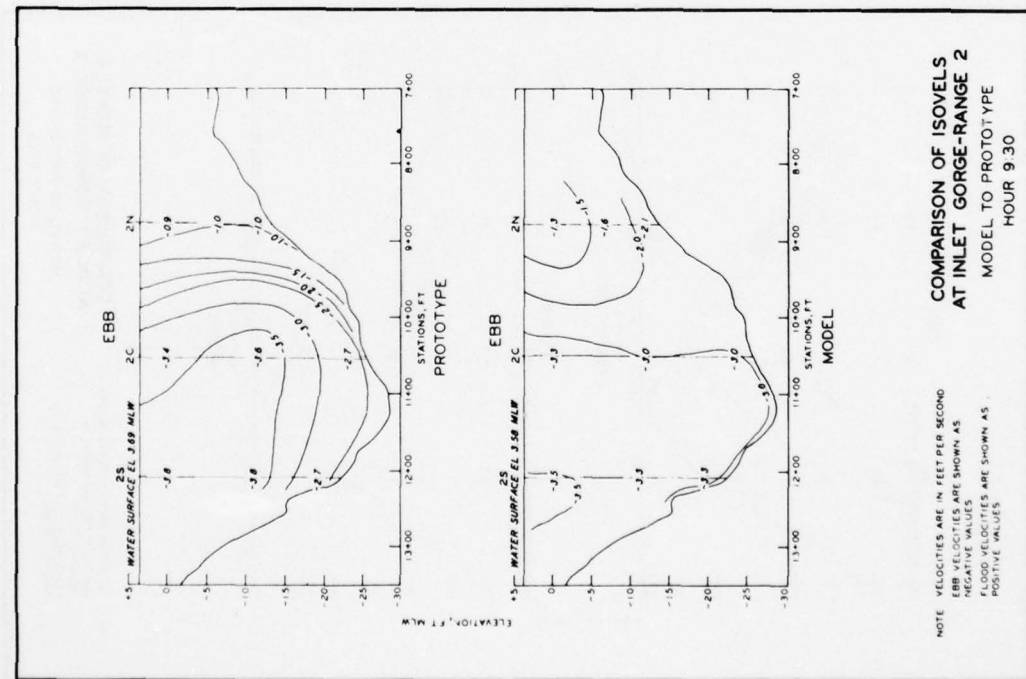


PLATE 156

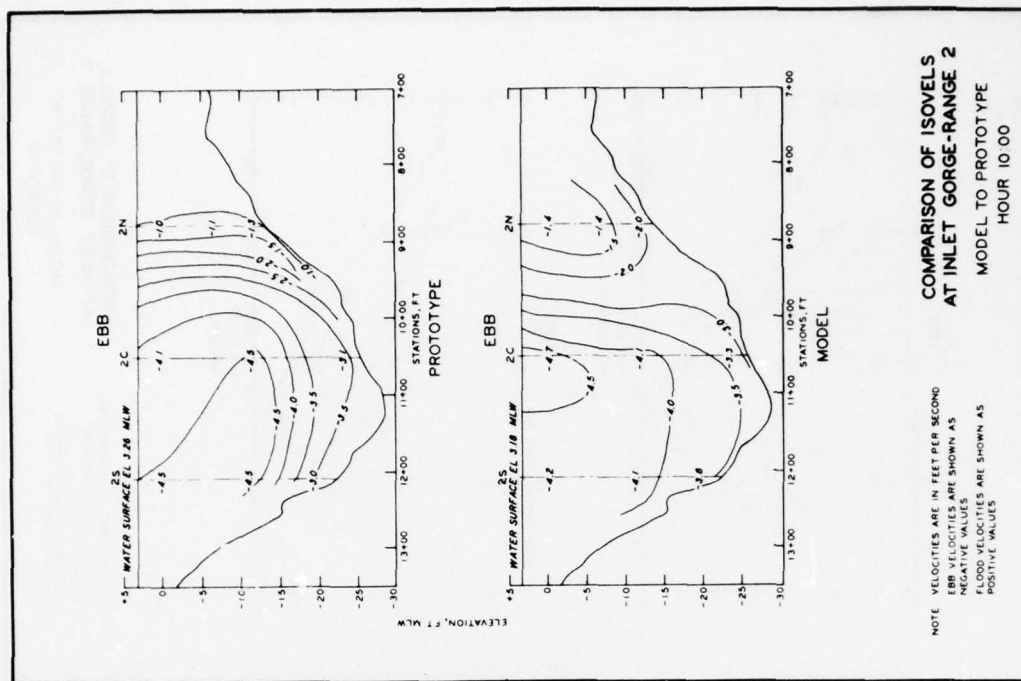


PLATE 157

AD-A055 523

ARMY ENGINEER WATERWAYS EXPERIMENT STATION VICKSBURG MISS F/G 8/3
PHYSICAL MODEL SIMULATION OF THE HYDRAULICS OF MASONBORO INLET,--ETC(U)
NOV 77 R A SAGER, W C SEABERGH

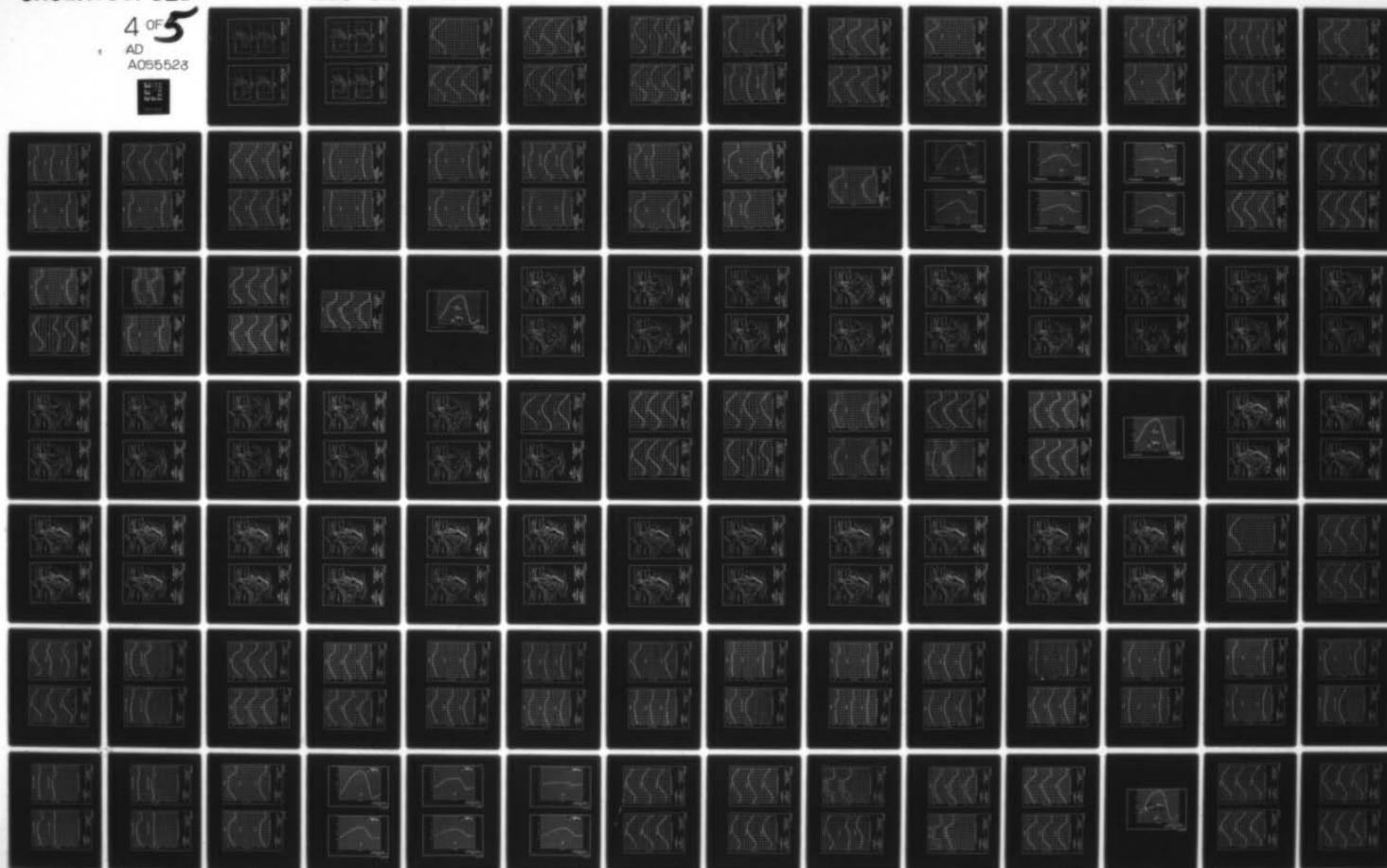
UNCLASSIFIED

WES-GITI-15

NL

4 OF 5

AD
A055523



IFIED

4 OF 5

AD

A055523



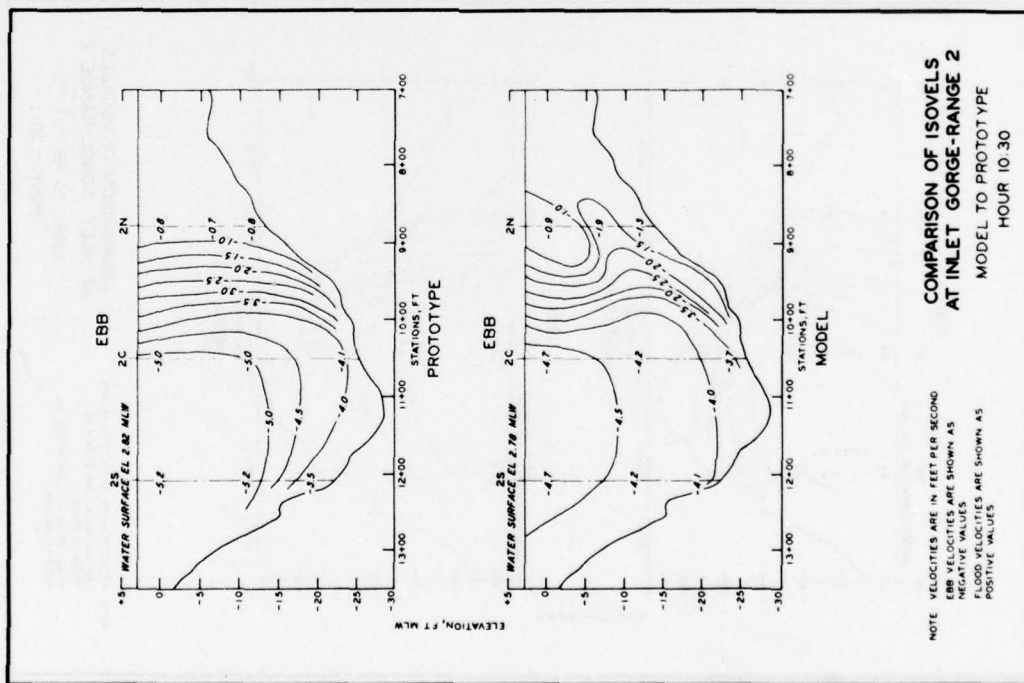


PLATE 158

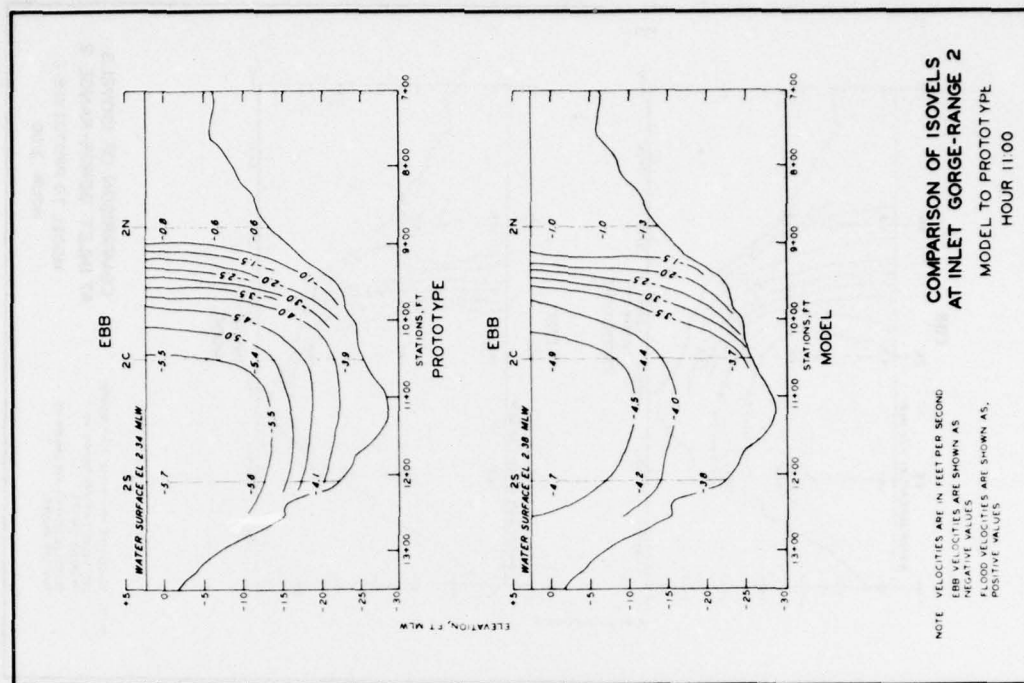


PLATE 159

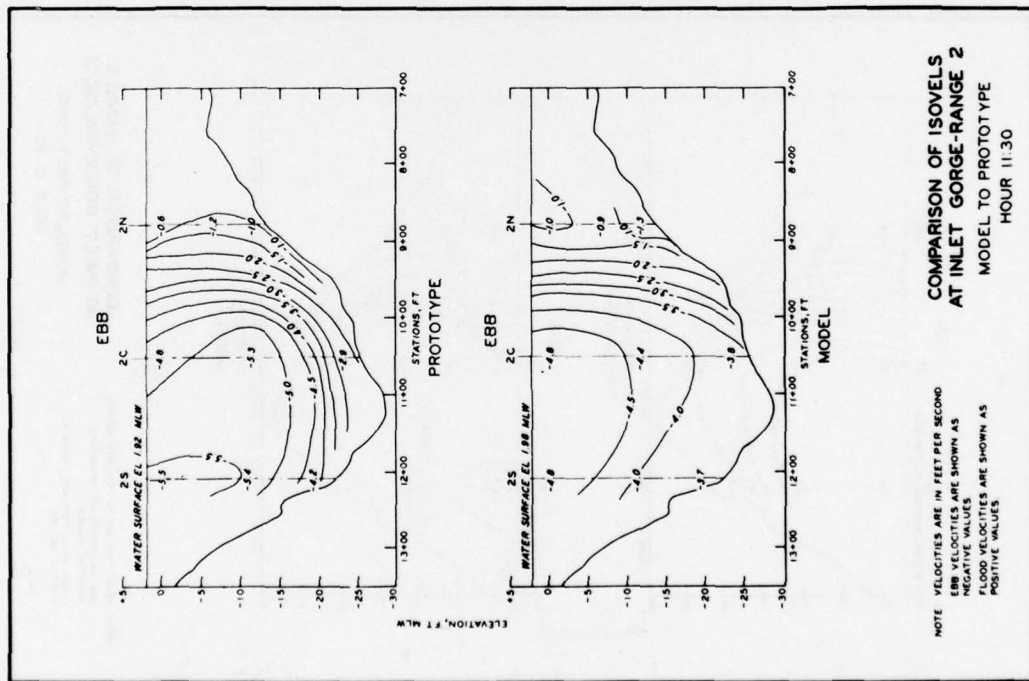


PLATE 160

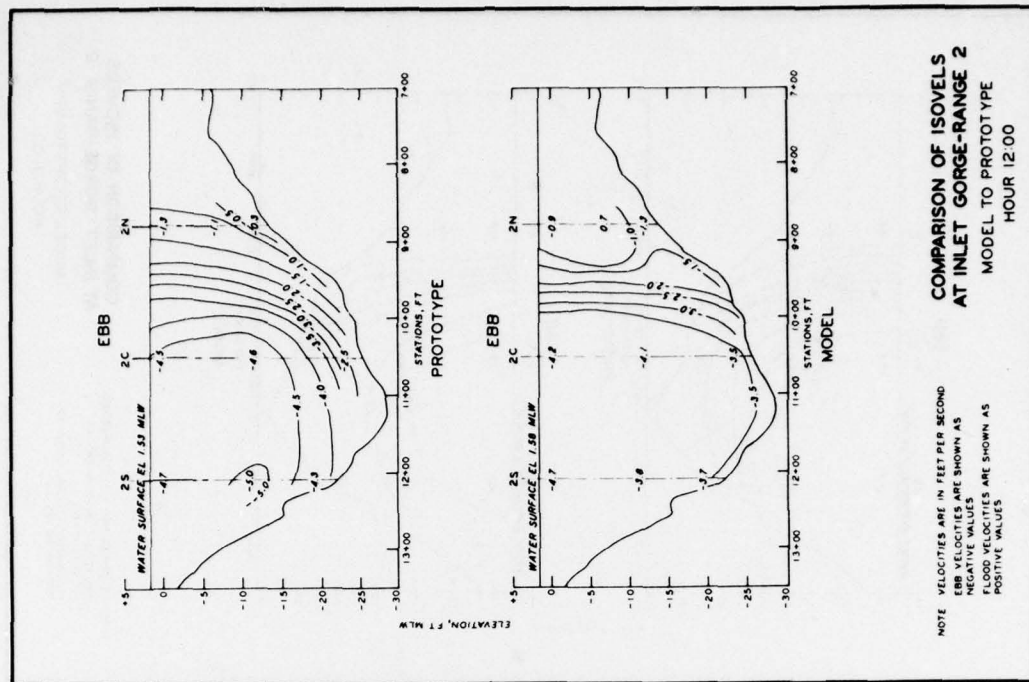


PLATE 161

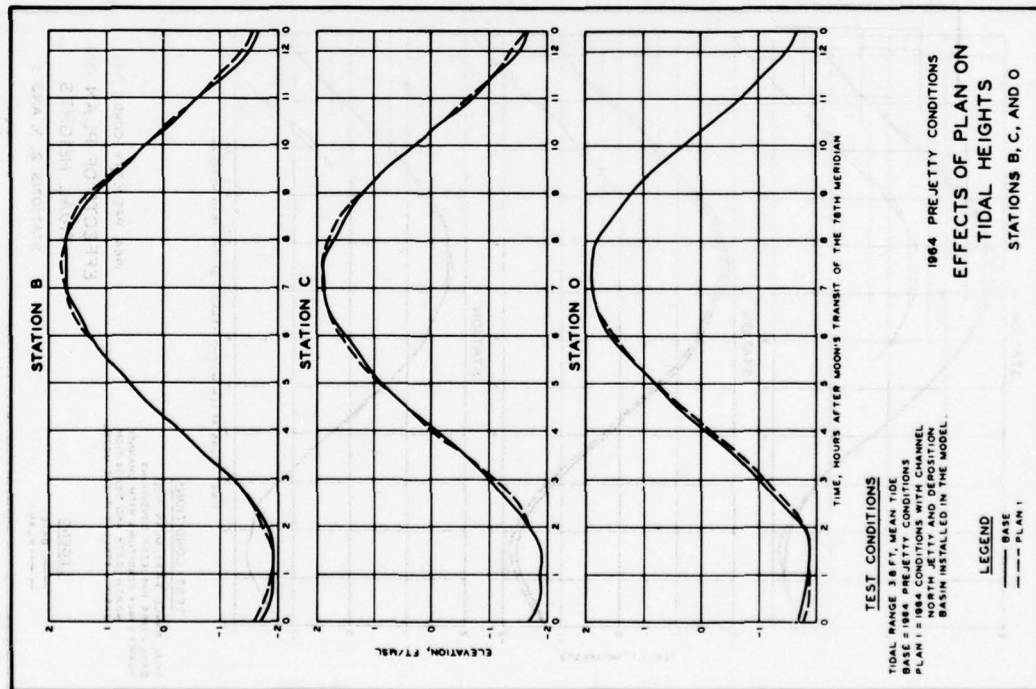


PLATE 162

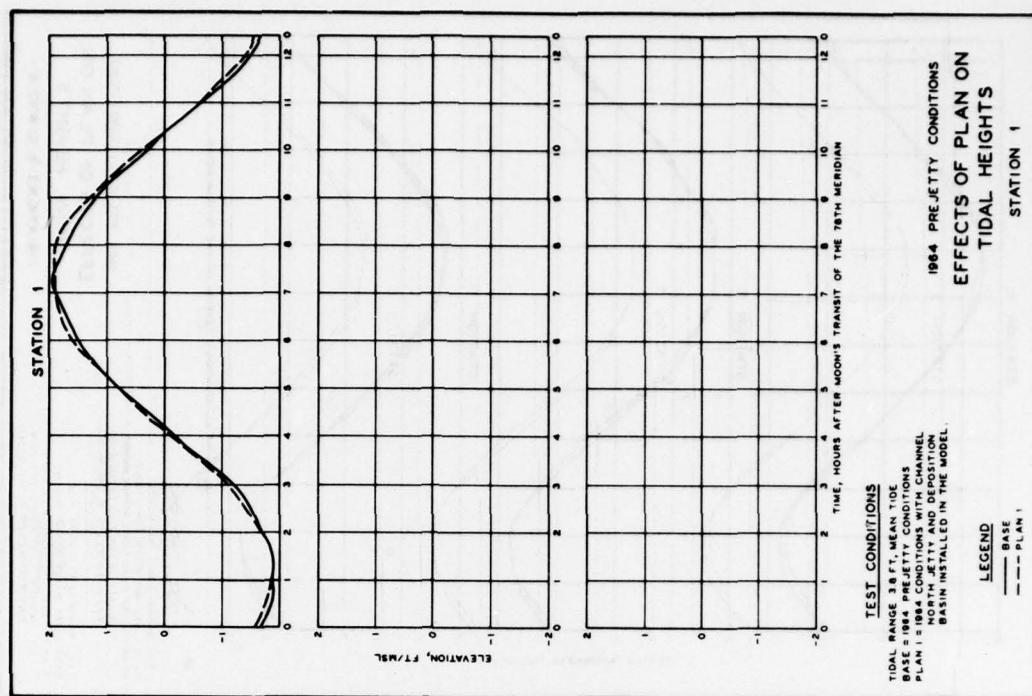


PLATE 163

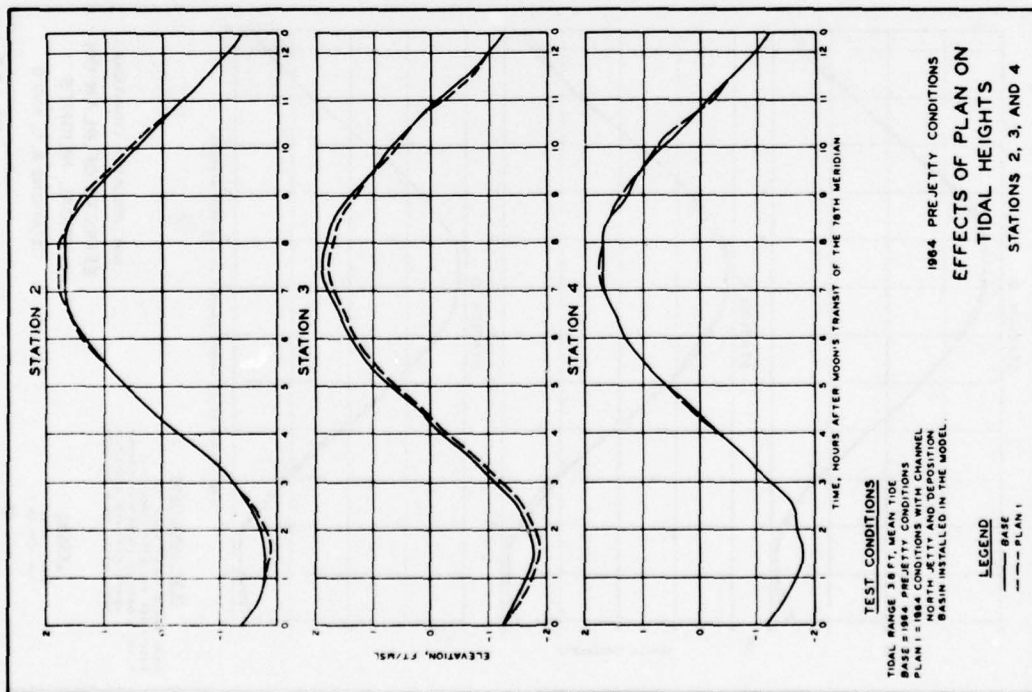


PLATE 164

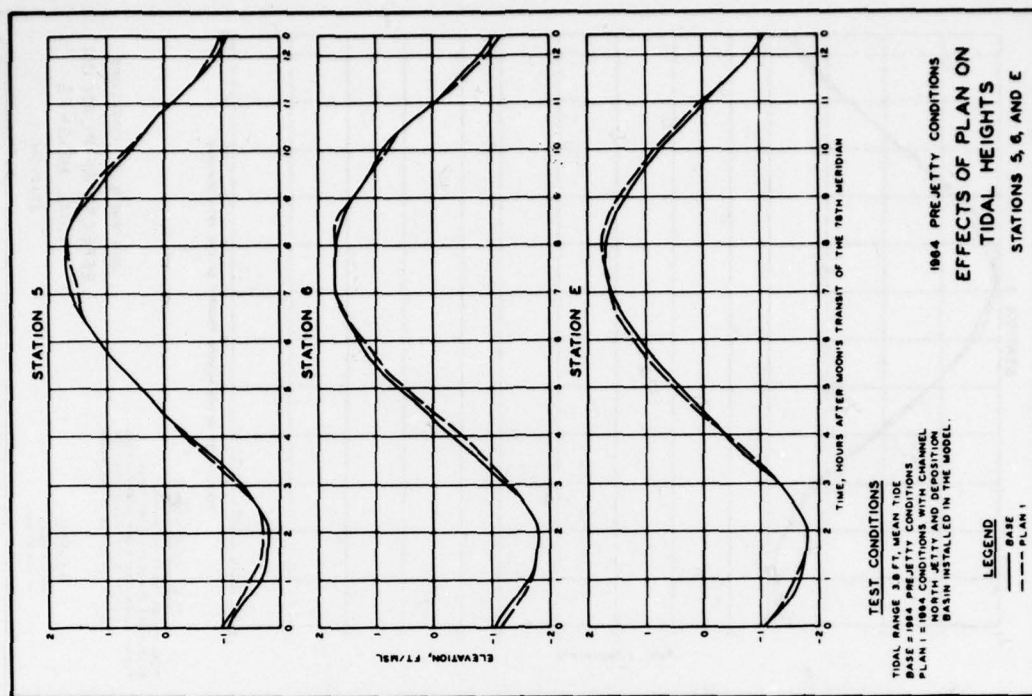


PLATE 165

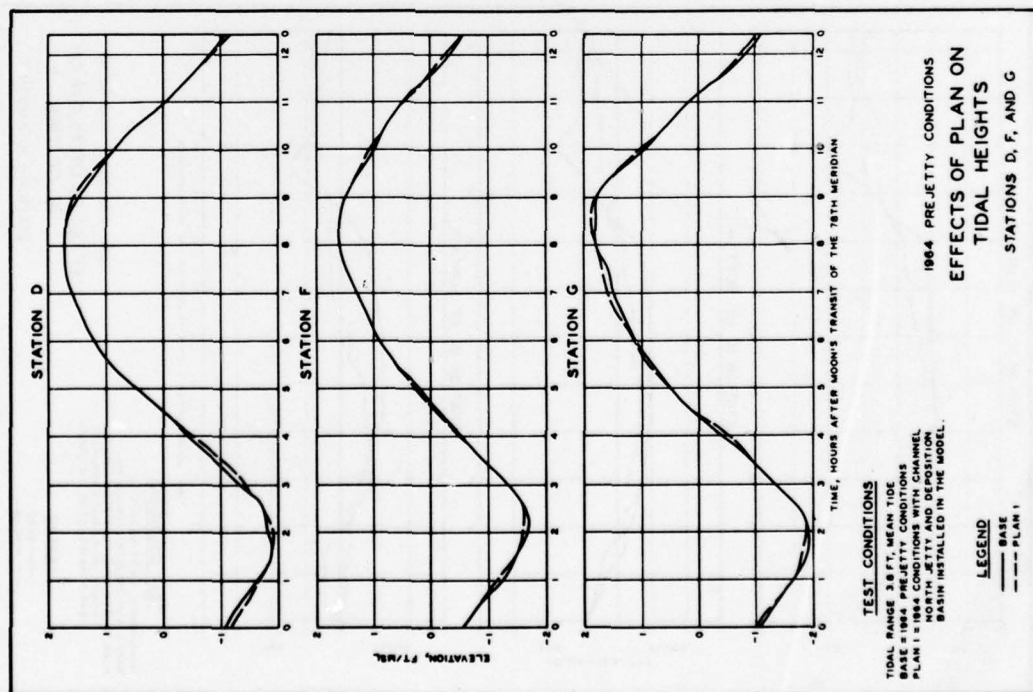


PLATE 166

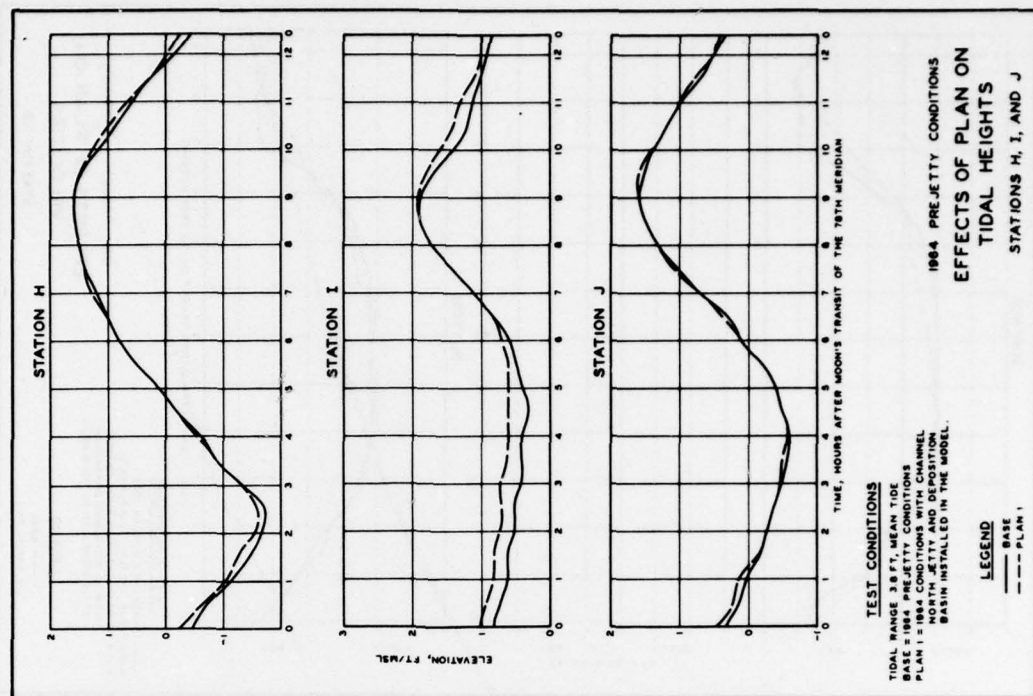


PLATE 167

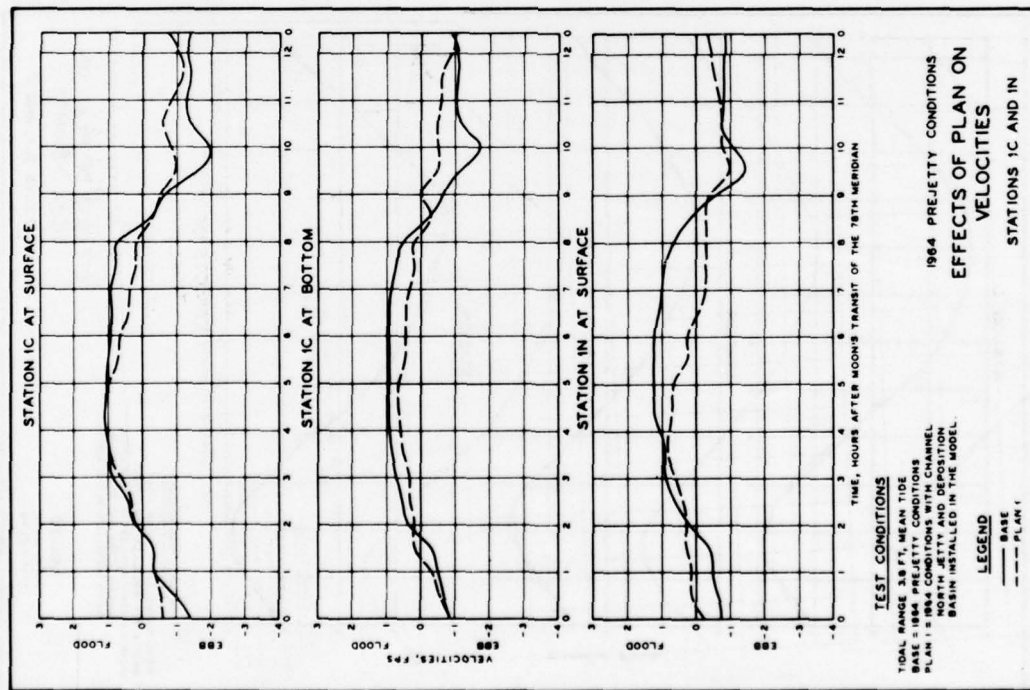


PLATE 168

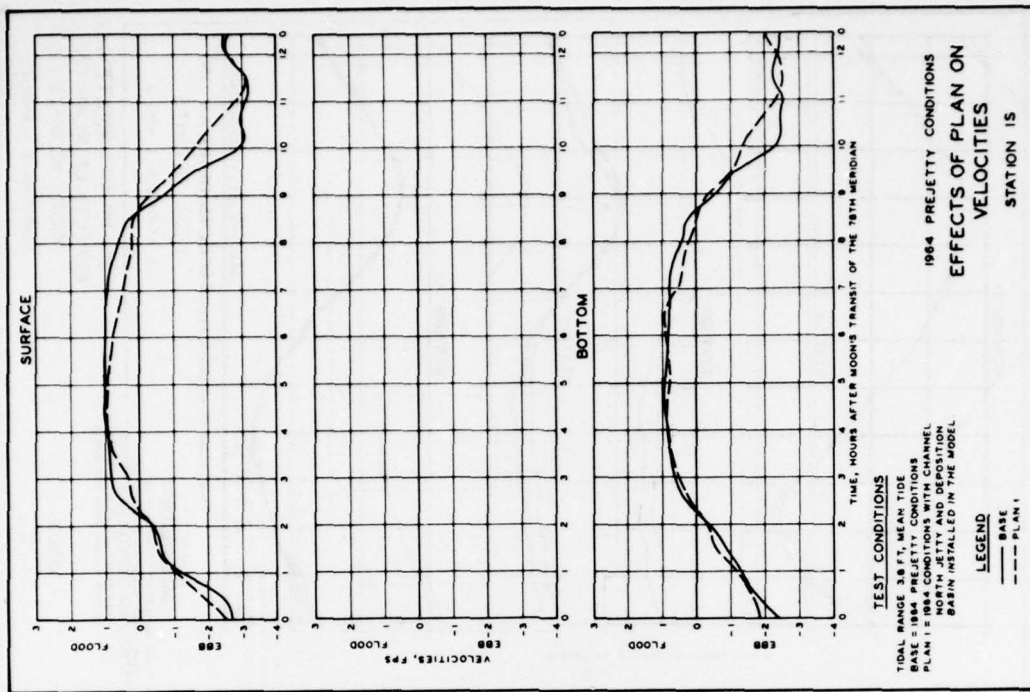


PLATE 169

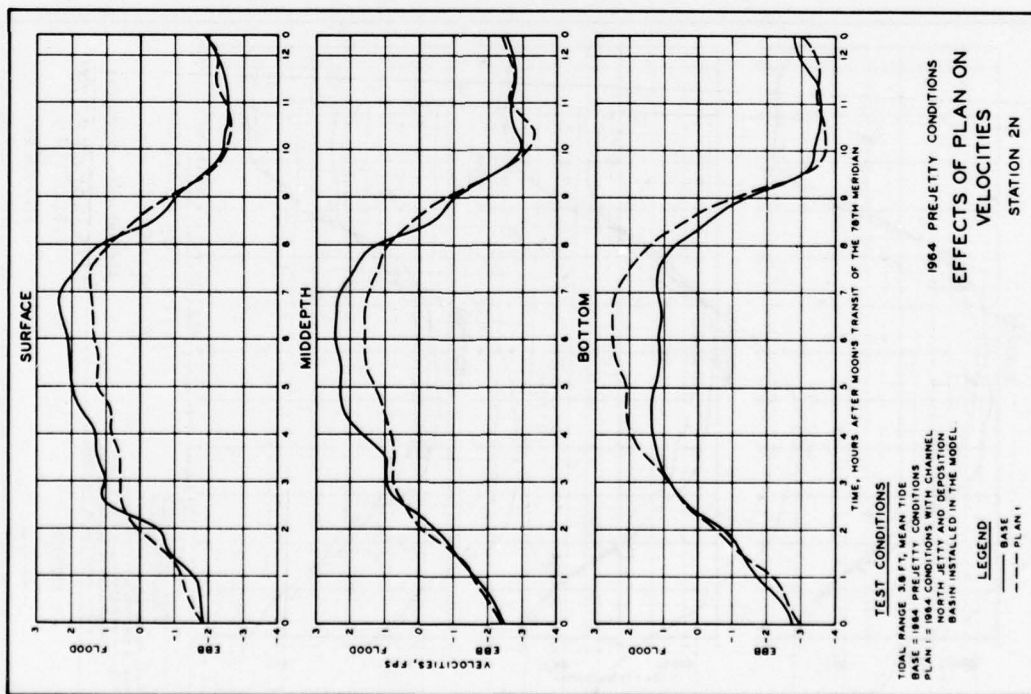


PLATE 170

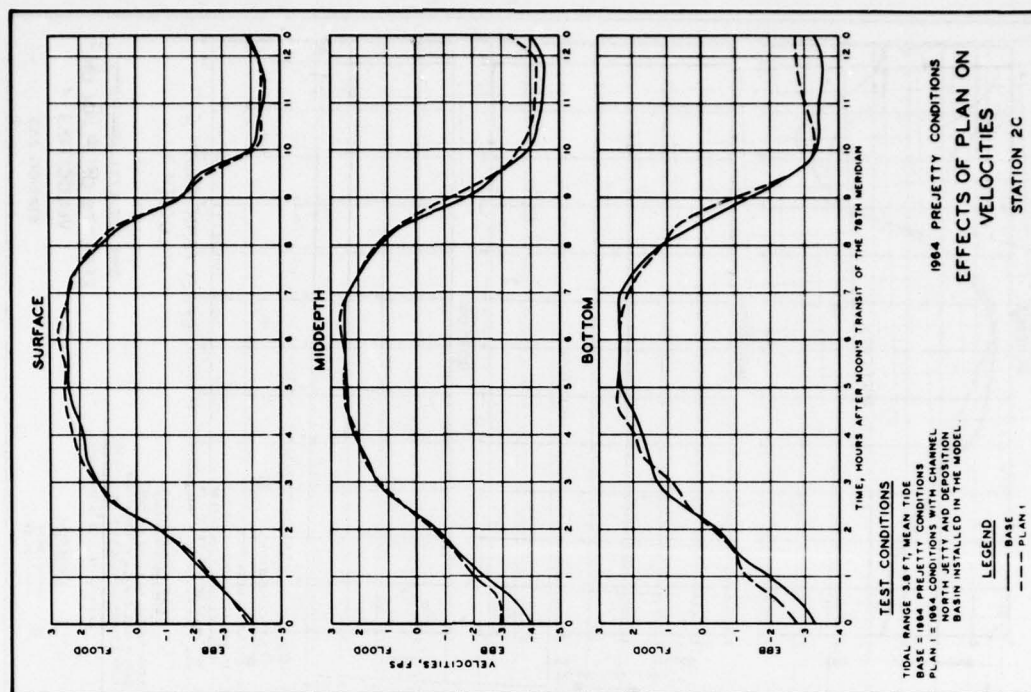


PLATE 171

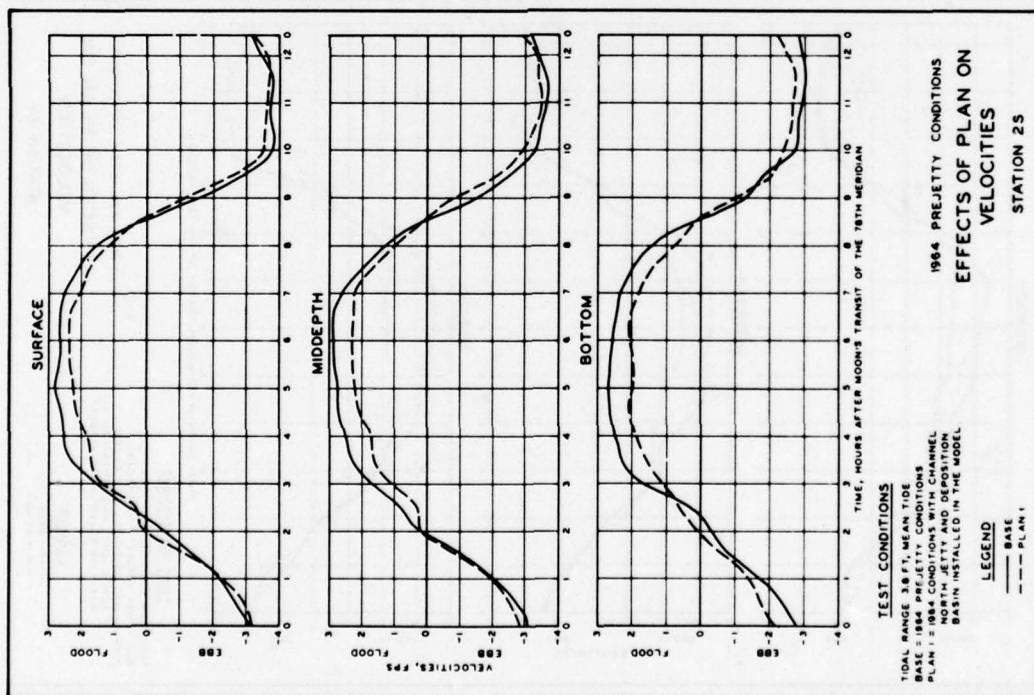


PLATE 172

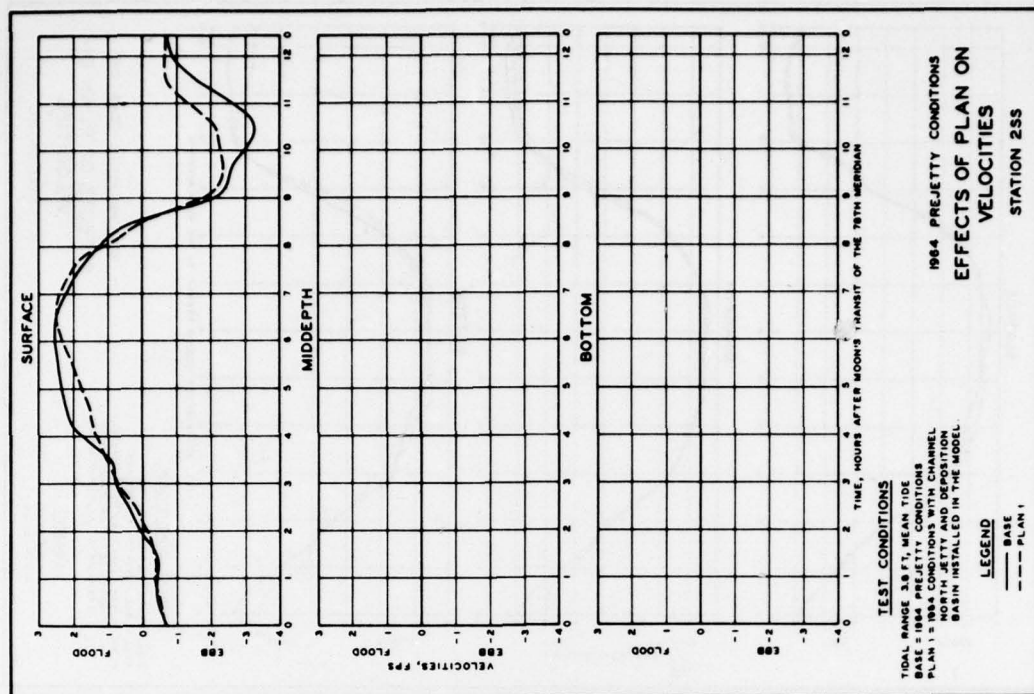


PLATE 173

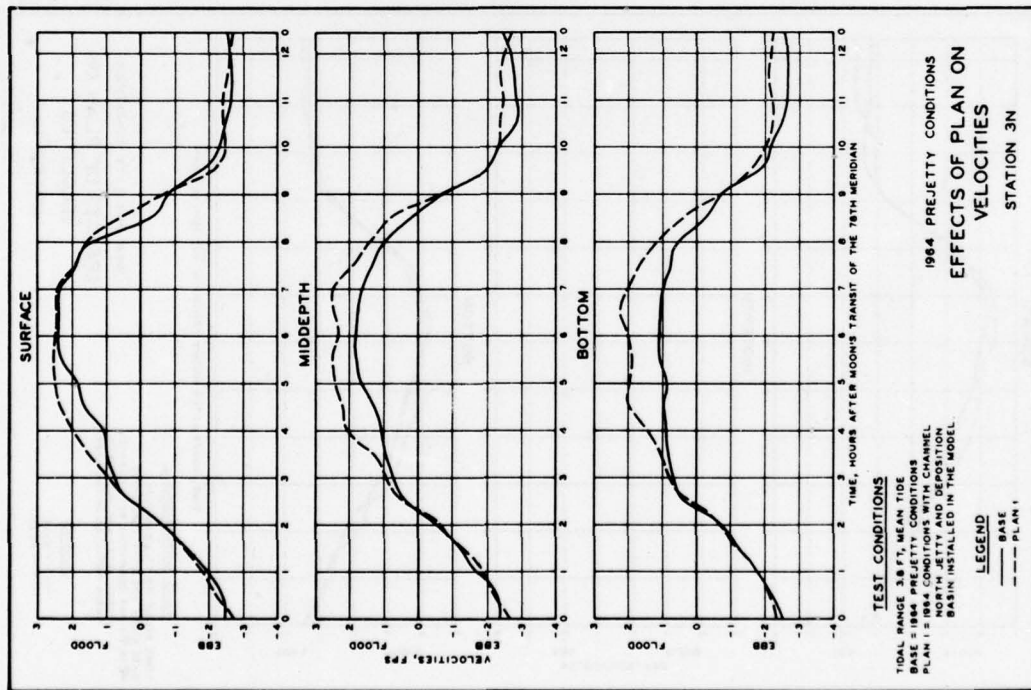


PLATE 174

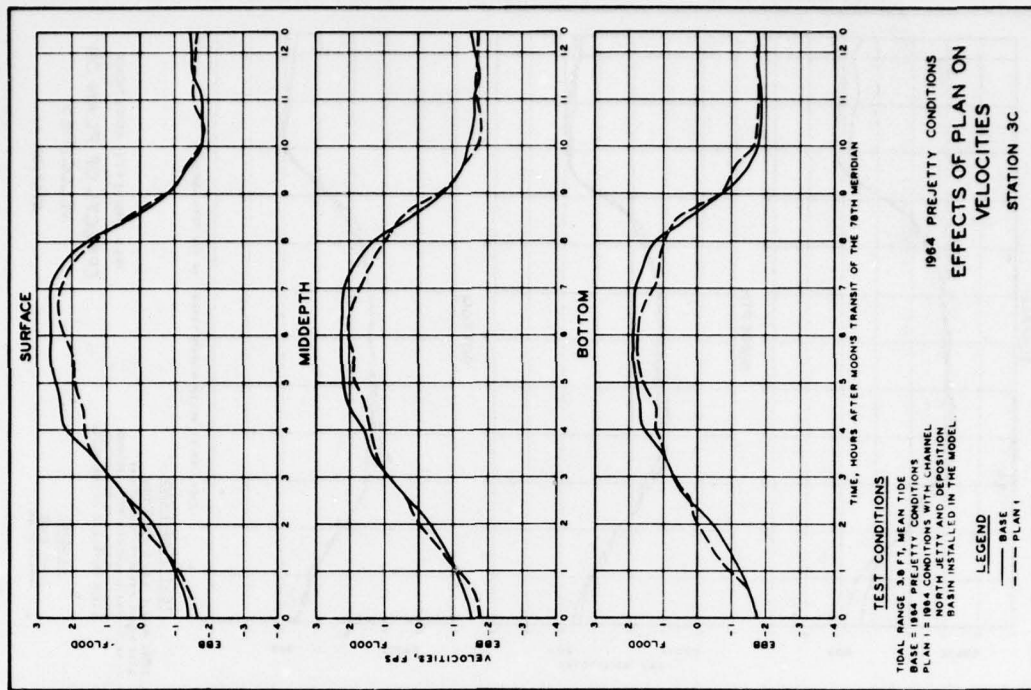


PLATE 175

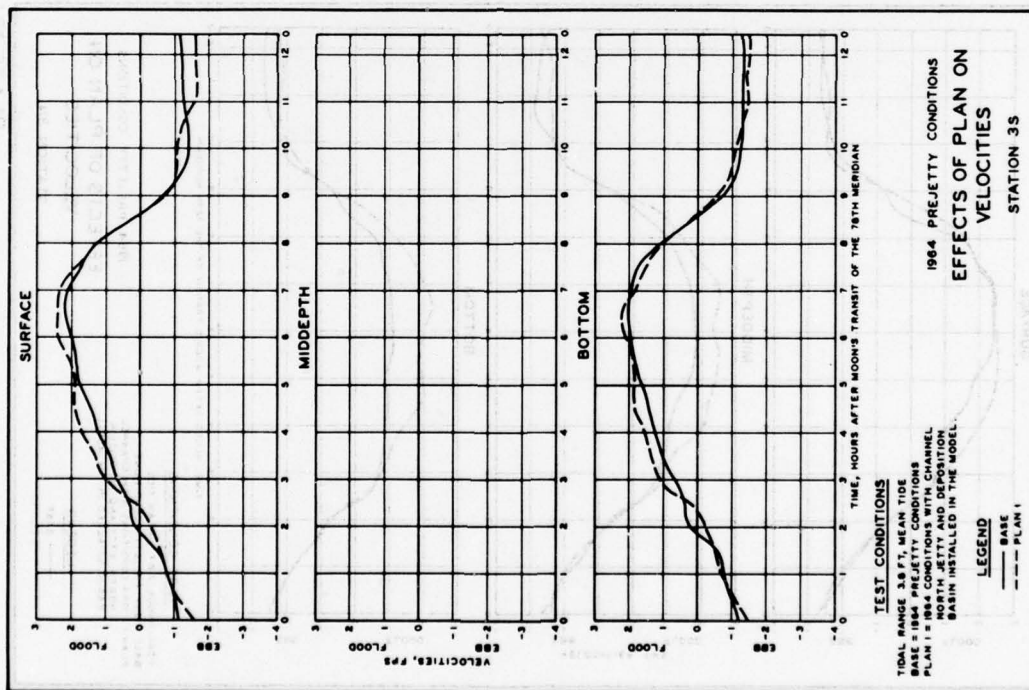


PLATE 176

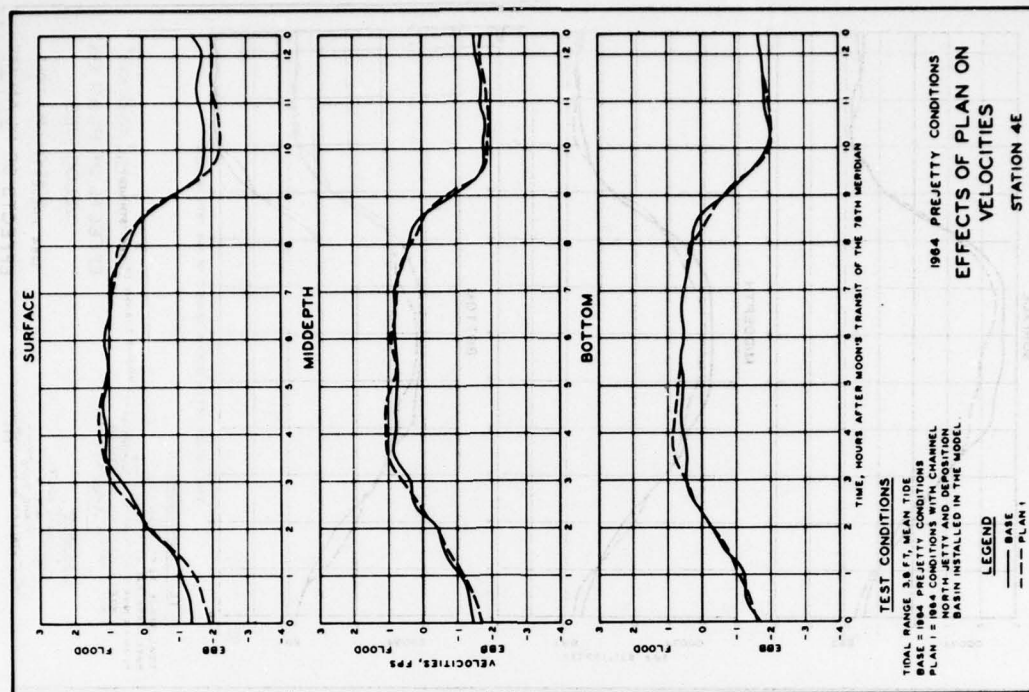


PLATE 177

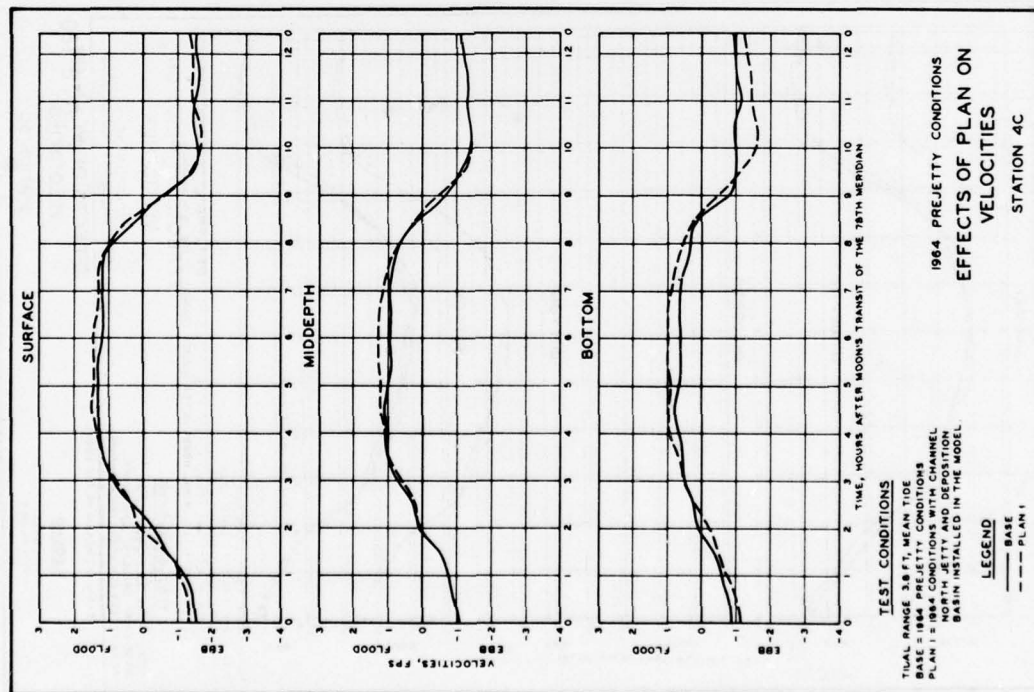


PLATE 178

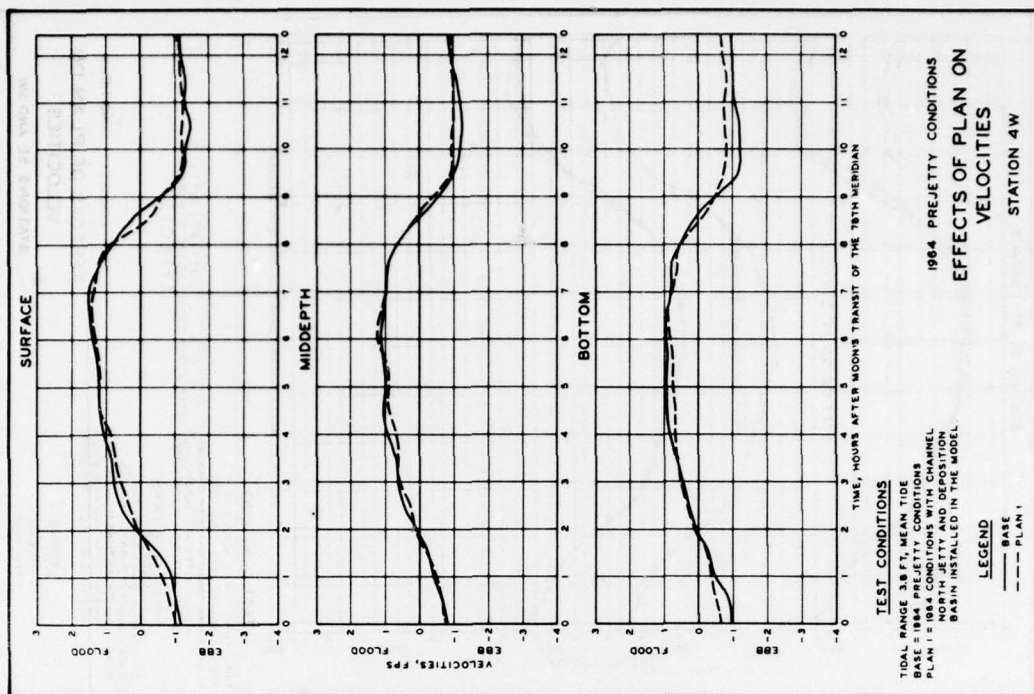


PLATE 179

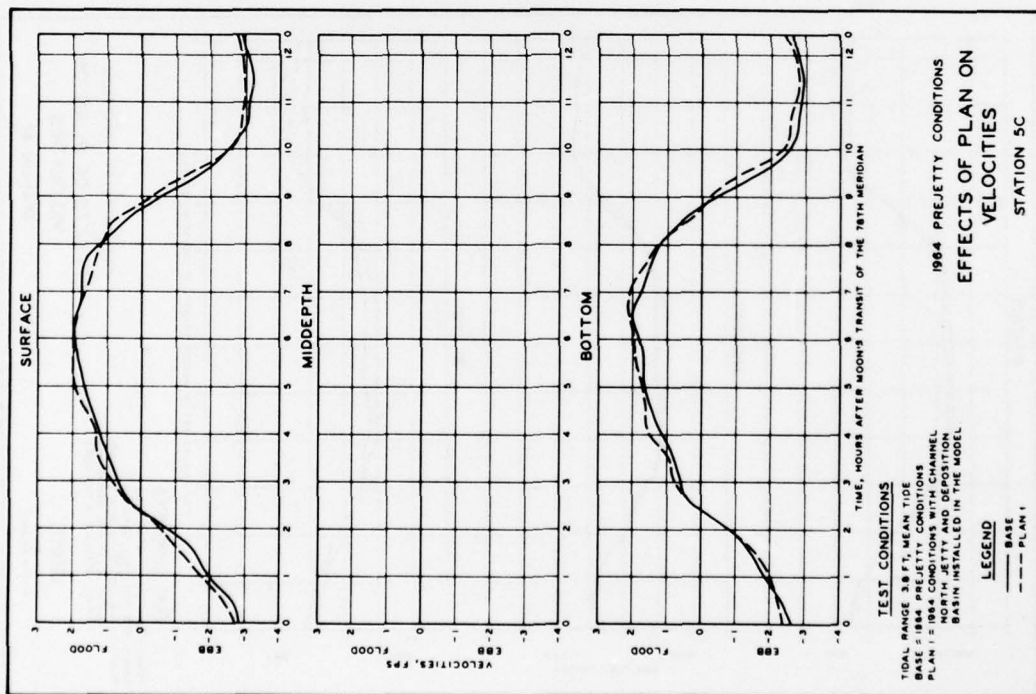


PLATE 180

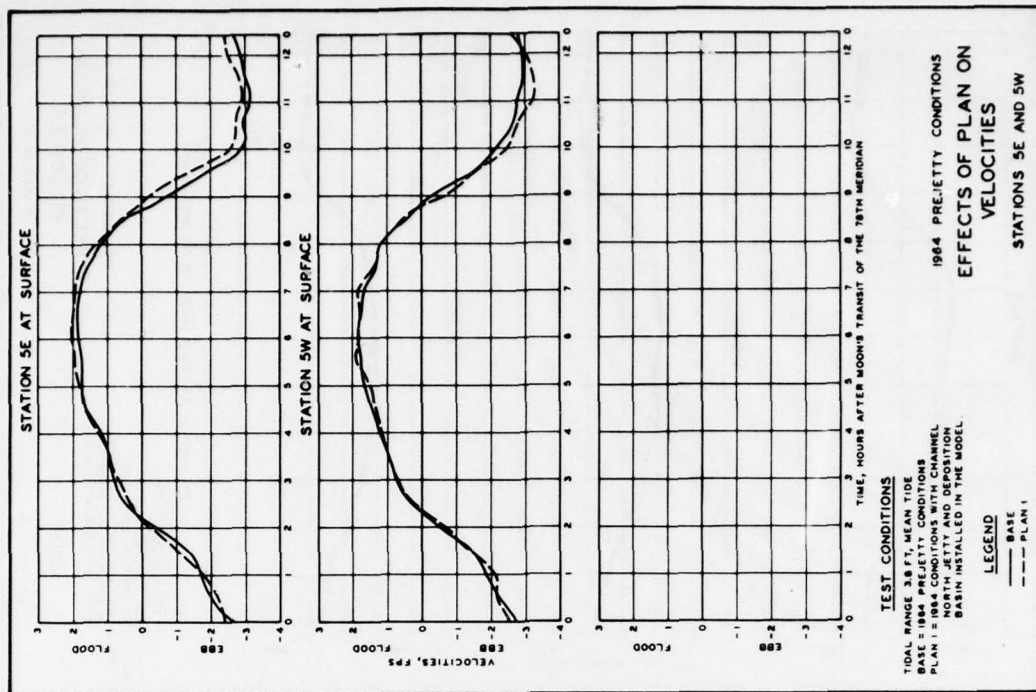


PLATE 181

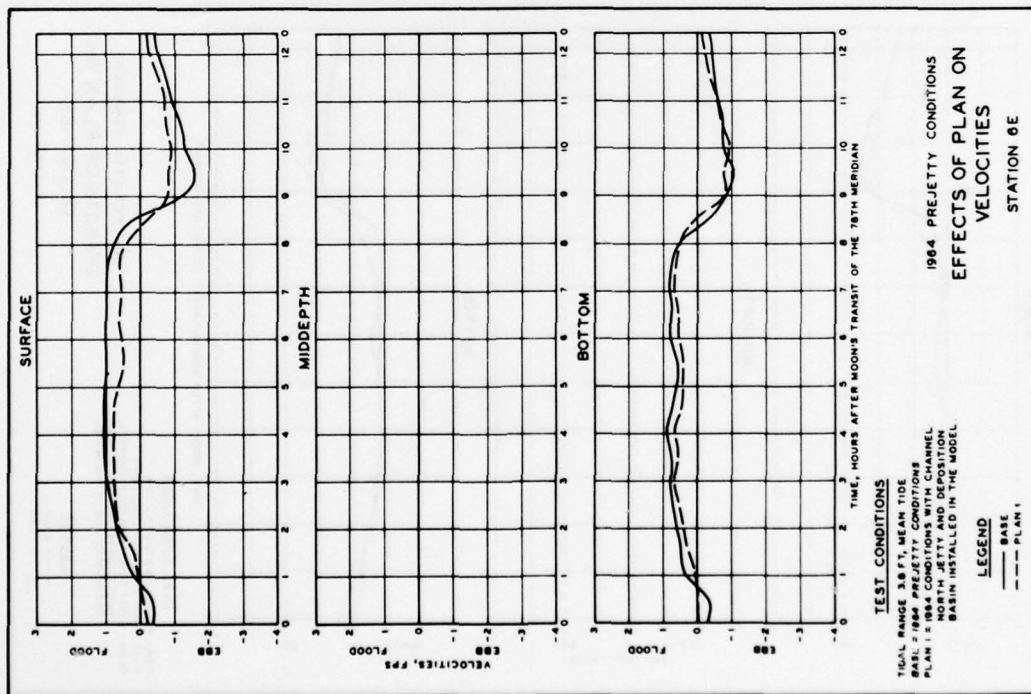


PLATE 182

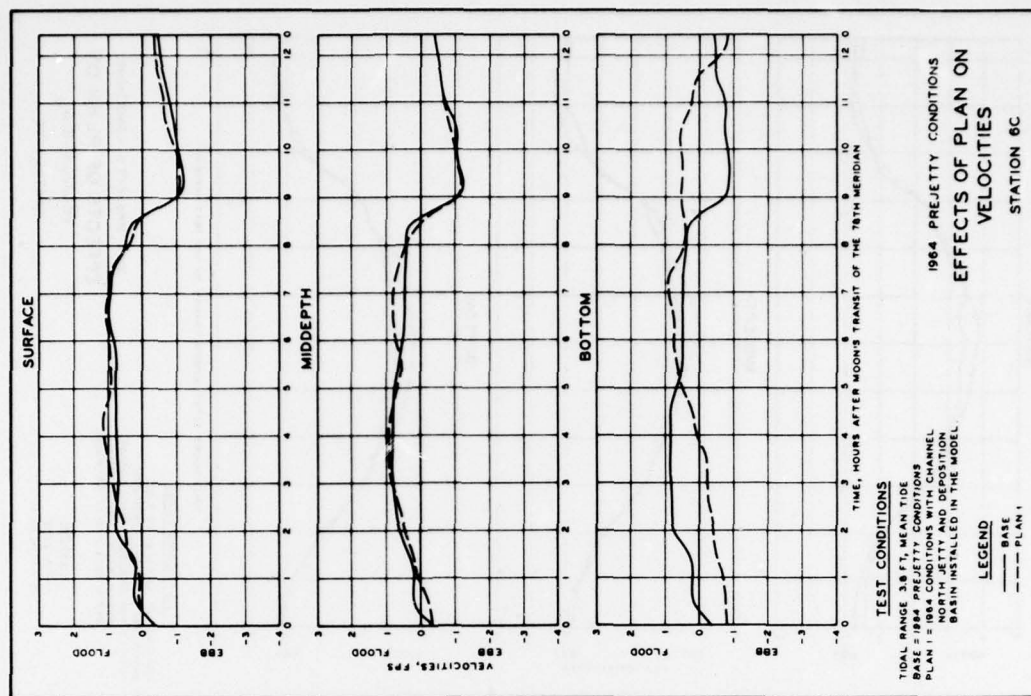


PLATE 183

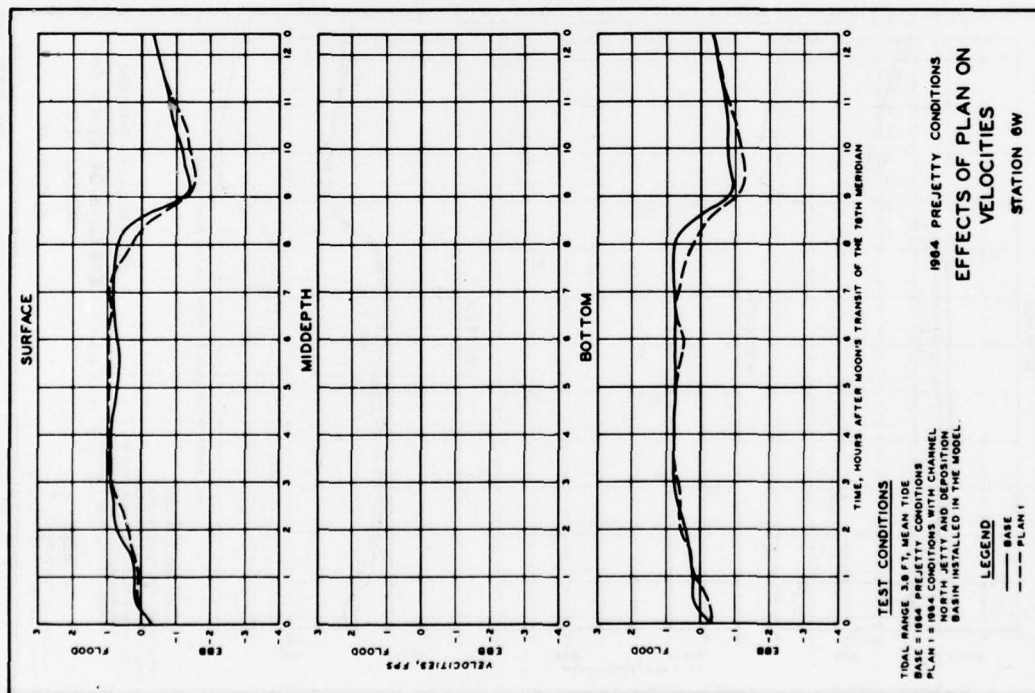


PLATE 184

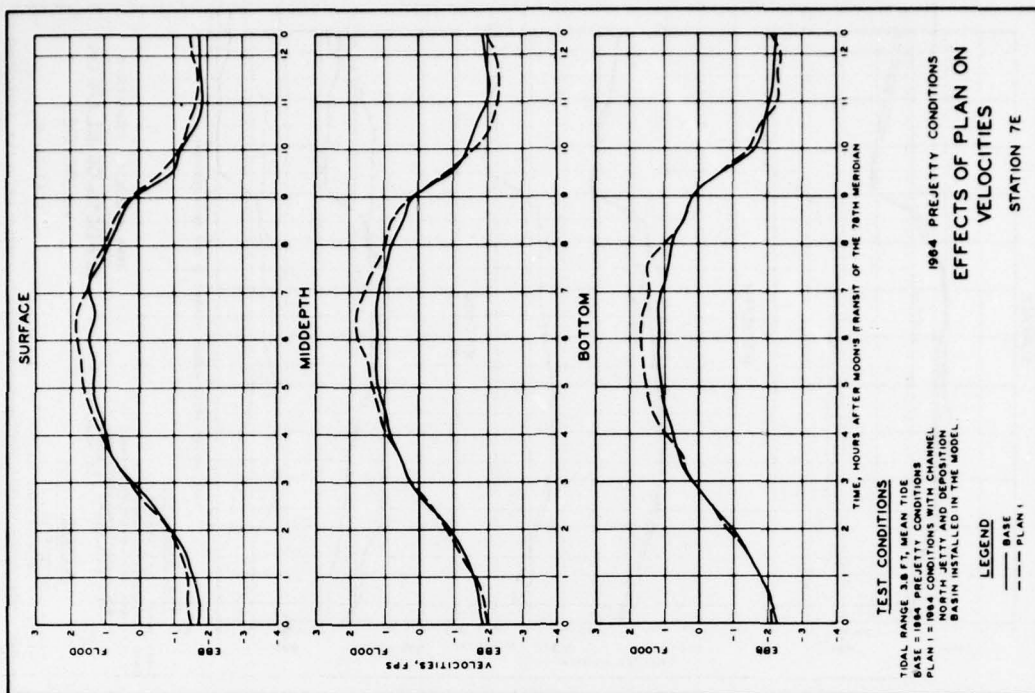


PLATE 185

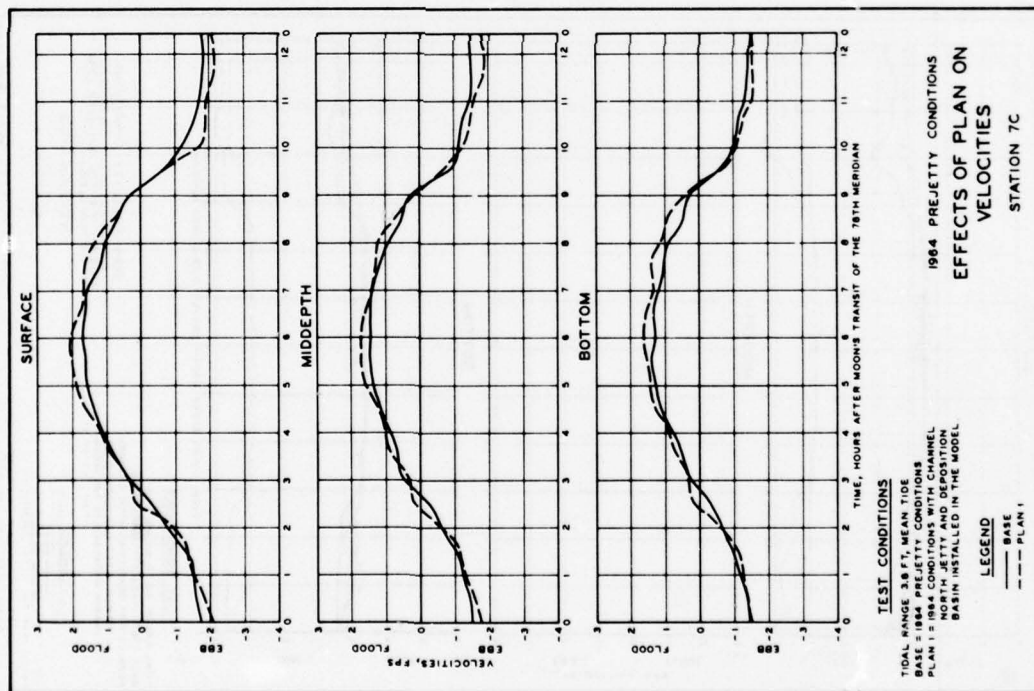


PLATE 186

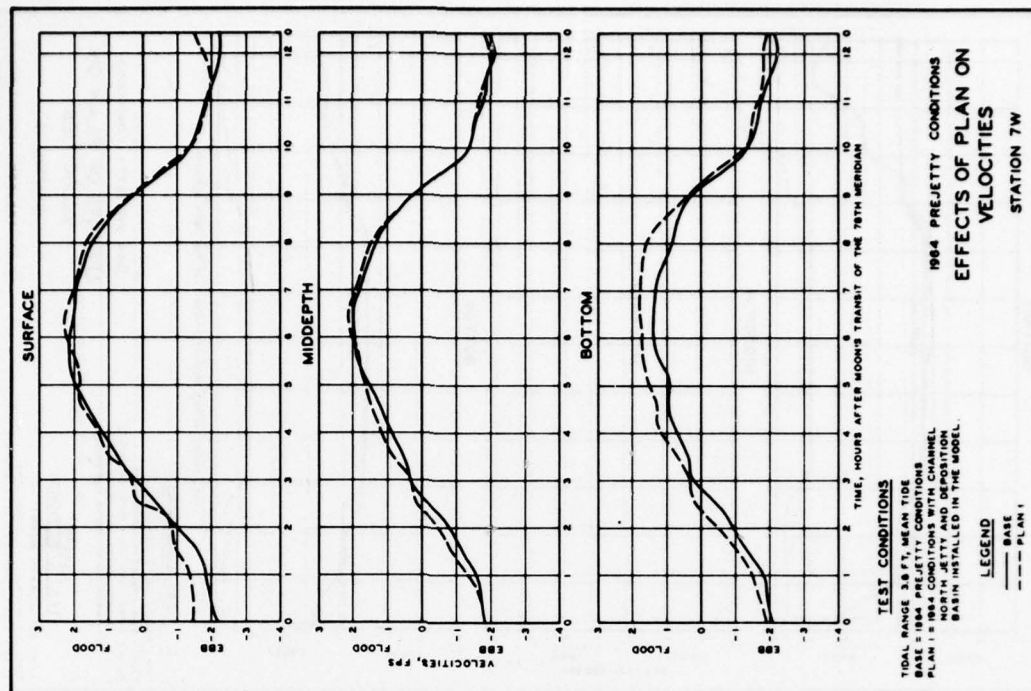


PLATE 187

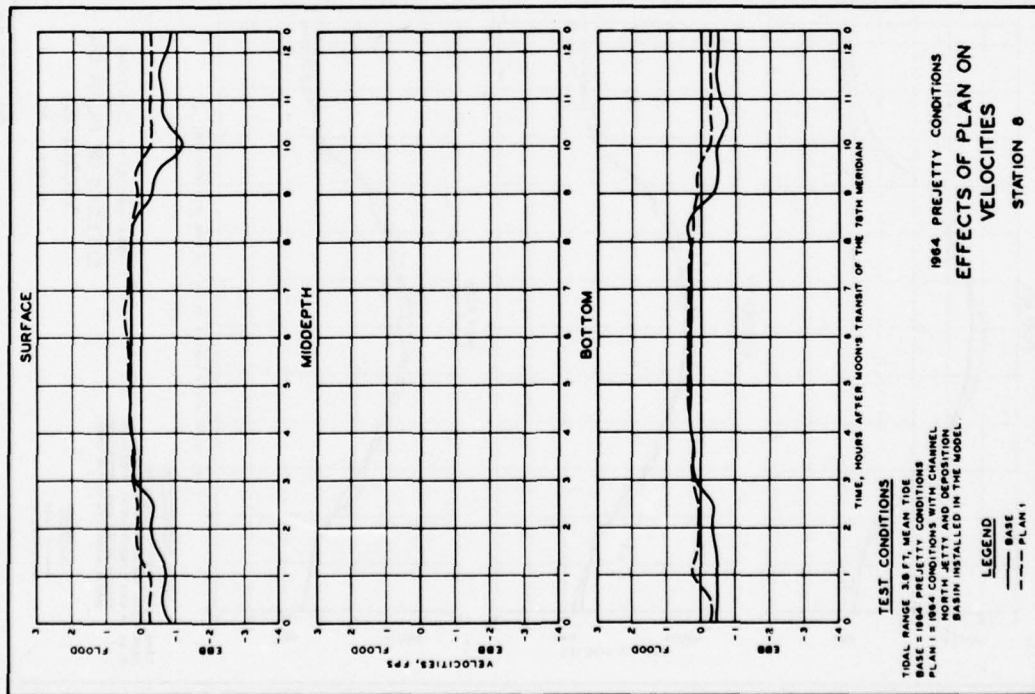


PLATE 188

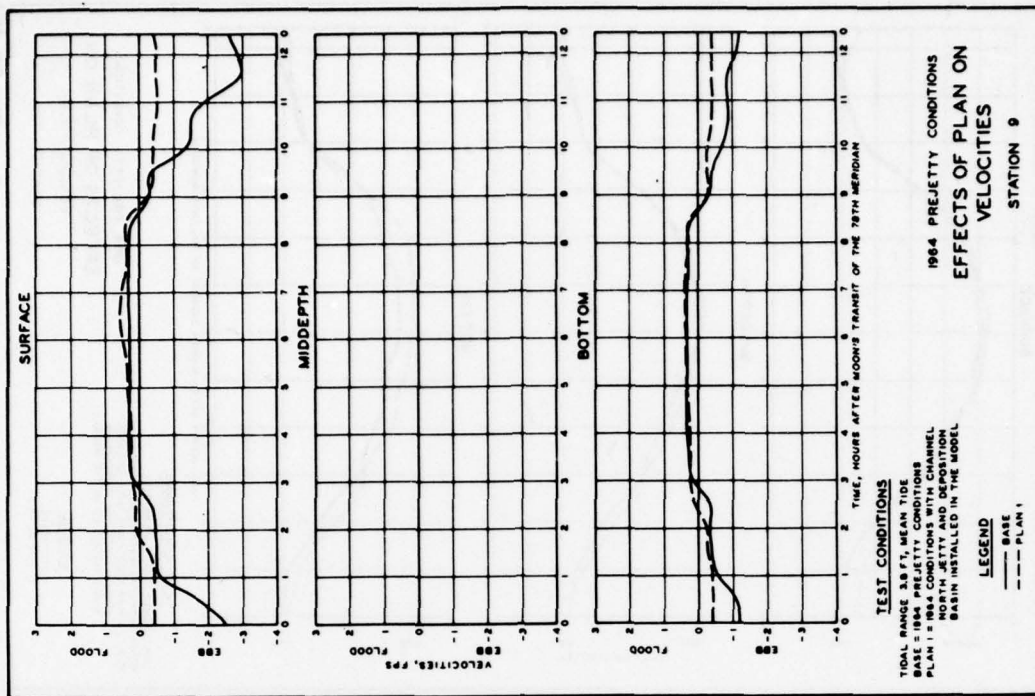


PLATE 189

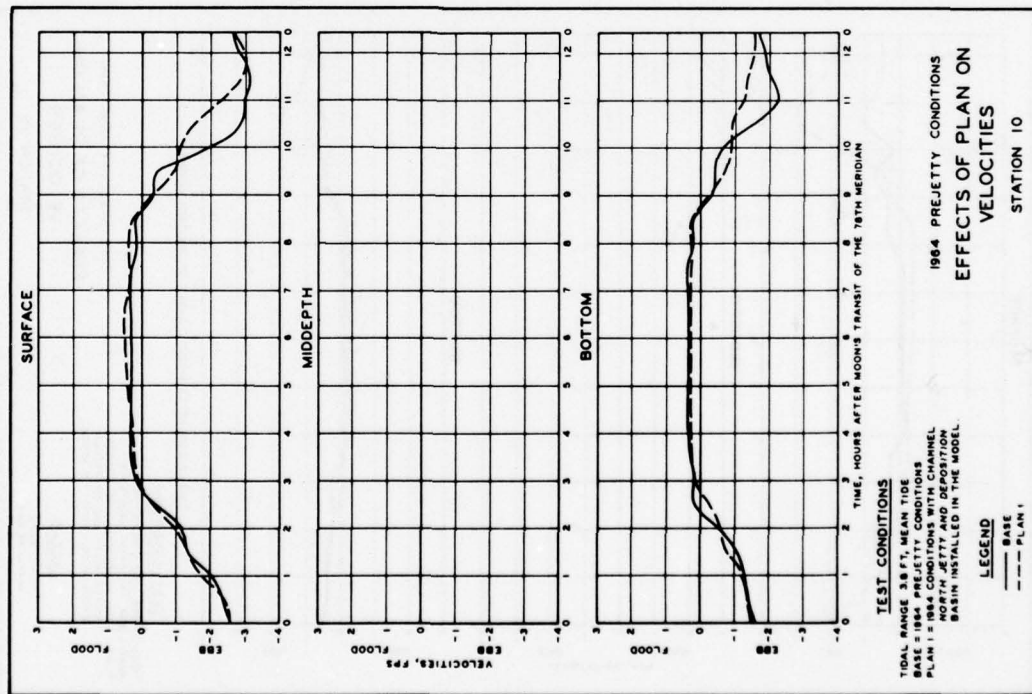


PLATE 190

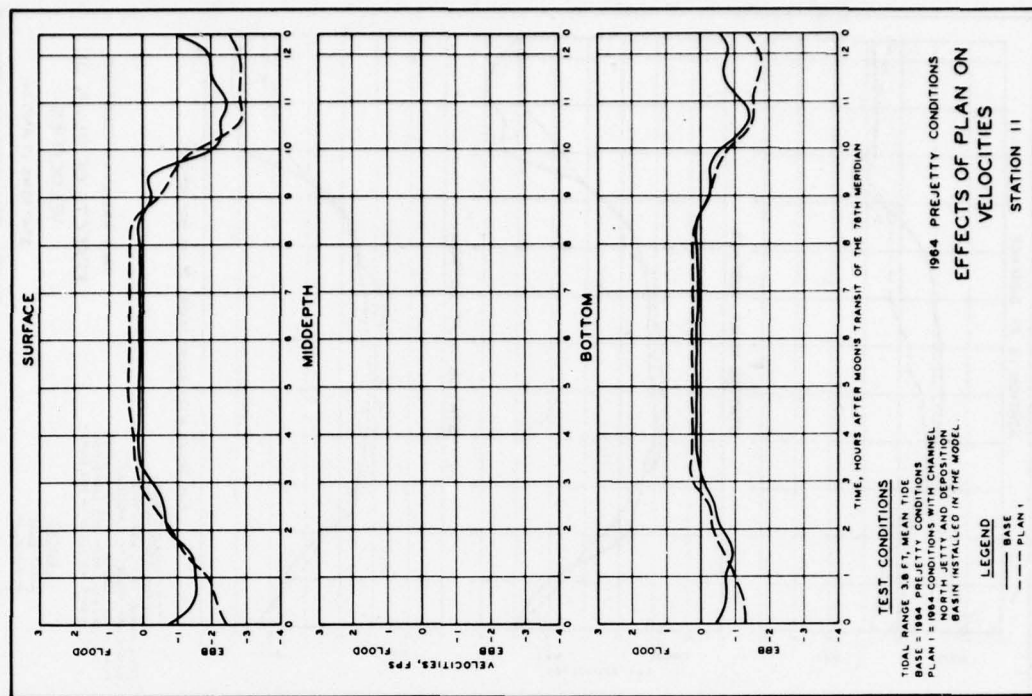


PLATE 191

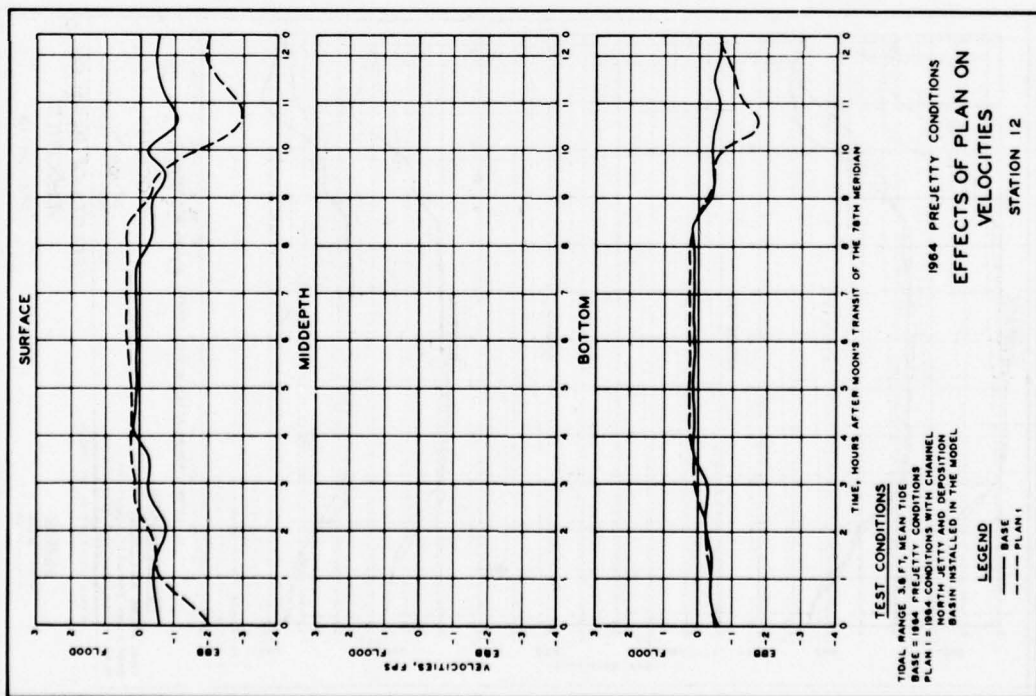


PLATE 192

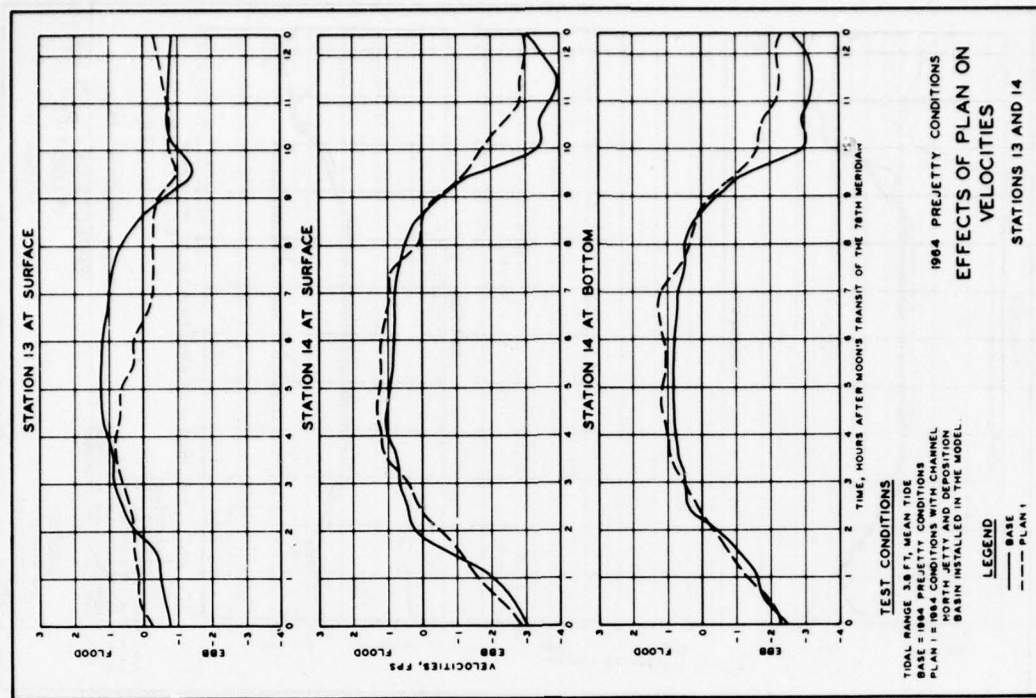


PLATE 193

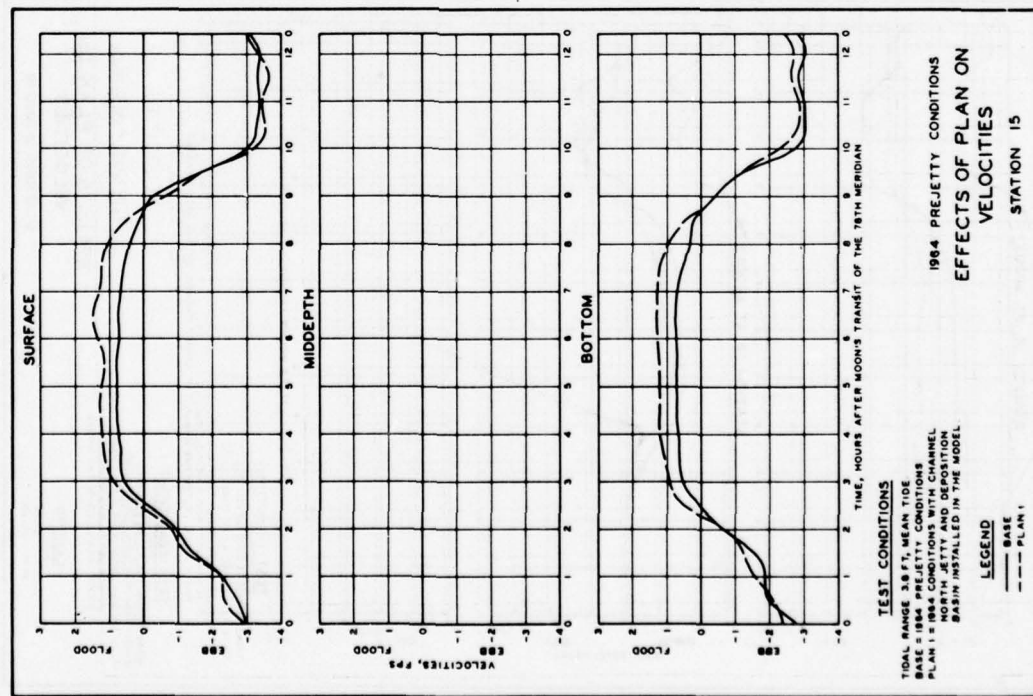


PLATE 194

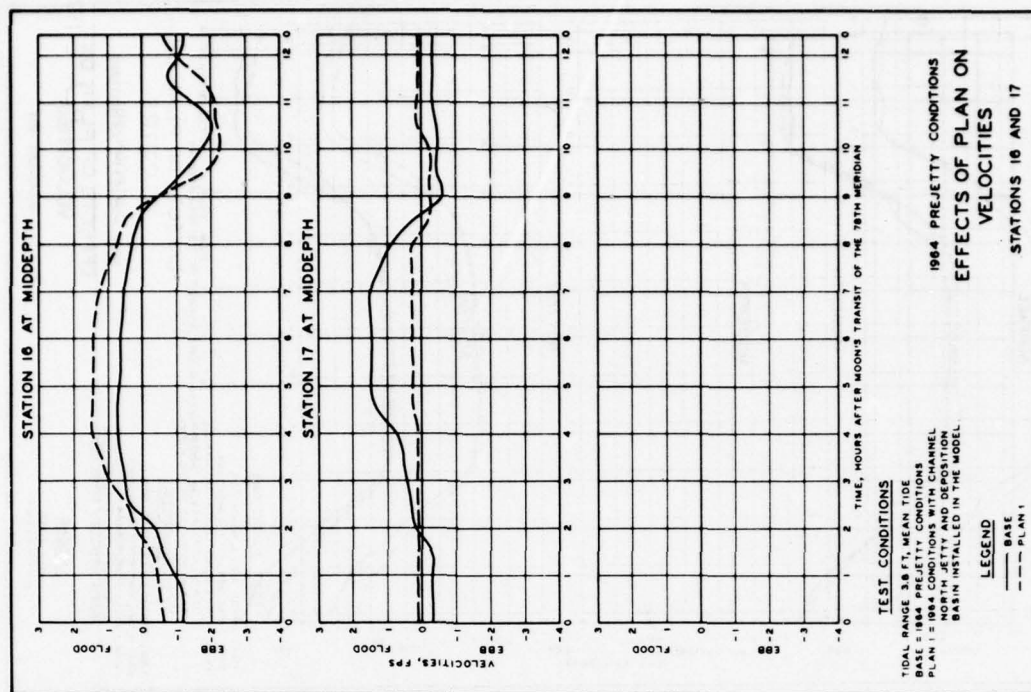


PLATE 195

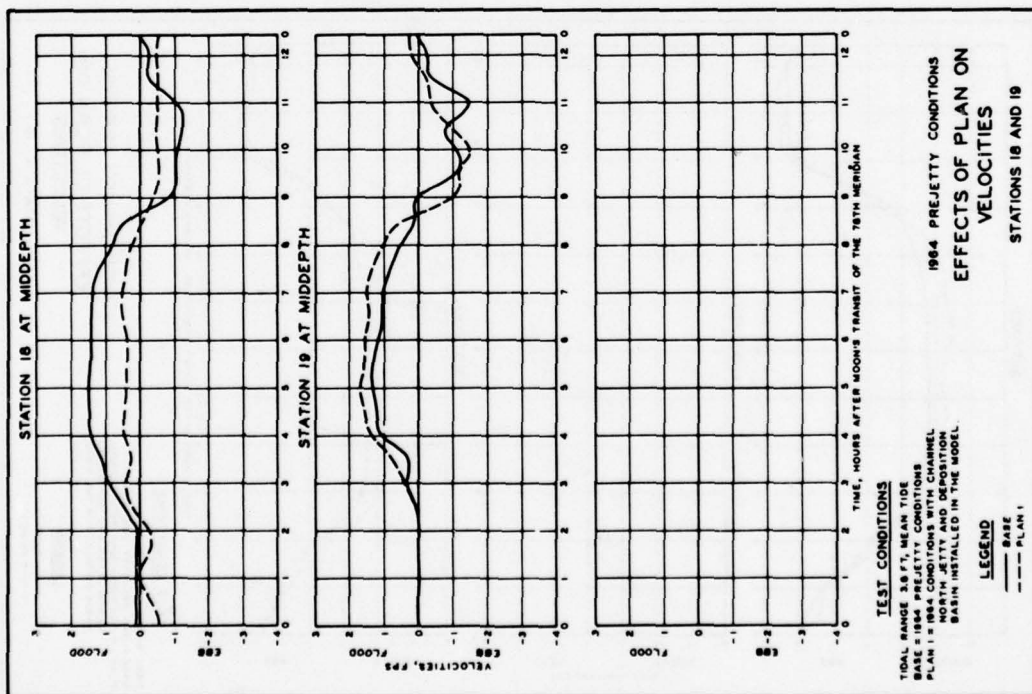


PLATE 196

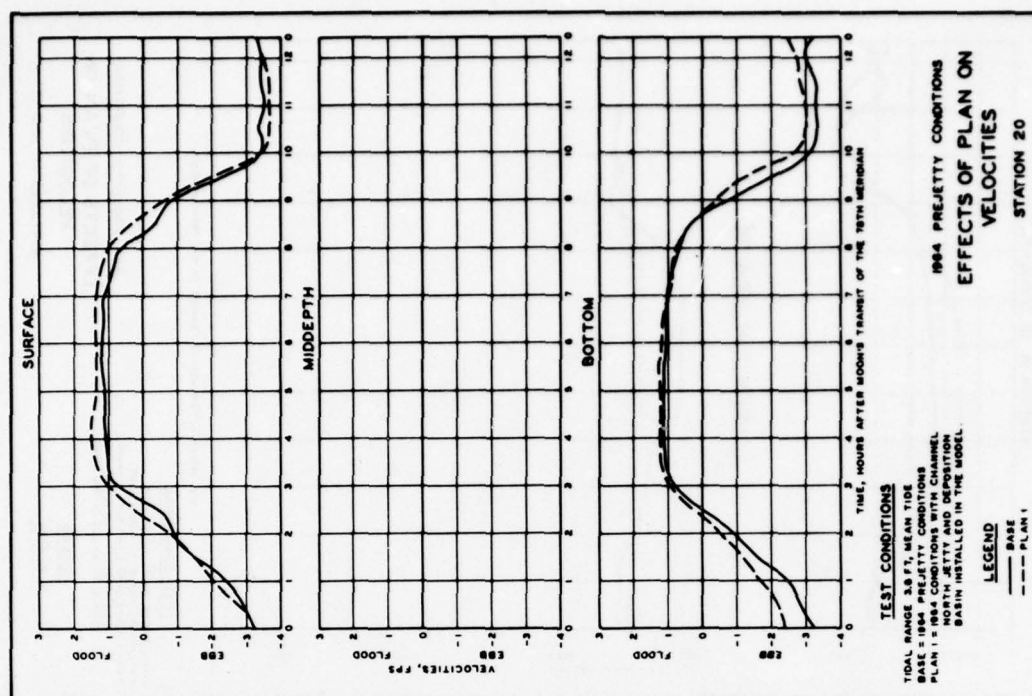
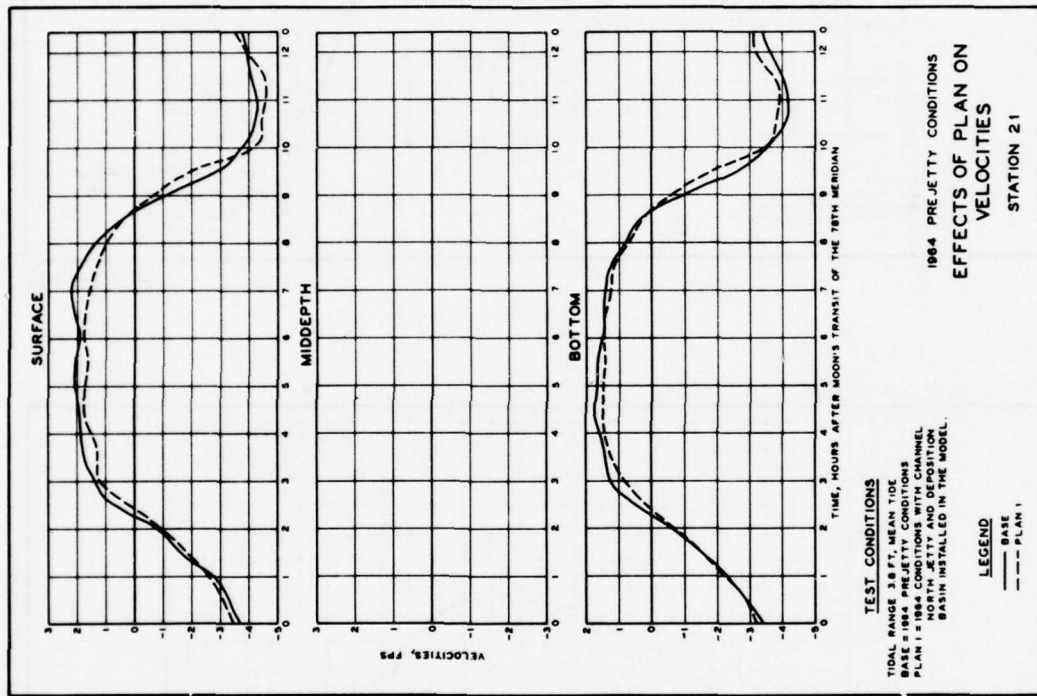


PLATE 197



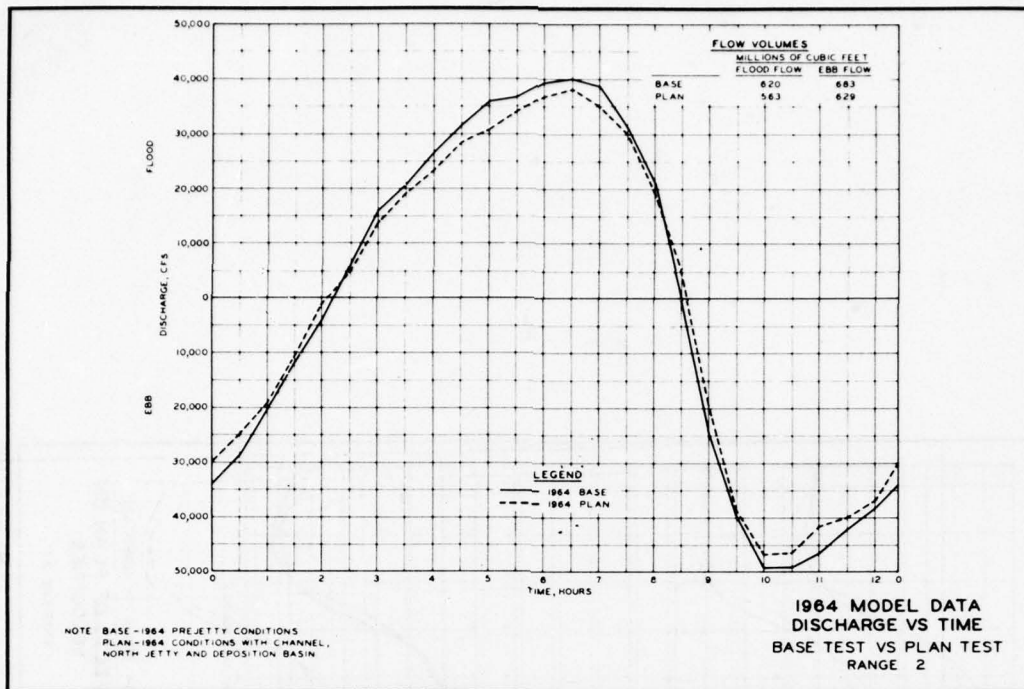


PLATE 199

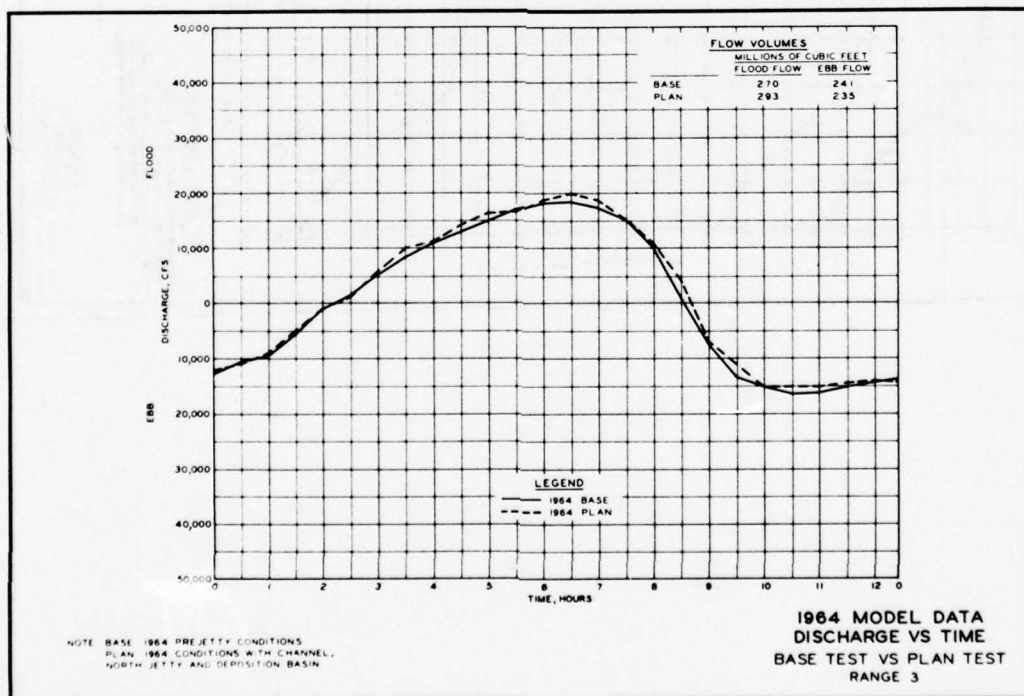


PLATE 200

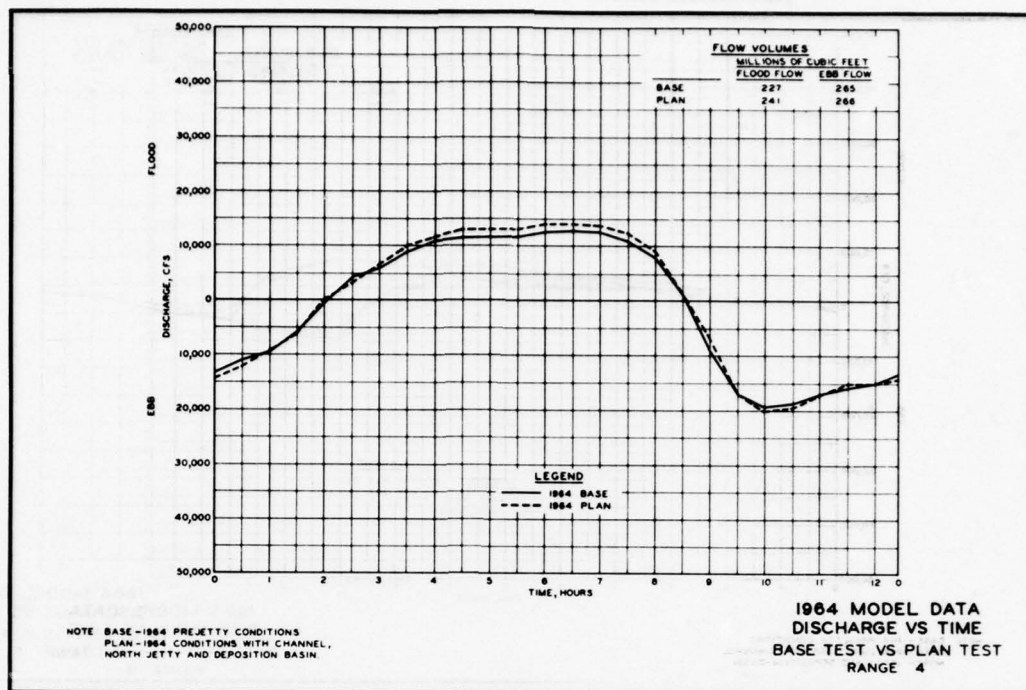


PLATE 201

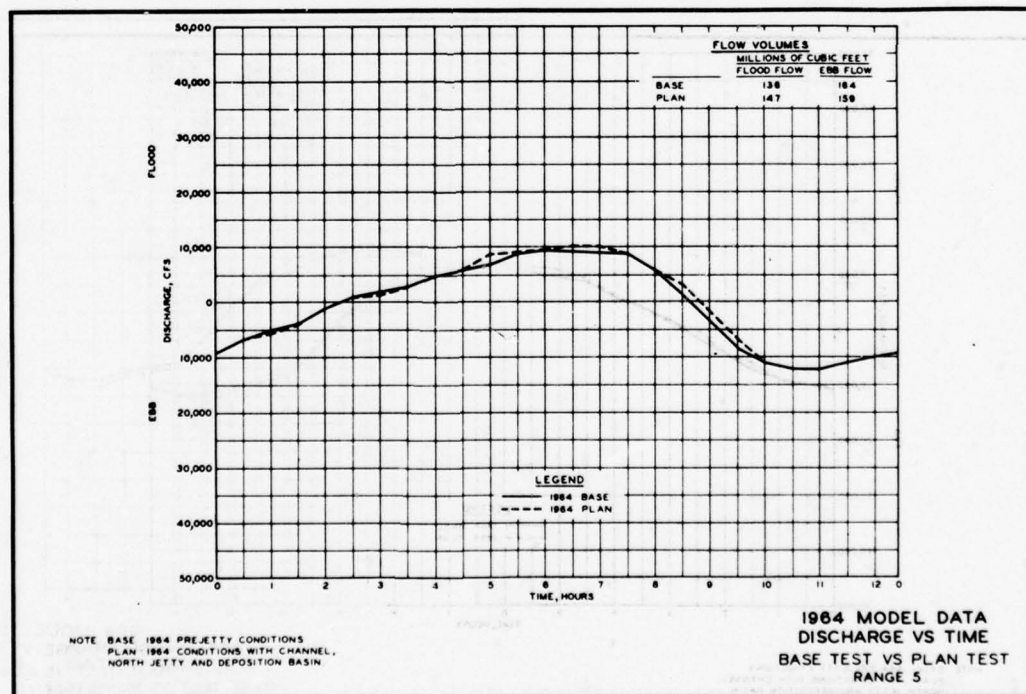


PLATE 202

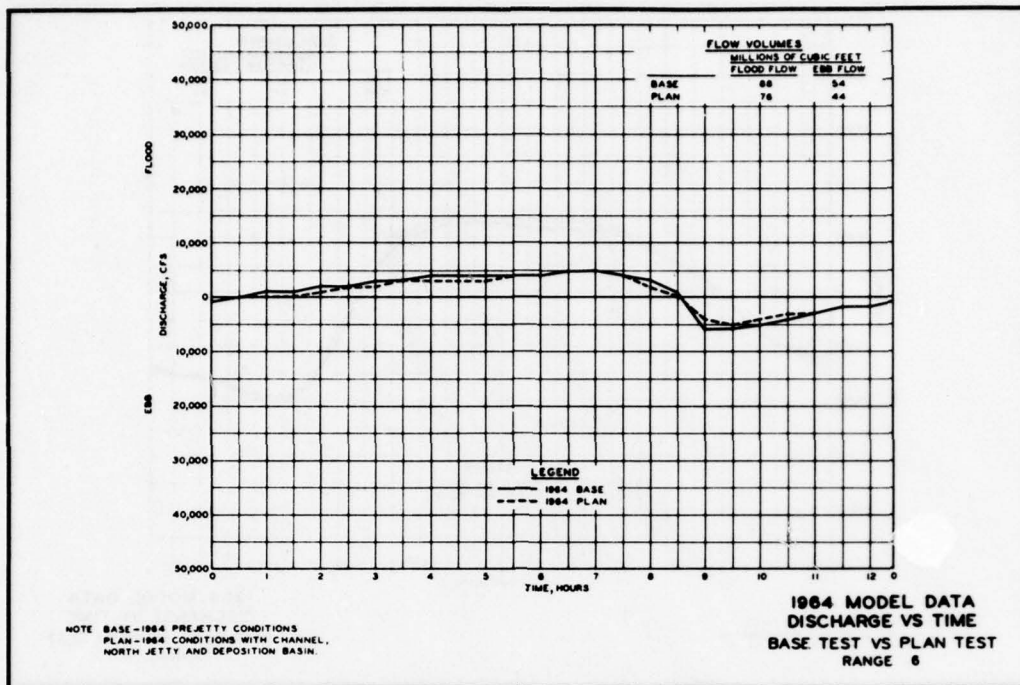


PLATE 203

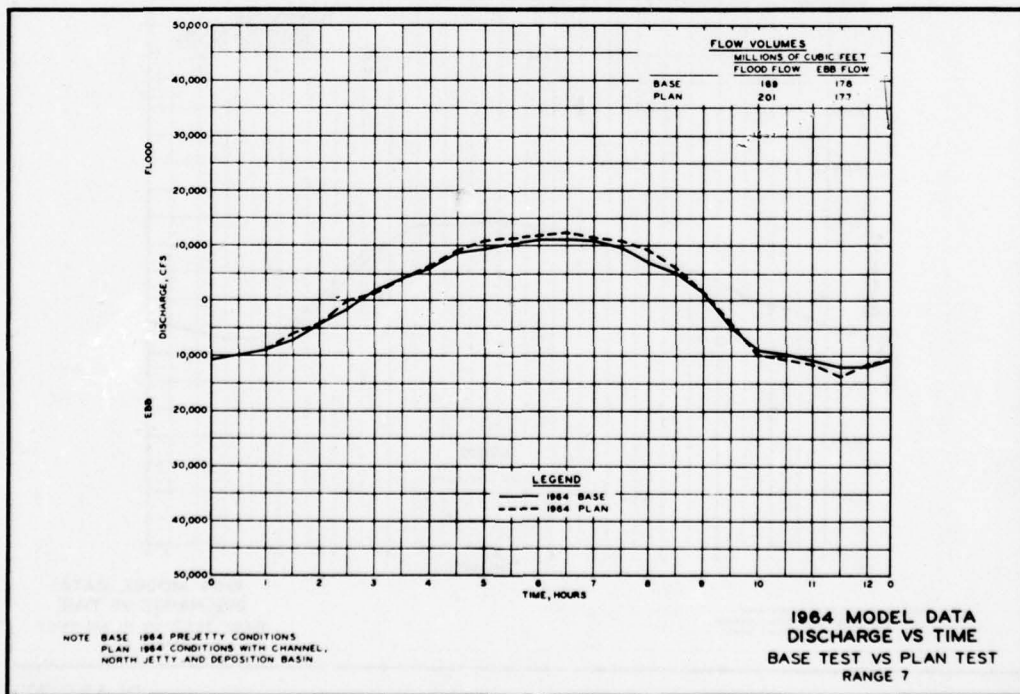


PLATE 204

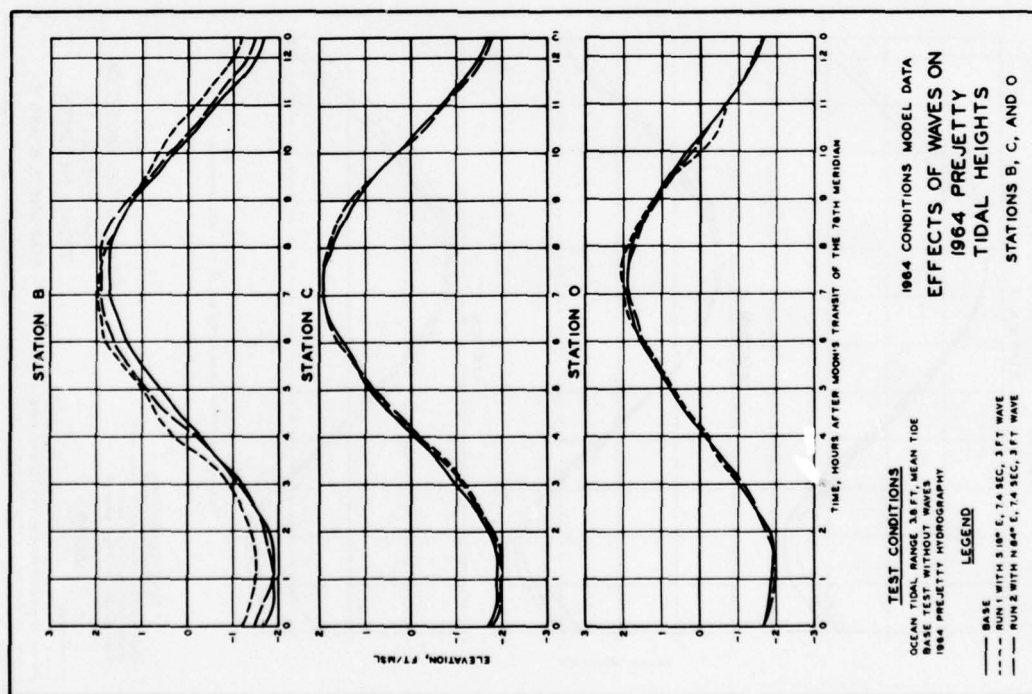


PLATE 205

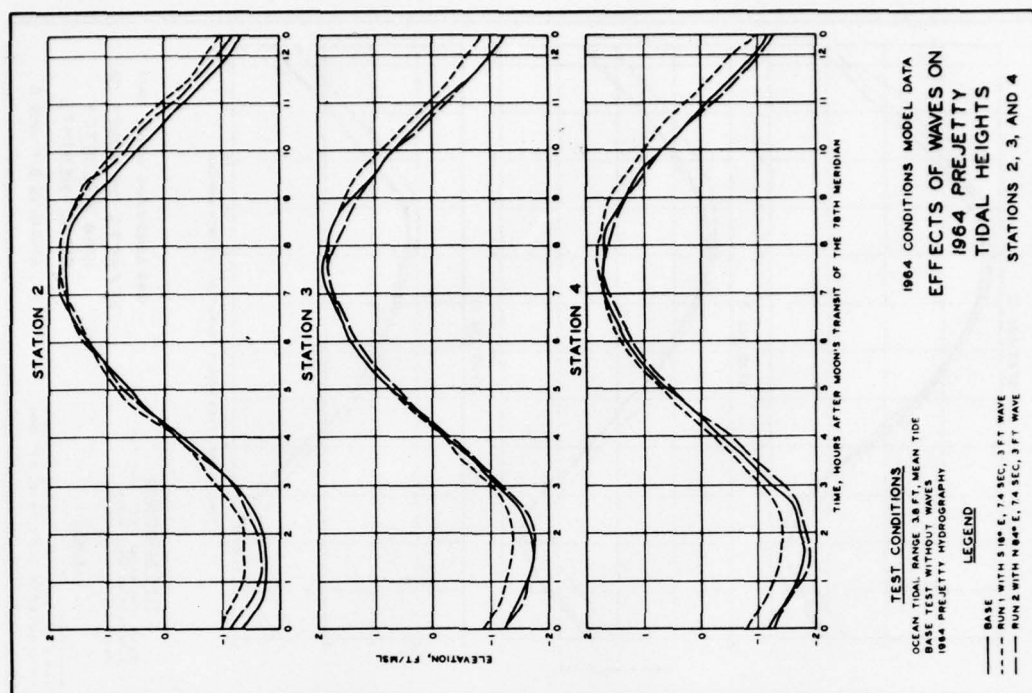
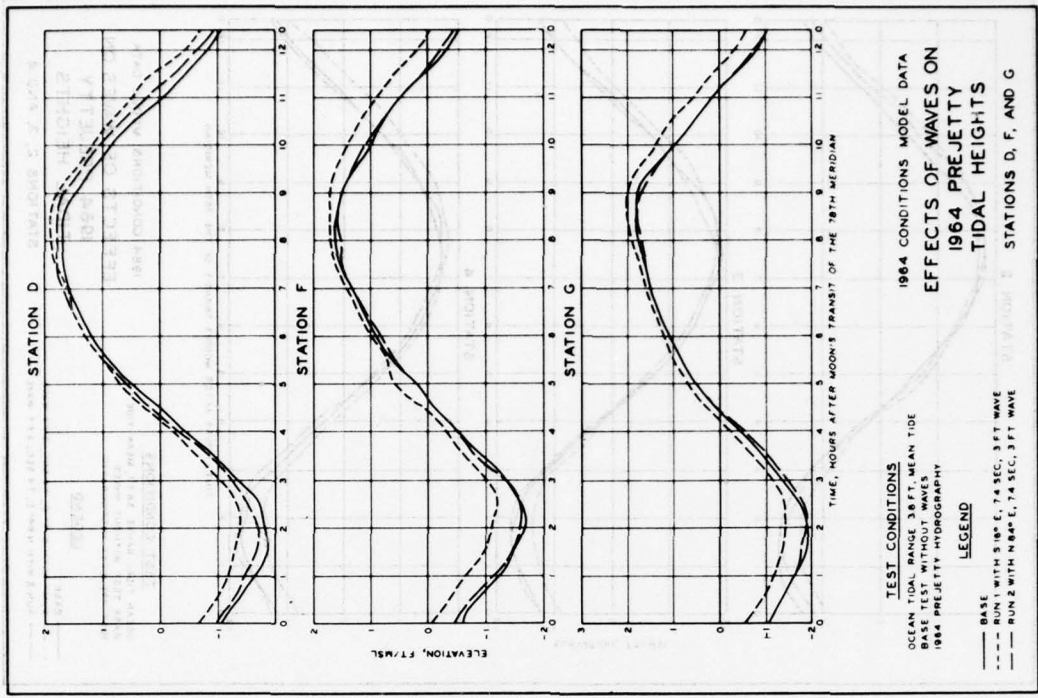
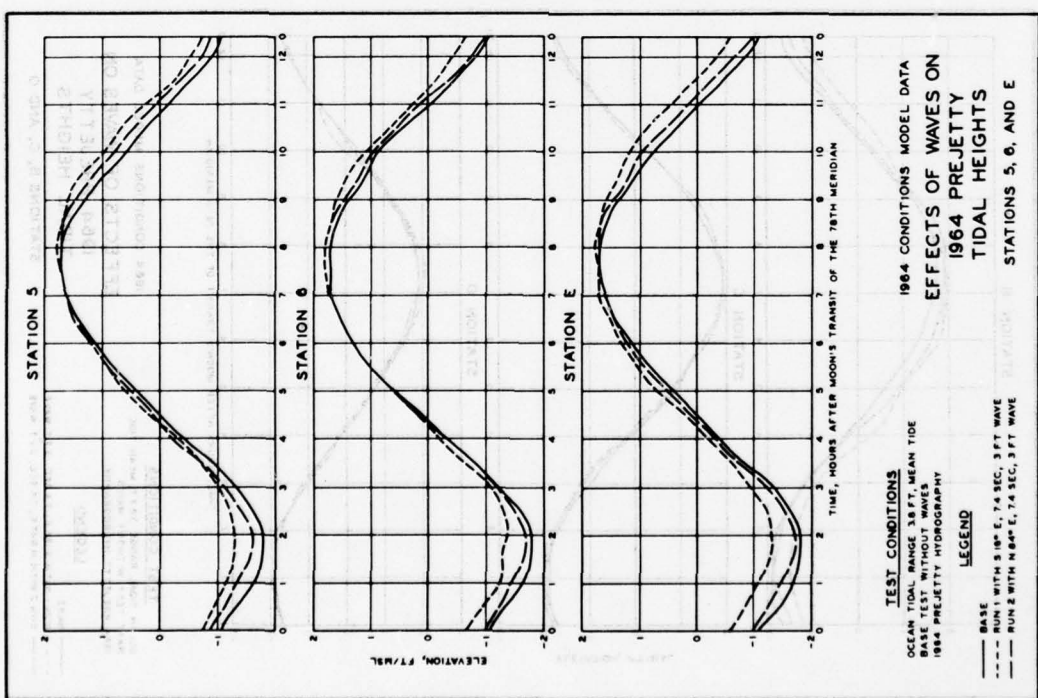


PLATE 206



67V1E313

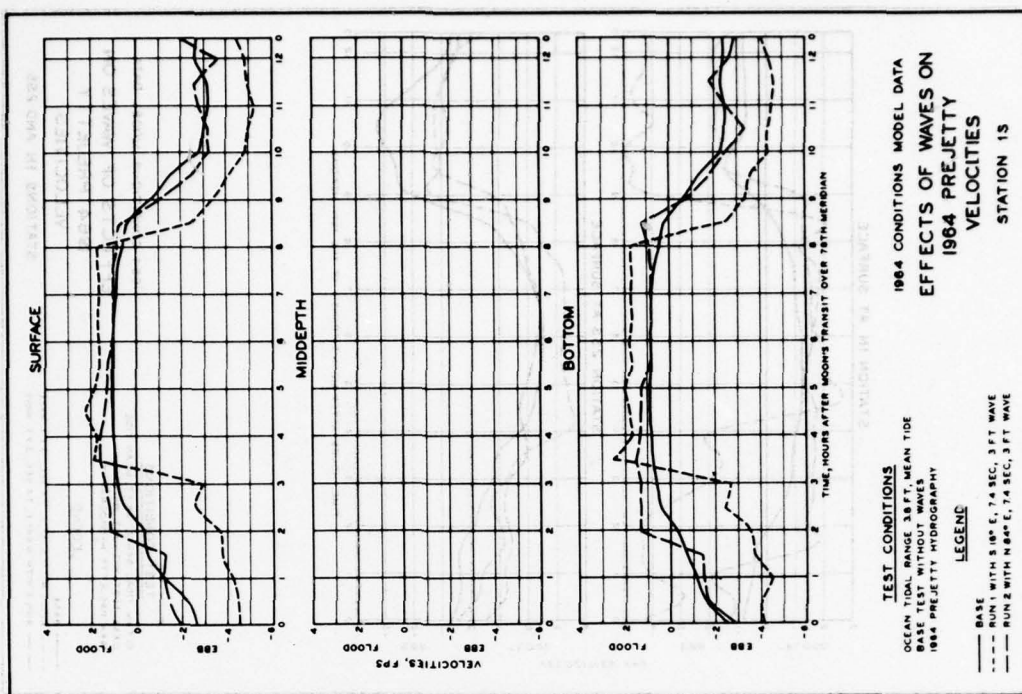


PLATE 210

67V1E313

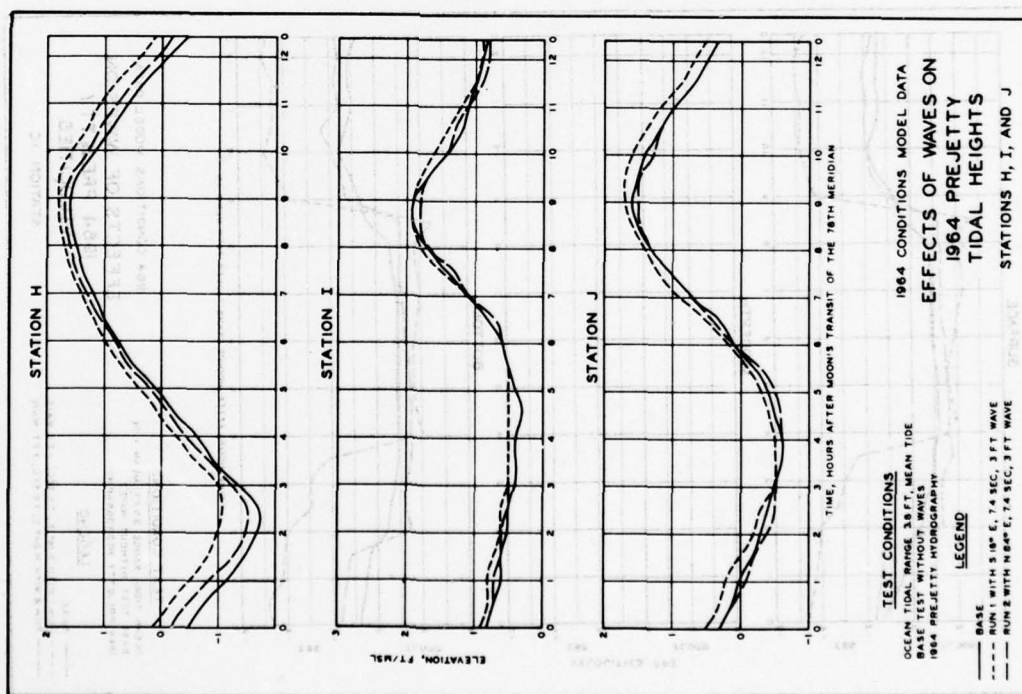


PLATE 209

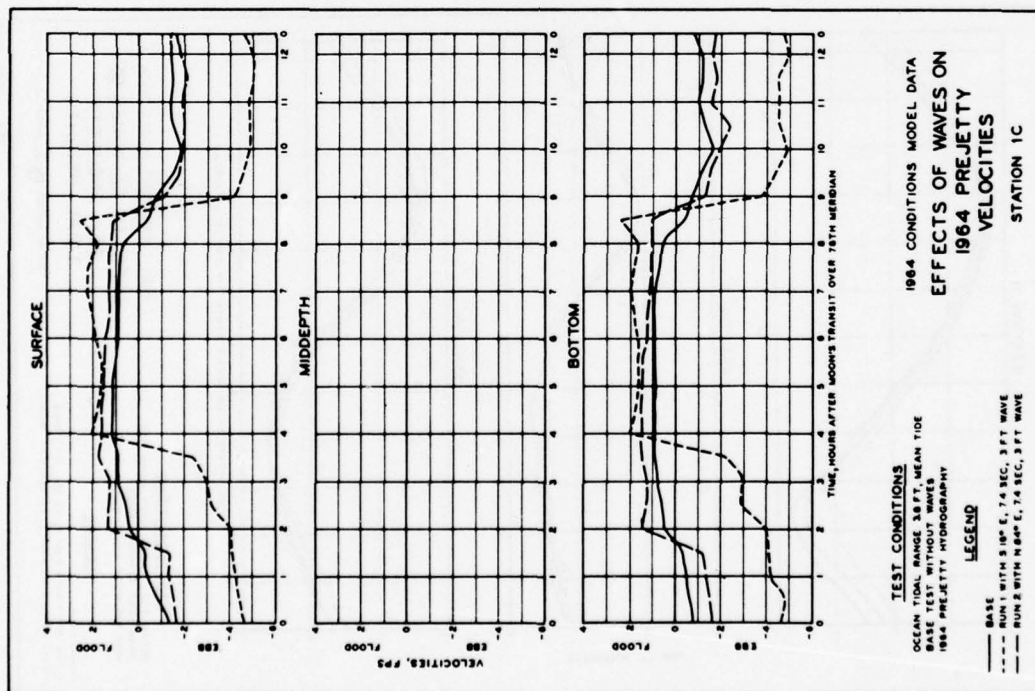


PLATE 211

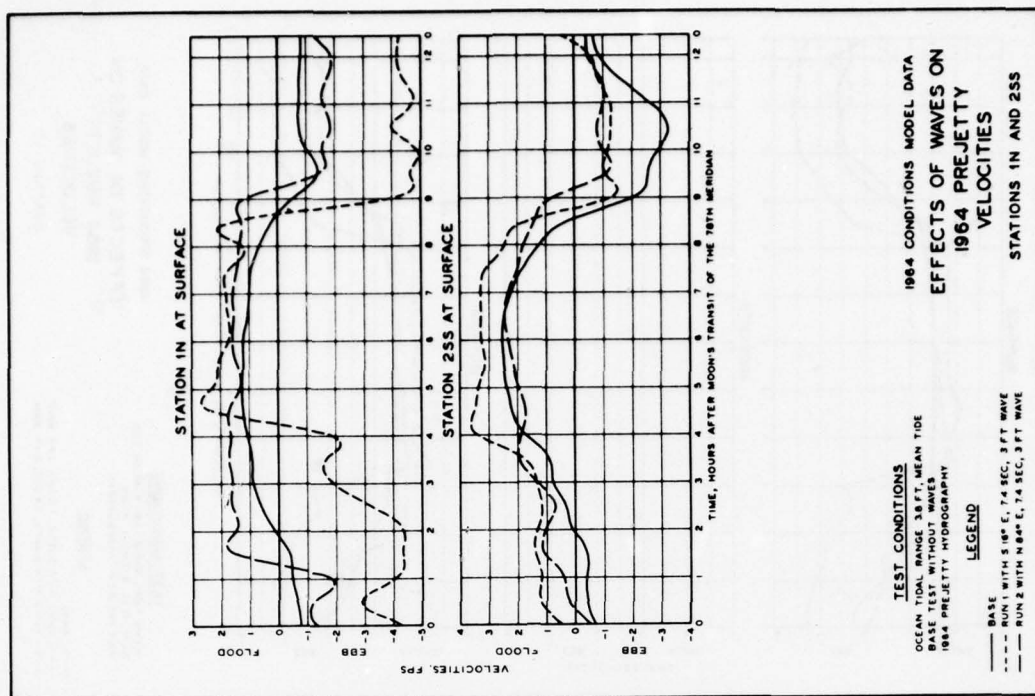


PLATE 212

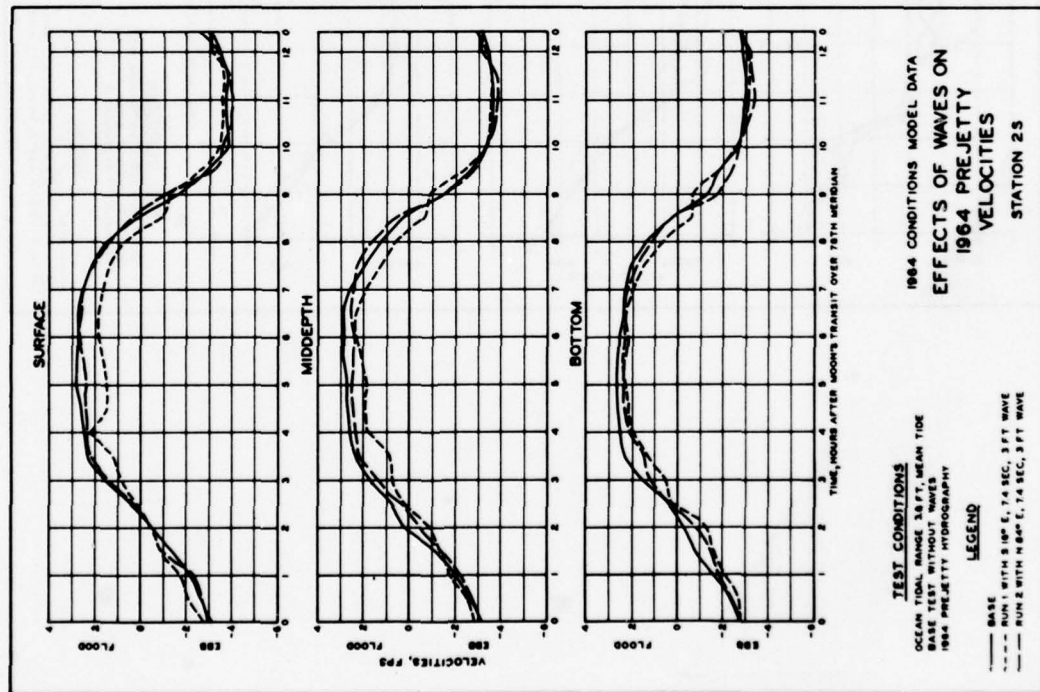


PLATE 213

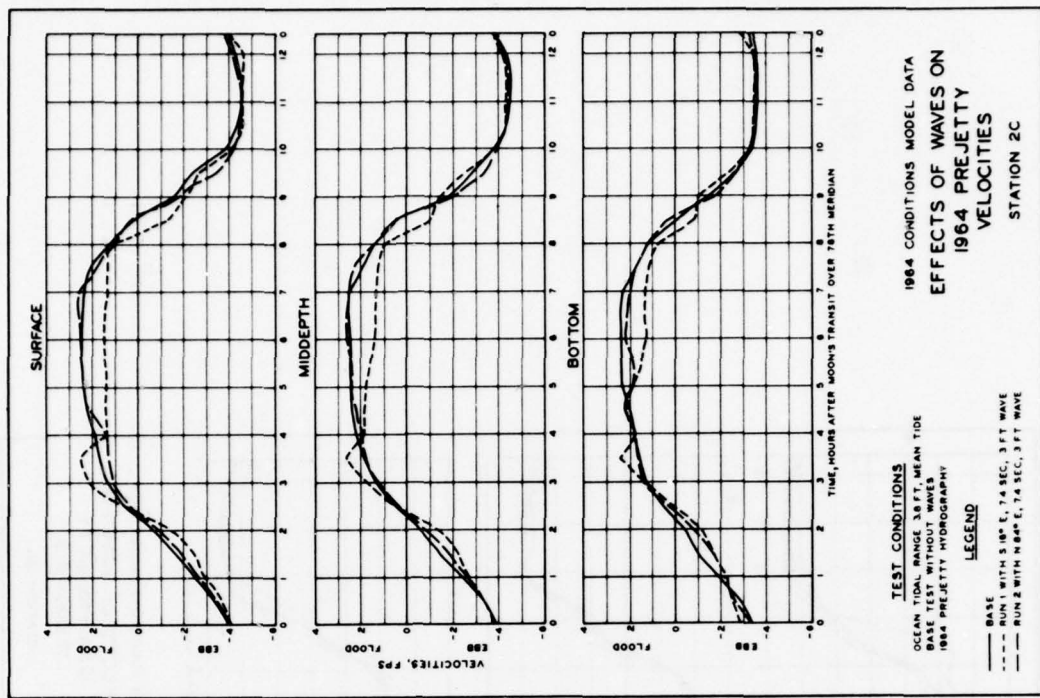
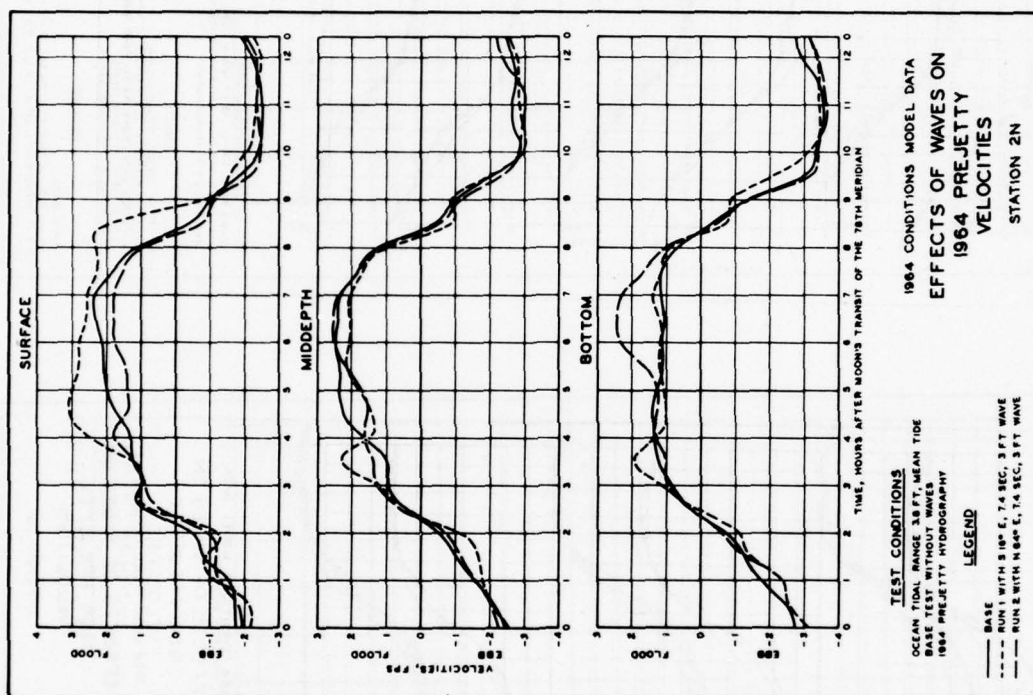
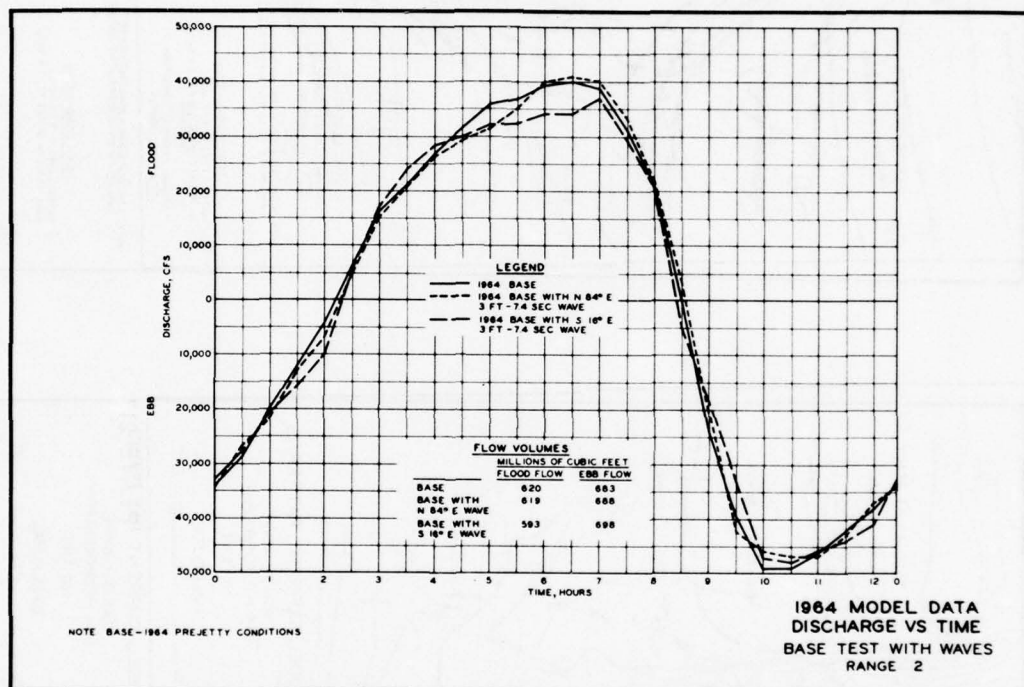


PLATE 214

67416 JIN





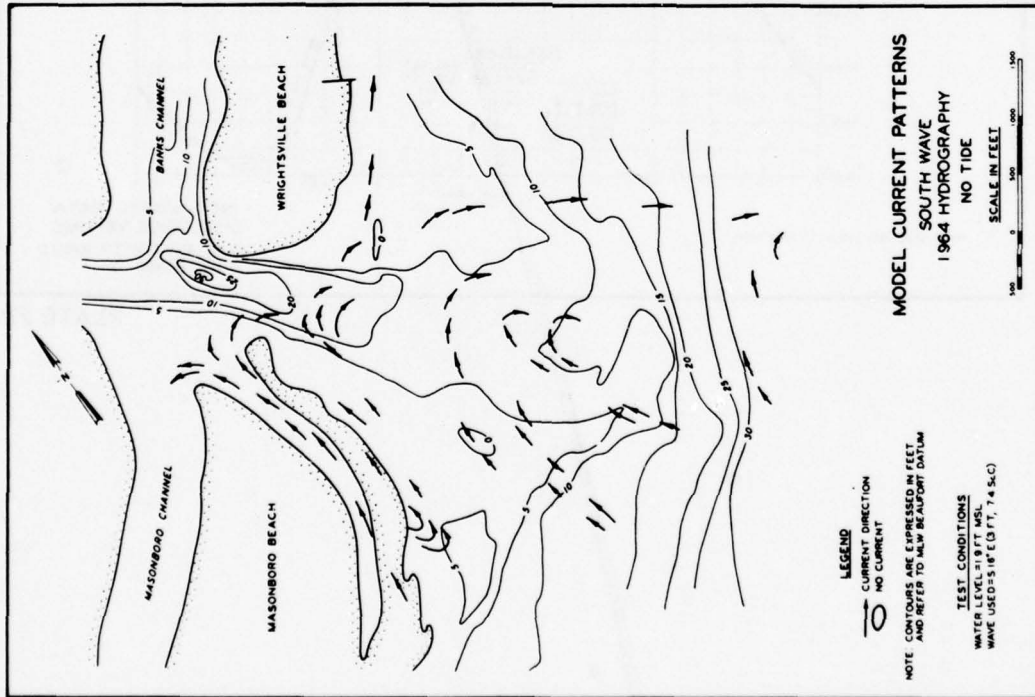


PLATE 217

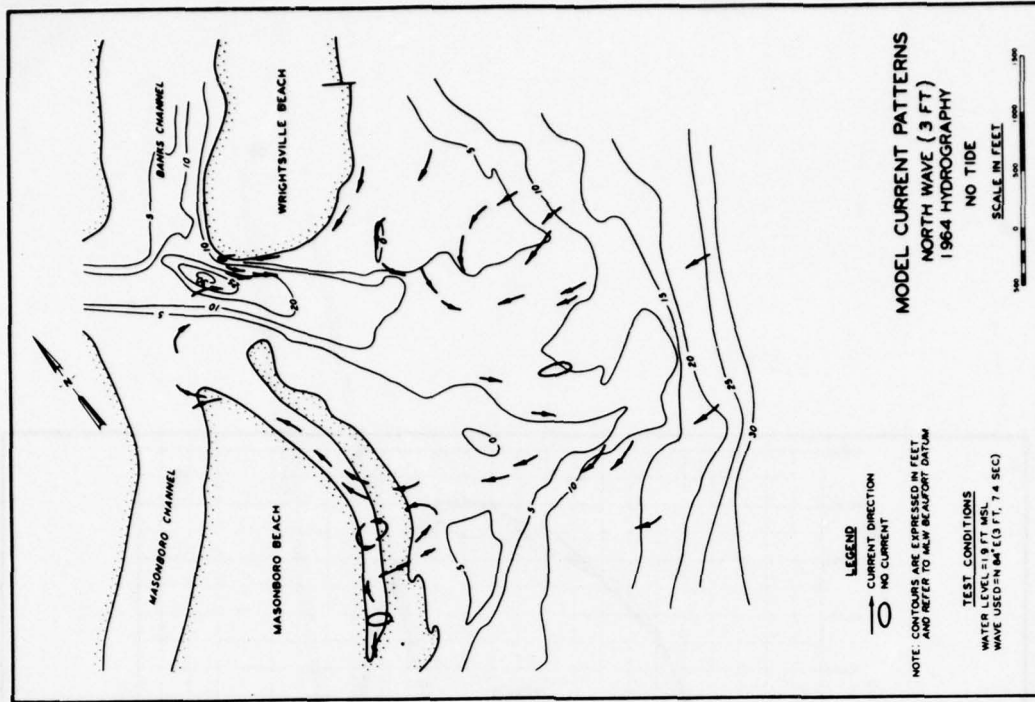


PLATE 218

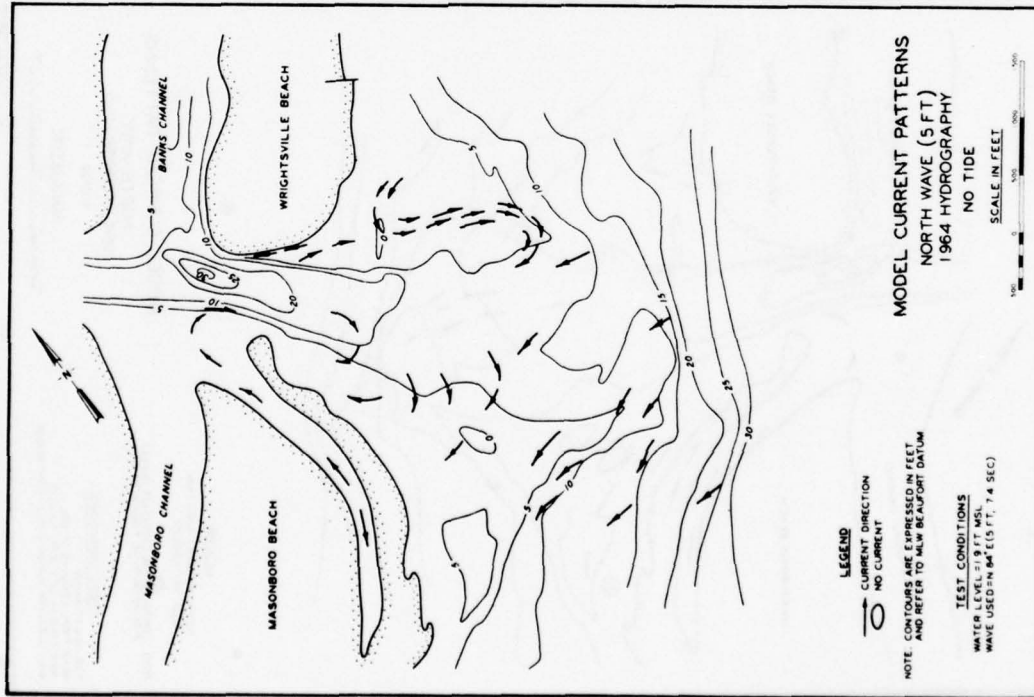


PLATE 219

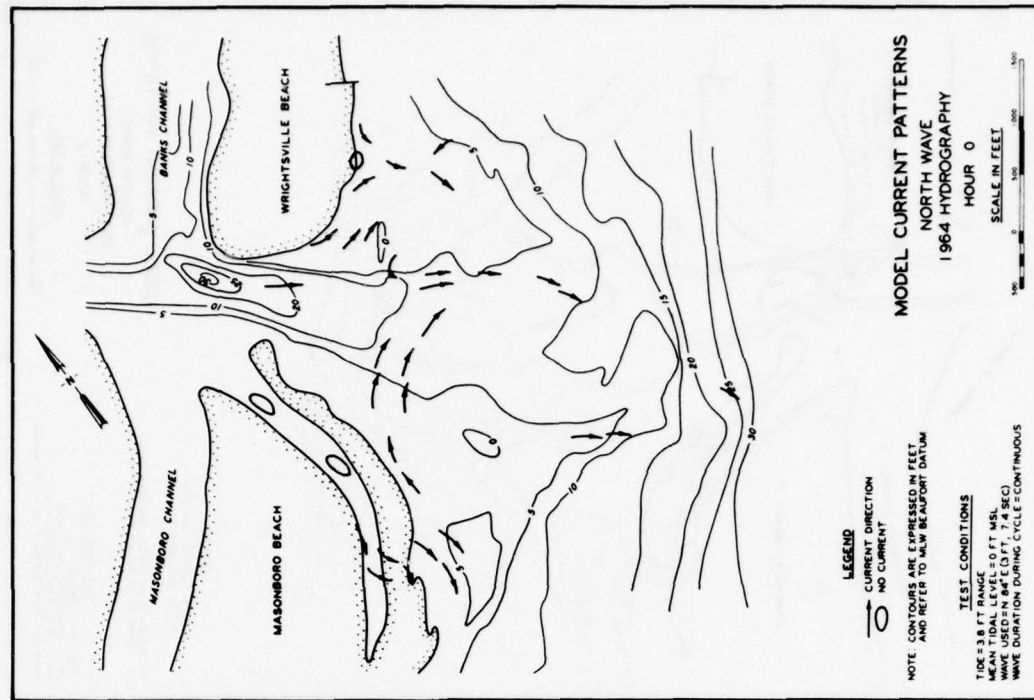


PLATE 220

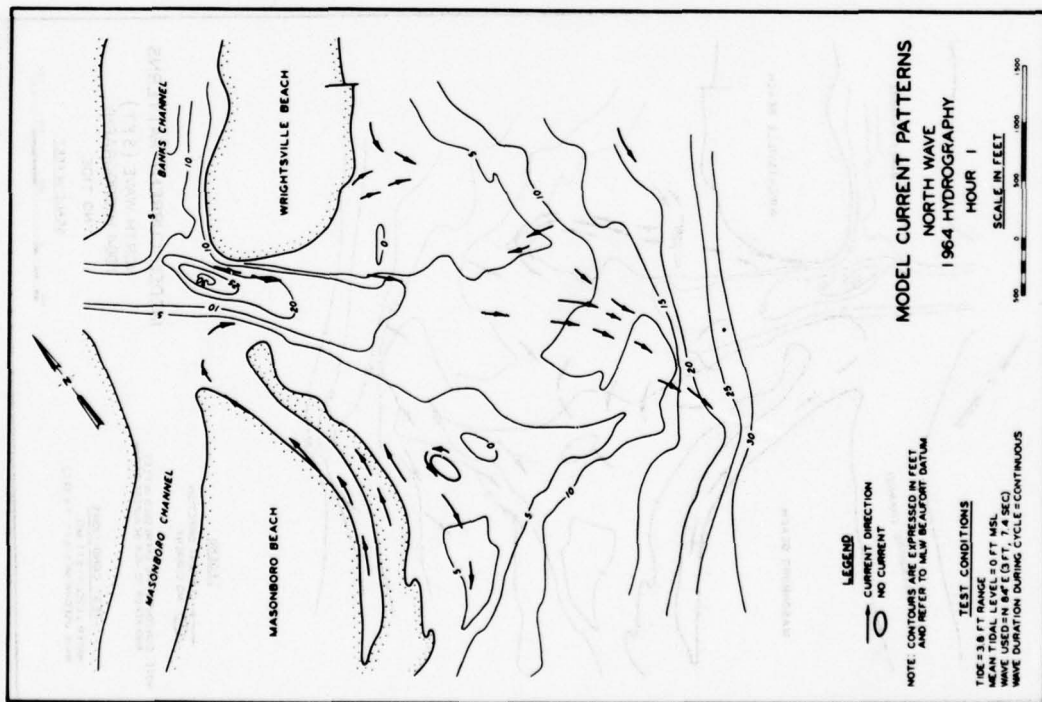


PLATE 221

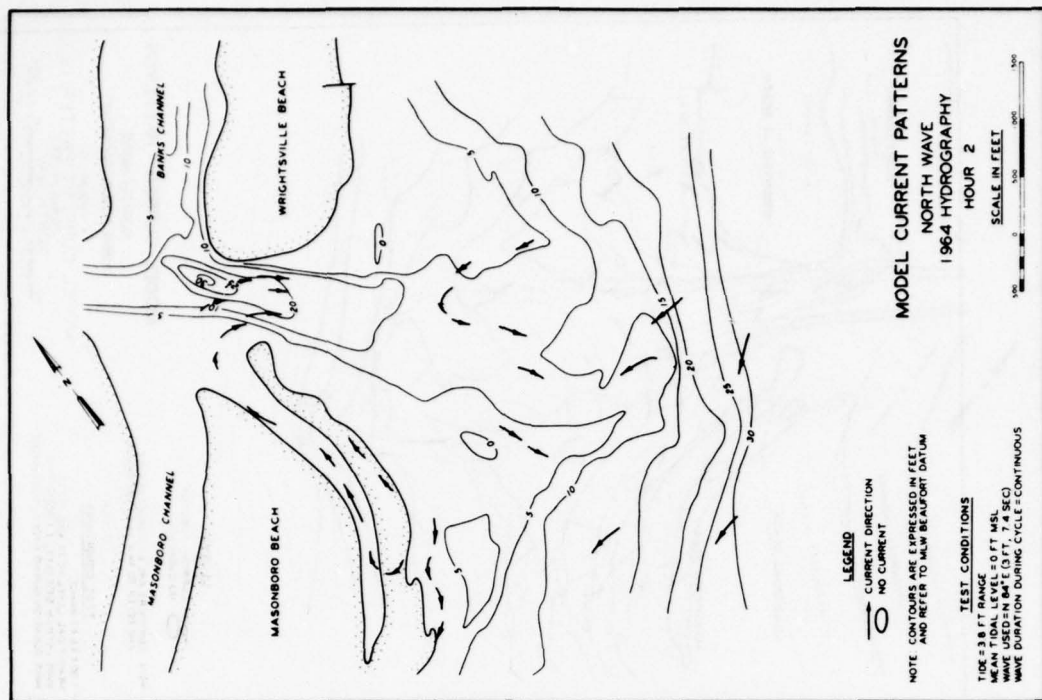


PLATE 222

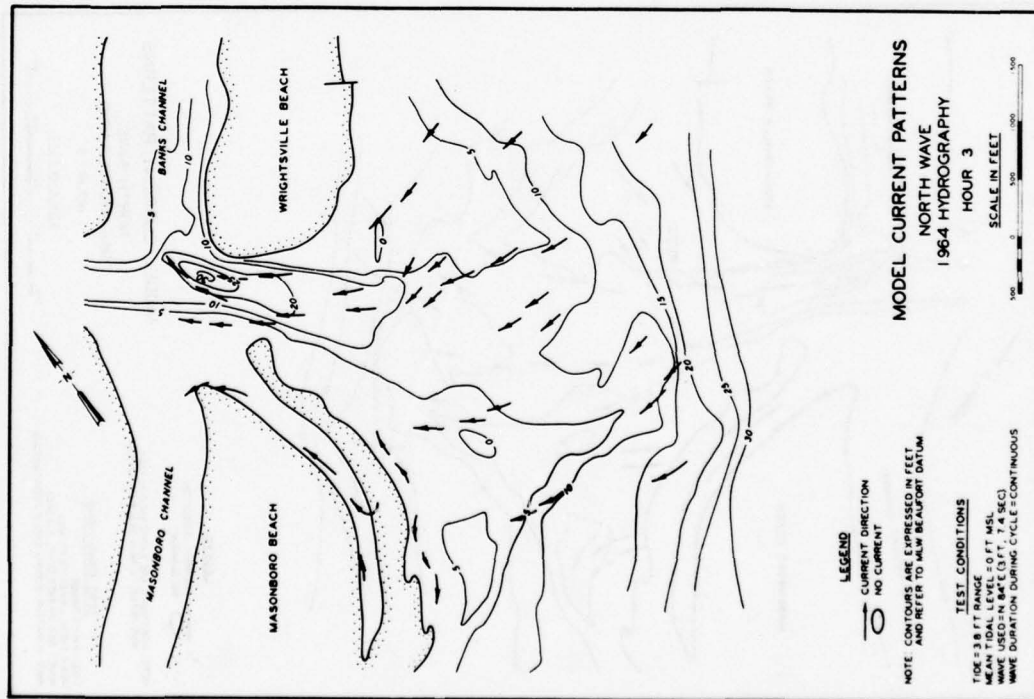


PLATE 223

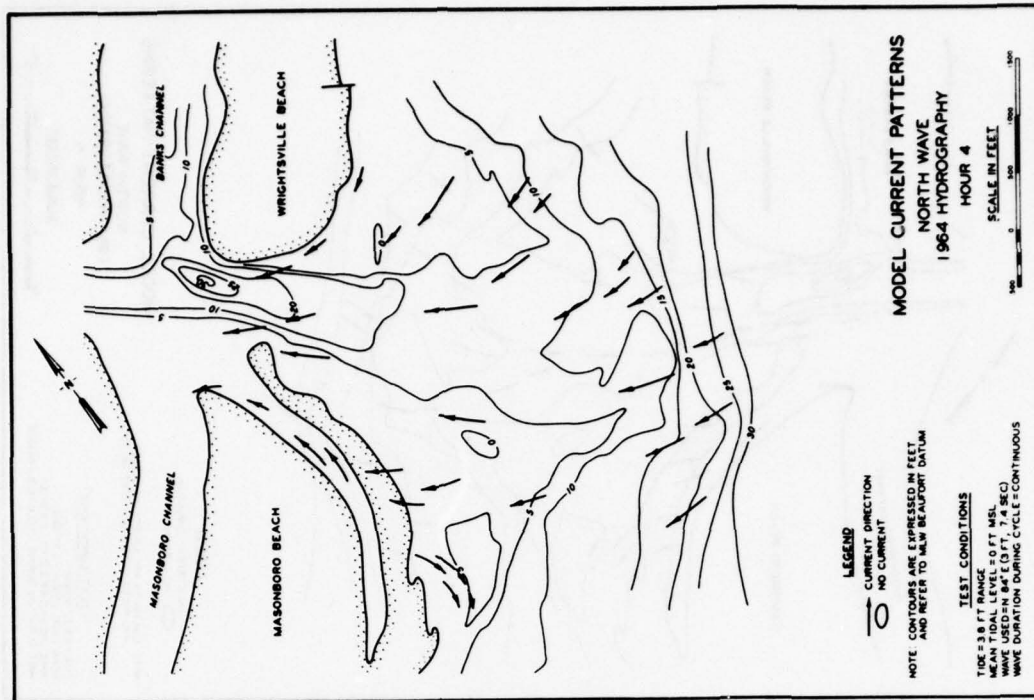


PLATE 224

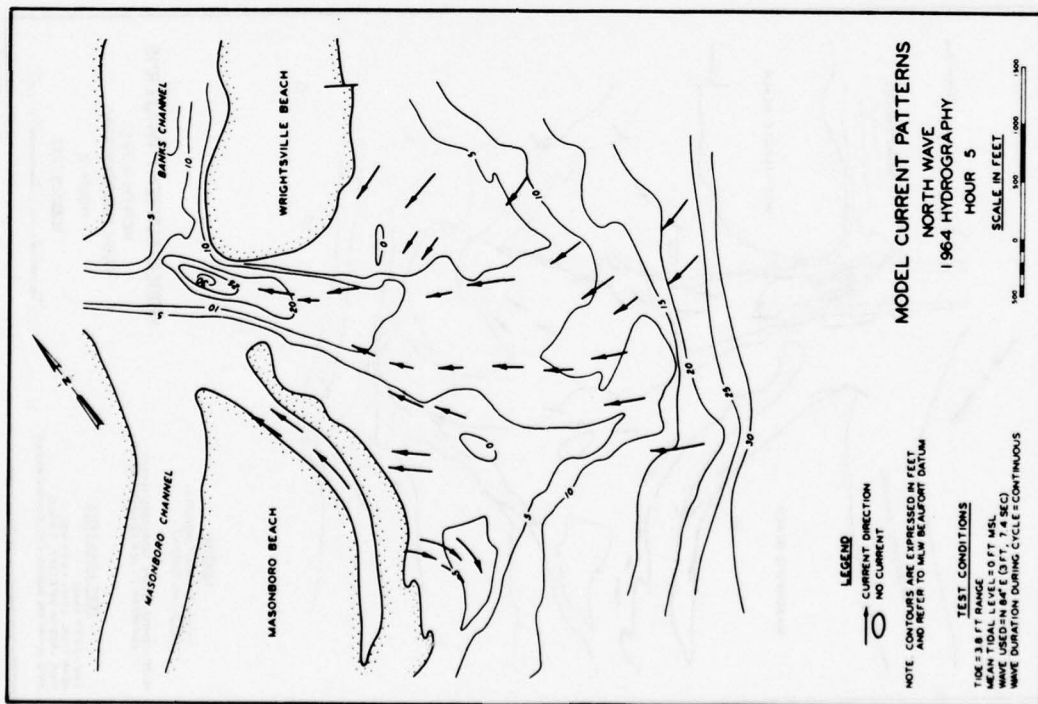


PLATE 225

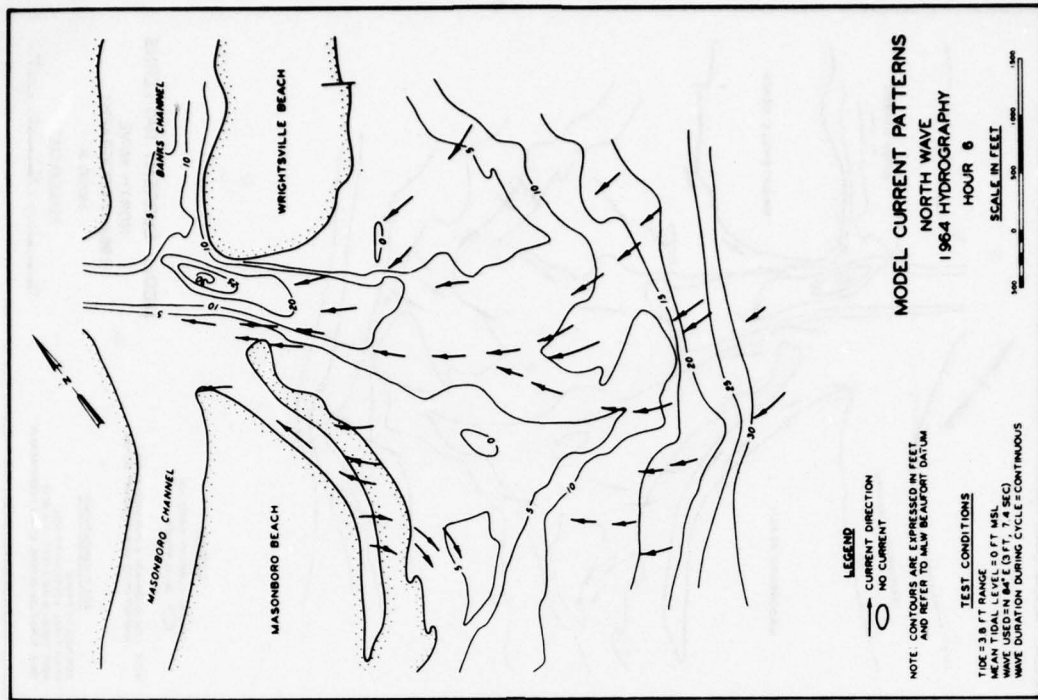


PLATE 226

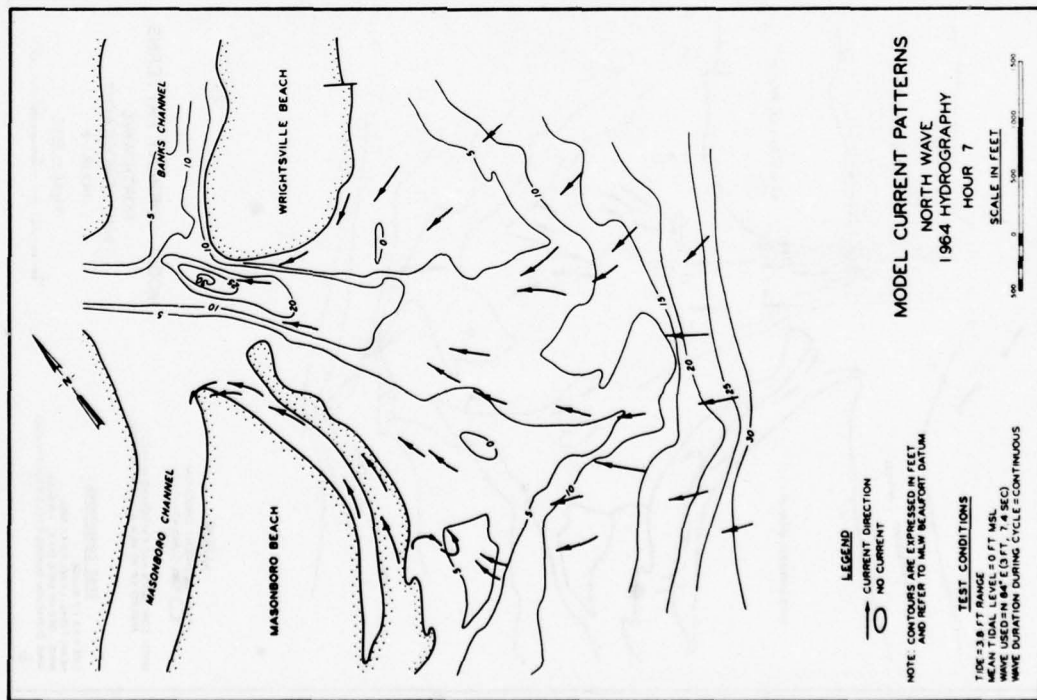


PLATE 227

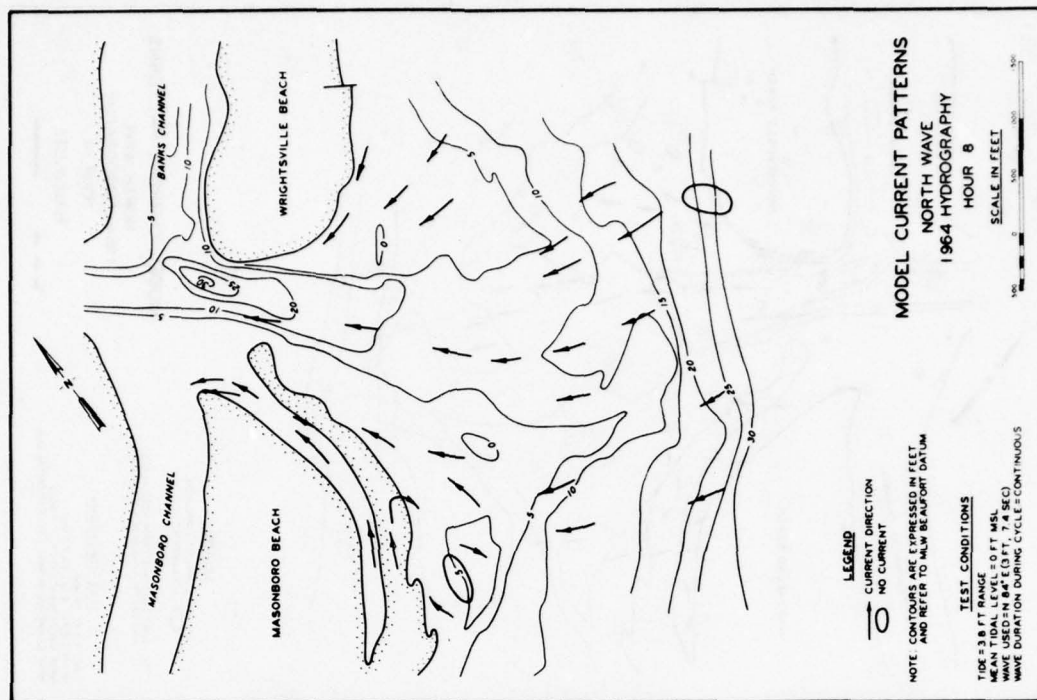


PLATE 228

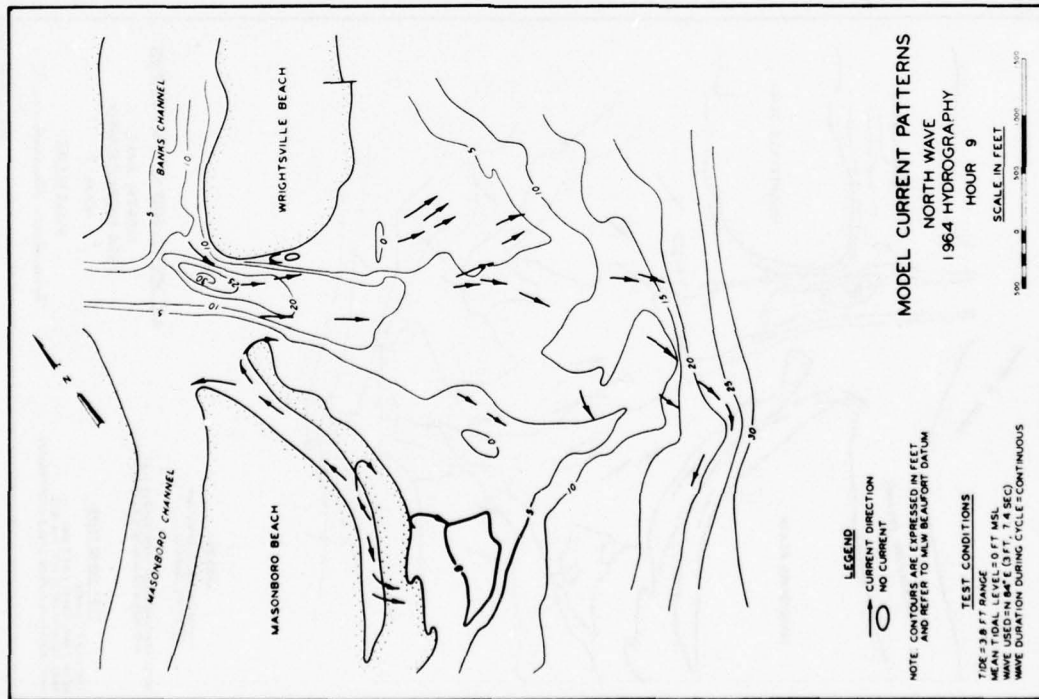
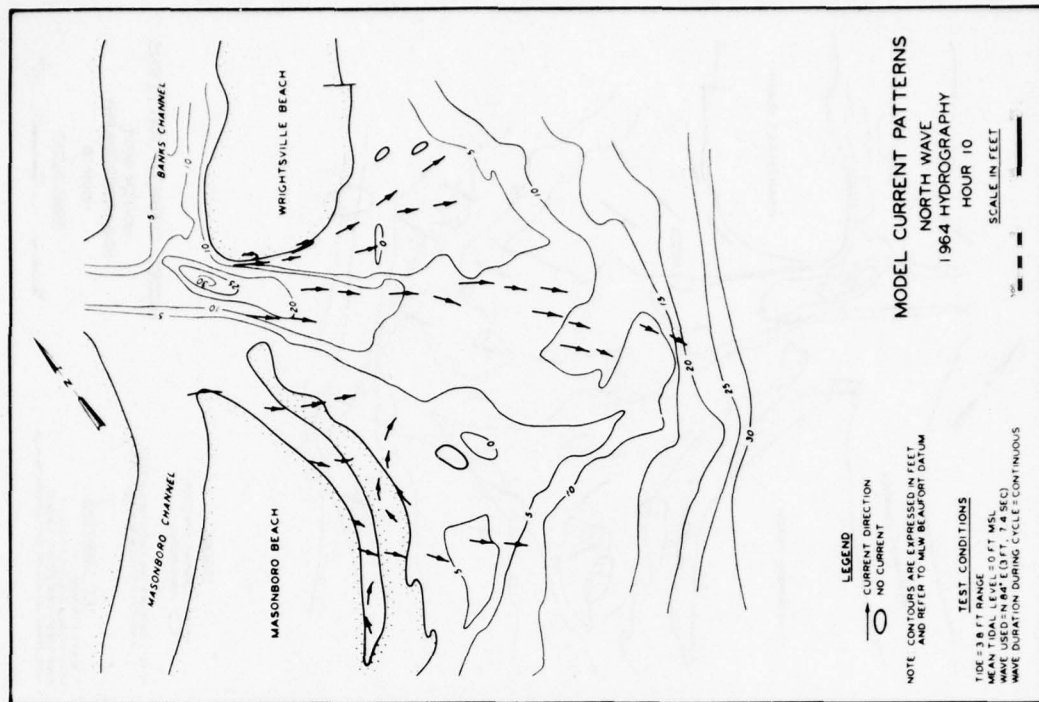


PLATE 229



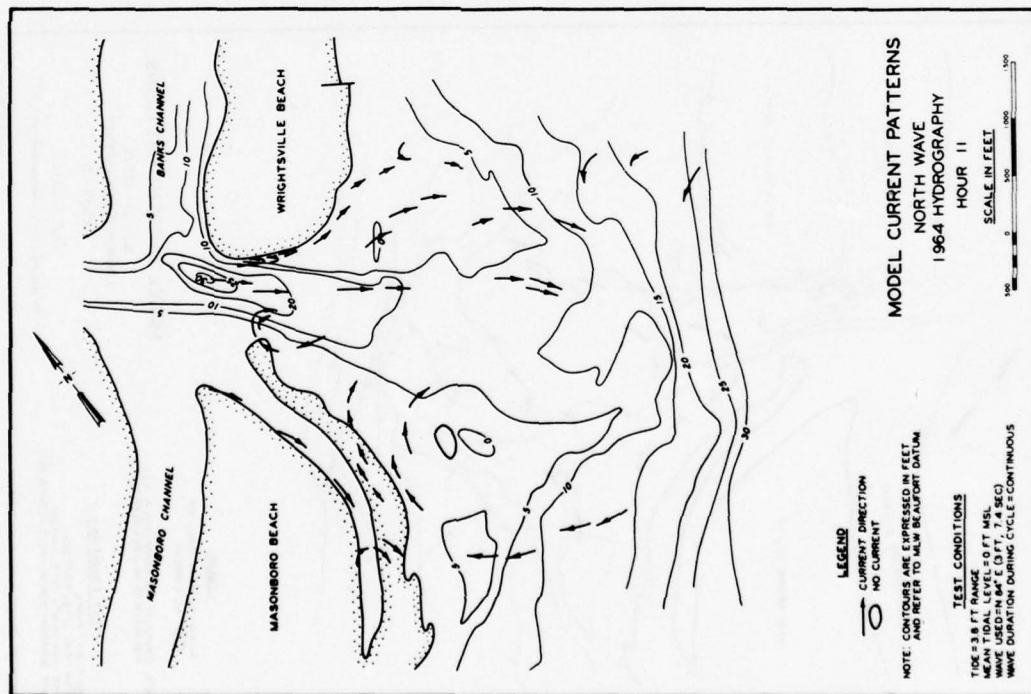


PLATE 231

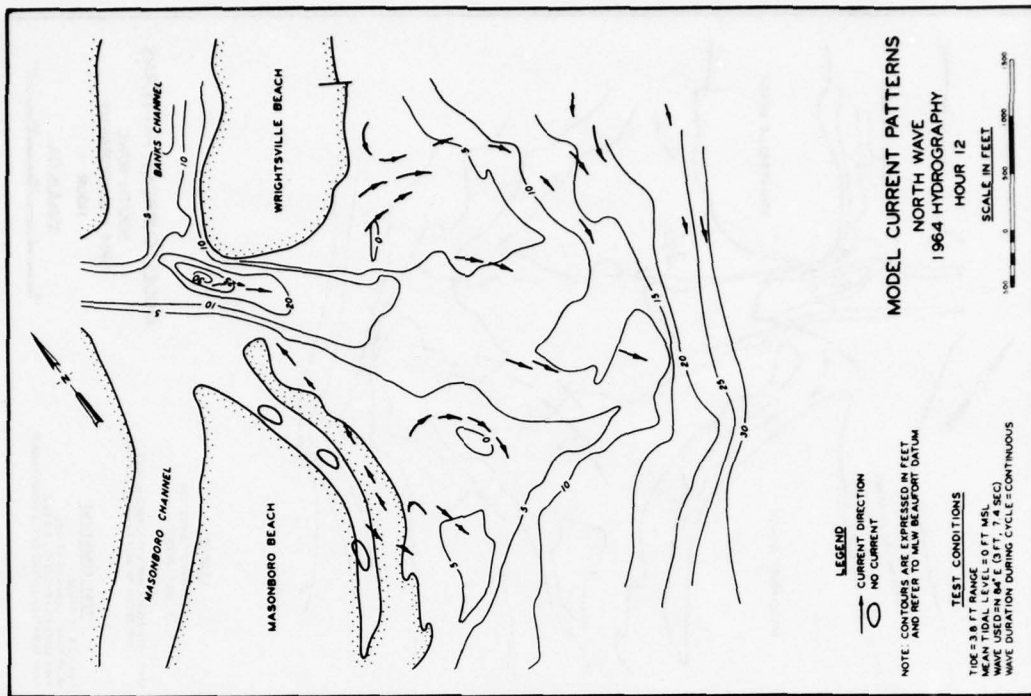


PLATE 232

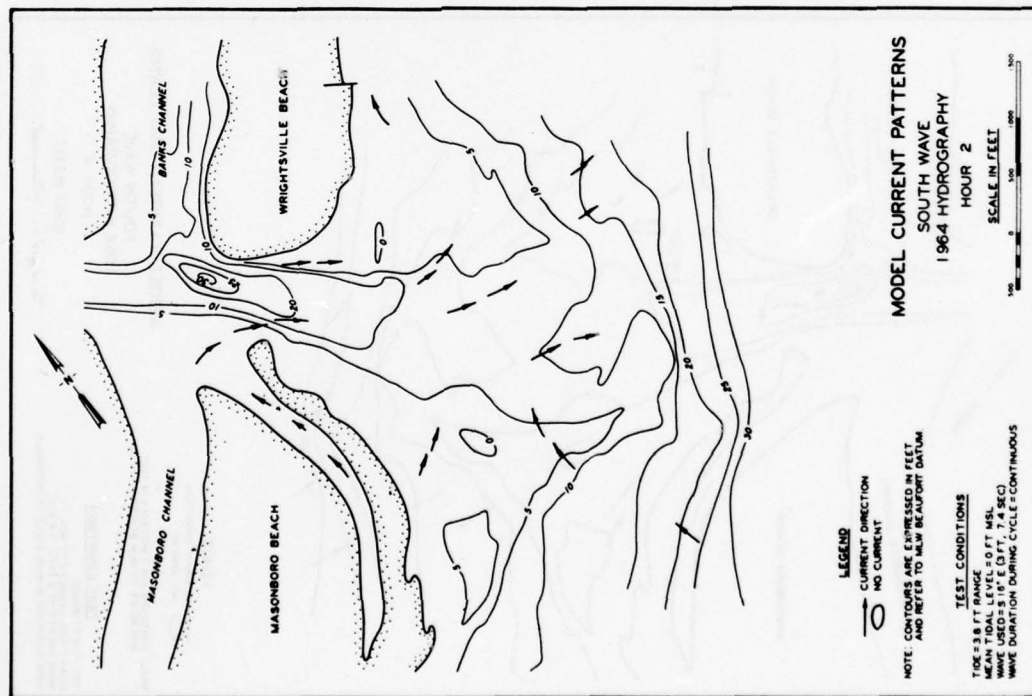


PLATE 235

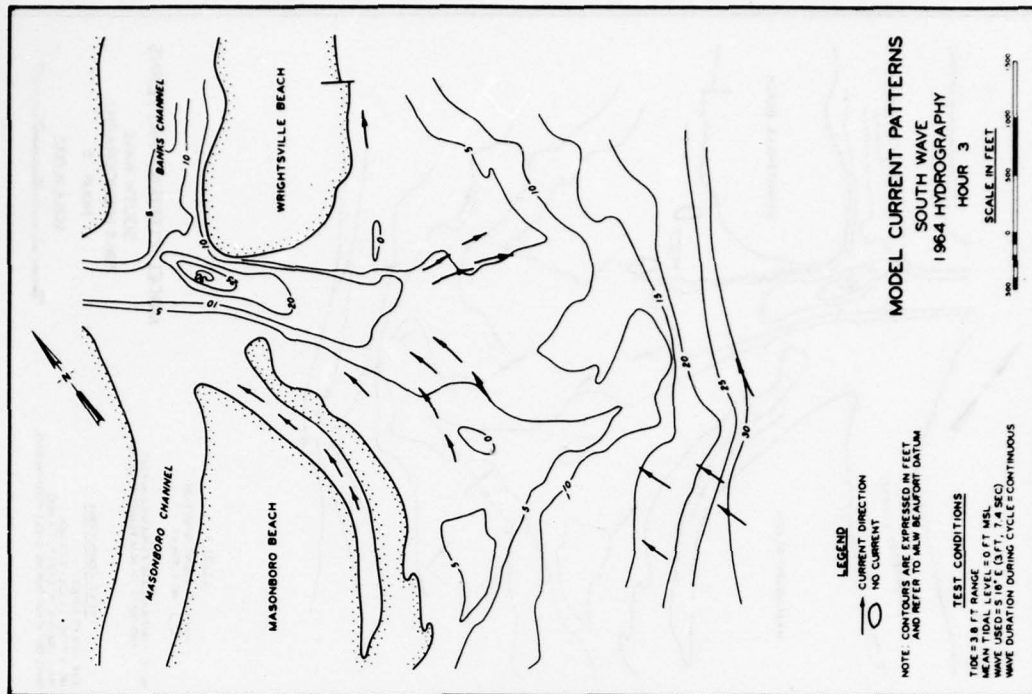


PLATE 236

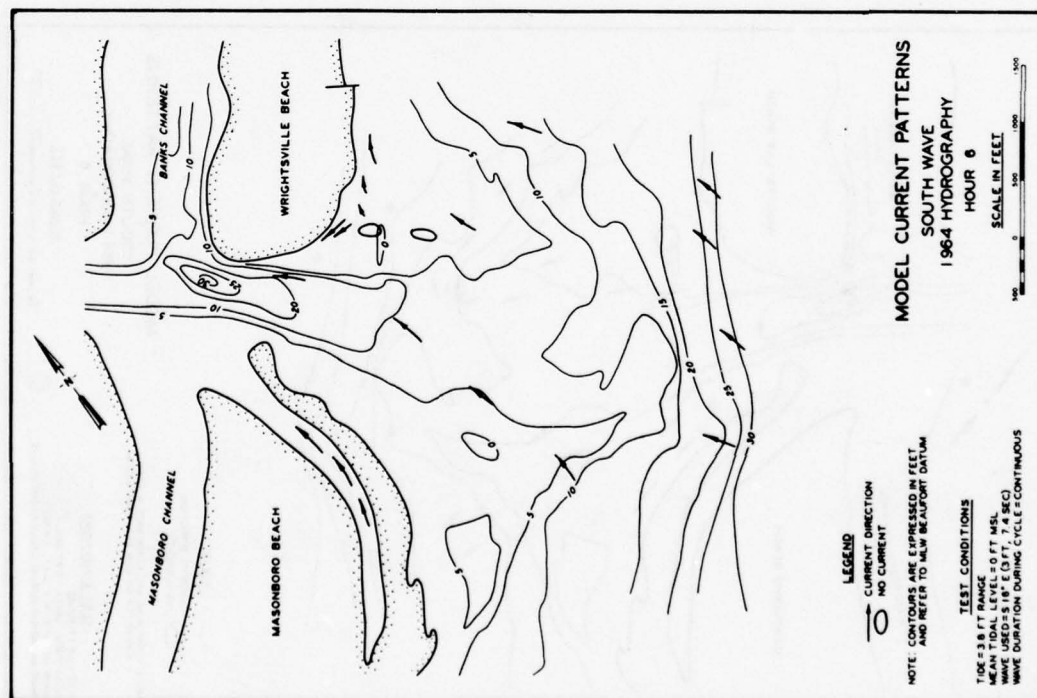


PLATE 239

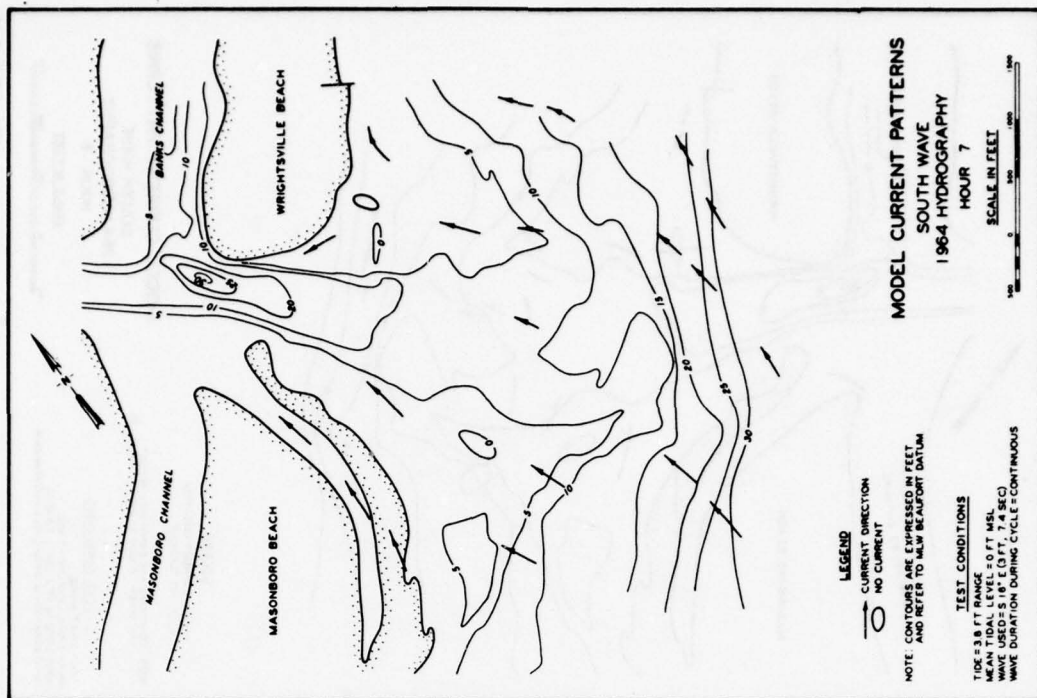


PLATE 240

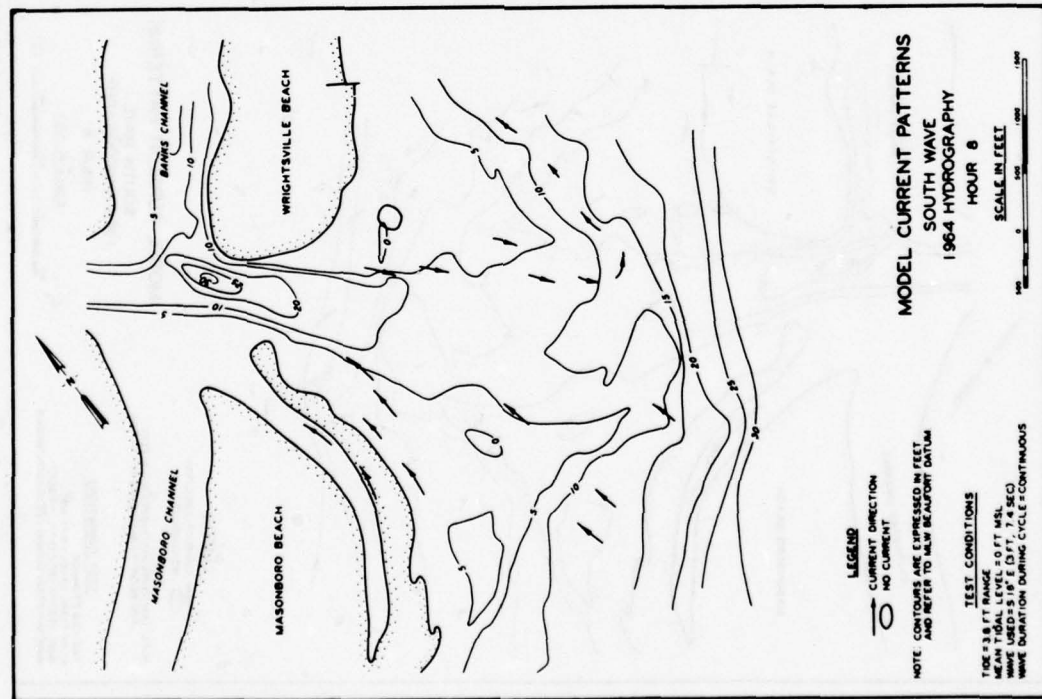


PLATE 241

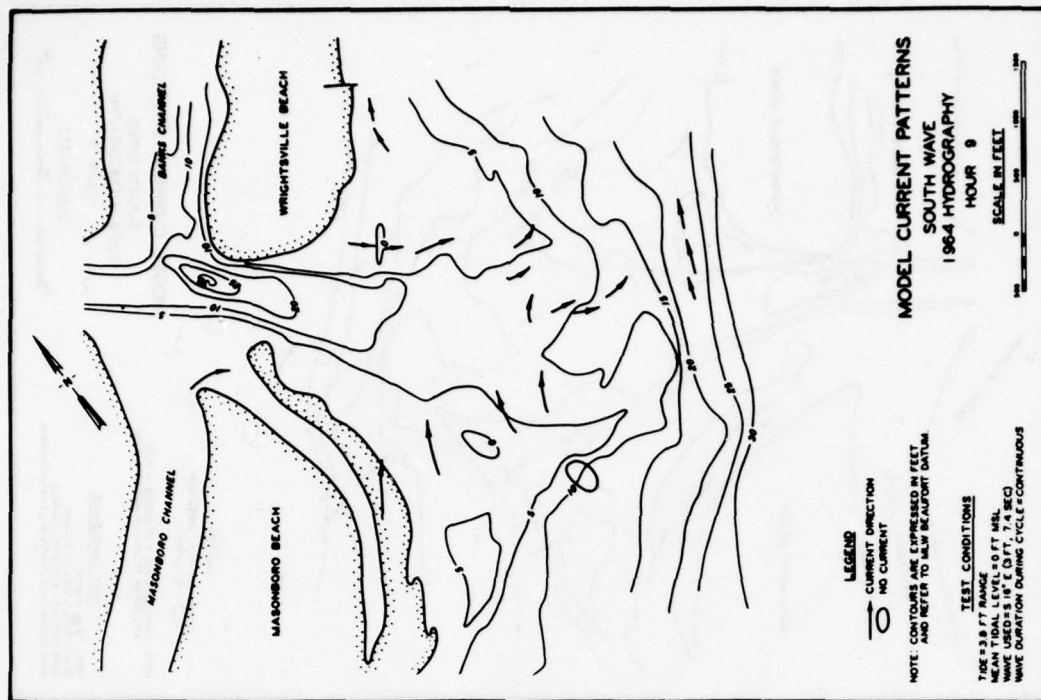


PLATE 242

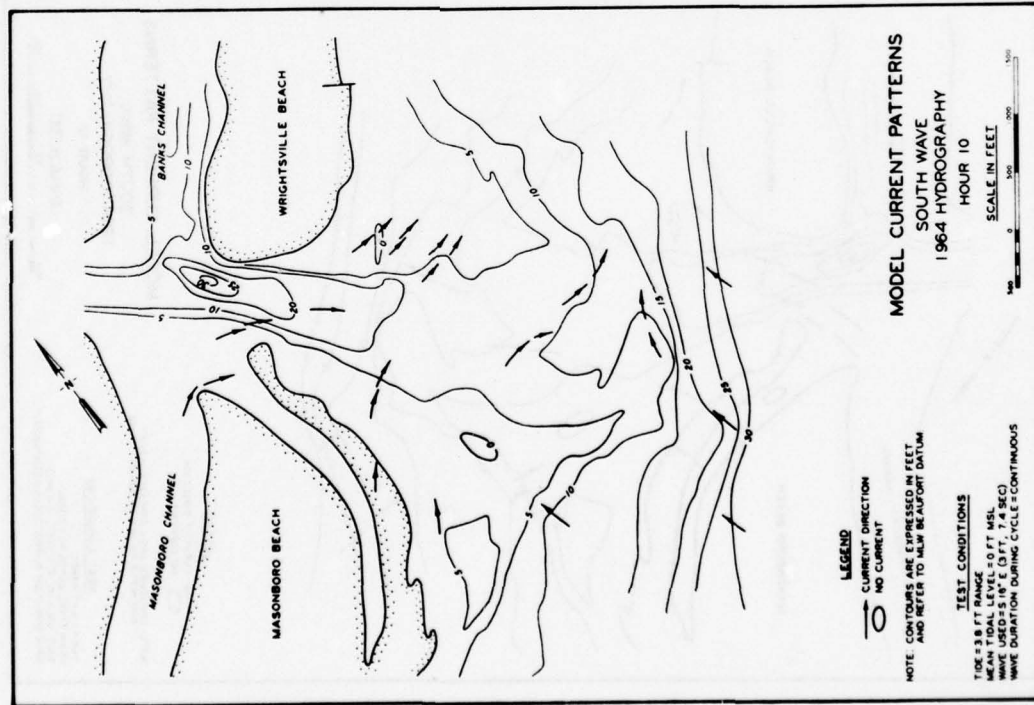


PLATE 243

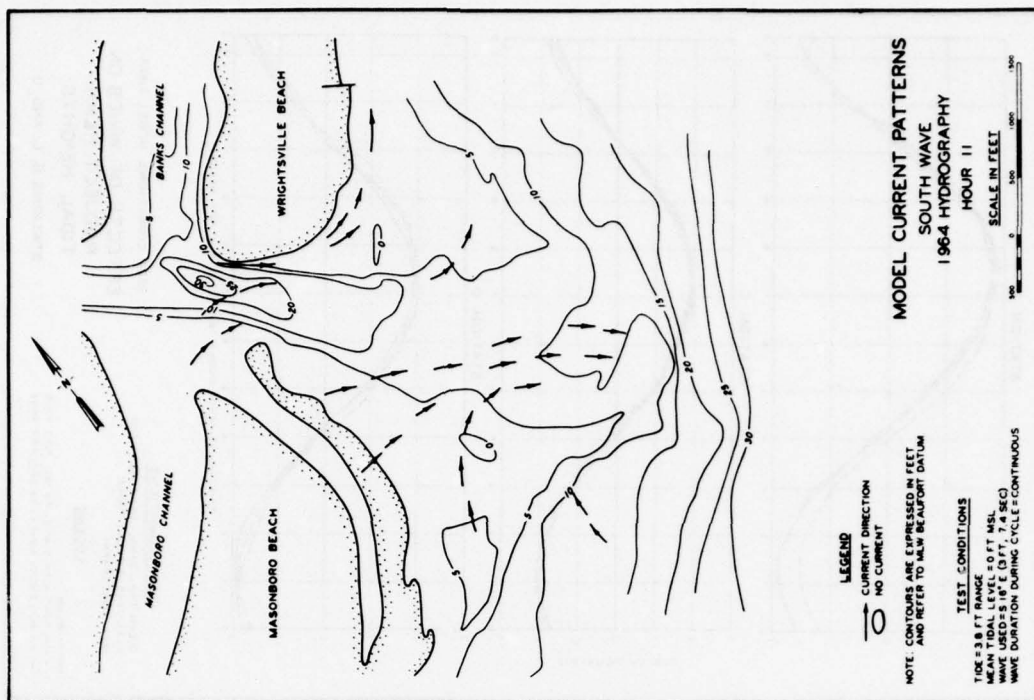


PLATE 244

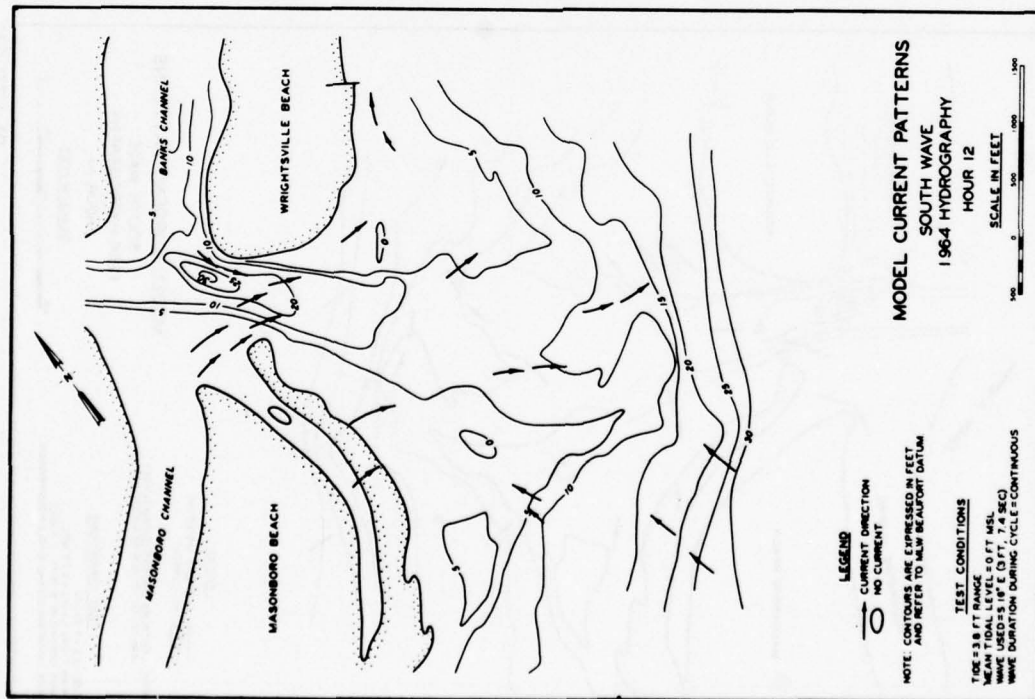


PLATE 245

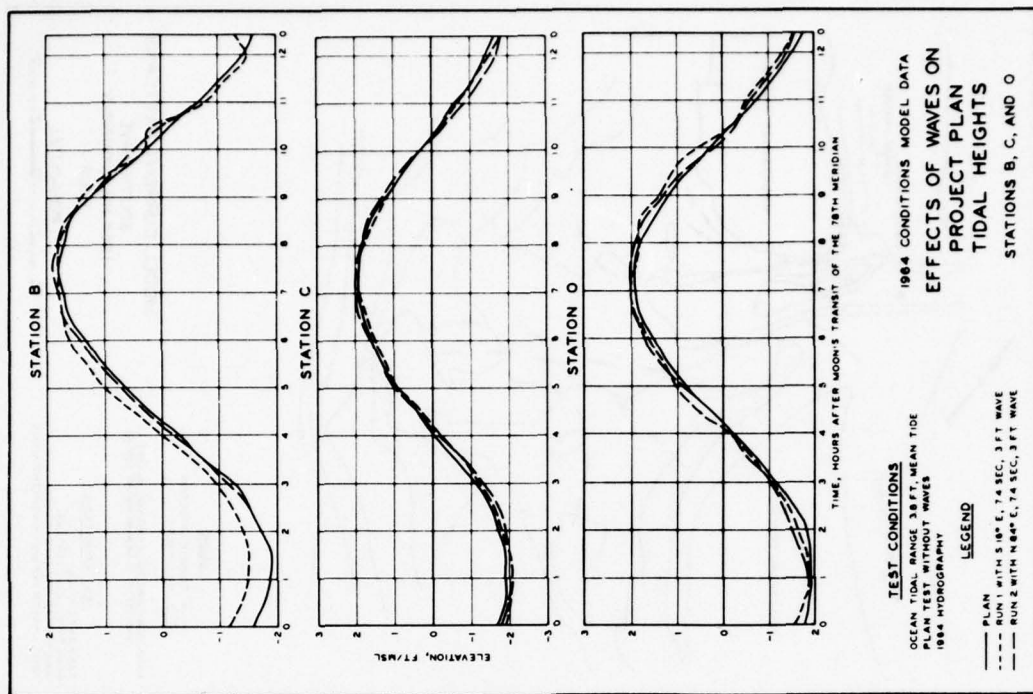


PLATE 246

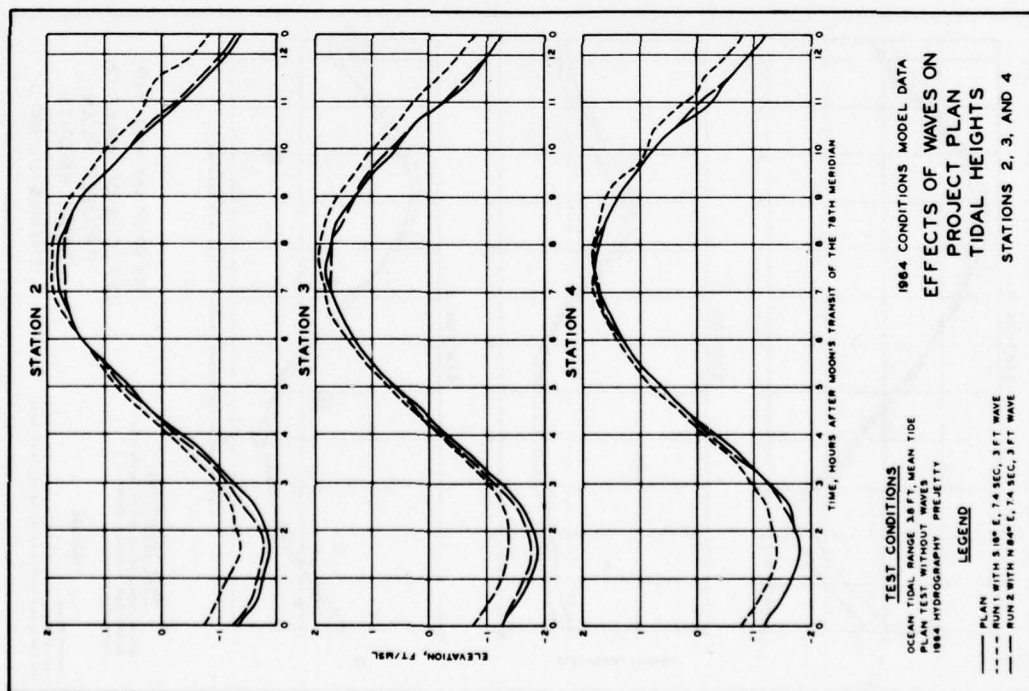


PLATE 247

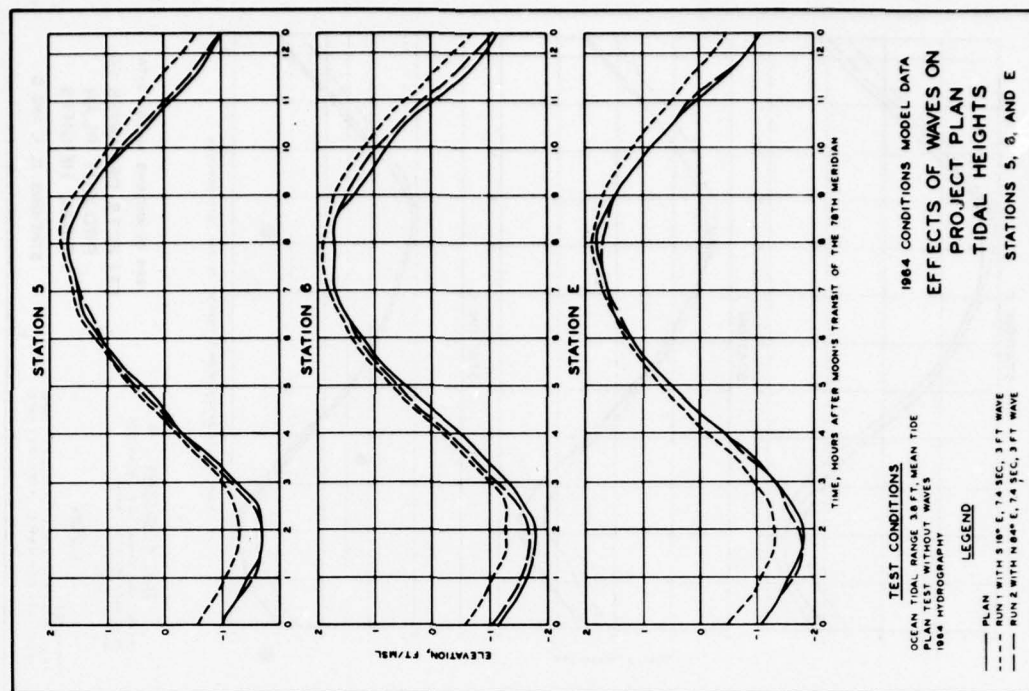


PLATE 248

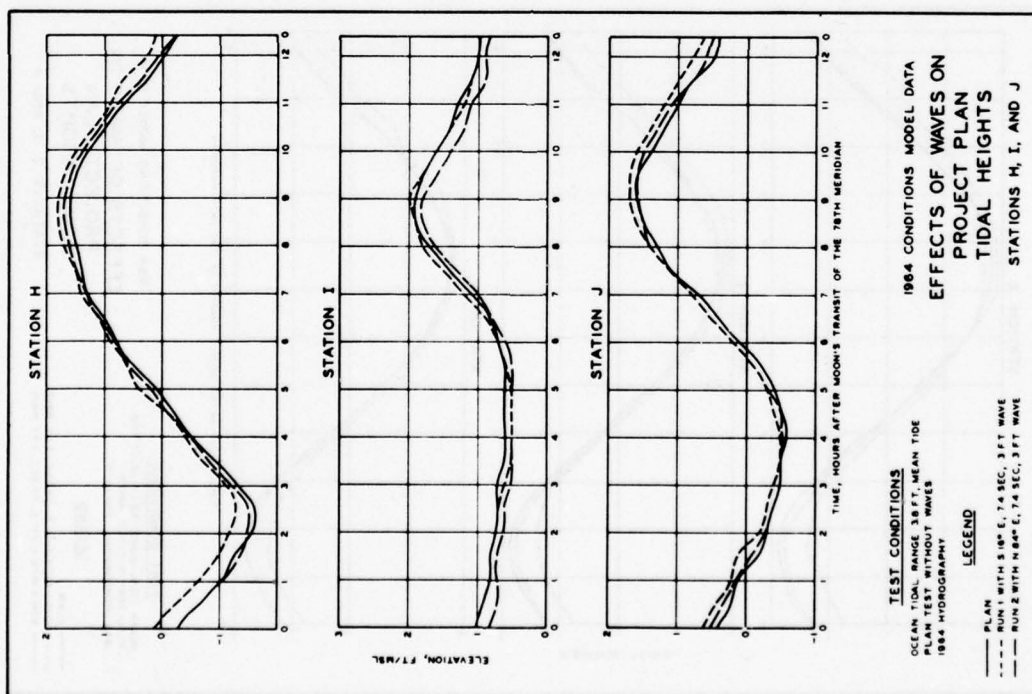


PLATE 249

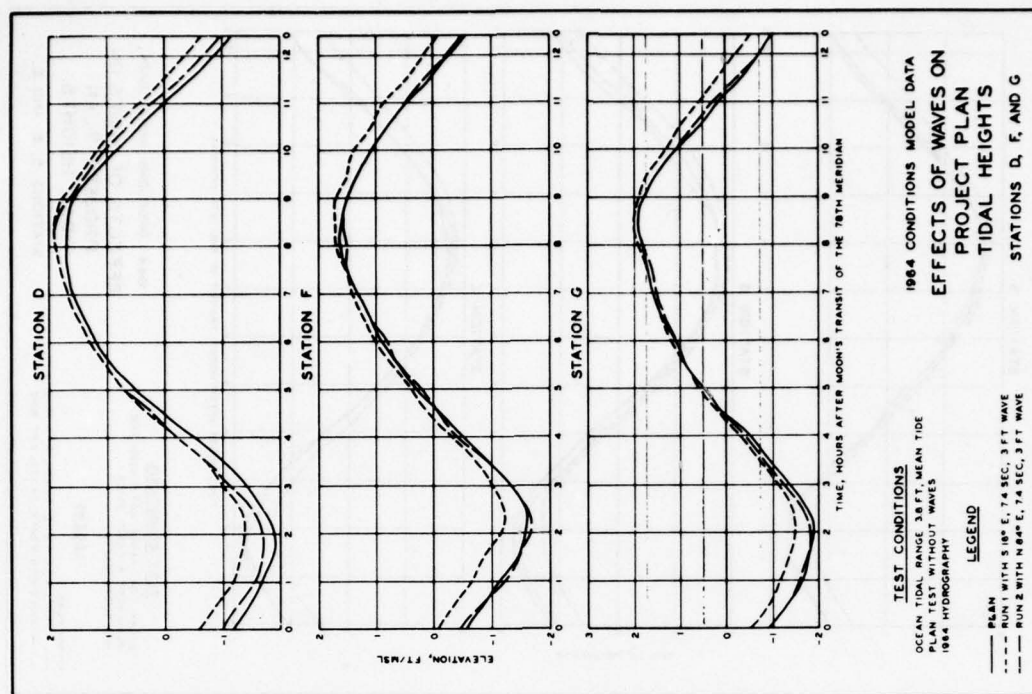


PLATE 250

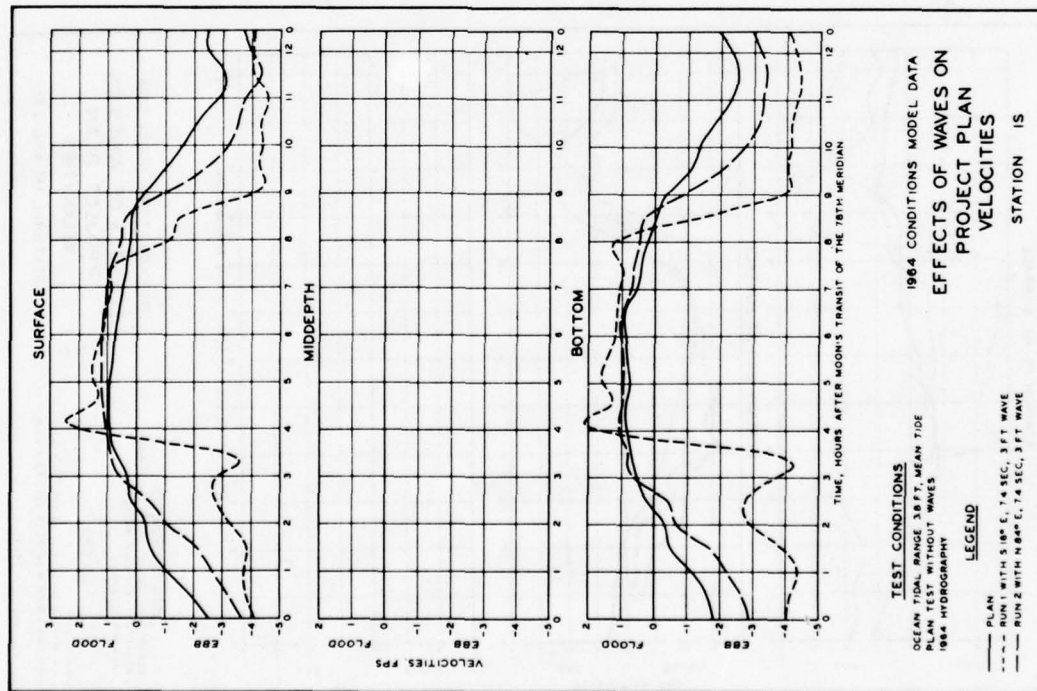


PLATE 251

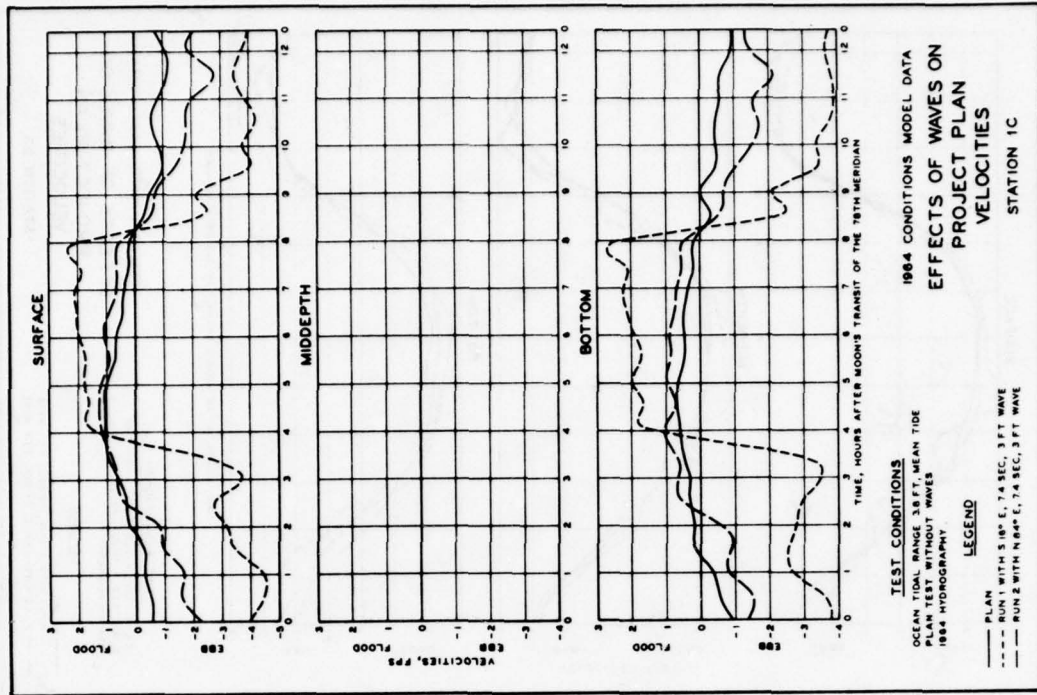


PLATE 252

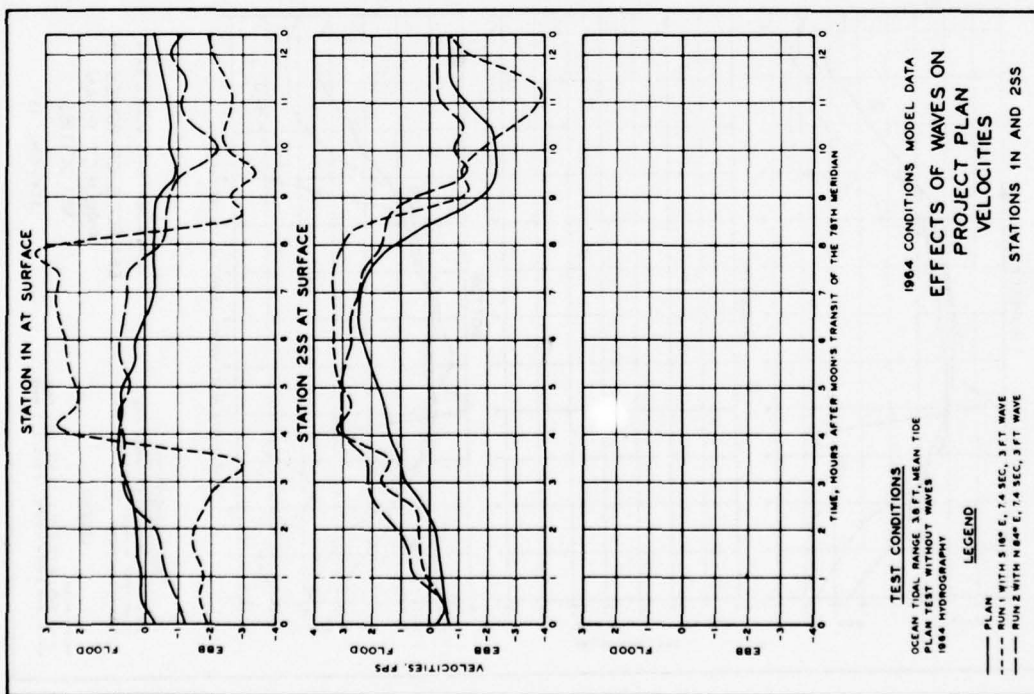


PLATE 253

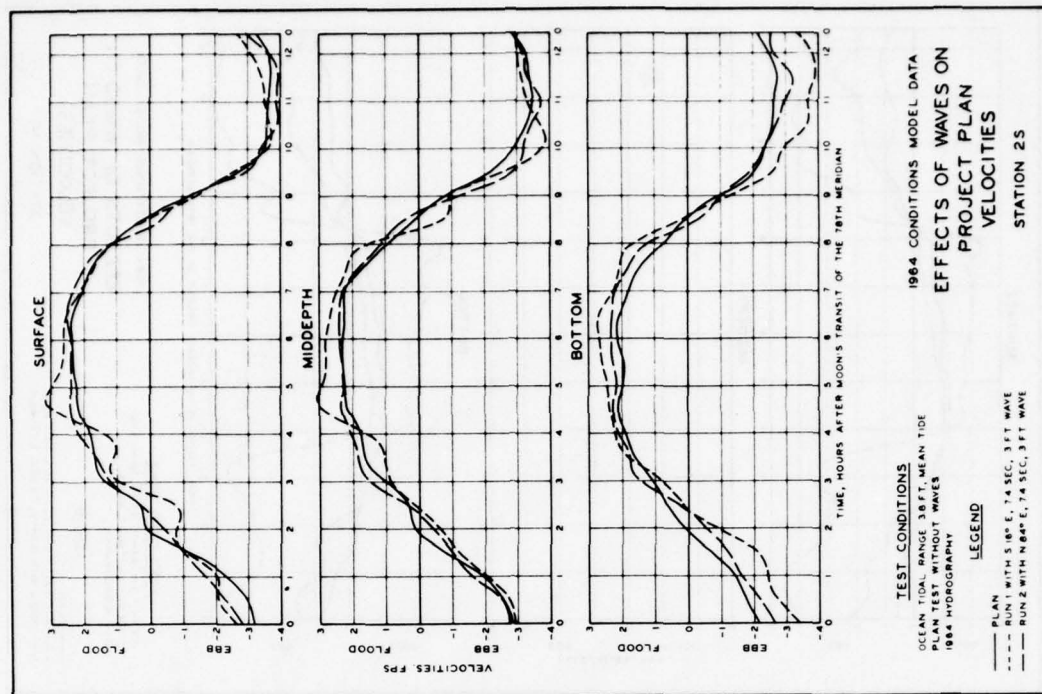


PLATE 254

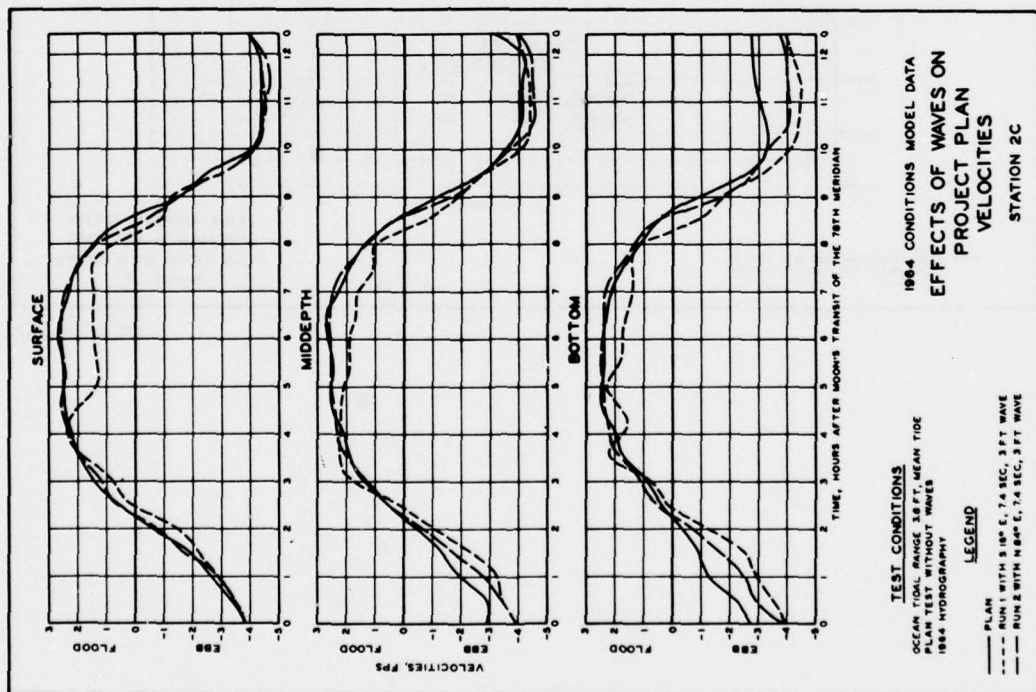


PLATE 255

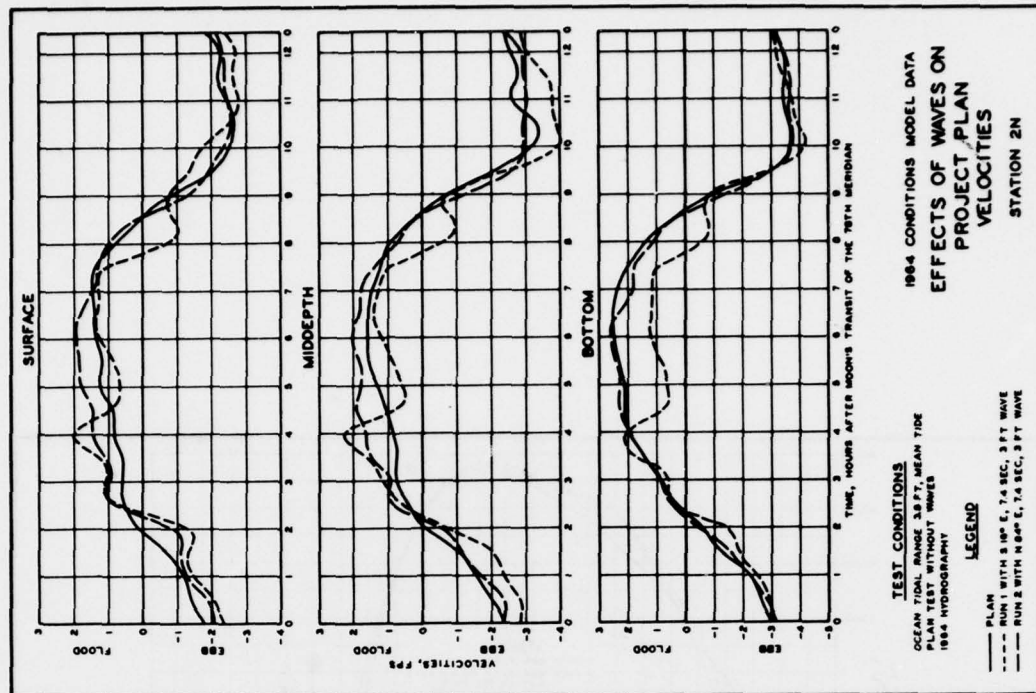
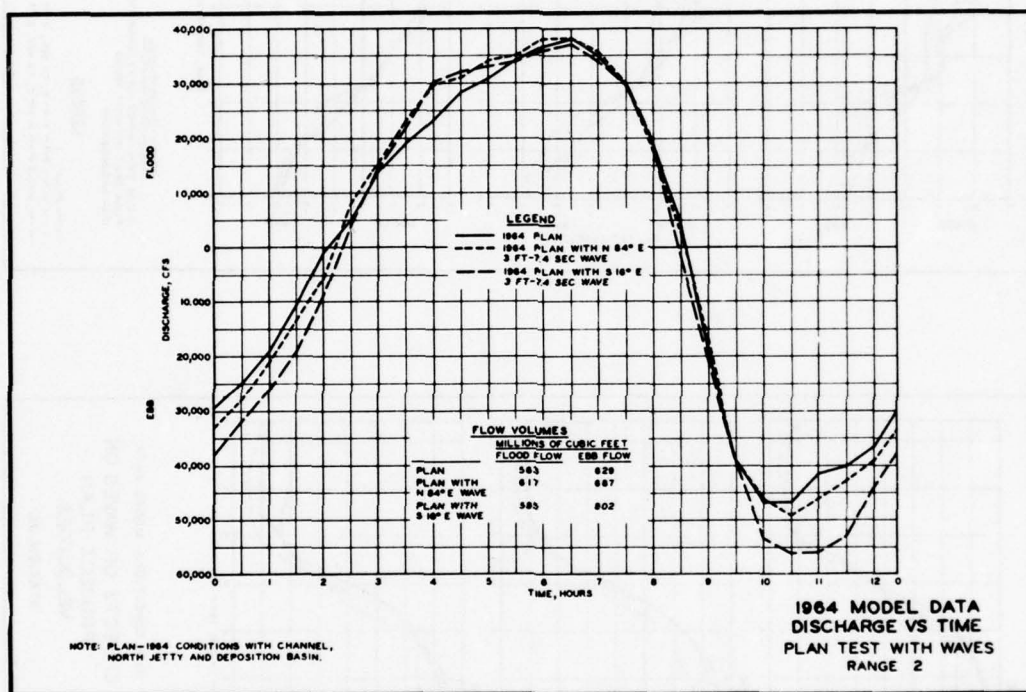


PLATE 256



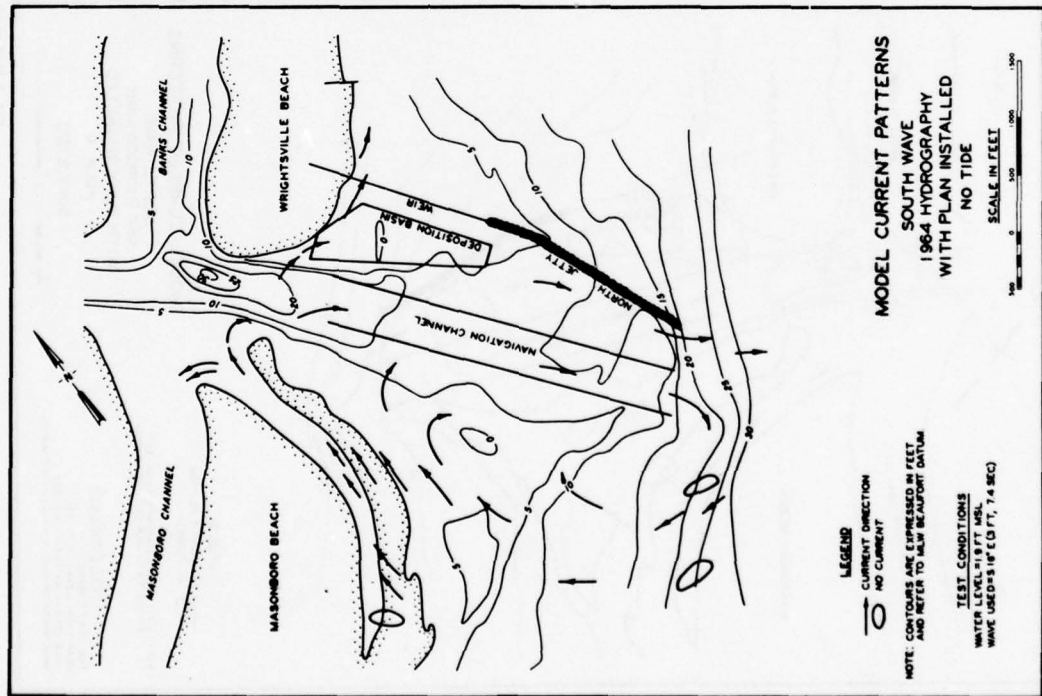


PLATE 258

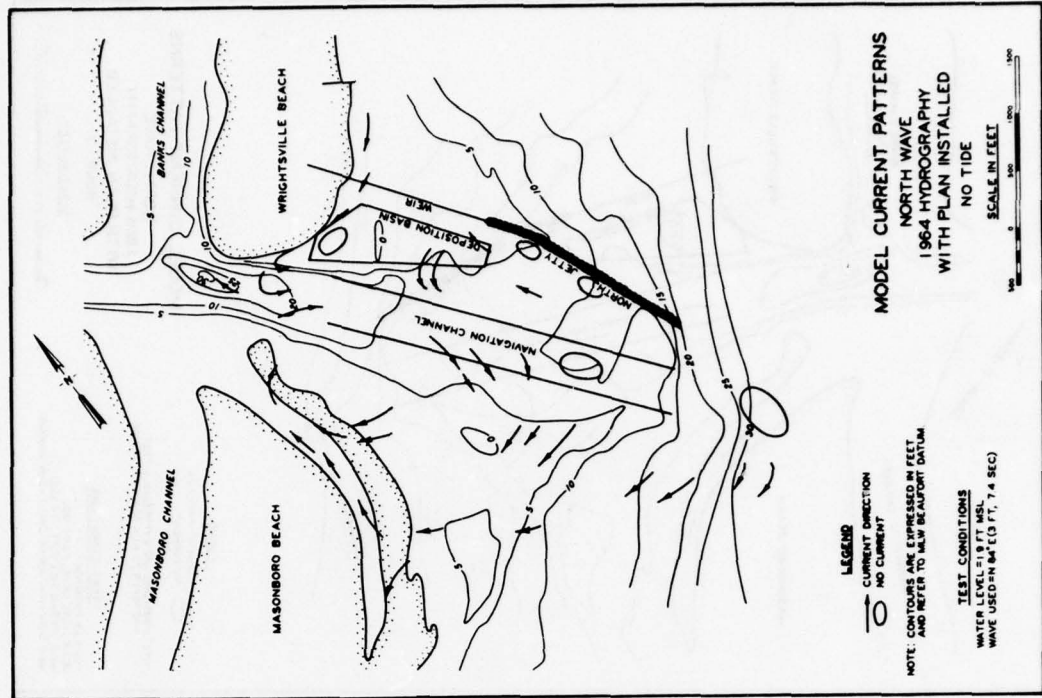


PLATE 259

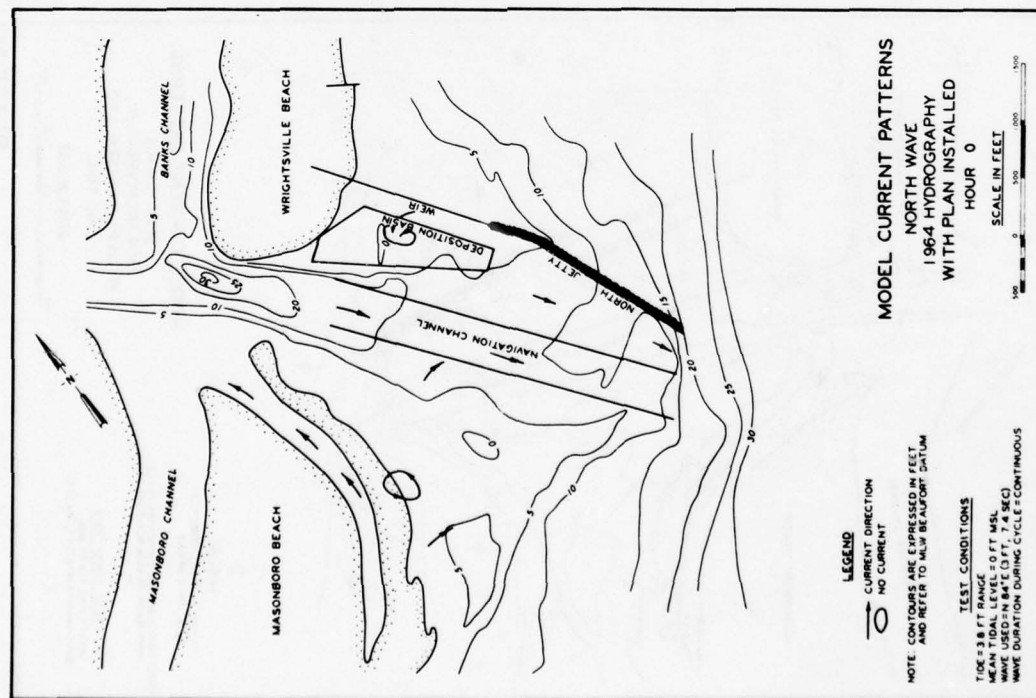


PLATE 260

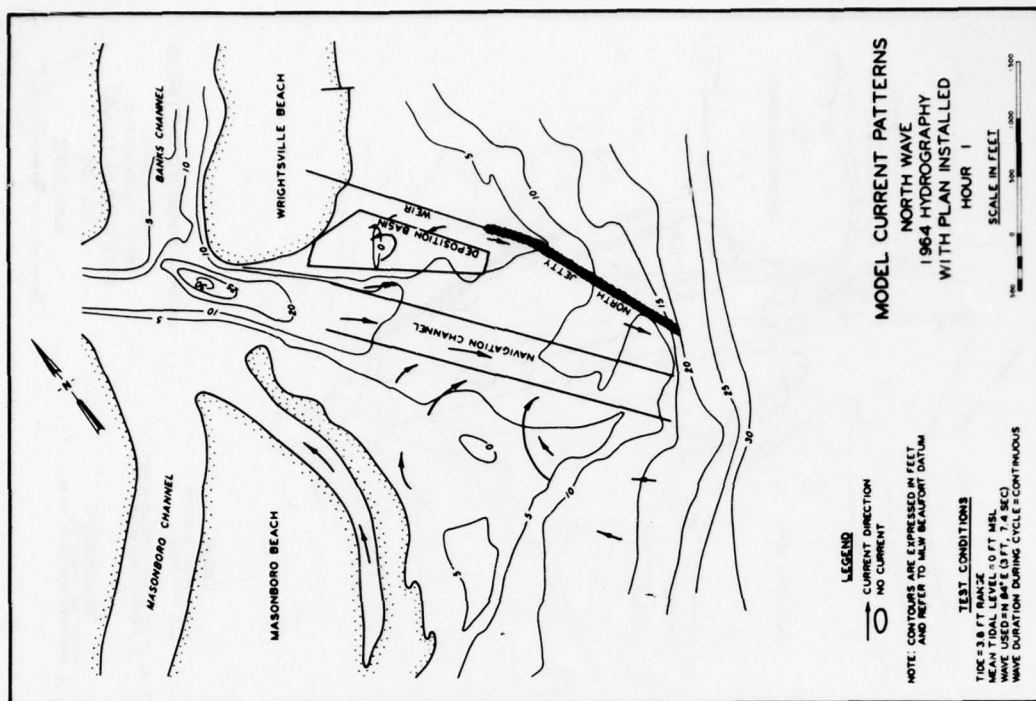


PLATE 261

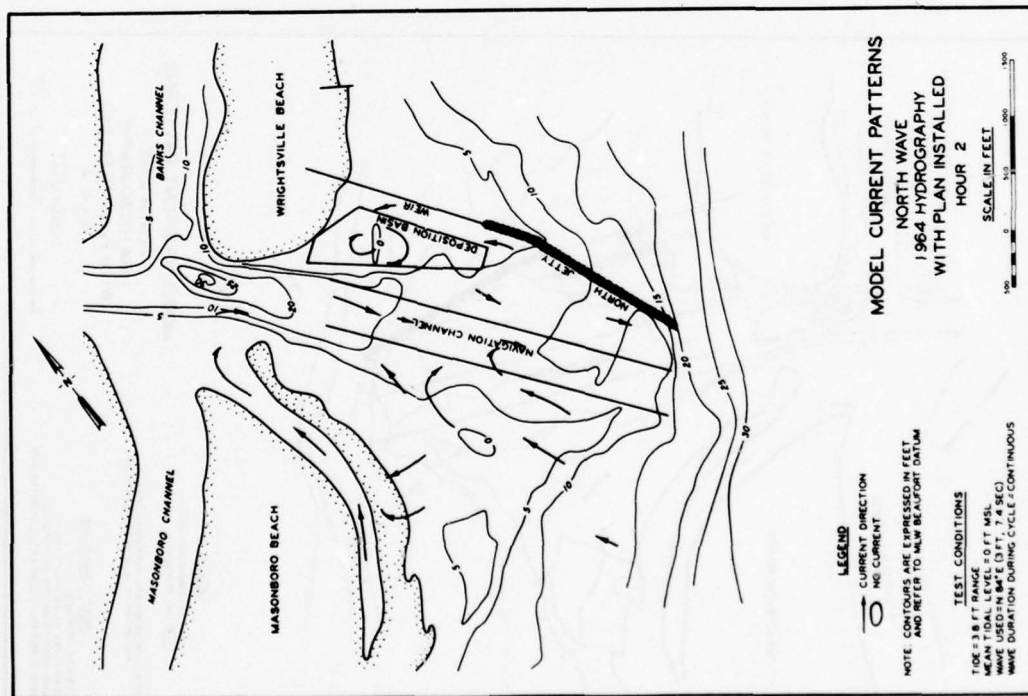


PLATE 262

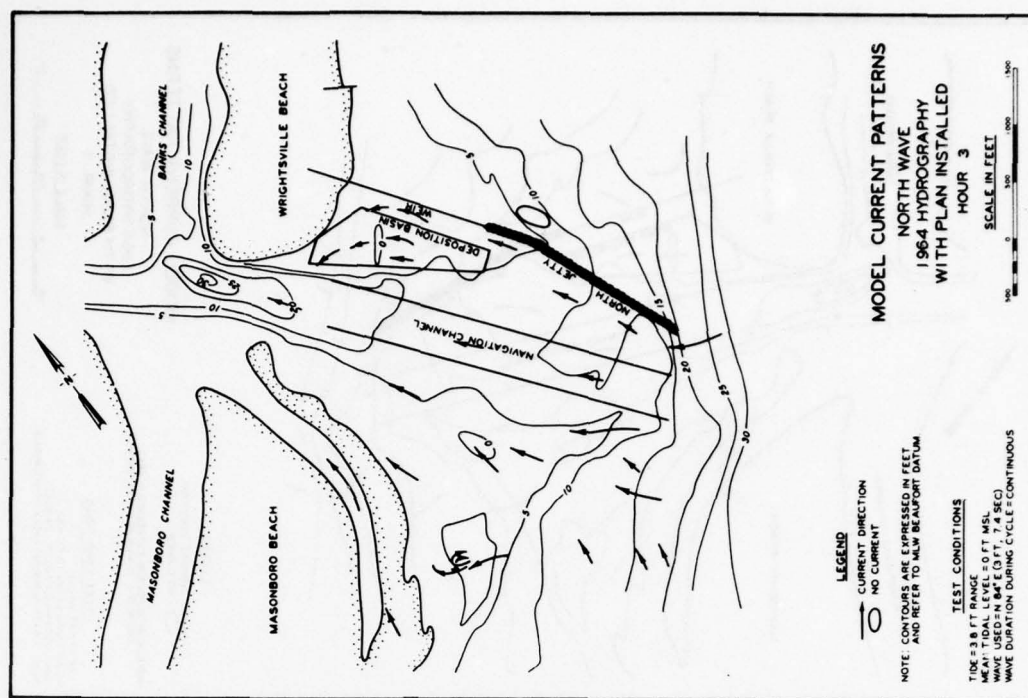


PLATE 263

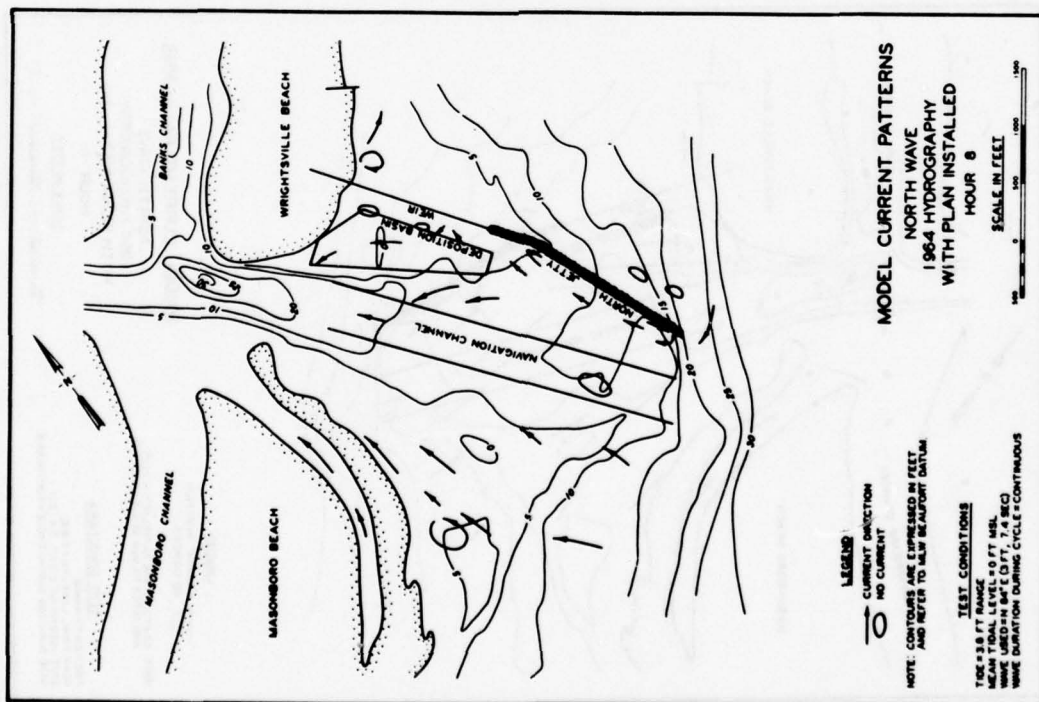
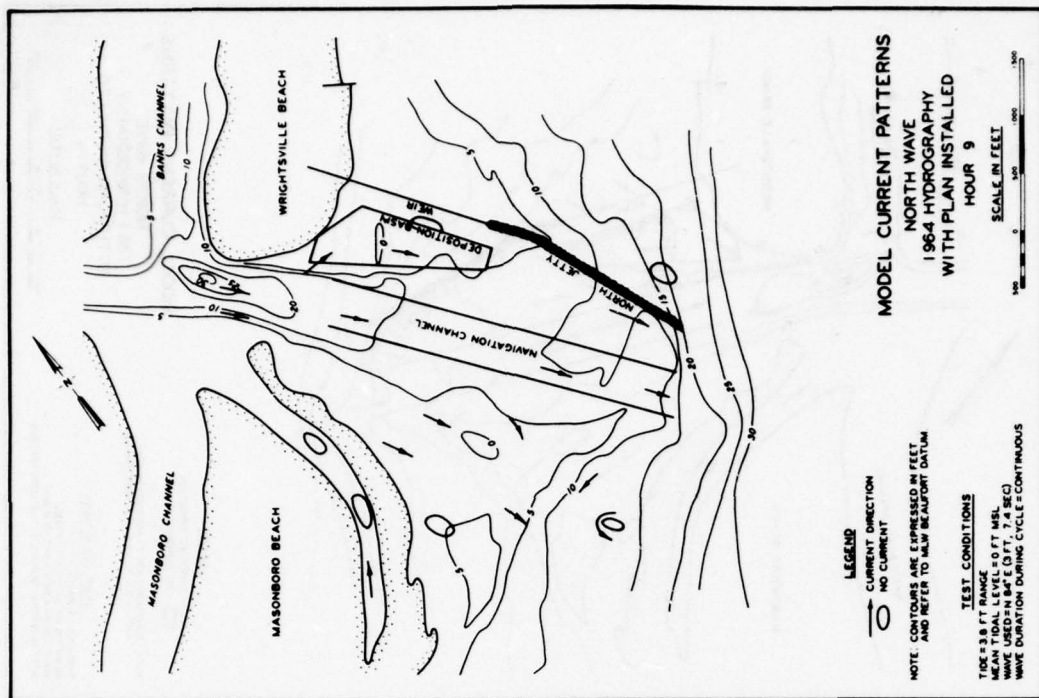


PLATE 268



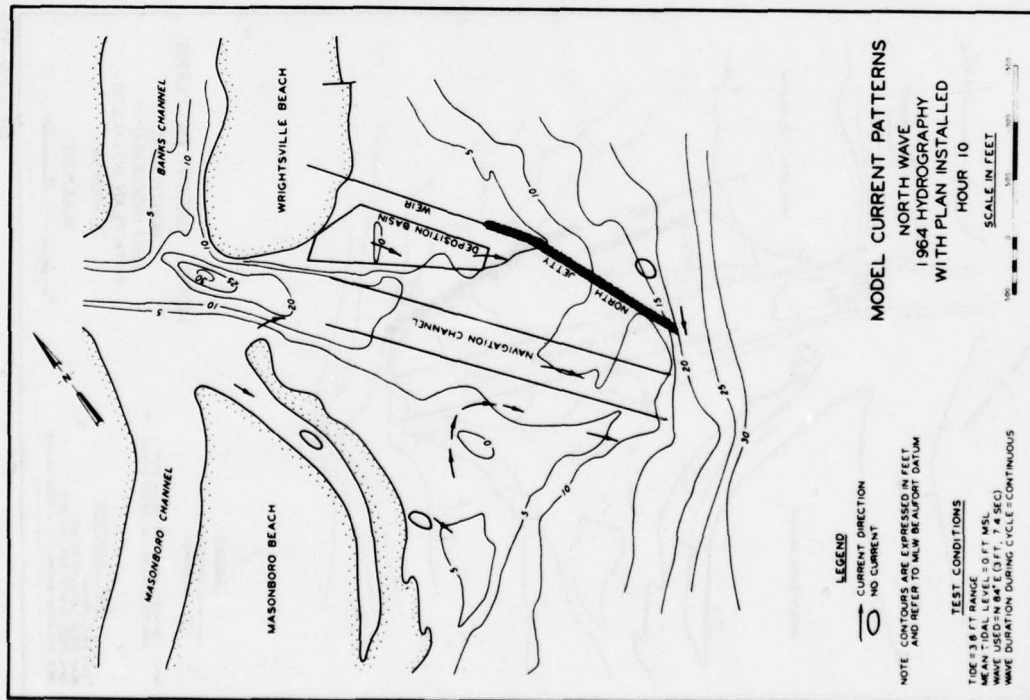


PLATE 270

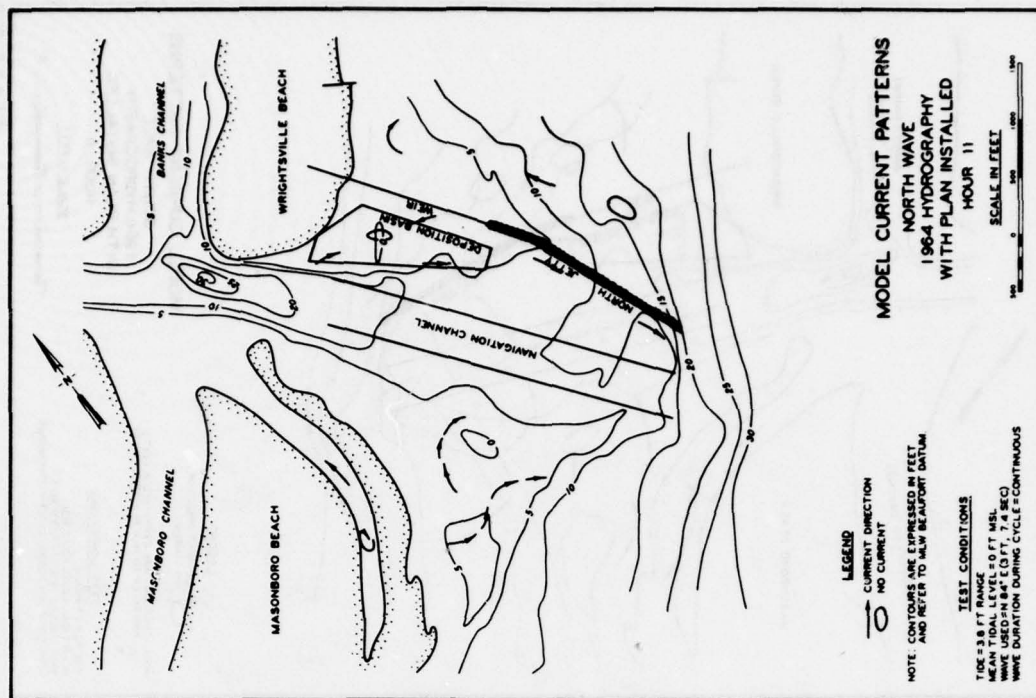


PLATE 271

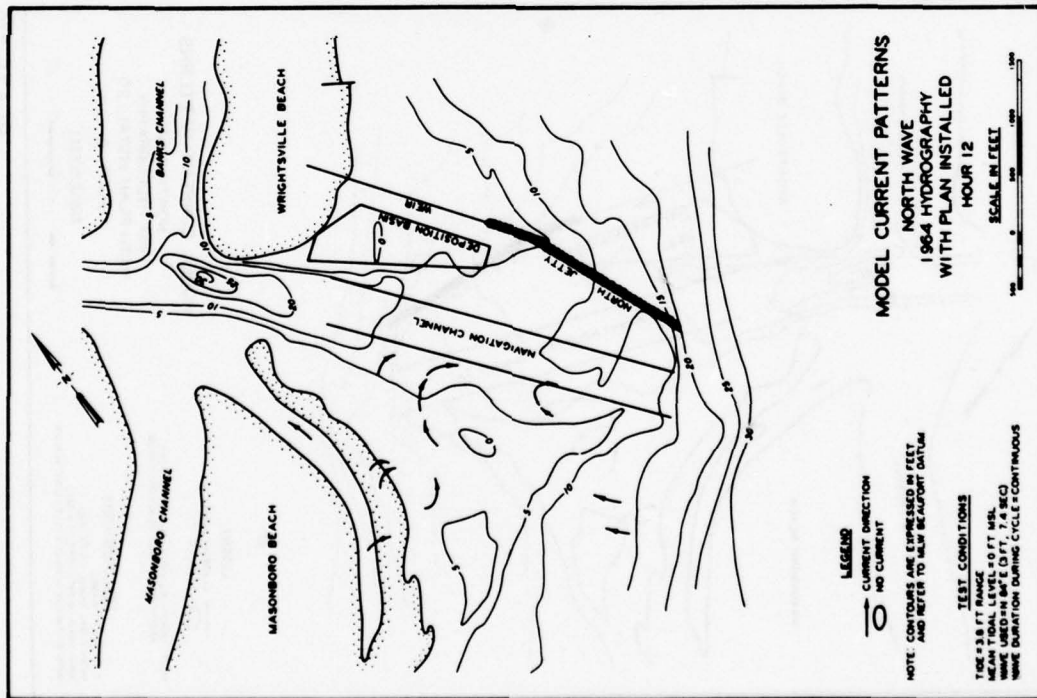


PLATE 272

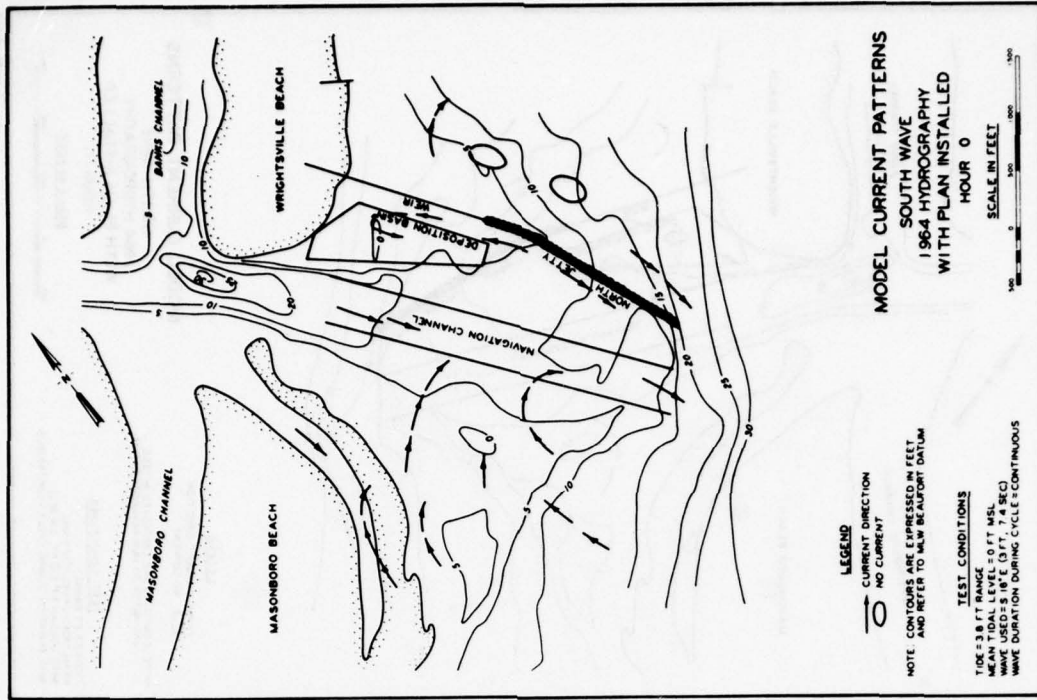


PLATE 273

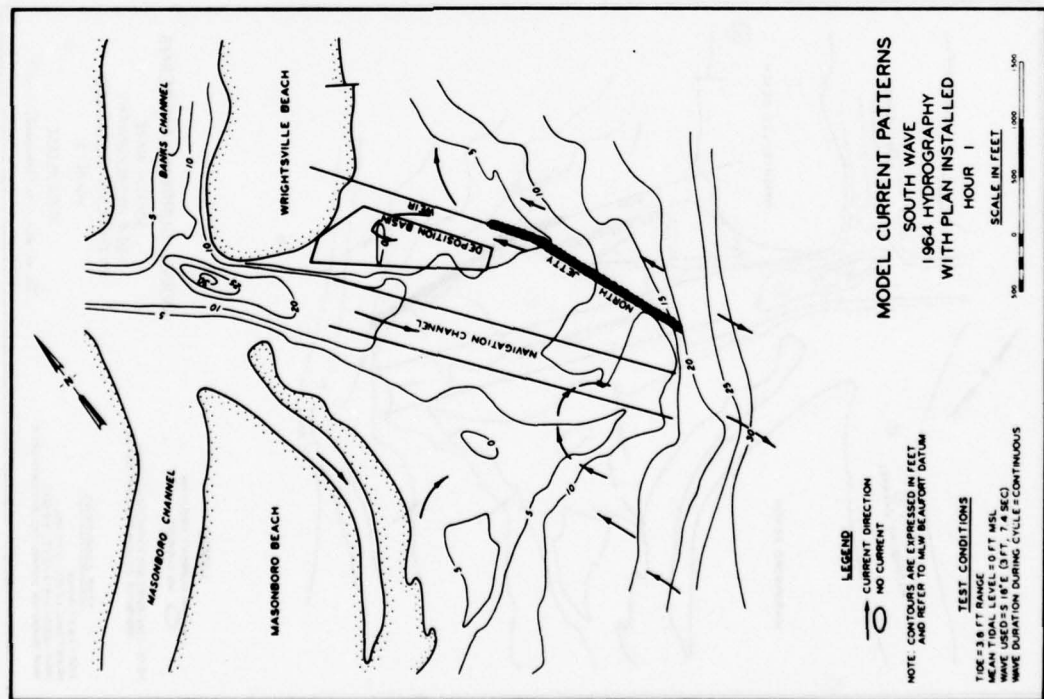


PLATE 274

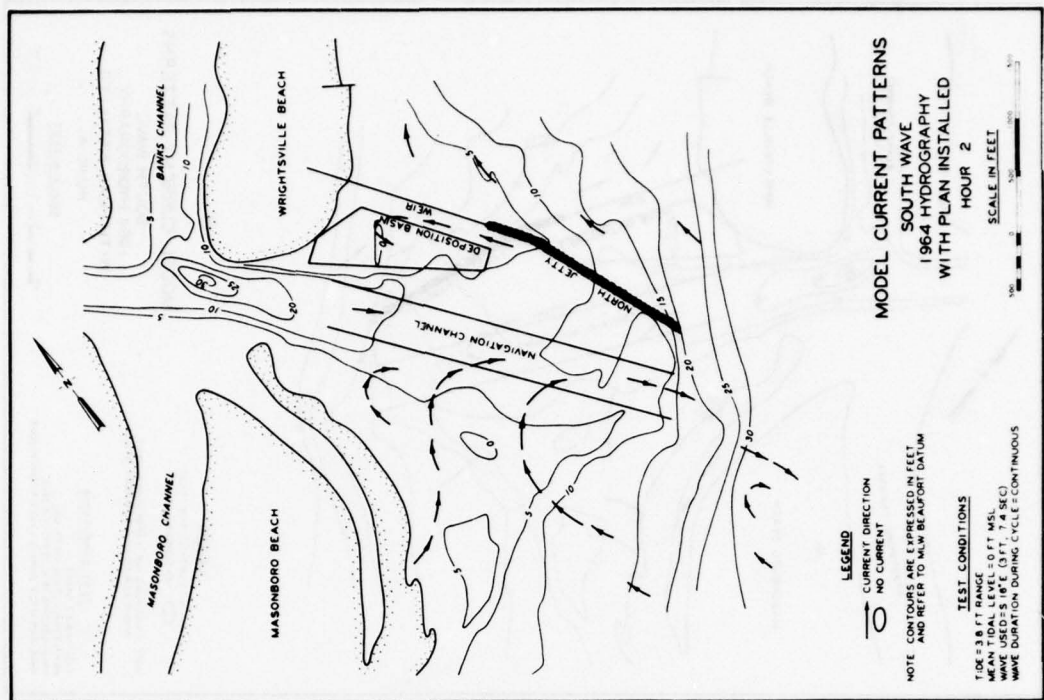


PLATE 275

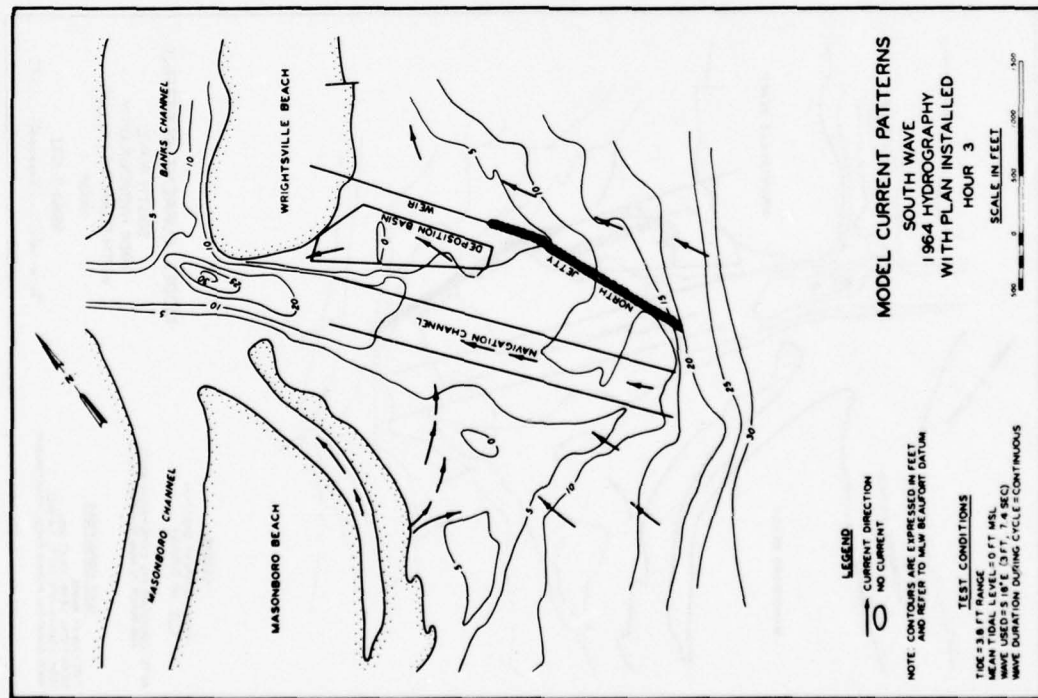


PLATE 276

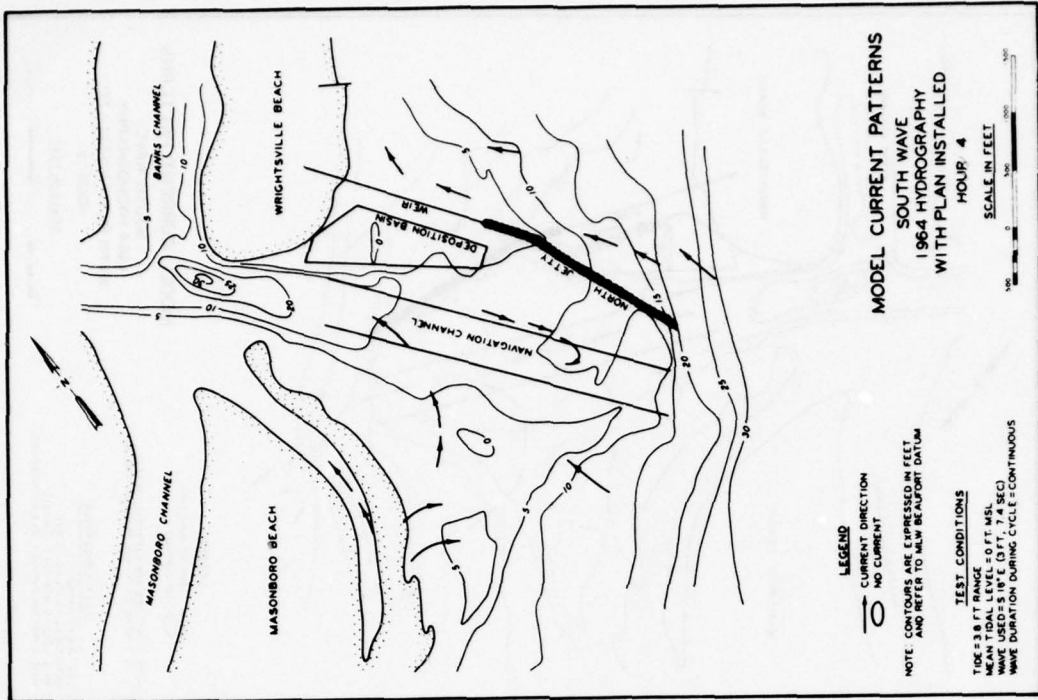


PLATE 277

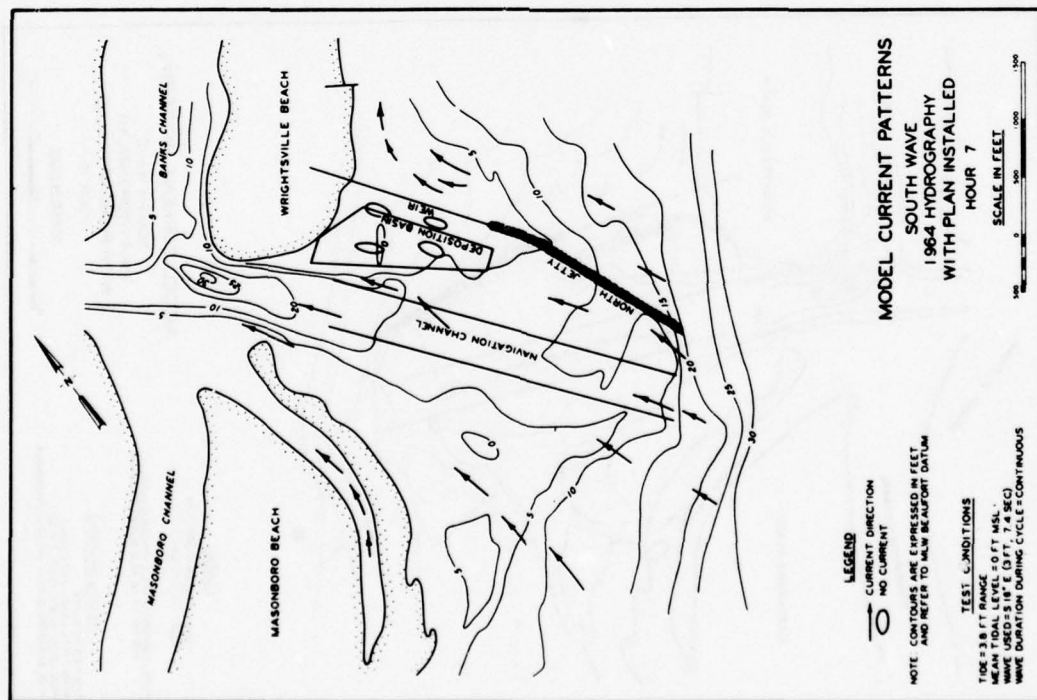


PLATE 280

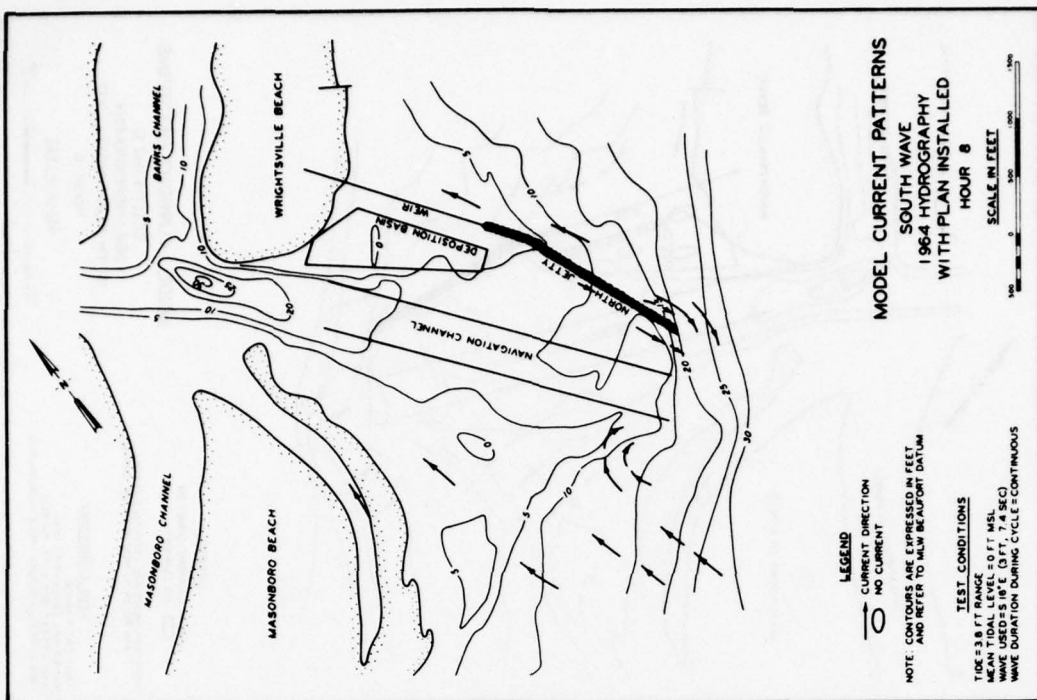


PLATE 281

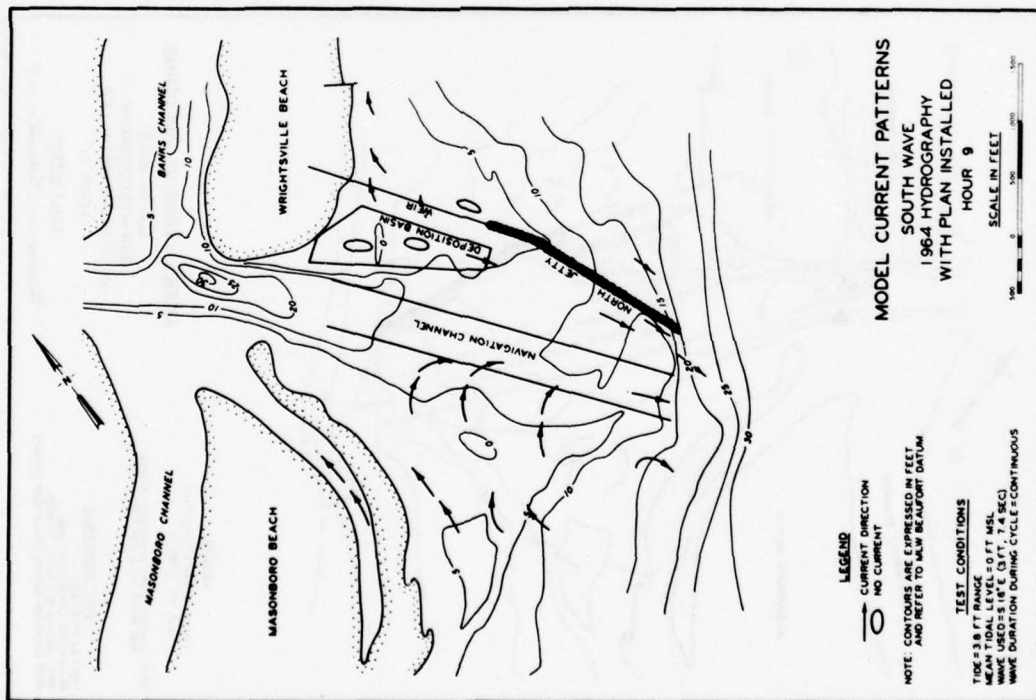


PLATE 282

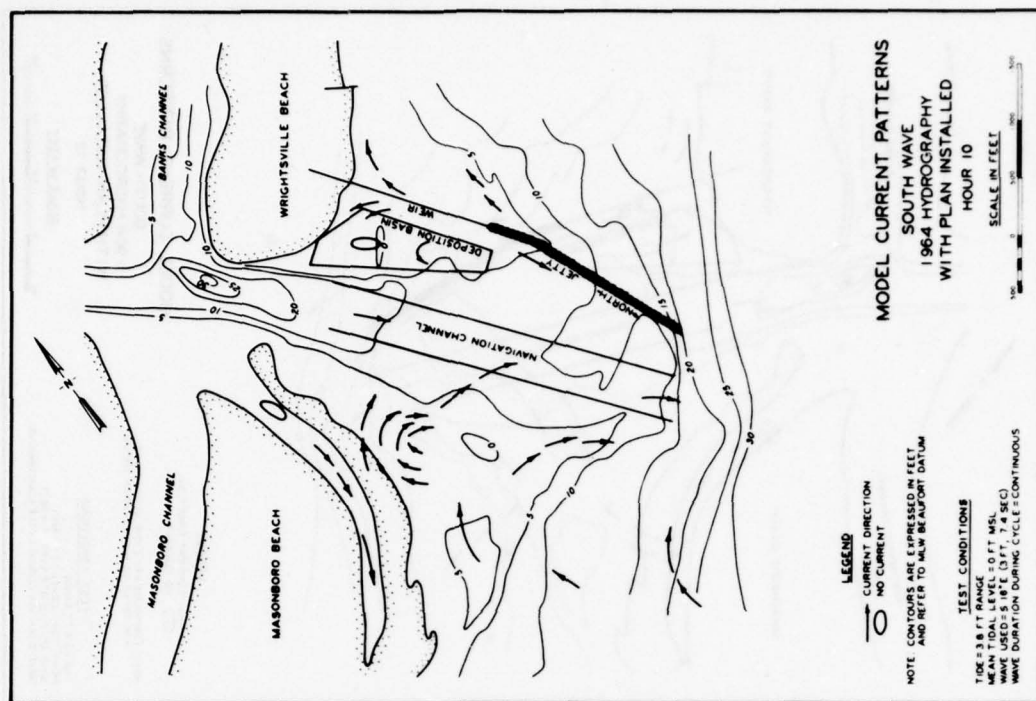


PLATE 283

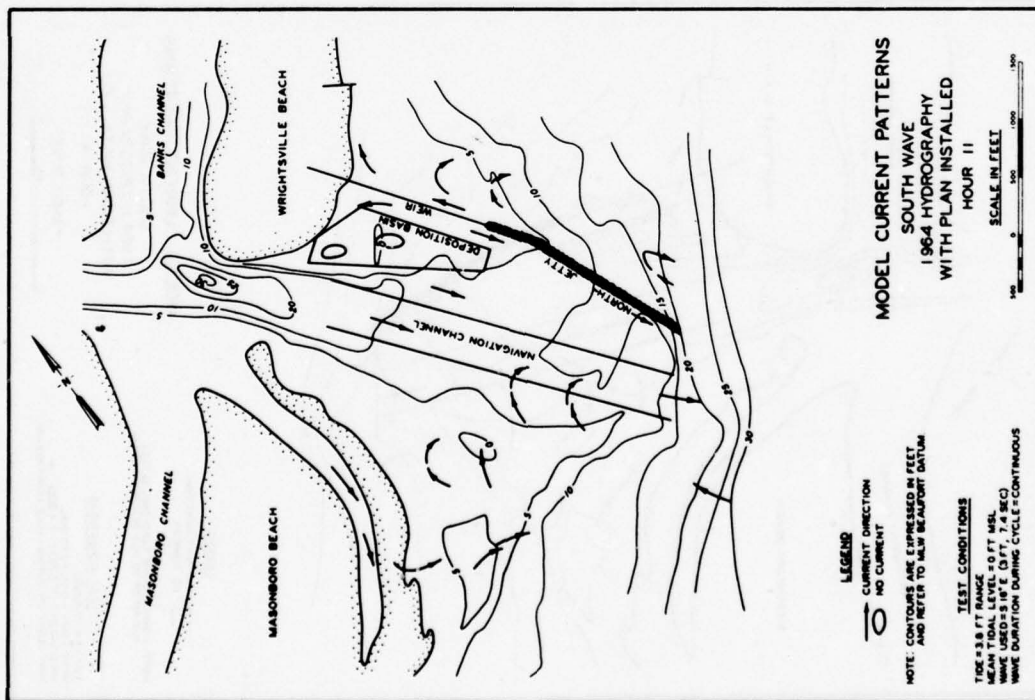


PLATE 284

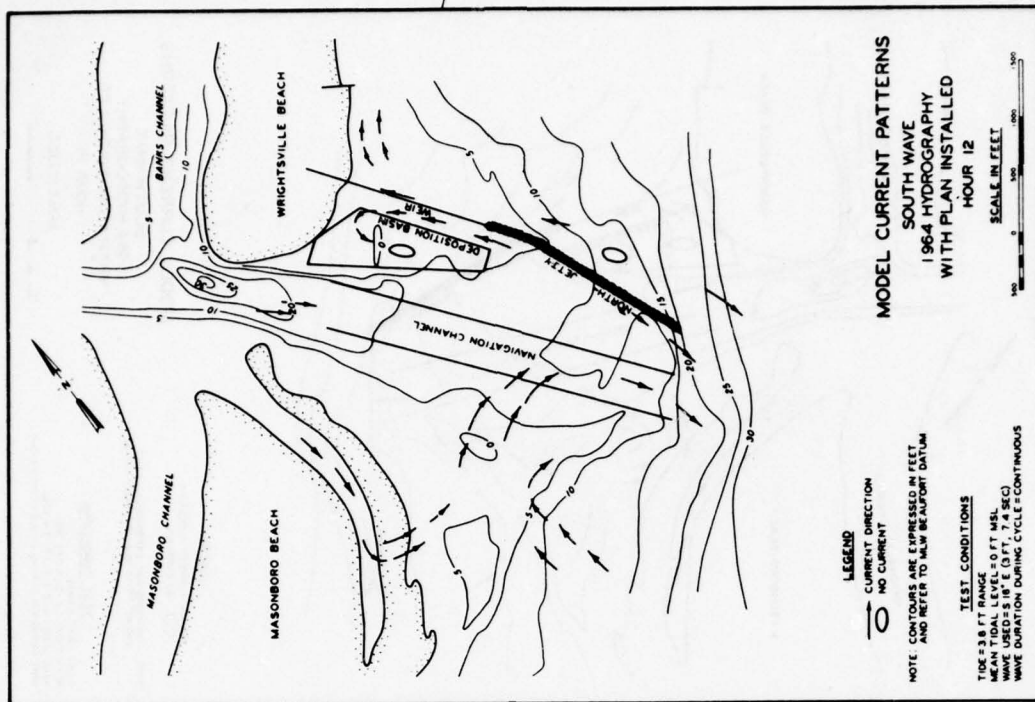


PLATE 285

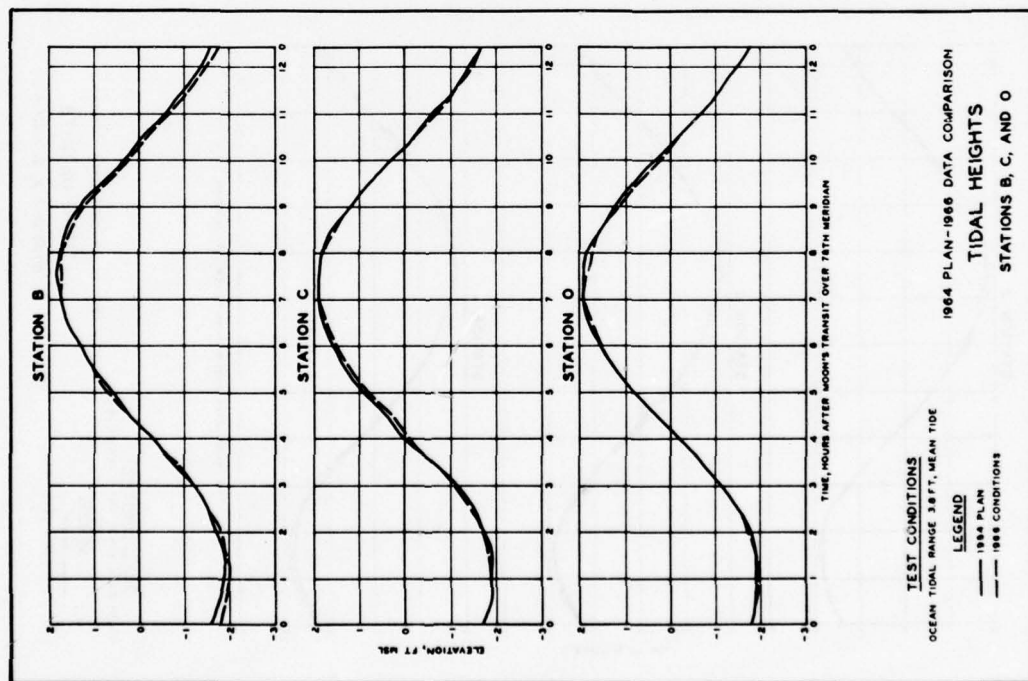


PLATE 286

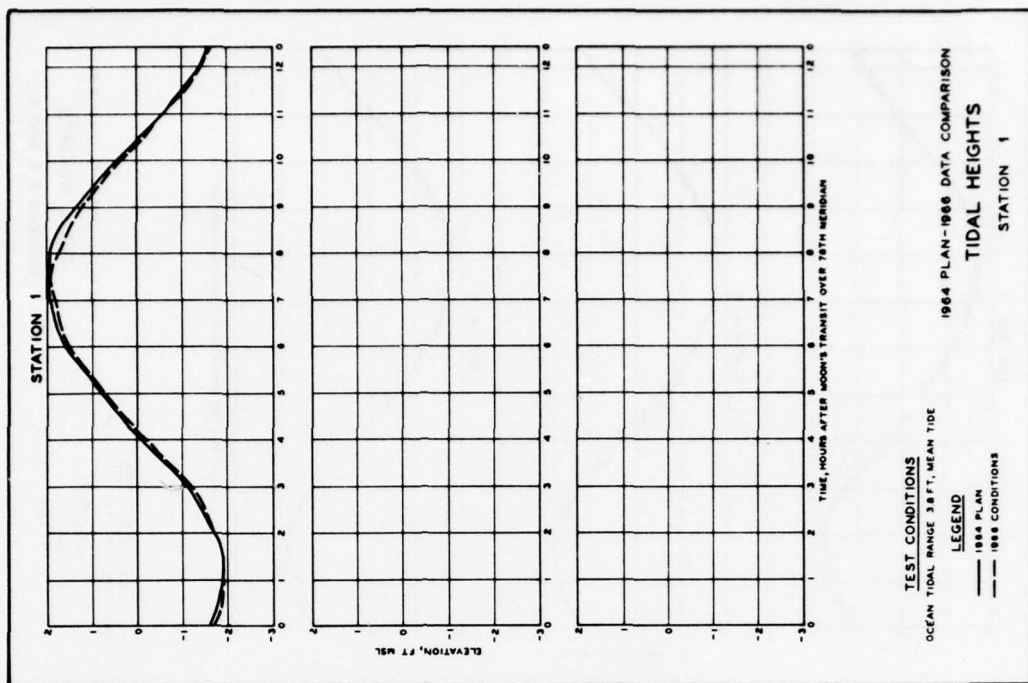


PLATE 287

PLATE 388

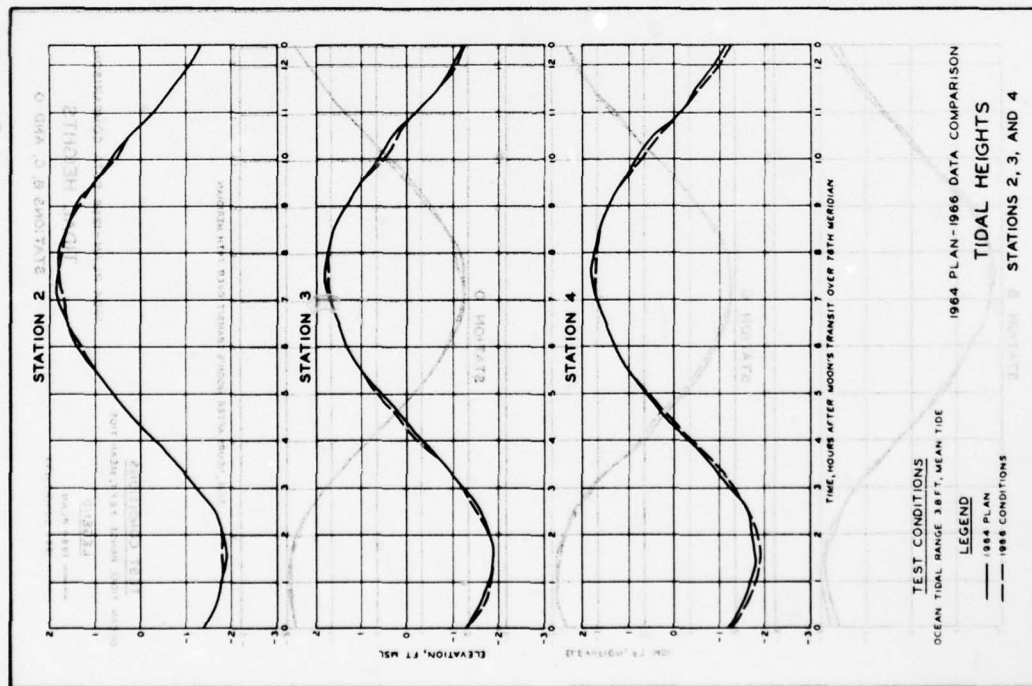


PLATE 288

PLATE 389

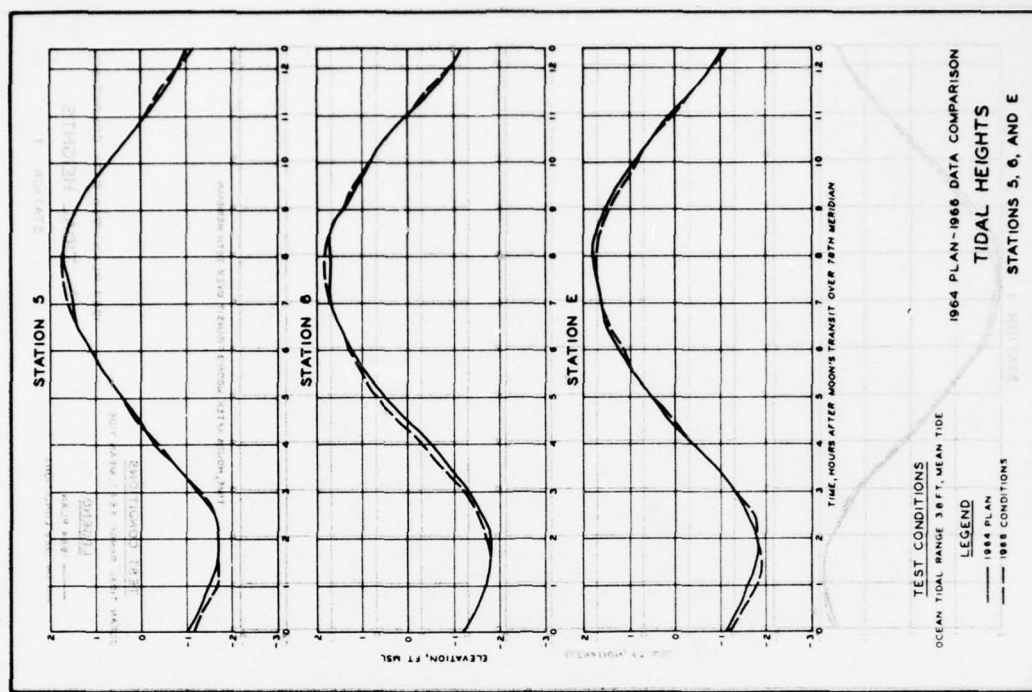


PLATE 289

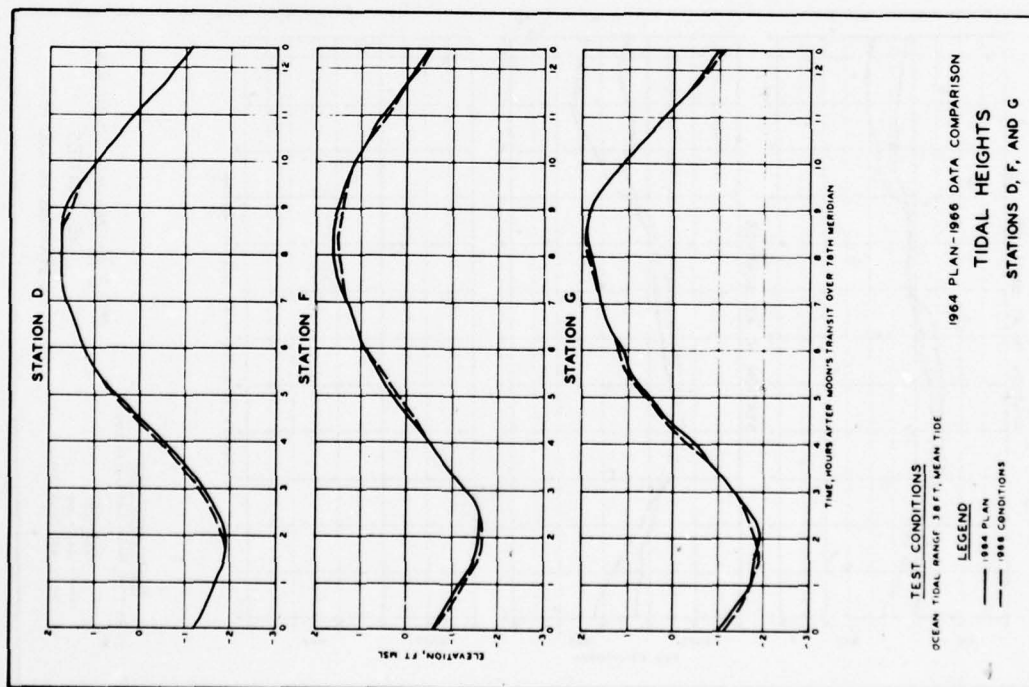


PLATE 290

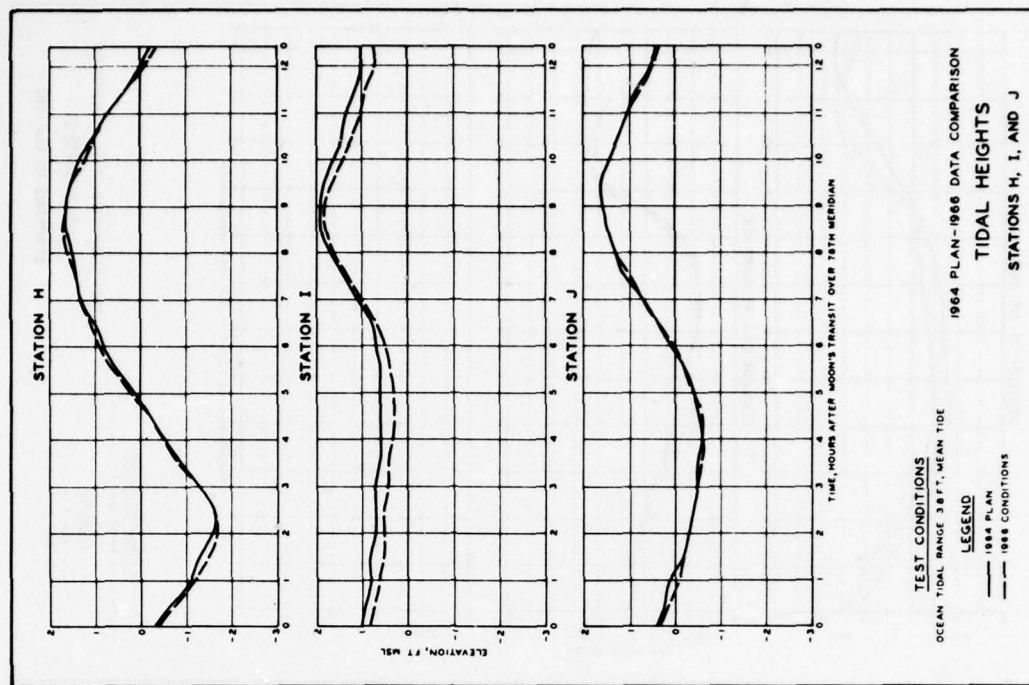


PLATE 291

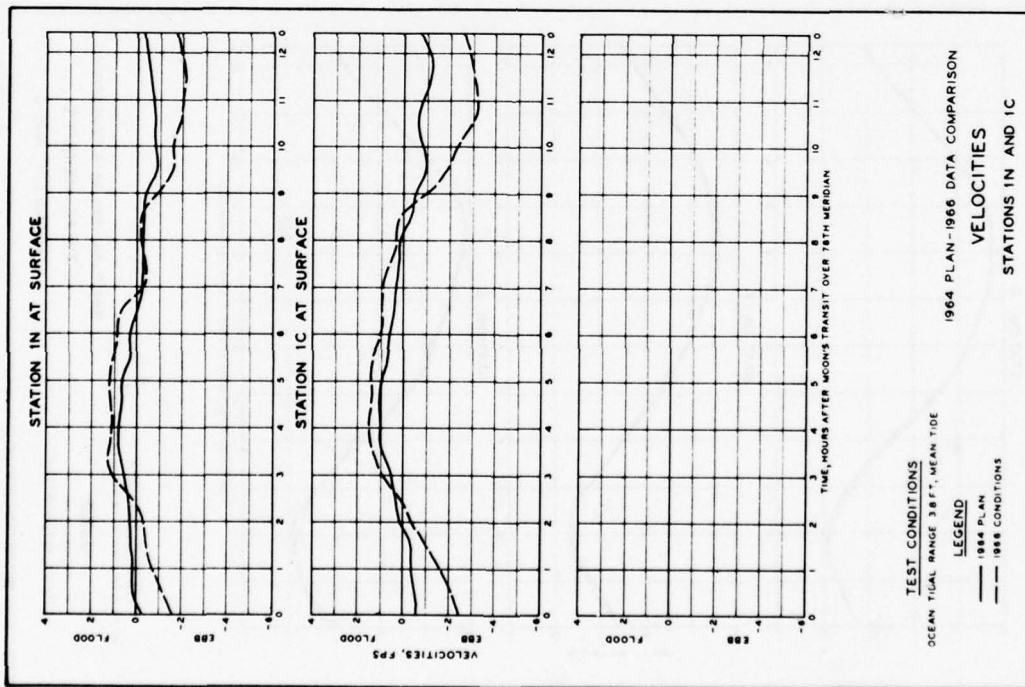


PLATE 292

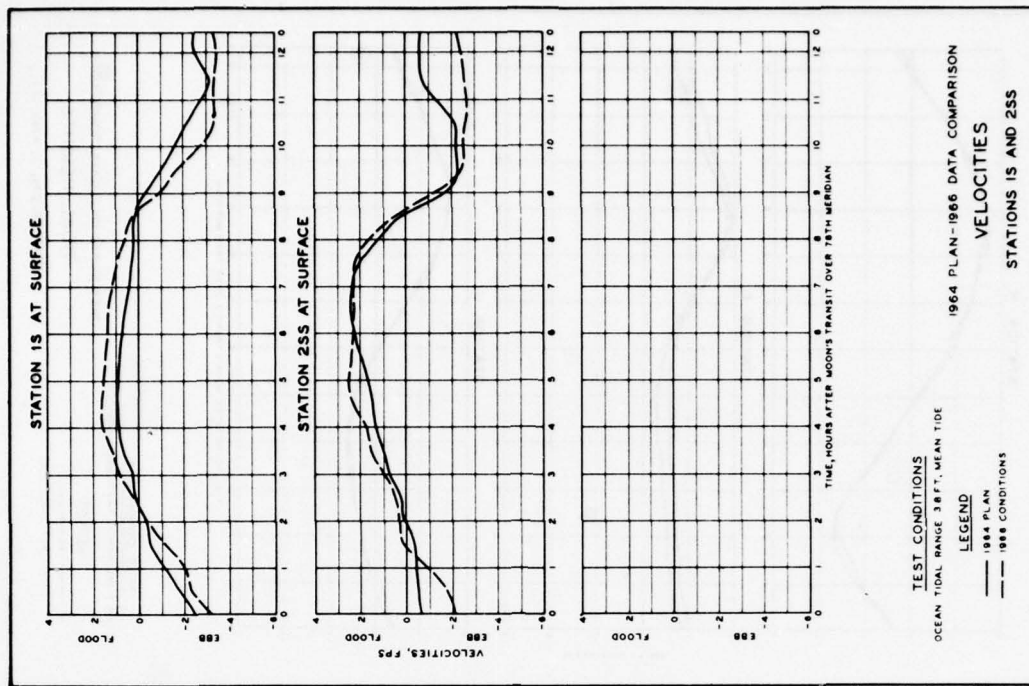


PLATE 293

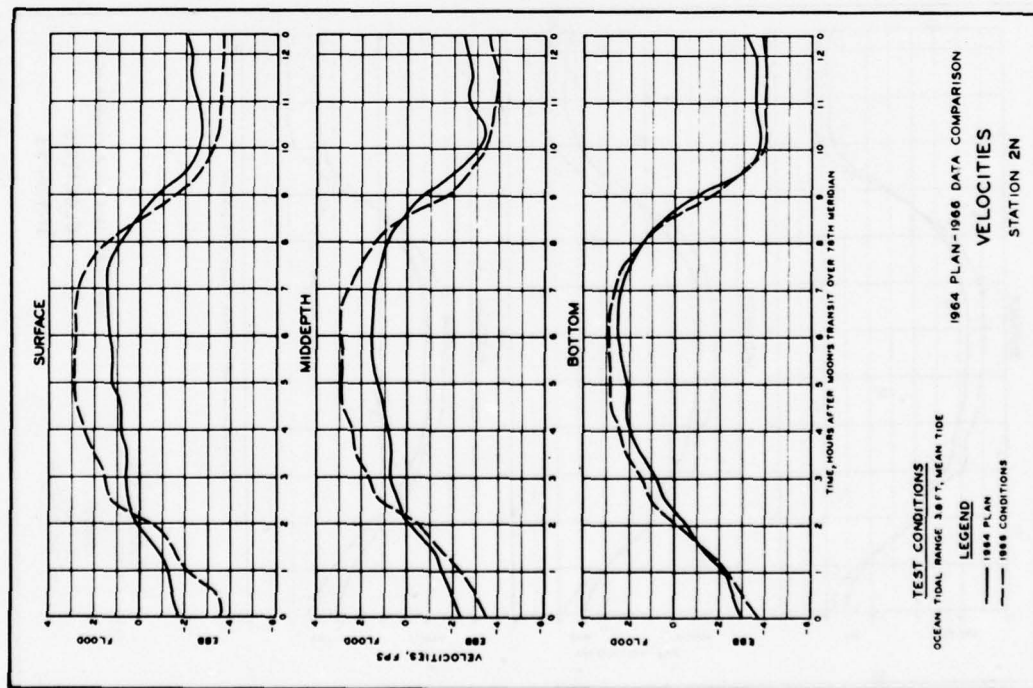


PLATE 294

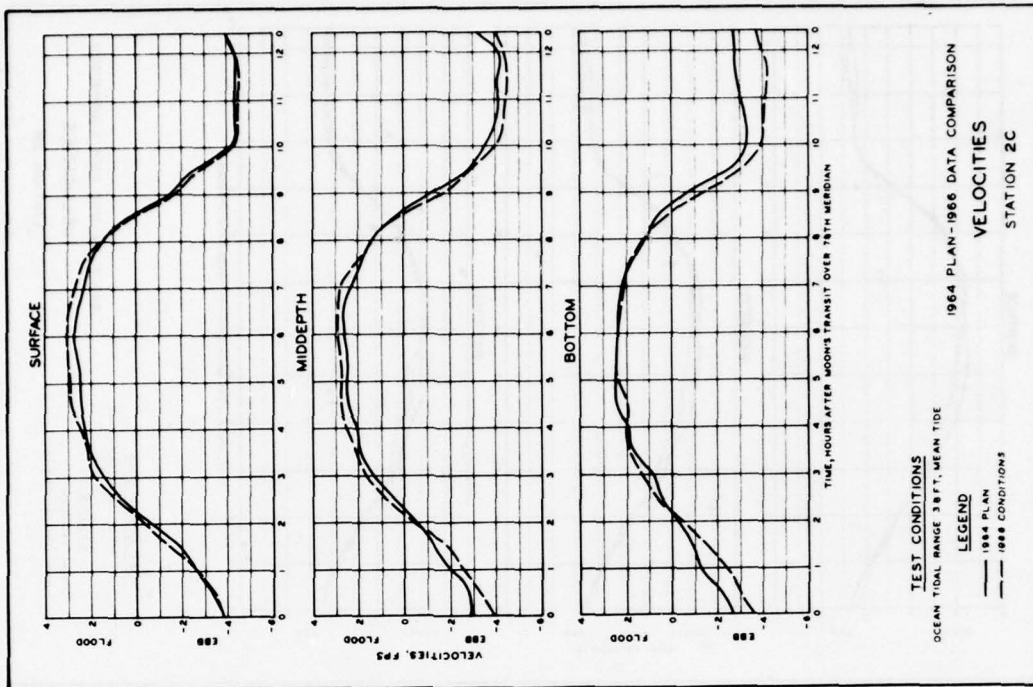


PLATE 295

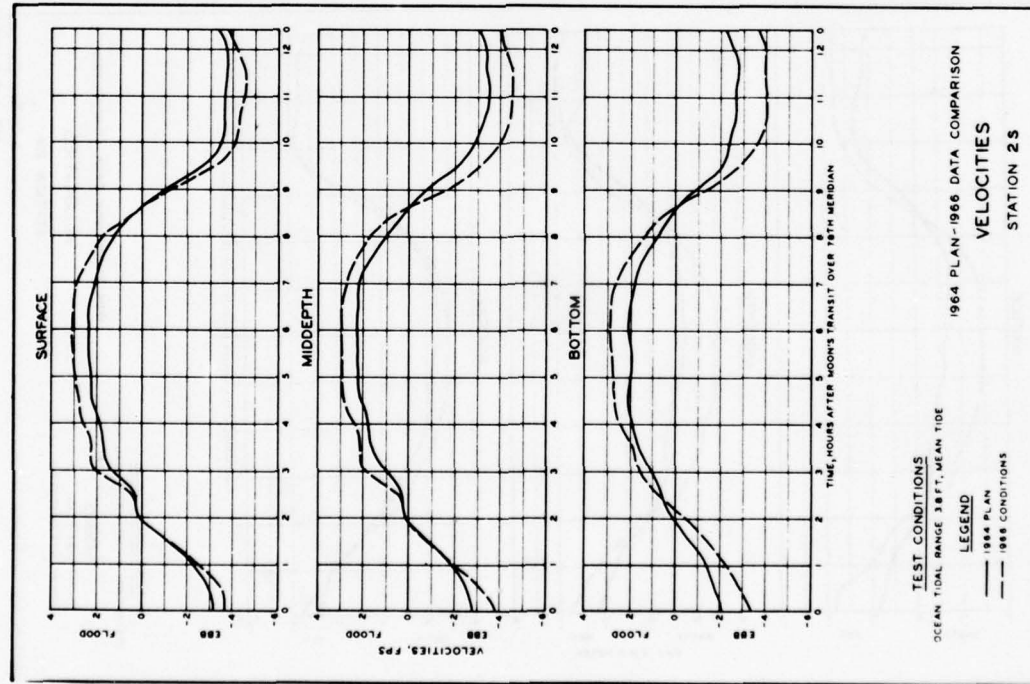


PLATE 296

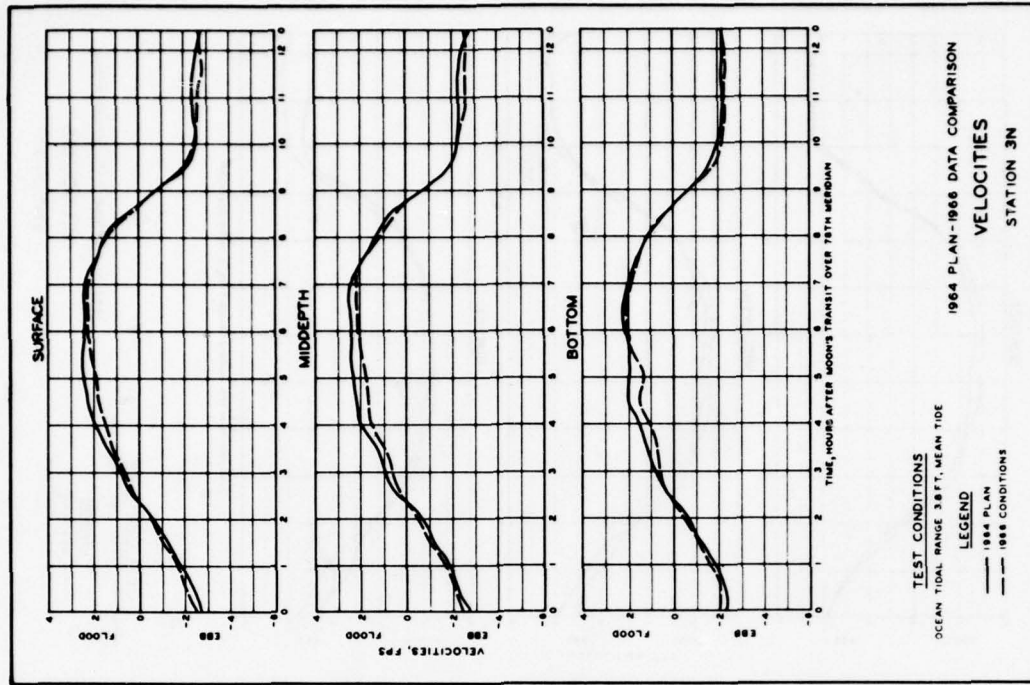


PLATE 297

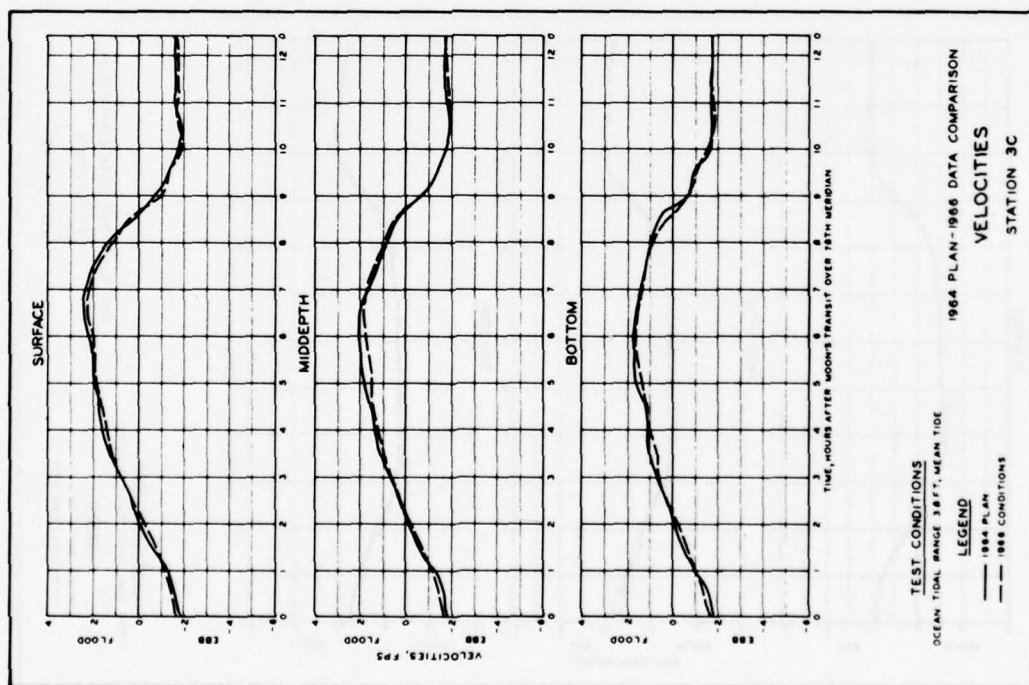


PLATE 298

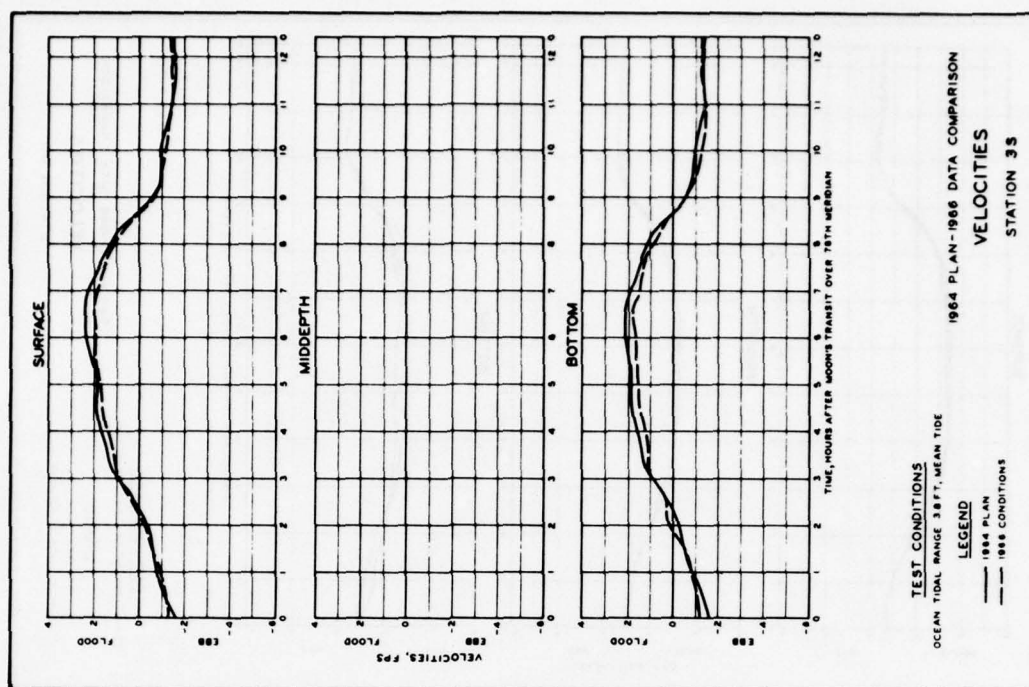


PLATE 299

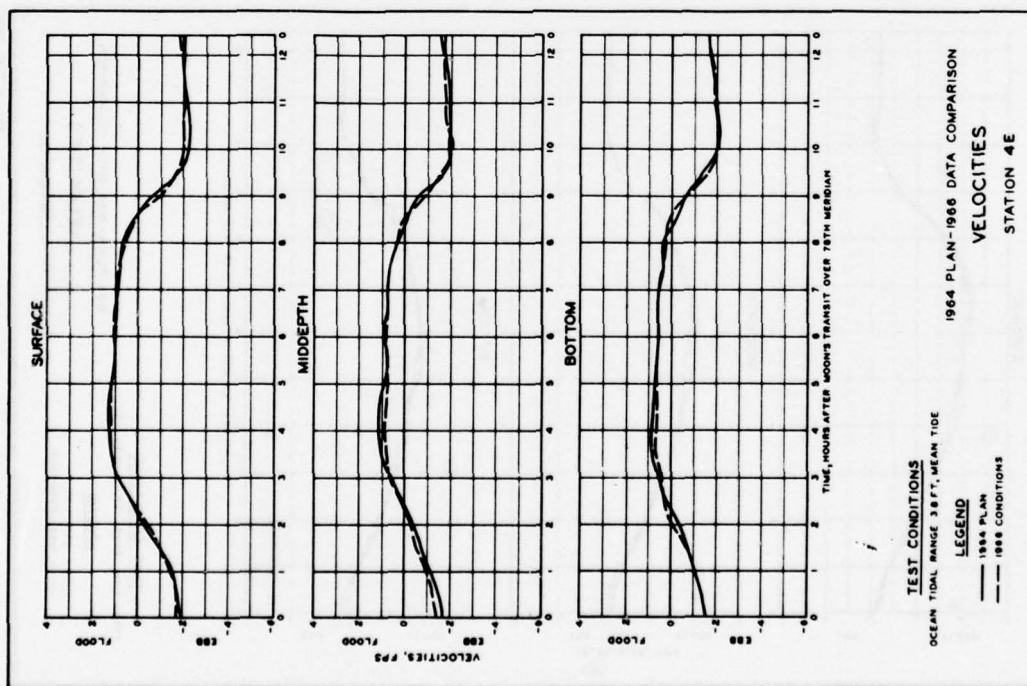


PLATE 300

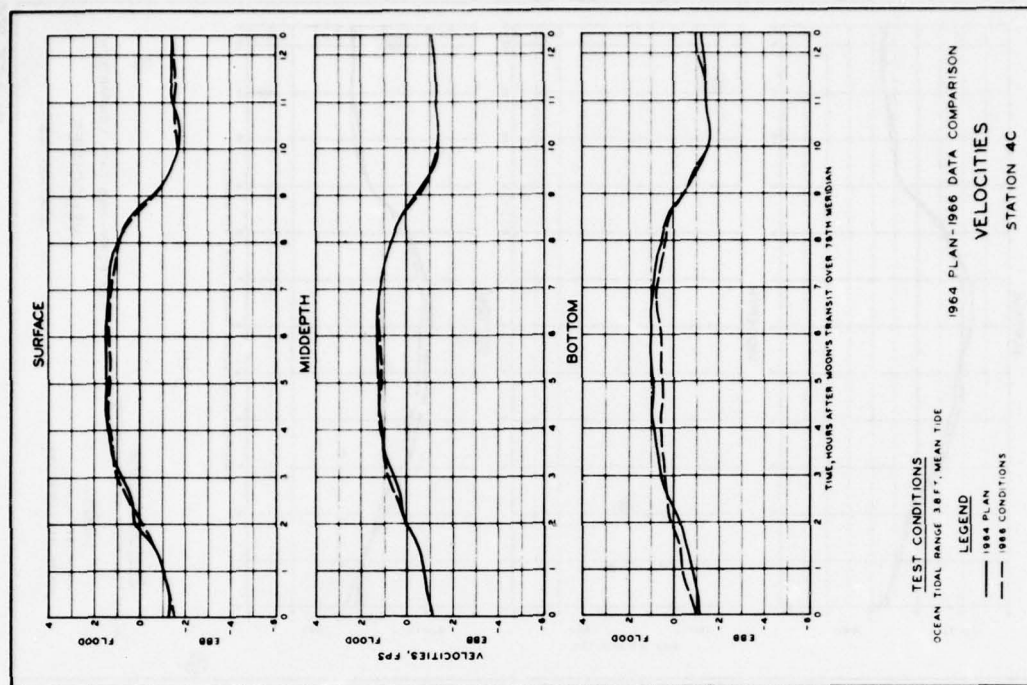


PLATE 301

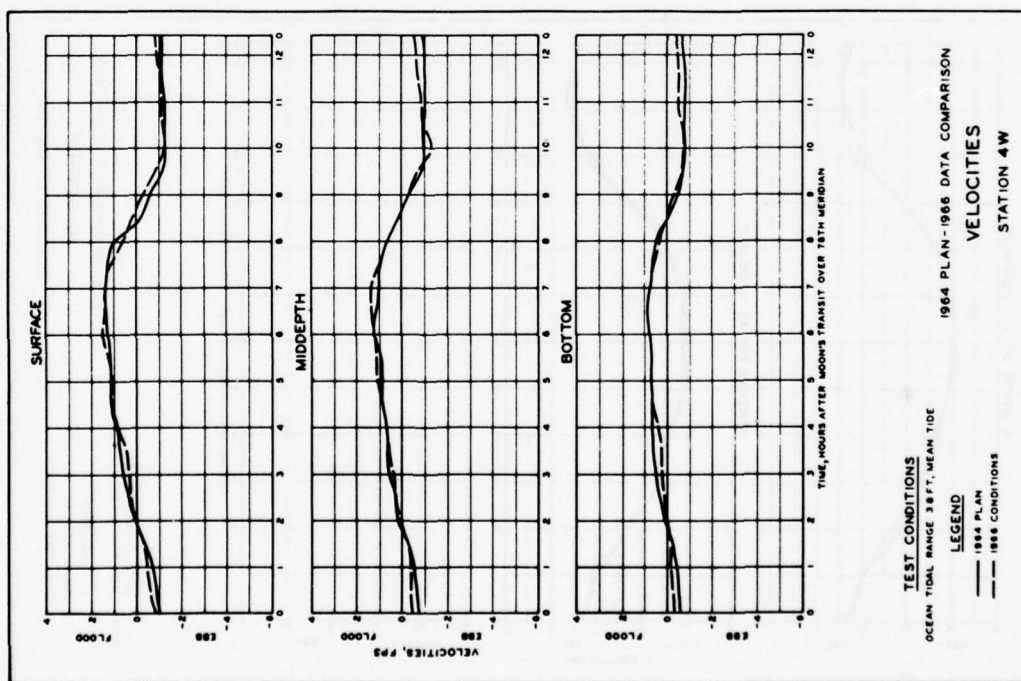


PLATE 302

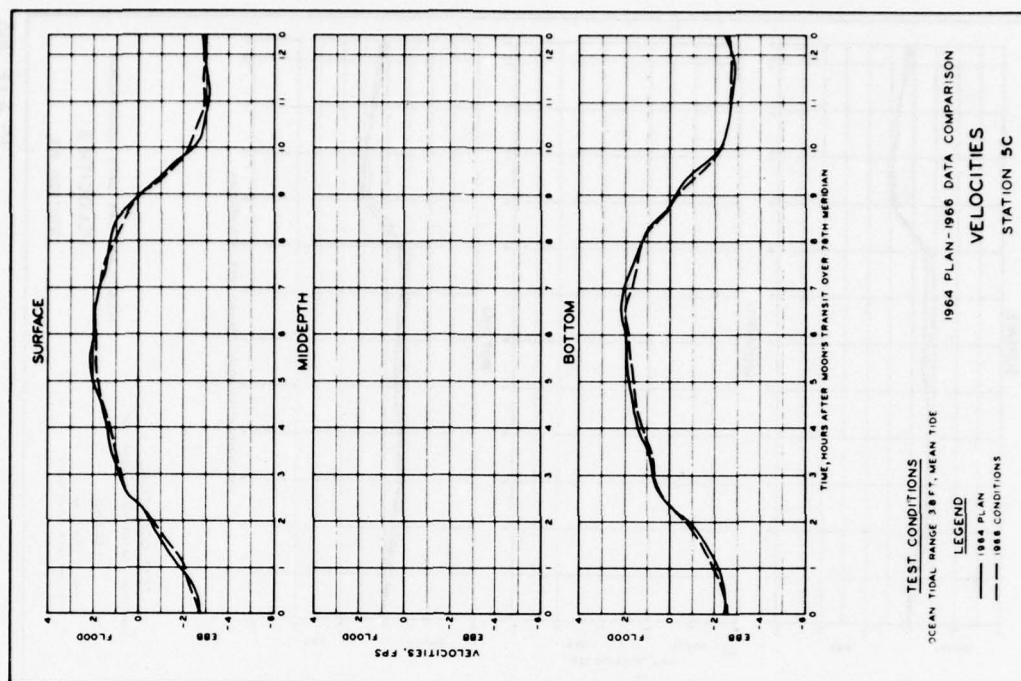


PLATE 303

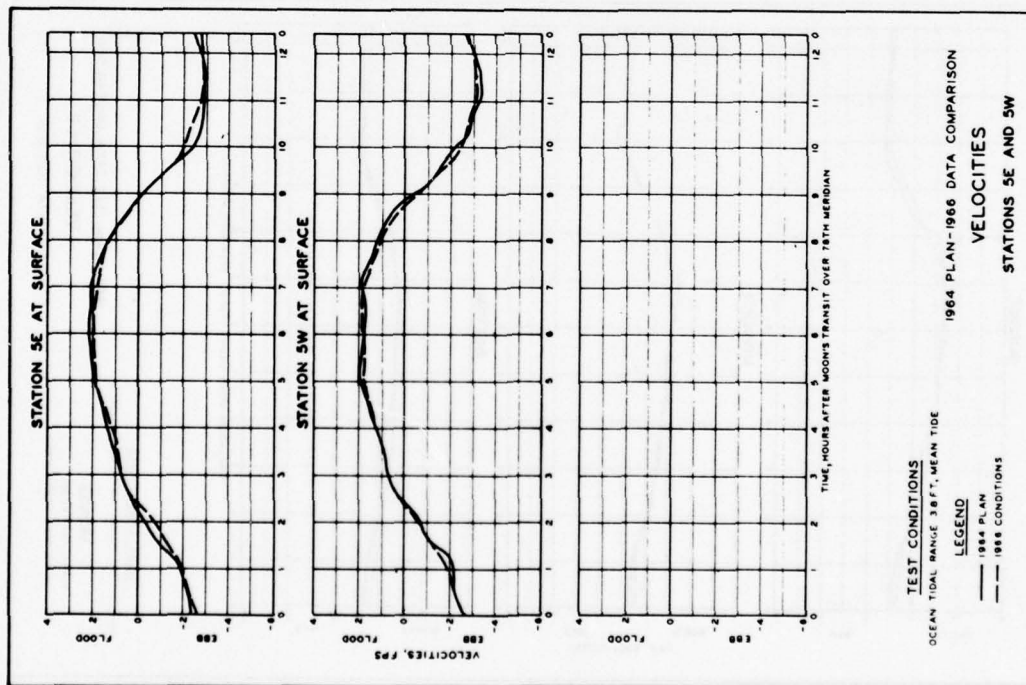


PLATE 304

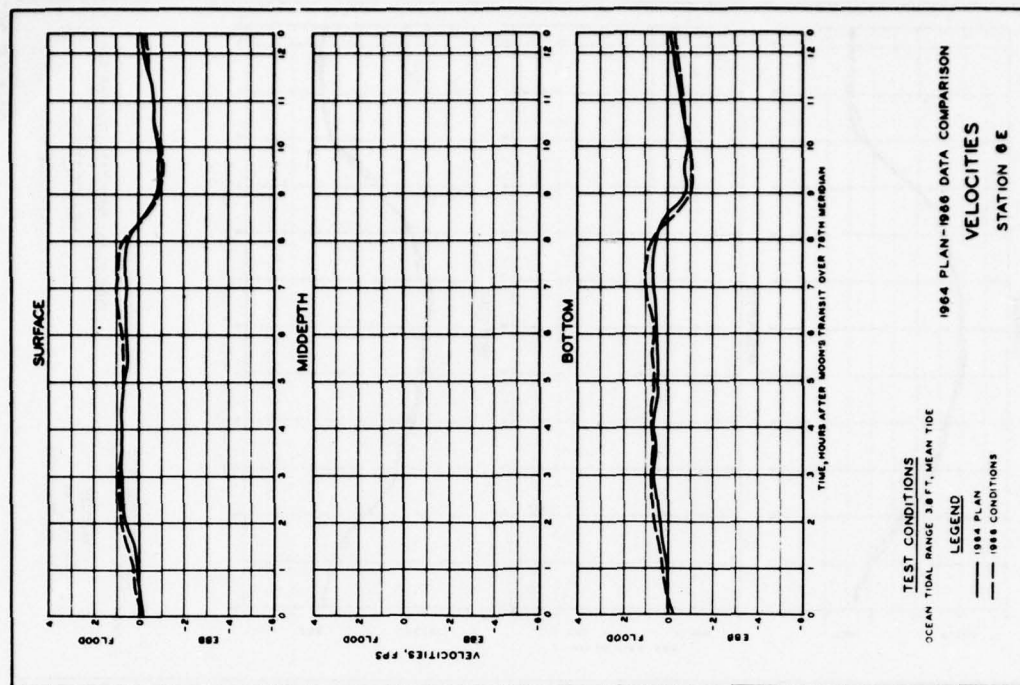


PLATE 305

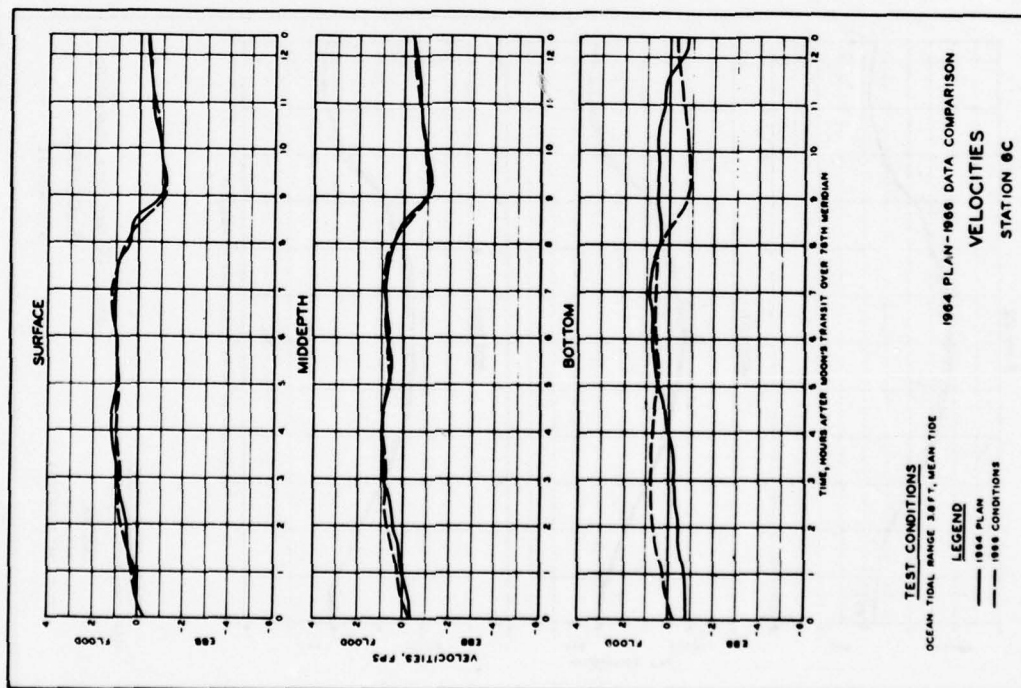


PLATE 306

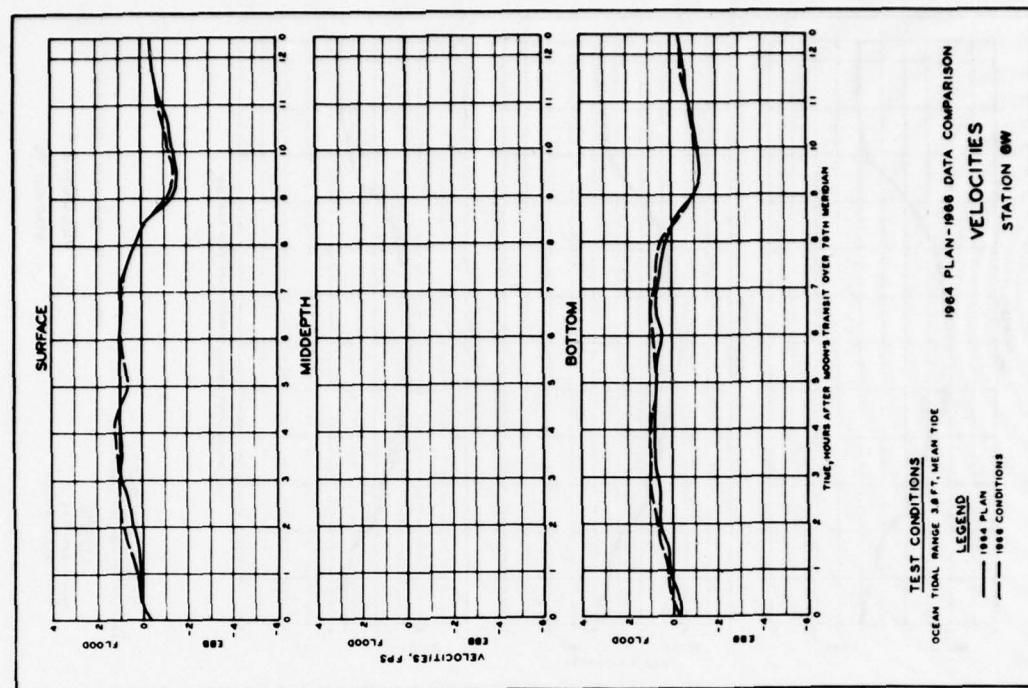


PLATE 307

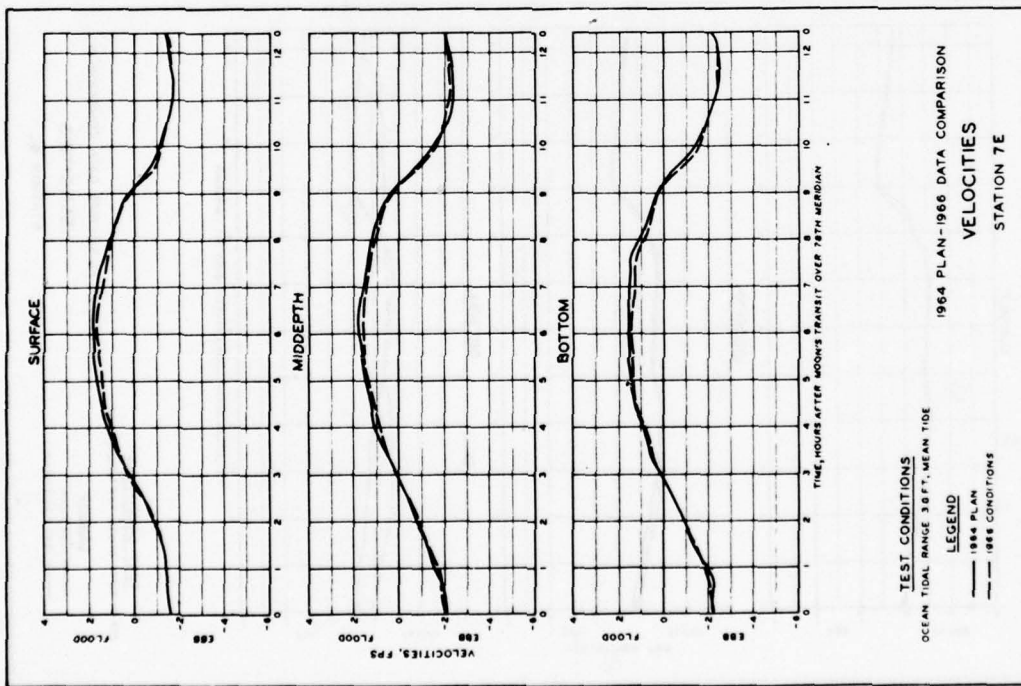


PLATE 308

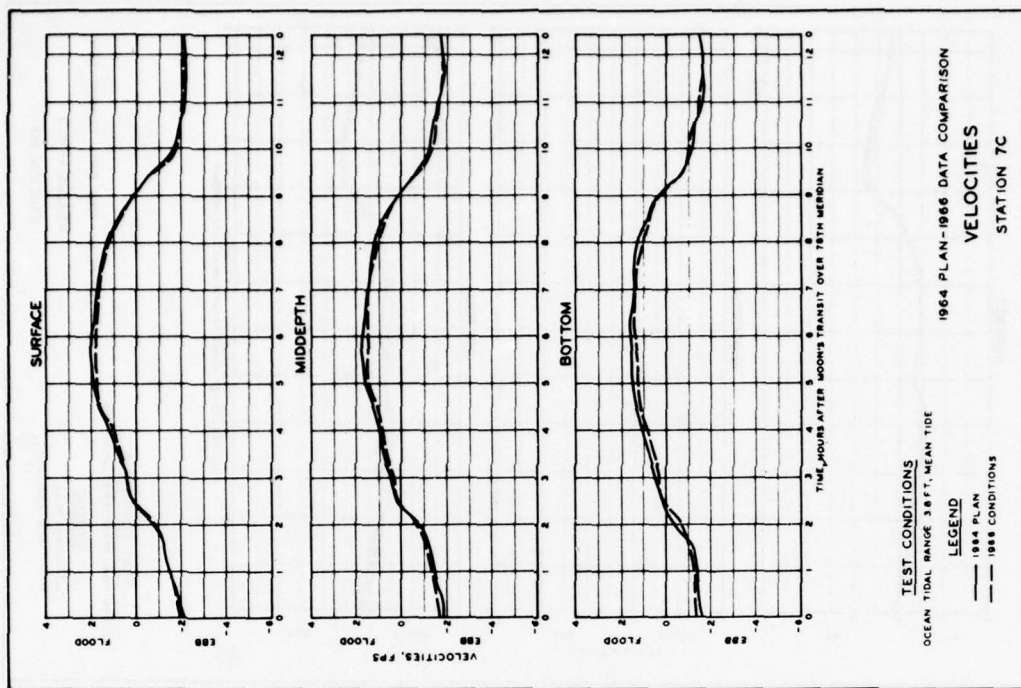


PLATE 309

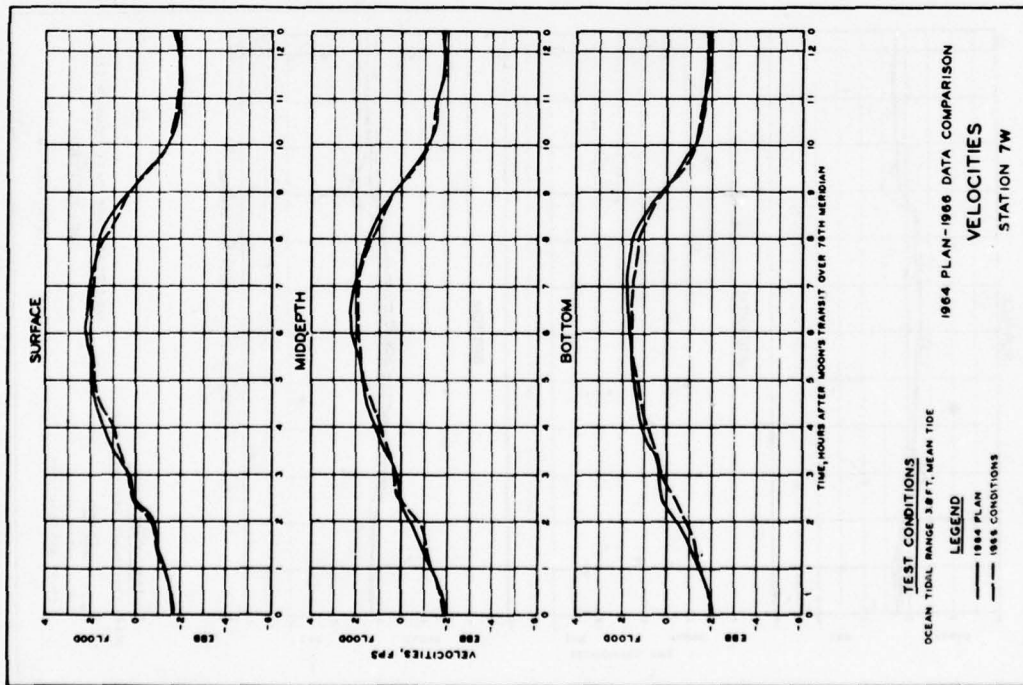


PLATE 310

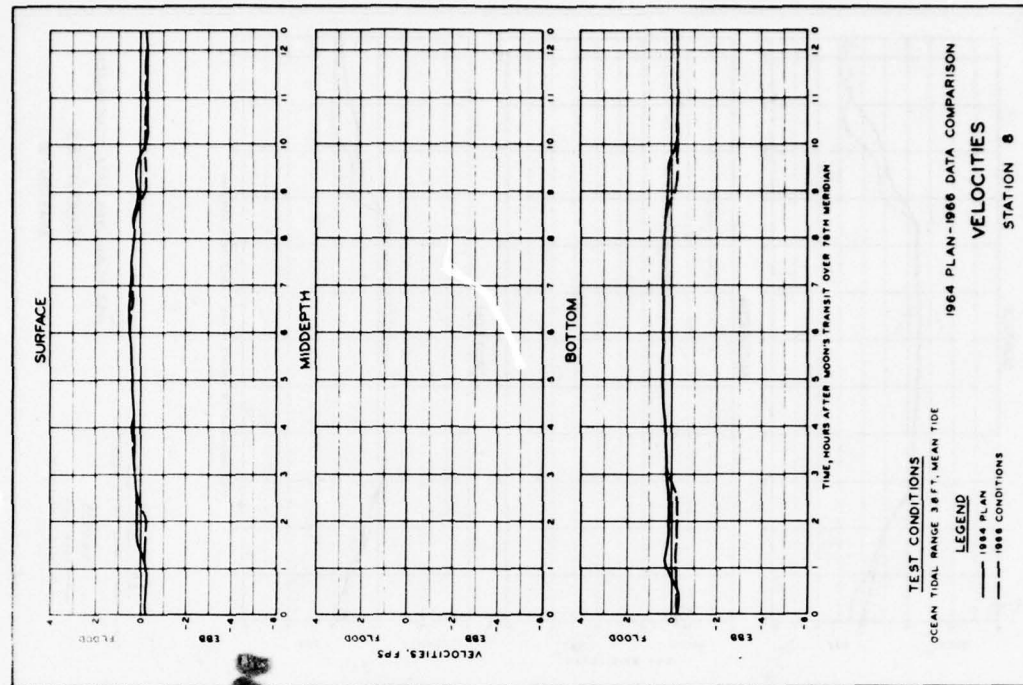


PLATE 311

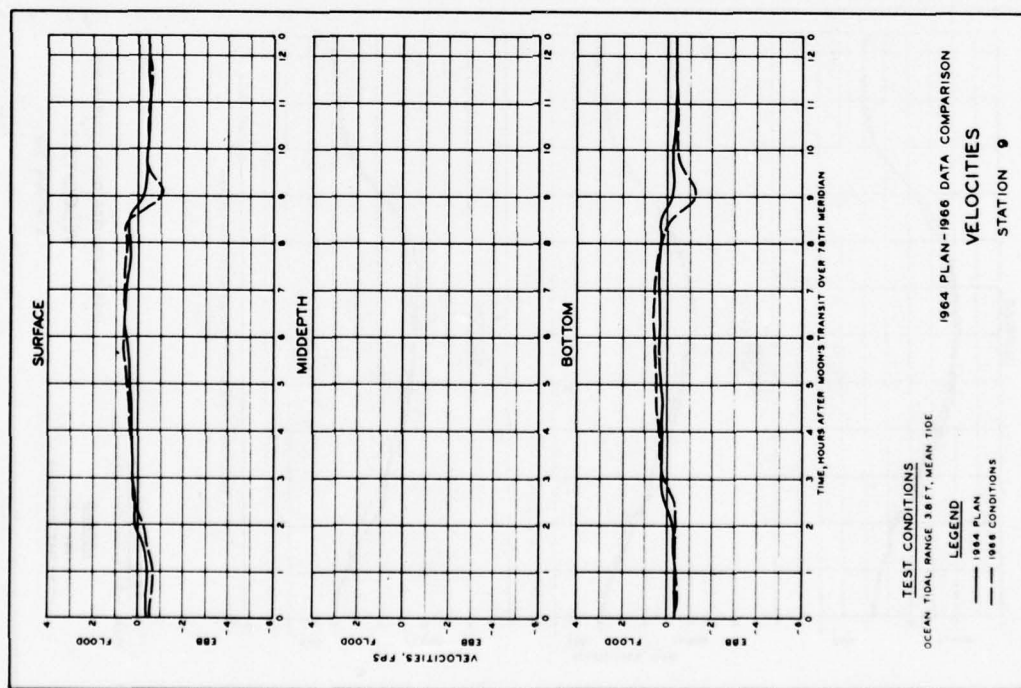


PLATE 312

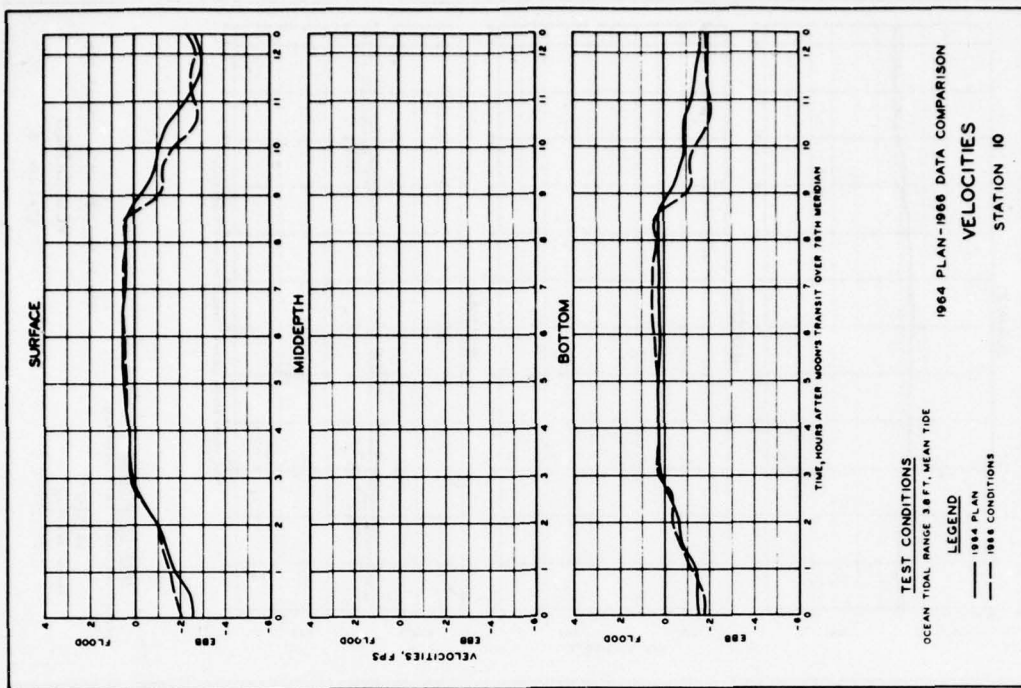


PLATE 313

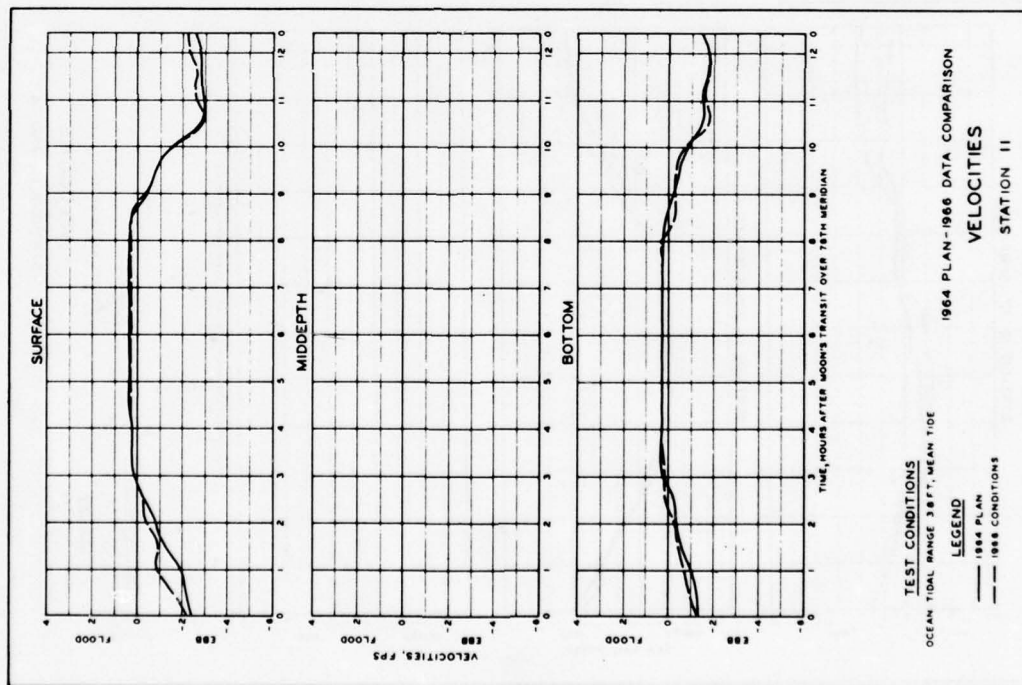


PLATE 314

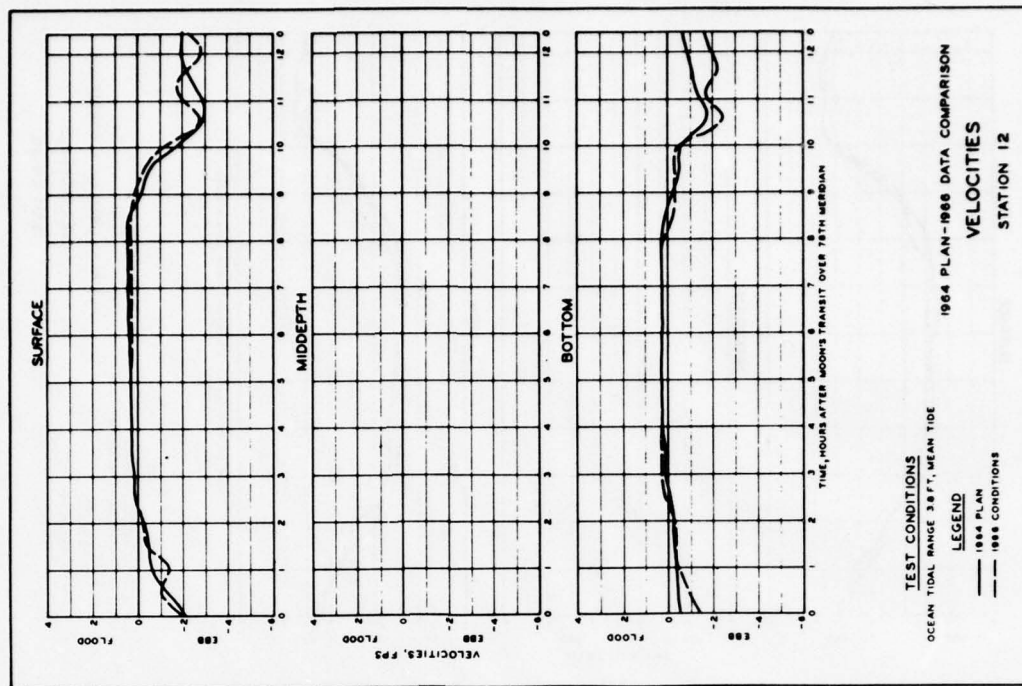


PLATE 315

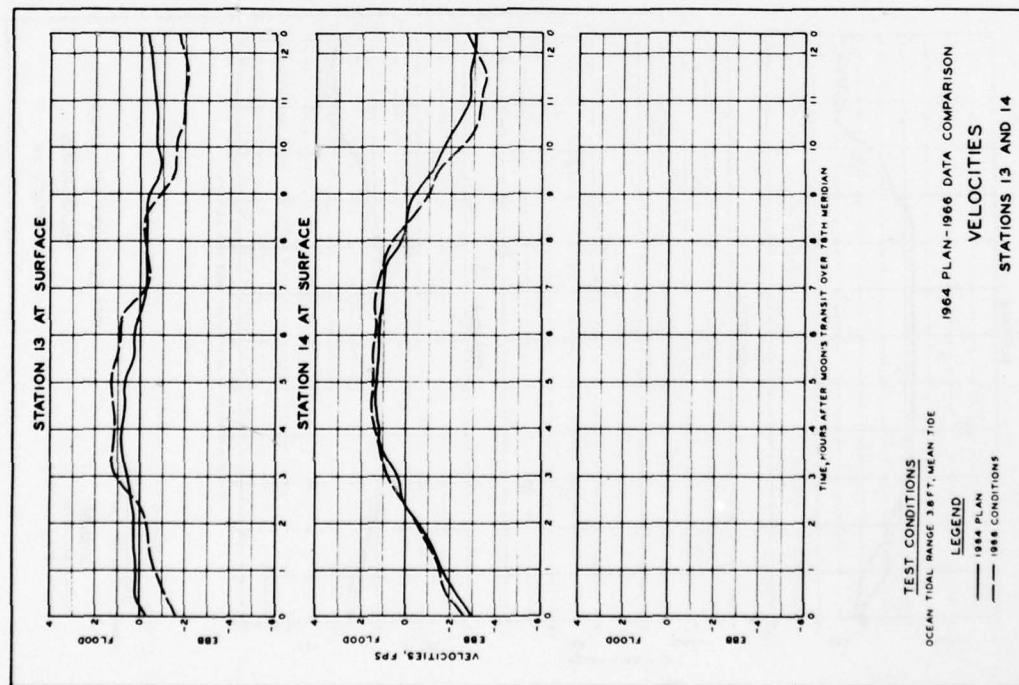


PLATE 316

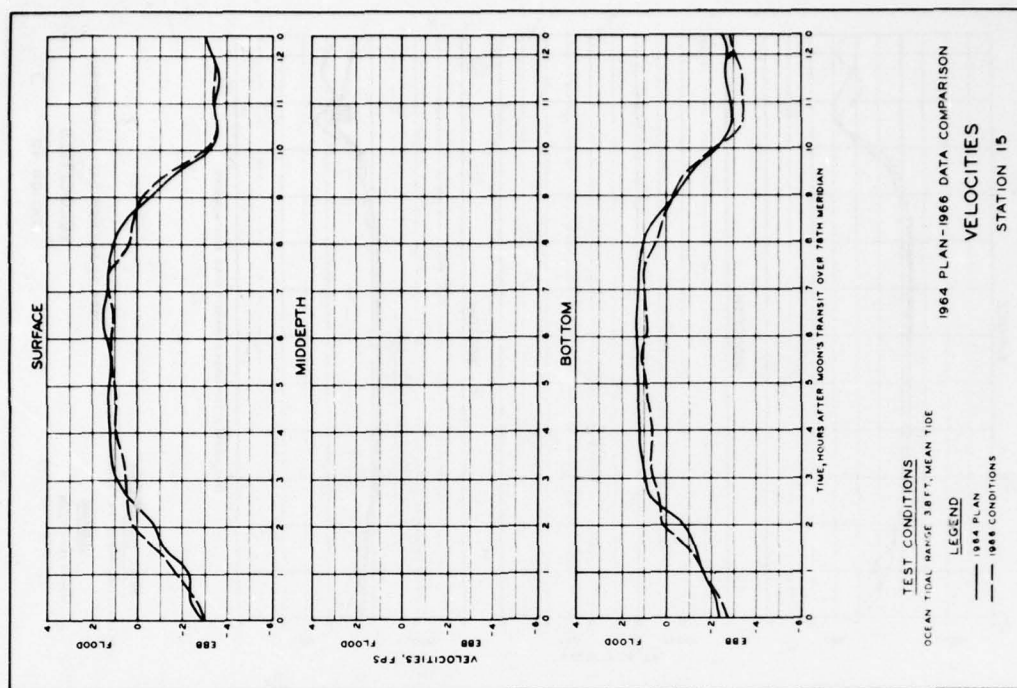


PLATE 317

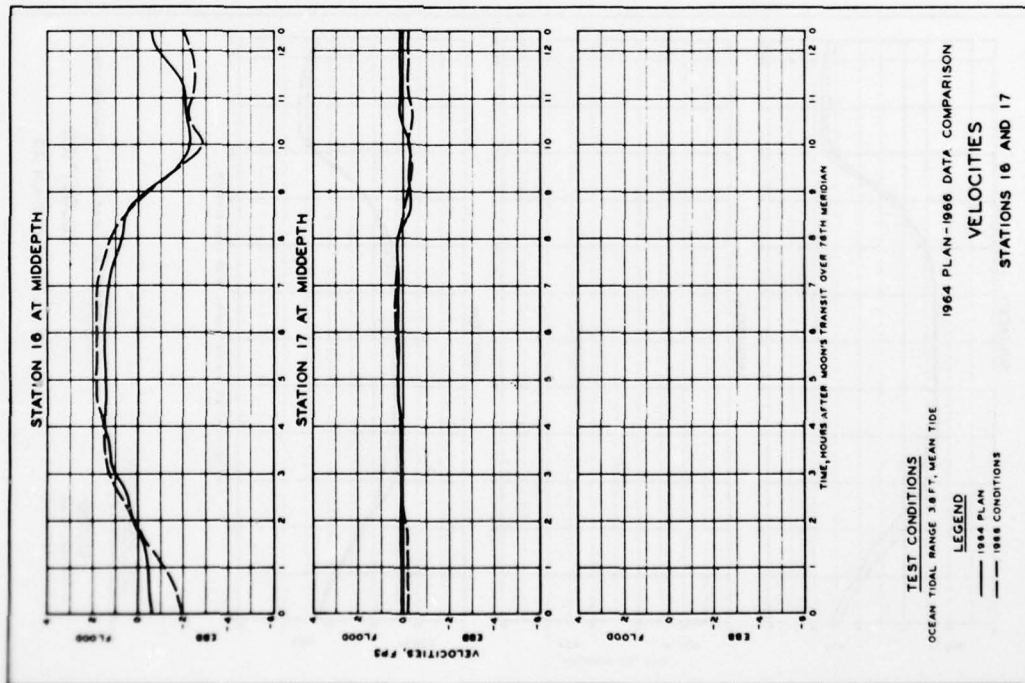


PLATE 318

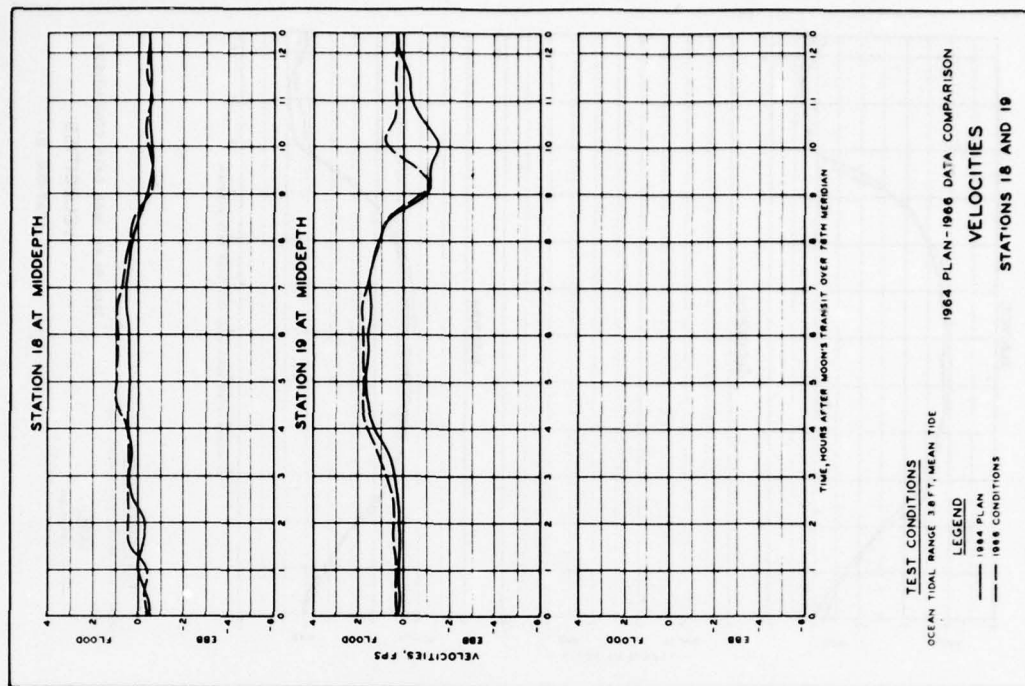


PLATE 319

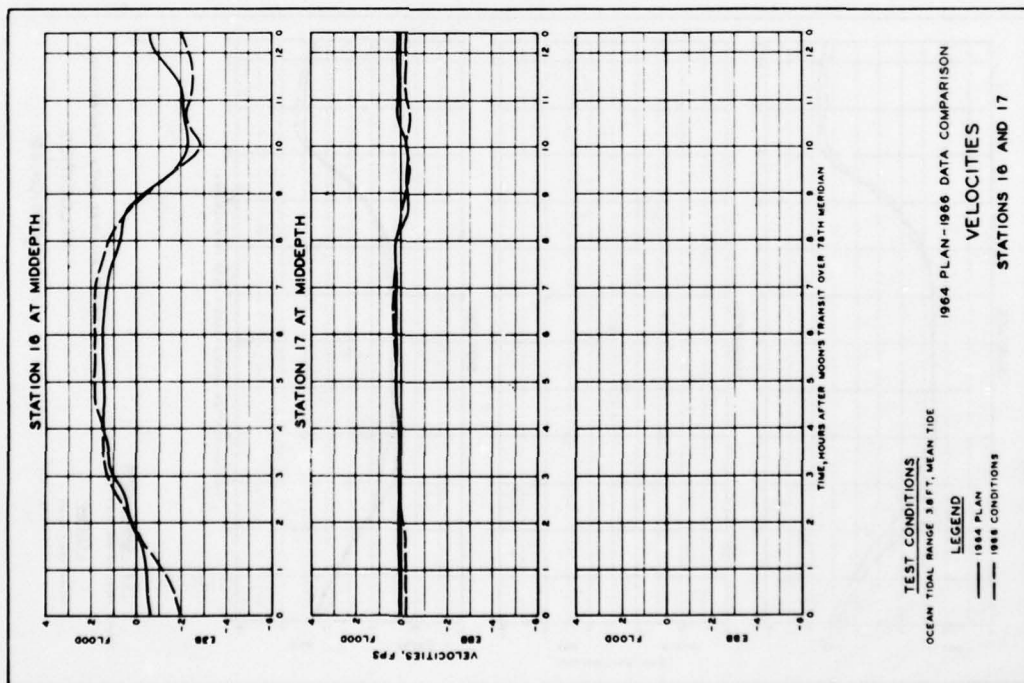


PLATE 318

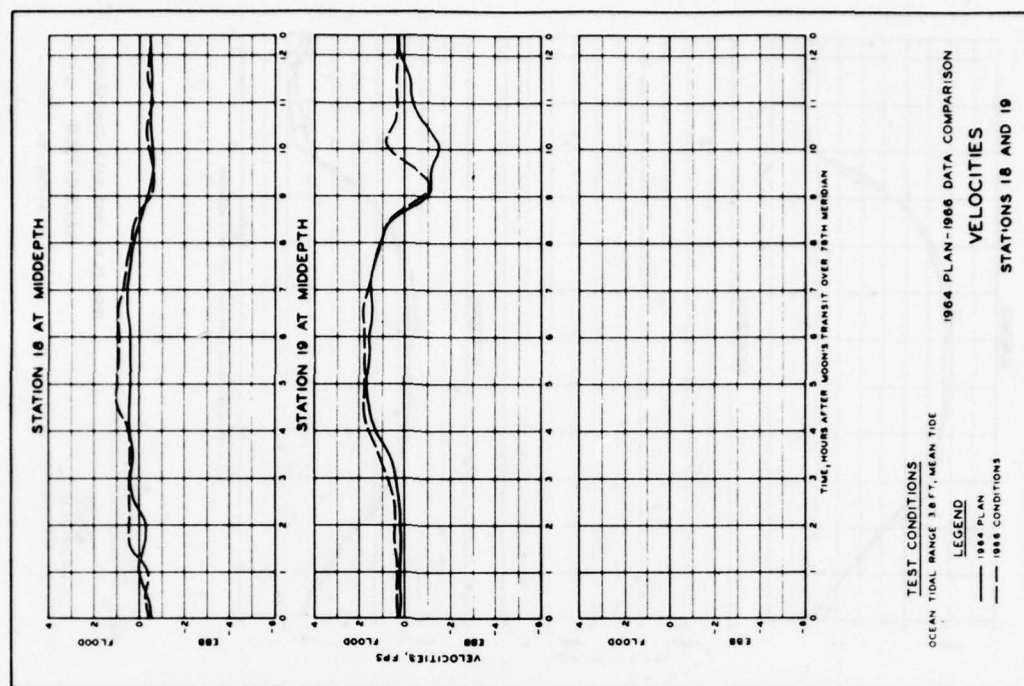


PLATE 319

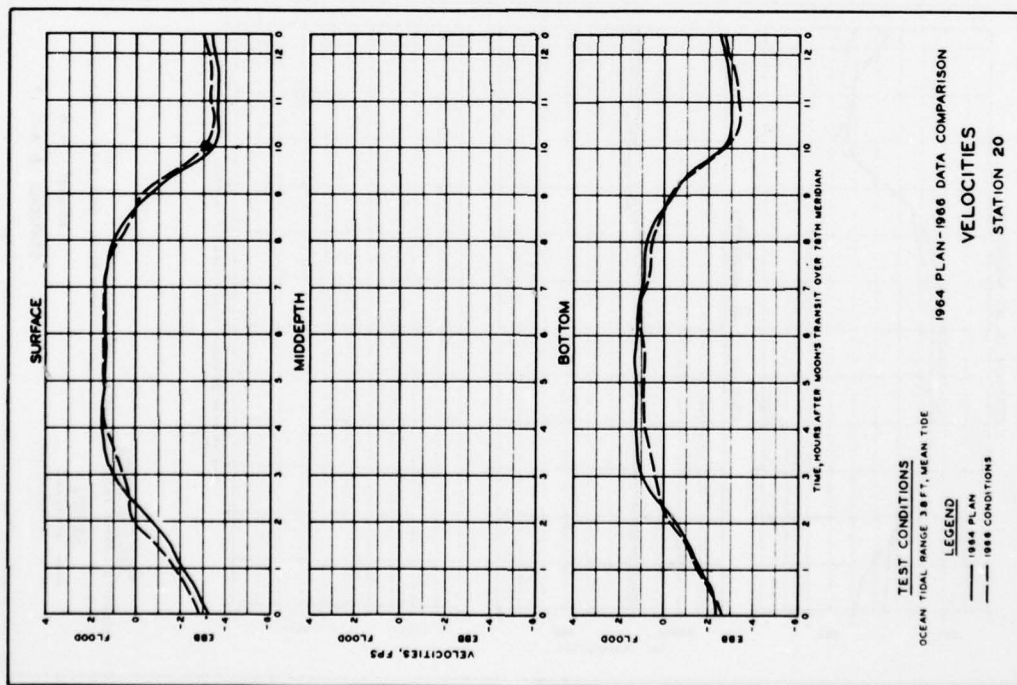


PLATE 320

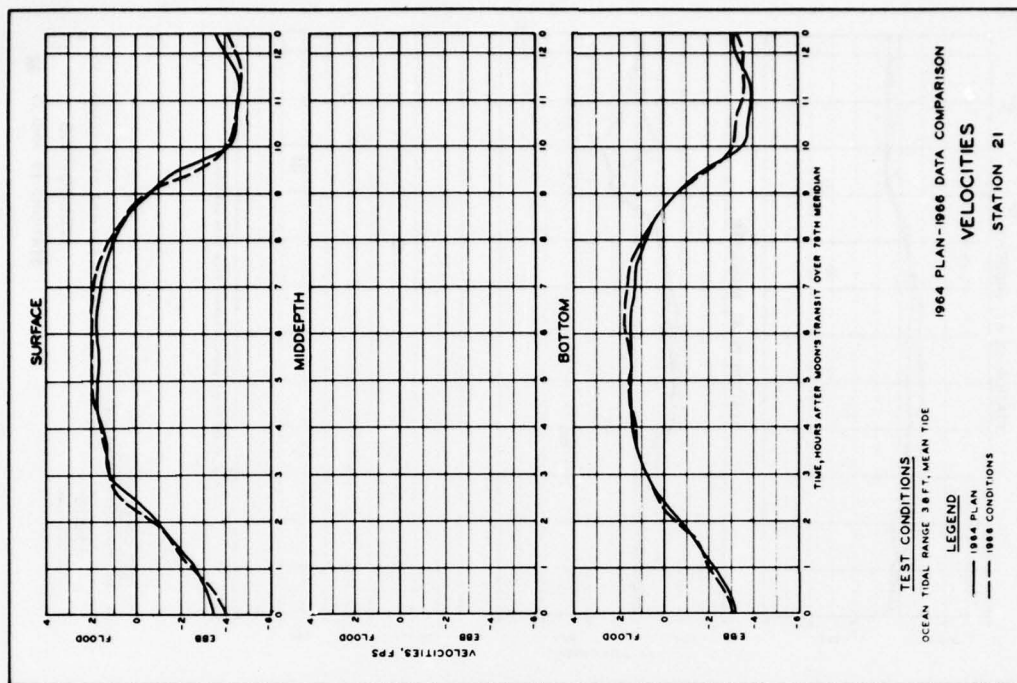


PLATE 321

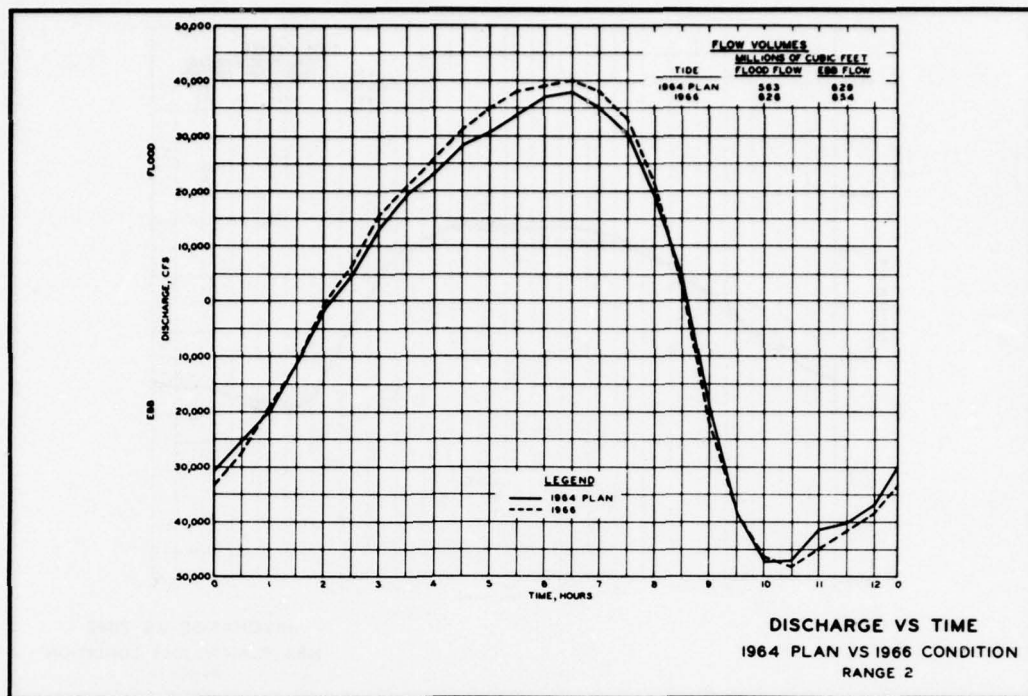


PLATE 322

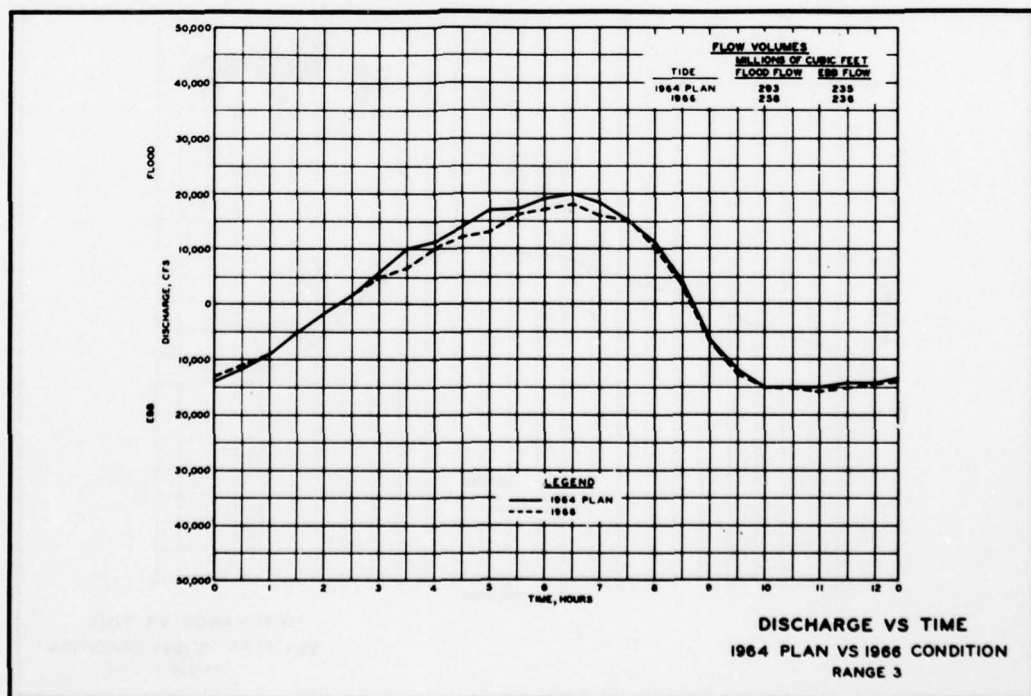


PLATE 323

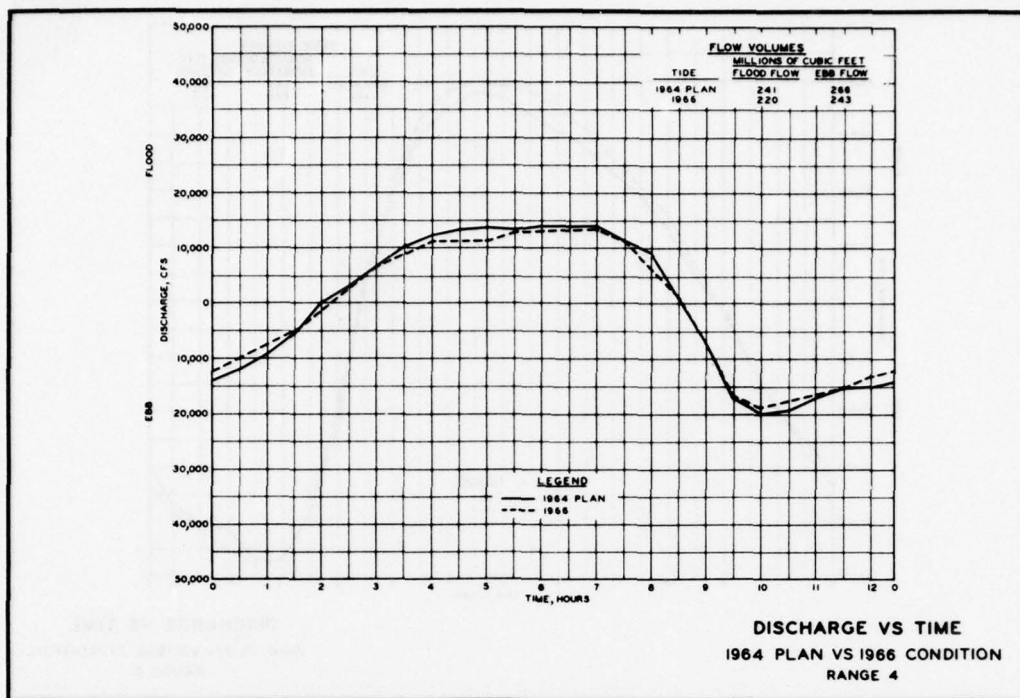


PLATE 324

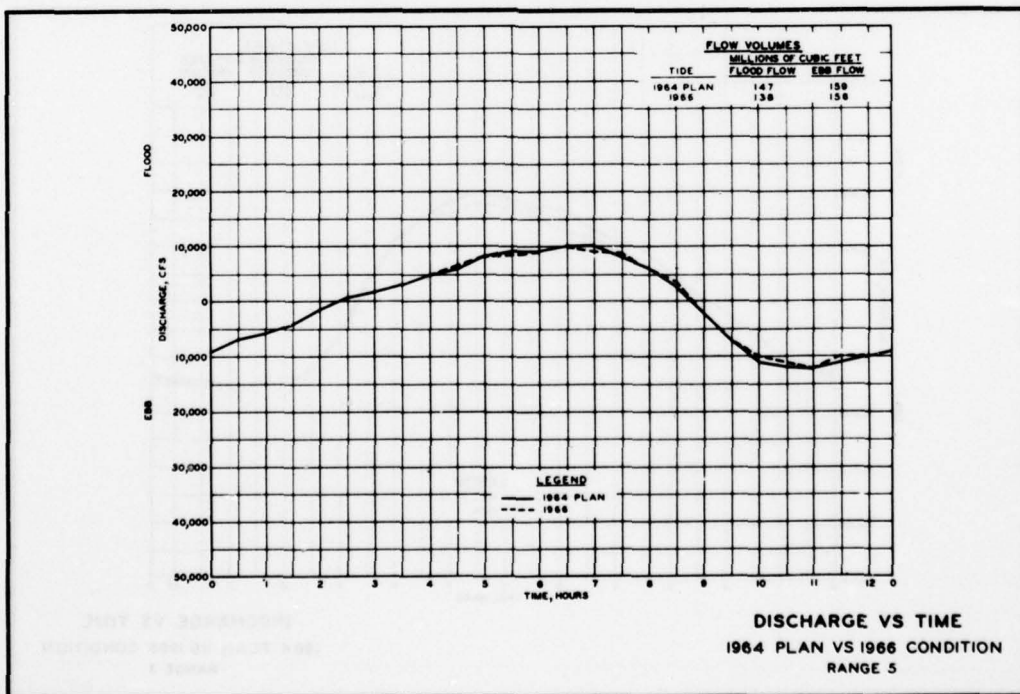


PLATE 325

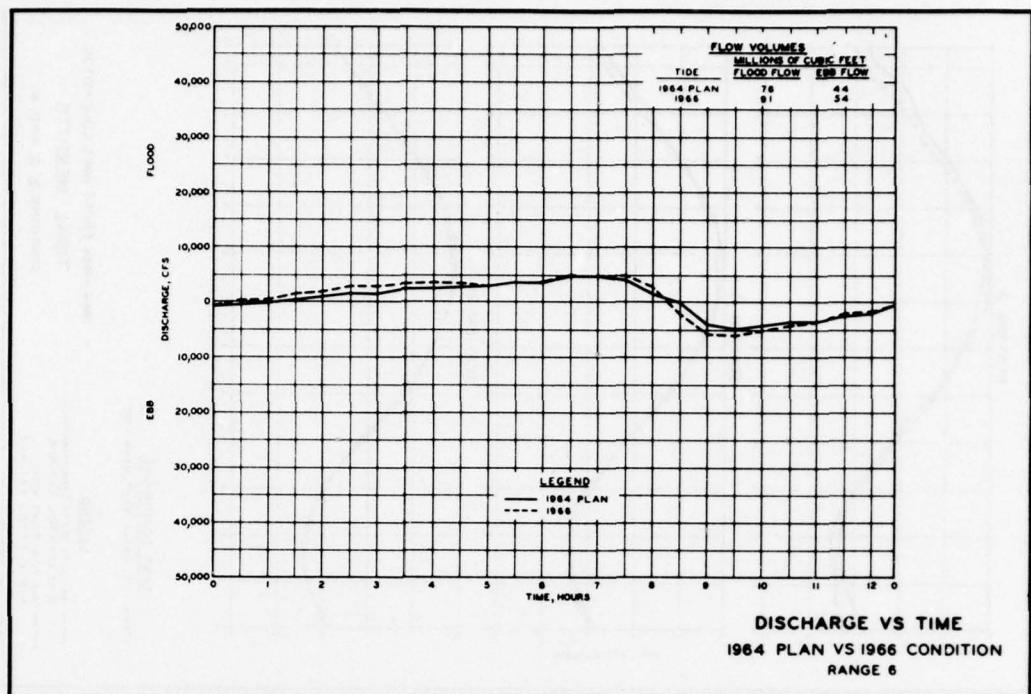


PLATE 326

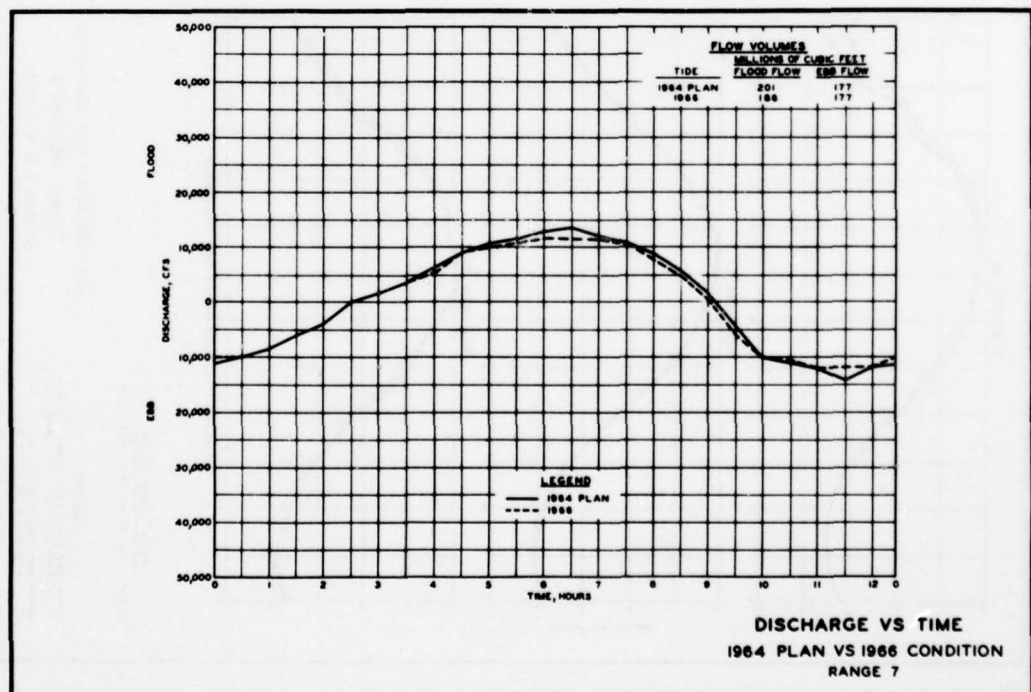


PLATE 327

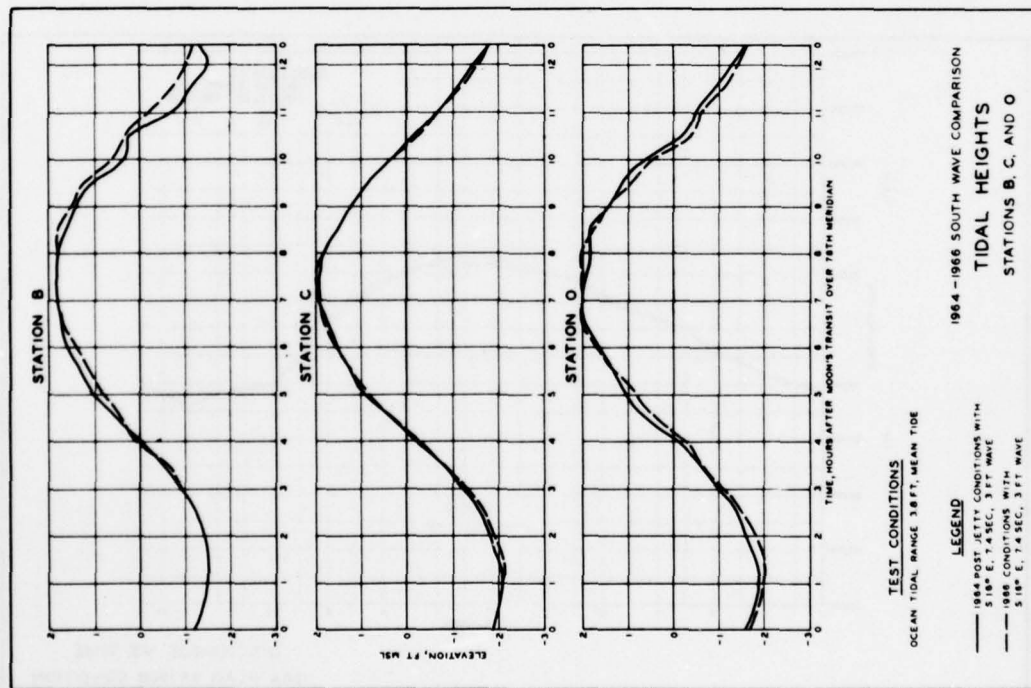


PLATE 328

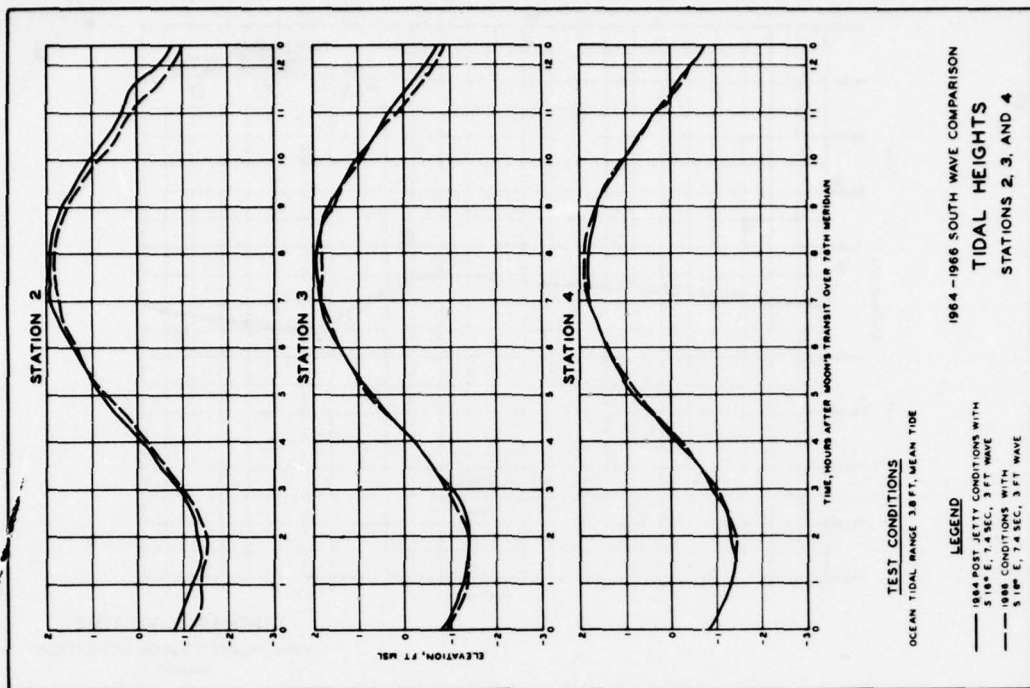


PLATE 329

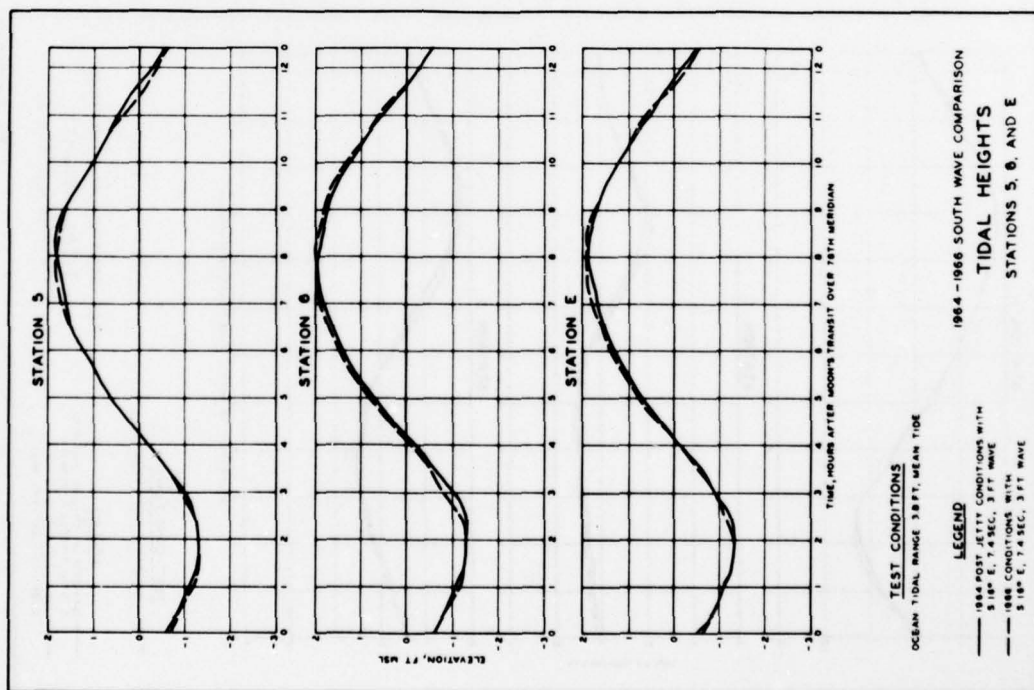


PLATE 330

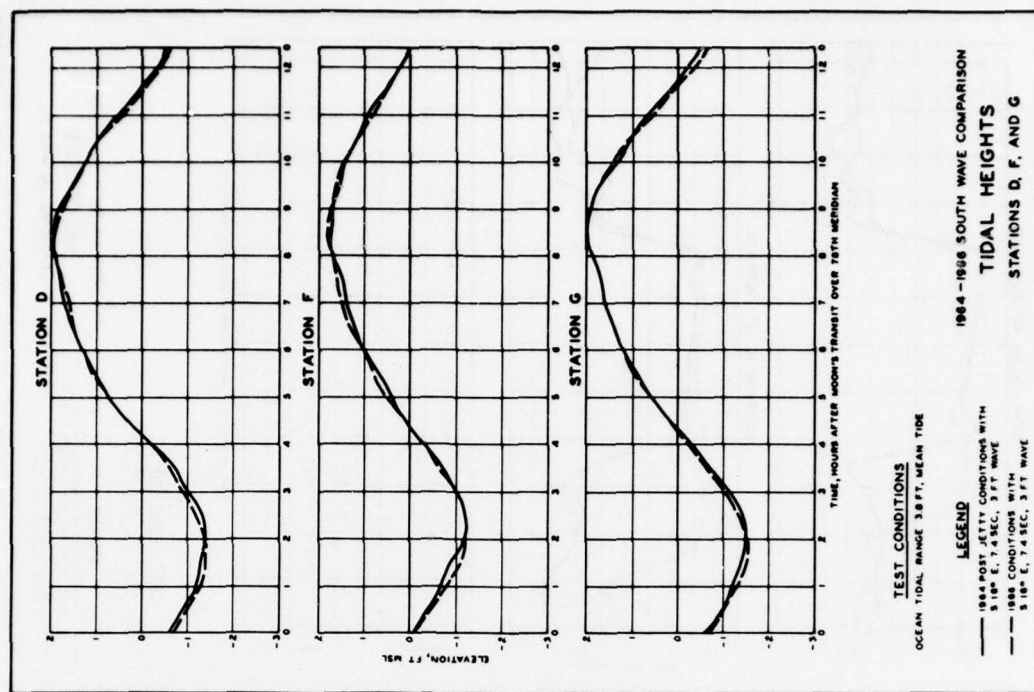


PLATE 331

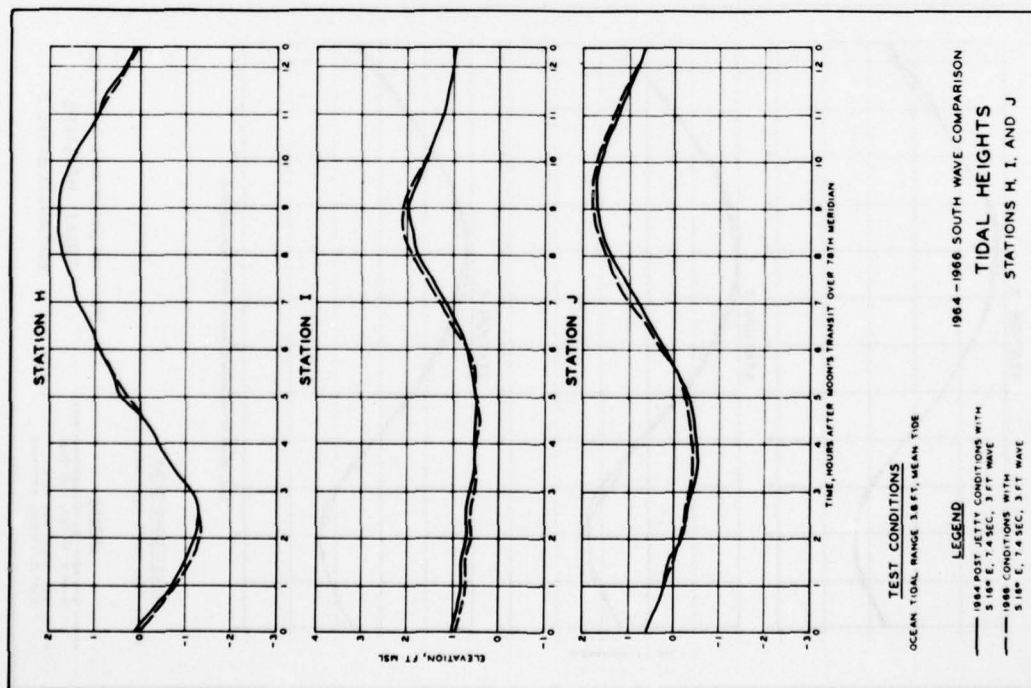


PLATE 332

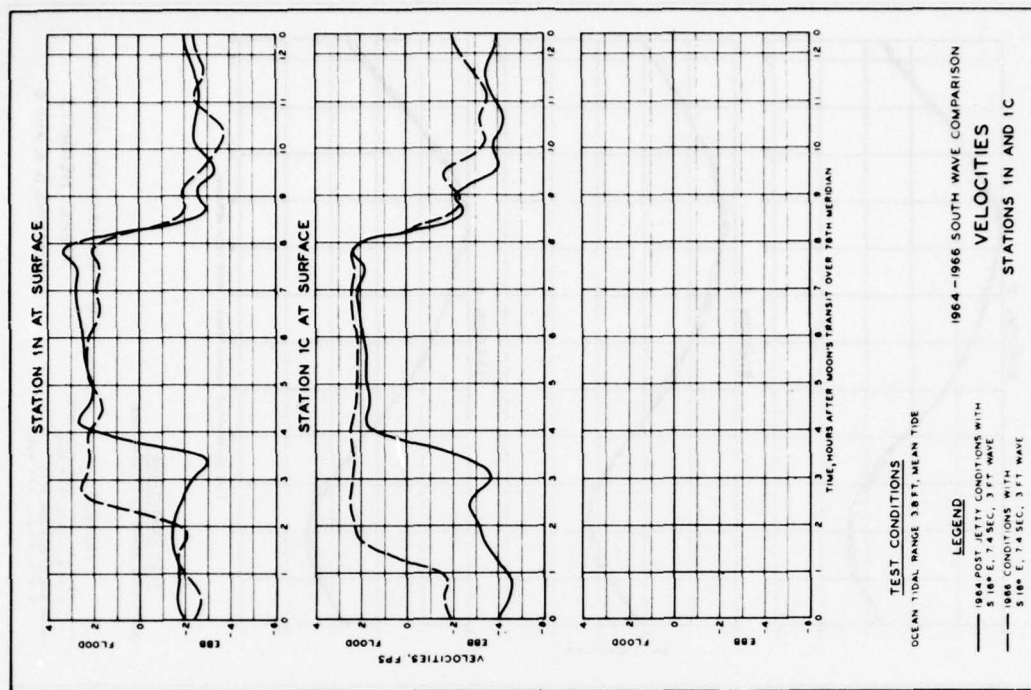


PLATE 333

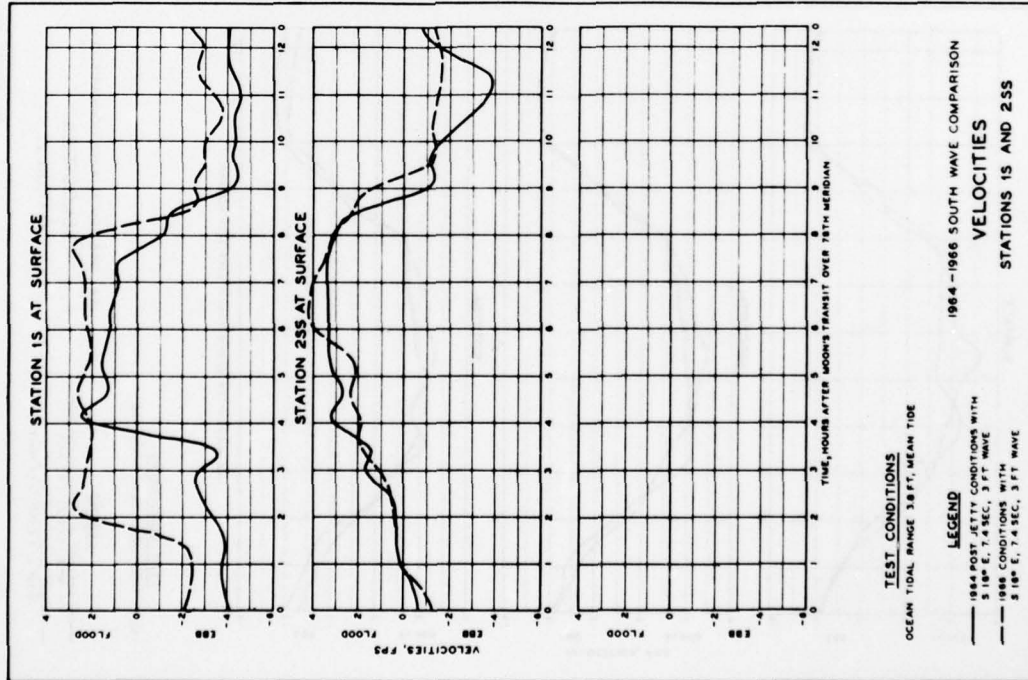


PLATE 334

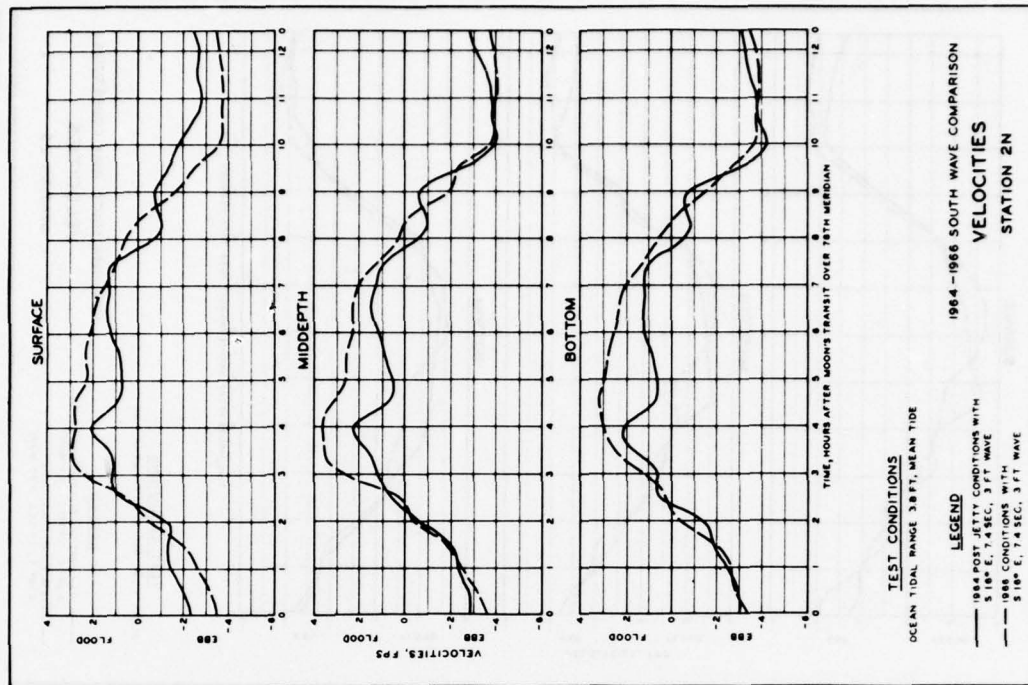


PLATE 335

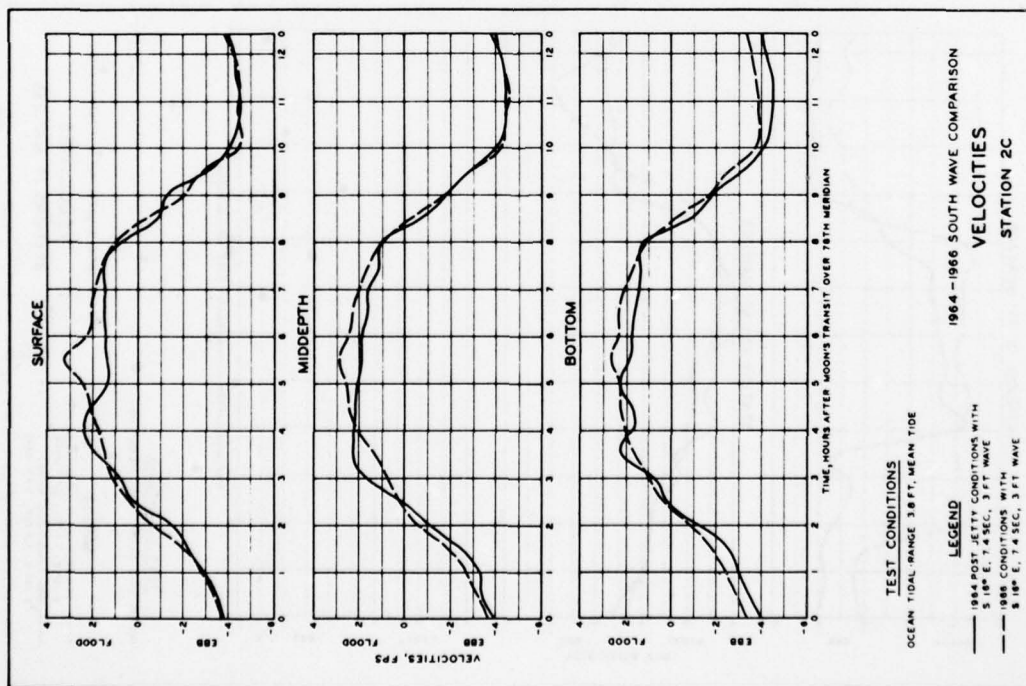


PLATE 336

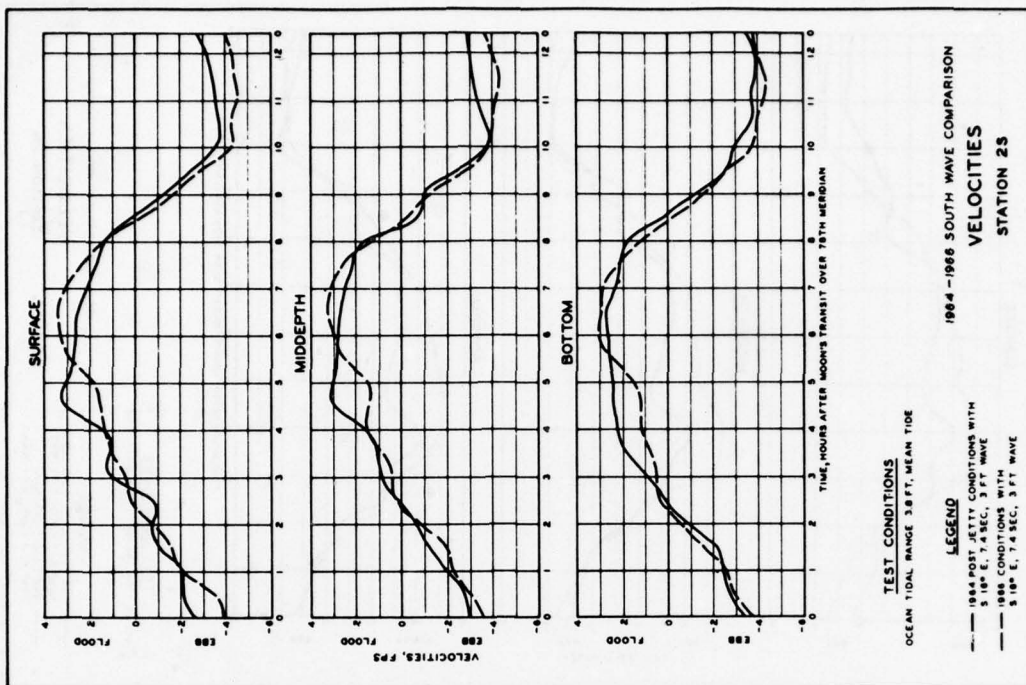
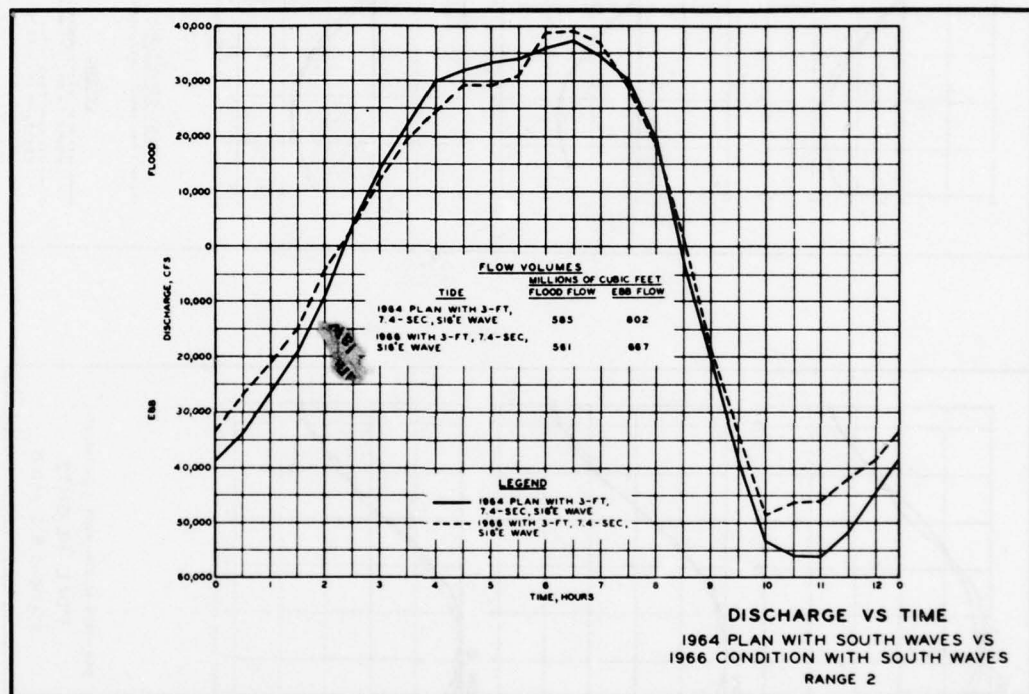


PLATE 337



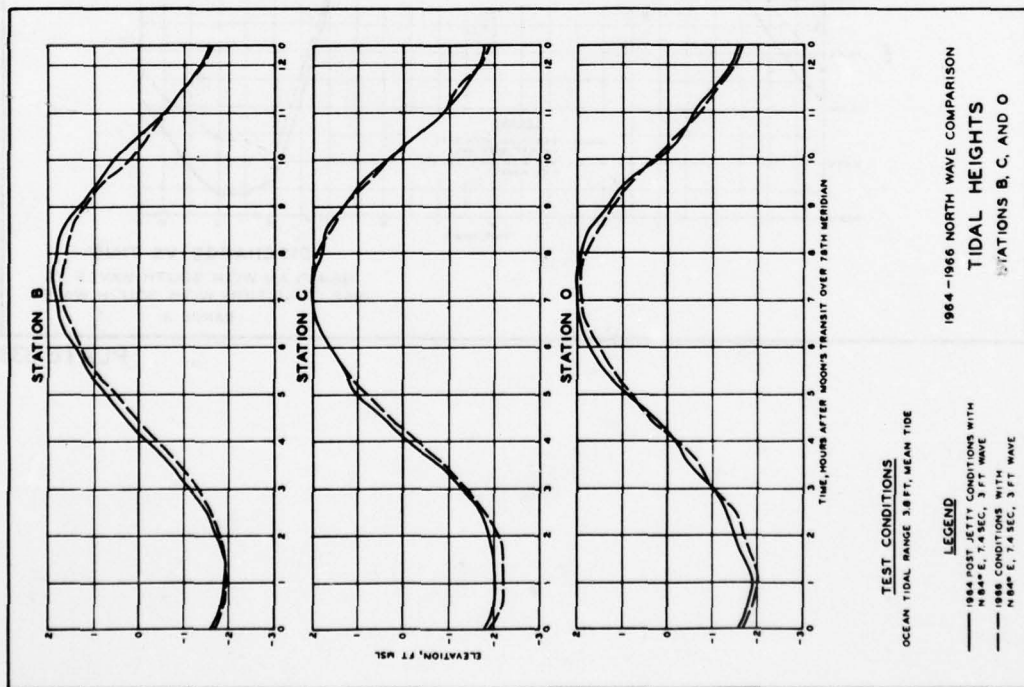


PLATE 339

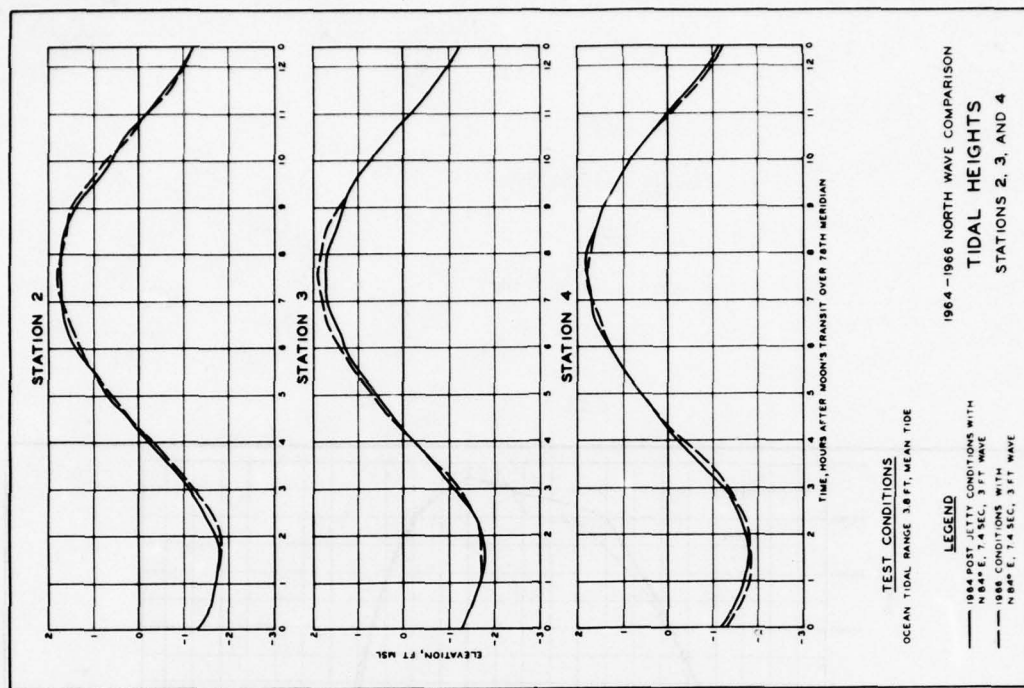


PLATE 340

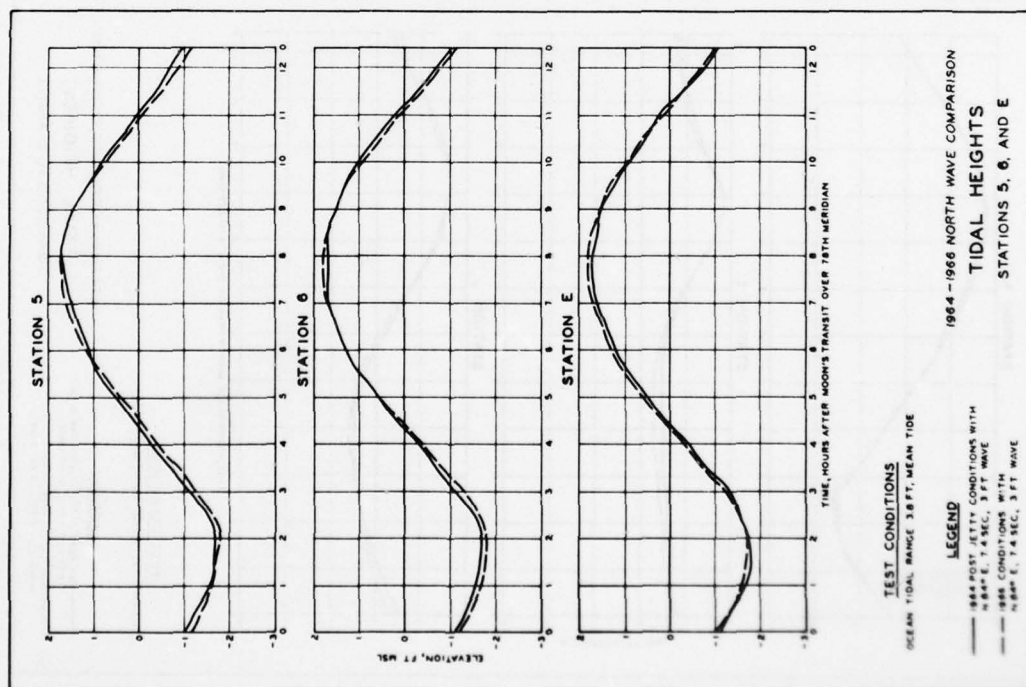


PLATE 341

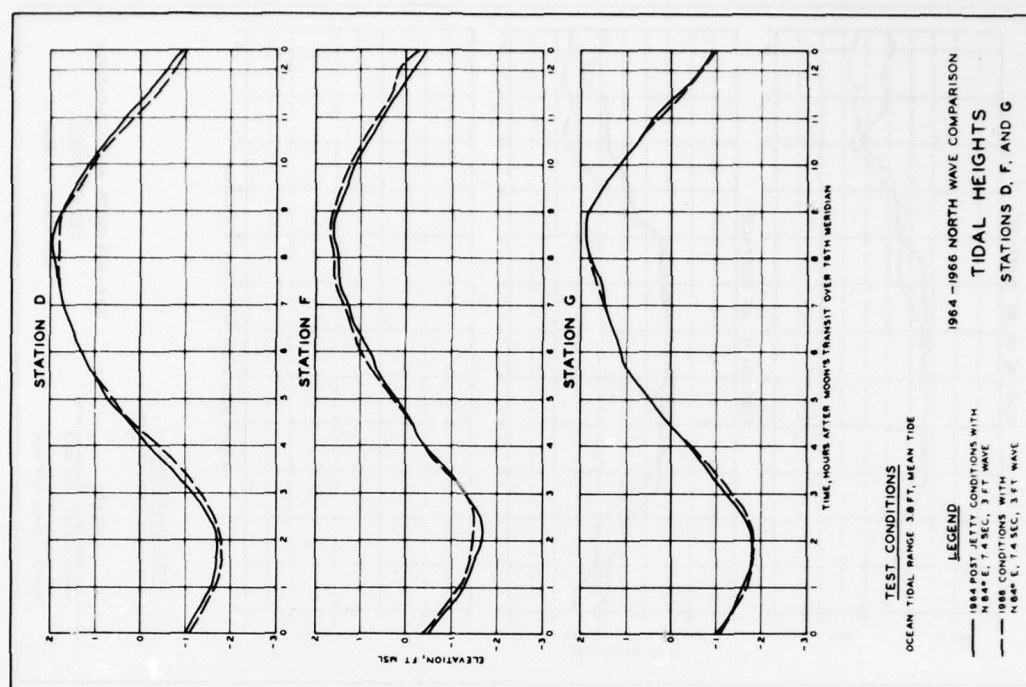


PLATE 342

AD-A055 523

ARMY ENGINEER WATERWAYS EXPERIMENT STATION VICKSBURG MISS F/G 8/3
PHYSICAL MODEL SIMULATION OF THE HYDRAULICS OF MASONBORO INLET,--ETC(U)
NOV 77 R A SAGER, W C SEABERGH

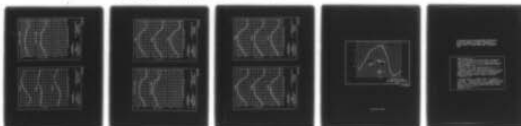
UNCLASSIFIED

WES-GITI-15

NL

5 OF 5

AD
A055523



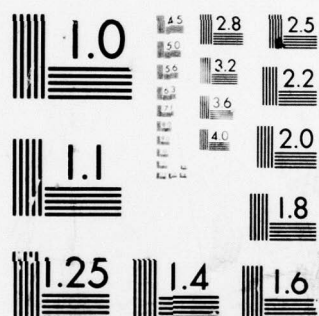
END

DATE

FILMED

7-78

DDC



MICROCOPY RESOLUTION TEST CHART
NATIONAL BUREAU OF STANDARDS-1963-A

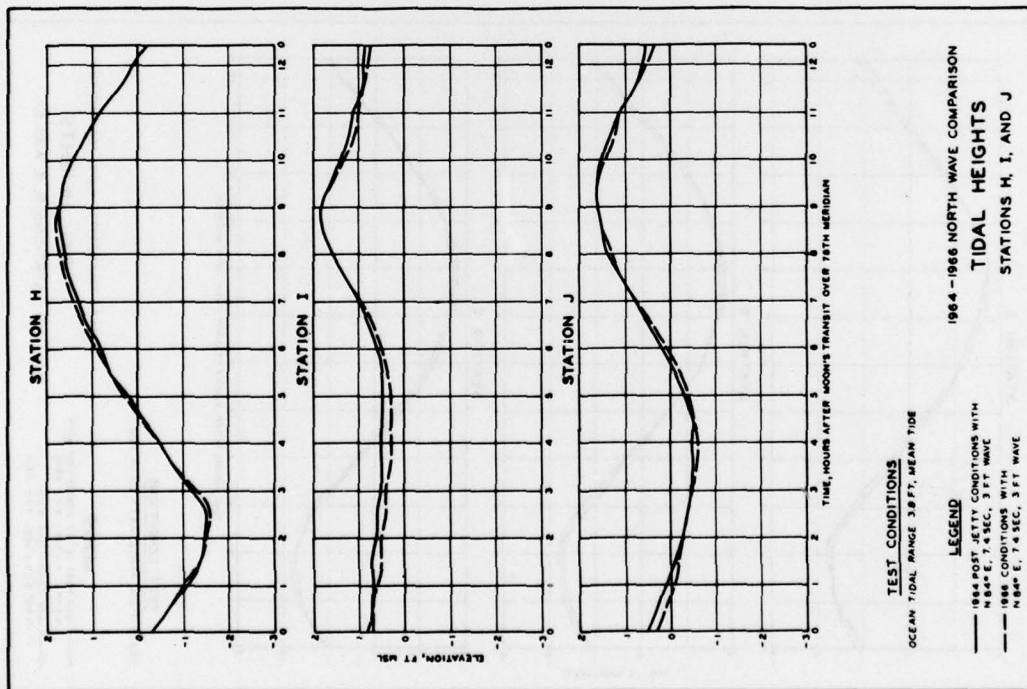


PLATE 343

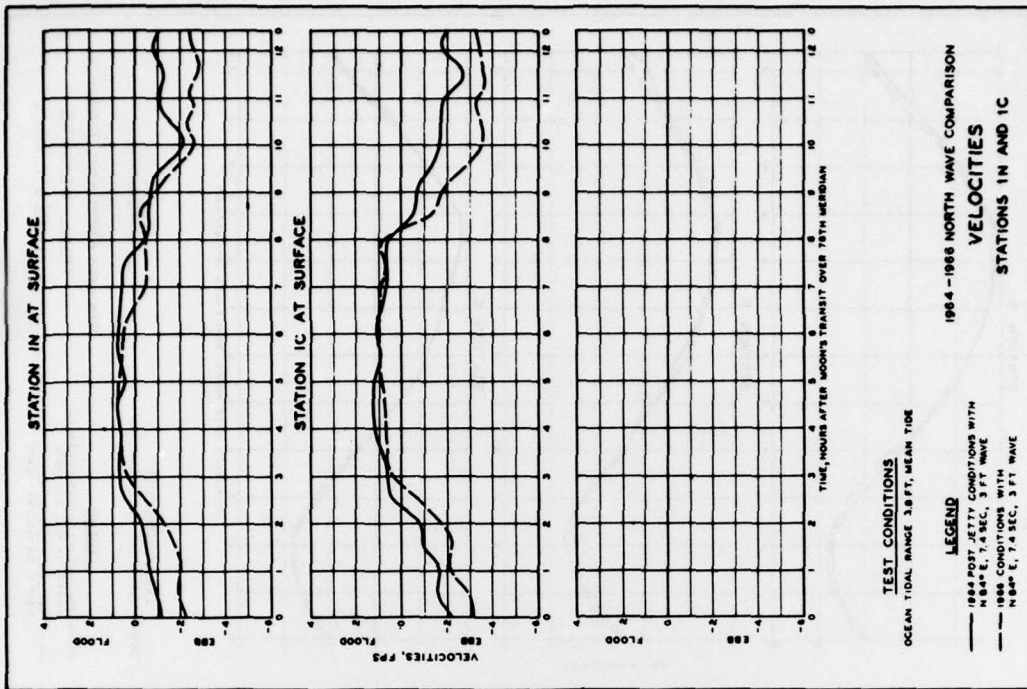


PLATE 344

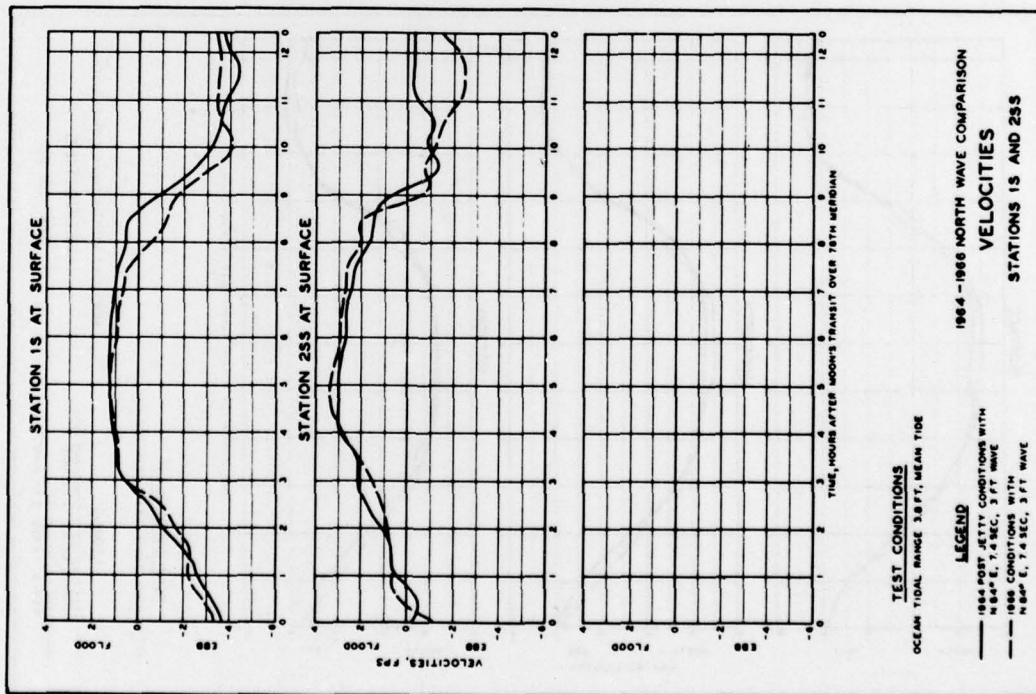


PLATE 345

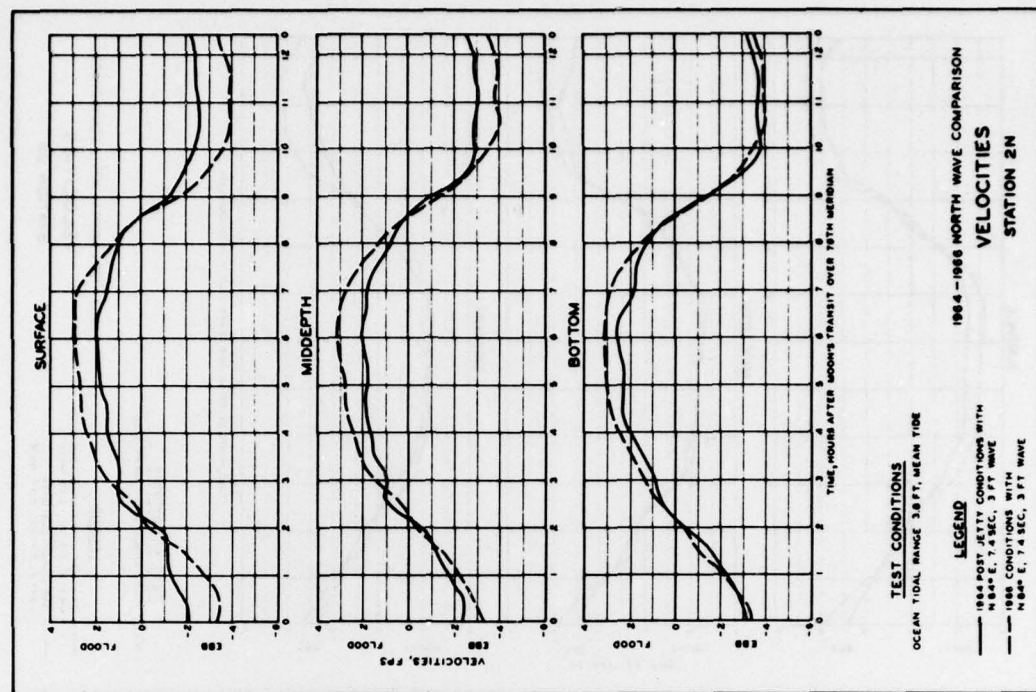


PLATE 346

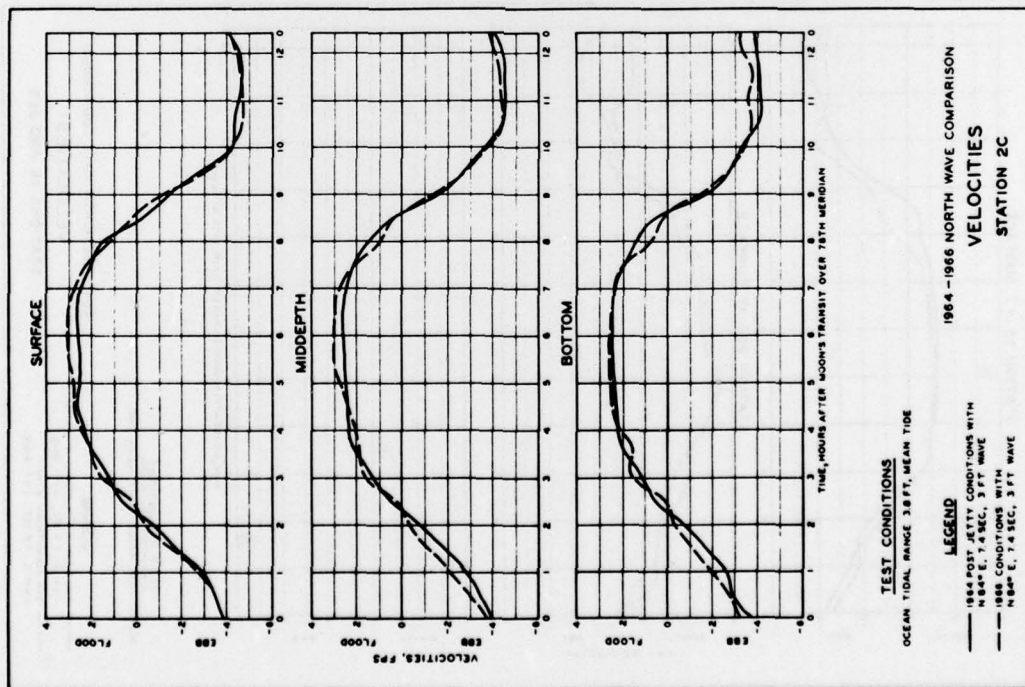


PLATE 347

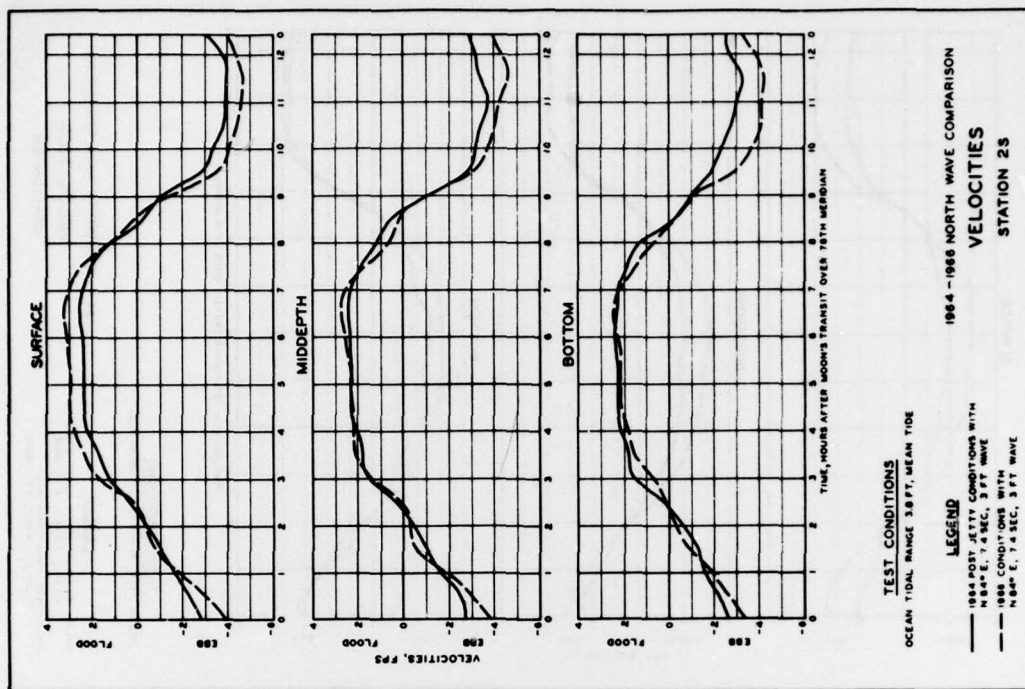


PLATE 348

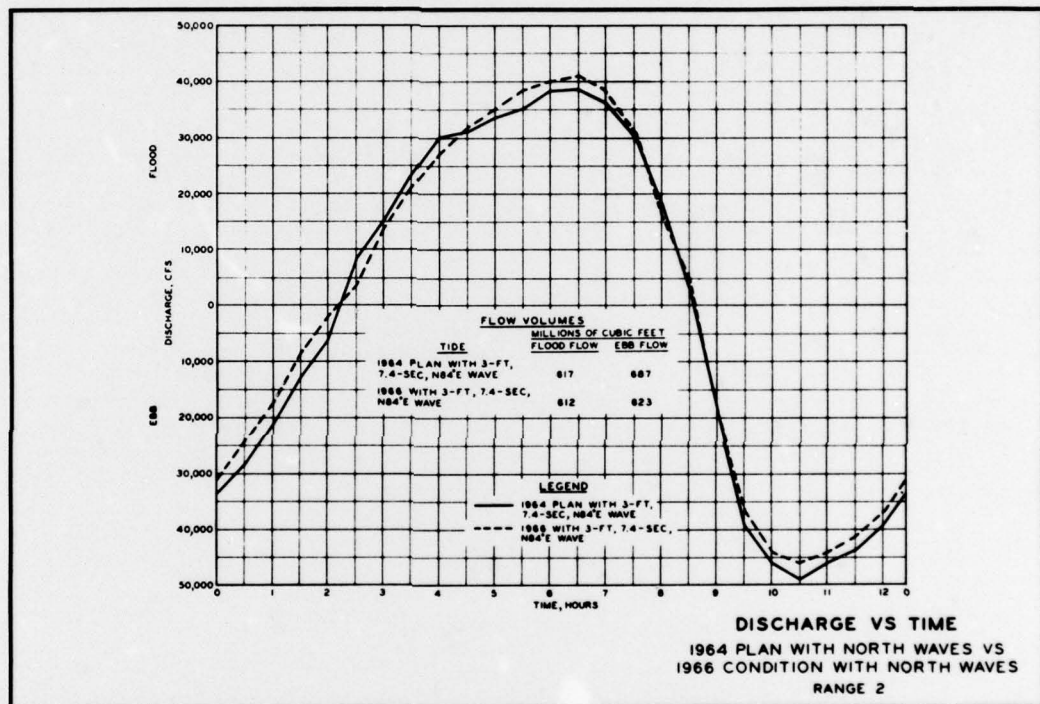


PLATE 349

In accordance with letter from DAEN-RDC, DAEN-ASI dated 22 July 1977, Subject: Facsimile Catalog Cards for Laboratory Technical Publications, a facsimile catalog card in Library of Congress MARC format is reproduced below.

Sager, Richard Allan

Physical model simulation of the hydraulics of Masonboro Inlet, North Carolina / by Richard A. Sager, William C. Seabergh. Vicksburg, Miss. : U. S. Waterways Experiment Station ; Springfield, Va. : available from National Technical Information Service, 1977.

94, 44, 105 p., 180 leaves of plates : ill. ; 27 cm. (GITI report - U. S. Army. Corps of Engineers ; 15)

General investigation of tidal inlets; a program of research conducted jointly by U. S. Army Coastal Engineering Research Center, Fort Belvoir, Virginia, and U. S. Army Engineer Waterways Experiment Station, Vicksburg, Mississippi.

References: p. 94.

1. Fixed-bed models. 2. Hydraulic models. 3. Hydraulic similitude. 4. Masonboro Inlet, N. C. I. Seabergh, William C., joint author. II. United States. Coastal Engineering Research Center. III. United States. Waterways Experiment Station, Vicksburg, Miss. IV. Series: United States. Army. Corps of Engineers. GITI report ; 15.
GB454.T5.U5 no.15

IED
78